ISEC 86

International Committee for Solvent
Extraction Chemistry and Technology

European Federation of Chemical Engineering

ISEC '86
International Solvent Extraction Conference

Preprints

Volume I

DECHEMA

München, Fed. Rep. of Germany
11 — 16 September 1986

BART

Carl Hanson Memorial Session

Contents

Volume I

Page

Processing needs in metal extraction
D.S.Flett, Stevenage, Herts/UK 3- 11

The future of solvent extraction in the nuclear fuel cycle
H. Eccles, A. Naylor, Preston/UK 13- 22

The kinetics of nitric acid extraction by TBP in a rotating diffussion cell
P.N.E. Lawson, M.A. Hughes, Bradford/UK 23- 30

The Purex-process computer-model "VISCO" and its applications
G. Petrich, Karlsruhe/D 31- 39

Axial mixing coefficients in reciprocating plate colums
A.E. Karr, S. Ramanujam, Fairfield, N.J./USA;
T.C.Lo, Nutley, N.J./USA; H.I. Baird, Hamilton, Ont/CDN 41- 48

Supercritical and new Extraction Systems

The process and the environment — is solvent extraction the answer?
G.M. Ritcey, Nepean, ONT/CDN 51- 62

Supercritical phase equilibria — theory and applications
A. Fredenslund, Lyngby/DK; E. Brignole, Bahia Blanca/RA 63- 73

PUREX: Process and equipment performance
D.A. Orth, Aiken, SC/USA 75-80

Application of the TRUEX process to the decontamination of nuclear waste streams
E.Ph. Horwitz, Argonne, IL, W.W. Schulz, Richland, WA/USA 81-90

Some chemical aspects of solvent extraction performance in the Tokai reprocessing plant
M. Ozawa, K. Koyama, T. Yamanouchi,Ibaraki-ken/J 91- 98

Process-control for reprocessing plant WA Wackersdorf
B. Kube, Hannover, A. Nothaft, Stuttgart/D 99-106

Long chain NN di alkyl aliphatic amides as extracting agents of actinides: progress in process development for high burnup fuel reprocessing
M. Casarci, G.M. Gasparini, G. Grossi, A. Moccia, Rome/I 107-115

Technical scale electroredox equipment for the separation of plutonium
H. Schmieder, H. Goldacker, Karlsruhe/D 117-129

REPROCX — a reprocessing flowsheet computational syste
J.W. Harrison, A.L. Mills, M. Wilkins, Harwell/UK 131-136

Technetium behaviour control in the PUREX process
E. Vialard, M. Germain, Fontenay-aux-Roses/F 137-142

Solvent regeneration development at the Idaho chemical processing plant
A.L. Olson, C.W. Mc Cray, Idaho Falls, ID/USA 143-149

Model reference adaptive control system of liquid-liquid extraction column
A.Al Khani, M.V. Le Lann, K. Najim, G. Casmatta, Toulouse/F 151-160

Solvent extraction of uranium and plutonium for the reprocessing of nuclear power reactor fuels by the Purex process. Comparison between simulation and experiment
A. Nothaft, E.D. Gilles, Stuttgart/D; H. Ramm, Hannover 161-168

Calculation and measurement of concentration profiles for the coupled fluxes of uranylnitrate and nitric acid in a pulsed column
E. Ihle, R. Ollenik, W. Nitsch, Garching/D 169-174

Nuclear Fuel Reprocessing

Calculation of the activity coefficient of TBP in water solution and in diluent by the cluster expansion method
Yun-Xiaon Zhong, Wenqing Xiaobo Wang, Beijing/China 175-176

Improvements and results acquired through six years of industrial uranium extraction from phosphoric acid by the PRAYON process
A. Davister, G. Martin, Engis/B 177-184

Estimation of equilibrium constants for the extraction of nitric acid by TBP-kerosene mixtures
J.M. Schaekers, Pretoria/ZA 185-192

Extractions of iodine from irradiated uranyl nitrate samples
M.G. Jalhoom, Baghdad/Iraq 193-200

Boundaries of third-phase formation by uranium (IV) and plutonium (IV) in TBP / diluent systems
P.D. Wilson, J.K. Smith, Cumbria/UK 201-208

Kinetics of uranium extraction and stripping in DEHPA-TOPO process of uranium recovery from phosphoric acid
R. Stevanović, Z. Ilić, S. Milojić, v. Pavasović, Beograd/YU 209-214

Study of extraction rate for uranyl-nitrate-TBP/n-dodecan in a single drop column
K.W. Kim, Y.J. Shin, J.H. Yoo, H.S. Park, Chung-Nam/Korea 215-222

Interphase transfer kinetics of plutonium and nitric acid in the system nitric acid — tributylphosphate, dodecane
C. Mas, G. Knittel, R. von Ammon, Karlsruhe/D 223-230

Kinetics of the extraction of uranium (VI) by synergistic mixtures: Di-2-ethyl-hexyl phoshoric acid (HDEHP) / Neutral organophosphorus extractants (TBP and TOPO)
A. Maher, D. Pareau, Chatenan-Malabry/ 231-238

Properties of heavy organic phases and their formation in the PUREX process
L. Stieglitz, R. Becker, H. Bautz, R. Will, Karlsruhe/D 239-244

Extraction of Cr, Nd, Ru and U in PUREX-Media monitored by an analytical ultacentrifuge
V. Friehmelt, Ch. Frydrych, R. Gauglitz, S. Kriegel, G. Marx, Berlin (West) 245-252

Studies on interfacial precipitation of the first PUREX extraction cycle
F. Baumgärtner, A. Huber, Garching/D 253-260

Extraction of actinides and fission products by non-chelating N, N'-tetra-alkylamides
M.-C. Charbonnel, C. Musikas, Fontenay-aux-Roses/F 261-266

Phoric acid and di-2-ethyl hexyl monothiophosphoric acid: sturcture of the complexes of the organic phase
D. Pattee, C. Musikas, A. Faure, C. Chachaty, Fontenay-aux-Roses/F 267-274

The reciprocical effect of iron (III) and uranium (VI) extraction by synergistic mixture di-2-(-ethylhexyl) phosphoric acid and triocylphosphine oxide from phosphoric acid solutions
S. Meleš, I. Fatović, M.V. Proštenik, J. Romano, Zagreb/YU 275-283

Improved URPHOS process to extrat uranium from phosphoric acid using new organo-phoshorous solvents
A. Bathelier, G. Lyaudet, A. Textoris, Bessines sur Gartempe;
P. Michael, Velizy Villacoublay/F 285-292

Analysis of the extraction tailing in Purex process
F. Baumgärtner, J.I. Kim, K. Stephan, Garching; B. Kanellakopulos, Karlsruhe/D 293-300

Non reductive partitioning of uranium and plutonium in the Purex process
D.O. Campbell, Oak Ridge, TN/USA; A.L. Mills, Harwell/UK 301-307

Demonstration of the electrochemical reduction of Pu (IV) in the Purex-process in the absence of hydrazine
M. Heilgeist, K. Flory, U. Galla, H. Schmieder, Karlsruhe/D 309-316

Investigation concerning lay-out of industrial extraction columns for the Purex-process: Influence of mixing effects on mass transfer parameters
K. Eiben, K. Haberland, Leopoldshafen; P. Feucht, A. Merz, R. Walter, Karlsruhe/D 317-324

THOREX process studies
E. Zimmer, J. Borchardt, Jülich/D 325-332

Separation of fission products from U and Pu in the highly radioactive cycle of the Purex process
Z. Kolarik. H.-J. Bleyl, H. Schmieder, Karlsruhe/D 333-341

Plutonium and americium extraction studies with bifunctional organophosphorus extractants
J.D. Navratil, Golden, CO/USA 343-345

The extraction of uranium (IV) from wet-process phosphoric acid in a centrifugal extraxtor
K. Grabas, Wrocław/PL 347-353

Separation of long alpha emitters from medium activity liquid wastes by solvent extraction with tri butyl aceto hydroxamic acid (TBHA)
M. Casarci, D. Carlini, G.M. Gasparini, G. Grossi, G. Torri, Rome/I 355-362

Preconcentration of uranium by membrane extraction with di-2-ethyl hexyl-phosphoric acid
F. Macašek, P. Rajec, V. Ngoc Anh, V. Řehaček, Bratislava/CS 363-369

The influence of plate surfaces on the hydrodynamics of pulsed plate columns
W. Batey, S.J. Lonie, P.J. Thompson, J.D. Thornton, Caithness/UK 371-378

The design, operation and performance of a pulsed columns pilot plant for fast reactor fuel reprocessing
J.A. Jenkins, D.H. Logsdail, E. Lyall, P.E. Myers, Harwell, Oxfordsh./UK 379

Efficiency of contactors
D.A. Orth, F.R. Graham, D.L. Holt, Aiken, SC/UK 381-386

The effect of phase ration on pulse column capacity for high volume/low uranium concentraction system
T.A. Todd, A.L. Olson, Idaho Falls, ID/USA 387-392

Tritium seperation from PUREX-solution
P. Feucht, G. Petrich, Karlsruhe; K. Eiben, H. Evers, Leopoldshafen/D 393-398

Transient behaviour of PUREX pulsed columns
J. Schön, H.-J. Bleyl, D. Ertel, E. Hamburger, M. Kluth,G. Petrich, W. Riffel, Karlsruhe/D 399-404

Hydrodynimacis in pulsed perforated plate extraction columns of annular and circular cross section
H. Schmidt, Karlsruhe/D 405-412

Development of low capacity centrifugal extractors for small scale reprocessing facilities
S.B. Koganti, V. Sreedharan, G.R. Balasubramanian, Kalpakkam/IND 413-420

Discosearch — a computerised storage and retrieval system for Purex distributation data
A.L. Mills, Harwell; R. Ross Oxford/UK 421-426

Application of the code PULCO for the simulation of pulsed column behaviour in the 1. extraction cycle of the PUREX-process
E. Gelfort, B. Heits, Hannover; H. Kühl, W. Weyer, Titz-Rödingen/D 427-432

The tri-n-butylphosphate (TBP) distruction owing nitric acid, zirconium and hafnium
O.A. Sinegribova, G.A. Yagodin, A.A. Varnek, R.P. Ozerrov, A.H. Kuznetsov, Moscow/USSR 433-440

Chemical degradation of amine solvents
Y. Sze, D.A. Archambault, C.G. Martin, T.E. McDougall, D.G. Boase, Pinava, Manitoba/CDN 441-448

Fundamental Studies

Measurement of liquid-liqiud interfacial kinetics: where do we stand?
R.D. Noble, Bouler, CO/USA 451-458

Reactions in monolayers between liquid phases
Th. Michel, K. Matt, A. Hamza, W. Nitsch, Garching/D 459-466

Laser light-scattering and laser fluorescense studies of solvent extraction systems
R.D. Neuman, Auburn, AL/USA 467-473

Effect of dissolved salts on the binary vapour-liquid equilibria and binary and ternary liquid-liquid equilibria
V.K. Srinivas, D. Srinivasan, Madras/IND 475-476

Selectivity and equilibria in extraction with macrocycles in synergistic combination with organophilic acids
W.J. McDowell, B.A. Moyer, S.A. Bryan, R.B. Chadwick, G.N. Case, Oak Ridge, TN/USA 477-482

Modelling of salting out effects and solvent extraction equilibria
H. Pitsch, Mexico/MEX; J. Ly, C. Poitrenaud, Gif-sur-Yvette/F 483-490

A general model for computing liquid-liquid equilibria. Application to the extraction of cobalt, copper and manganese by tri-iso-octylammonium choloride
P.A. Noirot, M. Wozniak, Villeneuve d´Arcq/F 491-498

To the tehory of mutual influence of metals in the extraction systems with aggregated extractants
V.V. Bagreev, Yu.A. Zolotov, S.O. Popov, V.I. Vernadsky, Moscow/USSR; C. Fischer, Dresden/DDR 499-506

Interfacial phenomena of liquid-liquid systems under electric, magnetic and gravitational fields
V. Mohan, P. Jayasankar, K. Padmanabhan, Madras/IND 457-510

Interfacial transfer under electrostatic field in solvent extraction
M. Hund, F. Lancelot, Saint-Etienne/F 511-517

Amine phase partitioning using emulsion liquid membranes
A. Kirkkopru, R.D. Noble, Boulder, CO; A.L. Bunge, Golder CO/USA 519-522

Liquid Membranes

Challenges and progress in ion selection and transport systems
O. Kedem, A. Warshawsky, Rehovot/IL 525

Supported liquid membranes in 1986: New technology or scientiffic curiosity?
P.R. Danesi, Wien/A 527-536

Extraction of metals using supported liquid membranes: the cooper/o-hydroxy-oxime system
M. Cox, D.A. Mead, Hatfield, J. Melling, Stevenage/UK 537-544

Selectivity in the extraction of metals by liquid membranes
M. Teramato, T. Sakuramoto, H. Takaya, Y. Katayama, A. Kojima, Kyoto/J 545-552

Seperation of metal species by emulsion liqiud membranes
J. Draxler, W. Fürst, R. Marr, Graz/A 553-560

Metal extraction with liquid surfactant membranes: The role of the emulsifying agent
B.A. Mikucki, K. Osseo-Asare, University Park, PA/USA 561-566

Separation of copper from a zinc solution by liquid membrane permeation
H.J. Bart, R. Wachter, R. Marr, Graz/A 567-571

Supported liquid membrne separation of aluminium from copper leaching liquors
L.E. Schultze, S.P. Sandoval, T.G. Carnahan, J.A. Eisele, Reno, NV/USA 572

Development of new surfactant in liquid surfactant membrane process
F. Nakashio, M. Matsumoto, M. Goto, J. Irie, K. Kondo, Fukuoka/J 573-579

Ionizable crown ethers for coupled transport of metals across liquid membranes
R.A. Bartsch, W.A. Charewicz, S.I. Kang, W. Walkowiak, Lubbock, TX/USA 581-583

Recovery of indium from industrial solutions by supported liquid membranes
R. Guerriero, L. Meregalli, I. Vittadini, Venice/I; X. Zhang, Beijing/China 585-592

Stationary mass transfer at inorganic substances membrane extraction
G.A. Yagodin, S.Yu. Ivakhno, A.V. Afanasjev, A.O. Sinegribova, Moscow/USSR 593-600

Use of liquid membrane in metal recovery from metal-containing wastes in the ppm-range
W. Gutknecht, H.-B. Hauertmann, K. Schürgerl, Hannover/D 601-609

Coupled transport of zinc using solid supported liquid membranes
L. Fernandaez, J. Aparcio, M. Muhammed, Stockholm/S 611-618

Appendix

Solvent extraction of metals by oligomeric extracting agents
V.I. Bukin, A.M. Reznik, S.A. Semenov, L.D. Yurchenko, Moscow/USSR 621-629

Author Index A-1 — A-16

Carl Hanson Memorial Session

Processing Needs in Metal Extraction

D S Flett, Warren Spring Laboratory, Stevenage, Herts, U.K.

Metal extraction, be it from ores or concentrates or from secondary scraps and wastes is carried out either by pyrometallurgy or hydrometallurgy. The relationship between pyrometallurgy, hydrometallurgy and the mining and preconcentration processes is shown in fig 1. It may be thought that there is no common ground between pyro- and hydrometallurgy but that is not so as much of the chemistry carried out in both types of process involves heterogeneous systems wherein mass transfer and phase separation are common critical parameters with regard to space-time yields within processing equipment. While the processing needs in metal extraction can therefore be considered as a whole within this broad framework, it is surely more appropriate at ISEC'86 to consider them in the context of the solution treatment step of fig 1 which of course includes, amongst the array of currently available separation and purification processes, the process of solvent extraction which is the theme of ISEC'86 and indeed for which mass transfer and phase separation are critical components. This paper therefore examines the current state of the art of solution treatment in metal extraction and seeks to identify what the future requirements may be.

General Considerations

Notwithstanding the current recession in world metal markets and the consequent downturn in activity on the mining and processing scene in response to market imbalances, some significant trends within the industry are discernable which are already having and will continue to have a considerable impact on processing needs. For example there is the need to mine and treat ever lower grade material where "simple" ores are concerned while on the other hand there is an upsurge in interest in higher grade complex ores. Furthermore, the concept of "total resource utilisation" is one which has become more common and thus deportment and recovery of cc-products and minor values in the materials being processed is of particular importance. Finally recycling and recovery of metals from scraps, wastes of all descriptions and from metalliferous effluents such as mine waters and plant waste liquors is assuming an ever-increasing importance which, technological requirements apart, also impacts upon the requirement for metal from primary sources.

Developments in Separation Science in Hydrometallurgy

Although hydrometallurgy has a history which is hundreds of years old (1) large scale use has only developed in the 20th century. In many ways this large scale development would have been impossible without the development of suitable separation science and technology which has led to the now-familiar processes of adsorption, ion exchange, solvent extraction and more recently membrane processes.

It is these processes and their successful engineering that have provided the vital bridge between the metalliferous feed materials by hydrometallurgical processes, the leach liquors therefrom and the final metal winning step for the production of pure metals. With the perceived trend to lower and/or more complex ores, hydrometallurgy may be expected to become increasingly important as the preferred process for metal winning, particularly where mineral processing techniques cannot economically succeed in producing concentrates which are acceptable feeds for the high temperature pyrometallurgical processes. Thus, particularly because of problems which will inevitably arise with selectivity in the leaching step and the difficulties (if not impossibility) in achieving high tenor leach liquors from low grade feedstocks then the burden of performance will increasingly fall on the solution treatment step in terms of providing purification, concentration and separation of the metal values of interest in the leach liquor and therefrom achieving optimal interface with the final metal winning process.

The developments in separation science in hydrometallurgy have been reviewed recently (2). From this review a number of points emerge. While precipitative processes and adsorption processes are of considerable importance in hydrometallurgy, they are likely to remain somewhat limited in their application not least because the development of solvent extraction and ion exchange has provided alternatives that are chemically much more efficient than precipitation processes for separating major metal values in leach liquors and are more easily engineered as continuous processes. Cementation however will continue to maintain its place in solution-purification applications particularly on a small scale while, in effluent treatment, chemical precipitation may continue to prove to be, for all its faults, a lower cost option than the more advanced technologies. Adsorption processes on the other hand are somewhat limited in their application with by far the largest application being for the recovery of gold on active carbon. Thus these two process options will not be considered further, and attention will be focussed on ion exchange, solvent extraction and membrane processes.

1. Ion Exchange Ion exchange is used in hydrometallurgy for the recovery and purification of uranium, thorium, rare earths, transition metals, transuranics, platinum group metals and chromium. By far the largest application has been in the uranium industry wherein the development of viable continuous ion exchange processes and equipment has provided the basis for the considerable commercial success that this process has achieved in this industry, wholly reversing the trend towards direct solvent extraction of uranium leach liquors that was prevalent in the late 1960's and early 1970's. It has been predicted that (3) continuous ion exchange would spread to other branches of hydrometallurgy but so far this has not happened to any great extent and solvent extraction seems to have too great a hold

and competes more favourable on the grounds of selectivity and high extraction rates. While quite a range of chelating ion exchange resins are now available, their exchange rates (2) are much lower than the extraction rates encountered in solvent extraction systems and for many, their selectivity for hydrometallurgy duty, leaves much to be desired. Thus it is considered that with current technology, resin inventories of any plants designed to use existing chelating resins for metal recovery from dilute primary leach liquors would probably be very large and thus the capital cost of such systems would be a major deterrent in any such proposed applications. In order to try to avoid these problems a combination of solvent extraction and ion exchange was devised to produce resin impregnates (2). While much work has been done on these systems throughout the world, commercialisation has been achieved only with the Levextrel products made by Bayer in Germany. However their encapsulation polymerisation manufacturing technique produces essentially hydrophobic products with low exchange rates. Work in Israel (4) aimed to avoid this problem by an impregnation technique that allowed carrier solvent used in the impregnation step to be washed out and replaced with water. However all these materials suffer from slow leakage of extractant with time and thus their lifetimes in industrial operations are limited. Production and material costs are high and thus applications with currently available materials are likely to be limited to low volume, high value metals and there is a clear need for cheaper, more stable materials if this technique is ever to be applied to low-tenor large volume metal-bearing liquors.

2. Solvent Extraction Solvent extraction is now a very well-established process in hydrometallurgy and is used to extract copper, nickel, cobalt, zinc, uranium, molybdenum, tungsten, vanadium, rare earths, zirconium, hafnium, niobium, tantalum, the platinum group metals, boron, wet process phosphoric acid, nitric acid etc and in the reprocessing of nuclear fuels. The whole field of solvent extraction in hydrometallurgy has been thoroughly reviewed recently (5) and some perceptive forward looking articles have also appeared (6,7). New reagents continue to appear and examples in recent years are the dialkyl phosphinic acid extractant, Cyanex 272, the dialkyl phosphine sulphide extractant Cyanex 471S both from American Cyanamid and CLX 20 from Acorga. Variations of the well known hydroxyoxime range of reagents also appear from time to time. Indeed it is worth pointing out that the leach-solvent extraction-electrowin approach to copper recovery from oxide ores in the USA is now producing some of the cheapest copper in the world so that the original work pioneered by General Mills back in the 1960's is really paying off for copper producers in what are particularly difficult times for them.

Research into solvent extraction systems continues unabated as shown by the number of papers to be presented at ISEC'86 on the chemistry, both equilibrium and kinetic, of metal extraction. However the whole subject in terms of applications and commercial use is now quite mature and even with such important equipment developments as the Davy CMS contractor (9) or the Krebs mixer-settler system (10), there have been very few major advances in process design and application in recent years. One process development that is of considerable interest however is that of microemulsion extraction. The chemistry of this process was presented by Bauer (11) at ISEC'83. This interesting development, which is already in commercial operation for gallium extraction from Bayer Process liquors (12), achieves very high extraction rates even for those systems which are characterised by very slow rates in conventional solvent extraction practice. Whether this novel development will have wider application in solvent extraction processing in general or will only be of useful application where specific problems arise such as with the extraction of gallium from Bayer Process liquors remains to be seen.

3. Membrane Processes The use of membranes in the process industries has increased significantly in recent years. Ion exchange membrane technology in particular has proved to be a considerable growth area, especially within the chlor-alkali industry while in hydrometallurgy generally the use of ion exchange membranes has been examined for tungsten processing (13), the regeneration of chromium plating baths (14), uranium processing (15) and in the regeneration of cupric chloride and ammoniacal etchants in the printed-circuit-board industry (16). These processing innovations have arisen from the development of new and improved membranes having high permselectivities and good conductivity, and new electrolytic cell designs such as ICI's FM21 and the Electricity Council's DEM cells (17).

In recent years one of the most exciting developments in the membrane field has been that of liquid membranes. These are considered to have several advantages over other separation processes ie. lower capital cost, low energy consumption and low solvent inventory which gives opportunities for economic use of exotic, expensive reagents. These are of two types a) emulsion (or surfactant) membranes and b) supported membranes. Full descriptions of such membranes and discussion of the basic transport mechanism have been given in the literature. Emulsion membranes are beginning to find commercial application in industry. For example this technology is now being used in Austria to recover valuable metals from industrial waste waters (18). Such systems however do suffer from the need to destroy and reform the emulsion in every process cycle and adventitious breakdown of the emulsion in the extraction step can be enhanced by osmotic flow between the two aqueous phases. While a variety of contactors have been considered for this technology it may be that column contactors will offer the best way forward in the immediate future.

Supported liquid membranes offer immediate opportunities for application through already available engineering concepts such as plate and frame type installations for flat polymer sheet supports or RO or microfiltration type engineering concepts for hollow fibre supports. From work done so far in this area it would appear that hollow fibre membranes are to be preferred over flat polymer sheet supports and by proper choice of fibres, long operating times (4000 hrs) can now be achieved in continuously running laboratory units (19). The major disadvantage of these membrane systems is the relatively low mass transfer rate per unit membrane area. It is believed that no commercial application of this technology has yet taken place, although work at Argonne National Laboratory (20), Bend Research (21), and Warren Spring Laboratory (19) has all shown considerable economic potential for this new technology.

FUTURE NEEDS

With the continuing trends in feed materials to hydrometallurgical operations noted earlier and the ever-increasing requirement to remove metals from mine waters and effluents, the need to effectively and economically process ever increasingly dilute solution (concentrations 0.1 gl^{-1} or less) will continue unabated. For water treatment where metal recovery is secondary, ion exchange, particularly continuous ion exchange will continue to play a dominant role. Where specific and selective recovery of metals is required then chelating ion exchange may be effective, provided that the pH of the liquor does not require adjustment to meet optimum absorption conditions and the metal ion exchange rate is high enough to avoid excessive resin inventories. Improvements in exchange kinetics of chelating resins will be essential to achieve this goal. Membrane processes have disadvantages when used to treat very dilute solutions. In particular, concentration polarisation is a problem when electrodialysis is used and deviations from zero order rate laws may limit recovery levels in practice. Direct electrolysis of dilute liquors using high surface area cathodes has some advantages but it is non-selective and there remain problems with further treatment of the cathode product. Conventional solvent extraction has a cut off point at somewhere around 0.5 gl^{-1} of metal in the feed. Thus selective recovery of metal ions from very dilute liquors remains a problem for the foreseeable future and no real alternative to non-selective ion exchange would appear to be in sight.

With regard to treatment of solutions containing greater than 0.1 gl^{-1} metal then selection of the appropriate separation technology will depend on ability to achieve the desired objectives and economic considerations. It does not appear likely that any quantum step in solvent extraction reagent technology is about to take place so that new tricks with existing reagents will be required and some very interesting possibilities arise from synergistic mixtures of reagents. The work carried out by Mintek (22) using mixtures of alkyl oximes and carboxylic acids to selectively extract nickel from cobalt is a good example of this technique. Also novel stripping processes have recently been the subject of study. The hydrolytic stripping approach developed at laboratory scale by Monhemius (23) has, on paper, considerable attractions and could offer a solution to the iron problem which pervades hydrometallurgy. A proper engineering assessment of this process based on larger scale and longer term continuous trials would seem overdue.

Although not particularly novel these days new information on direct reductive stripping of loaded organic phases has been provided recently by Demopoulos (24). It is again surprising that so little engineering design information and comparative economic data is available on this interesting process alternative. The application of this technique to direct production of platinum group metals from loaded organic phases in particular looks attractive. The direct production of metallic gold by water stripping gold loaded Kelex 100 extracts is surprising and the chemistry involved in this reaction bears closer examination.

Cost reductions in solid-liquid separation in hydrometallurgy are always welcome, particularly in current circumstances when marginal cost reductions in operating plants may achieve economic operation in an otherwise adverse climate. For continuous countercurrent column based resin-in-pulp processes the availability of denser resins would allow thicker pulps to be used than at present with a considerable impact on capital costs. The development of novel stirred vessel in-pulp contactors (25) is already well advanced and these avoid the operation limitation of the column contactors set by low resin density and pulp solids settling rate. Initial developments are aimed at the uranium industry.

Development of ion exchange resin based processes for gold to replace the carbon-in-pulp processes used currently would have advantages as resin capacities for gold are much higher than carbon and thus again capital costs could be reduced. Equipment identical to that cited above for uranium resin-in-pulp processing would be employed. The problem in the use of resins is not in the absorption step but in the elution. A very ingenious elution procedure which may well have solved this problem has been devised by Fleming (26) at MINTEK. It remains to be seen whether commercialisation of this technique will take place.

It seems unlikely that any really effective solvent-in-pulp process will be developed but liquid supported membranes may provide a basis for treatment of unclarified liquors as this technique provides the selectivity of the solvent extraction reagent without the need to intimately mix the organic phase with the pulps. Little information is as yet available for such processes and development work in this area could be very rewarding.

Much more research and development of membrane processes in hydrometallurgy is required. Insufficient information is available on relative transport numbers of multivalent ions in ion exchange membranes for typical hydrometallurgical process liquors containing copper, nickel, cobalt, zinc and iron and the provision of such data would be highly beneficial. For liquid membranes it is gratifying to see that well targetted work with column contractors (27) and the like is being carried out on the surfactant membrane systems in order to define engineering parameters for various potential processes. For supported liquid membranes, now choice of materials (hollow fibres) and the lifetime problem seems to be less of a problem, much more attention needs to be payed to enhancement of the mass transport rate.

In the longer term a wider interest in non-aqueous or mixed organic aqueous systems chemistry in hydrometallurgy seems likely (28). Certainly ion activities can be radically changed and interesting and potentially very useful chemistry is possible in such systems. The development of appropriate solvent-extraction systems with polar and non-polar organic solvents could be of considerable interest in the longer term and it is already well known that improved separations by ion exchange are possible in such systems.

In conclusion therefore, the increasing constraints of lower ore grades of simple ores and increasing complexity of higher grade ores seems to point to a much wider application of hydrometallurgy than is currently practised. Such an expansion of application will require the availability of cost effective separation processes in order to bridge the gap between leach liquor and final metal winning steps. Separation science and technology is the key to successful hydrometallurgy. It has served it well in the past and there is every reason to believe that it will serve it equally well in the future.

References

1) Flett, D S. Chemy Ind. 1981, June 20, 427-431.

2) Flett, D S. MINTEK 50, Proc. Int. Conf. Mineral Science and Technology. Haughton, L F. (ed), publ. The Council for Mineral Technology, Randburg. RSA, 1985, Vol 1, 63-75.

3) Streat, M. J. Sep. Process Technol. Vol 1, no 3, 1980, 10-18.

4) Warshawsky, A and Patchornik, A. The Theory and Practice of Ion Exchange: An International Conference, Streat, M. (ed) Paper no. 38, London Society of of Chemical industry 1976.

5) Flett, D S. Hydrometallurgy, Research, Development and Plant Practice Osseo-Asare, K and Miller, J D. eds. Warrendale, The Metallurgical Society, AIME, 1982, 39-64.

6) Hanson, C. Plenary lecture, Proc. ISEC'80, 80-I, 13pp, 1980.

7) Ritcey, G. Sep. Sci and Technol. 1983, 18 (14,15), 1617-1646.

8) Kordosky, G A; Sudderth, R B and House, J E. Extraction Metallurgy '85 IMM, London, 1985, 1057-1074.

9) Gillett, G A and Rowden, G A. Chemy Ind. 1985, Sept 2, 583-589.

10) Kohler, K L; Sonntag, AA and Szanto, I. Extraction Metallurgy '85 IMM, London, 1985, 849-876.

11) Bauer, D and Komornicki, J. Proc. ISEC'83, A.I. Chem.E. 1983, 315-316.

12) Fitoussi, R and Helgorsky, J. Poster Presentation, ISEC'83, Denver, Colorado, 1983.

13) Vadasdi, K; Olah, R; Szilassay, I and Jeszenszky, A. 11th Int. Plansee Seminar '85 Vol 1, 77-89.

14) Grot, W G. Electrochemistry in Industry: New Directions. Landau, U; Yeager, E and Kortan D. (eds) New York, Plenum, 1982, 73-87.

15) Seko, M; Miyauchi, K and Omura, J. Ion Exchange Membranes, Flett, DS. (ed) Chichester, Ellis Horwood Ltd, 1983, 179-193.

16) Anon, Materials Reclamation Weekly, 1985, May 25, 23.

17) Marshall, R J and Walsh, F C. Surface Technol. 1985, 24 45-77.

18) Anon, Materials Reclamation Weekly, Dec 7, 1985, 20.

19) Flett, D S and Pearson, D. Extraction Metallurgy '85, IMM, London, 1985, 1-21.

20) Danesi, P R. Paper presented at first ACS Award Symposium, in Separation Science and Technology, St Louis, Mo. April 8-13, 1984.

21) Parkinson, G; Short, H and McQueen, S. Chem. Engng. 1983, 90, (17), 22-27.

22) Preston, J S. Hydrometallurgy 1983, 11 105-124.

23) Monhemius, A J. MINTEK 50 Proc. Int. Conf. on Mineral Sci and Technol. Haughton, L F. (ed) The Council for Mineral Technology, South Africa, 1985, Vol 2, 599-609.

24) Pouskouleu, G and Demopoulos, G P. Paper presented at IPMI Int. Symp. Toronto, Canada, June 1984.

25) Naden, D; Bicker, E; Willey, G and Lunt, D. Ion Exchange Technology, Naden, D and Streat, M. (eds) Ellis Harwood Ltd, 1984, 690-697.

26) Fleming, C A. Extraction Metallurgy '85, IMM, London 1985 757-787.

27) Melzner, D; Tilkowski, J; Mohrmann, A; Poppe, W; Halwachs, W and Schügerl, K. Hydrometallurgy, 1984, 13, 105-123.

28) Muir, D M and Parker A J. Hydrometallurgy, Research, Development and Plant Practice. Osseo-Asare, K and Miller, J D. (eds) New York, The Metallurgical Society, AIME, 1983, 341-355.

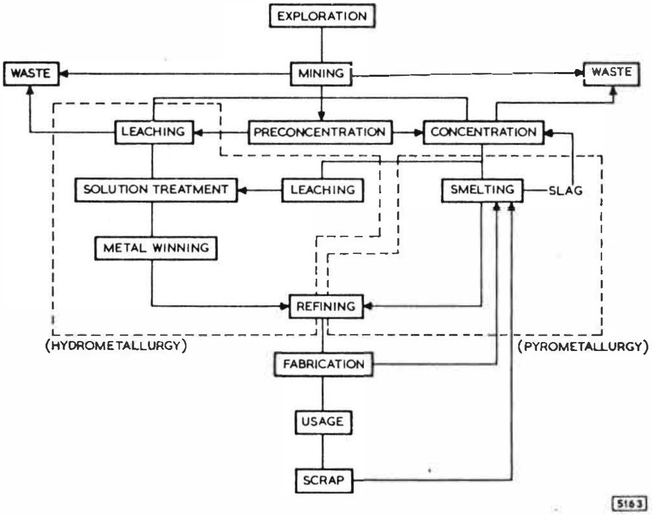
EXPLORATION
MINING
WASTE
WASTE
LEACHING
PRECONCENTRATION
CONCENTRATION
SOLUTION TREATMENT
LEACHING
SMELTING
SLAG
METAL WINNING
REFINING
(HYDROMETALLURGY)
(PYROMETALLURGY)
FABRICATION
USAGE
SCRAP
5163

FIG. 1 SCHEMATIC VIEW OF EXTRACTIVE METALLURGY

THE FUTURE OF SOLVENT EXTRACTION IN THE NUCLEAR FUEL CYCLE

H Eccles and A Naylor

Technical Department
BRITISH NUCLEAR FUELS PLC
Springfields Works
Preston
Lancashire, UK

The solvent extractive process has been used in the nuclear industry for about forty years. This paper briefly reviews the origin and scope of the technology within the industry. The current position of solvent extraction in each of the various stages of the nuclear fuel cycle, namely, mining, refining and reprocessing are considered. The future potential for solvents, contactors and complementary processes such as liquid membranes are predicted.

INTRODUCTION

Solvent extraction has dominated the scene in many areas of the nuclear fuel cycle for over forty years and has played a major role in achieving high standards of separation and purification under varying conditions.

The success of the application of solvent extraction to the mining/milling of uranium ore, refining of ore concentrates and in nuclear fuel reprocessing has been due to its adaptability to lend itself to cost-effective multi-stage operation needing little maintenance. The technology has been particularly useful when a consistently high quality product has been required, when purification/separation factors of 10^4 - 10^8 were necessary or when components (eg the actinides) were closely similar in their chemical properties.

In more recent years, solvent extraction in the nuclear fuel cycle has extended beyond the mainline processes to many ancillary areas concerned with recovery, recycle of certain transuranic elements and waste management.

The current position on solvent extraction is briefly outlined, developments in process flowsheets and contacting equipment are reviewed and the future role of the technology is discussed.

THE CURRENT SITUATION

1. Recovery of Uranium from Ores

The purpose of the technology in uranium ore processing is primarily to concentrate the uranium to a point where it can be recovered from solution economically and to reject impurities.

Originally many plants used ion exchange to recover uranium from the leach liquors, subsequently a combination of ion-exchange and solvent-extraction was employed but solvent extraction now alone predominates at many of the mines. The choice of extractant is determined largely by the choice of the leaching agent, which in turn is determined by the composition of the ore. Most commercial uranium is currently produced from ores which are leached with sulphuric acid, although other leaching agents, sodium carbonate/bicarbonate, nitric acid, etc are also employed. Some mills and the solvents employed are listed in Table 1.

Mixer-settler contactors appear to have found universal acceptance for the solvent extraction operations; however, several designs of the mixer, eg turbine or pump type have been used.

As the price of uranium increased in the 1970's, recovery from alternative resources, eg phosphate processing, was further developed and by the early 1980's commercial plants recovering about 2000 tons of U_3O_8 per year were in operation.

TABLE 1 - MILLS AND THEIR SOLVENTS

MINE AND LOCATION	SOLVENT EMPLOYED
Shiprock, New Mexico	D2EHPA/TBP
Split Rock, Wyoming	Alkyl amine
Palabora, South Africa	TBP
Buffelsfontein, South Africa	Alamine 336

2. Purification of Uranium Ore Concentrates (Yellow Cake)

The rejection of all other elements whilst recovering uranium from uranium ore concentrates or yellowcake is the prime aim of the solvent extraction procedure, in the refining operation. The recovery and purification of uranium from ore concentrates is almost exclusively achieved by a solvent extraction process based on the extractant TBP dissolved in a suitable diluent. The four major western world refineries employ similar solvent extraction processes except for the concentration of TBP and the choice of contactor (see Table 2).

TABLE 2 - OPERATING PURIFICATION CENTRES

OPERATING COMPANY AND LOCATION	PRESENT CAPACITY METRIC TONS OF URANIUM PER YEAR	EQUIPMENT	TBP CONCENTRATION EMPLOYED $^{o}/v$
Eldorado Nuclear Ltd, Canada	9,000	Mixco Columns	25
Comurhex, France	12,000	Agitated Columns	40
BNFL, UK	9,500	Mixer-Settlers	20
Kerr-McGee, USA	9,000	Pumper Decanters	30

3. Spent Fuel Reprocessing

The initial objective in the reprocessing of spent nuclear fuel was to recover plutonium. Present day processes are much more complex and represent a considerable extension of the original objective. It is now required to separate the uranium and plutonium from the fission products and to purify them to levels at which fissile materials can conveniently be re-used.

The solvent TBP is now universally used in a system generally known as the PUREX process. However, the choice of diluent varies from a mixture of linear branched cyclic alkanes. eg odourless kerosene (OK) to a relatively pure system, eg n-dodecane or even hydrogenated propylene tetramer (HPT).

Mixer-settlers and pulse columns are most commonly used, the latter being now favoured for the first cycle for spent light water reactor fuel. Centrifugal contactors have also been employed on a commercial scale.

The variation in the choice of diluent and other process conditions for some of the major reprocessing facilities is shown in Table 3.

TABLE 3 - PRINCIPAL OPERATING REPROCESSING PLANTS

LOCATION & COUNTRY	FIRST CYCLE CONDITIONS		SUBSEQUENT CYCLE CONDITIONS	
	SOLVENT	EQUIPMENT	SOLVENT	EQUIPMENT
Cap La Hague (France)	30°/v TBP-HPT	First Contactor, Centrifugal; Remainder, Mixer-Settlers	30°/v TBP-HPT	Mixer-Settlers
Karlsruhe (W Germany)	30°/v TBP-n Dodecane	Mixer-Settlers	30°/v TBP-n Dodecane	Mixer-Settlers
Tokai-Mura (Japan)	30°/v TBP-Dodecane	Mixer-Settlers	30°/v TBP-Dodecane	Mixer-Settlers
Sellafield (UK)	20°/v TBP OK	Mixer-Settlers	20°/v TBP OK	Mixer-Settlers
Savannah River (USA)	30°/v TBP-n Paraffin	First Contactor Centrifugal; Remainder, Mixer-Settlers	30°/v TBP-n Paraffin	Mixer-Settlers
Hanford (USA)	30°/v TBP-n Paraffin	Pulse Columns	30°/v TBP-n Paraffin	Pulse Columns

4. Associated Processes

In recent years solvent extraction technology has been extended within the nuclear industry into for instance:

i. Effluent cleanup, for the removal of transuranic elements from active waste liquors.

ii. The recovery of noble metals, eg Pd, Rh, Ru from highly active liquors with solvents such as tri-iso octylamine and trilaurylamine.

iii. The enrichment of the uranium isotopes U-235 as in the French CHEMEX process. However, although advances were made in high efficiency pulse column technology, it is envisaged that this route will not realise commercial importance in the nuclear fuel cycle. The centrifugation process and the proposed laser enrichment route are more competitive systems and offer a greater potential for further development.

THE FUTURE OF SOLVENT EXTRACTION

As an established technology in the nuclear fuel cycle over many years, more recent developments in process and equipment areas have been concerned with the optimisation of the mainline processes. However, technology changes in development of separation flowsheets and contacting equipment have been mainly associated with ancillary processes concerned with recovery and waste management.

There are many areas of change associated with the nuclear fuel cycle that indicate there is a further need for process and equipment development. Four criteria dominate the future requirements for these separation processes; namely:

i. The need to meet more stringent environmental conditions;

ii. The improvement of occupational hygiene standards;

iii. The desire to maintain capital and operating costs at economic levels;

iv. The requirement to develop alternative process routes to meet new or changing fuel specifications.

Currently mining/milling and reprocessing operations appear to be attracting most attention in the fields of environmental protection and process economics. Waste management and environmental concepts have impacted substantially on the overall economics of the nuclear fuel cycle, which can now contribute up to 20% of the total costs for nuclear power generation.

A further requirement for the industry is the need to recycle purified and separated materials back to various stages of the fuel cycle. This means that there is a stronger interplay between the various sections of the fuel cycle and the requirement to balance recovery of materials and purity of the materials recycled.

The impact of these changes on the fuel cycle is now considered in relation to future process and equipment developments.

1. Mining and Milling Operations

Recent technology aimed at reducing mining/milling capital and operating costs have been vigorously pursued. These developments can be divided into three groups:

i. elimination of operating steps by in-situ leaching, resin-in-pulp and/or solvent-in-pulp;

ii. modification of techniques or equipment, eg continuous ion exchange or solvent extraction, and

iii. pre-concentration of the ore body.

These objectives will continue even more actively in future years, particularly as primary ores become depleted and secondary uranium sources are mined and processed resulting in new feedstocks which may require alternative process routes. For example, alternative leaching agents to sulphuric acid may be employed or an ore pre-concentration step may be used resulting in a more concentrated uranium feed liquor being fed to the solvent extraction circuit. Under these conditions alternative solvents to amine extractants may be required and flowsheet parameters may require reassessment to compensate for the more concentrated uranium feed liquors. A specific need will be to prevent third phase formation resulting from higher solvent concentration in the organic phase and consequent higher uranium solvent loading.

The development of a viable solvent-in-pulp process presents a number of difficult technical problems. If these problems can be overcome this process could find extensive applications to both low and high grade ores.

Improvements have also been made in the design of solvent extraction contactors aimed essentially at the reduction of the solvent loss due to entrainment and equipment which can tolerate insolubles in the uranium aqueous feed. Optimisation of design is important because the solid-liquid separation stage of uranium ore processing accounts for up to 50% of the capital and operating costs. A number of new or modified solvent extraction contactors have been placed in commercial operation. These include the Krebs mixer-settler units at the COMUF mill in Gabon, pulse columns at two uranium milling operations in France, and the Davy-McKee combined mixer-settler at the Cooke Site Mine, South Africa.

As these contactors are successfully operated and more operating experience is gained, their incorporation as alternatives, to conventional box mixer-settlers currently employed at the majority of the mills, for refurbished and/or new mining/milling facilities will be seriously considered.

Any new or even existing U_3O_8 flowsheet may need for environmental reasons to consider the ultimate fate of other radionuclides, eg Th, Ra. Alternative leaching routes have already been proposed, principally to solubilise radium along with uranium.

Nitric and hydrochloric acid leaching routes have been examined, although the process economics did not appear to be economically competitive with sulphuric acid. However, in future years, economic factors may have to be weighed more seriously against environmental considerations. The disposal of thorium and radium nuclides to tailings dams may in future years be unacceptable and their removal, subsequent isolation and disposal in an encapsulated form or other controlled manner may be necessary.

The use of alternative leaching agents to overcome this potential environmental problem could lead to the development of new or modified solvents particularly if the selectivity of the existing reagents for uranium over other radionuclides is insufficient. Alternatively, complementary processes to solvent extraction such as liquid membrane technology could become a viable option, particularly if a "polishing technique" is necessary to reduce any radioisotope in waste liquors to extremely low levels.

2. Ore Concentrate Refining

It is difficult to envisage in the next two decades that any other technology would replace solvent extraction for the purification of uranium from ore concentrates to fuel grade specification. The combined cost of solvent extraction and ancillary processes, including dissolution, filtration and evaporation, represents less than 0.3% of the overall nuclear fuel manufacturing costs for either LWR or AGR fuel. Furthermore, so long as the purification of ore concentrates is dependent on uranyl nitrate technology, alternative solvents to TBP cannot be envisaged. However, flowsheet modifications at the refineries may have to be introduced to enable the processing of less pure concentrates which may be produced at any new future mining/milling operation.

A potential reduction in the "head-end" fuel manufacturing costs could be achieved by decreasing the number of process stages which produce uranium intermediates such as UF_4 or UF_6 (hex). Success in this field is likely to require a new purification route and a thorough re-examination of alternative solvents to TBP may be necessary.

Lower costs could be achieved in future years by using alternative contactors to those reported in Table 2, such as centrifugal, pulse column or the Davy-McKee combined mixer-settler. The latter could result in the filtration stage of the UOC purification cycle being omitted by all refining plants, as this contactor will handle suspended solids in the uranic feed liquor. The pulse column could find favour where potential emulsion forming impurities such as zirconium compounds and silica are present in the aqueous feeds to the solvent extraction circuit. Centrifugal contactors, which are small compact units capable of high throughputs, could assist in the reduction of building capital costs for the new refineries.

The removal of radioactivity deriving from the uranium daughters, Th-234 and Pa-234 (β emitters) and the other isotopes of Th (Th-230, Th-232, both α emitters) associated with the raffinate from the uranyl nitrate purification stage, is generally based on precipitation techniques. More efficient clean-up operations may be required in the future and in this context liquid membranes could complement these precipitation routes. Future discharge regulations may however require these radionuclides to be separated from other metallic species (eg Fe, Al), which may require solvent extraction procedures to be developed.

3. Spent Fuel Reprocessing

New plants that are now being developed for the reprocessing of either thermal or fast reactor fuels (eg THORP in the UK, Cap La Hague plant in France and EDR plant at Dounreay, UK), will use the purification/separation technology based on the nitrate-TBP/diluent system and it would seem that this technology will be maintained until the next century. Alternative solvents to the TBP/diluent system in mainline reprocessing schemes are not likely to replace this well tried and used solvent over the next two decades.

Future process developments will still examine the possibility of improved fission product decontamination to reduce the number of extraction cycles. However, with the need to minimise environmental discharges and the requirements of safe ultimate disposal of all wastes, there is an increased incentive to achieve maximum extraction efficiencies and the recovery of all alpha emitters that are destined for ultimate disposal. Two possible examples of this type of optimisation of process flowsheets are:

i. To recover Pu present in the various raffinate streams by the use of alternative solvents to TBP, which would be highly selective for its removal down to extremely low levels. Solvents such as hetrocyclic β-diketones and alkylated neutral crown ethers would seem to have potential. There would also be the need to obtain a better understanding of the mass transfer mechanisms at the "raffinate end" of the primary TBP extraction process, where species changes, impurities and low trace concentration effects interact and influence extraction performance.

ii. The presence of Neptunium-237 (an isotope of half life 2.2×10^6 years and of environmental significance) in the highly active raffinate stream could prolong the ultimate storage requirements and times for glass vitrification wastes. If Np could be removed later in the medium/lower radioactive extraction cycles and then selectively separated from other effluents, then it could be packaged and disposed of in a low volume storage system. To achieve this, the organic solvent developed will have to be highly selective for Np from various aqueous media and it may be worthwhile investigation of other solvents such as specific crown ethers and mixtures of amines and β-diketones or additional studies with solvents such as the hydroxamic group or TBP-modified systems.

With the move away from effluent treatments which involve evaporation, delay storage and some dispersal, to evaporation and incorporation of the waste in a solid matrix for ultimate disposal, then it is likely that salt-free flowsheets could become less important. A great deal of study has been carried out on investigating alternative reductants for the separation of plutonium from uranium and also for alternative reagents to sodium carbonate and sodium hydroxide for solvent purification and recycle. Under the policy of reducing discharges to as near zero as possible, compatibility of these latter reagents with the solid matrix to be used for disposal is an essential criterion and under some circumstances it could be advantageous to have some concentrations of salts present in the disposal matrix itself. However, for the U-Pu separation process, it may be advantageous to reassess and develop the nitric acid partitioning method for U-Pu separation or to extend the various development studies on electrolytic reduction, as most separation/reducing agents have some effect on waste management processes. For example, if the medium active aqueous effluents containing these agents are combined with the highly active raffinate for evaporation and then for disposal in a glass vitrification process, then sulphate ion (when ferrous sulphamate or sulphuric acid is used for separation) could cause phase separation in the glass whilst hydrazine (when U(IV)) is used for separation) could increase ruthenium-106 volatility in the vitrification stage.

The recovery of plutonium from various wastes and scrap material has been previously addressed. A considerable effort in this area has been expended by US workers, but no doubt this problem will be pursued universally as fast reactors and mixed oxide fuels become a commercial reality rather than speculation. Other separation techniques to those previously employed, such as solvent extraction or liquid membranes, should be considered. However, the choice would be primarily dependent on the dissolution process employed to solubilise the plutonium.

The established contacting equipment (eg mixer-settlers and pulse columns) again may continue to be used over the next two decades and, if so, the degree of mechanical development work required for the future plants would be limited. However, there is a potential for development in the areas of automated process and equipment control.

In the future development for contactors in any extraction process for reprocessing technology, it will be important to obtain large throughput equipment and with the minimum overall geometric dimensions to avoid large amounts of shielding and hence increased capital costs. Under these requirements, a further look at short residence time-large throughput contacting equipment is required and it may well be that the centrifugal contactor or similar equipment could play a role in achieving these objectives.

Also, for future development, it may well be that annular column could be further developed as they have the potential to avoid the use of solid poisons for criticality control.

SUMMARY

Solvent extraction will have a continued major role in the nuclear fuel cycle. Both process and equipment development will be required to meet future environmental and economic constraints.

THE KINETICS OF EXTRACTION OF NITRIC ACID BY TBP IN A ROTATING DIFFUSION CELL

by

P.N.E. Lawson & M.A. Hughes

Schools of Chemical Engineering
University of Bradford
Bradford, BD7 1DP
U.K.

Introduction

In the liquid-liquid extraction of spent nuclear fuels using tri-n-butyl phosphate (TBP), nitric acid plays an important role. However, the kinetics of extraction of this component has often been neglected.

The majority of the recent laboratory studies on this topic have been carried out with the aid of stirred cells. The work of Pushlenkov et al(1) and Nitsch et al(2) points towards organic phase diffusion control. Sovilj et al(3) and Olander(4) also concluded that the extraction is diffusion controlled but at higher concentrations the transfer rate is affected by interfacial turbulence. Bergeonneau et al(5), who used a centrifugal contactor, found the reaction to be primarily diffusion controlled with a slight contribution from the chemical step.

The present work reports results obtained in a rotating diffusion cell for both forward and reverse extraction (backwashing) of nitric acid. The rotating diffusion cell has been described in detail elsewhere(6). The hydrodynamics of the cell precisely define the thickness of the diffusion layers, thereby allowing the prediction of the film mass transfer coefficients. A comprehensive model is reported which includes an explanation of stripping data for the first time.

Experimental

The following table summarises the concentration ranges studied:

TABLE 1

Forward Extraction	Reverse Extraction
1 → 10.15M HNO_3 0.548, 1.096, 1.461M TBP/OK	0.2 → 1M HNO_3 in 1.096M TBP/OK 0.75M HNO_3 in 0.548, 1.461M TBP/OK

The rotation speed was varied between 1.5 and 3.5 Hz and the temperature was maintained at 25 ± 0.2°C. Small samples were withdrawn from the organic phase at intervals and analysed by non-aqueous titration.

Results

Figures 1, 2 and 3 present results for forward and reverse extraction experiments. Inspection of Figure 1 and similar graphs reveal that increasing the nitric acid concentration and increasing the rotation speed lead to an increase in the transfer flux. Such observations imply a substantial element of diffusion control in the extraction process.

Referring to Figure 2 it may be noted that in stripping experiments the initial rate (0 → 15 minutes) was up to six times faster than that observed during the remainder of the experiment. The reduction in rate has been attributed to either a dynamic interfacial tension effect(7) and/or to a slow blocking of the interface by either reactants or products(8), the latter again implies a diffusion limited process. The change in rate over initial periods is observed in forward extraction but to a lesser extent.

Figure 3 reveals that a limiting stripping flux is reached with increasing organic nitric acid concentration. This is again indicative of diffusion control, with the rate at which the stripping reaction occurs limited by how fast the loaded organic molecules can reach the interface.

Modelling

For the purpose of modelling the extraction process we consider the case where TBP diffuses to the aqueous reaction zone when the following reaction occurs(9):

$$TBP_{aq} + HNO_{3\,aq} \xrightarrow{k_R} TBP.HNO_{3\,aq}$$

Evidence for the formation of a stable equimolar complex is given by Collopy and Blum(10). These workers also find this is the only complex formed in the nitric acid - TBP system.

The rate equation is by inspection:

$$\frac{d[TBP]}{dt} = k_R \cdot [TBP] \cdot [HNO_3] \tag{1}$$

Applying Astarita's method(11) we obtain the interfacial flux of TBP, N_{TBP}:

$$N_{TBP} = \left(k_R \cdot D_{TBP} \cdot [HNO_3]_i\right)^{1/2} \cdot [TBP]_i \tag{2}$$

We now define the interfacial concentrations in terms of film mass transfer coefficients:

$$N_{TBP} = \overline{k}_{TBP} \cdot \left(\overline{[TBP]} - \overline{[TBP]}_i\right) \qquad (3)$$

and:

$$N_{TBP} = k_{HNO_3} \cdot \left([HNO_3] - [HNO_3]_i\right) \qquad (4)$$

Elimination of the interfacial concentrations in equation (2) by use of the relationships (3) and (4) leads to equation (5):

$$\left(1 - \frac{N_{TBP}}{\overline{k}_{TBP} \cdot \overline{[TBP]}}\right)^2 \cdot \left(1 - \frac{N_{TBP}}{k_{HNO_3} \cdot [HNO_3]}\right) = \left(\frac{N_{TBP}}{\theta \cdot [HNO_3]^{\frac{1}{2}} \cdot \overline{[TBP]}}\right)^2 \qquad (5)$$

where: $\theta = \frac{k_R \cdot D_{TBP}}{P_{TBP}^2}$

$\overline{k}_{TBP}$ and k_{HNO_3} are organic and aqueous film mass transfer coefficients and D_{TBP} is the diffusivity of TBP in the aqueous phase. P_{TBP} is the partition coefficient of TBP between aqueous and organic.

Superscript bar denotes the organic phase and subscript 'i' denotes an interfacial concentration.

If typical values are taken for the different parameters in the model it may be shown that the model predicts the following behaviour:

(i) The flux increases with increasing nitric acid concentration (at a constant TBP concentration).

(ii) The flux increases with increasing TBP concentration (at a constant nitric acid concentration).

(iii) The flux increases with increasing rotation speed (this is to be expected since the film thickness decreases).

(iv) The flux-concentration profiles flatten out because an upper diffusion limit, dictated by the organic phase, is reached(9).

All the above observations have been confirmed by experiment.

Film coefficients (k_{ij}), for species i in solvent j are defined as a ratio of diffusivity (D_{ij}) to diffusion film thickness (δ_j):

$$k_{ij} = \frac{D_{ij}}{\delta_j} \tag{6}$$

From the hydrodynamic theory(13) of the rotating diffusion cell the thickness of the diffusion layer is given as:

$$\delta_j = 0.643\ D_{ij}^{\ 1/3} \cdot \left(\frac{\mu_j}{\rho_j}\right)^{1/6} \cdot w^{-1/2} \tag{7}$$

μ_j is the phase viscosity (kg m^{-1} s^{-1})
ρ_j is the phase density (kg m^{-3})
D_{ij} is the diffusivity of species i in solvent j (m^2 s^{-1})
w is the rotation speed at which the experiment was conducted (s^{-1}).

Insertion of the necessary physical property data allows prediction of the film coefficients for a range of acid concentrations.

All the diffusion coefficients required for the model may be estimated using the Wilke-Chang correlation(14).

The partition coefficient, P, is essentially the ratio of the concentration of TBP in the organic phase to that of TBP in the aqueous phase. Experiments were conducted in order to determine the value of P; an infrared technique was used to analyse for TBP.

The group parameter θ consists of a diffusivity, a partition coefficient and the fundamental second order chemical rate constant. Both the diffusivity and the partition coefficient vary with nitric acid concentration whereas the rate constant should remain constant. An analysis of the behaviour of the model showed a strong relationship between flux and partition coefficient with the other parameters showing lesser degrees of sensitivity. The parameter θ is similar in form to that reported by Hughes and Rod(9), which was used successfully to model rate data obtained in three laboratory contacting techniques for the copper-hydroxyoxime system.

The optimum value of k_R was obtained by application of the Marquardt optimization technique(15) to the experimental data. A typical output is shown in Figure 1. The resulting value of the rate constant was approximately 3×10^3 m^3 $kg.mol^{-1}.s^{-1}$. The low value of the rate constant seems to rule out the possibility of a 'bulk' aqueous phase reaction and we postulate that the reaction occurs so close to the interface that 'water structuring' slows down the reaction(16).

Discussion

It might be noted here that Sovilj et al$^{(3)}$ studied the same system in a vibration cell and found the plot of flux versus nitric acid concentration to be a similar shape to that in Figure 1. However, these workers show decreasing fluxes in the upper diffusion limit, at high TBP concentrations. This is the opposite to our results and indeed the opposite to that predicted by the model.

Sovilj et al also report the presence of the Marangoni effect during the extraction process. Our own visual observation of forming aqueous drops in the organic phase showed no interfacial turbulence. The turbulence observed by Sovilj et al$^{(3)}$ could be caused by internal circulation resulting from drop formation at a drop Reynolds number, $Re_d > 10^{(17)}$. The absence or otherwise of the Marangoni effect is still the subject of discussion$^{(18)}$.

In conclusion we believe the extraction of nitric acid by TBP to be primarily diffusion controlled and that the reaction occurs in the aqueous phase close to the interface.

The extraction of uranium by TBP has also been studied by the same technique and a model based on the same approach successfully accounts for the extraction of $0.2 \rightarrow 3.6\ g\ell^{-1}$ uranium in solutions of up to 4.5 M nitric acid by TBP.

The authors would like to thank British Nuclear Fuels PLC, Sellafield for their continued interest in this work and for permission to publish the results. One of the authors (P.N.E.L.) thanks B.N.F. for the award of a Scholarship.

FIGURE (1) VARIATION IN TRANSFER FLUX WITH CONCENTRATION & ROTATION SPEED

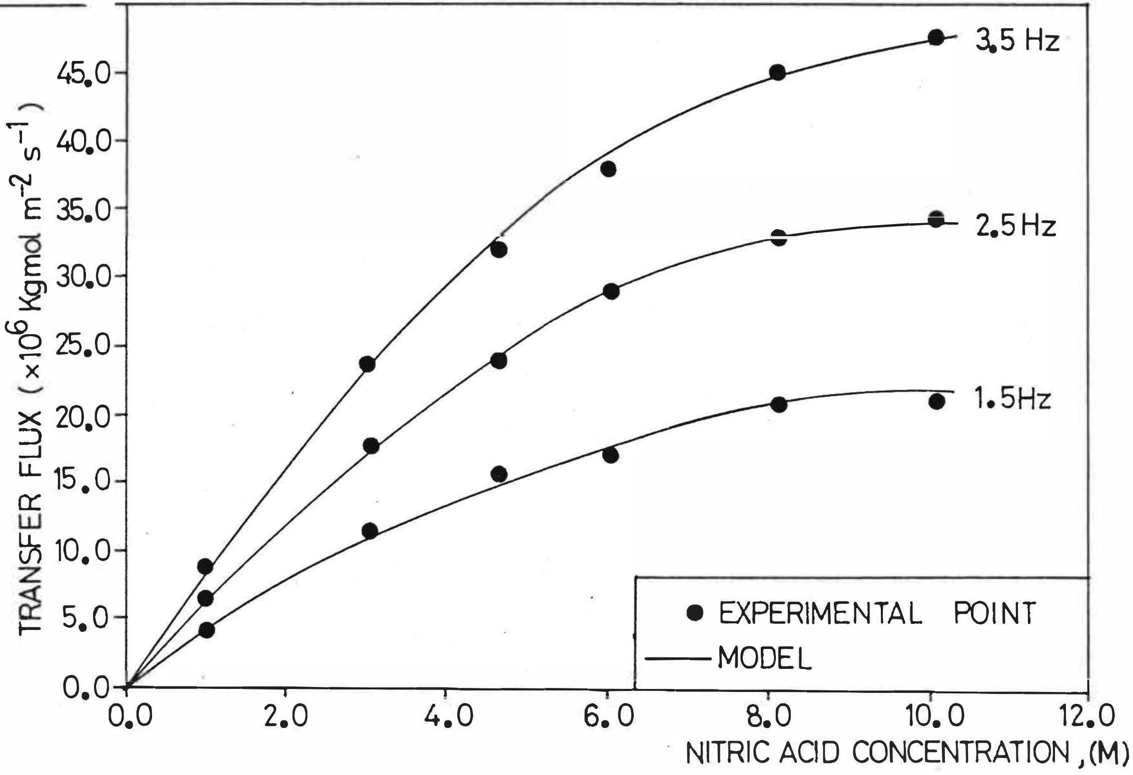

FIGURE (2)

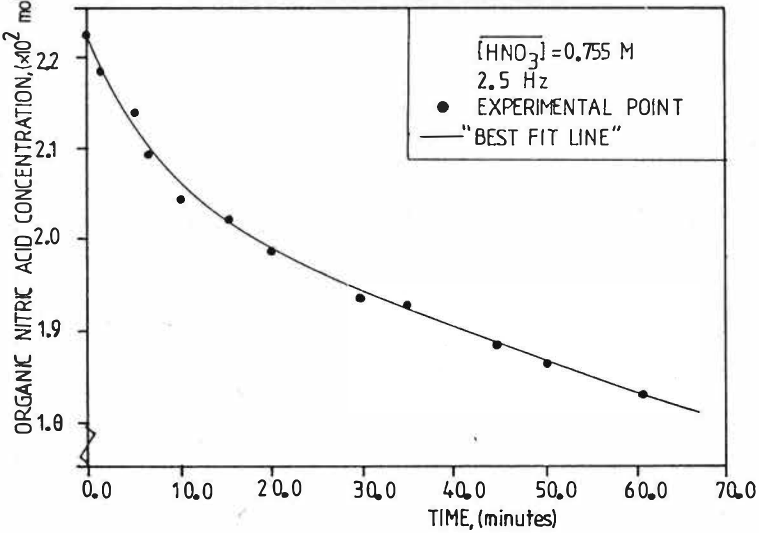

STRIPPING OF A LOADED ORGANIC PHASE WITH WATER

FIGURE (3)

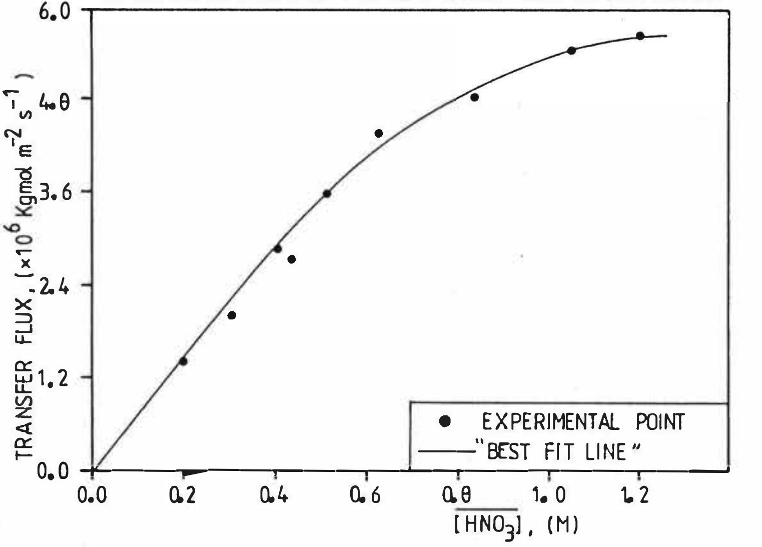

VARIATION IN STRIPPING FLUX WITH ORGANIC ACID CONCENTRATION

References

(1) Pushlenkov, M.F., and Shchepetil'nikov, N.N., Soviet Radiochemistry, (11), 16, 1969.

(2) Nitsch, W. and van Schoor, A., Chem. Ing. Tech., (54), 614, 1982.

(3) Sovilj, M., Lukesova, S. and Rod, V., Collect. Czech. Chem. Commun., (50), 738, 1985.

(4) Olander, D.R. and Benedict, M., Nucl. Sci. Eng., (15), 354, 1963.

(5) Bergeonneau, Ph., Jaonen, C., Germain, M. and Bathellier, A., Proc. Intern. Solv. Extr. Conf. C.I.M., Special Volume 21, p 612, 1974.

(6) Fisk, P.R., Ph.D. Thesis, Imperial College of Science and Technology, 1982.

(7) Yagodin, G.A., Ivakhno, S. and Tarasov, V.V., Proc. Intern. Solv. Extr. Conf., Vol. 3, Rep. 80-140, University of Liege, Belgium, 1980.

(8) MacRitchie, F., Interfacial Synth., (1), 103, 1977.

(9) Hughes, M.A. and Rod, V., Hydrometallurgy, (12), 267, 1984.

(10) Collopy, T.J. and Blum, J.F., J. Phys. Chem., (64), 1324, 1960.

(11) Astarita, G., 'Mass Transfer with Chemical Reaction', Elsevier, Amsterdam, 1967.

(12) 'Science and Technology of TBP', Volume 1, CRC Press, 1984.

(13) Levich, V.G., 'Physicochemical Hydrodynamics', Prentice Hall, 1962.

(14) Wilke, C.R. and Chang, P., A.I.Chem.E.J., (1), 264, 1955.

(15) Marquardt, D.W., J. Soc. Appl. Math., (11), 431, 1963.

(16) Danesi, P.R., Vandegrift, G.F., Horwitz, E.P. and Chiarizia, R., J. Phys. Chem., (84), 3582, 1980.

(17) Burkhart, L., Weathers, P.W. and Shearer, P.C., A.I.Chem.E.J., (22), 1090, 1976.

(18) Thompson, P.J. Batey, W. and Watson, R.J., 'Extraction '84', E.C.C.E., Publication Series No. 43, Publ. Pergamon Press, 1984.

THE PUREX-PROCESS COMPUTER-MODEL "VISCO" AND ITS APPLICATIONS

G.Petrich
Institut für Heiße Chemie
Kernforschungszentrum Karlsruhe
Postfach 3640, D-7500 Karlsruhe, F.R.G.

1. Introduction

Modelling and simulation of simple countercurrent liquid-liquid extraction processes is common practice. The Purex process for reprocessing spent nuclear fuel is a challenging example for an extremely intricate multicomponent system. To simulate this process detailed models of the distribution equilibria, the mass transfer kinetics and the redox reactions are needed. Due to the extensive experimental material of thermodynamic and kinetic data available for the Purex process a unique condition is found for chemical process modelling. This led to several computer models in the past, the best known of which is the SEPHIS code [1]. In a modern plant both mixer settlers and pulsed sieve plate columns are employed and fluiddynamic effects have to be adequately described. A varying number of extractors may be coupled countercurrently. Some extractors are equipped with additional electrochemical devices. Again the existing quantity of fluiddynamic and electrochemical data may serve to make up a reliable model.

The VISCO computer code has been developed in Karlsruhe since 1974. It was validated for a wide range of flowsheet conditions for mixer settlers and for pulsed columns, including those process steps where conventional redox chemistry or electrochemistry are involved. At present the species U(IV), U(VI), Pu(III), Pu(IV), Np(IV), Np(VI), HNO_3, HNO_2, hydrazine, hydroxylamine nitrate and Fe(II)sulfamate are incorporated into the model. Concentrations of the species along with temperature profiles are calculated for transients and steady state conditions.

2. Areas of application

Up to now the code was employed for the preparation and evaluation of experiments in the following test facilities of our institute:

- LABEX, a laboratory scale mixer settler based extraction cycle for Purex flowsheet studies, e.g. [2];
- MILLI, a very flexible highly shielded small scale mixer settler based reprocessing plant with three extraction cycles, e.g. [3];
- MINKA, small pulsed column extraction cycle for the study of transient phenomena [4];
- PUTE, pulsed column extraction cycle, throughput 10 kg Pu/d [5].

Other useful applications of the VISCO code included:

- General process flowsheet calculations;
- Support in the design of Purex extractors;
- Industrial scale pulsed columns.
- Studies of process dynamics;
- Estimation of the impact of operational fluctuations for control purposes;
- Studies of hypothetical maloperations;
- Behaviour of tritium in the scrub columns of the highly active cycle [6];
- Identification of process parameters inaccessible from batch experiments;
- Illustration of the complex interactions in multi-component counter-current extraction with and without simultaneous chemical reactions by monitoring the concentration profile transients on a CRT screen;
- Quantitative comparison of the major U/Pu separation processes [7];
- Parameter sensitivity study of an electroreduction pulsed column [8].

Development and experimental validation of the model and its computer implementation has been an iterative process and is still continuing. Examples of how theory compares with experiment can be found in most of the references quoted above.

3. Conceptual study of an electroreduction centrifugal extractor

The major research effort in our Purex process work throughout the past years has been a process optimization with regard to separation efficiency and product yield and a simplification of the process leading to reduced costs. Chemical engineering R&D work was directed to cut down the number of Purex extraction cycles and to improve the space-time yield of the equipment [9]. The latter may be achieved by the use of fast extractors and in particular of centrifugal extractors. Development and operation of this type of extractor started in the early 1960s, e.g. [10]. No application of centrifugal extractors for the reductive U/Pu separation in technical scale is known to us even though experiments demonstrated the applicability of U(IV) as a reductant [10], [11], [12].

In a previous publication [7] the major separation processes were compared and the principal advantages of in-situ electroreduction were shown. A first design study showed the feasibility of a centrifugal extractor equipped with electroreduction where single stages are arranged in a cascade similar to [13]. This paper presents the computer simulation results for an electroreduction centrifugal extractor battery based on this principle.

3.1 Basic model of a centrifugal extractor

Uniform phase concentrations are assumed for the mixers as well as for the settlers. No mass transfer takes place in the settlers. The following equations comprise the computational algorithm for one centrifugal stage in the absence of any redox reactions. x_i and y_i denote the aqueous and organic concentrations of solute i, F is the flowrate, V the volume, D the organic to aqueous distribution coefficient, T the temperature, σ the interfacial area and β the overall mass transfer coefficient. Subscript M refers to mixer, S to settler, a to aqueous and o to organic. X_i and Y_i are the aqueous and organic mixer feed concentrations of solute i (usually equal to the momentary settler concentrations x_{Si} and y_{Si} in the adjacent stages).

$$D_i = D_i\{T, [TBP], x_1, x_2, \ldots, x_n\} \tag{1}$$

$$\beta_i = (0.0038+-0.0009)\bullet\{\partial(D_i x_i)/\partial x_i\}^{\alpha\bullet(0.63+-0.16)} \tag{2}$$

$\alpha = +1$ for aqueous dispersed and $\alpha = -1$ for organic dispersed systems

$$V_{Ma}\bullet dx_{Mi}/dt = F_a\bullet(X_i-x_{Mi}) - \sigma\bullet\beta_i\bullet(D_i\bullet x_{Mi}-y_{Mi}) \tag{3a}$$

$$V_{Mo}\bullet dy_{Mi}/dt = F_o\bullet(Y_i-y_{Mi}) + \sigma\bullet\beta_i\bullet(D_i\bullet x_{Mi}-y_{Mi}) \tag{3b}$$

$$V_{Sa}\bullet dx_{Si}/dt = F_a\bullet(x_{Mi}-x_{Si}) \tag{3c}$$

$$V_{So}\bullet dy_{Si}/dt = F_o\bullet(y_{Mi}-y_{Si}) \tag{3d}$$

The algebraic distribution equation (1) for Purex multicomponent extraction is the foundation of all VISCO calculations and was built from a computerized data bank holding more than 4000 experimental distribution data [14]. It is based on thermodynamic considerations using an empirical activity coefficient submodel. Extracting species included are U(VI), U(IV), Pu(IV), Pu(III), Np(VI), Np(IV), HNO_3 and HNO_2 and the nonextracting species hydrazine, hydroxylamine nitrate and Fe(II)sulfamate.

The derivation of equation (2) for the overall mass transfer coefficients β_i was fully described in [15] for TBP concentrations of 3.9 to 16.2 vol% in dodecane. Later measurements for 30 vol% TBP [16] fitted the correlation (2) without any further tuning of the two parameters. This fact corroborates the choice of the equilibrium curve slope as the only independent variable and gives some confidence to the model extrapolation behaviour. For the U/Pu separation and Pu purification extractors this model is also used for the additional species U(IV), Pu(III) and HNO_2 for which no separate transfer measurements exist. The successful numerical simulation of Purex B-type pulsed columns [8] seems to justify this assumption.

The driving force for mass transfer between the phases in equ.(3) is assumed to be proportional to the interfacial area σ as calculated from the mean drop size and the holdup fractions in the mixing compartments. Our attempts to support this assumption in single drop mass transfer experiments with varying drop sizes were not successful. Drop diameters were inevitably of the order of 2 to 3 mm. Concentration profile calculations in pulsed columns with mean drop diameters of 0.5 to 1.5 mm seem to be in agreement with the assumption, however, when compared to measured profiles.

Fig.1 shows the measured steady-state profiles of U and HNO_3 coextraction performed with a 3-stage centrifugal extractor [17]. Since drop sizes were not determined, this parameter was varied in the course of the calculations. Below about 30 μ (calculated profiles are shown for this value) the results stay practically constant, indicating that chemical equilibrium is reached in the mixer compartments.

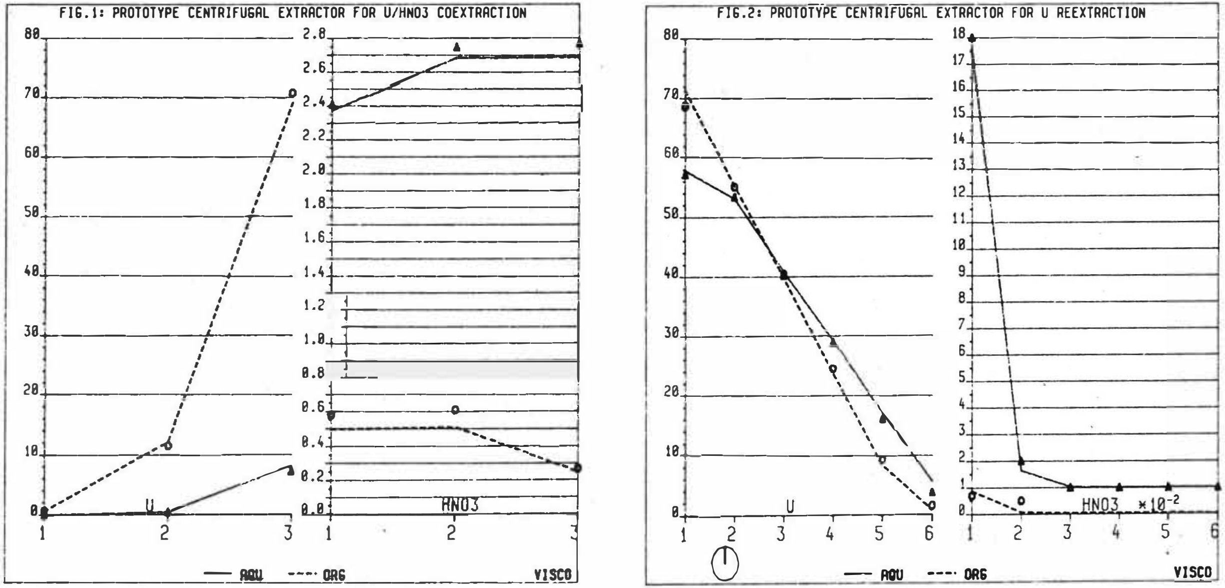

Figs.1 and 2: Measured [17] and theoretical concentration profiles of U and HNO_3 in prototype centrifugal extractors. Measured (o = organic, Δ = aqueous) and calculated (dashed lines = organic, solid lines = aqueous) concentrations (metals in g/l, otherwise M/l) are plotted vs. stage number. Coextraction (fig.1): organic feed (85 l/h) enters at stage 1, aqueous feed (130 l/h, 47 gU/l, 2.5 M HNO_3) at stage 3. U reextraction at 22°C (fig.2): organic feed (85 l/h, 77.3 g U/l, 0.22 M HNO_3) enters at stage 1, aqueous feed (115 l/h, 0.01 M HNO_3) at stage 6.

Fig.2 shows another result obtained with a 6-stage centrifugal extractor for U reextraction at 22°C. Calculated profiles are the least square fit result for the drop diameter found to be 25 µ. Chemical equilibrium is reached at drop diameters below about 10 to 20 µ in this case.
For both test cases all stages are essentially in chemical equilibrium. Thus the values for the drop diameters obtained from the profile calculations have to be considered as upper limits. This is well within the mean drop diameter range of 20 to 50 µ expected for centrifugal extractors [18]. Again, the assumption of mass transfer being proportional to the interfacial area as calculated from the drop size is at least not contradicted, even in the case of very small drops.

3.2 U/Pu separation in centrifugal extractors with external U(IV) feed

Early successful experiments with this type of extractor were conducted in the USA (e.g.[10]) and in France (e.g.[12]). To numerically simulate this extractor the material balance equations (3) for the mixing and settling compartments have to be extended by the following redox reactions [7]:

- Reduction of Pu(IV) by U(IV) [19]:
  $d[Pu(IV)]/dt = -k \cdot [Pu(IV)] \cdot [U(IV)] / \{([HNO_3]+K_P) \cdot ([HNO_3]+K_U)\}$
  k(aqu)=15200 mol/min, E_A=104 kJ/mol [20]
  The organic reaction is not well known. It is assumed to be a factor 100 slower than the aqueous reaction [21].
- Reduction of Pu(IV) by hydrazine [22]:
  $d[Pu(IV)]/dt = -k \cdot [Pu(IV)] \cdot [N_2H_5^+] / ([HNO_3]+K_P)$
  k=0.038/min, E_A=93 kJ/mol
- Oxidation of Pu(III) by HNO_2 (aqueous phase) [23], modified:
  $d[Pu(III)]/dt = -k \cdot [Pu(III)] \cdot [HNO_2] \cdot ([HNO_3]-0.4) \cdot [NO_3^-] = -2 \cdot d[HNO_2]/dt$
  k=144/(mol³•min), E_A=59 kJ/mol
- Oxidation of Pu(III) by HNO_2 (organic phase) [21], modified:
  $d[Pu(III)]/dt = -\exp\{7.28 \cdot ([HNO_3]+0.8)\} \cdot [Pu(III)] \cdot [HNO_2] = -2 \cdot d[HNO_2]/dt$
- Reaction of HNO_2 with hydrazine [24]:
  $d[HNO_2]/dt = d[N_2H_5^+]/dt = -60000 \cdot [HNO_2] \cdot [N_2H_5^+] \cdot [HNO_3]^2$

Material balances are calculated from the reaction stoichiometry. K_P and K_U are hydrolysis and dissociation constants for Pu and U respectively. The reaction constants k are given for 30°C.

Apart from previous validations of this system of equations for mixer settlers and for pulsed columns (e.g. [7], [25]) the experimental data of [10] for a U/Pu split centrifugal extractor were used as an input to the VISCO calculations. The internal holdup ratio of the phases was assumed to be equal to the external flow ratio. Good agreement between calculation and experimental findings [10] was obtained at mean drop diameters of about 35 µ. Though no experimental concentration profiles are reported in [10] the result confirms the expectation that a centrifugal extractor is principally well suited for U/Pu separation.

3.3 Simulation study of an electro-reduction centrifugal extractor ELSE

For mixer settlers and pulsed columns a simple way was found to install the electroreduction equipment. The problem to supply the space for the electrodes in the far more compact electroreduction centrifugal extractor ELSE without disturbance of the extraction function can be solved by arranging the individual stages in a cascade on separate drives. To model the redox reactions in ELSE the system of equations given above has to be extended by the following equations [26]:

- Cathodic reduction of Pu(IV):
  $d[\mathrm{Pu(IV)}]/dt = -k\cdot\Omega_c\cdot[\mathrm{Pu(IV)}]$, k(35°C, Ti-cathode, stirred)=0.25 cm/min
- Cathodic reduction of U(VI):
  $d[\mathrm{U(VI)}]/dt = -k\cdot\Omega_c\cdot[\mathrm{U(VI)}]$, k=0.012 cm/min
- Anodic reoxidation of Pu(III):
  $d[\mathrm{Pu(III)}]/dt = -k\cdot\Omega_a\cdot[\mathrm{Pu(III)}]$, k(35°C, Pt-anode, stirred)=0.25 cm/min

Ω_c and Ω_a are the specific cathode and anode areas of the electro-process in 1/cm. The rate constants for electroreduction of U and Pu were measured in individual

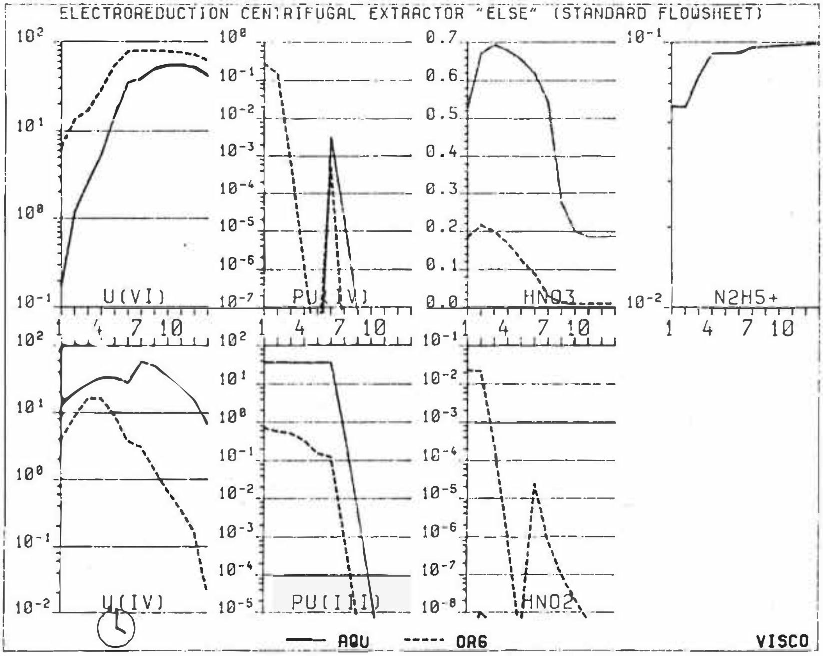

Fig.3: Calculated concentration profiles of an electroreduction centrifugal extractor ELSE for the separation of U and Pu at 35°C using a standard FBR fuel flowsheet with a 5-stage U-scrub BS section and a 7-stage Pu extraction BX section [29]. A standard drop size of 10µ is assumed. Electrolytic equipment is installed in the BX section (stages 6 to 12). Organic feed HSP (stage 6): 100 l/h, 30 % TBP, 75.7 gU/l, 9.3 gPu/l, 0.1 M HNO_3, 0.001 M HNO_2. Organic scrub BSX (stage 1): 20 l/h, 30 % TBP. Aqueous strip (stage 12): 25 l/h, 0.2 M HNO_3, 0.1 M $N_2H_5^+$.

laboratory experiments [27], [28]. These constants are functions of the degree of agitation of the fluid and of the applied current. The constants used in the model are estimated from the average current density applied to the extractor which is assumed to be constant over the full electrode area.

Fig.3 shows the theoretical concentration profiles of ELSE using a standard FBR fuel flowsheet [29] as indicated in the figure caption. The process works extremely well at Pu losses to the organic raffinate well below the usual specification of 1 mg/l. The Pu losses will be higher than the theoretical value though, since the model does not yet account for the small amounts of Pu complexed to HDBP which is known to strip poorly from the organic phase.

The HNO_2 feed concentration in the model flowsheet was assumed to be 0.001 M. Values of this order were repeatedly found for real process solutions [30]. Since process significant nitrite concentrations are only produced in the process itself by the reoxidation reaction with Pu(III), the initial concentration is of minor importance as long as a sufficient supply of hydrazine is guaranteed. The simulation result (fig.3) shows significant reoxidation in stages 1 and 2 as can be seen from the increased organic Pu(IV) and HNO_2 settler compartment concentrations. The short contact times of the two phases in the mixer compartments of ELSE in conjunction with the low metal loading of the solvent in the first stages allows the HNO_2 formed in the organic mixer phase only partially to extract to the aqueous phase where it can be destroyed by hydrazine. Consequently, sizable amounts of HNO_2 enter the settler and increase autocatalytic reoxidation.

The effect of Pu(III) reoxidation in the BS section of the extractor becomes even more pronounced when no hydrazine is fed with the BXS flow. Pu in the BX section is almost completely reoxidized to Pu(IV) then. But the Pu losses to the organic raffinate do even decrease in this case as compared to the standard flowsheet (hydrazine curve of fig.4). The solution to this apparent paradoxon is found in the following sequence of arguments:

1. Since no electrodes are installed in the BS section autocatalytic reoxidation of Pu(III) occurs in both phases in the absence of hydrazine.
2. Reoxidized Pu(IV) is carried with the organic flow to the BX section, due to its high extractability.
3. As long as the acidity in the BX section is kept low enough, U accumulates and enough U(IV) is produced by the in-situ electroreduction of U(VI) to fully reduce Pu(IV) to the almost inextractable Pu(III). In contrast to an electro mixer settler the short residence times inhibit full reoxidation in the organic BX settler compartments which would otherwise lead to a depletion of U(IV).
4. Trivalent Pu cannot leave the 7-stage BX section with the organic raffinate due to its low extractability. It is carried back to the BS section where finally after reoxidation it has to leave the extractor as Pu(IV) with the aqueous product.
5. Since there is no salting-out effect of hydrazine on Pu, theoretical Pu losses are somewhat smaller in this case.

As expected the most sensitive process parameter of the electroreduction centrifugal extractor turned out to be the organic to aqueous flow ratio in the BX section. This can be seen from either the aqueous scrub flow or the organic feed flow curves shown in fig.4. An increase of the BX flow ratio leads to higher Pu(III) concentrations in the BS section as long as enough U(IV) is electrolytically produced in the BX section for complete reduction of Pu. The strong salting-out effect of Pu(III) forces all extractive species to recycle more and more to the BX section according to their extraction factor. Since this holds for Pu(III) and HNO_2 as well, reoxidation is increased there. U(IV) does also increase initially and is therefore stabilizing the process. But the continuous cycle of Pu reoxidation and reduction is further accelerated by the rise in U(IV) concentration and produces more and more nitrite. This leads to increasing amounts of Pu(IV) in the BX section and eventually at a critical flowratio to a breakdown of the process.

The effect of a reduced cathode area in fig.4 on Pu losses is less complicated. Less U(VI) is reduced to U(IV) which is the major reductant for Pu(IV) in the process. Initially autocatalysis is slowed down but at still smaller cathode areas the process breaks down due to a lack of U(IV).

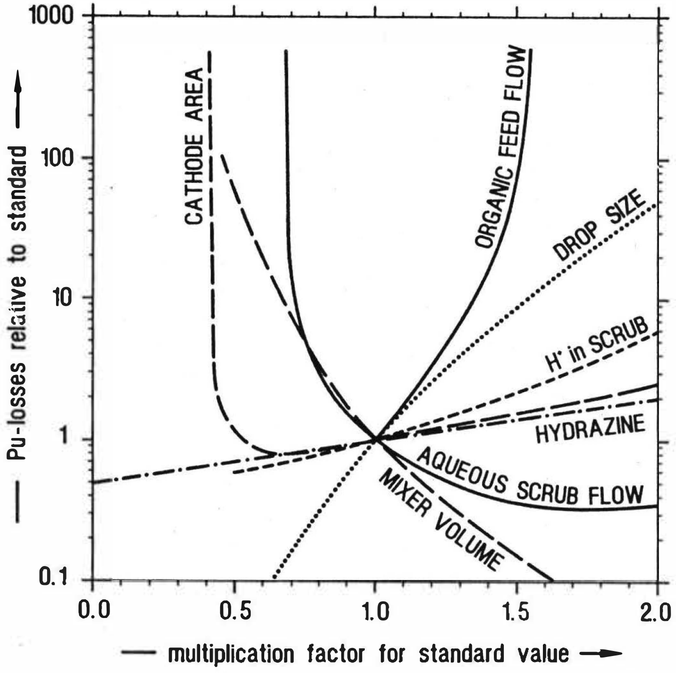

Fig.4: Theoretical parameter sensitivities of the electroreduction centrifugal extractor ELSE described in fig.3. Plotted are the Pu losses to the BU raffinate leaving stage 12 for a variation of the standard parameters of fig.3, normalized to the Pu losses in the standard case.

The effect of changing contact time and interfacial area is reflected by the mixer volume and drop size curves of fig.4. Decreasing mass transfer by decreasing mixer volume or increasing drop diameters generally leads to smaller concentration profile gradients and losses increase. Since less U(VI) is transfered to the aqueous phase less U(IV) is produced; therefore separation is still further reduced.

The tool of numerical simulation has led to a thorough a priori familiarity with the delicacies of the process. It is save to say that from the chemistry point of view an electroreduction centrifugal extractor should perform at least as well in the Purex process as the corresponding mixer settler or pulsed column equipment. Efficiency is increased due to improved mass transfer and reduced entrainment. The rates of the redox reactions are still fast enough. Short residence times keep reoxidation down under reasonable flowsheet conditions. There is a good chance to operate the process without any hydrazine; if the Pu product is fully oxidized to Pu(IV) in this case, additional equipment for subsequent reoxidation may be saved.

References

[1] W.S.Groenier, ORNL-4746 (1972)

[2] W.Ochsenfeld, H.J.Bleyl, D.Ertel, F.Heil, G.Petrich, Proc. Fast Reactor Fuel Reprocessing Conf., Dounreay 15-18 May 1979

[3] H.J.Bleyl, K.Ebert, D.Ertel, W.Ochsenfeld in Proc.Int.Solvent Extraction Conf. ISEC'83, p.327, Denver, Aug.26-Sep.2, 1983

[4] J.Schön et al., this conference

[5] G.Petrich, U.Galla, H.Goldacker, M.Heilgeist, M.Kluth, R.Schlenker, H.Schmieder, K.Ebert, Inst. Chem. Eng. Symp. Series 88, 267 (1985)

[6] P.Feucht et al., this conference

[7] G.Petrich, H.Schmieder in Proc.Int.Solvent Extraction Conf. ISEC'83, p.84, Denver, Aug.26-Sep.2, 1983

[8] G.Petrich, U.Galla, H.Goldacker, H.Schmieder, Chem.Engng Sci. (in print)

[9] H.Schmieder, E.Henrich, K.Ebert, Proc. ENC-4-Congress, June 1-6, 1986, Geneva

[10] C.S.Schlea, M.R.Caverly, H.E.Henry, W.J.Jenkins, USAEC report DP-808 (1963)

[11] M.Krumpelt et al., USAEC report ANL-7799 (1971)

[12] C.Bernard, P.Michel, M.Tarnero, Proc. ISEC'71, The Hague, 2, 1282 (1971)

[13] D.A.Orth, J.M.McKibben, USAEC report DPSPU 69-30-1 (1969)

[14] G.Petrich, Z.Kolarik, KfK-3080 (1981)

[15] G.Petrich, Proc.Int.Solvent Extraction Conf., Liège, Belgium, Sept.6-12, 1980; Liège Université 1980

[16] G.Petrich, in "Modelling of Chemical Reaction Systems", K.H.Ebert, P.Deuflhard, W.Jäger, Eds; Springer Series in Chemical Physics 18, Springer 1981.

[17] B.F.Roth, German report KfK-862 (1969)

[18] R.A.Leonard, G.J.Bernstein, R.H.Pelto, A.A.Ziegler, AIChE Journal 27, 495 (1981)

[19] P.Biddle, J.H.Miles, M.J.Waterman, J.Inorg.Nucl.Chem. 28, 1736 (1966)

[20] T.W.Newton, J.Phys.Chem. 63, 1493 (1959)

[21] P.Biddle, H.A.C.McKay, J.H.Miles, "Solvent Extraction Chemistry of Metals", Harwell, 27.-30. Sept. 1965

[22] W.S.Koltunov, Reaktionskinetik der Aktiniden, Atomizdat, Moskau 1974 (russ.)

[23] E.K.Dukes, J.Am.Chem.Soc. 82, 9 (1960)

[24] P.Biddle, J.H.Miles, J.Inorg.Nucl.Chem. 30, 1291 (1968)

[25] G.Petrich, U.Galla, H.Goldacker, M.Heilgeist, M.Kluth, R.Schlenker, H.Schmieder, K.Ebert in Inst. Chem. Engs., Symposium Series 88, 267 (1985)

[26] H.Schmieder, H.Goldacker, M.Heilgeist, M.Kluth, H.Hausberger, L.Finsterwalder, KfK-2957 (1980)

[27] H.Schmieder, F.Baumgärtner, H.Goldacker, H.Hausberger, KfK-2082 (1974)

[28] H.Schmieder, H.Goldacker, G.Petrich, Dechema-Monographien 94, 253 (1983)

[29] H.Schmieder, H.Goldacker, this conference

[30] D.Ertel, private communication

Axial Mixing Coefficients in Reciprocating Plate Columns

A.E. Karr and S. Ramanujam, Fairfield, NJ/USA, T.C. Lo, Nutley, NJ/USA and M.H.I. Baird, Hamilton, ON/CANADA.

Since its initial development (1) the open-type reciprocating plate extraction column (RPC) has found wide application in the pharmaceutical, chemical, hydrometallurgical and waste-water treatment industries. Performance data published for columns up to 914 mm diameter have been reviewed by Lo and Prochazka (2). A simple power-law relationship has been recommended for the scale-up of optimum mass transfer performance from pilot scale columns (subscript 1) to columns of larger diameter (subscript 2):

$$(\mathrm{HETS})_2/(\mathrm{HETS})_1 = (d_2/d_1)^n \tag{1}$$

This is based upon extensive mass transfer data from RPCs with between 25 and 914 mm diameter (3-5). The exponent n is 0.38 for "difficult" extraction systems requiring high levels of agitation, e.g. o-xylene/acetic acid/water. In general, "easier" systems requiring less agitation exhibit a lower value of n. A small alteration of agitation frequency (at constant stroke) is required to maintain optimum conditions in scale-up:

$$f_2/f_1 = (d_2/d_1)^{-0.14} \tag{2}$$

This paper presents some axial mixing data on a 508 mm diameter RPC. Although it was obtained only in single phase flow conditions, it is the first axial mixing data to be published for an industrial scale RPC. Previous work (6,7,8) has been carried out with columns no larger than 150 mm diameter. In addition, new data are presented here on axial dispersion in a 25.4 mm column.

The axial mixing data are used in calculating the scale-up criteria (9,10) and the results are compared with equations (1) and (2). This contributes to the objectives of the late Professor Carl Hanson (11) in improving the fundamental basis for scale-up procedures.

Apparatus and Procedure

The 25.4 mm column was built of flanged glass with an overall height of 4.02 m. The feed and sampling arrangements are shown schematically in Figure 1. The plate stack consisted of 3.35 m of Teflon plates (open area 58.4%) spaced on a stainless steel drive shaft at intervals of 25.4 mm. The aqueous phase was either tap water or deionized water, and the organic phase was n-heptane. The tracer was an aqueous solution containing 9% ammonium chloride (by weight) and sufficient methanol to bring its density close to within 1% of that of pure water. It was injected pulsewise and the tracer responses in the aqueous phase were measured by electrical conductivity probes CP1 and CP2. This technique was carried out both for aqueous phase continuous (to obtain E_c) and for aqueous phase dispersed (to obtain E_d). In the latter case, collecting funnels were employed on the sample tubes to ensure that only the aqueous phase was withdrawn to the conductivity probes.

The industrial scale RPC also shown in Figure 1 consisted of a 508 mm i.d. titanium shell containing a 6.18 m plate stack of Teflon plates. The plate stack was divided into two zones A and B. In the upper zone A there were groups of perforated plates, spaced at 55.6 mm intervals and separated by doughnut baffles. In the lower zone (B), groups of perforated plates were used with spacing 30.2 mm centre to centre. The perforated plates in both zones had hole diameters 15.9 mm and fractional open areas 0.603. The baffle diameters were 386 mm (internal) and 502 mm (external). Only a single phase, tap water, was used in the axial mixing studies with this column. The pulse injection of tracer was made at a T-junction in the water inlet flow as shown. The conductivity probes (CP1 and CP 2) were connected to sample points in the column wall by means of 3 mm i.d. polypropylene tubing. Electrical conductivity was found to be a linear function of tracer concentration and the axial dispersion coefficients were evaluated from the response curves using the method of Vergnes (12). In both sizes of RPC, the stroke length A was constant at 25.4 mm. Agitation was varied by means of the reciprocation frequency.

Results for Single Phase Operation

Figure 2 contains data for the two RPC sizes (25.4 and 508 mm diameter) used in this work, and some of the data of Hafez et al. (9) for a 150 mm RPC. The conditions and symbols used are given in Table 1.

In all columns the axial dispersion coefficient is relatively high at zero agitation, due to the tendency for the liquid velocity to become unevenly distributed with respect to radial position (13). As the agitation is

TABLE 1

Axial Mixing Data in Single Phase Flow

Column dia. d(mm)	Plate Spacing h(mm)	Donut Baffles in Stack	Flow Velocity U_c(cms − 1)	Ref.	Symbol (Fig. 2)
25.4	25.4	No	1.13	This work	×
150	52	No	0.83	Hafez et al (1979)	O
150	52	Yes #	0.83	Hafez et al (1979)	●
508	30.2 & 55.6	Yes	0.56	This work	▲
508	30.2 & 55.6	Yes	0.78	This work	■
508	30.2 & 55.6	Yes	0.93	This work	◆

# One baffle per group of 3 plates

increased, the non-uniformities are reduced and the axial dispersion coefficients generally decrease to a minimum value and then increase.

In order to reduce radial non-uniformity effects, it is common industrial practice (3) to include doughnut baffles at intervals in the plate stack of large scale columns. Rosen and Krylov (13) proposed that:

$$E = E_0 + f_0 d^2 (\Delta w)^2 / E_0 \tag{3}$$

where E_0 is the contribution due to agitation and fluid flow (approximately proportional to (U_c + Af)) and the second term relates to radial non-uniformity effects. The advantage of including doughnut baffles in large columns is that radial mixing is greatly increased, thereby reducing the second term in equation (3). From equation (3) it would be expected that under well-agitated conditions ($Af \gg U_c$) with good radial mixing,

$$E \simeq E_0 \propto Af \tag{4}$$

There is clearly an additional effect of column diameter which can be seen more clearly in Figure 3 which plots E/Af versus d, excluding those data for Af < 4 cm/s which are affected by radial non-uniformity. The dashed line indicates that in scaling from the 25.4 mm column (unbaffled) to the 508 mm column (baffled), E increases approximately as the 0.67 power of diameter.

Results for Two Phase Operation

Data for axial dispersion in the continuous phase are shown in Figure 4, with the single phase data in the 25.4 mm RPC also shown (crosses). The data shown from Bensalem (8) were selected for an amplitude (16 mm) and combination of flow rates to come as close as possible to those used in this work (open triangle points). Comparison indicates a similar effect of agitation, but with the data somewhat higher in the larger diameter RPC used by Bensalem (8). The data of Hafez (7) trend downwards to values similar to those of this work. The present axial dispersion curves are shifted upwards as the dispersed phase flow is increased. The effect is greatest at zero agitation, at which E_c is more than doubled when U_d increases from 0 (single phase flow) to 0.281 cm/s. Curves A and B are drawn through the present data from equations (3) and (4) with fitted parameters. In this work, the dispersed phase (n-heptane) tended to wet the Teflon plates and this effect, coupled with the large density difference (0.32 g/mL) between the phases, explains why agitation levels could be taken higher in this work than in previous investigations. Wetting of the plates by the dispersed phase is believed to enhance the radial non-uniformity effects of the dispersed phase. Thus Kim and Baird (8) using a 50.8 mm RPC with non-wetting plates, had found that U_d had little effect upon axial dispersion coefficients, U_d being varied up to 0.7 cm s^{-1}.

Dispersed phase axial dispersion was measured in this work with water dispersed in n-heptane, and Teflon plates. This combination provides a non-wetting dispersed phase, so that the system is not prone to the exaggerated radial non-uniformity effect mentioned above. The values of E_{ds} (based on superficial velocities) are presented in Figure 5 for both the present data and those of Bensalem (8). The values of E_{ds} from this work are about three times those obtained from Bensalem's (8) data. This is probably due to the larger interphase density difference and interfacial tension in the present systeother things being equal, the droplet velocities for the present system will be greater and so will the velocity differences for droplets of different size, which account for forward mixing.

Applications of Results to Scale-up

In this section, the effects of column diameter and plate agitation on calculated column height for given parameters (extraction factor, extract composition, etc.) are computed in the light of data obtained in this work and previous literature on the RPC. We are concerned only with the relative effect of the increase in agitation and column diameter on column height, rather than prediction of column height itself for a specific system, which is a much more complex problem.

The procedure used here for calculating the height of a countercurrent mass transfer column with axial dispersion is the simplified one developed by Pratt (10). The column length is obtainable if the height of a transfer unit, the dimensionless extract composition Y^0, the extraction factor E and the Peclet numbers P_x and P_y for each phase are specified. Peclet numbers are defined in terms of the superficial flow velocities and axial dispersion coefficients, and a characteristic dimension which may be taken as the column diameter.

$$P_x = U_x d/E_x \quad (5a)$$

$$P_y = U_y d/E_y \quad (5b)$$

In this work we consider phase x to be the continuous (feed) phase and phase y the dispersed (solvent) phase. Typically the extraction factor is slightly greater than 1.0; a value of 1.3 is selected. The dimensionless extract concentration Y^0 should approach 1.0; in this work it is set at 0.95. On the basis of plug flow, 6.42 theoretical stages would be required for this separation, or 5.61 transfer units based on the x phase. The height of a transfer unit is the value applicable for plug flow, calculated from the mass transfer parameters, i.e. $U_x/(k_{ox}a)$. On the basis of small scale experiments on mass transfer, drop size and holdup (14,15) it is found approximately that H_{ox} varies as the -3.2 power of Af. Here, it is assumed that

$$H_{ox} = 2.7 \times 10^{-5} (Af)^{-3.2} \quad (6)$$

where all quantities are in S.I. units. It should be noted that equation (6) is not supposed to be of general applicability for all systems; it is merely a typical variation that can be expected, based on recent data (15).

In the scale-up comparisons here, the flow velocities are both set at 0.5 cm/s. Hence in S.I units:

$$P_x = 0.005\, d/E_x \text{ and } P_y = 0.005\, d/E_y \quad (7)$$

The approximate dependence of E_x upon column diameter d and agitation level Af can be estimated from Figure 3, assuming that agitation is so large that equation (4) is applicable. In the absence of any two-phase axial mixing data for large diameter columns, it is assumed that the scale effect for two phase flow is the same as that measured for single phase flow. The working equations in S.I. units are:

$$E_x = 0.033\, Af d^{0.67} \quad (8)$$

$$P_x = 0.152\, d^{0.33}/(Af) \quad (9)$$

Axial dispersion data for the dispersed (y) phase are quite sparse and scattered as shown in Figure 5. It was decided to investigate two alternative assumptions regarding dispersed phase mixing. The first is that

$$E_y = E_x \text{ and hence in this case } P_y = P_x \quad (10)$$

An alternative simple assumption is that E_y has a constant value of 10 $cm^2\, s^{-1}$ regardless of agitation level or column diameter. In this case, for S.I. units,

$$P_y = 5d \quad (11)$$

While equation (10) indicates that axial mixing has the same effect in both phases, equation (11) suggests that the relative importance of continuous phase mixing increases with increase in column diameter.

Application of the column height calculation method (10) provided curves (Figure 6) showing minima in the plots of H.E.T.S. versus reciprocation frequency, as observed by Karr and Lo (3,4). The computed minimum column heights and the corresponding values of Af are plotted against column diameter in Figure 7 for the two different assumptions about the dispersed phase mixing. The scale-up exponent n (equation 1) of diameter for minimum column height has been established conservatively by Karr and co-workers at 0.38 but a recent study (16) on scaling from 52 mm to 1.52 m diameter shows an exponent of 0.33. The assumption that mixing is the same in both phases (equation (10)) gives a value of $n = 0.51$, significantly higher than observed. For the assumption of constant dispersed phase mixing, the plot of minimum height versus diameter (circles on Figure 6) is not quite straight on logarithmic coordinates. For scale-up from 25 mm to 1.5 m the equivalent exponent n is 0.31, while for scale-up from 150 mm to 1.5 m it is 0.36. These values are close to or within the range 0.33-0.38 obtained empirically. It may thus be concluded that the assumption of dispersed phase mixing independent of column diameter, and continuous phase mixing proportional to $d^{0.67}$, provides a satisfactory basis for scale-up. The exponents on agitation for optimum conditions are computed here to be -0.16 for assumed equal mixing in both phases, and -0.17 for the model using equation (12); these results are reasonably close to the value of -0.14 obtained by measurement (equation (2)).

Finally, it should be emphasized that more axial dispersion data from large columns are needed before this approach to design can be used with full confidence. Measurements of dispersed phase mixing are particularly lacking. There is also need for further study of coalescence and other effects on mass transfer, leading to better prediction of H_{0x} from system properties. However, this paper has shown that the dispersion model design equation of Pratt (10) has good potential for applications in the scale-up of RPCs.

Acknowledgements

The authors are grateful to Hoffman La Roche Inc. for permission to obtain data from the 508 mm column. M.H.I. Baird is grateful to the Natural Science and Engineering Research Council of Canada for financial assistance in preparing this paper.

Nomenclature

A	reciprocation stroke
a	specific interfacial area
d	column diameter
E	axial dispersion coefficient
E	extraction factor
f	reciprocation frequency
f_0	non-uniformity term, equation (3)
HETS	height of equivalent theoretical stage
H_{0x}	height of a transfer unit, overall basis (x phase)
h	plate spacing distance
k_{0x}	mass transfer coefficient, overall basis (x phase)
n	scale-up exponent
P	Peclet number
U	superficial velocity
Y^0	dimensionless extract composition

Greek letters

$\Delta\rho$	density difference between phases
Δw	non-uniformity term, equation (3)

Subscripts

c	continuous phase
d	dispersed phase
s	superficial basis
x	phase x
y	phase y
1	pilot scale column
2	large scale column

References

1. Karr, A.E., "Performance of a reciprocating plate extraction column", AIChE J. 5, 446-452 (1959).
2. Lo, T.C. and J. Prochazka, "Reciprocating-plate extraction columns", Ch. 12 in Handbook of Solvent Extraction (eds. T.C. Lo, M.H.I. Baird and C. Hanson), Wiley- Interscience, New York (1983).

3. Karr, A.E. and T.C. Lo, "Performance and scale-up of a reciprocating plate extraction column", Proc. Int. Solvent Extn. Conf. (ISEC 71), The Hague, pp. 299-322 (Soc. Chem. Ind., London, 1971).
4. Karr, A.E. and T.C. Lo, "Scale-up of large diameter reciprocating plate column extraction columns", Chem. Eng. Progr. 72 (11), 68-70 (1976).
5. Karr, A.E. and T.C. Lo, "Performance of 36-in. diameter reciprocating plate extraction column", Proc. Int. Solvent Extn. Conf. (ISEC 77), 1, 355-361 Canadian Inst. Min. Met. (1979).
6. Kim, S.D. and M.H.I. Baird, "Axial dispersion in a reciprocating plate extraction column", Can. J. Chem. Eng. 54, 81-89 (1976).
7. Hafez, M.M., M.H.I. Baird and I. Nirdosh, "Flooding and axial dispersion in reciprocating plate extraction columns", Can. J. Chem. Eng. 57, 150-158 (1979).
8. Bensalem, A. "Hydraulics and mass transfer in a reciprocating plate extraction column", Ph.D. thesis, E.T.H. Zurich (1985)
9. Pratt, H.R.C. and M.H.I. Baird, "Axial dispersion", Ch. 6 in Handbook of Solvent Extraction (eds. T.C. Lo, M.H.I. Baird and C. Hanson), Wiley Interscience, New York (1983).
10. Pratt, H.R.C., "A simplified analytical design method for differential extractors with backmixing. I. Linear equilibrium relationship", Ind. Eng. Chem. Proc. Des. Dev. 14, 74-80 (1975).
11. Pratt, H.R.C. and C. Hanson, "Selection, pilot testing and scale-up of commercial extractors", Ch. 16 in Handbook of Solvent Extraction (eds. T.C. Lo, M.H.I. Baird and C. Hanson), Wiley-Interscience, New York (1983).
12. Vergnes, F., "A simple and practical method for the determination of Peclet number in the longitudinal dispersion model", Chem. Eng. Sci. 31, 88-90 (1976).
13. Rosen, A.M. and V.S. Krylov, "Theory of scaling up and hydrodynamic modelling of industrial mass transfer equipment", Chem. Eng. J. 7, 85-97 (1974).
14. Baird, M.H.I. and S.J. Lane, "Drop size and holdup in a reciprocating plate extraction column", Chem. Eng. Sci. 28, 947-957 (1973).
15. Shen, Z.-J., N.V. Rama Rao and M.H.I. Baird, "Mass transfer in a reciprocating plate extraction column", Can. J. Chem. Eng 63, 29-36 (1985).
16. Karr, A.E. and S. Ramanujam, "Scale-up and performance of 5 ft. (1.52 m) reciprocating plate extraction column", Paper to be presented at Int. Solvent Extn. Conf. (ISEC 86), Munich (1986).

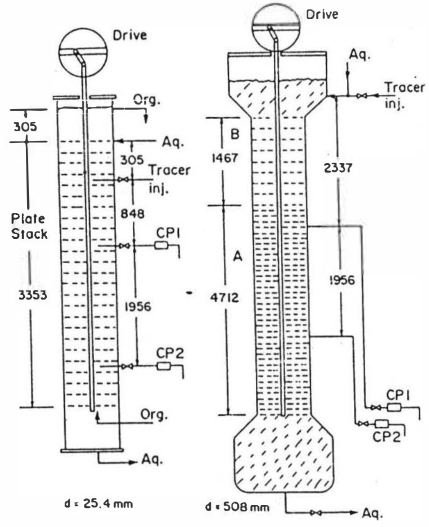

Figure 1. Columns used and sampling arrangements. Dimensions shown in mm., drawings not to scale.

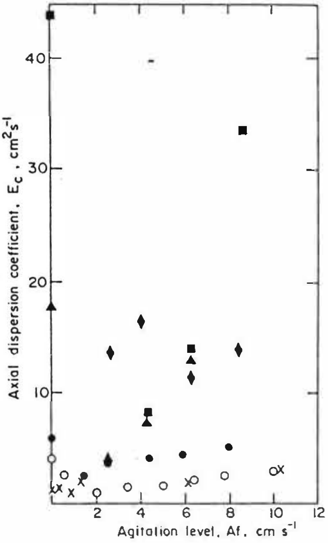

Figure 2. Effect of agitation level and column diameter on single-phase axial dispersion coefficient. See Table 1 for symbols.

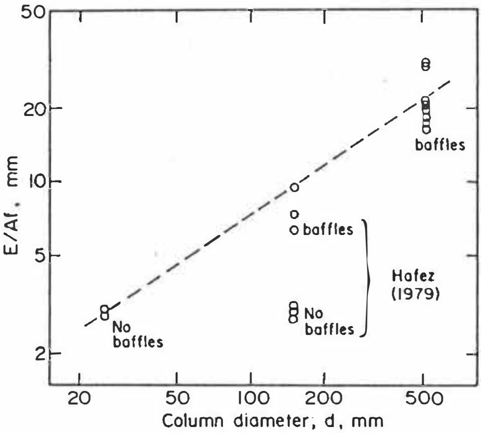

Figure 3. Effect of column diameter on ratio E/Af for single phase flow where Af ≥ 4 cm s^{-1}. Dashed line denotes slope 0.67.

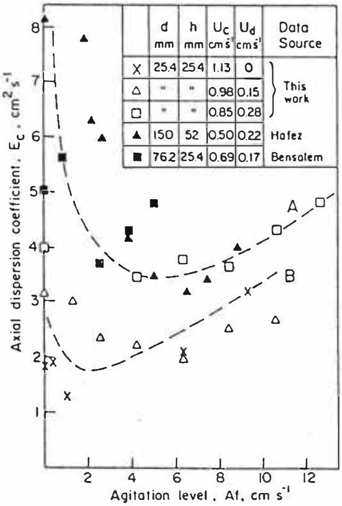

Figure 4. Effect of agitation level and column diameter on continuous-phase axial coefficient.

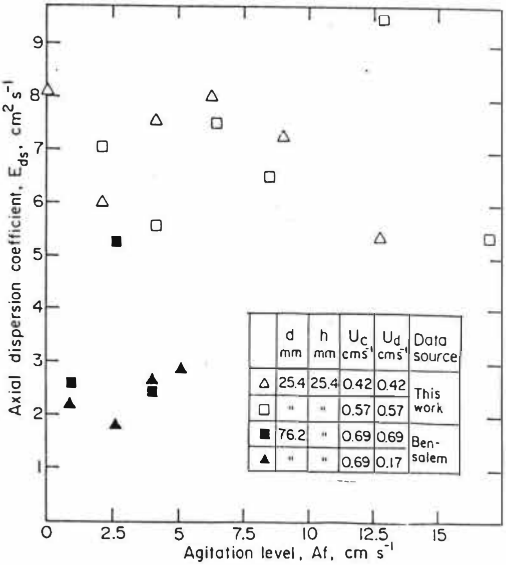

Figure 5. Effect of agitation on dispersed-phase axial dispersion coefficients, based on superficial velocities.

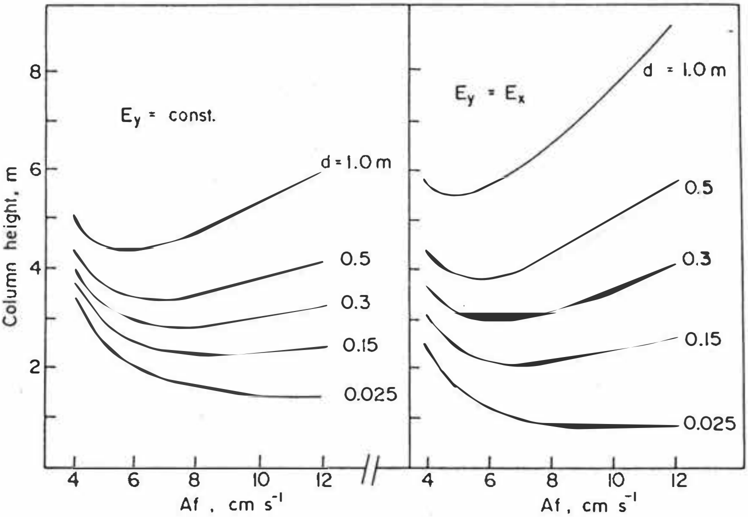

Figure 6. Computed effects of agitation and column diameter on required height.

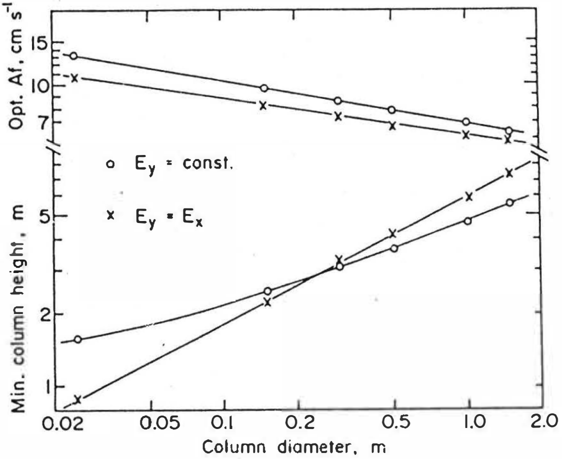

Figure 7. Scale-up relationships computed for minimum column height and optimum agitation level.

Supercritical and new Extraction Systems

Nuclear Fuel Reprocessing

The Process and The Environment - Is Solvent Extraction the Answer?

G.M. Ritcey, CANMET, Energy, Mines and Resources, Ottawa, Canada

Introduction

With the increasing awareness of the environmental hazard due to effluents, containing trace metals reaching streams, regulatory guidelines are and will be imposed as to the amount and volumes of solutions that can be discharged from a property. Guidelines and water quality objectives have been established in many countries. Thus a company may be forced to treat an effluent stream, even at high cost, in order to meet environmental regulations. Therefore, in the early development of the flowsheet, the process should incorporate steps to meet environmental constraints.

In spite of the fact that there can be solvent losses to the process raffinate, a number of processes have been developed and many put into practice for the treatment of waste streams for the removal and/or recovery of metals and other constituents that may be considered as potential pollutants to the environment.

This paper will review the various application possibilities of solvent extraction to the treatment of waste materials and effluents prior to discharge to the environment.

Removal and Recovery of Actinides from High Level Radioactive Wastes

Radioactive liquid wastes are produced at most stages in the nuclear fuel cycle. By incorporating efficient recycling within the various processes the volume of effluents that are discharged carrying contaminants are minimal. These bleed effluent streams therefore must be treated before final disposal. Solvent extraction has been used extensively.

Various reagents have been developed and evaluated by numerous researchers on the extraction of trivalent lanthanides and actinides from strong nitric acid radioactive waste solutions. Using three stages in contact with 30% dibutyl ((diethylcarbamoyl) methyl) phosphonate (DBDECMP) the Pu content was reduced by a factor of greater than 5000 and the Am by a factor of 600 (1). Subsequent investigations at Oak Ridge, Hanford and Idaho sites used the dihexyl derivative (DHDECMP) to compare it with other carbamoylmethylphosphonates (2,3) for the extraction of Am.

Many other extractants have been reported for the treatment of radio-active waste liquors for the removal of actinides. These include DEHPA (6), DBBP (4) and TRPO (5).

The recently developed TRUEX (transuranium extraction) process of Horwitz and Schulz is designed to treat such waste solutions to reduce the transuranium elements. TBP is used as the extractant together with a small amount of CMO (octyl (phenyl)-N-N-diibutylcarbamoylmethylphosphine oxide) (6). The presence of CMO permits the extraction of tri-, tetra- and hexavalent actinides in the presence of high nitric acid and salt concentrations. The Am and Tc are stripped with 0.05 M HNO_3 in the first stage and with a mixture of 0.05 M HNO_3 - 0.05 M HF in the second stage. Prior to extraction the addition of oxalic acid (0.15-0.25 M) prevents the subsequent extraction of zirconium and more than half of the yttrium and rare earths. Any oxalic acid on the solvent following extraction is removed by scrubbing with 0.005 M Fe^{III} in 0.5 M HNO_3. Otherwise rare earth oxalates would precipitate during the stripping stage.

Earlier work by Crouse and Horner at Oak Ridge National Laboratory indicated that strontium and mixed rare earths were co-extracts from a waste solution to which tartrate or citrate had been added prior to contact with DEHPA (7).

Liljenzin, Rydberg and Skarnemark in Sweden have described a process for treatment of reactor wastes using three-successive cycles of DEHPA and TBP (8). The extraction process removes the high level wastes from the solutions, including the lanthanides.

Investigation by Musikas, Vitorge and Patee in France was concerned with solvent mixtures for the synergistic separation of trivalent actinides from lanthanides from nitric acid waste solutions (9), using a mixture of an aromatic polyimine (TBTZ) and a carboxylic acid (α-bromocapric acid). Mixtures of HDNNS-TBTZ and HDEHDTP - dodecanoic acid also gave synergistic extraction and separation of the actinides from lanthanides.

Recovery of Metals from Wastes

MX Processors in Sweden described a process whereby zinc was recovered from drainage water from a rayon manufacturer (10). In a 2-stage extraction with DEHPA, the zinc is reduced to <2 ppm in the process effluent. Prior to discharge of the raffinate it is passed through a microflotation unit where entrained solvent is removed and recovered.

Ortega et al. have described the separation and recovery of mercury by SX treatment of nitric acid wastes from reactor fuels with a carboxylic acid containing a sulphide group (11) - dodecyl-thioglycolic acid (HDTG). Brine wastes resulting from chlorine-caustic production plants could also be similarly treated. Mercury is stripped efficiently using 2.5-4.5 M HCl.

The extraction of small quantities of cobalt from sulphuric acid plating baths has been described by the Ugine Kuhlman company in France, where the secondary di-lauryl (LA-2) and the tertiary tri-n-octyl amines were evaluated and compared with tributyl phosphate (12,13). Extraction from a solution containing 0.2 g Cr/L, in contact with 0.1 M extractants, resulted in higher extraction coefficients for the amines compared to the TBP. However, with increase in acidity, the loading capacity of the amines decrease while that of TBP increases. The TBP was shown to possess greater stability and was less soluble than the amines in the aqueous phase. Chromium is recovered as sodium chromate by stripping with sodium hydroxide at an equilibrium pH of 4.

MX Processors in Sweden describe processes for treating flue dust for the recovery of zinc and copper (14). The flue dust is leached in sulphuric acid under oxidizing conditions to dissolve the metals. Zinc is recovered by extraction with D2EHPA, stripping the zinc electrolyte containing 100-150 g Zn/L, and electrowinning. In the presence of copper, that metal is first extracted and separated from zinc using a chelating extractant such as LIX 64N. Following stripping, the copper solution is sent to electrowinning to recover cathode copper.

A process was developed by van Acker et al. (15) for the removal of the zinc and copper cyanide complexes using Adogen 464 (Sherex Chemical) in a single stage of extraction. The co-extracted species are stripped sequentially, first using 5 M NaOH for recovery of Zn and 2 M NaCN + 0.75 M NaOH for Cu.

In the presence of high iron-containing waste, MX Processors employ an ammoniacal ammonium carbonate leach to make the primary iron separation. The solubilized metal ammine complexes are recovered by solvent extraction (16). A small pilot plant treats a neutralization waste from the plating industry to recover copper by solvent extraction-electrowinning; the nickel by crystallization as nickel sulphate after solvent extraction separation, and the zinc by precipitation of zinc carbonate with CO_2 from the raffinate.

In another process, the authors describe the recovery of Ni and Cd from Ni-Cd batteries (16). Following dissolution in a NH_4-CO_2 leach, the Ni is recovered by LIX 64N and the $CdCO_3$ returned to production.

Branch et al. (17) have described the treatment of sludges containing metals, mostly copper, together with Ni, Fe, Co, Al, Na, Ca. Following dissolution in H_2SO_4 the leach solution is contacted with LIX 64N to extract the base metals, which are stripped with 150 g/L H_2SO_4.

In the treating of hydroxide slimes from the plating industry, MX Processors in Sweden developed a process to recover the metals (18). The slimes generally consist of iron, copper, zinc, nickel and chromium. Following leaching of the slimes in H_2SO_4, the filtered leach solution is contacted with LIX 64N to remove and recover copper. The raffinate is then contacted in DEHPA in a second circuit to co-extract Fe and Zn. In a third extraction circuit the nickel is extracted and stripped with sulphuric acid. Chromium remains in the raffinate.

Spisak and McClincy have described a route to process smelter dusts (19). It consists of dissolution in H_2SO_4 neutralization to pH 2.0 with limestone followed by extraction with Acorga P-5100 to recover the Cu.

In the purification of water by alum addition, a sludge is formed which is deposited in a settling pond (20). Following acidification treatment of the sludge to pH 2.0 the resultant solution is contacted with mono-di(2-ethylhexyl) phosphoric acid to recover the aluminum.

Recovery of Metals and Acids from Wastes

The Soderfors process in Sweden employs a solvent extraction route, using 75% TBP in kerosene for the extraction of HNO_3, HF and Mo from the process effluent after the addition of H_2SO_4 (21,22). The HNO_3 and HF are water-stripped and recycled to the pickling batch. The metals in the extraction raffinate (Cr, Fe, Ni) are precipitated in two stages. Thus the entire metal content as well as >95% HNO_3 and approximately 70% HF that is contained in the effluent is recovered and recycled to the plant.

French research by Societe Le Nickel and the Commissariat a l'Energie Atomique resulted in a process for the recovery of nitric acid by solvent extraction from a nickel sulphate solution using 50% TBP in dodecane (12).

Extraction of H_2SO_4 from a wash containing zinc (prior to zinc extraction) indicated isobutyl alcohol or isoamyl alcohol was satisfactory (23). However, although the acid could be extracted satisfactorily the solubility of the organic solvents were high in the aqueous phase. If the treated raffinate was neutralized prior to discharge, then 50-60% of the dissolved solvent would be released from the aqueous phase and could be recovered. Isobutyl alcohol was considered the most effective and least expensive of the two alcohols.

The Nihon Solex Process in Japan involves the treatment of pickling waste acids (24,25). In the process at Kawasaki, the waste acid containing, in g/L, 40 HF, 50 HCl and 200 HNO_3, together with Fe, Cr, Ni is sent to an iron extraction circuit. the iron is extracted using DEHPA, scrubbed with water followed by a precipitation-stripping operation in a specially-designed conical unit, using $NH_4F.HF$. The $(NH_4)_3FeF_6$ crystals are filtered, dried and heated to decompose to a α-Fe_2O_3 product. The gases are recycled to stripping.

The raffinate from extraction containing the acids, is sent to an air-pulsed column to extract the HNO_3-HF using 70% TBP in n-paraffin diluent.

Extraction of Oils

Work has been described for the use of solvent extraction in a mixer-settler process to remove oil from water (26). The water contains up to 1000 ppm of crude oil from the North Sea. By mixing with a paraffin solvent, aqueous dispersed, the amount of oil was reduced to 100 ppm.

Extraction of Organics

A mixture of toluene and o-nitrotoluene is used to extract organic pollutants from a waste solution from the manufacture of p-nitrobenzoic acid (27). The toluene extractant containing the extracted organics was then subjected to distillation, the toluene distalate recovered for re-use, and the bottoms containing the pollutants thermally decomposed.

Carboxylic acids, such as acetic acid, are removed from waste streams using Alamine 336 and diisopropyl ketone, while phosphoryl extractants (TOPO in DIBK) are better for phenols (28) in the extraction at pH 3.3-3.8.

Investigations by Inoue and Shishido in Japan concerned the comparison of various extractants for the removal of phenol from waste waters (29). From the study it was concluded that the tertiary amine Aliquat 336 was the best extractant, used in the H_2SO_4 or HCl form. Stripping is accomplished using alkali solutions.

Phenols have been extracted from waste water by benzene, toluene, isobutylene methylene chloride, isopropyl ether, n-butyl acetate, methyl isobutyl ketone and amines (30). Acetic acid has been removed by extraction with TOPO. Solvents such as toluene and carbon tetrachloride were used for the treatment of secondary municipal effluents (containing humic acids, carbohydrates, proteins, tannin, lignins, detergents, etc.).

The wastes from coal mining and processing contain mono and polysubstituted phenols, cresols, naphthols, intenols, pyridines, aromatic, polyaromatic and heterocyclic hydrocarbons, sulfur compounds, nitrogen heterocycles and arylamines. Isopropyl ether is used in one plant to reduce the phenols to <20 ppm.

Supported Extraction Systems

The use of solvent impregnated in various medium or in fibres or supported membranes can have application in the treatment of waste waters for environmental protection. Roux-Guerraz, Defives and Durandet in France have reported on the removal of aromatic and phenol from water (31).

A process was described by Nichols et al. (32) using bound liquid ion exchange (quaternary amine) membranes for removal and recovery of chromate from plating rinse waters. Although the transport rates were considered suitable for practical use, the membrane life was limited by a phase inversion process. This occurs when water droplets nucleate within the membrane and eventually halt ion exchange.

Fujinawa and Hozawa at the University of Tohoku in Japan have carried out considerable research on supported liquid membranes (33) for extraction of Cu and Zn from H_2SO_4 solutions. Properties that have been studied include stability of emulsion, breaking and swelling, viscosity and density. The continuous countercurrent testing has involved the examination of the mechanism of permeation and deterioration. One of the problems with membranes seem to be the loss of reagent to the aqueous phases as well as the low tolerance for the treatment of "dirty" metallurgical leach solutions.

Solvent Losses and the Environment

The raffinates from the solvent extraction process can, and usually do contain various amounts of the organic constitutents used in the metals recovery stage. The organic reagents can be present as entrained solvent, as stable emulsions or crud, and as dissolved organic in the aqueous phase. The solubility ranges from less than 1 ppm to several grams per liter depending upon the particular reagent, the pH of the aqueous phase and the anionic strength of the aqueous phase, and the degradation properties of the solvent extraction reagent with continued recycle (34).

Removal and Recovery of TBP from Raffinates

Kano, Togashi and Nagai in Japan have described the removal and recovery of TBP from a copper electrolyte which has had arsenic removed by using a 100% TBP extractant (35). By scrubbing the raffinate, containing 92 ppm, with CCl_4 the amount was reduced to <1 ppm when the CCl_4 contained 3% TBP and 1 ppm when 10% TBP was in the CCl_4. With recycle of the CCl_4 and build-up of TBP concentration, a bleed stream is taken to distillation for recovery of the TBP.

Germain and Pluot in France have described their technique for removing the TBP from process raffinates by washing the aqueous phase with the diluent (36).

Although the solvent extraction process has been demonstrated to be useful for the removal and recovery of trace constituents fom waste liquors (as well as from more concentrated leach liquors), nevertheless the nature of the process, type of solvent and solvent extraction contactors used could have an impact on the amount of solvent carried out in the process raffinates as soluble loss, entrainment and stable emulsions and cruds. Various types of coalescers, centrifuges and after-settlers can be used to recover entrained solvent and break emulsions and cruds (37,38). Activated carbon can be used to remove and recover most dissolved solvent from the raffinate (39). Any appreciable solvent remaining in the raffinate can ultimately impact adversely on the aquatic and other life in the environment (37). Acute toxicity testing on various fish and animals have demonstrated that some of the reagents used in solvent extraction processing are very lethal, and therefore must be removed.

The foregoing have been examples demonstrating the use of solvent extraction for the treatment of waste effluents. However, in the usual processing by solvent extraction it is also evident that no matter what plant controls are exercised, there could exist soluble solvent in the raffinate. Often this solvent is also composed of the metal chelate, in addition to the unextracted metal. Thus, even though the solvent concentration appearing in an effluent stream may meet the environment regulations regarding aquatic toxicity, the concentration level of metals present may indeed be well above the tolerable limits. Thus, it may be necessary to treat the effluent from solvent extraction processing for the removal of possible toxic metals (40). There are many instances where solid ion exchange should be used.

Activated carbon has been used for the removal and recovery of trace constituents such as gold, molybdenum, vanadium, oil, etc. from solutions. Activated carbon adsorption offers an effective means of removing, and perhaps recovering, the components of solvents from aqueous raffinates produced in the solvent extraction process (41).

Athough treatment of certain effluent streams and off-gas vapours containing metals, salts and solvents could be costly, it may be necessary in order to meet the environmental regulations.

Solvent losses to waste process stream effluents can be both uneconomical and unacceptable environmentally. Chemical and chemical engineering designs are therefore necessary to minimize the losses, coupled with biological studies to ensure that any losses that do occur will not adversely affect the receiving environment.

If solvent extraction is to have a prominent place in the future processing of waste streams for the removal of potential pollutants and recovery of values, then there are certain improvements that could assist in the success of the process, e.g.:

a) use of more easily biodegradable extractants
b) better engineering design and operation of equipment to minimize entrainment and physical losses
c) development of improved solvent removal and recovery method and equipment
d) design and improve on membrane extraction (to reduce leakage) so that technology might be used in waste treatment

References

1. McIsaac, L.D., Baker, J.D. and Tkachyk, J.W., ERDA, U.S.A., Report ICP-1080, August, 1975.

2. Shoun, R.R., McDowell, W.J. and Weaver, B. "Bidentate organophosphorus compounds as extractants from acidic waste solutions: A comparative and systematic study"; in Proceedings of International Solvent Extraction Conference, ISEC'77, Toronto, September 1977, Vol. 1, p. 101-105, Pub. Can. Inst. Mining and Metallurgy; 1979.

3. Schulz, W.W. and McIsaac, L.D. "Biodentate organophosphorus extractants: Purification, properties and applications to removal of actinides from acidic waste solutions"; in Proceedings of International Solvent Extraction Conference, ISEC'77, Toronto, September 1977, Vol. 2, p. 619-629, Pub. Can. Int. Mining and Metallurgy; 1979.

4. Richardson, G.L. "Americium recovery by DBBP solvent extraction pilot plant demonstration"; USAEC Report BNWL-CC-1503; 1968.

5. Yongjun, Zhu., Rongzhou, Jiaa., Shouzhong, Wang, Shoguo, Fan., Bingren, Liu., Hualing, Zheng., Shunli, Zhou, Shuming, Chen. "An extractant (TRPO) for the removal and recovery of actinides from high level radioactive liquid waste"; in Proceedings of International Solvent Extraction Conference, Denver, Colorado, p. 9, September 1983.

6. Horwitz, E.P. and Schutz, W.W. "Solvent extraction and recovery of the transuranic elements from waste solution using the Truex Process"; in Proceedings of Solvent Extraction and Ion Exchange in the Nuclear Fuel Cycle, Ed. Logstail and Mills, Pub. Ellis Horwood Limited, Chichester, pp. 138-144; 1985.

7. Crouse, D.J. and Horner, D.E. "Unexpected ratio effects in the extraction of rare earth by di-(2-ethylhexyl) phosphoric acid"; Solvent Extraction of Metal, p. 305, Ed. McKay, Healy, Jenkins by CRC Press 1965, in Proceedings of International Solvent Extraction Conference, Harwell, U.K..

8. Liljenzin, J.O., Rydberg, J. and Skarnemark, G. "Reducing the long-term hazard of reactor waste through actinide removal and destruction in nuclear reactors"; Separation Science Technology, 15(4), pp. 799-824; 1980.

9. Musikas, C., Vitorge, P. and Patee, D. "Progress in trivalent actinide lanthanide group separation"; in Proceedings of International Solvent Extraction Conference, Denver, Colorado, p. 6, September 1983.

10. Reinhardt, H. "Solvent extraction for recovery of metal waste"; Chemistry and Industry, March 1, pp. 210-213; 1975.

11. Ortega, J. and Gutierrez, J. "Recovery of mercury from wastes"; Proceedings of International Solvent Extraction Conference, Liege, Belgium, Paper 80-103, September 1980.

12. Demarthe, J.M., Tarnero, M., Miguel, P. and Goumondy, J.P. "Example of nitric acid recovery by solvent extraction"; Proceedings of International Solvent Extraction Conference, ISEC'74, Lyon, pp. 1275-1296, Pub. Soc. Chem. Industry, London; 1974.

13. Cuer, J.P., Stuckens, W. and Texier, N. "The techniques of solvent extraction applied to the treatment of industrial effluents"; Proceedings of International Solvent Extraction Conference, ISEC'74, Lyon, pp. 1185-1200, Pub. Soc. Chem. Industry, London; 1974.

14. Anderssen, S.O.S. and Reinhardt, H. "MAR-hydrometallurgical recovery processes"; Proceedings of International Solvent Extraction Conference, ISEC'77, Toronto, pp. 798-804, Pub. Canadian Institute of Mining and Metallurgy; 1979.

15. van Acker, P., Verhaege, M., van Peteghem, A., Cyselinck, L. "Recuperation and separation of copper and zinc from cyanide electroplating effluents by solvent extraction"; Proceedings of International Solvent Extraction Conference, ISEC'83, Denver, September 1983, p. 532, Pub. American Institute of Chemical Engineers; 1983.

16. Bozec, C., Demarthe, J.M. and Gandon, L. "Recovery of nickel and cobalt from metallurgical wastes by solvent extraction"; Proceedings of International Solvent Extraction Conference, ISEC'74, Lyon, pp. 1201-1229, Pub. Soc. Chem. Industry, London; 1974.

17. Branch, J., Dewey, J., Rousseau, L. "Industrial sludges processed by the use of solvents"; Proceedings of International Solvent Extraction Conference, Liege, Belgium, Paper 80-100, September 1980.

18. Reinhardt, H. "Solvent extraction for recovery of metal waste"; Chem. and Industry, p. 210-213, March 1975.

19. Spisak, J.F. and McClincy, R.J. "Solvent extraction of copper from smelter dust treatment liquor with Acorga P-5100"; Proceedings of International Solvent Extraction Conference, Liege, Belgium, ISEC'80, Paper 80-99, September 1980.

20. Cornwell, D.A. "Recovery of aluminum from water treatment plant sludges"; in Proceedings of International Solvent Extraction Conference, ISEC'80, Liege, Belgium, Paper 80-67, September 1980.

21. Rydberg, J., Reinhardt, H., Lunden, B. and Haglund, P. "Recovery of metals and acids from stainless steel pickling baths"; International Symposium on Hydrometallurgy, Chicago, 1973, pp. 589-611, Pub. AIME, New York; 1973.

22. Kuylenstierna, U. and Uttertun, H. "Solvent extraction of HNO_3-HF from stainless steel pickling solutions"; Proceedings of International Solvent Extraction Conference, ISEC'74, Lyon, pp. 2803-2816, Pub. Soc. Chem. Industry, London; 1974.

23. Buttinelli, D., Giavarini, C. and Mercanti, A. "Pilot-plant investigations on H_2SO_4 extraction by alcohol from spent electrolytes"; in Proceedings of International Solvent Extraction Conference, ISEC'83, Denver, September 1983, p. 422, Pub. American Chemical Society; 1983.

24. Nishimura, S., Watanabe, M. "Recovery process of acid and high purity metallic iron/iron oxide from pickling waste acid"; Presented at Recycle of Waste Acid from Stainless Steel Pickling Meeting, American Iron and Steel Institute, Pittsburg, July 1982.

25. Watanabe, T., Hoshino, M., Uchino, K., Nukazato, Y. and Nishimura, S. "A new recovery process for stainless steel pickling waste liquor with iron removal process using solvent extraction"; Paper to be presented at the International Symposium on Iron Control in Hydrometallurgy, Toronto, 16th Annual Hydrometallurgy Meeting, CIM, October 1986.

26. Robilliard, K.R., Thorsen, G., Grislingas, A. "Purification of only water by solvent extraction"; Proceedings of International Solvent Extraction Conference, Liege, Belgium, Paper 80-171, September 1980.

27. Wennensten, R. "Extraction of organic pollutants from an effluent stream in the manufacture of p-nitiobenzoic acid"; Proceedings of International Solvent Extraction Conference, Liege, Belgium, Paper 80-68, September 1980.

28. King, C.J. "Removal and recovery of carboxylic acids and phenols from dilute aqueous stream"; Proceedings of International Solvent Extraction Conference, Liege, Belgium, Paper 80-66, September 1980.

29. Inoue, Katsutoshi and Shishido, Hironori "Solvent extraction of phenol with quarternary ammonium compounds and various mineral acid salts of high-molecular-weight amines"; in Proceedings of Symposium in Solvent Extraction, Faculty of Science, Science University of Tokyo, p. 101-108, December 1985.

30. Mackay, D. and Medir, M. "The applicability of solvent extraction to waste water treatment"; in Proceedings of International Solvent Extraction Conferences, ISEC'77, Toronto, September 1977, Vol. 2, p. 791-797, Pub. Can. Inst. Mining and Metallurgy; 1979.

31. Roux-Guerraz, C., Defives, D. and Durandet, J. "Solvent extraction using impregnation in a porous medium"; Proceedings of International Solvent Extraction Conference, Liege, Belgium, Paper 80-69, September 1980.

32. Nichols, L.D., Obermayer, A.S. and Allen, M.B. "Bound liquid ion exchange membranes for recovery of chromium from wastewater"; Moleculon Research Corp., Cambridge, Mass., Bureau Mines Report OFR-109-82.

33. Private Communication to the author.

34. Ritcey, G.M. and Ashbrook, A.W. "Solvent extraction - principles and application to process metallurgy"; Vol. 1, p. 261, Pub. Elsevier Science Publishers, Amsterdam; 1984.

35. Kano, G., Togashi, R. and Nagai, T. "Removal and recovery of TBP in a raffinate by carbon tetrachloride scrubbing"; Proc. Symposium on Solvent Extraction, Japan Association of Solvent Extraction, Hamamatsu, Japan, pp. 42-44, December 1982.

36. Germain, M. and Pluot, P. "Diluent washing of aqueous phase using centrifugal contactors"; International Solvent Extraction Conference, ISEC'80, Liege, Belgium, Session 14, Vol. 3, Paper 80-218, September 1980.

37. Ritcey, G.M. and Ashbrook, A.W. "Chapter 6 - Solvent loss, recovery and environmental considerations"; Vol. 1, p. 230-289, Pub. Elsevier Science Publishers, Amsterdam; 1984.

38. Ritcey, G.M., Wong, E.W. "Influence of cations on crud formation in uranium circuits"; Hydrometallurgy, 15, p. 55-61; 1985.

39. Ritcey, G.M. and Ashbrook, A.W. "Chapter 6 - Solvent loss, recovery and environmental considerations"; Vol. 1, p. 269, Pub. Elsevier Science Publishers, Amsterdam; 1984.

40. Ritcey, G.M., Lucas, A.M. and Ashbrook, A.W. "Treatment of solvent extraction raffinates for the removal of organic reagents"; in Proceedings of International Solvent Extraction Conference, ISEC'74, Lyon, pp. 943-968, Pub. Soc. Chem. Ind., London; 1974.

41. Ritcey, G.M., Northern Miner, pp. 13, January 3, 1974.

Supercritical Phase Equilibria - Theory and Applications

Aa. Fredenslund, E.A. Brignole, Technical University of Denmark, Lyngby/Denmark and Plapiqui, Bahia Blanca/Argentina

Supercritical fluid equilibria and Supercritical fluid extraction (SFE) have been the topic of several thorough reviews:

Essen-Symposium, June 1978: Extraction with Supercritical Gases. ed. G.M. Schneider et al., Verlag Chemie 1980.

London, Febr. 1982, Chemistry and Industry, 19 June 1982, pg. 385-405.

Separation Science and Technology, 17, 1982, pg. 1-233.

Cambridge 1982, Fluid Phase Equilibria, Elsevier Scientific Publishing Company, Amsterdam, 10, 1983, pg. 141-344.

Chemical Engineering at Supercritical Fluid Conditions, ed. M.E. Paulaitis et al., Ann Arbor Science Publishers, Ann Arbor, Michigan, 1983.

A Review of Supercritical Fluid Extraction, Dec. 1983, of James F. Ely and Jolene K. Baker, Chem. Eng. Science Div., Nat. Eng. Lab., National Bureau of Standards, Boulder, Colorado 80303.

Königstein/Taunus-Symposium, April 1984, i Berichte der Bunsen-Gesellschaft für physikalische Chemie, 88, sept. 1984, pg. 784-923.

Erlangen-Symposium, Okt. 1984, ed. Verein Deutscher Ingenieure, GVC-VDI-Gesellschaft Verfahrenstechnik und Chemieingenieurwesen, Postfach 1139, Düsseldorf.

San Francisco-Symposium, Nov. 1984, Proc. Symp. of Supercritical Fluid Technology, Elsevier Science Publisher BV, Amsterdam.

F.M. Taylor, Carbon Dioxide, the solvent for the food and related industries. Wolviston Consultancy Services Ltd., 50, Cricket Lane, Lichfield Staffs, England WS14 9ER.

It is impossible in a few pages to give a just review of SFE. Below we give a brief survey of areas of application of SFE. Two examples are then given to illustrate the thermodynamics behind selective supercritical fluid extraction from solid and liquid mixtures, respectively.

Applications of SFE processen

Existing and potential areas of application of SFE extraction processes are given in Table 1

TABLE 1

POTENTIAL APPLICATIONS OF SUPERCRITICAL EXTRACTION PROCESSES

NATURAL PRODUCTS	SCF	References
Decaffeination of green cofee beans	CO_2	Zosel (1978)
Extraction of spices, e.g. peper, nutmeg and chili	"	Vitzhum et al. (1978)
Production of hop extract for the brewing industry	"	Vitzhum et al. (1978)
Fractionation of glycerides and fatty acids	"	Peter and Brunner (1978)
Oil extraction from seeds and foods	"	(cited by Paulaitis et al. (1983b), p. 228)
Fractionation of cod-liver oil	"	Zosel (1978)
Extraction of flavours and fragances	"	Caragay (1981), Schultz and Randell (1970)
Defattening of fryed potato chips and other snack foods	"	Paulaitis et al. (1983b), p. 230
Extraction of nicotine from tobacco	"	Vitzhum et al. (1978)
PETROLEUM AND COAL		
Deasphalting of heavy petroleum fractions	pentane propane	Gearhart and Garwin (1976) (1976), Zhuze (1960), Zosel (1978)
Tertiary oil recovery	CO_2, C_2, C_3	Hull (1970), Metcalfe and Yarborough (1979)
Coal processing for conversion to liquid fuels	toluene water	Paulatis et al. (1983b), part III
PETROCHEMICALS		
Recovery of chemicals from water streams (ethanol, isopropanol, butanol)	C_2H_6, C_3H_8, and others	Moses et al. (1982), Kuk and Montagna (1983), Brignole et al. (1985)

It is apparent from Table 1 that the solvent normally is a light gas (CO_2 or light hydrocarbon), and that the phenomena involved are either solid-fluid or fluid-fluid equilibria.

Solvent properties

Some order-of-magnitude properties of near-critical fluids are given in Table 2.

TABLE 2

Near-Critical Fluid Properties

Property	Dense Gas	Near-critical Fluid	Liquid
Density, ρ g/cm^3	10^{-3}	0^{-3}	1
Diffusivity, D cm^2/s	0.1	10^{-3}	$5 \cdot 10^{-6}$
Viscosity, η g/cm s	10^{-4}	10^{-4}	10^{-2}

This table shows that the near-critical fluid has liquid-like densities (and hence potentially high solute solubility), intermediate diffusivities, and gas-like viscosities. It is these properties which are exploited in SFE processes.

SFE: Solid-Fluid Equilibria

For two phases (S and F) in equilibrium, the following equation holds for each component i:

$$f_i^S = f_i^F \qquad i = 1,2..M \qquad (1)$$

where f_1 is the fugacity of component i in the mixture.

The component fugacities may be calculated from either activity coefficent (γ) models:

$$f_i = x_i \gamma_i f_i^o \qquad (2)$$

or from fugacity coefficient (φ_i) which may be obtained from equations of state:

$$f_i = y_i \varphi_i P \qquad (3)$$

In equation (2) and (3), x_i represents a solid or fluid phase mole fraction, f_i^o the reference fugacity, P the pressure, and y_i a fluid or vapor phase mole fraction.

For the solubility of solids in near-critical fluids, it is normally assumed that the solid phase is pure. The near-critical fluid phase is treated as a compressed gas phase using equation (3). The solubility of a solid (2) in near-critical fluid (1), y_2, is then given by:

$$y_2 = \frac{P_2^S}{P} \left[\frac{\varphi_2^S}{\varphi_2} \exp\left(V_2^S(P-P_2^S)/RT\right) \right] \qquad (4)$$

where P_2^S is the sublimation pressure of pure solid 2 at the temperature of the system, φ_2^S is the corresponding fugacity coefficient, and V_2^S is the molar volume of pure solid 2. The term in the square brackets is termed the enhancement factor. P_2^S/P is the ideal solid solubility.

The many normal applications, the enhancement factor is nearly unity. In near-critical fluid extraction, the enhancement factor may become considerably large.

Consider, for example, the solubility of solid naphtalene in ethylene at 15 K above the critical temperatures of ethylene as shown in Fig.1 (Bruh et al., 1982). The large difference between the ideal and the actual solubility of naphtalene in ethylene above approximately 60 bar is due to a sharp increase in the enhancement factor. This increase can only be explained a sharp decrease in the fluid-phase fugacity coefficient, φ_2, which may be obtained from an equation of state by the well-known relationship:

$$RT \ln \varphi_2 = \int_0^P \left(\bar{V}_2 - \frac{RT}{P}\right) dP \qquad (5)$$

where $\bar{V}_2$ is the partial molar volume of component 2 in the fluid phase.

Normally, φ_2 is described using a cubic equation of state such as the Soave-Redlich-Kwong or the Peng-Robinson equations. It should be noted that the results from the SRK and the PR equations are extremely sensitive to the value of the mixture parameter, "kij", especially in SFE applications.

If the solid phase is not pure, the fugacity of the components in the solid phase may be taken into account using Eq. (2). In this case not only the solubility (y_2), but also the selectivity become of primary concern. Selectivity is discussed in the section on fluid-fluid equilibria below.

Entrainers

When the supercritical fluids is mixed with another solvent, an entrainer, the properties of the (mixed) solvent become a strong function of the concentration of the entrainer, even at low entrainer concentrations. The function of the entrainer is to

- increase the solute solubility
- increase the P- and T-dependence of the system properties
- increase the selectivity

Example of entrainers used in CO_2 are: propane, hexane, ethanol, and acetone.

The effect of the entrainer is to reduce the pressure and/or temperature changes needed in SFE process flow sheets.

SFE: Fluid-Fluid Equilibria

SFE may be used to selectivity extract components from a liquid mixture. Some of these applications mentioned in Table 1 are: tertiary oil recovery and recovery of oxygenated hydrocarbons from water. In this case, one of the fluids (e.g. ethanol + water) is liquid-like, and the other fluid (e.g. ethane) is dense-gas-like. In this case, we may write the equilibrium relationship as follows:

$$f_i^L = f_i^V \qquad i = 1,2.. M \qquad (6)$$

where L is the liquid-like and V is the dense-gas-like phase.

Equation (3) is used to describe both f_i^L and f_i^V.

As an example, we will consider the extraction of ethanol from water using near-critical fluid extraction (Brignole et al., 1985). Simulation of such processes requires an equation of state to predict the component fugacity coefficients in Eq. (3). The group-contribution equation of state (GC-EOS) by Skjold-Jørgensen (1984) has been shown to be applicable to this purpose. Some examples of SFE calculations for Ethanol - Water - Near-Critical-Fluid mixtures using GC-EOS are given below.

Water - Ethanol - Carbon Dioxide experimental phase equilibrium data (Kuk and Montagna, 1983) are compared with GC-EOS predictions in Fig. 2. It is interesting to note the increase of ethanol and water solubility in the CO_2 phase when the system pressure exceeds the critical value for CO_2. However, the increase in solubility is much higher for ethanol than for water. The distribution coefficients of isopropanol between water and CO_2 are compared with experimental data in Fig. 3.

Based on the predictions of the GC-EOS, a better understanding of the behaviour of NCF extraction solvents like CO_2 and ethane is possible. Fig. 4 shows predicted ethanol distribution coefficients between a 10 wt % ethanol aqueous solution and CO_2. The critical coordinates of CO_2 are T_c = 305.2 K and P_c = 73 bar. At 75 bar the distribution coefficient shows a steep decrease with temperature in the ambient temperature range. The same behaviour, but less pronounced, is found at 100 bar. At 150 bar the distribution coefficient is no longer strongly affected by temperature. In the case of ethane, a similar variation of the distribution coefficient with temperature is observed in the ambient temperature range (Fig. 5). The critical temperature of ethane is 305.4 K.

The predicted ethanol concentration in extracting ethanol from a 10 wt % ethanol-water mixture, using CO_2, is shown in Fig. 6 as a function of extraction temperature at two isobars. The results agree with the experimental observations of Kuk and Montagna (1983), Paulaitis et al. (1981) and Moses et al. (1982). It is not possible to break the azeotropic composition working in the temperature range from 298 to 333 K. However, the predictions indicate that by extraction at subambient temperatures it is possible to break the azeotropic compositions, and that the operation at higher pressures favours this effect. Still, the distribution coefficients are rather low for practical applications. One of the limitations of CO_2 as a solvent is its relatively low critical temperature, which confines the extraction temperature to values close to ambient temperatures. The same limitation holds for ethane and ethylene. The use of solvents of higher critical temperature, like propane or butanes, will allow operation at higher temperatures with fluids of liquid-like densities.

Predicted distribution coefficients for ethanol in propane are shown at 43 bar and 75 bar in Fig. 7. The distribution coefficient of ethanol between water and propane increases monotonically with temperature when the pressure is above the critical of propane. This illustrates the favourable effect of using a solvent of greater critical temperature than those of CO_2 or ethane.

The above-mentioned effects are exploited by Brignole et al. (1985) in the development of a SFE process for recovering oxy-organic compounds from water using light hydrocarbons as a dual-effect solvents (entrainer and extractant).

Conclusion

SFE may be analysed and described using well-known thermodynamic principles and equations of state. The extraction of solid components is well described using well-known cubic equations of state such as SRK NPR. Fluid-phase extraction of for example oxyorganic compounds from water is well described using equations of state with density-dependent mixing rules such as the GC-EOS.

REFERENCES

Brignole, E.A., P.M. Andersen and Aa. Fredenslund, Submitted to Ind.Eng.Chem. Process Des. Dev. (1985).

Bruh, M.R., R.W. Corbett and S. Watanasiri, paper presented at the 47th API midyear Refining Meeting, New York, 1982.

Caragay, A.B., "Supercritical Fluids for Extraction of Flavors and Fragances from Natural Products", Perfume and Flavorist 6 43 (1981).

Gearhart, J.A. and L. Garwin, "Resid-Extraction Process Offers Flexibility", Oil Gas J., 74 (24) 63-6 (1976).

Hull, P., Oil Gas J. p. 57. 17 august (1970).

Kuk, M.S. and J.C. Montagna, "Solubility of Oxygenated Hydrocarbons in Supercritical Carbon Dioxide", in "Chemical Engineering at Supercritical Fluid Conditions", Paulaitis et al. (1983).

Metcalfe,R.S. and L. Yarborough, SPE. Journal 242 (Aug. 1979).

Moses, J.M., K.E. Goklen and R.P. De Filippi,"Pilot Plant Critical-Fluid Extraction of Organics from Water", A.I.C.h.E. Annual Meeting, Paper No. 127c Los Angeles (1982)

Paulaitis, M.E., M.L. Gilbert, C.A. Nash, "Separation of Ethanol-Water Mixtures with Supercritical Fluids", 2nd World Congress of Chemical Engineering, Montreal (1981).

Paulaitis, M.E., V.J. Krukonis, R.T. Kurmik and R.C. Reid, Reviews on Chem. Eng. 1 (2) 179 (1983b)

Peter, S. and G. Brunner, Angen.Chem.Int.Ed. 17 746 (1978).

Skjold-Jørgensen, Steen, Fluid Phase Equilibria. 16, 317 (1984).

Vitzhum, O., Hubert, P. and Sirtl, W., "Production of Hops. Extracts", US Patent 4104409 (1978).

Zhuze, T.P., Petroleum (London) 23 298 (1960).

Zosel, K., Angew.Chem.Int.Ed. 17 702 (1978).

List of figures

Number	Title and Captions
1	Actual and ideal solubility of naphtalene in ethylene.
2	Ethanol(1)-Water(2)-CO_2(3) Phase Equilibria at 313 K. Comparison of Experimental Data of Kuk and Montagna (1983) with GC-EOS predictions.
3	Distribution Coefficients of Isopropanol between Water and CO_2. Isopropanol mole fraction (CO_2 free basis) in the aqueous phase is 0.114.
4	Ethanol Distribution Coefficient between Water and CO_2. Ethanol concentration in the aqueous phase is 10 wt % (CO_2 free basis).
5	Ethanol Distribution Coefficient between Water and Ethane. Ethanol concentration is the aqueous phase is 10 Wt % (ethane free basis)
6	Ethanol Concentration is the Extract as a Function of Temperature and Pressure of Extraction. Extraction with CO_2 of a 10 wt % ethanol in water feed.
7	Ethanol Distribution Coefficient between Water and Propane. Ethanol concentration in the aqueous solution is 10 wt % (propane free basis).

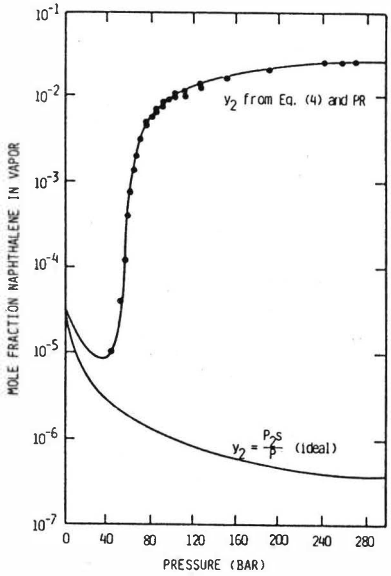

FIGURE 1

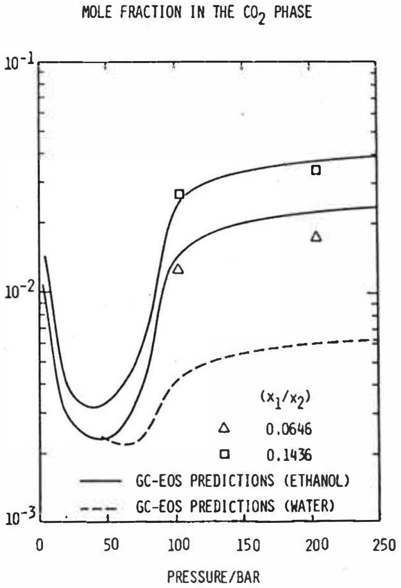

FIGURE 2

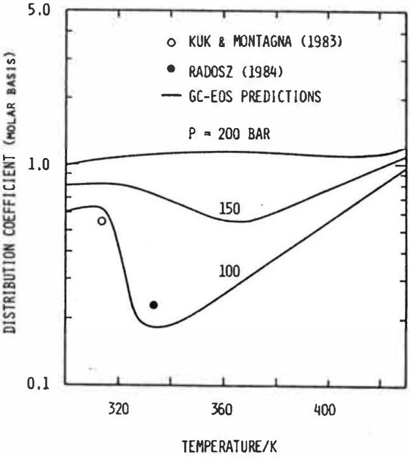

FIGURE 3

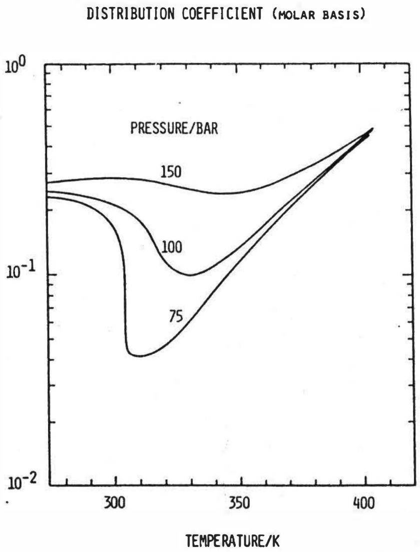

FIGURE 4

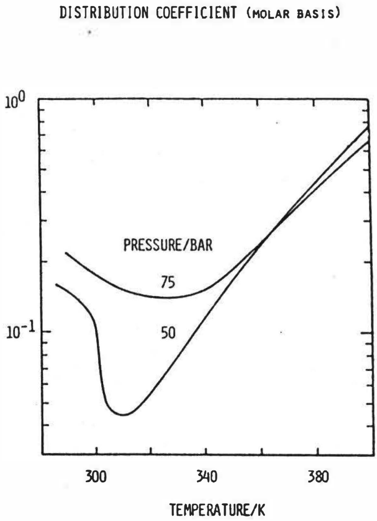

FIGURE 5

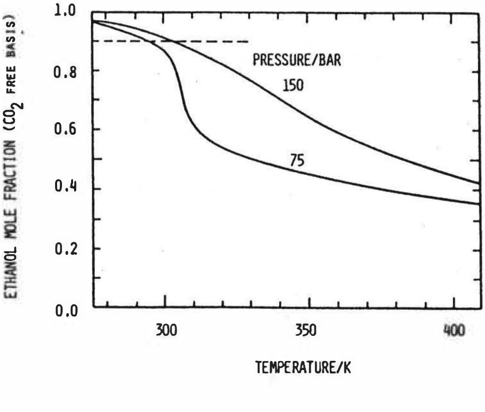

FIGURE 6

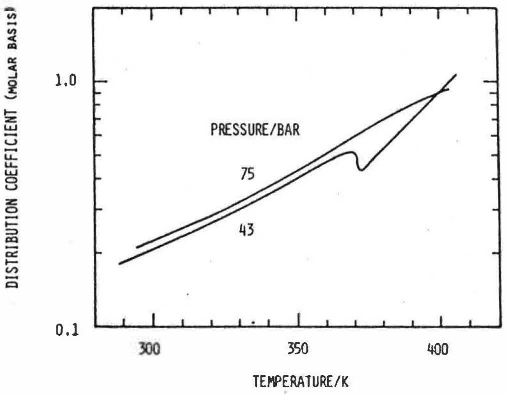
DISTRIBUTION COEFFICIENT (MOLAR BASIS)
1.0
0.1
PRESSURE/BAR
75
43
300
350
400
TEMPERATURE/K

FIGURE 7

PUREX: PROCESS AND EQUIPMENT PERFORMANCE*

D. A. Orth, E. I. du Pont de Nemours and Co., Savannah River Laboratory,
Aiken, South Carolina, 29808 USA

INTRODUCTION

The Purex process is the solvent extraction system that uses tributyl phosphate (TBP) as the extractant for separating uranium and plutonium from irradiated reactor fuels. Since the first flowsheet was proposed at Oak Ridge National Laboratory in 1950, the process has endured for over 30 years with only minor modifications. The spread of the technology was rapid, and worldwide use or research on Purex-type processes was reported by the time of the 1955 Geneva Conference. The overall performance of the process has been so good that there are no serious contenders for replacing it soon.

Purex has also had a substantial affect on solvent extraction science. The desire by many establishments and countries to investigate nuclear materials processing has led to a large investment in fundamental research. This research has covered the mechanisms of extraction, metal-organic compounds, mixing phenomena, thermodynamics, kinetic effects, interphase transfer, analytical techniques, and many other areas of direct application to solvent extraction.

The many papers of the McKay group at Harwell are examples of the contributions. This is not to say that Purex is responsible for the major advances in solvent extraction technology, just that the association with nuclear processing has made funding easier for solvent extraction research.

Two papers on nuclear fuel processing, given at these Conferences in the past, would be difficult to improve on. Spence, at ISEC '71, covered the early history of solvent extraction for nuclear materials recovery. A subsequent comprehensive description of some of the varied approaches was given by A. Chesne' at ISEC '80. I will discuss the evolution of the Purex system, the comparative performance over the years, the areas of science and engineering that have been involved, and some possible areas of continued development.

Some other Purex-related systems that utilize different strengths of TBP for the separation of heavy elements can be operated in the equipment used for Purex. Indeed, one of the original Savannah River Plant (SRP) Purex plants has operated with the following variations:

- Thorex, which separates and recovers thorium target material and U-233
- Interim 23, which recovers only U-233, and sends thorium to waste
- 25 Process, which recovers irradiated highly or medium enriched uranium
- Assorted flowsheets for recovery of higher isotopes of plutonium from irradiated plutonium fuel
- Assorted flowsheets for recovery of transplutonium elements.

---

* The information contained in this article was developed during the course of work under Contract No. DE-AC09-76SR00001 with U.S. Department of Energy.

The ranges of TBP strength utilized in these processes have ranged from 1.5% to 42% at different sites.

PUREX PROCESS DESCRPITION

A brief outline of the basic Purex process is warranted. The first cycle involves coextraction and decontamination of uranium and plutonium in a first contactor, reductive partition of plutonium from uranium in a second contractor, and recovery of the uranium in a third contactor. Separate second cycles then give further decontamination of the plutonium and uranium. The spent solvents are washed with alkaline solutions and recycled. Many variations of this basic outline have been utilized on a large variety of irradiated fuels. Extraction contactors are generally center-fed units with an extraction section and a scrubbing section for decontamination, while stripping contactors are generally end-fed. Center-fed contactors can be and have been replaced by two end-fed units. Extra cycles have been provided in some installations to obtain higher decontamination with less restrictive conditions. Other flowsheet variations include backcycle and reflux flowsheets. In backcycle, overall waste volumes can be reduced by utilizing the waste from one cycle as chemical adjustment for a previous cycle. Solvent streams can also be backcycled to reduce losses or add some operating versatility.

Reflux flowsheets have been used to obtain high concentrations by recycling a product stream back to a feed stream and drawing off a small product stream after the desired concentration has been reached. Finally, completely separate solvent systems may be provided for each cycle, or two or more may be combined. The net result of all these possibilities is that few, if any, Purex installations have had exactly the same flowsheets or cycle arrangements. However, the many variations have all had at least satisfactory performance.

EQUIPMENT PERFORMANCE

The requirements for a high decontamination factor (at least 10^7), low losses of valuable fissile materials, and minimum space for very expensive shielded facilities, mean that the solvent extraction contactors must be highly efficient and reasonably compact. The contactors primarily utilized for Purex operations have been pulse columns and mixer-settlers, with some limited use of centrifugal units. Pulse columns were ushered in with Purex processing in 1949 and 1950 at Oak Ridge National Laboratory, following development work at Hanford and Oak Ridge in the recovery of uranium from stored waste. The emergence of pulse columns at this time is illustrated by the 1950 edition of Perry's Chemical Engineers' Handbook, which does not even include pulse columns in its discussion of contactor types, even though a patent for the concept was issued in 1935.

Mixer-settlers, on the other hand, have been used in a variety of sizes and configurations following the first description of one in 1904 (which was amazingly similar to some present day units). Overall, mixer-settlers in production work have ranged from small units for enriched uranium and plutonium-rich fuels (as at Eurochemic and Dounreay), to large units like those at Sellafield and Savannah River. Even these units are very small compared to industrial units.

Pulse columns and assorted designs of mixer-settlers were adopted as the number of Purex installations grew. The Savannah River Plant adopted mixer-settlers of a pump-mix design (developed at Knolls Atomic Power Laboratory) for its two Purex plants that began operating in 1954 and 1955. The Hanford Purex Plant,which began operating in 1956, utilizes scaled-up pulse columns. Many other installations that use pulse columns and mixer-settlers were described in the Geneva Conferences of 1955, 1958, and 1964, and at ISEC conferences.

Mixer-Settlers

General factors that determine the efficiency of mixer-settlers have been reviewed many times. Some of the earliest production Purex units were those at Savannah River. The KAPL pump-mix impeller design moves the heavy phase through the bank, and balances the mixing and pumping functions to give good efficiency at a restricted flowrange. Above the design range, the high impeller speeds necessary for high flows result in excessive mixing, with consequent excessive entrainment in the reduced residence time that accompanies high flow. Below the design range, low impeller speeds for low flow provide insufficient mixing and low efficiency. Units with separate pumping and mixing functions in a variety of configurations are used at other installations. Such units can maintain a high stage efficiency and reasonable entrainment over a wide flow range.

Mixer-settler stage efficiencies in most Purex applications can be held at 70% to near 100% relatively easily where the bulk transfer of uranium and plutonium is involved. Efficiencies can be low in extreme flow ratio regions, such as some scrub sections, where transfer of a small amount of material from the bulk phase into a small volume of dispersed phase is desired.

One requirement for the continued efficient operation of mixer-settlers is that solids not accumulate in the banks, particularly at the interfaces in the settlers. Such material can cause excessive solvent degradation if fission products accumulate and become a localized high radiation source. Such a phenomenon involving fission product zirconium was reported from Marcoule; it was solved by the addition of fluoride ion, which dissolved the zirconium. Such behavior appears to depend on the characteristics of the feed solutions and specific flowsheets. Mobile solids in the aqueous phase can move through some banks without accumulations. Also, no large solids problem has been found at Savannah River, where all feed is centrifuged for clarification after treatment to coagulate silicic acid, which originates from aluminum associated with the fuels.

Pulse Colummns Performance

Efforts to increase the efficiency of pulse columns have continued since their inception in Purex service. Many variables have been explored: amplitude, frequency, and shape of the pulses; size, number, and shape of sieve-plate holes; configuration and spacing of plates; wetting characteristics of surfaces, etc. For the nuclear applications specifically, a high efficiency is necessary to avoid undue height that must be enclosed in heavily shielded facilities. To decrease overall height, columns that might be center-fed in a small-scale installation have been divided into two end-fed units. The height of an equivalent theoretical stage increases somewhat with column diameter. However, actual individual columns that have been built are in the same height range for plants of considerably different capacity. Eurochemic, the Barnwell plant (at five-tons-per-day design basis), and the Hanford plant all had assorted columns in the 10- to 15-meter range, with diameters for the largest in each plant ranging from 150 mm to 812mm.

Pulse columns have many favorable features for nuclear fuel processing. First-stage extraction columns tolerate substantial solids in the feed when operated organic-continuous with a bottom organic-aqueous interface. The solids follow the aqueous down and out of the column, and the organic overflow is quite clean. Such operation has become essentially standard. Also, columns with reasonable throughputs have been designed and operated with diameters favorable for nuclear criticality safety, where concentrated fissile materials have been present. Additionally, relatively short residence times limit the amount of solvent degradation when highly radioactive solutions are being processed. Overall, pulse columns have provided good service in many Purex installations.

Rapid Contactors

Rapid contactors that utilize centrifugal force to aid in separating the phases allow rapid startup and shutdown. In Purex operations, the two primary types of contactors whose uses have been reported are the SGN-Robatel multi-stage unit, and the Savannah River single-stage unit which is arranged in banks. The Robatel unit can provide high efficiency, but demands highly clarified feed since solids can clog the small passages. Test work in Purex applications at Marcoule and other CEA facilities was reported at ISEC '71. Good efficiency and uranium capacities of 5 and 8 tons per day were reported for different units. A Robatel unit was installed as the first contactor in the Allied General Nuclear Services Barnwell Plant, but no performance data in this demanding service have been obtained because the plant did not start up.

An 18-stage bank of the Savannah River centrifugal contactors was installed in 1966 as a replacement for the large mixer-settler bank that had demonstrated large solvent degradation effects. As reported in 1971, the unit provided low solvent degradation and allowed rapid startup and shutdown. The small holdup volume and rapid response have made the standard discontinuous operation, with weekly startup and shutdown, relatively simple. The contactor has given good mechanical service. The primary reason for replacing a motor unit has been excessive leakage of the weir-control air at the rotating seal, although many seals have lasted ten years or more (one operated for 18 years). Still, new bearings and seals that should extend life have been designed and are being installed. Vibration analysis is also recommended. A fatigue failure at a weld occurred at the same position on each of the six-stage sub-units after 7, 10, and 13 years respectively. Reinforcement appears to have solved the problem.

Kinetic effects still appear to limit zirconium decontamination in the nine rapid scrub stages in the bank, as noted in the report at ISEC '71. Only recently has further experimental work started to explore the effect of slow scrubbing stages following the rapid centrifugal stages.

A variation of the single-stage centrifugal contactor has been introduced by Argonne National Laboratory personnel and developed further at Savannah River. Mixing takes place in the annular space between the bowl and housing, and the seal for the air for interface control has been simplified. Banks with bowls in a range of sizes have been built, but none have been used in production operations yet.

FISSION PRODUCT DECONTAMINATION

The fission product elements that determine the final decontamination that can be attained in the Purex process are ruthenium, zirconium, and niobium. As a result, many studies have been undertaken to understand the fundamental chemistry and extraction behavior of these elements. Ruthenium has been found to form a large number of nitroso and nitro species in aqueous nitrate solutions. These species have different distribution coefficients and relatively slow equilibration times between species. Further, slowly equilibrating complexes with TBP are formed in the organic phase. The additional effects of degraded solvent on ruthenium decontamination are generally small, but they have been important in a few cases. The zirconium problems have been due primarily to interactions with solvent degradation products. The simplest of these is the well-known complex with dibutyl phosphate. However, the limits on performance with highly active feed result from interactions with the other components of degraded solvent. Studies on the fission products continue, as attested to by papers at this conference. But note again, that lack of knowledge has not prevented 35 years of successful operation.

Differences in fission product performance have been reported with different flowsheets and equipment. At Savannah River, the original, small 16-stage mixer-settler banks provided about the same first-cycle decontamination as the Oak Ridge Pilot Plant pulse columns. The small 1A 16-stage bank in one plant was replaced with a 24-stage, jumbo bank as part of a general plant revision in 1959. As reported at the 1962 Gatlinburg Symposium, the many long-residence stages initially gave excellent decontamination factors for zirconium and ruthenium (up to 2×10^4 for zirconium and near 10^5 for ruthenium). However, the 7- to 15-minute-per-stage residence times caused serious solvent degradation problems that resulted in low decontamination and high solvent activity. Improved solvent washing, dodecane diluent, and limitations on feed activity finally provided a stable, but low, decontamination. In 1966, an 18-stage bank of centrifugal contactors replaced the jumbo 1A bank. This solved the solvent degradation problem and improved decontamination somewhat, but the fewer, short-residence scrub stages limit decontamination.

Zirconium presented a different problem at Marcoule, as reported at ISEC '71. Zirconium-accumulating solids gathered in the mixer-settlers, accelerating solvent degradation and decreasing the decontamination. A small concentration of fluoride was added to the feed to complex the zirconium. The fluoride eliminated the solids and increased the decontamination factor to greater than 10^4 for zirconium, and to greater than 3000 for ruthenium.

Essentially, all sites have operated at a high degree of saturation of the organic phase by uranium during the initial extraction. This condition leaves less TBP available to complex the fission products and increases the decontamination from fission products markedly. The Windscale Purex Plant represented another departure with a low-saturation flowsheet that accepted a lower fission product decontamination to keep solids and recoverable plutonium out of the waste. At lower saturation, both Pu(IV) and the somewhat less extractable Pu(VI) that may be formed during fuel dissolution are recovered efficiently, resulting in low losses without the addition of valence adjustment chemicals.

Still other systems have provided variations in the initial extraction acidity, scrub acidity, and temperature to improve fission product decontamination. The distribution coefficient of zirconium increases as acid increases, while that of ruthenium decreases as acid increases; hence, compound scrub sections with high and low acid sections are used in some cases to improve decontamination. Also, ruthenium equilibrates more rapidly at high temperatures, allowing it to be scrubbed more efficiently.

SOLVENT EFFECTS

The nature of the diluent used with the TBP and the treatment of the spent solvent from the process steps are very important to the performance, when decontamination factors on the order of 10^7 are needed. Originally, the chief worry was the decomposition of TBP to dibutyl phosphoric acid and monobutyl phosphoric acid by radiolysis and acid hydrolysis. Washes with sodium hydroxide or sodium carbonate solutions to remove these acidic species were part of the original flowsheets. It was found early that dibutyl phosphate complexes zirconium, carrying it through the process, and decreasing the decontamination. The dibutyl phosphate also complexes plutonium strongly and can cause high plutonium losses to the solvent washers.

Soon after production-scale operations began, it became apparent that degradation of the diluent was having a large influence on performance. Other compounds in the solvent besides the butyl phosphates were transporting zirconium, niobium, and ruthenium through the process, reducing decontamination, and causing high levels of activity in the circulating solvent. Several areas of study followed: the relation between the structure of the hydrocarbon diluent and its stability; identification of the degradation products as an aid to their removal; solvent regeneration techniques and alternative washing agents.

Empirical tests in the late 1950's demonstrated that excessive branched chains and aromatic compounds in the hydrocarbons used as diluent could be the precursors of the unidentified degradation products. Straight-chain paraffins in the twelve-carbon range had a desirable combination of density, viscosity, flash point, and radiation resistance. Dodecane became almost a standard to measure other diluents against. Solvent degradation problems led Savannah River to adopt n-dodecane as a diluent in 1961. The first inventories of n-dodecane were quite expensive. Thanks to the demand for biodegradable detergents, supplies of mixed n-paraffins that were predominately dodecane became available at reasonable prices, and their use spread. Note that other hydrocarbon diluents offer advantages where radiation degradation is not a problem. Some metal-TBP complexes, such as plutonium and thorium, have a limited solubility in the hydrocarbon diluent, and at high concentrations will separate out as a heavy organic phase. The complexes are considerably more soluble in aromatic diluents; hence, aromatics may be the diluent of choice in some concentrated flowsheets. Overall, diluent can have substantial influence on the performance of a given system, and process requirements should be considered carefully in its selection.

Solvent Degradation Products

The identification of the degradation products responsible for the decrease in decontamination has been the subject of investigation and speculation for 25 years. Even as early as the 1962 Gatlinburg Solvent Extraction Chemistry Symposium, one paper had 58 references on solvent degradation. Some of the most definitive work has been done at Karlsruhe, Germany with identification of several classes of compounds formed from the primary activation of the diluent and TBP. These include carbonyl, nitro, and nitroso compounds from diluent alone, long-chain acid phosphates from diluent and TBP combinations, and polymeric butyl phosphates from TBP interactions. Some of these compounds have the zirconium retention properties observed in plant operations. The conductivity techniques developed at Karlsruhe for determining the amounts of these compounds can be very useful in determining whether poor performance is due to their presence or to some other operating variable.

Sodium carbonate still appears to be the primary solvent cleanup solution in use at nearly all sites reporting. Various other cleaning systems have been tried, such as permanganate added to the alkaline washers and absorption columns of many materials, including ion exchange resins, calcium oxide, lead oxide, and alumina. Given the assortment of compounds that have been found in the solvent, some of them could be removed by almost any of the reagents. Recent Karlsruhe work has utilized hydrazine carbonate as a washing agent that does not contribute to waste solids; a trial of hydrazine carbonate also has been reported at La Hague. The prime advantage of this reagent is the small amount of waste solids generated as compared with sodium carbonate and sodium hydroxide. The solids are important when the cost of final waste disposal is considered.

PARTITIONING OF URANIUM AND PLUTONIUM

The agents used to reduce Pu(IV) to Pu(III) and partition it from uranium varies between sites. Ferrous sulfamate was the agent in the original Purex flowsheet and is still used extensively. The efforts to reduce waste solids early led to the consideration of U(IV) as a substitute that would be more efficient because it acts on plutonium in both the aqueous and organic phases.

Two methods have been utilized for the reductions with U(IV): the introduction of an externally generated U(IV) solution at multiple positions along the 1B contactor, and the electrolytic generation of U(IV) in situ. Typical utilization of U(IV) solution was reported from Marcoule and Eurochemic at ISEC '71. An early installation for electrolytic reduction was at the WAK mixer-settlers at Karlsruhe for the stripping of plutonium in the second plutonium cycle. Successful test work with both mixer-settler and pulse column units for the first-cycle uranium-plutonium partition also has been reported there. A large pulse column unit was built for the five-ton-per-day Barnwell Plant, but its performance was never determined.

A typical problem with the partitioning of plutonium with either ferrous sulfamate or U(IV) is the large consumption beyond the stoichiometric requirement, leading to significant excess waste with ferrous sulfamate. Considerable study has taken place on the mechanisms of consumption and on methods to reduce the amount of reductant required. Low acid in the bank is favorable, and both hydroxylamine nitrate and hydrazine nitrate can substitute for some ferrous sulfamate.

The overall selection of the method of partitioning rests upon the importance of waste, equipment flexibility in a given installation, the tolerable uranium contamination in the plutonium product, and the uranium separation capability of any subsequent plutonium cycles.

CONCLUSION

Many different arrangements of the basic Purex process have been designed, involving different equipment and chemicals, with specific details resting on the goals and restrictions set for a given installation. Flowsheets can be designed for almost any required level of product purity, for concentrated or dilute products and for low solids in the waste. Systems are also versatile, capable of processing many different feeds and products. Other processes for reactor fuel processing have been explored, but the Purex process has had no major competitors in the past 35 years, and none are apparent in the foreseeable future.

01DA0001:ksr

Application of the TRUEX Process to the Decontamination of Nuclear Waste Streams*

E. Philip Horwitz

Chemistry Division, Argonne National Laboratory
9700 South Cass Avenue
Argonne, IL, 60439, USA

Wallace W. Schulz

Rockwell Hanford Operations
Post Office Box 800
Richland, Washington, 99352, USA

The TRUEX (transuranium extraction) is a generic actinide extraction/recovery process (1-3). The process is designed to reduce the TRU (transuranic element) concentration in nitric and hydrochloric waste solutions to <100 nCi/g of disposed form. (In the USA, non-TRU waste is defined as <100 nCi/g of disposed form.) In many cases, waste solution in which the TRU concentration has been reduced to <100 nCi can be safely and cheaply converted to grout for surface storage. Only the recovered TRU fraction, at a volume reduction of two to three orders of magnitude, need be buried in a deep geologic repository.

The key ingredient in the TRUEX process is a new, actinide-lanthanide selective, bifunctional extractant called octyl(phenyl)-N,N-diisobutylcarbamoylmethylphosphine oxide, abbreviated OϕD(iB)CMPO or simply CMPO. The structure of OϕD(iB)CMPO is shown in Figure 1. This extractant contains a unique combination of donor and substituent groups which enable it to extract trivalent actinides [which are much less extractable than tetra- and hexavalent actinides] over a wide range of nitric acid concentrations and over moderate to high hydrochloric acid concentrations. In nitrate media OϕD(iB)CMPO has good selectivity over non-lanthanide fission products, especially in the presence of a small concentration (0.1 M) of oxalic acid. OϕD(iB)CMPO also has good stability towards hydrolytic and radiolytic degradation. In addition, the behavior of OϕD(iB)CMPO towards hydrolysis and radiolysis is favorably augmented by the fact that the primary degradation product of the CMPO, methyl(octyl)(phenyl)phosphine oxide (MOϕPO), is capable of replacing

---

*Work performed under the auspices of the Office of Basic Energy Sciences, Division of Chemical Sciences, U. S. Department of Energy, under contract number W-31-109-ENG-38.

a portion of the OϕD(iB)CMPO molecules coordinated to the americium nitrato complex (4). The net effect of this replacement is that the distribution ratio of americium, D_{Am}, does not decrease as rapidly as expected based on the loss of CMPO.

Figure 2 shows the acid dependencies for the extraction of Am(III) from nitric and hydrochloric acids using 0.5 M OϕD(iB)CMPO in tetrachloroethylene (TCE). The data show that efficient extraction of Am can be obtained above 0.25 M HNO_3 or 5 M HCl. The extraction equilibria for Am(III) from nitric and hydrochloric acids may be represented by the following equations:

$$Am^{3+} + 3NO_3^- + \overline{3E\cdot(HNO_3)_n} \qquad \overline{Am(NO_3)_3\cdot E_3\cdot(HNO_3)_m} + (3n-m)\ HNO_3 \tag{1}$$

$$Am^{3+} + 3Cl^- + \overline{3E\cdot(HCl)_n} \qquad \overline{AmCl_3\cdot E_3\cdot(HCl)_m} + (3n-m)HCl \tag{2}$$

where E = OϕD(iB)CMPO and the bar denotes the species in the organic phase. The values of n and m range from 0 to 2 and 0 to 3, respectively for Eq. 1 and from 0 to 1 for Eq. 2. In the case of the extraction of Am from nitric acid, CMPO is able to function effectively at high acidity because the carbonyl group is able to bond to nitric acid which suppresses the attack on the Am-phosphoryl oxygen bond (1). In the corresponding chloride system, this process occurs to a much lesser extent because HCl is much less extractable than HNO_3 (5). The extremely rapid rise in D_{Am} with increasing concentration of HCl is due to the rapid increase in the mean activity coefficient of chloride ion and the third power chloride ion dependency (see eq. 2).

Three different TRUEX process solvents are employed, depending on the type of waste to be processed. The compositions and uses of the process solvents are shown in Fig. 3. Tributylphosphate (TBP) is always used in conjunction with CMPO in TRUEX solvents used for processing nitric acid waste solutions. Its role is essentially that of a phase modifier but it has a number of beneficial effects on the behavior of OϕD(iB)CMPO. TBP enhances D_{Am} and reduces its sensitivity to acid above 1 M HNO_3 (extraction conditions), lowers D_{Am} below 1 M HNO_3 (stripping conditions), reduces third phase formation (especially when a normal paraffinic hydrocarbon diluent is used), reduces the loss of CMPO to the aqueous phase, reduces radiolytic degradation of CMPO, and reduces the effect of acidic degradation products on D_{Am} at low acidity. TRUEX process solvent used for processing chloride salt waste does not normally require TBP unless the organic phase is loaded to near saturation with plutonium and/or americium. The influence of TBP on the nitric acid dependency for the extraction of Am(III) by 0.25 M OϕD(iB)CMPO in TCE is shown in Fig. 4. The nitric acid dependency for the extraction of Am by

0.20 M OϕD(iB)CMPO - 1.4 M TBP in Conoco (C_{12}-C_{14}) is shown in Fig. 5. [Conoco (C_{12}-C_{14}) is a NPH with an average carbon chain of thirteen.]

Figures 6 and 7 show the ranges of distribution ratios of inert constituents (e.g. Fe, Al), fission products, and actinides found in nitric acid and chloride salt wastes (6 M in HCl). Figures 8 and 9 show the generic TRUEX process flowsheets for both nitric acid waste and chloride salt waste. The composition of the TRUEX process solvent used for each flowsheet are given in Fig. 3.

Acidic nitrate waste solutions containing fission products, i.e. HLLW, require the addition of oxalic acid to the feed, unless high concentrations (3 to 4 M) of fluoride are present. The oxalic and hydrofluoric acids suppress the extraction of Zr, and to a lesser extent Mo, by the formation of inextractable oxalato and fluoro complexes. The concentration of oxalic acid required is dependent on the concentration of Al in the waste solution. High concentrations of Al require high concentrations of oxalic acid. Generally oxalic acid concentrations in the range of 0.15 to 0.25 M are sufficient to suppress D_{Zr} when Al is in the range of 0.4 to 0.7 M.

Extensive scrubbing of the loaded organic phase is usually unnecessary since a few percent of non-rare earth fission products or inert constituents, e.g. Fe, in the Am, Cm-R.E. product does not significantly increase its weight. However, a dilute nitric-oxalic acid scrub, e.g. 0.25 M HNO_3-0.001 M $H_2C_2O_4$ can be used to remove the remaining quantities of Zr, Mo, and Fe. If the nitric-oxalic acid scrub is used, a basic aluminum nitrate (BAN) scrub is also used to remove all traces of oxalic acid (and excess HNO_3) from the organic phase prior to the stripping of Am and Cm from Pu and Np. This is necessary to prevent rare earth oxalates from precipitating and/or Pu from back extracting during the first stripping operation. The organic to aqueous phase ratio (O/A) used in scrubbing is generally 3 for nitric acid or nitric-oxalic acid and 10 for BAN. The spent BAN scrub is routed directly into the feed rather than into the first scrub.

An important feature of the flowsheet is the selective partitioning of Am and Cm from tetravalent Pu and Np. This partitioning is feasible because OϕD(iB)CMPO has an actinide(IV)/actinide(III) separation factor of ~10^3, even from 0.04 M HNO_3. After stripping Am and Cm from the loaded solvent, Pu(IV) and Np(IV) are effectively stripped using a dilute nitric-hydrofluoric acid mixture. If Pu is present in macro-concentration, i.e. $>10^{-3}$ M, it can be selectively reduced with a solution of hydroxylammonium nitrate in dilute nitric acid. This results in a separation of Pu from Np. The O/A used in stripping is generally 1 for Am-Cm and 2 for Pu-Np. Uranium(VI) is removed from the organic phase during the solvent cleanup step.

The flowsheet for processing the chloride salt waste is similar, in principle, to the flowsheet for processing nitric acid waste (6). However, OϕD(iB)CMPO is less selective for TRU's in chloride media than in nitrate. If certain transition and post-transition metals are present in the salt waste, e.g. Fe, Zn, the TRUEX process is preceded by a head-end extraction process using trioctylphosphine oxide (6). The head-end extraction removes all transition and post-transition metals which CMPO would have extracted, as well as tetra- and hexavalent actinides. The aqueous raffinate from the head-end extraction is then the feed for the TRUEX process. Trivalent Pu, which is its primary oxidation state in chloride salt waste, together with Am(III) are now the only constituents extracted from the feed. If Am is to be separated from Pu, the Pu is oxidized in the feed to its tetravalent state using sodium chlorite.

The selectivity for tetravalent over trivalent actinides is greater in chloride media than in nitrate media. For example, D_{Pu}/D_{Am} is $>10^5$ from 2 $\underline{M}$ HCl (6). Therefore, the selective stripping of Am and Cm from Pu and Np is readily achieved using an O/A in the range of 2 to 4. Stripping of Pu from 0.5 $\underline{M}$ CMPO is effectively achieved by reducing Pu(IV) to Pu(III) with ascorbic acid (AA). An O/A of 2 or greater is feasible depending on the concentration of Pu in the organic phase. The reduction is very rapid (<15 sec) and thus can be performed in high speed centrifugal contactors.

In both flowsheets, effective stripping of all TRU elements from TRUEX solvent before its recycle is essential to avoid TRU contamination of solvent wash streams and to achieve a large reduction of the TRU concentration in the feed. Effective stripping of TRUEX process solvent is dependent on maintaining low concentrations of acidic compounds produced from hydrolysis and radiolysis of TBP and CMPO. Solvent cleanup generally involves a sodium carbonate wash (analogous to PUREX process solvent cleanup) and periodic passage through a macroporous anion exchange resin (Amberlyst® A-26) on the hydroxyl cycle.

To date the TRUEX process has been tested on a variety of synthetic and a few real TRU liquid wastes. The following synthetic high-level wastes have been studied: 1) current acid waste (1 to 2 $\underline{M}$ in HNO_3); 2) high acid waste (5 $\underline{M}$ in HNO_3); 3) dissolved sludge waste (1 $\underline{M}$ in HNO_3 and 0.3 $\underline{M}$ in oxalic acid); and 4) complexant concentrate waste. Numbers 1, 2, and 4 are representative of waste streams generated at Rockwell Hanford Operations. Number 3 is a simulated waste which would be generated by dissolving the sludge formed by NaOH neutralization of HLLW generated in PUREX processing. Number 4 is a waste stream generated during the recovery of ^{90}Sr from dissolved sludge. Number 4 contains high concentrations of chelating agents such as EDTA, NTA, and citric acid as well as fission products. The following non-fission product TRU salt wastes have been studied: 5)

PUREX raffinate generated from Pu scrap processing; and 6) mixed chloride salt waste generated from Pu electrorefining, molten salt extraction, and direct oxide reduction operations. Numbers 5 and 6 have been studied using both synthetic and real waste. The major TRU constituent by activity in all wastes (1 through 6) was ^{241}Am. Testing involved both batch and continuous countercurrent modes. In all tests, the TRU concentration was reduced to <10 nCi/g of solid raffinate. This reduction in TRU content usually involved decontamination factors of 10^4 to 10^5.

References

1. E. P. Horwitz, D. G. Kalina, H. Diamond, G. Vandegrift, and W. W. Schulz, Solvent Extr. Ion Exch. 3, 75 (1985).
2. E. P. Horwitz, D. G. Kalina, H. Diamond, L. Kaplan, G. F. Vandegrift, R. A. Leonard, M. J. Steindler, W. W. Schulz, TRU Decontamination of High-Level PUREX Waste by Solvent Extraction Utilizing a Mixed Octyl(phenyl)-N,N-diisobutylcarbamoylmethylphosphine Oxide/TBP/NPH (TRUEX) Solvent, in Lanthanide/Actinide Separations, (Eds.) G. R. Choppin, J. D. Navratil, and W. W. Schulz, World Scientific Publications, Singapore, 1985, p. 43.
3. E. P. Horwitz and W. W. Schulz, Solvent Extraction and Recovery of the Transuranic Elements from Waste Solutions using the TRUEX Process, in Solvent Extr. Ion Exch. in the Nuclear Fuel Cycle, (Eds.) D. H. Logsdail and A. L. Mills, Ellis Horwood Limited, Chichester, England, Sept. 1985, p. 137.
4. R. Chiarizia and E. P. Horwitz, Solvent Extr. Ion Exch. 4 (In press).
5. E. P. Horwitz, H. Diamond, K. A. Martin, and R. Chiarizia, Solvent Extr. Ion Exch. 4 (In press).
6. E. P. Horwitz, H. Diamond, K. A. Martin, and C. Herrick, Solvent Extr. Ion Exch. 4 (In press).

Octyl(phenyl)-N,N-diisobutylcarbamoylmethylphosphine Oxide

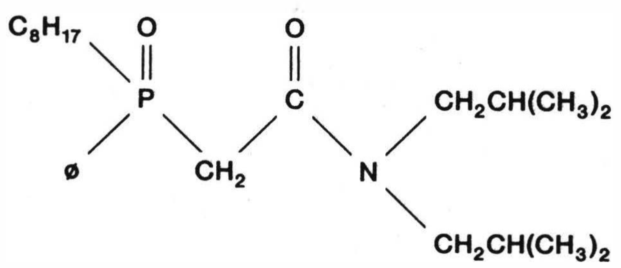

OøD(IB)CMPO

Fig. 1.

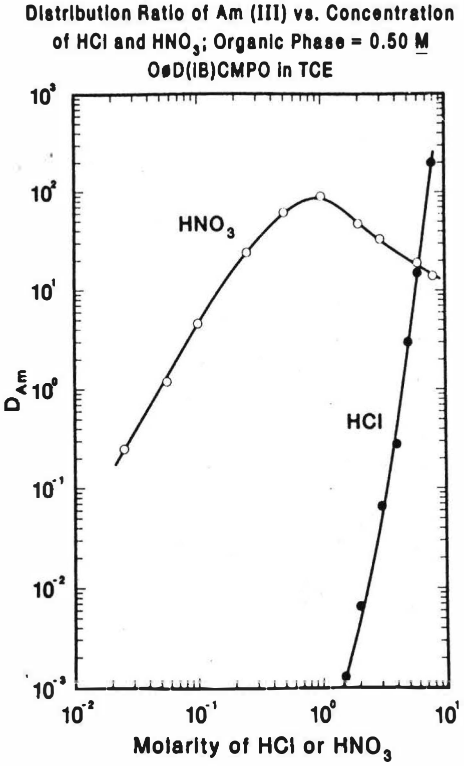

Distribution Ratio of Am (III) vs. Concentration of HCl and HNO_3; Organic Phase = 0.50 M OϕD(IB)CMPO in TCE

Fig. 2.

TRUEX Process Solvents

CMPO, M	TBP, M	Diluent	Use
0.20	1.2 to 1.4	NPH(C_{12} to C_{13})	HLW
0.25	0.75 to 1.0	CCl_4, TCE	Pu Scrap Waste
0.50	-	TCE	Chloride Salt Waste

Fig. 3.

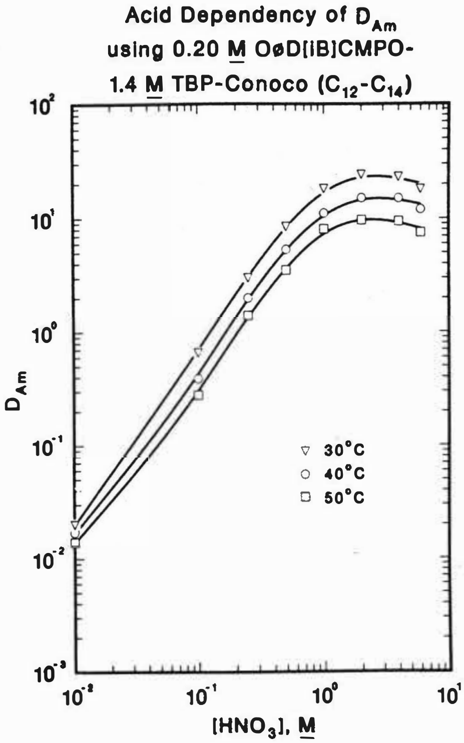

Acid Dependency of D_{Am} using 0.20 M OøD[iB]CMPO-1.4 M TBP-Conoco (C_{12}-C_{14})

Fig. 5.

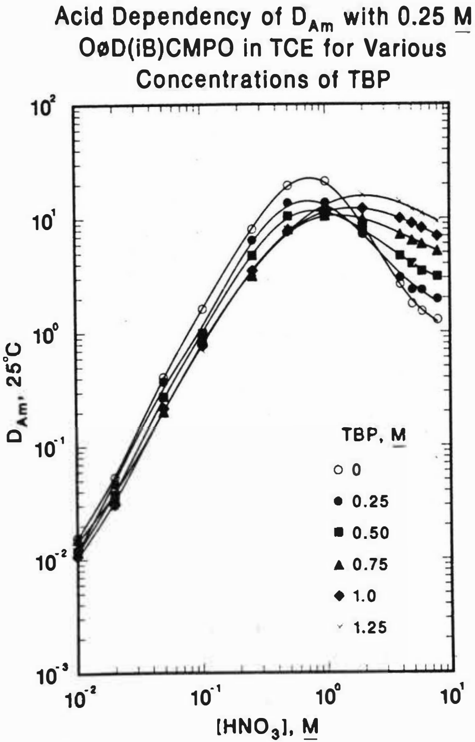

Acid Dependency of D_{Am} with 0.25 M OøD(iB)CMPO in TCE for Various Concentrations of TBP

Fig. 4.

Extractabilities of Elements from Nitric Acid (1 to 3 M) Waste using TRUEX Process Solvent

Distribution Ratio Range

<0.05		0.01 to 1	1 to 20	>20
Be	Rb	*Zr	Y	Th
Na	Sr	*Mo(VI)	Tc	U(VI)
Mg	Rh	Ru	La	Np(IV)
Al	Ag	*Pd	Ce	Pu(IV)
K	Cd		Pr	
Ca	In		Nd	
Cr(III)	Sb		Pm	
Mn(II)	Te		Sm	
Fe(III)	Cs		Eu	
Co(II)	Ba			
Ni			Am	
Cu			Cm	
Zn				

*D's lowered by oxalate ion

Fig. 6

Extractabilities of Elements from Hydrochloric Acid (6 M) using TRUEX Process Solvent

Distribution Range

$<10^{-2}$	10^{-2} to 10^{0}	10^{0} to 10^{2}	$>10^{2}$
Be	Mn(II)	V	Fe
Na	Co(II)	Zn	Ga
Mg	Ni	Cd	Zr
Al	Pb(II)	Sn	Mo
K			
Ca		Am	Th
Cr(III)		Cm	U(VI)
			Np(IV)
			Pu(IV)

Fig. 7.

Generic TRUEX Process Flowsheet for Nitric Acid Waste

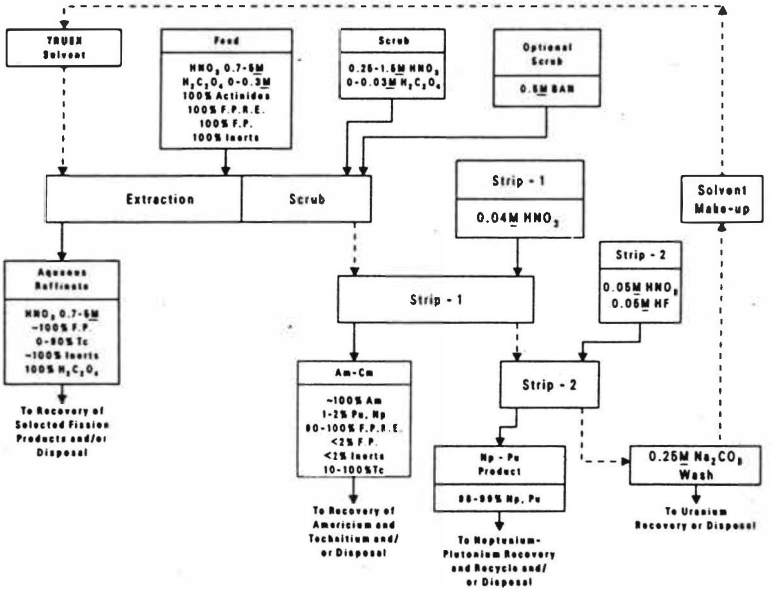
TRUEX Solvent
Feed
HNO_3 0.7-5M
$H_2C_2O_4$ 0-0.3M
100% Actinides
100% F.P.R.E.
100% F.P.
100% Inerts
Scrub
0.25-1.5M HNO_3
0-0.03M $H_2C_2O_4$
Optional Scrub
0.5M HAN
Extraction
Scrub
Strip - 1
0.04M HNO_3
Solvent Make-up
Aqueous Raffinate
HNO_3 0.7-5M
~100% F.P.
0-90% Tc
~100% Inerts
100% $H_2C_2O_4$
To Recovery of Selected Fission Products and/or Disposal
Strip - 1
Strip - 2
0.05M HNO_3
0.05M HF
Am-Cm
~100% Am
1-2% Pu, Np
90-100% F.P.R.E.
<2% F.P.
<2% Inerts
10-100%Tc
To Recovery of Americium and Technitium and/or Disposal
Strip - 2
Np - Pu Product
98-99% Np, Pu
To Neptunium-Plutonium Recovery and Recycle and/or Disposal
0.25M Na_2CO_3 Wash
To Uranium Recovery or Disposal

Fig. 8.

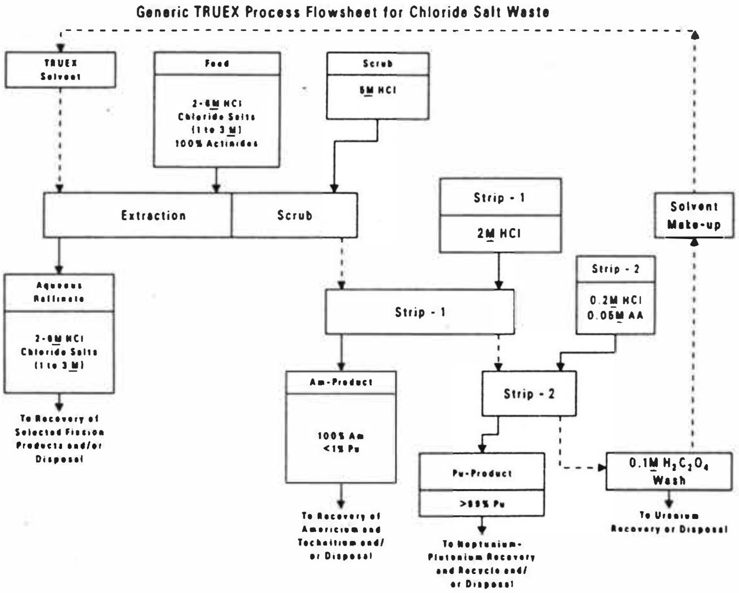
Generic TRUEX Process Flowsheet for Chloride Salt Waste
TRUEX Solvent
Feed
2-6M HCl
Chloride Salts
(1 to 3 M)
100% Actinides
Scrub
5M HCl
Extraction
Scrub
Strip - 1
2M HCl
Solvent Make-up
Aqueous Raffinate
2-6M HCl
Chloride Salts
(1 to 3 M)
To Recovery of Selected Fission Products and/or Disposal
Strip - 1
Strip - 2
0.2M HCl
0.05M AA
Am-Product
100% Am
<1% Pu
To Recovery of Americium and Technetium and/or Disposal
Strip - 2
Pu-Product
>99% Pu
To Neptunium-Plutonium Recovery and Recycle and/or Disposal
0.1M $H_2C_2O_4$ Wash
To Uranium Recovery or Disposal

Fig. 9.

Some chemical aspects of solvent extraction performance in the Tokai reprocessing plant

M. Ozawa, K. Koyama and T. Yamanouchi

Power Reactor and Nuclear Fuel Development Corporation
Tokai-Mura, JAPAN

Introduction

PNC's Tokai reprocessing plant reprocessed 253t of LWR spent fuels in the period of 1977 to December 1985, with the result that some of the produced 1.6t of plutonium has been recycled back to PNC's Advanced Thermal Reactor (ATR) as the mixed oxide fuel. During these 9 years of the Tokai plant operation, there has been no trouble affecting the plant availability in the extraction system, but serious difficulties, occurred due to the corrosion in dissolvers and an acid recovery evaporator, have forced lengthening operational interruptions. The general experience including the characteristics and amounts of reprocessed fuel in the Tokai reprocessing plant has been reported elsewhere$^{(1)}$.

Third phase formation is widely known to be present in the process utilizing the liquid-liquid extraction process. This has been one of the major problems in the Purex reprocessing plant$^{(2)\sim(5)}$. In the Tokai reprocessing plant as well, formation of various kinds of third phase has been observed: one was an interfacial crud formed in the first extraction cycle, and the other was a heavy plutonium-rich third phase formed once during the early operation stages of the rework process. Even in such cases of third phase formation, however, an improved alkali-scrubbing method and a plutonium stripping technique using uranous nitrate solution has been utilized successfully to eliminate both of these problems. The outline of the methods and results are described as follows.

Description of process

A brief explanation of dissolution, clarification and extraction process of the Tokai reprocessing plant was given in Ref.(1); the extraction process consists of three extraction cycles with providing mixer-settlers as extractor for every cycle, and performing U/Pu partition in the second extraction cycle. In the first extraction cycle, 9 stages are provided for extraction, 8 stages for scrubbing and 12 stages for stripping, respectively. Adjusted dissolver solution enters the 9th stage, where it comes into contact with the solvent fed in the first stage by means of counter-current method. 6 electrodes of different lengths are installed in order to detect the interfacial level of organic phase in each settler, with measuring directly the difference of electric conductivity of aqueous and organic phase, as shown in Table 1. The densimeters installed for measuring aqueous and organic phase are also available for the same purpose. Furthermore in the feed stage settler, a γ-monitor, which can move up and down in a vertical line, is provided for detecting crud formation.

The rework process, composed of several vessels, has different roles for temporary storage of aqueous and organic solution, waste solvent, and waste diluent. Some vessels of this process therefore have a function of phase separation. This process is also capable of receiving and storing the concentrated plutonium nitrate solution, provisionally. Thus the related vessels are made in the shape of thin slab-type to avoid reaching in critical state at any given plutonium concentrations.

Interfacial crud in the first extraction cycle

When the highly burned spent fuels were reprocessed, abnormal indications of the lamps in electric interfacial detector and in densimeter have become more predominant at the feed stage settler. Table 1 shows the measured electric resistances of electric interfacial detector in the case of both normal and abnormal state in the feed stage settler. Lamps indicate the abnormal condition when the electric resistance of middle and upper zones decreases. This phenomenon could be interpreted in terms of a hypothesis that the crud possessing higher electrical conductivity formed and tended to build up from the interphase upward, contributing to the formation of bridges among the electrodes and the wall of settler. The adherent and electroconductive natures of the crud were tested in the bench-scale test(6) performed in OTL (Operation Testing Laboratory). Once, the crud being formed in the settler, it seemed to spread out gradually to the whole stage of the extraction section by being continuous detached and carried toward the raffinate outlet with aqueous stream. Such a crud formation was quickly increased when clarification occurred not to be in service.

It is reported by other authors, that the complex of degraded phosphates and fission products, e.g. zirconium, was the main component of the interfacial crud, and in the meantime the suspended insoluble residues acted as an accelerator for developping the crud and they also became a stabilizer once they were absorbed in the crud. In the Tokai reprocessing plant, on the other hand, estimated exposure rates of solvent in the first extraction cycle were usually too low(1) (up to ca. 0.1wh/l per pass through) to induce such a type of crud formation. In addition, small paradium particles of <0.1μ mainly could lead to crud formation even in pure TBP 30% in n-dodecane system(6). Although the nature of the crud has not been identified, these results pointed to the conclusion that the insoluble residues suspended in the dissolver solution were considered to be the major cause of interfacial crud formation in the case of the Tokai reprocessing plant.

In the actual operation, the crud never caused difficulties regarding to transferring of elements between the various phases and emptying them from the mixer-settlers during the operation, but it was difficult to be removed completely by means of the regular rinsing procedure carried out after reprocessing. The rinsing procedure is as follows: (Step 1) Flush out fission products and plutonium with UNH solution (FPs-PuFO); (Step 2) Flush out uranium with nitric acid (UFO); (Step 3) Flush out solvent with filling nitric acid (SFO). As the measured dose variation in some campaign shown in Fig. 1, maximum activity appeared near the interphase level (point 2) in the course of FPs-Pu FO and then only shifted to upper zone (point 3) without diminishing, even after emptying the solvent. In other words, it was obvious that drastic removal of the activity due to the interfacial crud could not be achieved by these rinsing steps. Therefore alkali-scrubbing using 1$\underline{\mathrm{M}}$ caustic soda solution (Step 4) was carried out in addition to the regular rinsing procedure. With this procedure, the activity in the settler has decreased effectively to reach about 20 R/h after Step 4, which was one hundredth of initial activity. The typical compositions of fission products in a dissolver solution and a crud are given in Table 2. The activity of crud, dark brown of a color, exceeded 750R/h/10 mℓ, even it was sampled during the regular rinsing operation. The crud showed relatively high specific activity of ^{106}Ru compare with the rest of the fission products in the dissolver solution. The major activity removed from the extractors was also ^{106}Ru in a series of rinsing steps including alkali-scrubbing, and alkali-scrubbing step mainly contributed to the removal of ^{106}Ru, in accordance with the composion of removed fission products contained in a waste alkali-scrubbing solution, as shown in Table 2. In addition, the operational experience showed that the signal from electric interfacial detectors returned to the normal operational condition after completion of alkali-scrubbing, thus leading to the conclusion that alkali-scrubbing was one of the effective method to remove the interfacial crud.

Despite the interfacial crud formation in the first extraction cycle, it has been possible to manage the operation without such attendant problems as lowering the decontamination factors of fission products, increasing the losses of uranium and plutonium, and clogging the mixer-settlers. Furthermore, even faced with the cases of considerable degree of crud formation, or preparing for the long-term interruption in operation, alkali-scrubbing has been successfully adopted to achieve the effective decontamination.

Third phase in the rework process

In the early operation stage, third phase formation was recognized at the bottom of the rework vessel relating to the plutonium purification and concentration process. Visual observations revealed that sampled third phase was brownish-black in color and viscous, tar-like substance with a density higher than the aqueous phase. The infrared spectra as shown in Fig. 2 indicated that the third phase was mainly composed of TBP containing some n-dodecane, and was considered to be contained nitrate esters that corresponded to the absorption at 1640 cm^{-1}. Thus, PNC named the third phase Heavy Organic Phase (HOP) at a moment. Plutonium and also uranium were contained in HOP, however, HOP did not capture any fission products. Although no special verification has been made to investigate the cause of HOP formation, the relatively high plutonium (Pu^{IV}) loadings to the solvent in the rework vessel was probably responsible as described in the preceding studies(4),(7)~(9). Laboratory tests showed that HOP was soluble in both pure TBP and methanol but insoluble in n-dodecane, and that plutonium could be stripped out from HOP by treating with uranous nitrate (U^{IV}) in nitric acid solution containing some hydrazine. Namely, under defined process condition, reductive stripping of plutonium can be applied to HOP treatment. As shown in Fig.3, an addition of 6-fold excess U^{IV} was adequate to strip plutonium completely from HOP in the actual plant scale operation. As a result of the plutonium stripping operation, HOP became light phase, i.e., it did not any longer exist as a heavy third phase. The plutonium (Pu^{III}) stripped out from HOP in the rework equipments was recycled to the plutonium purification cycle, and where successively reoxidized, purified, concentrated in order to be recovered as the plutonium products.

Conclusions

(1) Experience covering a 9-year period in the Tokai reprocessing plant has proved that reprocessing LWR spent fuel with a burn-up of up to ca.35000 MWD/T could be performed successfully with mixer-settler extractor in a three-cycle Purex process.

(2) Formation of two types of third phase was observed during the early operation stages.

(3) The interfacial crud, formed in the first extraction cycle, could be removed effectively with an alkali-scrubbing method using caustic soda solution.

(4) Heavy organic phase (HOP), formed in the rework process, was successfully treated with uranous nitrate solution for stripping plutonium and for eventual elimination HOP itself.

References

(1) T. Yamanouchi, M. Ozawa and M. Yamamoto, "Experience in thermal and fast reactor fuel reprocessing in JAPAN" International meeting on Solvent Extraction

& Ion Exchange in the Nuclear Fuel cycle, Harwell, UK (1985)

(2) P. Faugeras and X. Talmont, "Radiolysis and hydrolysis of TBP and their effects" CEA-CONF 1265 (1968)

(3) C. Breschet and P. Miquel, "Improvement of the procedure used to treat highly irradiated fuels" Proc. Int. Solvent Extraction Conf. (1971)

(4) J. van Geel, G. Joseph, E. Detilleux, W. Heinz, J. Centeno and B. Gustafsson, "Chemical aspects of solvent extraction on plant scale at Eurochemic" Proc. Int. Solvent Extraction Conf. (1971).

(5) K.L. Huppert, W. Issel and W. Knoch, "Performance of extraction equipment in the WAK-pilot plant" Proc. Int. Solvent Extraction Conf. (1974)

(6) K. Gonda, K. Oka and T. Nemoto, "Characteristics and behavior of emulsion at nuclear fuel reprocessing" NUCLEAR TECHNOLOGY VOL.57 (1982)

(7) A.L. Mills and W.R. Logan, "Third phase formation between some actinide nitrates and 20% tri-n-butyl phosphate/odourless kerosene" SOLVENT EXTRACTION CHEMISTRY, NORTH-HOLLAND, AMSTERDAM (1967).

(8) D.E. Horner, "Formation of third phases and the effect of temperature on the distribution of plutonium and uranium in extractions by tri-n-butyl phosphate" ORNL (1971)

(9) Z. Kolarik, "The formation of a thrid phase in the extraction of Pu (IV), U(IV), and Th(IV) nitrates with tributyl phosphate in alkane diluents" Proc. Int. Solvent Extraction Conf. (1977)

Table 1. Typical electric resistances and lightings of interfacial detectors observed at the feed stage of the first extraction cycle

Electrode	Normal interphase state		Existence of interfacial crud	
	Resistance (Ω)	Lighting of lamps	Resistance (Ω)	Lighting of lamps
A	2	ON	2	ON
B	2	ON	3	ON
C	5	ON	7	ON
D	> 1000	OFF	40	ON
E	> 1000	OFF	15	ON
F	> 1000	OFF	> 1000	OFF

Note;

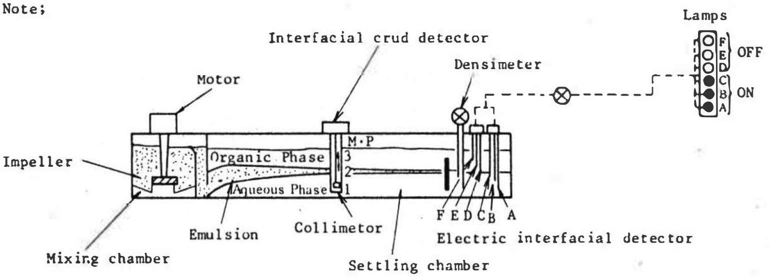
Lamps
F
E
D
C
B
A
OFF
ON
Interfacial crud detector
Densimeter
Motor
M·P
3
2
1
Organic Phase
Aqueous Phase
Impeller
F E D C B A
Electric interfacial detector
Emulsion
Collimetor
Mixing chamber
Settling chamber

Table 2 Typical compositions of fission products contained in a dissolver solution, an interfacial crud and a waste alkali-scrubbing solution.

FPs(ci)/Total FPs(ci), %

Nuclide	Dissolver solution(*1)	Interfacial crud	Waste caustic (1M) solution
^{95}Zr	0	0	0
^{95}Nb	0	0	0
^{106}Ru	6	59	98
^{125}Sb	1	3	1
$^{134+137}$Cs	75	32	1
^{144}Ce	11	1	0
$^{154+157}$Eu	5	5	0
^{241}Am	1	0	0

Note; (*1) Fuel characteristics:

initial ^{235}U	2.3%
burn-up	ca. 20000MWd/T
cooling-time	1840 days
specific power	30 MW/T

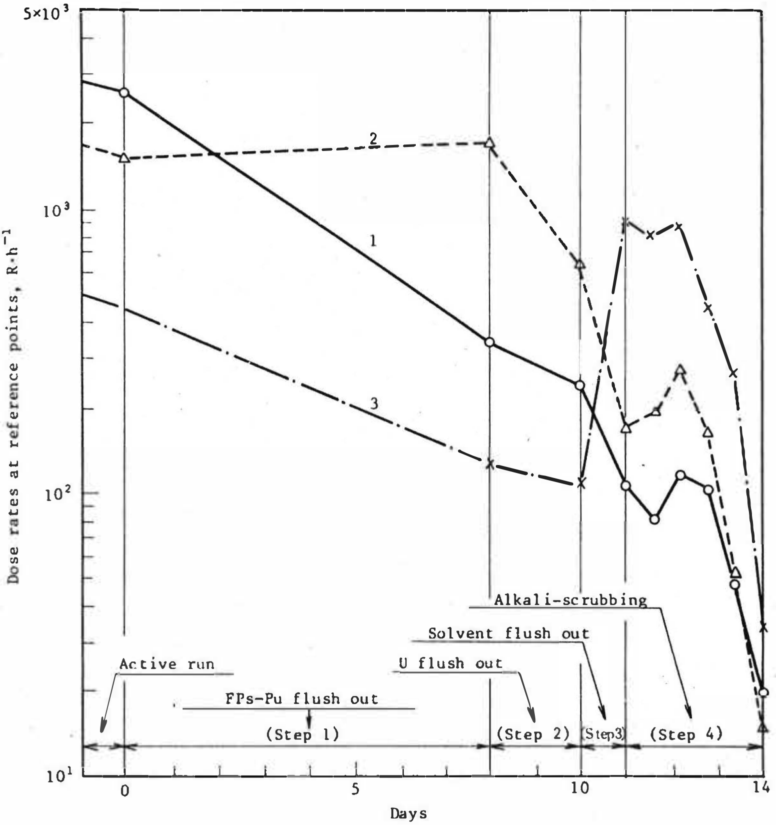

Fig. 1 Radiation measured by interfacial crud detector in the feed stage settler of the first extraction cycle as a function of the rinsing actions.

Measured points; (see Table 1)
1: Bottom-level
2: Middle-level
3: Top-level

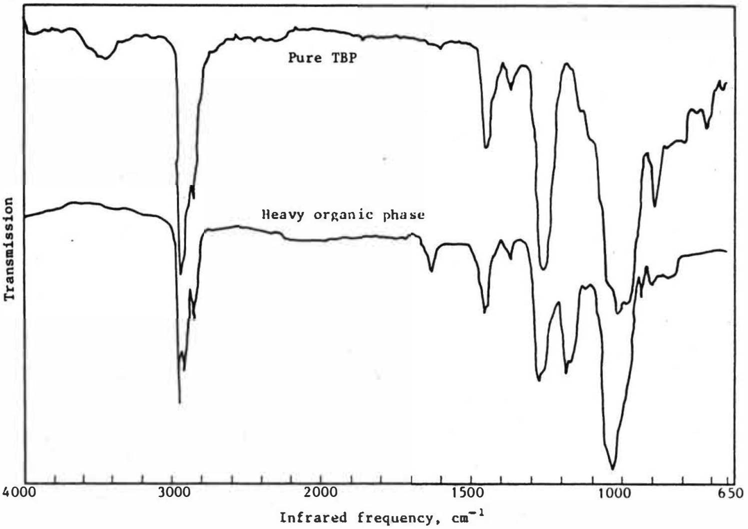

Fig. 2 Infrared spectra of Heavy organic phase

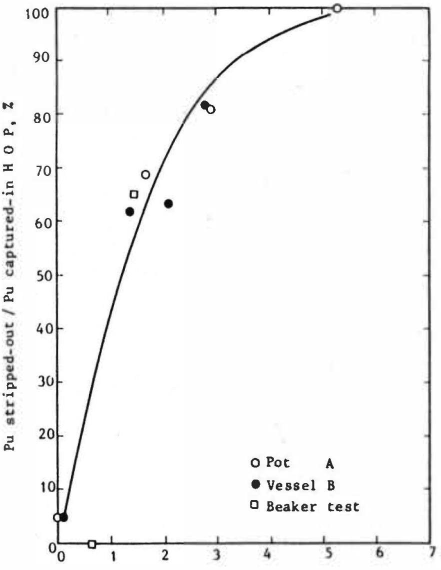

Fig. 3 The stripping of plutonium from Heavy organic phase with hydrazine-stabilized uranous nitrate (U^{IV}).

Process Control for Reprocessing Plant WA Wackersdorf

B. Kube, DWK, Hannover/Germany
A. Nothaft, University of Stuttgart/Germany

The process control equipment for the reprocessing plant Wackersdorf consists, like that of any conventional chemical plant, of the following components:

- sensors to determine the process parameters and product properties;
- actuators by whose assistance the flow of material and energy is directed in a way that the desired values given by process technique are met in the actual process;
- mathematical-technical equipment for linkage and demonstration of information, for operation, control and monitoring of process proceedings, for reports, self-acting control of proceedings and self-acting control of process parameters;
- equipment for communication, alarm and safety technique;
- facilities for power supply.

Some examples shall demonstrate what requirements must be set for this equipment, and how DWK meets these requirements.

The chemical industry requires all control components to be practically proven, robust and easy to maintain. These requirements apply in particular for appliances in hot parts of the reprocessing plant, as maintenance and repair are made more difficult exceeding the usual degree in chemical industry. Also, there is the requirement for a low degree of sensitivity to radiation in these appliances (electronics, lenses of cameras, cable insulations).

In order to make maintenance and repair in radioactive areas possible without decontamination it is planned to use remote-controlled manipulators. All control equipment in these areas must therefore be constructed in a way that it can be operated by means of the manipulators.

The following examples are to demonstrate in particular how the requirements due to the radioactive surroundings are met without unduly straining the manipulators.

Levels and densities of liquids in containers are determined by the dip tube method (fig. 1). The dip tubes reach from non-radioactive rooms (transmitter galleries) at the far side of the concrete shielding to the container, in case of level measuring on the floor and in the gas room, in case of density measuring both in the liquid. Air comes in through the pipes, and the pressure difference between the two feed pipes which corresponds with the hydrostatic pressure of the respective liquid column is measured in the transmitter gallery. The respective variable can be concluded from these measurements.

The flow of liquids is often measured by danaides (fig. 2). The actual measuring element is a horizontal orifice in a container over which the liquid is accumulated. The height of liquid level is the measurement for the flow and is again determined by the dip tube method.

The arrangement keeps the danger of fouling at a minimum. In addition, a duct for cleaning facilities is provided which reaches into the transmitter gallery.

In many places resistance thermometers or thermo-elements are slid through ducts from the outside to the measuring point.

As to radiation monitors, the electronics are separated from the detector and installed in the transmitter gallery.

The above examples are relevant to sensors. As actuators, there are mainly airlifts (fig. 3) in the hot areas of the plant and steam jets for particular processes (evacuation). As for airlifts, the density variations of the product liquid in the two sides of a U-shaped pipe arrangement produced by air inlet are utilized for transport. Steam jets convey according to the principle of the water jet pump. The valves for air or steam inlet are in both cases outside of the hot cells.

The requirements for the mathematical-technical equipment of process control technique mainly result from our aspiring to provide a degree of automation for the plant according to the state of technology in chemical industry. This is very useful because an automatic system which is properly developed and adjusted converts process data to characteristic values and graphs with more information and decides necessary action via the actuators in the process far more quickly and correctly than man. It increases safety and availability, and it is possible to utilize the plant and the ressources in the best way.

By automation, we understand automatic data processing, data compacting and evaluation as well as self-acting controls.

As an example for DWK's planning, control concepts for the 1st column of the PUREX process, the HA-column (fig. 4), are illustrated. In order to do so, the task of the column in the process has to be explained.

After cutting the fuel rods into short pieces, the fuel is solved from the hulls by means of nitric acid. In the HA-column, the valuable materials uranium and plutonium are now extracted from the watery solution into the organic phase by means of the organic extraction agent tributylphosphate (30 % TBP in kerosene or dodecane). For that purpose the organic phase is fed into the bottom and the watery phase into the top of the column, and they emerge at the respective opposite end of the column. The emerging organic phase should possibly be loaded with all of the uranium and plutonium, but with as little acid and fission products as possible which are also extracted.

In order to maintain the desired specification of the emerging organic flow it is important to retain a particular ratio between the incoming organic and watery phases. The value of this ratio depends on the specifications of the incoming flows and on changing column parameters. We therefore want to control the incoming flows in order to exclude disturbances due to varying flow. In addition to that, the relation of the organic to the watery flow is controlled, that is the set point of the organic flow controller is commanded in an adjustable ratio to the fuel solution flow, as this must be constant.

If a disturbance occurs (change of specifications or of the column parameters) this means that the phase-ratio must be altered in order to maintain the specifications of the emerging flows at the correct levels. For achieving automatic adjustment, a suitable control variable is required.

Our analysis of the system, the experiences gained from a test plant and the information from other users show, that most disturbances appear as a change of the temperature profile along the column, because the extraction is an exothermic process. The heat generation of the uranium extraction in the upper part of the column is sufficient for the development of a temperature maximum, which is well measurable. We consider using a characteristic variable of the profile as a control variable, for example the position of its point of concentration.

Because the most important specification of the emerging organic flow is its load of uranium, and a useful measurement for that is its density, also a combination of temperature and density measurements could be considered for a control variable.

Controlling of the separation process of the HA-column by those quantities which are not directly measurable is desirable or even required. Such quantities include the concentrations of the components in both phases. It is well known that the "observer" is a powerful tool to estimate or reconstruct those quantities from process variables which can be easily measured like the temperatures. A characteristic feature of the observer technique is that the estimation is based on an a priori knowledge of the process in form of a mathematical model. This "model based measuring technique" gains increasing significance in controlling and monitoring the complex process.

The described requirements show that the process control equipment must have a high potential of functions at the user's disposal in order to keep the effort for calculations and the realization of control structures and for modifications as little as possible. Under potential of functions we understand the extent of pre-manufactured software moduls, like adders, multipliers, controllers, etc. which still only have to be linked by the user and equipped with data. Additional requirements regard economy of projecting, installation, maintenance, etc.

Fig. 5 shows the control system which, for this reason, has been chosen for each process area. It is a distributed or structural process control system consisting of 5 levels.

The process components (transmitters, signal contacts, valve and engine drives etc.) are connected to the lowest level, the single control level. It has the tasks of signal preparation and drive control. This includes, for example, the electricity supply of transmitters, the conversion of signals to a form suitable to be passed on, if necessary, the filtering of signals, and the checks of process components and signals.

Above the single control level, there is the linkage control level. It consists of linkage processors which, on the one hand establishes the connection between the components of the single control level and the automation appliances of the group control level and on the other hand contains logic controls for the protection of process systems units and aggregates, with which the operator may not interfere.

In the group control level, the automation appliances are installed, which are respectively assigned to one part of the process area. As software they contain all functional modules which are essential for the compliance with the tasks of measured value processing, alarm processing, control, interlocking and signal operation. The modules can be used several times. They are programmed to be linked to each other in accordance with the tasks.

The highest level, the process control level, consists of monitoring and operating stations. Operation is effected via monitor terminals with light pen and keyboard. Printers and coloured hard copy devices are connected for recording. The operator gains all information required for observation and operation from the monitors (alarm list, flow charts, measuring arrangements, open-loop and closed-loop controls, curves).

The connection between process control level and group control level is the bus system of the communication level to which a process computer is also connected. It is essentially used for balance sheets, reports, as a temporary memory of selected data for several days, and also for the data interchange with other process areas and with a superior information system.

By means of the example of the control tasks of HA-column the working procedure of the control system is briefly indicated.

The measuring devices (transmitter outputs, connections for resistance thermometers) are connected to the analogous input assemblies, the drives of controlling valves for the input flows of the column to the output assemblies. The analogous measuring signals (very often load-independent d-c) are interrogated at regular intervals by the input assembly, digitized, and checked for plausibility. They are then available via the appropriate coupling processor at the input of the automation device which treats the tasks of the process control of the HA-column. The described complete link of the measuring signals is carried out by calculating programs of the automation device. As previously mentioned the pattern of these programs is extensively supported by pre-made program parts.

As result of the calculation the control signals for the valve drives appear digitized at the output of the automation device. They are transferred to the appropriate output assembly, which converts them into the suitable analogous mode and passes them on to the drives.

The measuring- and calculation results which are processed by the automation device are also supplied to the responsible operating station in that the automation device and the station are programmed accordingly. The results are focused into the graphical illustrations (e.g. flow diagrams), which are stored in the station and can be called upon on monitors. Selected results are stored in the station for a certain time and can be graphically represented at all times.

Via the control keyboard the operator can, on the other hand, transmit numerical values (e.g. set points for controllers) to the automation device or can effect switching actions like reversing of controllers from "automatic" over to "manual" (possible for every controller). In the last case the operator himself has the possibility to work the appropriate actuator via the automation device and the output unit.

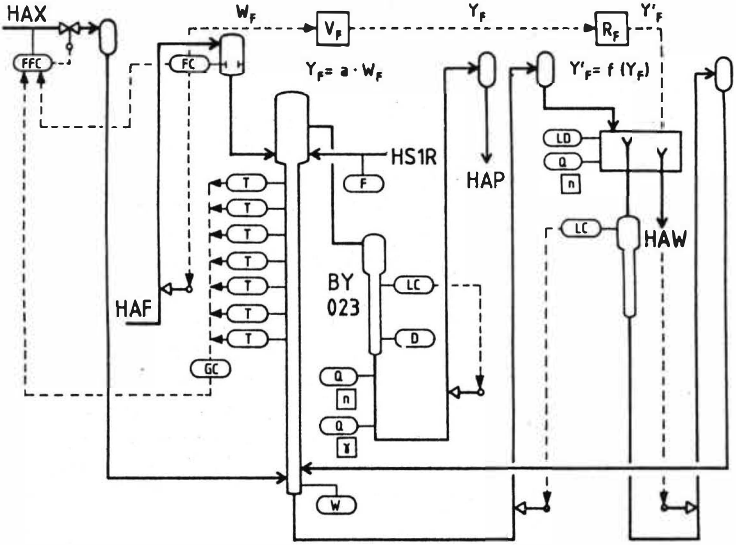
HAX
FFC
W_F
FC
V_F
Y_F
Y_F = a · W_F
R_F
Y'_F
Y'_F = f (Y_F)
HS1R
F
HAP
LD
Q
n
T
LC
HAW
BY
023
HAF
LC
D
GC
Q
n
Q
W

Fig. 4 HA-Column

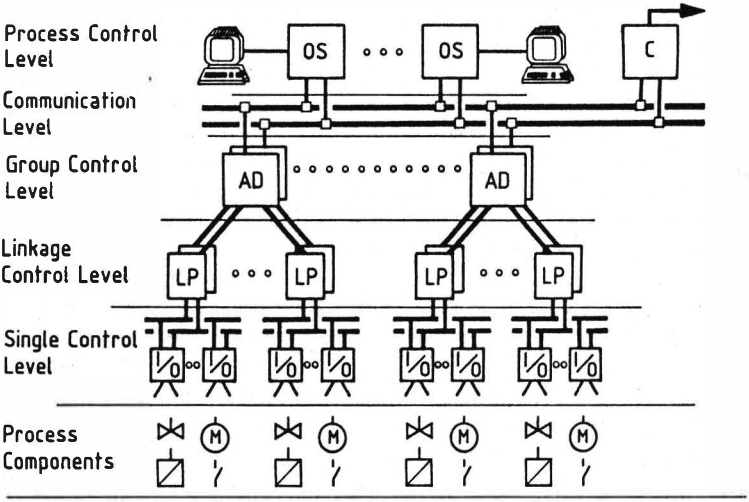
Process Control Level
OS
OS
C
Communication Level
Group Control Level
AD
AD
Linkage Control Level
LP
LP
LP
LP
Single Control Level
I/O
Process Components
M

OS Operating System
LP Linkage Processor
C Process Computer
AD Automation Device
I/O Input/Output Assembly

Fig. 5 Control System

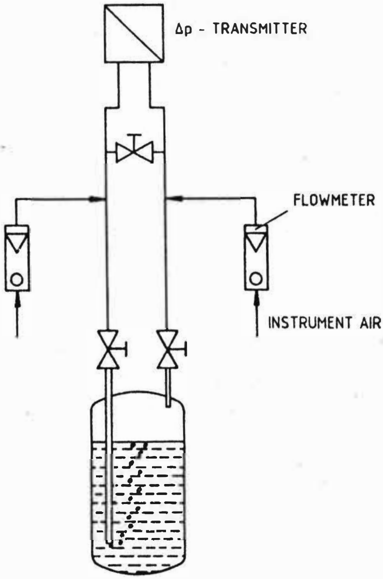
Δp - TRANSMITTER
FLOWMETER
INSTRUMENT AIR

Fig. 1 Measurement By Dip Tubes

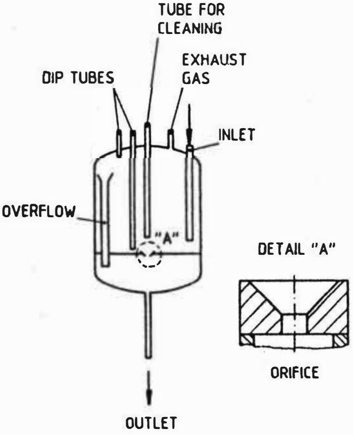
TUBE FOR CLEANING
DIP TUBES
EXHAUST GAS
INLET
OVERFLOW
"A"
DETAIL "A"
ORIFICE
OUTLET

Fig. 2 Danaide

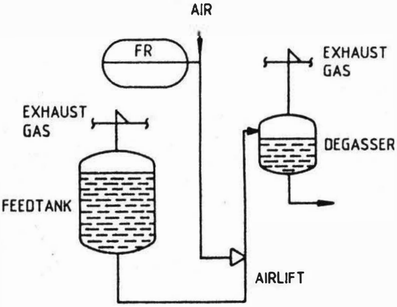
AIR
FR
EXHAUST GAS
EXHAUST GAS
DEGASSER
FEEDTANK
AIRLIFT

Fig. 3 Airlift

Long chain NN'di Alkyl Aliphatic Amides as extracting agents of actinides: progress in process development for high burnup fuel reprocessing

M.Casarci, G.M.Gasparini, G.Grossi, A.Moccia, V.Pagliai*

ENEA-Fuel Cycle Dept.-CRE Casaccia-P.O.Box 2400-00100 ROME, Italy
ENEA-Fuel Cycle Dept.-CRE Saluggia*

1. INTRODUCTION

Long chain NN'di alkyl aliphatic amides are under study in our laboratory since longtime, both as alternative in PUREX-type chemical processes, and as suitable extracting agents for special application such as the selective separation of actinides and other metal ions(1)(2).

This family of organic compounds has the following general structure:

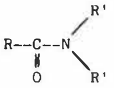

where R and R' are aliphatic chains with 4-8 carbon atoms.

In our previous(3)investigations we have pointed out some favourable aspects and some disadvantages of these compounds.

The possibility to modify their selectivity with a wide number of variables is one of the most interesting aspects of these amides.

Another favourable aspect is the low complexing capacity of the degradation products which, on the other side, are easily removed and soluble in water.

By comparison with TBP, other advantages are a better coalescence time and the easier stripping of Uranium.

On the other side, long chain aliphatic amides expecially those with a branched structure may give third phases.

Studies are still in progress in order to obtain more informations on the nature of the third phase and on the possibility to avoid their formation.

2.AMIDE FLOW-SHEET DEVELOPMENT FOR REPROCESSING OF "TRINO C" HIGH BURNUP FUELS

2.1 General remarks

Recently, in view of the next hot campaign to be carried out in the ENEA pilot reprocessing plant EUREX, a comparative study for the development of similar flowsheets with TBP and amides has been performed.

Due to the particular layout of the EUREX plant, it is not possible to use a classical PUREX-type flow-sheet,that's why we have focused our attention on a "coprocessing scheme", with a final product having an Uranium/Plutonium fixed ratio(4).

To fix a reference flow-sheet, the experience of coprocessing already successfully tried with TBP by others(5) have been take into account. In Fig.1 is reported the reference flow-sheet with TBP.

The flow-sheet with an amide is now under development, and some of the most significant steps are shown in this work.

The amide chosen is the Di-n-Butyl-Octanamide(DBOA).

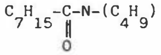

$$C_7H_{15}-\underset{\underset{O}{\|}}{C}-N-(C_4H_9)$$

This amide shows the best behaviour with regards to the third phases formation, as it does not give third phases at any Uranium and Nitric Acid concentrations.

Mesitylene has been chosen as diluent;the possibility of using aliphatic diluents is still under study.

The most"critical"points of these flow-sheets both with TBP and with DBOA have been tested in laboratory scale mixer-settlers.

During these experiments we had also the opportunity to verify the good agreement between the experimental and the theoretical values obtained using the SEPHIS code(6).

2.2 First cycle(Codecontamination,Scrubbing,Stripping)

The codecontamination and scrubbing section in the first cycle, with the DBOA,has been expecially investigated.

The results, illustrated in Fig.2, show that:

- The Plutonium losses in HLW stream are satisfactorly low;
- An Uranium loading greater than 90 g/l has been reached.
- During the mixer-settler runs two phases looked always clear and their separation resulted quicker than in the experiments using TBP.

These consideration can be extended to the experiments of the first cycle stripping section(Fig.3).

In this case we can see also that, with an amide solvent, the complete reextraction of Uranium and Plutonium is possible even without any reducing agent.

2.3 Second cycle(Coprocessing with fixed U/Pu ratio)

The "coprocessing"second cycle has been developped in order to obtain a "mixed product" U/Pu with a pre-fixed U/Pu ratio.

This means that, starting to the additional co-decontamination-scrubbing step(U+Pu in the organic phase), a special stripping section should be foreseen, in which, while all the Plutonium must be recovered in the aqueous phase, only a "calibrated" fraction of the overall amount of Uranium must be co-stripped with Plutonium.

This could be obtained with a "reducing partition flowsheet" using Hydroxylamine Nitrate(HAN) as aqueous reducing and salting agent.

Figure 4 shows the behaviour of a mixer-settler run with DBOA.

With this amide, due to its U(VI) distribution coefficent, Pu/U+Pu ratios in the range of 1-10% can be obtained.

In order to be able to reach higher Pu/U+Pu ratios(in the range 10-20%), a branched chain amide should be utilized,for example Di-Butyl-3,3DiMethyl-Butyramide.

Studies are now in progress in order to develop a suitable flow-sheet in this connection.

2.4 Fission products behaviour (fully active tests).

Comparative tests in batch using an organic phase(TBP or DBOA), and an aqueous phase containing U=272g/l,Pu=1.244g/l and Fission product= 296 GBq. have been carried out.

The experiments have been carried out to simulate the extraction, the re-extraction and the solvent regeneration steps.

After the equilibration and the phase separation the Uranium concentration and Fission products content in the organic phase have been determined. The results of these comparative extraction tests(Fig.5) show clearly that the amide is more selective and extracts less Fission products than TBP.

Moreover, Cerium, Antimony and Yttrium, seem not be extracted by amide. As a consequence the reextraction and the solvent regeneration(Fig.6 and 7)are easier and the amide solvent appears to be cleaner than the TBP solvent.
Taking into account these results, it seems to be to reach a good F.P. decontamination with only one codecontamination cycle.

These investigations concerning further flow-sheet optimizations will be carried out during the current year.
At the end of the 1986 we hope that we will be able to define in all process section also the amide flow-sheet.

The authors are indebted for the helpful contribution of D.Carlini,G.Puzzuoli,
A.Tieri COMB-MEPIS-ATTIN and D.Boretto,M.Gilardi COMB-EUREX

REFERENCE

1- The N,N' Di-Alkyl-Amides as Alternative Extractants of some Actinides:A Rewiew of Research Work carried out at ENEA
M.Casarci,G.M.Gasparini,G.Grossi
Proc. 1st International Conference on the Chemistry of the Lanthanides and Actinides-Venice(1983)

2- Application of N,N' Di-Alkyl Aliphatic Amides in the separation of some Actinides
G.M.Gasparini, G.Grossi
Sep.Science and Tech., 15(4), 825-844,1980

3- Alkyl Aliphatic Amides as alterative extractants for actinides:further studies on the influence of the chemical structure on the extractive behaviour
G.Grossi, G.M.Gasparini, M.Casarci
Proc.ISEC '83 Denver, California

4- Bench scale demonstration of a coprocessing operation with an amidic solvent
D.Carlini, M.Casarci, G.M.Gasparini, G.Grossi, A.Moccia
Proc. Fuel Reprocessing and Waste Management,1984, Jackson, Wyoming

5- Coprocessing Solvent Extraction Studies
M.S.Okamoto, M.C.Thompson
Nucl. Technol. 43, 126-131 (1979)

6- Modification of the SEPHIS computer code for calculating the Purex extraction system.
S.B.Watson, R.H.Raney
ORNL-TM-5123(1975)

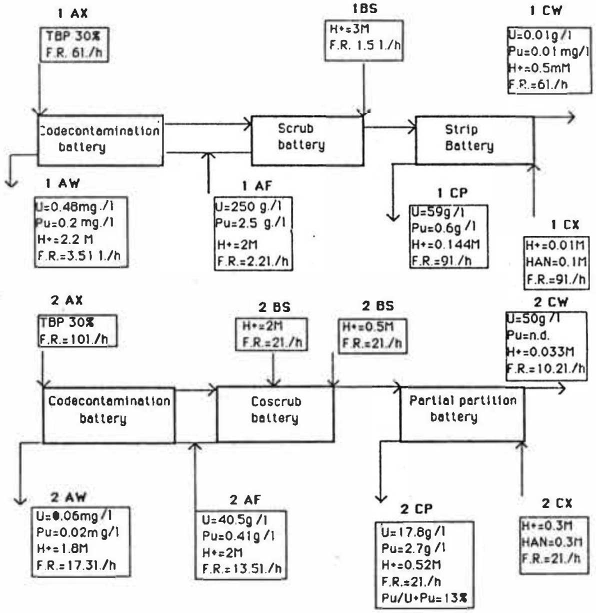
1 AX
TBP 30%
F.R. 6l./h
1BS
H+=3M
F.R. 1.5 l./h
1 CW
U=0.01g/l
Pu=0.01 mg/l
H+=0.5mM
F.R.=6l./h
Codecontamination battery
Scrub battery
Strip Battery
1 AW
U=0.48mg./l
Pu=0.2 mg./l
H+=2.2 M
F.R.=3.51 l./h
1 AF
U=250 g./l
Pu=2.5 g./l
H+=2M
F.R.=2.2l./h
1 CP
U=59g/l
Pu=0.6g/l
H+=0.144M
F.R.=9l./h
1 CX
H+=0.01M
HAN=0.1M
F.R.=9l./h
2 AX
TBP 30%
F.R.=10l./h
2 BS
H+=2M
F.R.=2l./h
2 BS
H+=0.5M
F.R.=2l./h
2 CW
U=50g/l
Pu=n.d.
H+=0.033M
F.R.=10.2l./h
Codecontamination battery
Coscrub battery
Partial partition battery
2 AW
U=0.06mg/l
Pu=0.02mg/l
H+=1.8M
F.R.=17.3l./h
2 AF
U=40.5g/l
Pu=0.41g/l
H+=2M
F.R.=13.5l./h
2 CP
U=17.8g/l
Pu=2.7g/l
H+=0.52M
F.R.=2l./h
Pu/U+Pu=13%
2 CX
H+=0.3M
HAN=0.3M
F.R.=2l./h

Fig. 1. REFERENCE FLOW-SHEET FOR THE TBP PROCESS.
(R.F.= flow rate)

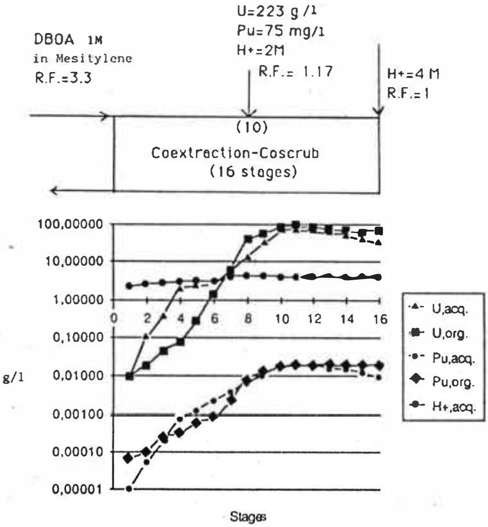

Fig. 2. CODECONTAMINATION-COSCRUB EXPERIENCE WITH AN AMIDE
(R.F. = flow rate)

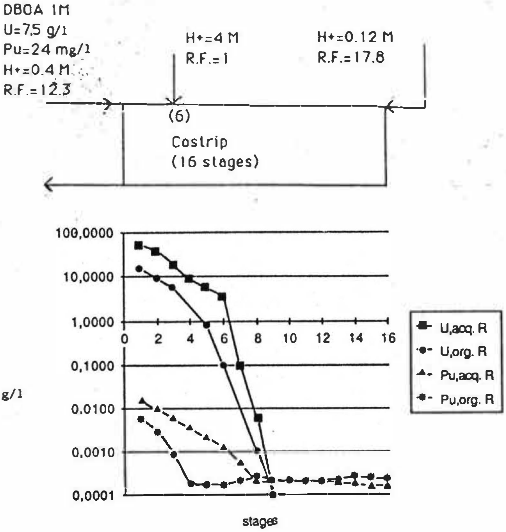

Fig. 3. COSTRIP EXPERIENCE WITH BBOA 1M IN MESITYLENE
(F.R.= flow rate)

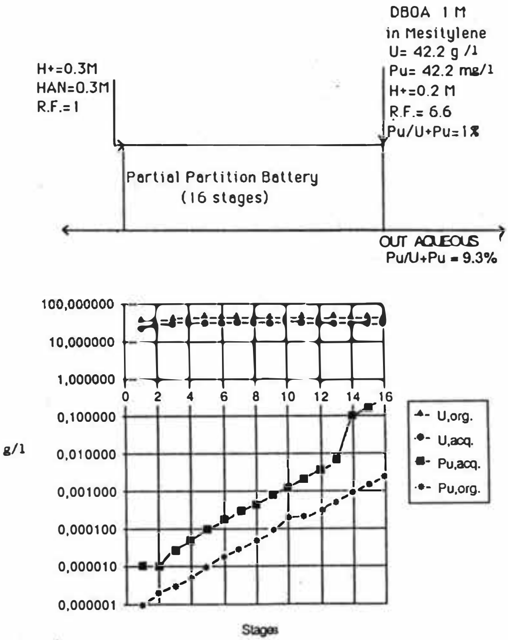

Fig. 4. **PARTIAL PARTITION EXPERIENCE**
(R.F. = flow rate)

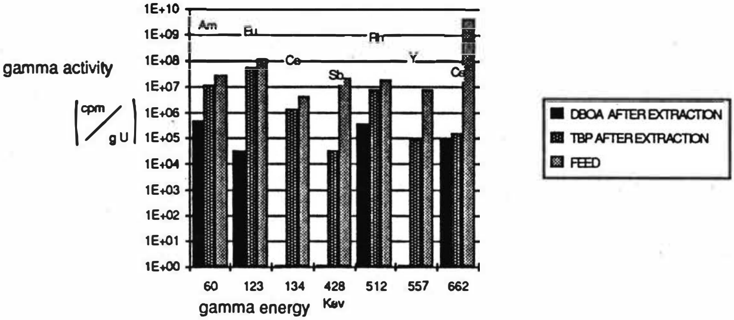

Fig. 5. COMPARATIVE EXTRACTION TEST

(TBP 30% in Kerosene;DBOA 1M (3O%) in Mesitylene;
phase ratio (o/a) =O.25, shaking time =5';

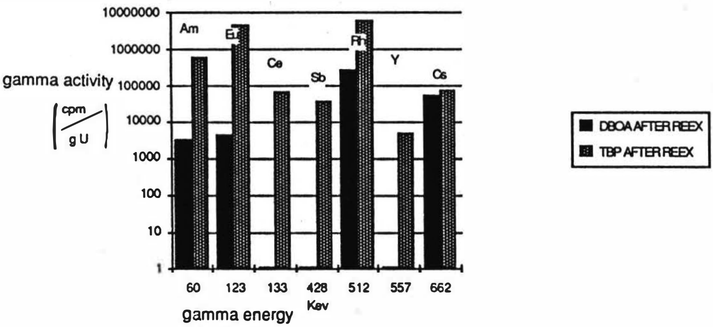

Fig. 6 **COMPARATIVE REEXTRACTION TEST**
(TBP 30% in Kerosene;DBOA 1M (30%) in Mesitylene;
phase ratio (o/a) =0.25, shaking time =5';
aqueous Ph. = 0.01M HNO_3 + 0.1M Hydroxylamine Nitrate)

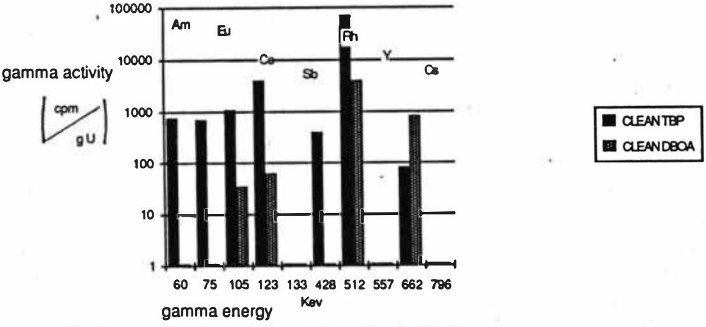

Fig. 7. **COMPARATIVE CLEANING TEST**
(TBP 30% in Kerosene;DBOA 1M (30%) in Mesitylene;
phase ratio (o/a) =0.25, shaking time =5';
Aq. Ph. = 0.5 M Na_2CO_3 + 0.025M Na tartrate)

TECHNICAL SCALE ELECTRODEDOX EQUIPMENT FOR THE SEPARATION OF PLUTONIUM

H. Schmieder and H. Goldacker
Institut für Heiße Chemie, Kernforschungszentrum Karlsruhe,
D - 7500 Karlsruhe, FRG

INTRODUCTION

For the separation of Pu from U in the PUREX process four processes were developed to technical maturity with the following reductants:

- Ferroussulfamate;
- Uranium-(IV)-nitrate;
- Hydroxylammoniumnitrate;
- Electroreduction within the extractor.

Externally fed U(IV) is usually applied in industrial reprocessing today. U(IV) shows at least two drawbacks:

- demand for a high U(IV) excess
- occasionally observed failure of the process caused by the autocatalytic reoxidation of Pu(III) and U(IV) starting in the organic phase.

These facts initiated activities in different countries to develop the in-situ electroreduction process already at the end of the sixties /1,2,3,4/.

A comparison of the chemical process with the electrochemical process was made in an earlier publication and resulted in a preference of the electroreduction process /5/. According to our experience this process shows all advantages of the U(IV)-process but avoids its draw-backs.

This paper describes the design principles of the electroreduction extractors (mixer-settler EMMA and pulsed column ELKE) and summarizes the results achieved.

In addition the experience with the electrooxidation cell (ROXI) for reoxidation of the Pu(III) product solutions which was developed in parallel is also described.

DESIGN AND APPLICATION OF THE ELECTROREDOX EQUIPMENT

Disregarding the specific advantages in the PUREX process /5,8/ the use of an electrochemical reactor can have principal advantages compared to a chemical reactor. Fig.1 shows schematically the layout of both reactors for redox purposes. The figure shows that in the case of a chemical reactor either waste is produced formed by the consumed redox chemicals or the redox chemicals have to be regenerated and recycled to the reactor. This requires a regeneration reactor, metering equipment, additional piping etc. Disadvantage for many technical applications can be the necessity of a diaphragm (risk of break, blockage) and insufficient corrosion stability of containment and electrode material. After the first successful electroreduction experiments performed in the Institut für Heisse Chemie /1/, our efforts to design simple, compact and reliable electroredox equipment for industrial applications led therefore to the following design criteria:

1 - no diaphragm
2 - use of apparatus casing as cathode
3 - current or voltage constant operation.

Basic chemical investigations and corrosion tests of different materials showed that these criteria can be fulfilled for both the electroreduction extractors and the electrooxidation cell /6,7/. Mainly the irreversible character of the U(VI)-electroreduction and of the hydrazine-electrooxidation permits to avoid diaphragms. Titanium was found to be well suited as containment and cathode material, with corrosion rates less then 50 micrometer per year under process conditions. Experiments with current or voltage constant operation showed that side reactions (hydrogen formation, nitrate reduction) can be suppressed to a tolerable amount. Therefore, reference electrodes necessary for potential constant operation are not required.

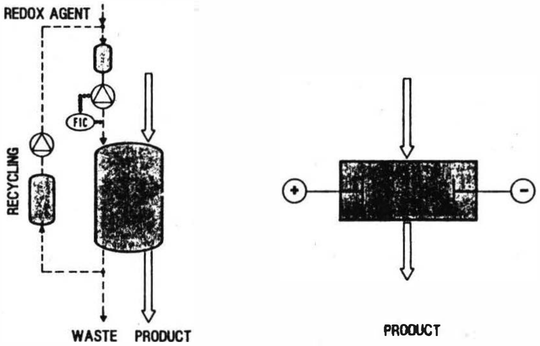

IHCH

Fig. 1 LAYOUT OF EQUIPMENT FOR A CHEMICAL AND AN ELECTROCHEMICAL REACTOR

Fig.2 shows schematically the construction of the mixer-settler, pulsed column and electrooxidation cell. The mixer-settler is made out of titanium and the containment is connected with the ground and acts as cathode. The anodes are installed in the settler chambers where consequently electroreduction takes place. The most stable anode material is platinum with corrosion rates of few micrometers per year. For technical equipment platinized Ta, Ti or other materials are used.

The pulsed column is constructed in a similar way. Column pipe and sieve plates are made out of titanium and function as the cathode. The platinized central rod is the anode. It is insulated against the sieve plates by rings made out of nonconductive material. In the top decanter of the column separator sheets are installed to support the separation of electrolytic gas from the organic drops.

The area ratio of cathode to anode is choosen as large as possible for both apparatus to reduce anodic reoxidation of Pu(III).

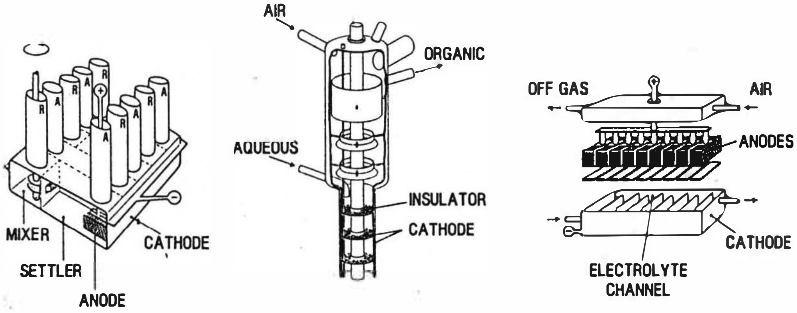

MIXER-SETTLER, EMMA

PULSED COLUMN, ELKE

OXIDATION CELL, ROXI

KfK IHCH

Fig.2 PRINCIPLES OF DESIGN FOR ELECTROREDOX EQUIPMENT

To eliminate any risk of hydrogen explosion the mixer-settler and the top decanter of the pulsed column are sparged with air to dilute the hydrogen below the explosion limit. The hydrogen current yield can be kept below 10% under typical conditions. The design of the electrooxidation cell shows the characteristics of an electrochemical flow reactor. The course of the electrolyte channel is meander-shaped to minimize axial mixing by the high ratio of total length to cross-section of the channel. The electrolytic gas leaves the cell diluted with sparging air. The containment (cathode) is again made out of titanium and connected to ground. The anode packages are made out of platinized metal sheets. The major advantage of electrooxidation as compared to chemical oxidation by nitrogen oxides is the compactness of the apparatus. The chemical process requires one absorption column for the complete oxidation of hydrazine and Pu(III) and one additional column to desorb the excess of nitrogen oxides /8/.

Comprehensive experiences with the electroredox equipment in different sizes have been made since 1970. Tab.1 summarizes these experiences along with the application purpose, apparatus size and throughput. The earliest results come from experimental work with a mixer-settler (MILLI-EMMA, 16 stages) and an electro-oxidation cell (MILLI-ROXI) in the scale of the miniature reprocessing plant, MILLI (throughput: ca. 1 kg/d, highly shielded). The electro equipment has been used for Pu-purification and for Pu/U split at lower activity levels than found in the highly active cycle /6,9/. Experimental experiences with pulsed columns (ELKE) were gained in the extraction cycle PUTE which is equipped with pulsed columns of about 5 cm diameter. The electroreduction column has an effective height of 800 cm. Pu inventory for the experiments in the PUTE facility is about 4 kg and the total throughput amounts 260 kg Pu up to now. Two electrooxidation cells are installed in the facility; one is made out of titanium and the other out of hafnium (cathode).

The Pu purification cycle of the Wiederaufarbeitungsanlage Karlsruhe, WAK, was equipped with an electroreduction mixer-settler (WAK-2B-EMMA, 12 stages) and an electrooxiation cell (WAK-2B-ROXI) in 1980. Both units work reliably since then /11/. The fission product content of Pu product solution is less than 1 mCi/ l on the average. The two units were extensively tested in the Institut für Heisse Chemie prior the installation in the plant. This allowed to study parameter variations /10/. Satisfied with the 2B-EMMA, the Wiederaufarbeitungsanlage Karlsruhe has equipped its first highly active cycle with an electroreduction mixer-settler in 1984. Due to a licensing problem (court decision pending) this extractor is at present only operated with externally produced U(IV).

	APPARATUS	APPLIED FOR	THROUGHPUT kg/d	OPERATION SINCE
EXPERIMENT	[1] MILLI-EMMA	Pu/U split cycle	1 Pu • U	1970
		Pu purific. cycle	0.1 Pu	1970
	MILLI-ROXI	split cycle purific. cycle	≤ 0.3 Pu	1973
	[2] PUTE-ELKE	Pu/U split cycle	100 Pu • U	1983
		purific. cycle	10 Pu	1982
	PUTE-ROXI	split cycle purific. cycle	≤ 15 Pu	1982
PLANT	[3] WAK-2B-EMMA	2nd Pu cycle	~ 2.5 Pu	1980
	WAK-2B-ROXI	2nd Pu cycle	~ 2.5 Pu	1980
	WAK-1B-EMMA	Pu/U split cycle	~ 200 Pu • U	(1984)[4]

[1] MILLI: Miniature Reprocessing Plant, shielded; U/Pu split demonstrated only without fission products up to now
[2] PUTE : Extraction cycle with pulsed columns, glove boxes, [3] WAK : Wiederaufarbeitungsanlage Karlsruhe
[4] no license for electrochemical operation up to now .

IHCH

Tab.1 EXPERIENCES WITH ELECTROREDOX EQUIPMENT

RESULTS AND DISCUSSION

ELECTROREDUCTION MIXER-SETTLER

Tab.2 summarizes the results of the counter current experiments with the electroreduction mixer-settlers in the scale of MILLI and WAK /6,9,10/. The 16-stage MILLI-EMMA was used for U/Pu split as well as for Pu purification, without U scrub in the latter case. The behavior of Np under the conditions of U/Pu split was investigated by Warnecke /20/. Because the miniature size of the apparatus only a low extraction stage efficiency could be realized with the extractor especially in experiments with a high organic to aqueous flow ratio. The major parameter variations were:

- 20V % and 30V % of TBP in kerosene
- Pu content
- current density
- HNO_3 concentration in the aqueous strip solution
- HDBP concentration in the organic solvent
- flow ratios
- total volume flow (residence time)

	PURPOSE OF TEST	FLOW RATIO $\frac{BF_0}{BX_0}$	Pu PRODUCT CONCENTR. g/l	SEPARATION		STAGE EFFICIENCY	VOLTAGE V
				Pu-DF	U-DF		
MILLI - EMMA	U/Pu split[1] FBR model fuel	5-6,7	≤ 22	≤ 4500[2]	~ 3000[2]	low	2.8-8
	U/Pu split LWR model fuel	7.1-9.3	≤ 4.8	≤ 2000[2]	~ 3800[2]	low	2.8-8
	Pu purification cycle	2-3.5	≤ 46	≤ 20000[3]	—	low	≤ 6
WAK-2B-EMMA[4]	Pu purification cycle	2-3	≤ 36	≤ 100000[5]	—	high	2-8

[1] 20 % V TBP-alkane, 30 % V for all other experiments,

[2] 9 practical stages used for Pu strip, 7 for U scrub,

[3] 16 practical stages used for Pu strip, without U scrub,

[4] results of test operation at Inst. f. Heisse Chemie,

[5] 12 practical stages used for Pu strip, without U scrub,

IHCH

Tab.2 RESULTS OF TEST RUNS WITH ELECTROREDUCTION MIXER-SETTLERS

The most significant influence on the separation (Pu-DF) was found for variations of the total volume flow. All other parameters have less importance when varied within reasonable limits. A decrease of the total volume flow causes complex interactions in a counter-current extractor due to the increase of residence times for both phases. In the case of the miniature mixer-settler the increase of extraction stage efficiency seems to be the dominant factor which improves the separation. For the Pu purification experiments an upper limit of the applicable organic to aqueous flow ratio was found at Pu product concentrations of about 40 g/l. A similar effect was observed during the test of the WAK-2B-EMMA. The flow ratio could not be raised beyond 3, corresponding to a Pu product concentration of about 36 g/l, although this apparatus has a significantly higher stage efficiency. One reason for the limitation of the Pu-DF to a maximum of 10^5 are the very long residence times because the volume flows used in these experiments had to be low for technical reasons /10/. To obtain a better understanding of the reductive Pu-separation processes we developped a mathematical model describing the complex system /12, 5/. This model VISCO has proved its reliability by comparison with many experimental results /13/. The raw structure of the model is given in Fig.3 /9/. Besides the equilibrium distribution of all chemical components the model contains the extractive transfer equations, assuming that transfer takes place only in the mixing chamber, the chemical and electrochemical reduction equations (the electroreduction occurs only in the settling chamber), the autocatalytic oxidation of Pu(III) by HNO_2 and the reaction of hydrazine with HNO_2.

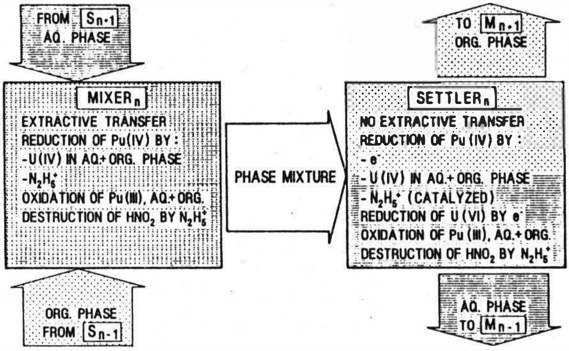
FROM S_{n+1} AQ. PHASE
MIXER$_n$
EXTRACTIVE TRANSFER
REDUCTION OF Pu(IV) BY :
-U(IV) IN AQ.+ORG. PHASE
-$N_2H_5^+$
OXIDATION OF Pu(III), AQ.+ORG.
DESTRUCTION OF HNO_2 BY $N_2H_5^+$
ORG. PHASE FROM S_{n-1}
PHASE MIXTURE
TO M_{n+1} ORG. PHASE
SETTLER$_n$
NO EXTRACTIVE TRANSFER
REDUCTION OF Pu (IV) BY :
- e⁻
- U (IV) IN AQ.+ORG. PHASE
- $N_2H_5^+$ (CATALYZED)
REDUCTION OF U (VI) BY e⁻
OXIDATION OF Pu (III), AQ.+ORG.
DESTRUCTION OF HNO_2 BY $N_2H_5^+$
AQ. PHASE TO M_{n-1}

Fig. 3 STRUCTURE OF MODEL (VISCO) USED FOR FLOW-SHEET CALCULATIONS OF ELECTROREDUCTION MIXER-SETTLER

Simulations on the basis of VISCO were carried out to determine the sensitivity of the individual parameters for Pu separation in multistage extractors. Tab.3 shows an example for a U/Pu split standard flow-sheet for FBR-fuel with a 12stage electroreduction mixer-settler (electroreduction only in the 7 stage BX part). The simulation results confirm the importance of the stage efficiency for a cascade extractor. Stage efficiencies below 75% finally result in a reoxidation starting in the organic phase caused by a depletion of the stabiliser, hydrazine. The importance of the organic to aqueous flow ratio and the Pu product concentration (40 g/l) were confirmed. The limitation by the Pu product concentration can be explained by the strong salting out effect of Pu(III) for U(VI), Pu(IV), and HNO_3 /14/. The transfer of U(VI) and Pu(IV) to the aqueous phase is inhibited under these conditions and nitric acid accumulates in the strip part of the mixer-settler resulting, finally in a lack of U(IV) and a decrease of the Pu-DF. The upper limit of hydrazine ($>$ 0,30 M) is explainable by the salting out effect of hydrazine nitrate on U, Pu and HNO_3. The upper limits of nitric concentrations and the lower limit of the hydrazine concentration are not surprising for the selected standard flowsheet.

ELECTROREDUCTION PULSED COLUMN

Tab.4 summarizes the results of the experiments with the electroreduction pulsed column (ELKE) used for U/Pu split and for Pu purification /18,19/. For the Pu purification cycle experiments the organic feed concentration was kept between 9,4 g/l and 15 g/l Pu. Total volume flow, flow ratio and U content in the organic feed solution were varied. The results show also for the pulsed column a limitation of the Pu product concentration to about 43 g/l (see flow ratio variation) where the Pu-DF falls below 6000. Next to this, the most significant parameter influencing the Pu-DF is the total volume throughput. Below 30% of the flooding flow a drastically increased effect of axial mixing in the continuous aqueous phase was observed. The highest DF (almost 10^6) was achieved at a flow ratio of two and an U/Pu ratio of 0,8 in the organic feed solution, but the U/Pu ratio has much less influence on the Pu-DF than the other parameters.

STANDARD	PARAMETER	LIMIT	——→ EFFECT
80%	STAGE EFFICIENCY	< 75%	drastic decrease of Pu-DF caused by reoxidation.
4	FLOW RATIO, $\frac{\text{org. feed}}{\text{aq. strip}}$	> 4,4	decrease of Pu-DF caused by lack of U(IV).
0,1 M	$[HNO_3]$, org. feed	> 0,25 M	
0,2 M	$[HNO_3]$, aq. strip	> 0,35 M	
0,1 M	$[N_2H_5^+]$, aq. strip	> 0,30 M	
		< 0,04 M	decrease of Pu-DF caused by reoxidation.

CONSTANT PARAMETERS

organic feed : $[Pu] = 9{,}3\,g/l$, $[U] = 75{,}7\,g/l$, $[HNO_3] = 10^{-3}\,M$
flow ratio, org. feed/org. scrub = 5
Pu strip = 7 stages , U scrub = 5 stages , T = 30°C

Tab.3 CALCULATED LIMITS OF A STANDARD FLOWSHEET (Pu-DF ~ 10^5, U-DF ~ 45) FOR AN ELECTROREDUCTION MIXER-SETTLER (U/Pu SPLIT)

PURPOSE OF TEST	PARAMETER				SEPARATION
	$\frac{\text{total volume flow}}{\text{flooding volume flow}}$ %	flow ratio $\frac{\text{org. feed}}{\text{aq. strip}}$	U/Pu org. feed	strip solution $[NH_2H_5^+]$ M/l	Pu - DF
Pu PURIFICATION CYCLE	16 - 47[1]	3	0.3 - 0.4	0.15 - 0.3	$1.6 \cdot 10^3$ to $2.7 \cdot 10^4$
	35	2.5 - 2.85[2]	0.3 - 0.4	0.15 - 0.3	$4.3 \cdot 10^5$ to $<6 \cdot 10^3$
	24	2.0	0.06 - 0.8[3]	0.15 - 0.3	$4.1 \cdot 10^4$ to $9.1 \cdot 10^5$
Pu/U SPLIT[4]	35	4 - 5	100	0.1	$4 \cdot 10^2$ to $3.1 \cdot 10^2$
	25	4	100	none to 0.1	$\sim 3.2 \cdot 10^2$
	25	2.4	100	none to 0.002	$\leq 2.1 \cdot 10^3$

[1] [Pu] org. feed = 10 g/l , [2] [Pu] org. feed = 15 g/l , [3] [Pu] org. feed = 9.4 g/l , [4] without U scrub .

Tab.4 RESULTS OF TEST RUNS WITH ELECTROREDUCTION PULSED COLUMN

voltage ~ 3 - 4 V , current yield for Pu ~ 25 %

The major objective of the U/Pu split experiments was the minimization of the hydrazine concentration in the aqueous strip solution. Basic experiments had shown that without any hydrazine the process should work if the nitric acid concentration is kept low enough. The column results confirm the principal possibility to operate the electroreduction without hydrazine. A discussion of these experiments in is given in detail by Heilgeist et al. /15/. The experiments showed also an unexpected finding, however. The achieved Pu-DF's are surprisingly low in comparison with the experiments in the Pu purification cycle, especially when considering the high U content in the organic feed which guarantees high concentrations of U(IV) electrochemically produced in the extractor. This effect is not well understood up to now. The most probable explanation is a transport of Pu rich aqueous phase by organic drops from the bottom of the column to the top of the column. If this assumption should be confirmed in further experiments, the mixer-settler could possibly be the better extractor for U/Pu split if high Pu-DF's are wanted. The effect is supported by poor Pu-DF's found in the Eurochemic reprocessing plant in Mol, where U(IV) was used as reductant in a pulsed column /16/. Moreover, calculations by VISCO show that the best separation should be achieved by the use of a centrifugal contactor equipped with electroreduction /13/. This extractor permits also the widest parameter variation and possesses other advantages such as a high space-time-yield and a favourable transient behavior. A first design study confirmed the principal feasibility of such an extractor.

Since 1983 the VISCO model can also be used for calculations of pulsed columns taking into account axial mixing, drop size etc. /17/. The result of a simulation series to determine the parameter limits of a standard flowsheet for the Pu purification cycle is given in Tab.5. The results confirm the experimentally observed limitation by the Pu product concentration of approximately 40 g/l caused by the salting

STANDARD	PARAMETER	LIMIT ——→	EFFECT
2	FLOW RATIO, $\frac{\text{org. feed}}{\text{aq. strip}}$	> 2,7	decrease of Pu-DF
9,3 g/l	[Pu] , org. feed	>20 g/l	
18,6 g/l	[Pu] , aq. product	>40 g/l	
0,1 M	$[HNO_3]$, aq. strip	> 0,35 M	
0,15 M	$[N_2H_5^+]$, aq. strip	none[*]	none
0,2 M	$[HNO_3]$, org. feed	> 0,2 M	
9,3 g/l	[U] , org. feed	traces	

[*] $T_{max} \leq 30°C$, $[HNO_3]$ aq ≤ 0.4 M

CONSTANT PARAMETERS

eff. height = 700 cm, volume flow, total = 190 l dm^{-2}h^{-1}, drop diam. < 3 mm, disp. coeffic. aq. < 800 cm^2 min^{-1}, org. feed $[HNO_2]$ = 10^{-3} M, T_{max} = 45 °C

IHCH

Tab.5 CALCULATED LIMITS OF A STANDARD FLOWSHEET (Pu-DF ~ 10^5, U-DF ~ 5) FOR AN ELECTROREDUCTION PULSED COLUMN (Pu PURIFICATION CYCLE) out effect of Pu(III) as already discussed above for the mixer-settler. The parameter limit for the flow ratio is nearly in agreement with the experiment. The limitation in the concentration of HNO_3 in the strip solution agrees with our experimental experience. Even for HNO_3 concentrations as high as 0,6 M in the organic feed solution no limitation is indicated by the simulation. For the standard flowsheet with a flow ratio of two the column should work well without hydrazine, and even without U in the organic feed. However, both variations are not experimentally tested up to now.

ELECTROOXIDATION

The main reactions occuring in an electrooxidation cell are summarized in Tab.6 /21/. The anodic destruction of hydrazine is assisted by the consumption of hydrazine in the reaction with Pu(IV) which is formed by anodic oxidation. Furthermore hydrazine is consumed by the reaction with HNO_2, which is cathodically produced with a small yield. The yield of the direct anodic oxidation of Pu(III) depends on the nitric concentration. Under typical conditions the major part of Pu(III) is oxidized autocatalytically by HNO_2. The accompanying U(IV) is consumed by reduction of Pu (IV).

The formation of Pu(VI) is suppressed at a HNO_3 concentration higher then 2 M. The formation of ammonium by cathodic reduction of HNO_3 depends on the electrolyte composition and was measured to be 0.03 to 0,46 mM/Ah for an electrolyte without hydrazine /21/.

The average values achieved with the two electrooxidation cells installed in the PUTE facility are given in Tab.7. For typical feed compositions current demands for

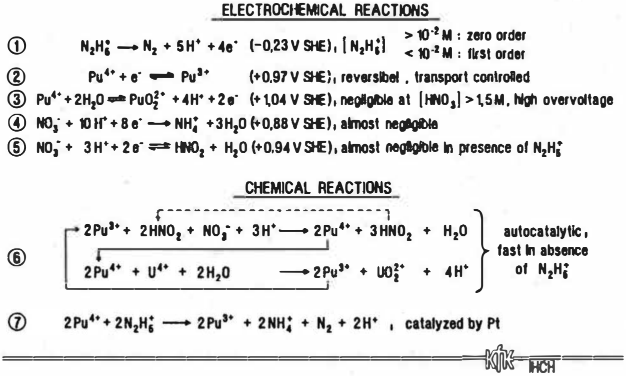

ELECTROCHEMICAL REACTIONS

① $N_2H_5^+ \longrightarrow N_2 + 5H^+ + 4e^-$ (-0,23 V SHE), $[N_2H_5^+]$ > 10^{-2} M : zero order; < 10^{-2} M : first order

② $Pu^{4+} + e^- \rightleftharpoons Pu^{3+}$ (+0,97 V SHE), reversibel, transport controlled

③ $Pu^{4+} + 2H_2O \rightleftharpoons PuO_2^{2+} + 4H^+ + 2e^-$ (+1,04 V SHE), negligible at $[HNO_3] > 1{,}5$ M, high overvoltage

④ $NO_3^- + 10H^+ + 8e^- \longrightarrow NH_4^+ + 3H_2O$ (+0,88 V SHE), almost negligible

⑤ $NO_3^- + 3H^+ + 2e^- \rightleftharpoons HNO_2 + H_2O$ (+0,94 V SHE), almost negligible in presence of $N_2H_5^+$

CHEMICAL REACTIONS

⑥ $2Pu^{3+} + 2HNO_2 + NO_3^- + 3H^+ \longrightarrow 2Pu^{4+} + 3HNO_2 + H_2O$

$2Pu^{4+} + U^{4+} + 2H_2O \longrightarrow 2Pu^{3+} + UO_2^{2+} + 4H^+$

autocatalytic, fast in absence of $N_2H_5^+$

⑦ $2Pu^{4+} + 2N_2H_5^+ \longrightarrow 2Pu^{3+} + 2NH_4^+ + N_2 + 2H^+$, catalyzed by Pt

Tab.6 MAIN REACTIONS IN AN ELECTROOXIOATION CELL (ROXI) the hydrazine destruction of about 100 Ah/M N_2H_5 were measured in the Ti-ROXI. This value corresponds to an anodic current yield higher than 100% explainable by the contribution of the other reactions mentioned above. For the Hf-ROXI a higher current demand is measured which is probably caused by by a smaller fraction of cathodic reactions supporting the hydrazine destruction. The ammonium formation is low, but still higher than expected in some cases. This can be explained by the formation of ammonium (reaction 7, Tab.6) in parallel to electroreduction of HNO_3. A higher ammonium content is found in the Pu product solutions of the extractors shown in Tab.8. The high specific yield of up to 14, 1 mM NH_4/Ah (column 4, Tab.8) can only be explained by reaction 7 i.e. of hydrazine with Pu(IV) which is catalyzed by Pt /21/. The high value of up to 6 M NH_4^+/M Pu (column 3) found in mixer-settlers using externally produced U(IV) as reductant is surprising. Probably part of the NH_4^+ is already formed in the U(IV)-production cell.

APPARATUS	FEED SOLUTION, M				CURRENT CONSUMPTION Ah/M $N_2H_5^+$	Pu(VI) FORMATION % of Pu	NH_4^+ FORMATION $10^3 \cdot$ M/Ah
	HNO_3	Pu	U	$N_2H_5^+$			
TITANIUM-ROXI	1.5-2	0.075- 0.105	0.0008- 0.004	0.03- 0.15	$\leq$ 100	$\leq$ 2	~ 1
HAFNIUM-ROXI	1.5-2	0.075- 0.105	0.0008- 0.004	0.03- 0.15	$\leq$ 170	$\leq$ 2	0.1-2
	1.4-2.6	0.012- 0.03	0.33	0.01- 0.07	~ 150	< 1	~ 0.6

I- anode ~ 2 to 4 mA cm^{-2}, $T \leq 48{,}5\,^\circ C$

IHCH

Tab.7 AVERAGE RESULTS OF ELECTROOXIDATION CELLS

APPARATUS	STRIP SOLUTION	AMMONIUM FOUND IN Pu PRODUCT SOLUTION		HN_3 FOUND IN ORGANIC RAFFINATE $10^3 \cdot$ M/l
	$[N_2H_5^+]$, M	NH_4^+/Pu	$10^3 \cdot$ M NH_4^+/Ah	
MIXER-SETTLER[1)] U(IV) as reductant	~ 0.2	1 to 6		
ELECTROREDUCTION MIXER-SETTLER[2)]	0.2 to 0.5	0,2 to 3		
ELECTROREDUCTION PULSED COLUMN[3)]	0.02 to 0.1	< 0.04 to 0.2	1.5 to 8.7	
	0.16 to 0.2	$\leq$ 0.47	$\leq$ 8.8	4.6 to 9.4
	0.31	0,88	14.1	11.5

[1)] laboratory and industrial used mixer-settler for U/Pu split
[2)] industrial mixer-settler used for Pu purification cycle only, laboratory mixer-settler used for both purposes
[3)] Tc content 350 ppm (Pu)

IHCH

Tab.8 AMMONIUM AND HYDRAZOIC ACID FOUND IN THE AQUEOUS PRODUCT AND ORGANIC RAFFINATE SOLUTIONS OF DIFFERENT EXTRACTORS

The behavior of technetium under the conditions of U/Pu split by electroreduction was studied by Kanellakopulos /22/. More than 95% of Tc fed to the extractor left with the Pu product; no increased $N_2H_5^+$ consumption (additional source of NH_4^+) was observed.

The last column of Tab.8 shows the hydrazoic acid concentrations found in the organic raffinate of the ELKE. The values measured in the organic U product (U/Pu split) are smaller. A comparison with the U/Pu split using U(IV) as reductant (MILLI) shows that HN_3 production is significantly lower in the electroreduction process.

CORROSION

The corrosion of Ti under cathodic conditions depends sensibly on the electrolyte composition and on the current density. Average corrosion rates estimated by different methods are shown in Tab.9. For the relevant and maximum HNO_3 concentration of 2,5 M gravimetric experiments show a drastic decrease of corrosion in presence of reducible cations (row 1, Tab.9); no definite influence of current density is detected in this case. Traces analysis in the product solutions confirms this effect for the various pieces of equipment. Only a small increase of corrosion is observed at higher ROXI current densities (row 2 and 3). Thickness measurements of the PUTE-ROXI channel sheets show after an operating period of 1950 h comparably small corrosion rates of 23 micrometer per year even at current densities up to 135 $mAcm^{-2}$ (last row). The corrosion rate of hafnium estimated from traces analysis amounts to 7,7 micrometer per year at current densities of 50 mA cm^{-2}.

The anodic corrosion of platinum increases with decreasing of HNO_3 concentration and increasing current-density and temperature /23/. The corrosion estimated by gravimetry, traces analysis and activation analysis /24/ for relevant electrolyte composition and current density amounts to a few micrometer per year. Fig.4 shows the rates as a function of current density.

CONCLUSIONS

- Compared with chemical separation processes for Pu, the electroreduction is the simpler process in the engineering and operation point of view. The process has all the advantages of the U(IV) feed process and avoids its drawbacks.
- Because of its simplicity and compactness electrooxidation has significant advantages as compared to the chemical oxidation process.
- The usual materials titanium, platinum and also hafnium show sufficiently low average corrosion rates to guarantee a long life-time of the electroredox equipment.

METHOD	ELECTROLYTE, M				AVERAGE CURRENT DENSITY in A cm^{-2}	ESTIMATED CORROSION RATE mm/a	REMARK
	$[HNO_3]$	$[N_2H_5^+]$	[U]	[Pu]			
GRAVIMETRIC	2.5	0.2			5 50	0.34 0.67	ca. 500 h
	2.5	0.2	0.1		5 15 50	0.022 0.088 0.018	
TRACES ANALYSIS OF Pu PRODUCT SOLUTION	≤ 0.5	≤ 0.5	≤ 0.01	≤ 0.1 - 0.15	≤ 5	≤ 0.009 < 0.002	2B - EMMA test operation WAK operation
	≤ 0.7 1.5 - 2	≤ 0.3 ≤ 0.1	≤ 0.04 ~ 0.002	≤ 0.16 ≤ 0.15	3 - 7.3 25 - 94	≤ 0.002 < 0.017	PUTE - ELKE PUTE - ROXI
MEASUREMENT OF SHEET THICKNESS	0.6 - 2.5	< 0.5	0 - 0.36	0 - 0.17	5 - 135	0.023	PUTE - ROXI after 1950 h operation

Tab. 9 TITANIUM CORROSION RATES OF ELECTROREDOX EQUIPMENT, T ≤ 50°C

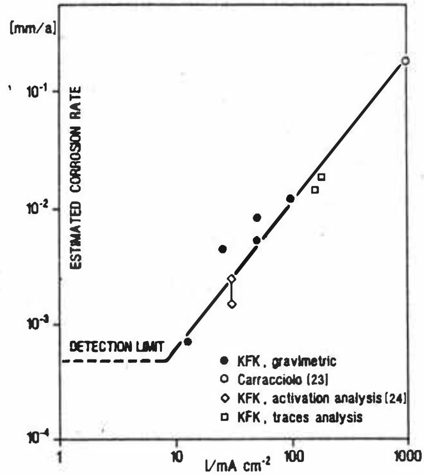

Fig. 4 PLATINUM CORROSION RATES AS FUNCTION OF ANODIC CURRENT DENSITY, T ≤ 60 °C

LITERATURE

/ 1/ F. Baumgärtner, E. Schwind, P. Schlosser
Deutsche Patentschrift 1905 51 (1970).

/ 2/ A. Schneider, A. L. Ayers
US-Patent 3616 276 (1971)

/ 3/ M. Krumpelt, et al., USAEC-Report ANL-7799 (1971)

/ 4/ Charvillat, Fabre, Le Bouhellec, Henry
Extraction'84, Dounreay, 27-29 Nov. 1984, EFCE Publication
Series No.43, p.1-17

/ 5/ G. Petrich, H. Schmieder, Proc. Int. Solv. Extr. Conf. ISEC'83.
Denver, Aug.26-Sept.2, 1983, p.84

/ 6/ H. Schmieder, F. Baumgärtner, H. Goldacker, H. Hausberger
KfK-Bericht, 2982 (1974)

/ 7/ F. Baumgärtner, H. Schmieder
Radiochimica Acta 25, 191-220 (1978)

/ 8/ H. Schmieder, H. Goldacker, M. Heilgeist, G. Petrich
"Fast Reactor Fuel Cycle", Conf., Proceed. British Nuclear Energy
Society, Paper No.47, London 1981

/ 9/ H. Schmieder
These, Institut National Polytechnique de Grenoble, 1984

/10/ H. Schmieder, H. Goldacker, M. Heilgeist, M. Kluth, H. Hausberger,
L. Finsterwalder
KfK-Bericht, 2957 (1980)

/11/ H. Goldacker, H. Hausberger, H. Schmieder, H. Wiese
Proceed. ANS-Conf., Sept.29 - Oct.2 1980, Gatlinburg, Tenn., USA

/12/ G. Petrich, Proc. Int. Solv. Extr. Conf., ISEC'80
Liège, Sept.6 - 12, 1980

/13/ G. Petrich, this conference

/14/ H. Schmieder, G. Petrich, A. Hollmann
J. Inorg. Nucl. Chem. 43, 3373 (1981)

/15/ M. Heilgeist, K. Flory, U. Galla, this conference

/16/ private communication

/17/ G. Petrich, U. Galla, H. Goldacker, M. Heilgeist, M. Kluth,
R. Schlenker, H. Schmieder, K. Ebert
Inst. Chem. Eng. Symp. Ser., 88, 267, (1985)

/18/ H. Goldacker, U. Galla, M. Kluth, R. Schlenker, H. Schmieder,
H. Evers, Proc. Int. Solv. Extr. Conf. ISEC'83, Denver, Aug.26 -
Sept.2, 1983, p.329

/19/ H. Schmieder, H. Goldacker, U. Galla, M. Heilgeist, M. Kluth,
G. Petrich
Proceed. ANS Meeting "Fuel Reprocessing and Waste Management"
Aug. 26 - 29, 1989, Jackson, Wyoming, USA

/20/ E. Warnecke, Dissertation, Universität Heidelberg 1975

/21/ M. Heilgeist
KfK-Bericht 3517 (1983)

/22/ B. Kanellakopulos, Kernforschungszentrum Karlsruhe,
private communication

/23/ V.P. Caracciolo, A.A. Kishbaugh, USAEC-Report, DP-896, 1964

/24/ J. Vehlow, Kernforschungszentrum Karlrsuhe, LIT, unpublished

REPROCX - A Reprocessing Flowsheet Computational System

J. W. Harrison, A. L. Mills, M. Wilkins, Chemistry Division, AERE, Harwell

Introduction

The preparation of flowsheets for nuclear fuel reprocessing comprises a number of well defined steps most of which involve the use of main frame computers for the solution of the many equations involved. Transfer of numerical data from one stage of the procedure to the next is by hand with a possible corruption or loss of data. The final flowsheet is drafted manually with manual insertion of numerical data. In some instances a 'Data Manual' is produced, again usually by manual methods.

This method of flowsheet production is time consuming and is open to error from the considerable amount of manual transcription of data involved. In the form described flowsheet calculation requires specialist knowledge and effort not usually available in Design Offices. The REPROCX suite of programs eliminates transcription errors and enables the total calculation and drafting procedures to be completed within minutes. Additionally a Data Manual can be obtained either as a 'hard' copy or on disc for further use. Due to the rapidity with which the calculations can be made, updating presents no problems and if an accessible file is maintained on a central computer difficulties arising from the use of 'old data' can be eliminated.

The REPROCX system comprises of a number of established computer programs which have been linked together to provide the required flowsheet. Since it is intended that the procedure shall be used generally in Design Offices an effort has been made to make the procedure as 'user friendly' as possible. Thus the total package is menu driven for the benefit of the non expert. The present procedure can accommodate various plant layouts and would appear to be capable of further development to include costing and process optimisation.

REPROCX

The principal steps in REPROCX are as follows:

Calculation of fission product and actinide inventories for a given fuel irradiated under specified conditions in a given reactor configuration. The user also specifies the post irradiation decay period for the fuel in question. The present version of REPROCX uses the UK program FISPIN to make the above inventory calculation. FISPIN output refers to single sub assemblies only and if the sub assembly is a compound unit such as a Fast Reactor sub assembly having a core section and integral top and bottom axial breeder sections then the calculation is done separately for each section. FISPIN outputs its data in gm atoms, gms, curies, becquerels, watts, etc. separately for each component section of the sub assembly. The data refer to the complete fission product and actinide spectrum produced in the reactor.

These FISPIN data are stored on file in the computer and are read by a second program, PROCESS. PROCESS requires that the mass of heavy metal (U + Pu, say) to be reprocessed per day is input together with the volume of liquor assumed to arise at fuel dissolution. If there is an increase in liquor volume from the dissolver stage of the flowsheet to the solvent extraction feed stage then this information is also input.

PROCESS then adds (for a compound sub assembly) the individual fission product and actinide nuclides from FISPIN and scales these data to the required heavy metal throughput for the reprocessing scheme. It then computes the concentration of the nuclides in terms of g/l, Bq/l, watts/l etc. for all these individual nuclides.

The next part of the procedure is to compute the solvent extraction flowsheet. There are a number of solvent extraction computation procedures in use although some of them have not been published in the open literature.

The programs in use can be split into three general classes, mixer settler type systems, e.g. SEPHIS, QUANTEX etc., column contactor type systems, e.g. PULCO, VISCO etc., and programs for centrifugal machines. Other classifications of solvent extraction programs might be made but the above will be used in the present paper. At the present time REPROCX incorporates the QUANTEX program and is therefore designated as REPROXQ(uantex), if PULCO were to be incorporated then the REPROCX version would be REPROCP(ulco) and so on.

The REPROCQ version considered in the present paper assumes a three cycle solvent extraction process with coprocessing in the first cycle (extraction, scrub and strip), and in the second cycle (extraction and scrub). This is followed by the U-Pu partition contactor and there are then parallel cycles of extraction, scrub and strip for the separated U and Pu streams. It is a relatively simple matter to change the configuration of the plant and process to fit any required scheme.

REPROCX requires that the inactive feeds, flows and compositions are input together with data such as stage number requirements and other information required by the solvent extraction program selected for use. This is identical to the procedure required for use of the solvent extraction program in the normal manner except that in REPROCX the necessary data for all the contactors in the total process are input at this time. Thus in the example flowsheet noted above, data for nine contactors are required. Any intercycle chemical adjustments to streams are carried out automatically provided that the necessary input reagents are stipulated together with the required adjusted conditions. The procedure then computes the solvent extraction flowsheet for the total process, feeding the appropriate product streams from one contactor to the next and listing raffinate streams together with the data usually obtained from the computational procedure if the program, say QUANTEX, were used in a more orthodox manner.

In addition to defining the distribution of U,Pu and acid throughout the process, REPROCX will select certain nuclides from PROCESS, say 95Zr, 95Nb, 103Ru, 106Ru etc. and will distribute these through the process according to decontamination factors input by the user. These decontamination factors are not computed from first principles. (If the necessary algorithm were available they could be included.)

The current version of REPROCX then sums the contents of the various waste streams as required by the user and will distribute the individual components of these streams as defined by the treatments to which they are to be subjected, e.g. precipitation, ion exchange, evaporation etc. Again the user inputs either the decontamination factor algorithm or the numerical decontamination factor expected. If the waste treatments take place at such a time after the waste is generated that the radioactive decay of certain species is important then the program will automatically correct for such decay. Where chemical procedures such as neutralisation and precipitation are used then the program will compute such items as alkali/acid requirements if requested. Similarly in the U and Pu conversion processes, say to oxide, where a distribution of fission products may occur between product and waste streams, these can also be quantified if the user specifies the decontamination factors. Since the sequence of work described above reads data from FISPIN or PROCESS data files then the numbers calculated are arithmetically correct.

Although the solvent extraction part of REPROCX gives the solvent extraction arisings, product and raffinate streams, it might be desirable to make some off line calculations based on U and Pu data to check that the process is chemically viable prior to using REPROCX. Although REPROCX will do this, if there is an error in the solvent extraction process, much of the computation will be wasted.

The output from REPROCX takes several forms:

The total FISPIN, PROCESS, QUANTEX (say), waste/product output listings for all the data calculated can be obtained. This can include graphical representation of the solvent extraction solute profiles showing the approach to steady state contactor by contactor. This output is voluminous and would not be required by most users of the system.

A data manual is also available. This summarises the waste streams and products from the solvent extraction, waste and product conversion processes and also tabulates any intermediate streams. All feeds as input by the user together with other input data are also summarised.

The data noted above may also be output to disc. As REPROCX data are calculated they are put on to disc storage on the main frame computer which can then be accessed via remote terminals. These data are always maintained as updated 'current' data. They may also be output to floppy disc for local use via a PC.

The last alternative is to output the data via a CAD computer to provide a fully drawn up fully quantified flowsheet. This latter is the form preferred by most users of REPROCX.

The main frame records are accessed via a menu system, REPDATA.

In addition to providing formal design data, REPROCX enables Design Offices to examine process, fuel or reactor variations easily and rapidly. Further, dependant upon the output device very high quality printed or drawn copy may be obtained, quickly and accurately.

The ability to read data directly from one program or data file to another has eliminated transcription faults from flowsheet production and calculation.

Having described the functions of the component parts of REPROCX the organisation of the system will now be examined together with a description of the menu drive system for REPDATA and REPROCQ.

Program Data Organisation

The acronym for the programs FISPIN, PROCESS, QUANTEX is REPROCQ and is the presently implemented member of the general set REPROCX where X can be Q(QUANTEX), S(SEPHIS), P(PULCO) etc. Since a fairly large amount of data has to be input into the scheme described above a facility is provided which reduces the input data to a 'form filling' exercise. Following the command REPROCQ at a suitable terminal (VDU) the user is presented with a consecutive set of display panels. Each panel is in the form of a questionnaire containing instructions to the user to provide information in the form of names and numbers. Default values are supplied on each panel and warnings are issued to the user if incorrect data are entered. As well as assembling the input data the panel entry system also generates data sets required for the computation. When the input of data is complete the calculation is started.

Output from the Calculation

The output from the calculation has been basically described above.

In addition to what has already been noted a summary is provided of the whole plant calculation as a description of the plant interconnections, U, Pu, acid concentrations and main fission product isotope radioactivities in all the input and output streams, times to reach mass balance in the contactors and any warning messages generated in the calculation, e.g. low acid may cause Pu hydrolysis, too high an organic Pu concentration might give rise to third phase etc. A second part of the output consists of a data set stored in the computer comprising all the flowsheet tables generated in the calculation. The main purpose of this output is as source input data for the flowsheet drawings themselves. The drawings are stored separately on the CADAM (Computer Graphics Augmented Design and Manufacturing-CADAM Incorporated) system. These drawings are separately prepared and contain blank spaces which are allocated table numbers. After the REPROCQ calculations have been performed a separate computer operation transfers the stored tables to the blank spaces provided in the stored flowsheets. A secondary use for the stored tables is as a source of data for plant operators who may easily access the tables from a terminal (VDU).

Other Features of REPROCX

Since the organisation of REPROCX is as a sequential series of steps in which separate programs are executed obtaining data from and writing data to disc storage, it is a simple matter to add further programs to the system. This has already been done to provide table generating facilities for the flowsheet for tables not associated with plant streams themselves but with other plant operations such as waste treatment and product finishing.

Performance of REPROCQ

REPROCQ has been implemented on an IBM3084Q system at Harwell with FORTRAN77 as the source code language and using software of the SAS Institute Inc of North Carolina for the graphical output of QUANTEX. Typical running time for the FISPIN section of the calculation is about five minutes with a further one and a half minutes for a nine contactor solvent extraction plant. The transfer of tables to a flowsheet is accomplished in about fifteen seconds.

The panel entry system for the input of data was written using IBM TSO command language with the IBM ISPF (Interpretive System Productivity Facility) facility.

REPDATA

REPDATA is the program used for the retrieval of data from the data sets in REPROCX. It is operated via a menu system. A sequence of VDU screen displays requires the user to enter the reactor name, fuel zone, (for a fast reactor this could be inner, outer or radial breeder zone), the fuel burn up and the post irradiation decay time. The data sets from REPROCX contain data relevant to various reactors, fuels and irradiation conditions of interest and the user of REPDATA is obliged to select from the data on offer. This selection results in the generation of an identifier, e.g. CFI15#OP.C1#5Y which is interpreted as: Commercial fast reactor inner core fuel 15% peak burn up at 1.5 years decay, the 'hash' symbol is used to denote the decimal point in this identifier. After confirming the correctness of the identifier the user then has access to the index of tables of stored data. He may then scan the index and select the required data. This will be displayed on the VDU screen and if required a hard copy may then be printed off.

Although REPDATA and REPROCX do not necessarily cover all the possible combinations of irradiation and cooling times for any fuel, REPDATA enables a selection to be made from the most likely combination of these variables. If the exact burn up or cooling time is not available then REPROCX may be used to generate the data.

Conclusion

REPROCX is a suite of computer programs accessed via a menu system which enables a 'non expert' user to obtain quantitative data for irradiated nuclear reprocessing flowsheet design. The output from REPROCX is in several forms subject to selection by the user.

The subsiduary program REPDATA enables pre computed data relevant to specific fuels at given irradiation and decay times to be readily accessed.

The complete suite of programs represents a considerable saving in time in the calculation and drafting of nuclear fuel reprocessing flowsheets.

Technetium behaviour control in the Purex Process

E. VIALARD, M. GERMAIN
CEA-IRDI-DERDCA-DGR-SEP-SCPR
92265 - Fontenay-Aux-Roses Cédex

Technetium has been neglected for a long time in reprocessing nuclear fuels, but recent studies have emphasized its anomalous behaviour : it is fairly extracted by TBP and it catalyses hydrazine decomposition by nitric acid. With today's increased burn-up fuels a low technetium decontamination factor is expected and reoxidation risks are enhanced in the uranium-plutonium partition.

This paper deals with an examination of technetium behaviour and an attempt to limit the risks using slight modifications of the flowsheets.

Technetium extraction :

Pertechnetic acid, the heptavalent state found in the fuel dissolution liquor, is extracted by TBP. From 3N nitric acid extraction by 30 % TBP-dodecane is however rather low (D(Tc) = 0.1) and of little importance in Purex systems. The main extraction process is coextraction with extractible cations. It was observed the first time by SIDDALL [1] with uranyl nitrate : technetium extraction is enhanced by the formation of a uranyl pertechnetate complex in the organic phase.

Since SIDDALL's work other cations were found to give the reaction which is the most effective with tetravalent metals like thorium [2], plutonium [3] and zirconium [4].

In the Purex process, the main elements involved in technetium extraction are uranium, plutonium and zirconium. Literature data as well as our own measurements indicate that the reaction is roughly described by :

$$M(NO_3)_{n\,org} + TcO^-_{4\,aq} \rightleftarrows NO^-_{3\,aq} + M(NO_3)_{n-1}\,TcO_{4\,org}$$

and expressed by

$$D_M(Tc) = K_M \frac{K_A}{K_A + [H^+_{aq}]} \quad \frac{[M_{org}]}{[NO^-_{3\,aq}]}$$

where K_A is the dissociation constant for $HTcO_4$, if we suppose that technetium is at a trace level.
The linear dependance of the partition coefficient on the organic concentration of the cation is shown on the figure 1 for the three metals.

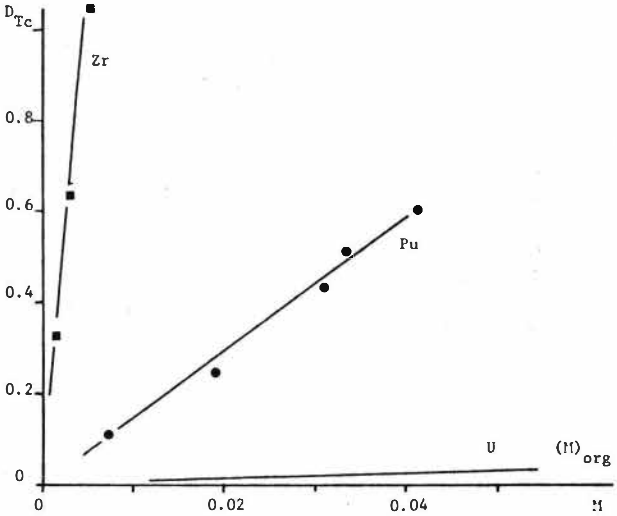

Fig.1:Variation of the Technetium partition coefficient from 4N HNO_3 with the organic concentration of the metal.

We measured the following values for the extraction constants :

$K_U = 8$; $K_{Pu} = 160$; $K_{Zr} = 2500$

If we try to estimate technetium extraction in the Purex process we must take into account the abundance and the extractibility of these metals. Uranium and plutonium are both quantitatively extracted but zirconium, which is slightly extractible (figure 2), is removed from the solvent by scrubbing.

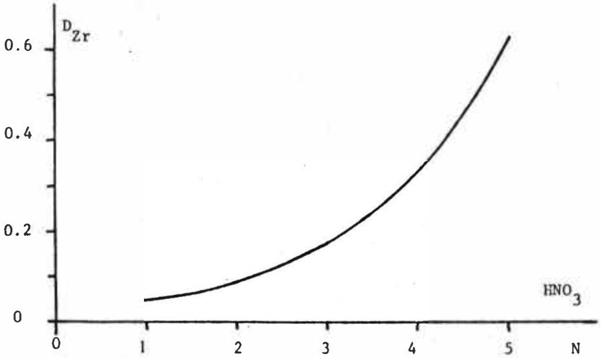

Fig.2:Zirconium extraction by 30% TBP.

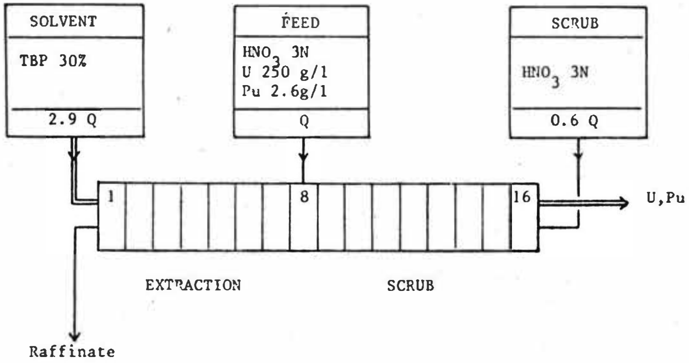
SOLVENT
TBP 30%
2.9 Q
FEED
HNO_3 3N
U 250 g/l
Pu 2.6g/l
Q
SCRUB
HNO_3 3N
0.6 Q
1
8
16
U,Pu
EXTRACTION
SCRUB
Raffinate

Fig.3:Standard flowsheet for PWR reprocessing first extraction.

If we consider a typical first extraction flowsheet for reprocessing standard PWR fuels (figure 3) the uranium and plutonium profiles are rather flat in the scrub section and the first extraction stage and they decrease sharply in the following extraction stages (figure 4). Zirconium profile is very different. This FP is fairly extracted in the absence of fissile materials (80 % yield in the extraction stages) and effectively stripped in the scrub.

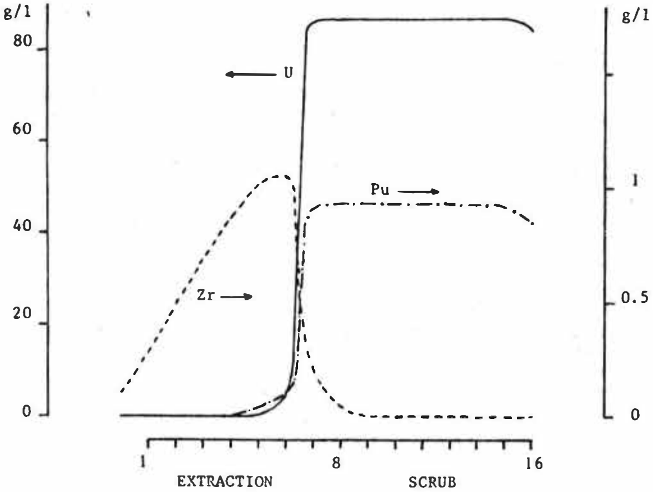

Fig.4:Organic concentrations profiles for a standard flowsheet.

We obtain therefore a zirconium accumulation with a peak height reaching sixfold the feed concentration.
Hence, in the extraction section, technetium is quantitatively coextracted with zirconium (D(Tc) being greater than 1) and is hardly removed from the solvent in the scrub section because of the coextraction with uranium and to a lesser extent with plutonium (D(Tc) ≈ 0.35).
Thus limiting technetium extraction may be achieved by complexing zirconium in the aqueous phase in order to decrease its extractibility [5]. We proposed to use oxalic acid which also complexes plutonium and uranium.
Equilibria constants however show that zirconium complexation by one or two oxalate is favoured :

	Zr^{4+}	Pu^{4+}	UO_2^{2+}
Log β_1	10.5	8.7	5.8
Log β_2	21	16.9	6.9

It is therefore possible to adjust the oxalate addition to a level permitting a quantitative zirconium complexation without any decrease of the fissile material extraction : the optimal oxalic to zirconium molar ratio R stands at 2 (figure 5).

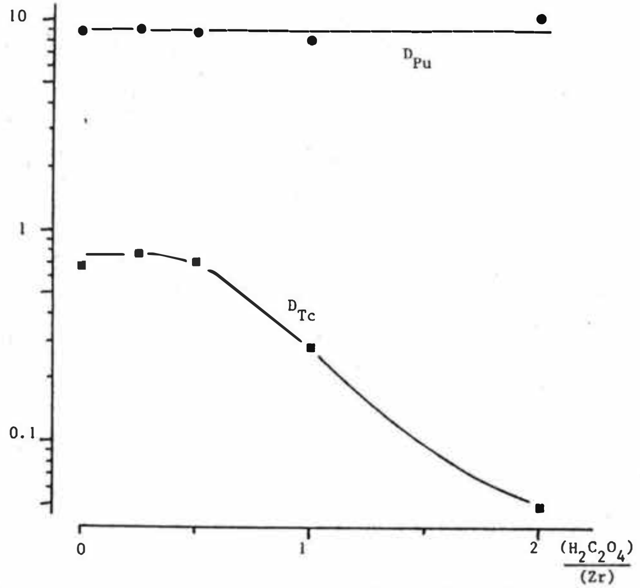

Fig.5: Influence of the oxalic to zirconium ratio on the extraction of technetium and plutonium.

Counter-current runs were performed with a standard flowsheet but a limited number of stages (extraction : 6 and scrub : 2). Oxalic acid was added to the feed. Different R ratio values up to 2 were tested and the technetium DF increased up to fourfold which means a significant reduction of the hydrazine consumption in the U/Pu partition.

$R = \frac{[H_2C_2O_4]}{[Zr]}$	DF_{Tc}
0	1.2
0.5	1.3
1.5	3.7
2	5.1

A higher DF seems rather impossible because of the slight technetium coextraction with uranium.

Technetium behaviour in plutonium reduction

WILSON and GARRAWAY [6] indicated that technetium catalyses hydrazine decomposition by nitric acid. From our own measurements in Purex conditions (figure 6) the reaction may be considered in first approximation as zero order with respect to hydrazine concentration ; but its rate depends largely on the technetium concentration.

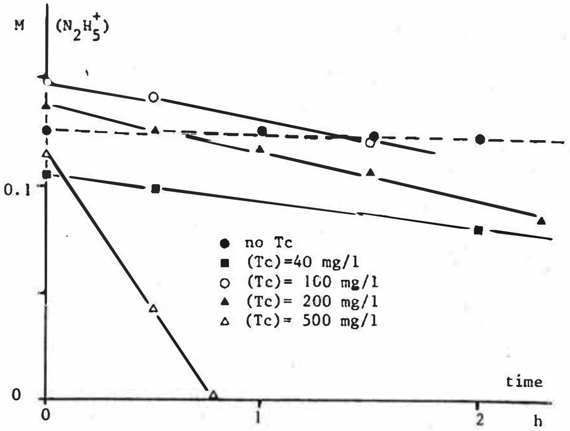

Fig.6: Decomposition of hydrazine in 1N HNO_3 at 40°C(Pu present).

A stabilizing agent is however necessary when uranous nitrate is the reductant and none is better than hydrazine. In order to keep stable reducing conditions we have to change the reductant. Hydroxylammonium nitrate (HAN) is suitable for the partition and can be used without hydrazine because of its little nitrous scavenging power. Figure 7 shows it is unaffected by the presence of technetium.

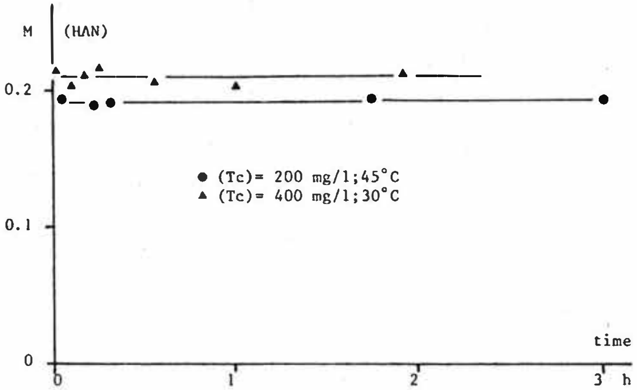

Fig.7: Stability of HAN in 1.5N HNO_3.

The use of HAN is therefore another good answer to the technetium problem in the U/Pu partition.

References :

[1] T.H. Siddall, DP - 364 (1959)

[2] F. Macasek and J. Kadrabova, J. Radioanal. Chem., 51, 97 (1979)

[3] E. Vialard and M. Germain, Internat. Conf. on Nucl. and Radiochem., Oct. 8-12, 1984. Lindau, FRG.

[4] T.N. Jassim, G. Persson and J.O. Liljenzin, Solv. Ext. and Ion. Exch., 2, 1079 (1984)

[5] A. Bathellier, J.Y. Pasquiou and E. Vialard, (submitted for publication).

[6] P.D. Wilson and J. Garraway, Inter. Meeting on Fuel Reproc. and Waste Manag., Aug. 26-29, 1984, Jackson Hole, Wy, USA.

Solvent Regeneration Development at the Idaho Chemical Processing Plant

A. L. Olson, C. W. McCray, Westinghouse Idaho Nuclear Company, Inc., Idaho Falls, ID, USA

The Idaho Chemical Processing Plant (ICPP) is a reactor fuel reprocessing facility which uses a variation of the PUREX solvent extraction process for the recovery of fissionable material from spent reactor fuel elements. Also located at the plant are spent fuel storage facilities, high level liquid waste storage, high level liquid waste solidification facilities, and low level liquid waste treatment systems.

The fissionable material recovery process consists of total dissolution of the fuel elements in an aqueous acidic environment to yield a solution containing 1 to 10 grams per liter of heavy metal. The heavy metal is extracted from the aqueous stream utilizing a 6 to 30 volume percent solution of tri-n-butyl phosphate (TBP) in a n-dodecane diluent. Scrubbing of this organic phase with aluminum nitrate and ammonium hydroxide or with nitric acid to achieve better fission product decontamination, and stripping of the heavy metal from the organic phase with dilute nitric acid completes the solvent extraction cycle. Three solvent extraction cycles are employed at ICPP to produce a heavy metal nitrate product solution.

The most significant single parameter which affects solvent extraction process operability and product purity is the quality of the solvent. Hydraulic stability of the solvent extraction contactors and decontamination of the heavy metal from fission products is directly traceable to the solvent quality. The solvent quality in the PUREX process is compromised by the formation of degradation products.

Degradation products are formed in the solvent due to contact with highly radioactive aqueous solutions containing nitric acid and other chemicals which cause radiolysis and hydrolysis. The primary degradation products of TBP are dibutylphosphoric acid (HDBP), monobutylphosphoric acid (H_2MBP), and butyl alcohol. The primary diluent degradation products are thought to include nitro alkanes, hydroxamic acids, carbonyls, and alkyl nitrates. It is postulated that the chemically complex and troublesome fission product ruthenium complexes with and is carried along with these compounds. These compounds can combine with metal ions and result in the formation of emulsions, interfacial cruds, and potential product losses. The solvent degradation rate is enhanced by increasing the metal ion and acid concentration, radiation exposure and temperature.(1,2)

The most widely used solvent treatment method is sodium carbonate scrubbing, which is presently used at ICPP. Its effectiveness has been well demonstrated at various fuel reprocessing facilities. Its success can be attributed to the acidic nature of most degradation products, especially those of TBP. It has not, however, been proven as effective with diluent degradation products. Potassium permanganate as an additive to the sodium carbonate has been somewhat successful.(3) The disadvantage of this method is that it produces a quantity of permanent salts which increase waste volumes and significantly interferes with the ICPP high level liquid waste solidification process. Alternative chemical washes have been suggested, such as hydrazine oxalate and hydrazine carbonate. These have been discarded at ICPP since they are no more efficient than sodium carbonate, they do not remove diluent degradation products, they are difficult to prepare and store, and they present potential safety hazards.

Diluent degradation products and their removal from the solvent are not as well understood as TBP degradation products. Recent research (4,5) has shown that the diluent degradation products can be removed by passing the solvent through a solid sorbent bed packed with activated alumina. This bed was also shown to remove TBP degradation products. Engineering problems could be foreseen with this process since it has not been used in an operating plant. They included the potential generation of additional radioactive solid waste, how to extend the bed life and what bed regeneration techniques might be available to make the process more operable in a radiochemical plant. Many other treatment methods have been considered and tested.(2)

Following a thorough literature survey, a solvent treatment scheme was chosen for the ICPP and development initiated. The method chosen is as follows. Two primary treatment systems would be utilized. The solvent would be separated into two distinct systems; one system for the first and second extraction cycles and one for the third extraction cycle. This would prevent contamination of the third cycle product with compounds contained in the solvent from the first extraction cycle. The primary treatment method for both systems (depicted in Figure 1) would be sodium carbonate scrubbing followed by a dilute nitric acid wash and would take place in pulse column contactors. Familiarity and effectiveness were the prime considerations in these choices. A pulse column pilot plant was also available for testing purposes.

The sodium carbonate scrub solution would be recycled within the system. It is estimated that the sodium discharge to waste storage could be reduced by 75% to 80%. With recycle of the sodium carbonate and controlling the removal rate of spent scrub solution by monitoring the pH of the scrub solution. The effectiveness of the sodium carbonate scrub solution is dependent upon the pH.

By closely monitoring this parameter it is felt that this sodium discharge reduction can be achieved. Very light flocculant precipitates have been observed floating in the solvent during laboratory experiments at ICPP. These are believed to be metal complexes, primarily of zirconium and ruthenium. Sintered metal filters, with a mean pore diameter of 40 microns have been placed downstream of the sodium carbonate scrubber to remove these. The precipitates are easily driven back into solution by contact with nitric acid solution and the filters will be backwashed as needed with this method. The use of a dilute nitric acid wash is thought to remove additional organic sodium soluble compounds not removed in the first sodium carbonate scrubbing contactor.

A secondary treatment method was identified to provide the best solvent quality possible for the third extraction cycle. The solvent would pass through a bed of solid sorbent material, which would adsorb diluent degradation products not removed in the primary sodium carbonate-nitric acid washes. The sorbent bed would be placed downstream of the primary treatment system to extend the life of the sorbent material. The active sites on the surface of the adsorbent would not then be occuppied by a larger concentration of TBP degradation products. In addition to its use as a third cycle solvent polish, the solid sorbent bed could be utilized to remove a buildup of diluent degradation products from the first and second cycle solvent when required.

Plant experience was not available for the solid sorbent method of solvent treatment and several questions needed to be answered prior to development of the system. Some of these questions included: What is the most efficient solid sorbent material and what would the loading capacity be?; Could the bed be regenerated, and if so, by what method and how many times?; How much and what type of solid waste would be generated?; Since the solvent contains a quantity of dissolved water which could take up available adsorbent sites in the bed, how could the water be removed? Could the process be remotely operated in a radioactive environment?; What were the operating conditions and parameters? Laboratory scale testing was initiated to answer some of these concerns.

Experiments using plant solvent revealed that the solvent could be dehydrated by contact with dry air. A packed column contactor was proposed and scoping tests performed. These were very successful. From a saturation level of about 7 grams per liter, the water content could be reduced to less than 0.2 grams per liter. Bed loading capacity tests using activated alumina showed that about 1800 bed volumes could be treated before breakthrough occurred. The solvent was dehydrated prior to passage through the bed. This would result in solid waste volume generated of less than 0.1 cubic meters per year of ICPP operation, if the bed could not be regenerated. Further tests indicated that a crude steam-strip regeneration of the bed would allow a reloading capacity of about 1000 bed volumes before breakthrough.

After the laboratory testing was completed, it was felt that enough data were available to build an engineering scale pilot facility (Figure 2). The solvent dehyration and solid sorbent bed steps were integrated and the pilot plant constructed. The pilot plant is approximately full-scale with respect to the third extraction cycle of the proposed plant unit. Simulated degraded plant solvent was used during initial testing and solvent from the pulse column pilot plant will be used as available. Since the pilot facility is not shielded, testing with radioactive solvent cannot be achieved. However, it is believed that through extrapolation of laboratory data and use of the pilot facility data, enough information will be available to accurately predict system performance.

Initial data analysis indicates that the process has the potential of returning solvent with a quality level much higher than as-received from the manufacturer. Delivered solvent contains about 1 volume percent impurities which include dibutyl and monobutyl phosphate and aromatics. ICPP solvent quality in the plant is measured by its interfacial tension, which is directly related to the phase separation time, and the retention of metal complexants such as zirconium and heavy metals. The presence of diluent degradation products, although not directly monitored in the plant, is verified by an infrared scan. Solvent treated by the solid sorbent bed possesses an interfacial tension of 0.023 to 0.014 N/m for 10 and 30 volume percent TBP, respectively. Essentially no complexants are measurable and an infrared scan shows no diluent degradation products. This is as compared to untreated solvent which may have an interfacial tension of approximately 0.007 N/m, contain about 1×10^{-4} molar complexants, and contain significant concentrations of nitro alkanes, alkyl nitrates and carbonyls.

Further basic solvent research is being supported at the University of Idaho. It is felt that if the solvent degradation compounds can be identified and characterized, more effective solvent treatment chemicals and methods can be developed.

REFERENCES

1. D. A. Orth and T. W. Olcott, "PUREX Process Performance Versus Solvent Exposure and Treatment", Nucl. Sci. Eng. 17, (1963)

2. J. C. Mailen and O. K. Tallent, "Solvent Cleanup and Degradation: A Survey and Recent ORNL Results", ANS Topical Meeting, Fuel Reprocessing and Waste Management, Jackson, WY, August (1984)

3. Rockwell Hanford Operations, "PUREX Technical Manual", US-DOE Report RHO-MA-116.

4. O. K. Tallent, J. C. Mailen and K. D. Pannell, "Solvent Cleanup Using Base (NaOH or LiOH) Treated Silica Gel Solid Adsorbent", UD-DOE Report ORNL/RM-8948 (1984)

5. J. C. Neace, "Diluent Degradation Products in the PUREX Solvent", Separation Science and Technology, Vol. 18, Nos. 14 & 15, (1983)

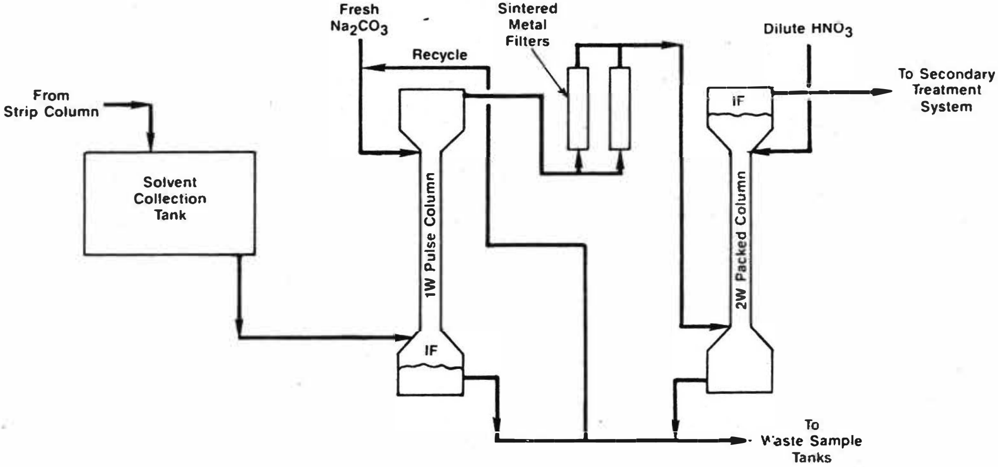
Fresh
Na_2CO_3
Sintered
Metal
Filters
Dilute HNO_3
Recycle
To Secondary
Treatment
System
From
Strip Column
Solvent
Collection
Tank
IF
1W Pulse Column
IF
2W Packed Column
To
Waste Sample
Tanks

ICPP-S-12872
(3-86)

Figure 1.
Primary Treatment System

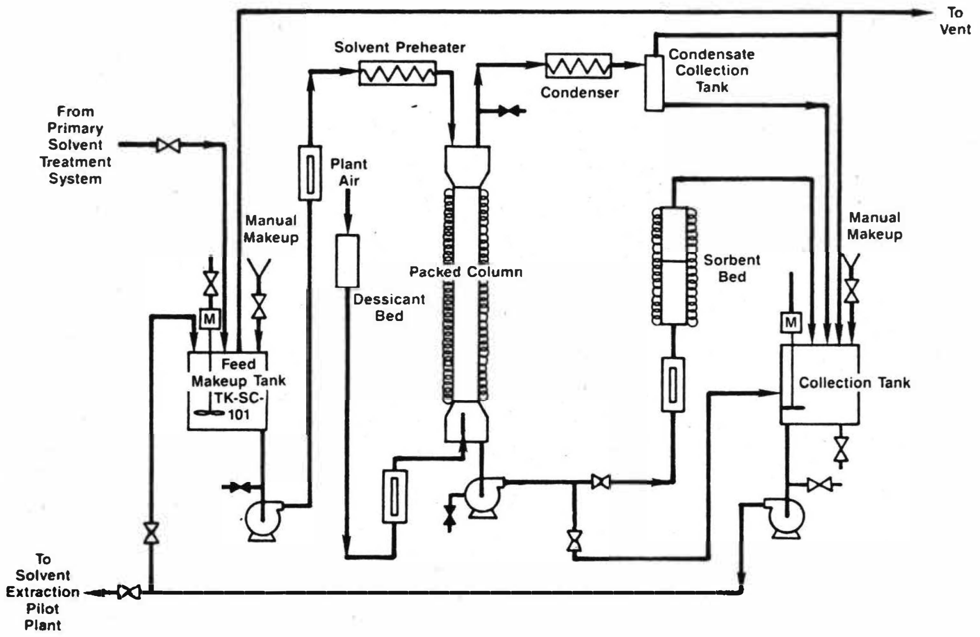
To Vent
Solvent Preheater
Condenser
Condensate Collection Tank
From Primary Solvent Treatment System
Plant Air
Manual Makeup
M
Packed Column
Dessicant Bed
Sorbent Bed
Manual Makeup
M
Feed Makeup Tank TK-SC-101
Collection Tank
To Solvent Extraction Pilot Plant

ICPP-S-12871
(3-86)

Figure 2.
Secondary Treatment System Solvent Cleanup Pilot Plant

Model Reference Adaptive Control System of Liquid-Liquid Extraction Column.

A. AL KHANI. M.V. LE LANN, K. NAJIM and G. CASAMATTA, ENSIGC, U.A. 192 CNRS,
Chemin de la Loge 31078 TOULOUSE CEDEX/FRANCE /GRECO 69/

Application of the well-developed optimal control theory to industrial plants is generally confronted with difficulties. Firstly, there is necessity of elaborating an adequate model of the controlled process. This is often quite a difficult task, especially in the industrial sectors such as chemical, mining, metallurgical and biological sectors where, usually the developed models are static. Secondly, even in the case where a mathematical model is worked out, the necessary conditions of optimality need excessive computer time and memory to be solved on-line ; Therefore, it is more preferable to establish approximate on-line control policies which can be applied to practical situatins, and adapt themselves to varying conditions. The theory and application of adaptive control have been developped very intensively and the developed of microcomputers permits now the implementation of complex adaptation algorithms.Among these approaches, the self-tuning regulator and the model reference adaptive system seems to be more attractive. Extraction columns are well known and widely used equipements for separation purposes in the field of the heavy and in the fine chemical industries. The behaviour of columns is strongly non linear, with varying dynamics, more over they are exposed to a lot of non expected of non controlled perturbations, such as the solvent purity and quality (fresh or recuperated), temperature, the feed flow rates and the presence of surface active impurities. All these perturbations may put out of work any controlling system with fixed parameters or with tuff dynamics.The present work is related to the application of model reference adaptive control M.R.A.C. system to a sieved plate pulsed extraction column. The control purpose is to maintain it in its optimal operating gone, i.E. close to the flooding point. The control action is based on a low order discrete model with time varying parameters. This paper is organized as follows :

section A : A description of the column and of the property of the Liquid system is shown
section B : The adaptive algorithm which is evaluated is described
section C : The hardware end software control aspects are presented
section D : Experimental results are shown that illustrate the successfull application of such an adaptive algorithms to an extraction column
section E : References - bibliography

SECTION A : DESCRIPTION OF THE INSTALLATION :

a) A pilot plant column as shown on fig(1), consisting of :

1: A 1.10 m in high extraction column, constructed from glass tubing of 0.05 m in diameter ; two wider sections, the head and the bottom are fitted to the active section. The bottom section contains the agitation mechanism which is composed of a pulse line of 0.05 m in diameter and a pulsor ; the active section contains 23 stainles steel sieve plates of 0.05 m in diameter, which are drille drilled with holes 0.002 m on a triangular pitch giving nearly a 19% free area These plates are setted on a fixed distance of 0.05 m between each of them ; the total volume of the column is about 7 liters. While the feeding light solvent dispersed phase pass throw a distributor located at the bottom of the column, the heavy continuous one is intruduced in from the column head. The head section contains the settling zone, the interface level of which is controlled by means of a capacity probe, which deliver a tension proportionnally to the interface level ; the delivered tension is compared respectively to two desired lowest and highest values for the interface level.

The resulting signal from the capacity probe commands a relay, which provides an on and off actions on an electromagnetic valve controlling the output of the heavy phase. By means of a conductivity sond which is implanted below the light dispersed phase distributor we can detect the apparition of the flooding zone in the column.

2: Two electromagnetic flow meters are used for measuring the feed flow rates of the two phases.

3: A continuous differential refractometer is used to measure the concentration of solute in the raffinate heavy phase.

4: Two feed pomps, one for each phase.

5: Three DC electrical motors are used to drive the pulsing mechanism and the two feed pomps ; a speed control box can command the motors by a 0-10 V continuous tension, so that we can achieve the automatical control of the feed flow rates and the agitation frequency.
0 : A conductimeter is used to measure the conductivity signal obtained from the conductivity sond, described latter.

b) Hydrodynamic Behaviour and Flooding of a Pulsed sieve Plate Column :

It has been proved that the pulsed column operates within five modes of hydrodynamical behaviour /1/ which depend on the agitation intensity and the input flow rates /2/.
The five operating modes can be described as follows

1 - Mixer - settler mode
2 - Emulsion mode
3 - Cyclic local flooding mode
4 - Flooding by intensive pulsation frequency
5 - Flooding by weak pulsation intensity

Flooding is exhibited by the apparition of a fluidized-like liquid-liquid swarm of drops below the dispersed phase distributor /3/.

Optimal operating and efficiency

Among there modes of functioning, the optimal operation can be characterized by the efficiency of the extraction mass transfer process ; on the other hand, the best efficiency of the column is corresponding to the maximum of the residual concentration measured in the heavy phase effluent. It has been found that the optimum operating functioning was achieved at the transition operating zone between the emulsion and the cyclic local flooding mode ; therefore we can get to this zone on tracing the decreasing conductivity sond signal, this signal is related to the fluidized like liquid-liquid swarm layer thickness developing below the distributor /3/.
In order to keep the operation within the optimal range, it is convenient to use the pulsing frequency as the command variable due to its dynamics. We have to mention that while operating within the transition zone, that column will be in its critical operating point, so it is easy to be slopped into the weak efficacy cyclic local flooding mode under the influence of a perturbation over the feed flowrates or an inconvenient excessive agitation intensity.

c) Operating conditions

We've realized two series of experiments using two systems :
1: Deminerized water and commercial toluen
2: Deminerized water, commercial toluene and pure aceton, the aceton concentration in the continuous phase inlet was about 5 % weight. There are standard system /4/.

In our experiments we've used extraction factors nearly E = 1. For the purpose of automatical control we had to test the column using step functions and to determine its response time delay constant, and the operating interval within which the column is completely commandable and in the sometime is keeping its maximum efficiency

- STEP function tests :

We've realized two series of echelons experiments over the pulsing frequency :

$$0.0 \text{ HZ} < F < 2.0 \text{ HZ}$$

the higher frequency value was fixed at 2.0 HZ because of mechanical safety reasons, while the pulsing amplitude has been fixed and equal to 0.015 m.

The first series correspond to the first system ; it has been carried out with the following feed flow rates :

light dispersed phase : 12.0 LIH < Qd < 14.0 LIH

heavy continuous phase : 10.0 LIH < Qc < 12.0 LIH

its shown on table (1) below, that we've traced the changement from the steady state under the action of the following step echelons :

fig	F(HZ) starting value	F(HZ) final value	% F(HZ) relative steps amplitude
2	1.1	1.35	28
3	1.35	1.50	16

table(1)

Presented results on fig (2,3) allow to analyse the column reactions to the echelons and to understand its sensibility at the different points within the whole operating interval ; we can easily distinguish the emulsion mode from the cyclic local flooding mode which results in a periodical movement, which may be detected by the conductivity probe.

The second series of tests was for the ternary system : we can see on fig(4) the column reactions under different step echelons from different steady states points

fig.4	F(HZ) starting value	F(HZ) final value	% F(HZ) relative steps amplitude
I	0.87	1.45	48.3
II	0.83	1.60	64.1
III	0.83	1.95	93.3

table(2)

After our analysis of the column dynamic behaviour we have determined an operating interval, between 0.55 ms/cm for the first system, and a second between 0.45ms/cm and 0.25 ms/cm for the second system, within which the column is completely controlable.

SECTION B : THE MODEL REFERENCE ADAPTIVE ALGORITHM :

We will present the broad out lines of the algorithm developed by I.D. Landau and Lozano /5/. The control purpose is to design a control signal so that any initial perturbation will be canceled with the dynamics defined by :

$$C_2(q-1)\ y(t+k) = 0 \qquad \ldots (1)$$

where

$$C_2(q-1) = 1+C^1 2\ q^{-1} + \ldots + C^L 2\ q^{-1} \qquad \ldots (2)$$

is an asymptotically stable polynomial. Therefore, the control law is given by :

$$P(t)\Phi(t) = C_2(q-1)\ y^M(t+k) \qquad \ldots (3)$$

where

$$\Phi(t) = \left\{ \mu(t),\ \mu(t-1), \ldots,\ \mu(t-k-n_B+1),\ y(t), \ldots,\ y(t-n_R) \right\} \ldots (4)$$

$y^M(t)$ is the output of the reference model and n_R is equal to :

$$n_R = \max\ (n_A-1,\ L-1) \qquad \ldots (5)$$

The controller parameter P(t) will be adapted by the following algorithm :

$$P(t) = P(t-1) + F_\delta(t)\ \Phi(t-k)\ \gamma(t) \qquad \ldots (6)$$

$$F_o(t+1) = \frac{1}{\lambda_1(t)}\left\{F_o(t) - \frac{F_o(t)\phi(t-k)\,\phi^T(t-K)\,F_o(t)}{\frac{\lambda_1(t)}{\lambda_2(t)} + \phi^T(t-k)F_o(t)\phi(t-k)}\right\} \quad \ldots (7)$$

with $$\gamma(t) = \frac{C_2(q^{-1})y^M(t) - P(t-1)\phi(t-k)}{1 + \phi^T(t-k)F_o(t)\phi(t-k)} \quad \ldots (8)$$

where $0 < \lambda_1(t) \leqslant 1 \quad ; \quad 0 \leqslant \lambda_2(t) \leqslant 2 \quad ; \quad F_o(0) > 0 \quad \ldots (9)$

A general block diagram of the Adaptive Algorithm

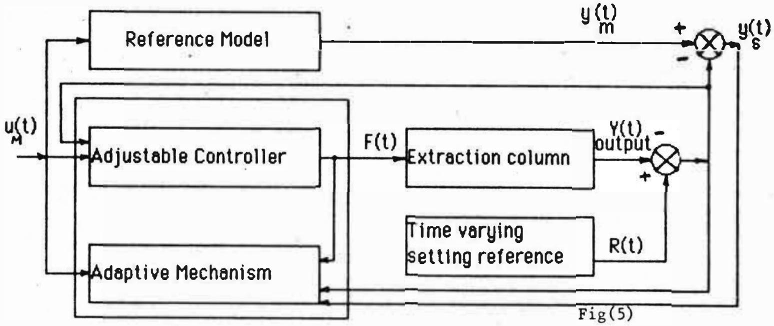

Fig(5)

where $y_M(t)$: reference model output
$y(t)$: real output (the measured conductivity)
$R(t)$: output of the time varying setting reference
$F(t)$: pulse frequency (HZ)
$\mu_M(t)$: model reference input
fig(5): block diagram of the M.R.A.C.

SECTION C : HARDWARE AND SOFTWARE CONTROL ASPECTS :

a) As shawn on fig(1), the apparatus are interfaced with an APPLE II microcomputer, associed to 12-bit digital-analog and analog-digital converters devices, throw which the conductivity signal, the refractive idex, and both florates signals are inputted. The hardware conception allows :
- on-line acquisition of the flow rates of both feed phases, of the conductivity measured signal, of the concentration of solute at the outlet of heavy continuous phase
- digital command of the pulsing frequency and the two feed pomps
- programming of the controller algorithms.

The controlling programm has been realized in PASCAL UCSD. It calls external assembly routines performing D/A and A/D conversions, and the clock reading for real-time control and on-line data sampling period.
- The sampling interval has been determined as equal to 10 seconds, and the occupied volume from the programm is about 8 k bytes. On fig(6) we present a general structure of the controlling algorithm.

b) Applied strategy and initialization :

I- Getting in consideration the non linear behaviour of the column and the previously described tests, we have applied a new controlling strategy consisting in the following points :

1: we bring manually the column to a desired initial steady state choosen within the operating interval determined in section (C), where we can trust the column stability. This is necessary because during the early moments when the algorithm is identifying it's parameters, the control may provide erratic commands.

2: Then we switch the computer to get the control of the column, as shown on figs(7,8).

3: We approach step by step towards the desired final operating point, by progressively modifying the reference value of the conductivity, The examination of figs(7,8) proves that our strategy of convergence based on a time varying reference value has revealed itself satisfactory and that it can helps the adaptive strategy, by smoothing the reseach of the critical desired operating point.

II The initialization step is very important, it consist of :

- The sampling interval equal to 10 sec.
- The pure time delay of the system.
- The order of the model
- The trace of the matrix of adaptation gain F(t).
- The polynam $C_2(q^{-1})$.
- The initial vector P(t).
- The initial observation vector $\phi(t)$.
- The initial adaptation gain matrix $F_o(t)$.
- The factors $\lambda_1(t)$, $\lambda_2(t)$
- The coefficient Bo which is the first element in the vector P(t).

Among these parameters we have to note here the important of the initial values of certain parameters like :

- Bo
- The matrix $F_o(t)$ and its trace.
- The polynom $C_2(q^{-1}) = (1+\alpha q^{-1})^L$

SECTION D : EXPERIMENTS AND RESULTS:

We have carried out two series of experiments, first of all we have tested the performance of our controlling algorithm on using the binary system : on fig(7) we can see clearly that the system has maintained itself very well. As we've noted before a second series has been realized using the ternary system water-aceton-toluene, the conditions and the results are presented on fig(8) ; it is shown that the described control policy actually results in increasing the efficiency of the column. It is very interesting to scrutinize the behaviour of our algorithm and its immediate reaction in front of an echelon on both feed flow rates.

CONCLUSION :

We have implanted successfully an algorithm of model reference adaptive control on an microcomputer type APPLE II to control a pulsed extraction Liquid-Liquid Column.
We've studied the dynamic behaviour of this column and we have determined the variation intervals of several parameters like flow rates, frequency, corresponding to an optimum operation of the column and the presented results show that the proposed controlling policy is efficient.

SECTION E : REFERENCE :

1 - SEGE G. and WOODFIELD F.W., Chemical Engineering Progress, 50, 396 (1954)
2 - SMOOT L.D., MAR B.W. and BABB A.L., Ind.Engng.Chem., 51, 1005-1010 (1959)
3 - CARRIER J., Thèse de Docteur-Ingénieur, I.N.P. Toulouse (1981)

4 - European Federation of Chemical Engineering, Recommanded systems for Liquid Extraction studies, 1978
5 - LANDAU, I.D. and LOZANO R.
Unification of discrete time explicit model reference adaptive control design : Automatica, Vol 17, n°4, pp 593-611, 1981
6 - K. NAJIM, "Commande adaptative des processus industriels" MASSON, Paris, 1982
7 - DALE E. SEBORG, SIRISH L. SHAH, and THOMAS F. EDGAR "Adaptive control strategies for process control : a survey" AICHE DIAMOND Jubilee Meeting Washington, D.C. (novembre 1983
8 - M. SAAD MOHAMMED "Commande adaptative avec modèle de référence d'un four industriel de séchage de phosphate" Thèse (1982) Faculté des Sciences-Rabat.

Fig.(1)

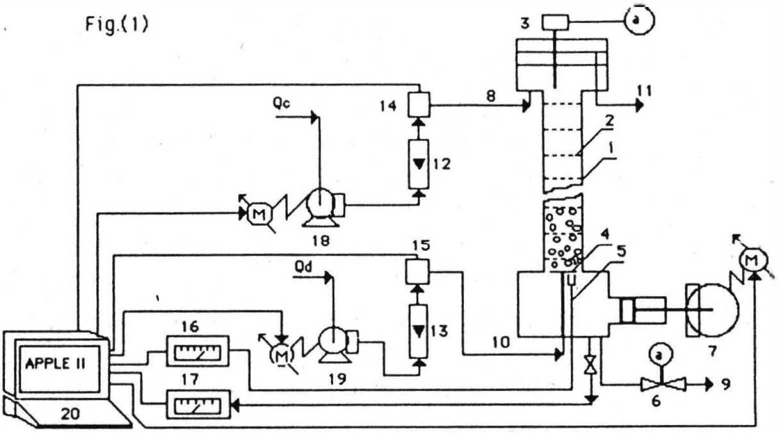

1-PULSED EXTRACTION COLUMN
2-SIEVE-PLATE
3-INTERFACE CONTROLLER
4-DISTRIBUTOR
5-CONDUCTIVITY SOND
6-ELECTROMAGNETIC VALVE
7-PULSING MECHANISM
8-CONTINUOUS PHASE INLET
9-CONTINUOUS PHASE OUTLET
10-DISPERSED PHASE INLET
11-DISPERSED PHASE OUTLET
12,13-ROTAMETERS
14,15-ELECTROMAGNETIC FLOWMETERS
16-CONDUCTIMETER
17-REFRACTOMETER
18,19-FEED FLOW RATES POMPS
20-APPLE II

Fig(2)

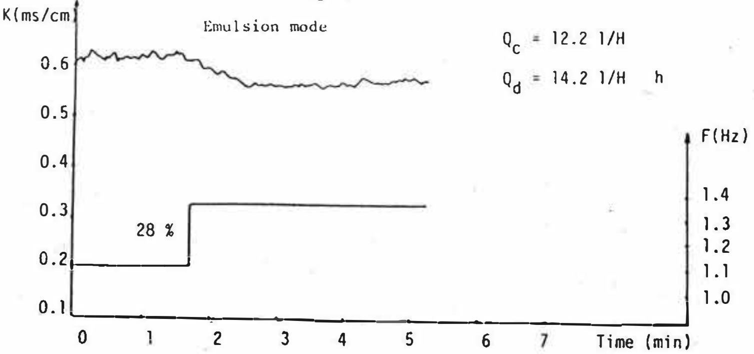

Fig(3)

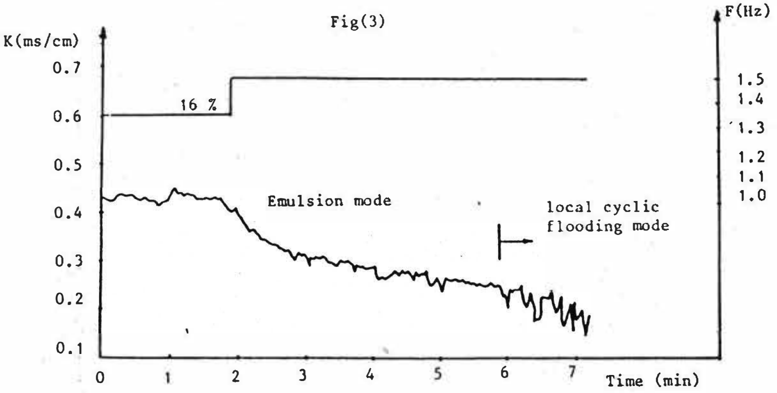

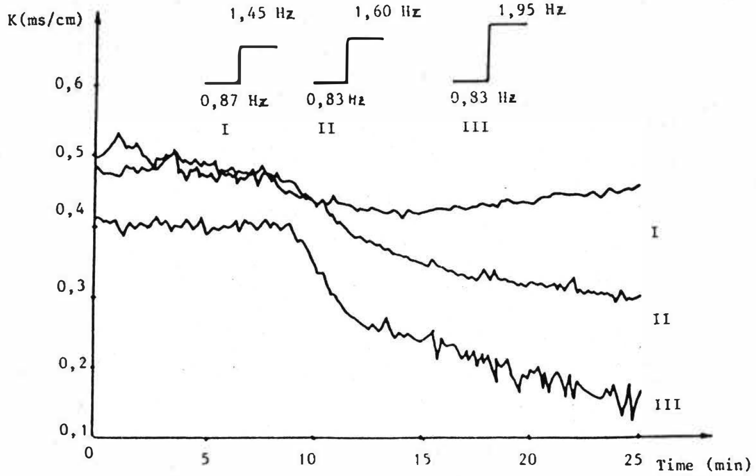

Fig(4)

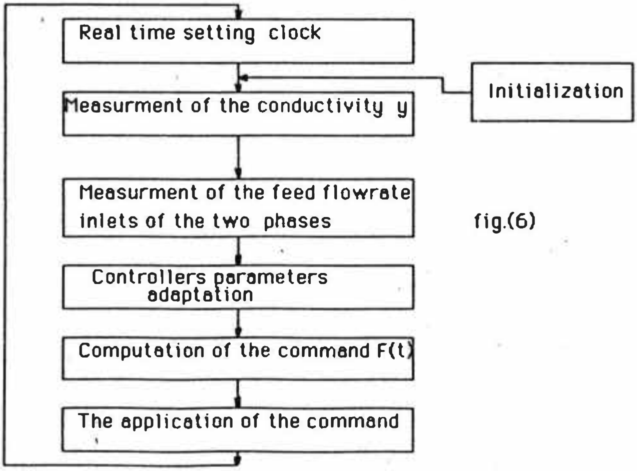
Real time setting clock
Measurment of the conductivity y
Initialization
Measurment of the feed flowrate inlets of the two phases
Controllers parameters adaptation
Computation of the command F(t)
The application of the command

fig.(6)

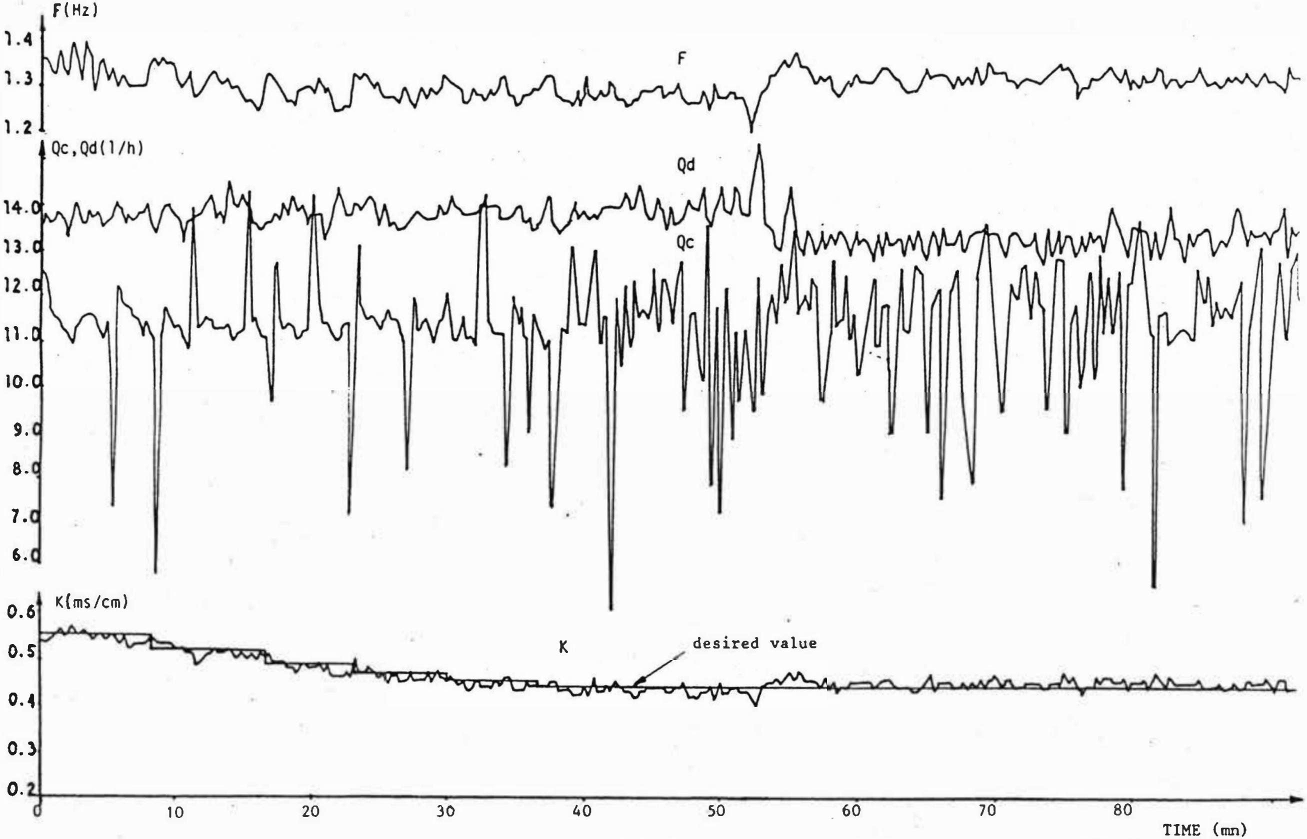

Fig(7) : M.R.A.C. performances (system without mass transfer) in front of a heavy perturbations over the continuous phase feed flowrate.

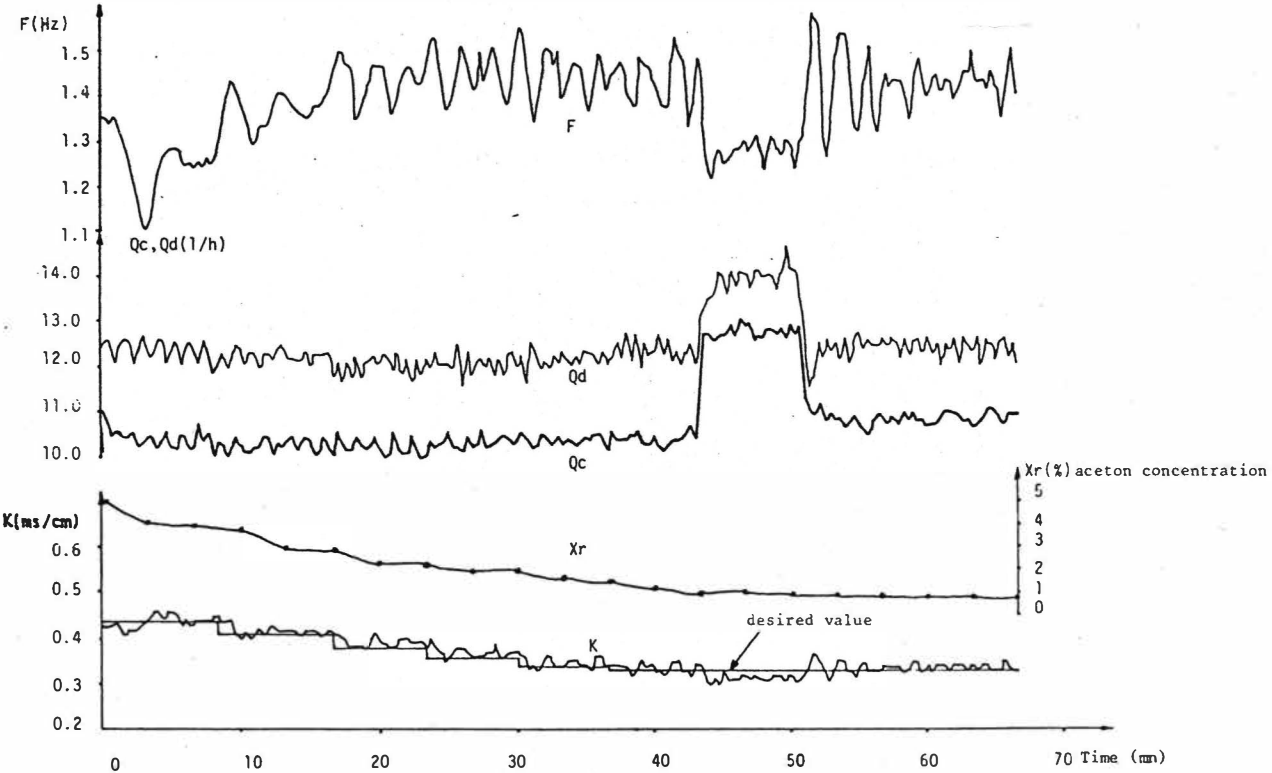

Fig(8) : M.R.A.C. performances (system with mass transfer)

Solvent Extraction of Uranium and Plutonium for the Reprocessing of Nuclear Power Reactor Fuels by the Purex Process.

Comparison between Simulation and Experiment.

Nothaft, A., University of Stuttgart/Germany
Ramm, H. DWK, Hannover/Germany
Gilles, E.D., University of Stuttgart/Germany

Introduction

For the reprocessing of nuclear power reactor fuels the Purex process is designed to separate uranium and plutonium from each other and from the fission products. The recovery of product species is accomplished by solvent-extraction, in which the components are separated from one another by controlling their relative phase distribution between aqueous solution and an immiscible organic solvent, tributyl phosphate (TBP) in a dodecane diluent.

The areas of concern in regard to the reprocessing of spent nuclear fuels are especially the operating conditions, optimal control and supervision of the process, control of inventory for nuclear material safeguards, nuclear criticality analysis, abnormal operating conditions and dynamic behavior. These concepts influence the design and application of the process in order to guarantee a high throughput and optimal operation.

For such a complex system it is useful to gain these ideas from well balanced theoretical development of computational models and practical research. On one hand process simulation reveals parametric sensitivity and shows the transient of the process states caused by an input change and, on the other hand, experiments are necessary to support the theoretical concepts.

Great interest in dynamic process simulation is reflected in a number of publications, which investigate the validity of computational models and provide the experimental data for the modelling of the parameters [1-6]. Here a profound knowledge of the steady-state and dynamic behavior for the first cycle of the Purex process will be considered with our solvent extraction computational model. The practical use of this computational model will be evident by comparing simulated results with experiments.

Purex process

The complex system consists of two pulsed-plate columns and a five-stage mixer-settler as shown in Figure 1. In the first column of the counter-current liquid-liquid Purex process the aqueous uranium and plutonium will be extracted from nitric acid into the organic tributyl phosphate - dodecane diluent. In the second column the loaded organic phase is scrubbed from low coextracted fission products. In the five-stage mixer-settlers tritium will be retained in the aqueous solution.

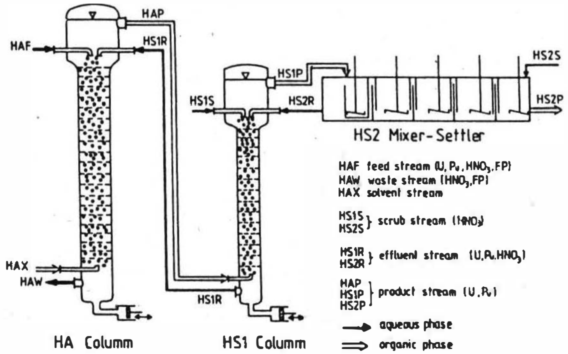
HAP
HS1R
HAF
HS1P
HS2S
HS1S
HS2R
HS2P
HS2 Mixer-Settler
HAF feed stream (U, Pu, HNO3, FP)
HAW waste stream (HNO3, FP)
HAX solvent stream
HS1S
HS2S } scrub stream (HNO3)
HS1R
HS2R } effluent stream (U, Pu, HNO3)
HAP
HS1P } product stream (U, Pu)
HS2P
aqueous phase
organic phase
HAX
HAW
HS1R
HA Columm
HS1 Columm

Fig. 1: Schematic flow chart of the Purex process

Mass transfer kinetic

The fission-product elements are relative non-extractable by tributyl phosphate and therefore leave the so called high active HA-column in the waste stream (HAW) at process operation. Furthermore the separated radioactive elements do not effect other sections of the first cycle of the Purex process. Hence the modelling of the Purex process can be reduced to the mass transfers of uranium und plutonium controlled by the strength of nitric acid.
At the interphase of the two immiscible fluids the components react with TBP, given by

$$UO_2^{2+} + 2\ NO_3^- + 2\ TBP \rightleftharpoons UO_2(NO_3)_2 \cdot 2TBP \ , \qquad (1)$$

$$H^+ + NO_3^- + TBP \rightleftharpoons HNO_3 \cdot TBP \qquad (2)$$

and

$$Pu^{4+} + 4\ NO_3^- + 2\ TBP \rightleftharpoons Pu(NO_3)_4 \cdot 2TBP \ , \qquad (3)$$

where the complexes are soluble in the organic phase.

Experiments [7] revealed, that the complex reactions and the decomposition of uranium and nitric acid occur at the interphase, are chemically coupled and are not controlled by the reaction, i.e. the transport to and from the interphase of the components is slow compared to the complex reaction at the interphase. Hence the concentrations at the interphase are considered to be at equilibrium [2]. The same mechanism will be proceeded from the third complex reaction, formed by plutonium [8].

Figure 2 shows schematically a concentration profile for the two phases of one component at the interphase. For the mass transfer into the solvent and into the aqueous phase the flux for an individual species is conveniently described by following equation:

$$j_i' = \beta_i'(c_i'-c_i^{*\prime}) = \beta_i''(c_i^{*\prime\prime}-c_i'') \tag{4}$$

with

β_i' individual mass-transfer coefficient of the aqueous phase,

β_i'' individual mass-transfer coefficient of the organic phase,

c_i' concentration of component i in the aqueous phase,

c_i'' concentration of component i in the organic phase,

$c_i^{*\prime}$ interfacial concentration of component i in the aqueous and

$c_i^{*\prime\prime}$ interfacial concentration of component i in the organic phase

Corresponding to the fast reactions at the interphase, the interfacial concentrations will be determined by the distribution coefficient D_i, which is defined as the ratio of the organic to aqueous concentration at equilibrium

$$D_i = \frac{c_i^{*\prime\prime}}{c_i^{*\prime}} \tag{5}$$

and represents a nonlinear function of concentration and temperature [9-10].

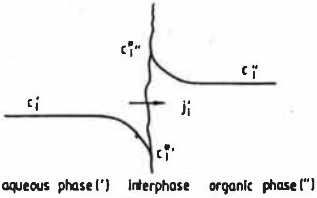

Fig. 2: Schematic concentration profile for component i at the interphase

Process model

To cope with competing and interacting phenomena of the complex Purex process, i.e. the coupled two pulsed-plate columns and the five-stage mixer-settlers, a reliable prediction of concentration and temperature states and the dynamic behavior is desirable. On the basis of the laws of conservation of mass and energy, and the principles of thermodynamics of mixtures a solvent extraction computational model will be derived. Figure 3 shows a finite element for the heterogeneous two-phase system of the aqueous and organic streams.

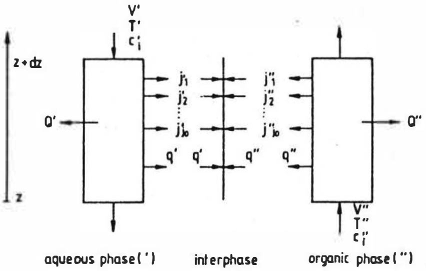

Fig. 3: Heterogeneous two-phase system

The mathematical equations are modeled by balancing this heterogeneous two-phase system. Neglecting the influence of the spatially varying flow rates, densities, heat capacities and thermal conductivities, and assuming that the two phases are immiscible and only the complex reaction of uranium generates heat, modelling leads to the following system of equations for the pulsed-plate column

$$\frac{\partial c'}{\partial t} = D' \frac{\partial^2 c'}{\partial z^2} + \frac{\dot{V}'}{\varepsilon A} \frac{\partial c'}{\partial z} + \beta' \frac{a}{\varepsilon} \left[c^{*\prime} - c'\right] \tag{6}$$

$$\frac{\partial c''}{\partial t} = D'' \frac{\partial^2 c''}{\partial z^2} - \frac{\dot{V}''}{(1-\varepsilon) A} \frac{\partial c''}{\partial z} + \beta'' \frac{a}{(1-\varepsilon)} \left[c^{*\prime\prime} - c''\right] \tag{7}$$

$$\left[\rho' c_p' \varepsilon + \rho'' c_p'' (1-\varepsilon)\right] \frac{\partial T}{\partial t} = \left[\lambda' \varepsilon + \lambda'' (1-\varepsilon)\right] \frac{\partial^2 T}{\partial z^2} +$$

$$\left[\rho' c_p' \dot{V}' - \rho'' c_p'' \dot{V}''\right] \frac{1}{A} \frac{\partial T}{\partial z} - \sum_{i=1}^{i_o} \beta_i'' a (c_i^{*\prime\prime} - c_i'') \, \Delta h_i - \frac{2}{R} \alpha (T - T_u) \tag{8}$$

The difference between the equilibrium concentration $c^{*\prime}{}_i (c^{*\prime\prime}{}_i)$ and the bulk concentration c_i' (c_i'') is considered to be the driving force of the mass transfers. The distributed parameter system of the pulsed-plate column results in parabolic partial differential equations, whereas for the mixer-settler the problem reduces to a lumped parameter system of ordinary differential equations including the additional assumption of chemical equilibrium in each mixing stage.

The desired computational model incorporates all essential dynamic properties of solvent extraction. It will be used in the next section to demonstrate with the dynamic process flowsheet simulator DIVA [1] a comparison between experimental and computational results.

Results

Figure 4 shows the comparison between theoretical and experimental results for the concentration profiles of uranium and nitric acid in case of normal operation. Evidently there is a sufficient agreement for practical application. The HA column is designed with sufficient extraction length for compensating abnormal operating conditions without increasing substantially uranium losses in the waste stream.

New steady state profiles present Figure 5, where the scrub nitric acid concentration for the scrub stream HS1S is replaced by water. Again the computational results agree well with experimental data. Due to the favoured reextraction of uranium at low nitric acid concentration in the HS1 column, the uranium inventory increases essentially in the HA column compared by the undisturbed case. A slightly increase of uranium concentration in the product stream HAP is also notable and causes an increase of internal uranium flux in the HA and HS1 columns. As can be seen the extraction length is sufficiently designed for compensating this disturbance.

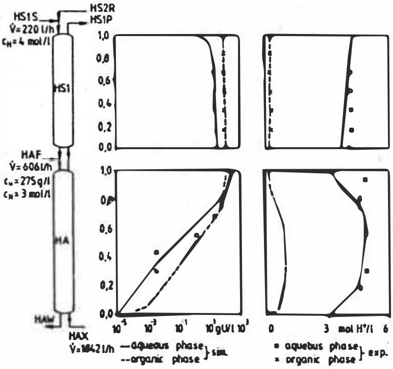

Fig. 4: Uranium and nitric acid concentration profiles at steady-state

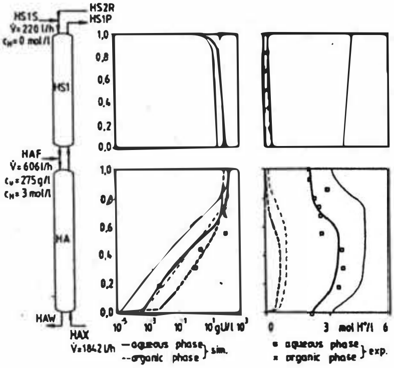

Fig. 5: Uranium and nitric acid concentration profiles at steady-state after changing the nitric acid of HS1S

After one day the decrease of the solvent stream HAX by 15 % leads to a new steady state condition as shown by the concentration profiles in Figure 6.

This good agreement between experiment and simulation by such a severe disturbance indicate the usefulness of the proposed theoretical model. Differences in the region of low uranium concentration are part of insufficient modelling of physical phenomena, e.g. the distribution coefficient or fluid dynamics.

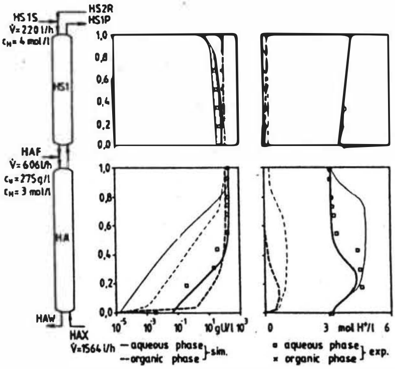

Fig. 6: Uranium and nitric acid concentration profiles at steady-state after reducing the solvent stream

Modelling looks not quite satisfactory in case of the related temperature profiles for the normal and disturbed process operation, shown in Figure 7. Temperature profiles are a useful information for the operator, estimating the extraction of the column. The comparison of measurements and theoretical results enable the application for applying model-based measuring techniques to reconstruct those variables, i.e. concentration, which neither can be measured easily on-line, nor at each location of the column.

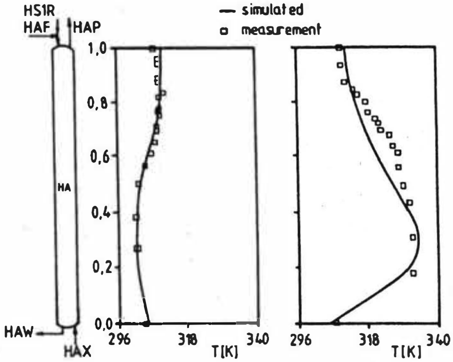

Fig. 7: Temperature profiles at steady-state
a) operation condition
b) after reducing the solvent stream

Figure 8 illustrates the transient to the new steady-state for a 15 % change in the solvent stream (HAX). The dynamic behavior of the more interesting HA column is slow, so that the operator is able to influence the process condition.

Besides the accumulation of uranium, the inventory of plutonium increases also in the HA column. But the plutonium concentration significantly increases higher than the inlet concentration. During the transient the concentration profiles of plutonium show a bulge, which is more evident at lower sections of the HA column. The bulge will remain at the new steady-state.

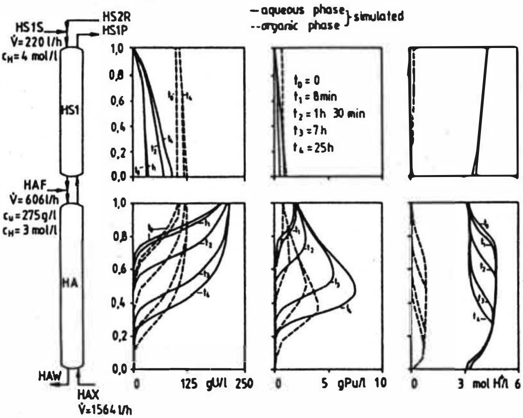

Fig. 8: Dynamic response to a change in HAX stream (U, Pu and HNO_3)

Conclusions

The presented solvent extraction computational model showed satisfactory results with measured concentration and temperature profiles at steady-state. Changing the solvent stream or the nitric acid concentration in the scrub stream, the model revealed realistic dynamic characteristics of the process behavior. For each disturbance the new obtained steady state profiles agreed well with experiments. The simulations demonstrated that the plutonium concentration, as the third component, can increase significantly over the height of the column compared with the inlet concentration. Furthermore the maximum amount and the location of plutonium can be determined for the process by this model. It would be interesting to verify this specific effect by experiments.

Acknowledgement

We are particularly grateful to Dr. Eiben and his collaborators for their experimental support.

Nomenclature

A cross sectional area cm^2
a interfacial area/volume cm^2/cm^3
c concentration, mol/l, g/l
c_p heat capacity cal/(g·grd)

D	distribution coefficient
D'	axial dispersion cm^2/s in aqueous phase
D"	axial dispersion cm^2/s in organic ohase
R	radius of the column cm
V	flow rate l/h
T	Temperature
z	coordinate
α	heat-transfer coefficient $cal/(cm^2 \cdot s \cdot grd)$
β	individual mass transfer coefficient cm/s
ρ	density g/cm^3
ε	holdup
λ	thermal conductivity $cal/(cm \cdot s \cdot grd)$

References

[1] Gilles, E.D., Holl, P. und Marquardt, W.: Dynamische Simulation komplexer chemischer Prozesse in der chemischen Verfahrenstechnik. Chem. Ing. Techn. 56, 1986.

[2] Nitsch, W., van Schoor, A.: The Kinetics of Coextraction in the System Uranylnitrate, Nitric acid, Tributyl-phosphate. Chem. Eng. Sci. 38, 1983, 1947-1957.

[3] Petrich, G.: Problems in Modelling the Purex Process. Springer Series in Chemical Physics, 18, 1980.

[4] Petrich, G. et al.: Comparison of Experiment and Simulation for Purex-B-type Electroreduction Pulsed Columns. Symposiums on Liquid/Liquid Extraction Science, 1984.

[5] Steiner, L., Berger, J. and Hartland, S.: Mass Transfer Rates in Liquid/Liquid Extraction with Partially Miscible Solvents. Solvent Extraction and Ion Exchange 2, 1984, 553-577.

[6] Ihle, E., Dissertation TU München 1985.

[7] van Schoor, A., Dissertation TU München 1982.

[8] Nitsch, W.: Plutonium-Extraktion im Purex-Medium. Classified paper.

[9] Baumgärtel, G., Ochsenfeld, W. und Schmieder, H.: Die Verteilung der Metallnitrate im System $Pu(NO_3)_4$-$UO_2(NO_3)_2$-HNO_3/TBP-Dodecan. KfK 680, 1967.

[10] Petrich, G., Kolarik, Z.: The 1981 Purex Distribution Data Index. KfK 3080, 1981.

Calculation and measurement of concentration profiles for the coupled fluxes of uranylnitrate and nitric acid in a pulsed column.

E. Ihle, R. Ollenik, W. Nitsch
Technical University of Munich, Garching/D

Introduction

For the design and scale up of extraction columns two processes are decisive: mixing and mass transfer

The event of mixing is determined by the apparatus itself and by the conditions of operation. This means, that investigations of mixing-processes must performed inside of a relevant column.

Mass transfer however, can be investigated outside the technical apparatus at a suitable laboratory scale. Because of the complex behavior of extraction columns all the possibilities should be used to clear up the kinetics of mass transfer in order to improve the approach to the design of columns.

For the coupled mass transfer of uranylnitrate and nitric acid into a kerosene phase, loaded with tributylphosphate (TBP), performed in a pulsed column, concentration profiles are accessible, provided that the corresponding kinetics of mass transfer is known as a "white box".

The Concept

The developed concept, having analogous application for other extraction systems, is characterized by three different experimental procedures:

1. With measurements of mass transfer in dependence on the forced convection conclusions are possible concerning the rate controlling step (transport or chemical reaction). Such results together with reasonable assumptions about the location of the chemical reaction enable one to formulate the appropriate set of equations. These equations are to be used instead of the usual "overall-term" for the description of mass transfer.

2. The second procedure is necessary in order to get values of suitable individual transport coefficients. The corresponding method is the mass transfer in beds of monodisperse drops, being equivalent for the dispersed phase inside a column. Computer aid is necessary in order to find the concentration region in which the individual coefficients are accessible. The applied evaluation is based on the set of equations formulated in the first procedure. With such equations and coefficients it is possible to calculate concentration profiles in columns, provided a suitable model describes the fluid dynamic behavior.

3. Finally with measured concentration profiles in a real column - the third procedure - one can estimate the efficiency of the calculation method based on the kinetic results.

Results

For the investigated liquid/liquid system, considered as an example for reactive mass transfer, the following results are remarkable:

Stirred Cell:

In such an apparatus, calibrated with known transport systems, the observed linear dependence of flux from stirring number shows, that the chemical reactions are controlled by transport processes. Together with the assumption, that the chemical reactions are located at the interface, the appropriate set of equations can be formulated. Corresponding to the scheme in

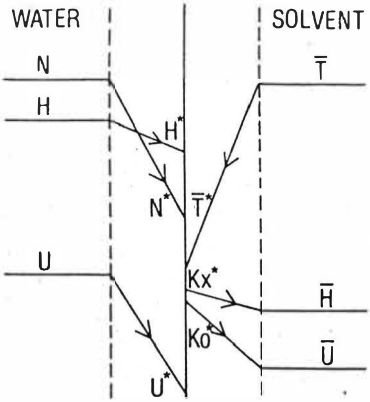

figure 1 and to the concept of taking all involved individual species into consideration for the relevant 6 species (H^+, No_3', TBP, Uo^{2+}, Kx, Ko) because of the condition for electroneutrality, 5 equations of the generalized kind

$$\dot{n}_i = \pm \beta_i \ (c_i - c_i^*)$$

are necessary to describe the kinetics. The individual fluxes $\dot{n}_i$ are connected with the stoichiometric relations for both reactions. Besides, the interfacial concentrations c_i^* are coupled together with the equilibrium conditions:

$$K_H = \left[\overline{Kx}\right]^* \Big/ \left[H^+\right]^* \left[No_3'\right]^* \left[\overline{TBP}\right]^*$$

$$K_U = \left[\overline{Ko}\right]^* \Big/ \left[Uo_2\right]^* \left[No_3'\right]^{*2} \left[\overline{TBP}\right]^{*2}$$

(Kx for $\overline{HNO_3TBP}$, Ko for $\overline{UO_2(NO_3)_2 \ 2 \ TBP}$)

Both "equilibrium constants" depend on the concentration. Figure 2 illustrates such a dependence.

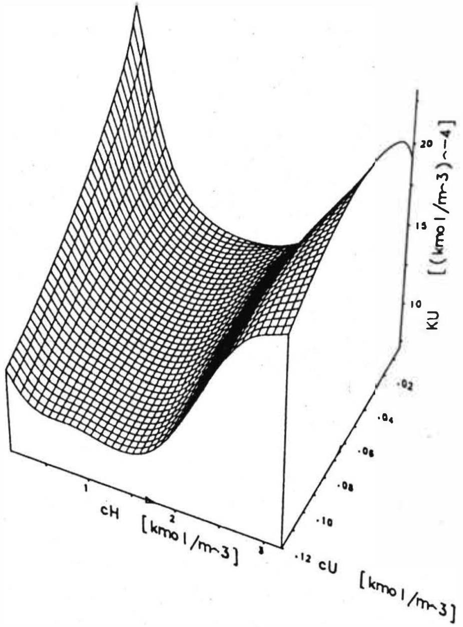

Fig. 2:
The influence of the nitric acid concentration cH and of the uranyl ion - concentration cU upon the equilibrium constant KU

Drops:

Measurements of mass transfer in beds of monodisperse drops for suitable concentrations are leading to individual coefficients. The values of these coefficients are comparable with the corresponding coefficients, calculated from correlations for circulating drops. This result supports the specific mechanism of mass transfer, provided for the evaluation. An additional support lies in the agreement of measurement and calculation concerning the coupling of nitric acid and uranium-transfer: The overshooting of the nitric acid concentration in the organic phase is only observed in the predicted region.

Fig. 3:
The transient development of the concentration profiles to the stationary behavior.
points are measured, lines are calculated

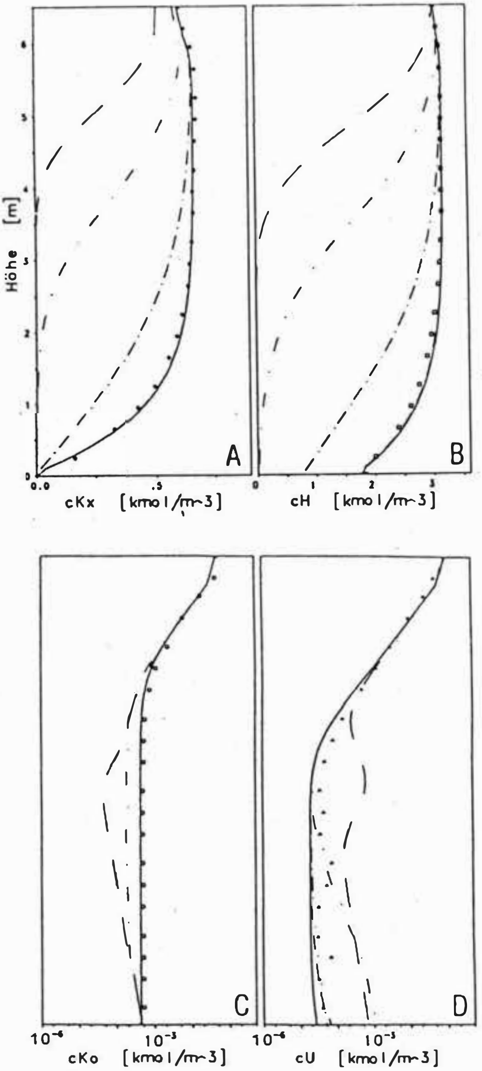

A: concentration of nitric acid (cKx) in the dispersed solvent phase

B: concentration of nitric acid cH in the continuous water phase

C: concentration of the uranium complex cKo in the solvent phase

D: concentration of uranyl ion cU in the continuous water phase

Pulsed Column:

In such a column with an active height of 6 m, 38 mm diameter, stages with a height of 10 cm, the concentration profiles were always measured for extraction and re-extraction for the organic phase being dispersed.

The most important result was, that for both directions of mass transfer and for both cases (nitric acid resp. nitric acid- and U-flux) the measured profiles agree very well with the calculated ones, if the column operates in the region of the mixer/settler regime. In the corresponding calculations the back-flow model without backmixing between the plates was used. This result is the best proof for the efficiency of the applied procedure. Same examples are presented in the figure 3. If the column operates in the region of dispersion, the observed deviations between experiment and calculation are not to be neglected; backmixing is the reason.

It is shown with examples, that the knowledge of kinetics enables one to calculate the back-flow or the dispersion-coefficients, provided measured c-profiles are known. This approach to the dispersion coefficients is a very reliable one, because the method operates at conditions of mass transfer. One does not need the specific fluid dynamic conditions being difficult to realize in the tracer techniques.

Resume

Especially for cases of reactive mass transfer ("chemical extraction"), where "overall coefficients" are usually dependent on the concentrations, the individual treatment is efficient for the kinetics. The key function of mass transfer for the design of columns is shown in the presentation. These results are most important for the extraction in the PUREX-medium because of the perspective of being able to calculate concentration profiles for plutonium.

Calculation of the activity coefficient of TBP in water solution and in diluent by the cluster expansion method

Yun-Xiao Zhong, Wenging Xiaobo Wang,
Department of Technical Physics, Peking University, Beijing/China

We have measured the activity coefficient of TBP in various diluents,such as benzene,chloroform,carbon tetrachloride,chlorobenzene by ^{32}P-labeled TBP distribution method and vapour presure method. The results of two method are contradictory to each other. Activity coefficient of TBP in water may be extracted for the analysis of the discrepancy.

In the ^{32}P-labeled TBP method, the activity coefficient of TBP in diluent is given by

$$\gamma_2 = \frac{\gamma_2'}{\gamma_{20}'}\,\frac{A}{x_2} \qquad (1)$$

where γ_2' is activity coefficients of TBP in water solution which is in equilibrium with TBP in the diluent and γ_{20}' is the same coefficient but equilibrium with pure TBP, A is the ratio of radioactivities of aqueous phase in both cases and x_2 is the mole fraction of TBP in the diluent. AS the solubility of TBP in water is very low, the activity coefficients of TBP in water was assumed to be unity. thus equation (1) become

$$\gamma_2 = \frac{A}{x_2} \qquad (2)$$

For comparision the activity coeficients of the diluent γ_1 were obtained by the Gibbs-Duhem law from γ_2 . If we used equation (2) for γ_2 , the value of γ_1 so obtained differs wildy with the value of γ_1 from vapour presure method. In certain systems the former is great than 1 and the latter is less than 1. It is conjectured that the assumption $\gamma_2' = \gamma_{20}' = 1$ may be in error. Comparing carefully the data of two methods of four systems we obtained the γ_2' / γ_{20}' vers A as show in figure 1.Using this γ_2' / γ_{20}' values, the γ_1

obtained from two methods are consistent with each other.

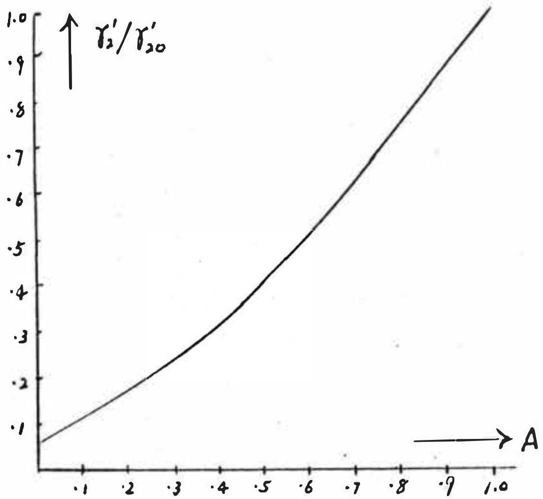

figure 1

As the manuscript was not available at the 28th May 1986, the deadline for printing this book, we only print the short abstract of the paper.

Improvements and results acquired through six years of industrial uranium extraction from phosphoric acid by the PRAYON process

A. Davister and G. Martin,
PRAYON DEVELOPPEMENT - B-4130 Engis, Belgium

The UMIPRAY plant extracts uranium from phos-acid since 1980 by the PRAYON Process

UMIPRAY S.A., a Belgian Limited Company wholly owned by PRAYON, started recovering uranium from phosphoric acid in May 1980.

The PRAYON process used is based upon fundamental works of the Oak Ridge National Laboratory, U.S.A. (1), (2), (3) and utilizes the two-cycle extraction/stripping technique with the DEHPA/TOPO* as solvent (* see last page). From the origin and during the six-year operation now completed, important and particular design features have been introduced in the process, making it different from other processes using the same DEHPA/TOPO solvent and operated in North America.

In spite of the depressed price displayed by the uranium since several years, the UMIPRAY plant is still in profitable operation and is the only one remaining on stream outside America. This is due to the high level of reliability, efficiency of operation and quality of uranium concentrate achieved by the process.

The main characteristics of the PRAYON uranium recovery process

The PRAYON process (formely called I.M.C./PRAYON process), is the property of PRAYON DEVELOPPEMENT S.A., the Engineering Division of PRAYON and has been developed in 1978-79.

To this end, PRAYON has entrusted METALLURGIE HOBOKEN-OVERPELT, a world leader in liquid/liquid extraction of non ferrous metals, with the extraction part of the research and has shared with I.M.C. the first year of industrial experience of their respective plants.

Basically, the process is outlined in the block-diagram hereafter. It has been described in several papers (4), (5), (6) and we only recall here some of its features.

1. The phosphoric acid pretreatment

From our view-point, the acid pretreatment is nearly as important as the extraction itself.

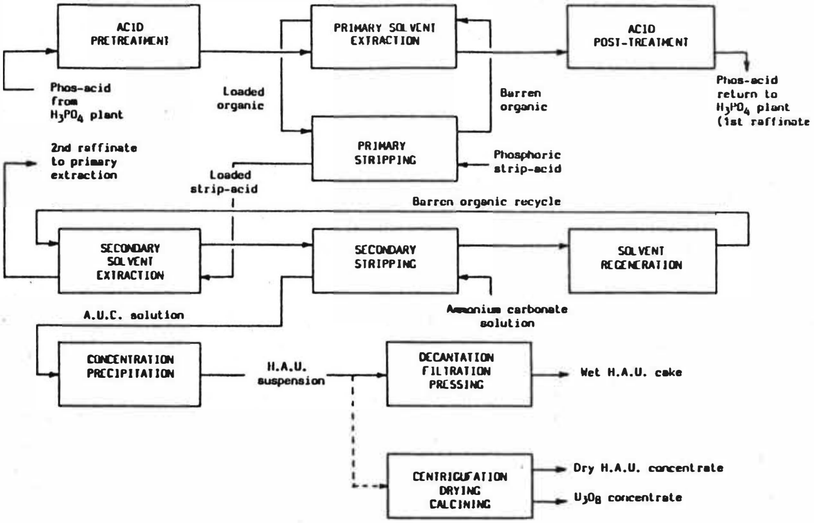
ACID PRETREATMENT
Phos-acid from H_3PO_4 plant
PRIMARY SOLVENT EXTRACTION
Loaded organic
Barren organic
ACID POST-TREATMENT
Phos-acid return to H_3PO_4 plant (1st raffinate
PRIMARY STRIPPING
Phosphoric strip-acid
2nd raffinate to primary extraction
Loaded strip-acid
Barren organic recycle
SECONDARY SOLVENT EXTRACTION
SECONDARY STRIPPING
SOLVENT REGENERATION
A.U.C. solution
Ammonium carbonate solution
CONCENTRATION PRECIPITATION
H.A.U. suspension
DECANTATION FILTRATION PRESSING
Wet H.A.U. cake
CENTRIFUGATION DRYING CALCINING
Dry H.A.U. concentrate
U_3O_8 concentrate

BLOCK DIAGRAM OF PRAYON URANIUM RECOVERY PROCESS

High performances in extraction step depend, indeed, on a strict control of the solvent and acid flows, on a clear-cut division between the two phases after each mixing, on the absence of any "organic cruds" formation that would inevitably reduce the efficiency and cause losses of acid and solvent. That is why we give the primary phosphoric acid an extensive preparation including cooling, desaturation, clay treatment, filtration and adsorption through activated carbon.

In these conditions, the resulting clear "GREEN ACID" is perfectly desaturated, free of any mineral or organic solid, free of its soluble humic material and is prepared to be processed by liquid/liquid extraction.

2. First Cycle of Extraction/Stripping

Both extraction and stripping are made in a 3 or 4-stage battery of rectangular mixer-settler units.

The DEHPA/TOPO solvent requires the uranium to be at the U^{6+} state for the extraction and, inversely, to be at the U^{4+} state for the reductive stripping.

The judicious utilization of scrap iron added to the small flow of phosphoric strip acid to lower its Redox potential during the stripping is a major factor for the operation of the plant.
After the extraction step and the separation of the solvent entrained, the main flow of phosphoric acid (the 1st raffinate) returns to the H_3PO_4 facility with the same clean aspect as the "green acid".

3. Second Cycle and Refinery

The same DEHPA/TOPO solvent is utilized in the 2nd cycle but with slightly different concentrations. The strip acid from 1st cycle enters the secondary extraction with a concentration of 10 to 12 g U_3O_8/litre.
The secondary stripping is made in a precise range of conditions such that the ammonium-uranium carbonate formed (A.U.C.) remains perfectly soluble, while other metallic compounds can precipitate.
Uranium precipitates naturally by concentration of the clear A.U.C. solution and gives a hydrated salt ($3\ UO_3\ .\ NH_4\ .\ 5H_2O$) called H.A.U. The purity of this product lies well beyond the requirements of all the converters.

Two ways of conditioning are then possible :

1°- The H.A.U. suspension is filtered and washed in a pressure filter and the WET YELLOW CAKE can be put directly in drums.
This concentrate does not need any calcination and it does not create any problem of radioactive dust recovery and environment protection.

2°- The H.A.U. precipitate can be, at will, either dried or calcined, giving in this case a U_3O_8 concentrate with more than 80 % U.

A few data about the UMIPRAY plant

Location :	at Puurs (near Antwerp) - Pretreatment of acid - Cycle I	at Engis (near Liège) - Cycle II - Refinery
Capacity :	130.000 t P_2O_5/year (outside UMIPRAY plant)	55 t U_3O_8/year (presently) 115 t U_3O_8/year (by possible modification)
Current output :	about 115.000 t P_2O_5/year	45 to 50 t U_3O_8/year

Phosphate raw material : Khouribga 70-71 BPL with 115-125 ppm U

Phosphoric acid to Sx-U : 45 to 50 m^3/hour with 30-32 % P_2O_5

Table of main performance figures :

Year	Uranium Concentrate Production (t U_3O_8)	Phosphoric Acid available		Uranium Extraction Yield (%)	Operating Factor (vs. time available)
		P_2O_5 content (%)	U_3O_8 content (ppm)		
1980	20,4 (a)	28,92	129	91,1	87,0
1981	41,1	28,96	129	94,8	96,7
1982	43,7	29,0	124	96,5	99,0
1983	45,1	30,1	132	96,8	98,2
1984	50,3	29,8	135	97,0	99,2
1985	44,1 (b)	31,2	125	94,0 (c)	99,0

(a) : 6 months of operation in 1980

(b) : the production is evidently subject to the U_3O_8 content of phosphate. A changement of phosphate rock composition has affected the production in 1985.

(c) : the new phosphate, strongly laden with humic material has caused a reduction of yield in 1985.

Recent innovations brought to the process with a view to improve its efficiency and reduce the production cost

1. Improvement of the phosphoric acid cooling in the Pretreatment by the use of two Low Level Flash Coolers working in series

The two-superposed-stage evaporator utilized originally has several process and operation disadvantages : incrustation build-up in the apparatus due to a high temperature drop, important kWh and water consumption, etc...

The new design includes two "Low Level Flash Coolers" (L.L.F.C.) similar to the ones used successfully in recent PRAYON phosphoric acid plants, working with a very low temperature drop (1 to 2 K) and a high circulation flow. These coolers are installed at a much lower level and partially flooded by the acid when put under vacuum. The circulation of acid is ensured by an axial-flow circulator with low manometric head. Each cooler has an individual circulation tank, the acid overflowing freely from 1st cooling circuit to 2nd one.

This design brings important savings of investment and operation costs to the acid pretreatment :

- less kWh consumed by the circulators (large capacity but very low manometric head);
- less cooling water needed by the condenser thanks to the higher temperature of water vapours leaving the 1st circuit;
- less steam for the ejectors of the vacuum unit (less dissolved air to be exhausted from the cooling water.

The following table gives the main figures for new and previous cooling designs on the basis of a 1.500 t P_2O_5/day pretreatment unit :

	Previous device	Use of 2 L.L.F.C.	Saving
Investment * (M FB)	16,7	12,3	26 %
Electrical power (kWh/h)	84,5	14,4	83 %
Cooling sea water (m^3/h)	447	312	30 %
Steam for ejectors (kg/h)	600	500	17 %

* investment relating to equipments differing in the two alternatives.

2. Improved control of the reductive stripping of uranium in the first cycle

The limitation of iron consumption during the stripping step of uranium is a major concern. Presence of Fe^{2+} ions is permanently required in the strip acid to reduce U^{6+} to U^{4+}, but both iron and uranium are exposed to re-oxidation by the ambient air. The resulting ferric iron passing into the acid can cause undesired precipitation of ferric phosphate compounds in the mixer-settler units.

A patented device of "interstage reduction" has been implemented in our process. Controlled amounts of scrap iron are dynamically dissolved at every stripping stage, ensuring a constant and minimum presence of Fe^{2+} ions at the right place with a minimum of fatal ferric iron passing in the acid.

In terms of consumption, the following figures have been recorded at UMIPRAY plant :

	kg scrap iron per t P_2O_5 available	kg scrap iron per kg U_3O_8
Average for 1982	1,43	3,54
Average for 1983	1,60	3,76
After start-up of new device :		
2nd half-year 1984	1,18	2,67
Average for 1985	1,17	3,12

3. Modification of the post-treatment of first raffinate

The first raffinate, that is the main flow of acid going back to the H_3PO_4 facility, is polluted by traces of solvent (DEHPA, TOPO and their diluent kerosene). For economical and technical reasons, it is important to sharply separate them. In UMIPRAY plant, the post-treatment presently includes one lamellas-settler followed by two activated carbon columns. The final quality of the raffinate is excellent, but the carbon must be periodically regenerated and the solvent absorbed in the columns is lost.

Another scheme of post-treatment has been experimented at industrial scale. After the lamellas-settler, the raffinate is treated in air-induced flotation cells. They practically require no maintenance and deliver the acid with less than 25 ppm (vol/vol) of solvent. The additional recovery of solvent is estimated to be 75 ppm of the raffinate volume (the average in/out contents being 100/25 ppm).

The corresponding saving in DEHPA + TOPO amounts to 16/g m^3 of raffinate, i.e. 95 g/kg U_3O_8 in the yellow cake. This represents about one third of the DEHPA + TOPO consumption of the first cycle.

4. Reduction of the cost of oxidation agent in the second cycle by utilization of gaseous oxygen

The substitution of gaseous oxygen to hydrogen peroxide for the oxidation of the uranium-loaded acid entering the 2nd cycle is gradually proceeding in the UMIPRAY plant. When the full changement will be achieved, it is expected that the cost of this reactive will be cut by four.
The efficiency of gaseous oxygen is less good than the one of hydrogen peroxide but this is amply compensated by its low cost.
So far, the oxidation cost evolves as follows :

YEAR	Cons. per kg U_3O_8	Unit cost	Cost per kg U_3O_8
1982+83	2,10 kg H_2O_2 (35 %)	25 FB/kg	52,5 FB
1984	1,01 kg H_2O_2 (35 %) 0,53 Nm^3 O_2	25 FB/kg 4,8 FB/Nm^3	25,25) 27,8 FB 2,55)
1985	0,66 kg H_2O_2 (35 %) 0,74 Nm^3 O_2	25 FB/kg 4,8 FB/Nm^3	16,5) 20,05 FB 3,55)

5. Improvement of the yellow cake purity and moisture

The handling and dissolution of the wet yellow cake (H.A.U.) at the converter's facility had given some unpleasant annoyance due to the :

- appearance of some spongy "gums" during dissolution of Y.C. in nitric acid (and caused by traces of solvent trapped in the H.A.U. precipitate);
- difficulty of handling the wet and sticky cake.

The origin of the first trouble has been quickly identified by laboratory tests. A simple solution has solved this problem : the A.U.C. solution is polished by filtering it through a paper-filter before entering the lamellas-settler. The bright clear solution then flows to the precipitation step.

The second problem has been definitely solved by pressing the H.A.U. cake in a tube-press under a pressure of about 120 bars.
The dewatered cake falls from the tube-press in the form of narrow strips having a compact and solid aspect and witholding only 10 to 15 % moisture.
This yellow cake is now easy to handle and has lost its thixotropic character.

6. Advance in the monitoring of uranium through the process, leading to a automatic control of the operation

The plant has demonstrated to be easily controlled and technical performances have reached a high level. The next task of our R & D staff is now to progressively introduce an automatic control of the operation in the plant.
The first step is the development, in laboratory, of a "continuous flow" uranium analysis method valid for organic and aqueous phases.
This has been achieved last year and it is based on the photo-colorimetric technique.
The next step will include the construction of a semi-automatic apparatus and its experimentation in cycle II of the plant.

---

* **DEHPA**

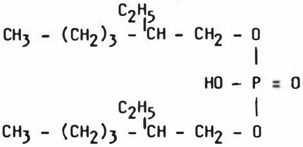

$$\begin{array}{l} CH_3 - (CH_2)_3 - \overset{C_2H_5}{\overset{|}{C}}H - CH_2 - O \\ \qquad\qquad\qquad\qquad\qquad\qquad | \\ \qquad\qquad\qquad\qquad\qquad HO - P = O \\ \qquad\qquad\qquad\qquad\qquad\qquad | \\ CH_3 - (CH_2)_3 - \overset{C_2H_5}{\overset{|}{C}}H - CH_2 - O \end{array}$$

TOPO

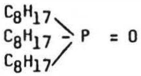

$$\begin{array}{l} C_8H_{17} \searrow \\ C_8H_{17} - P = O \\ C_8H_{17} \nearrow \end{array}$$

References

(1) F.J. HURST, D.J. CROUSE, K.B. BROWN, Recovery of uranium from wet process phos-acid, Industrial and Engineering Chemistry Process Design and Development, Vol 11, N° 1, 1972.

(2) F.J. HURST, D.J. CROUSE, K.B. BROWN, Solvent Extraction of Uranium from Wet Process Phos-Acid, ORNL Publ., ORNL. TM - 2522, 1969.

(3) F.J. HURST, D.J. CROUSE, Actinide Recovery from Waste and Low Grade Sources, Hardwood Academic Press, N.Y., 1982, p. 201-224.

(4) F.T. NIELSSON, A. DUBREUCQ, The IMC/PRAYON Uranium Recovery Process, I.S.M.A. Proceedings, Vienna (Austria), Nov. 1980.

(5) A. DAVISTER, A. DUBREUCQ, Interfacial Phenomena in Uranium Extraction from Wet Phosphoric Acid, I.S.E.C. Conference, Denver (U.S.A.), 1983.

(6) A. DAVISTER, A. DUBREUCQ, G. GRANVILLE, H. GRAY,
Récupération de l'uranium contenu dans l'acide phosphorique de voie humide et sa transformation en un concentré uranifère de grande pureté, Industrie Minérale - Les Techniques, April 1984.

ESTIMATION OF EQUILIBRIUM CONSTANTS FOR THE EXTRACTION OF NITRIC ACID BY TBP/KEROSENE MIXTURES

J M Schaekers, Atomic Energy Corporation of South Africa, Pretoria, South Africa

INTRODUCTION

Tri-n-butyl phosphate (($(CH_3CH_2CH_2CH_2O)_3$ PO, TBP) is a well known organic extractant which is frequently used for the separation and purification of metals, especially uranium and other compounds of interest to the nuclear industry. In this case extraction/purification is normally effected from aqueous acid nitrate solutions, and for this reason the system HNO_3-H_2O-TBP, with or without kerosene, has been studied extensively.

Numerous investigators have tried to describe it mathematically in order to be able to predict equilibrium HNO_3 concentrations in aqueous and organic phases under a variety of conditions. Originally it was assumed (1, 2) that only the compound HNO_3.TBP existed in the organic phase although it was accepted that the water, which was also present, could form secondary adducts of the type HNO_3.TBP.xH_2O. Later on it was established (3, 4, 5) that, at aqueous acid concentrations of $\geq$ 6 moles/dm^3, deviations did occur which were ascribed to the formation of high acid adducts of the type $(HNO_3)_x$.TBP with x = 2, 3 or even 4.

Apart from Collopy (2), who proposed undissociated HNO_3 as the active species during the extraction process, the other investigators used the total aqueous acid concentration, HNO_3 (4), or the completely dissociated acid, H^+ and NO_3^- (3, 5, 6), which can be represented by equations [1] and [2] respectively, unfortunately only with limited success. More recently (7) it has been accepted that lower adducts, such as HNO_3.2TBP, are also formed.

$$HNO_3 + TBP \rightleftarrows HNO_3.TBP \qquad [1]$$

$$H^+ + NO_3^- + TBP \rightleftarrows HNO_3.TBP \qquad [2]$$

A critical evaluation of IR-studies (5, 8, 9) indicates that only a very weak bond exists between H_2O and TBP in the organic phase and that H_2O containing adducts with TBP should not play an important role in the equilibrium between nitric acid and TBP/kerosene mixtures. This was also evident from Davis's (4) results, which indicated that the molar volume of H_2O and TBP dit not change appreciably in the absence of HNO_3.

DESCRIPTION OF THE MATHEMATICAL MODEL

Based on the above information it was concluded that the extraction of HNO_3 by TBP/kerosene mixtures could possibly be described by equations [3], [4] and [5], in which HNO_3 represents the undissociated nitric acid in the aqueous phase, and the horisontal bar above a compound means that it is present in the organic phase.

$$HNO_3 + 2\overline{TBP} \rightleftarrows \overline{HNO_3.2TBP} \qquad [3]$$

$$HNO_3 + \overline{HNO_3.2TBP} \rightleftarrows 2(\overline{HNO_3.TBP}) \qquad [4]$$

$$HNO_3 + \overline{HNO_3.TBP} \rightleftarrows \overline{(2HNO_3).TBP} \qquad [5]$$

The corresponding thermodynamic equilibrium constants, K_{12}, K_{11} and K_{21}, and conditional equilibrium constants, k_{12}, k_{11} and k_{21}, can then be represented by equations [6], [7] and [8] respectively (γ = activity coefficient, o = organic phase and a = aqueous phase).

$$k_{12} = K_{12} \cdot \frac{\gamma_a \cdot \gamma_{o(TBP)}^2}{\gamma_{o(HNO_3.2TBP)}} = \frac{[\overline{HNO_3.2TBP}]}{[HNO_3]\,[\overline{TBP}]^2} \qquad [6]$$

$$k_{11} = K_{11} \cdot \frac{\gamma_a \cdot \gamma_{o(HNO_3.2TBP)}}{\gamma_{o(HNO_3.TBP)}^2} = \frac{[\overline{HNO_3.TBP}]^2}{[HNO_3]\,[\overline{HNO_3.2TBP}]} \qquad [7]$$

$$k_{21} = K_{21} \cdot \frac{\gamma_a \cdot \gamma_{o(HNO_3.TBP)}}{\gamma_{o((2HNO_3).TBP)}} = \frac{[\overline{(2HNO_3).TBP}]}{[HNO_3]\,[\overline{HNO_3.TBP}]} \qquad [8]$$

$$K_{a(HNO_3)} = \frac{[H^+]\;[NO_3^-]}{HNO_3} = 24{,}00 \qquad [9]$$

To solve this set of equations, use was made of the acid dissociation constant for nitric acid, [9], which is equal to 24,00 (10), the proton balance, and the mass balances for total acid, acid in aqueous, acid in organic and for TBP. In these it was assumed that the volume of the aqueous and organic phases are equal and remain constant during the extraction process and that the activity coefficients do not change for a specific TBP concentration. This last assumption is only acceptable because $[H^+]$, $[NO_3^-]$ and $[HNO_3]$, which are used in [9], are actually based on the thermodynamic acid dissociation constant and therefore nearer to activities than to molar concentrations.

Finally the acid equilibrium concentrations in organic and aqueous phases were calculated by an iteration method and with varying values for k_{12}, k_{11} and k_{21} until the results differed less than 5 % from Davis's (4) experimental data and our own values (11) covering the total range from 0,5 to 12 moles/dm^3 HNO_3 for each TBP concentration. The initial values were then plotted and smoothed graphically to give the results in Table 1, which are represented graphically in Figures 1 and 2.

Table I: Conditional equilibrium constants and % difference between calculated and experimental HNO_3 concentrations in the organic phase

	Conditional equilibrium constants			% difference for various moles/dm^3 HNO_3 in aqueous phase at equilibrium						
% TBP	k_{12}	k_{11}	k_{21}	1,00	2,00	4,00	6,00	8,00	10,00	12,00
5	0,220	100,0	0,108	+25,0	+12,4	-2,3	-1,0	+2,7	+2,5	-2,0
10	0,608	35,7	0,120	+7,2	+4,3	-5,0	-2,0	+0,1	+0,8	-2,7
15	1,80	12,2	0,134	+5,0	-2,8	-3,4	-2,6	+2,2	+2,0	-5,0
30	3,50	6,34	0,162	+8,6	+4,6	-3,4	-1,4	+4,5	+6,4	+0,9
65	3,95	5,71	0,207	+2,0	+3,5	-2,3	-0,3	+4,0	+3,4	$-^{(b)}$
100	4,41	5,10	0,240	+4,7	+4,5	-4,1	-1,5	+2,4	+1,5	$-^{(b)}$

b: No experimental data available

DISCUSSION OF RESULTS

Experimental and calculated acid equilibrium concentrations for 30 % TBP are graphically shown in Figure 3. The percentage differences between these two values are also given in Table I for selected acid concentrations in aqueous phase and for all the TBP mixtures investigated. From these it is obvious that an excellent correlation is obtained, with a difference of generally less than 5 % except for $\leq$ 2 moles/dm^3 HNO_3 and 5 % TBP or for $\leq$ 1 moles/dm^3.

However, it is also clear that there is a general trend with positive differences up to 3 moles/dm^3 and between 7 and 11 moles/dm^3 and negative ones in the other regions. These are probably caused by the assumptions made in order to obtain a manageable mathematical equation and conditional equilibrium constants which are essentially constant for a specific TBP concentration.

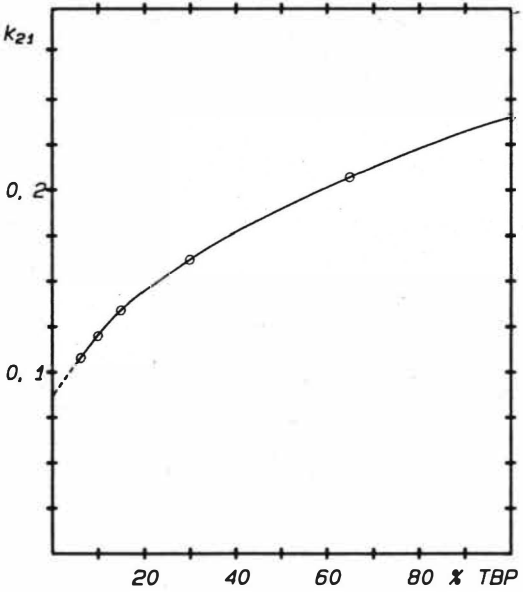

Fig 1 : VARIATION OF k_{21} WITH % TBP.

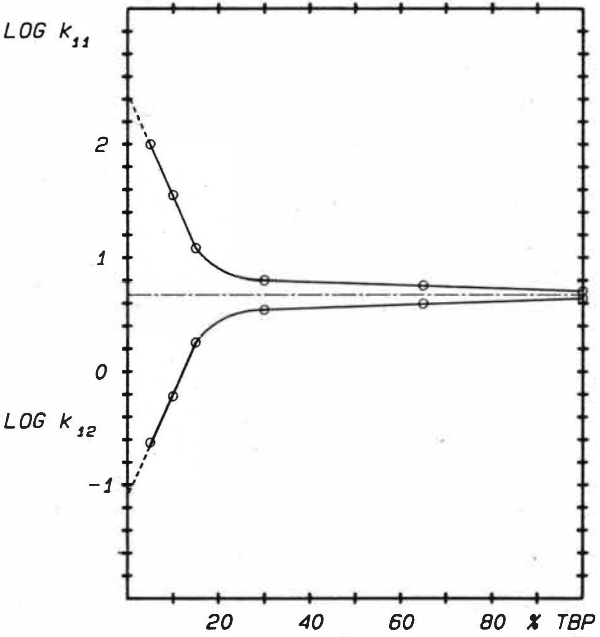

FIG 2 : VARIATION OF LOG k_{12} AND LOG k_{11} WITH % TBP.

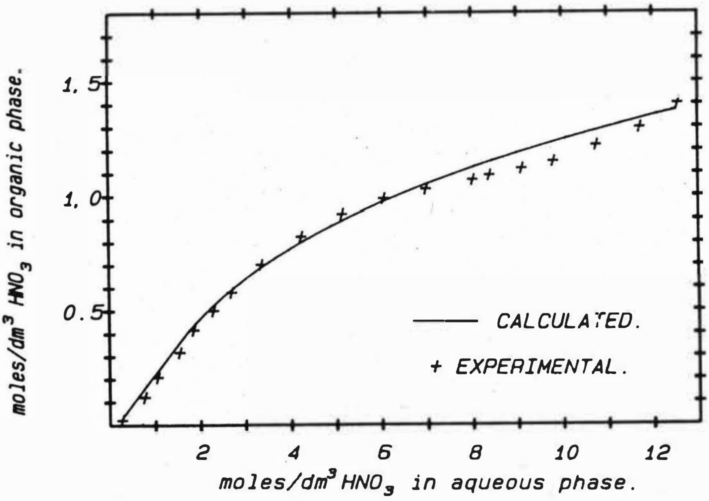

FIG 3: EXTRACTION OF HNO_3 BY 30 % TBP/KEROSENE.

Examination of the variation of the conditional equilibrium constants with % TBP shows that for k_{21} and k_{11} two regions can be identified, viz. $\leq$ 15 % TBP and $\geq$ 30 % TBP. In both cases $\log_{10}$ of k_{12} and k_{11} is linearly related to % TBP but the slopes differ greatly indicating that two systems must be considered i.e. TBP dissolved in kerosene and kerosene dissolved in TBP respectively. Extrapolation of these data to 0 % TBP to derive thermodynamic equilibrium constants is therefore only justified for the region $\leq$ 15 % TBP giving values of $K_{12} = 0{,}083$ ($\log_{10} k_{12} = -1{,}08$) and $K_{11} = 263$ ($\log_{10} k_{11} = 2{,}42$). It is also interesting to note that the product of these two values remains fairly constant at $22{,}0 \pm 0{,}5$ ($\log_{10} = 1{,}34$), indicating that $\gamma_a^2 \cdot \gamma_{o(TBP)}/\gamma_{o(HNO_3.TBP)}^2$ is also a constant (see equations [6] and [7]), which can eventually be used to estimate values of γ_o once γ_a is also taken in consideration.

From the variation of k_{21} with % TBP (Figure 1), however, it is evident that $\gamma_a \cdot \gamma_{o(HNO_3.TBP)}/\gamma_{o((2HNO_3).TBP)}$ does not remain constant but increases with a factor of nearly 2,5 from 5 % to 100 % TBP. k_{21} can nevertheless be extrapolated to 0 % TBP to obtain a value of 0,91 for K_{21}.

An attempt was also made to calculate the concentration of the various TBP compounds in the organic phase at equilibrium. The results are summarized in Table II.

Table II: % of TBP-species in the organic phase at equilibrium

		% of TBP-species(a) at various moles/dm^3 HNO_3 in aqueous phase (equilibrium)						
% TBP	Species	1,00	2,00	4,00	6,00	8,00	10,00	12,00
5	TBP	85,2	58,7	28,5	15,6	9,7	6,6	4,7
	HNO_3.2TBP	0,1	0,2	0,1	0,1	<0,1	<0,1	<0,1
	HNO_3.TBP	14,6	40,5	67,7	75,7	76,3	74,1	70,7
	(2HNO_3).TBP	0,1	0,6	3,7	8,6	13,9	19,2	24,5
10	TBP	83,9	57,6	26,4	13,3	7,5	4,6	3,0
	HNO_3.2TBP	0,6	1,0	0,7	0,4	0,2	0,1	0,1
	HNO_3.TBP	15,3	39,4	62,0	63,7	58,2	52,0	45,7
	(2HNO_3).TBP	0,2	2,0	10,9	22,6	34,1	43,3	51,2
15	TBP	82,6	56,8	27,4	15,0	9,4	6,2	4,4
	HNO_3.2TBP	2,4	4,1	3,2	2,1	1,3	0,9	0,6
	HNO_3.TBP	14,9	38,4	64,9	72,8	73,0	70,2	66,5
	(2HNO_3).TBP	0,1	0,7	4,5	10,1	16,3	22,7	28,5
30	TBP	77,6	51,5	25,0	14,0	8,5	5,8	3,1
		77,8(c)	*46,4*	*11,2*	*3,0*	*0,0*	*0,0*	*0,0*
	HNO_3.2TBP	8,1	12,7	10,6	7,0	4,5	2,9	1,9
		16,8	*28,6*	*20,2*	*7,0*	*2,1*	*0,0*	*0,0*
	HNO_3.TBP	14,2	35,0	59,4	67,7	68,2	65,7	61,9
		7,4	*25,0*	*67,5*	*86,0*	*89,7*	*82,3*	*69,4*
	(2HNO_3).TBP	0,1	0,8	5,0	11,3	18,8	25,6	32,1
		0,0	*0,0*	*1,1*	*4,0*	*8,2*	*17,7*	*30,6*
65	TBP	66,6	45,9	22,3	12,6	7,8	5,2	-(b)
	HNO_3.2TBP	17,0	21,7	18,4	12,6	8,3	5,4	-(b)
	HNO_3.TBP	16,2	31,5	53,7	61,7	62,3	59,7	-(b)
	(2HNO_3).TBP	0,2	0,9	5,6	13,1	21,6	29,7	-(b)
100	TBP	67,2	42,0	20,4	11,6	7,3	4,8	-(b)
	HNO_3.2TBP	20,5	28,4	24,4	17,2	11,5	7,7	-(b)
	HNO_3.TBP	12,2	28,6	49,2	57,0	57,9	55,5	-(b)
	(2HNO_3).TBP	0,1	1,0	6,0	14,2	23,3	32,0	-(b)

a: Based on Σ [TBP-species] = 100 %

b: No experimental data available

c: Cursive values estimated from (7)

From these it is clear that an appreciable amount of HNO_3.2TBP is only present for $\geq$ 15 % TBP and that the 1:1 adduct, HNO_3.TBP, is always the predominant species. It is also evident that ($2HNO_3$).TBP is already formed at 4 moles/dm^3 HNO_3 in the aqueous phase and reaches a value of approximately 30 % at 10 to 12 moles/dm^3 HNO_3. A comparison with literature values (7) for 30 % TBP (see Table II) shows appreciable differences for the individual figures but the general trend remains the same. Unfortunately, insufficient information is available to explain these differences, although it must be pointed out that the estimated organic acid concentration differs greatly from typical experimental values and that the total TBP mass balance does not remain constant over the entire acid concentration.

In order to test the applicability of the equilibrium constants to systems containing metal nitrates, Mailen's (6) experimental results were used to calculate expected undissociated HNO_3 in the aqueous phase and corresponding equilibrium concentrations in the organic phase. The results (Table III) clearly indicate that the estimated equilibrium constants and the associated mathematical model are at least useful for the range 0,1 to 2 moles/dm^3 HNO_3 with 0 to 4 moles/dm^3 metal nitrate. At higher nitrate concentrations very large errors are found which could probably be explained by an increasing change in the total activity of the aqueous solutions.

Table III: Application of model for aqueous HNO_3-$NaNO_3$ solutions (30 % TBP)

Aqueous concentrations: moles/dm^3			Organic acid concentrations: moles/dm^3		
Total HNO_3	Total $NaNO_3$	Undissociated HNO_3	Experimental reference(6)	Calculated	
				Present*	Reference(6)
0,365	1,00	0,0194	0,124	0,133	0,111
0,306	2,00	0,0265	0,175	0,170	0,162
0,256	3,00	0,0303	0,200	0,186	0,220
0,209	4,00	0,0310	0,225	0,190	0,248
0,129	6,00	0,0261	0,275	0,169	0,268
1,913	1,00	0,195	0,525	0,536	0,536
1,765	2,00	0,227	0,575	0,571	0,605
1,635	3,00	0,253	0,638	0,597	0,657
1,488	4,00	0,266	0,681	0,609	0,692
1,225	6,00	0,275	0,765	0,618	0,739

*: Graphical estimate based on concentration of undissociated acid in aqueous phase

CONCLUSIONS

To summarize, it can be concluded that the suggested model and the equilibrium constants that were derived are very useful to predict equilibrium concentrations for the extraction of HNO_3 in TBP/kerosene mixtures, containing from 5 to 100 % TBP, from 0,5 to 12 moles/dm^3 HNO_3 or from 0,1 to 2 moles/dm^3 HNO_3 with 0 to 4 moles/dm^3 metal nitrates. Deviations from experimental results were tentatively explained on the basis of the assumptions made. However, more detailed calculations will be needed to verify these. It was also shown that the equilibrium constants can be used to calculate the concentration of the various TBP-species in the organic phase, which is essential for the derivation of a similar model for the extraction of metal nitrates.

ACKNOWLEDGEMENT

I would like to thank the Atomic Energy Corporation of South Africa for the opportunity to carry out the work described above and for permission to publish the results.

LITERATURE REFERENCES

(1) K Alcock, F C Bedford, W H Hardwick, H A C McKay, J. Inorg. Nucl. Chem., (1957), 4, pp. 100.

(2) T J Collopy, J H Cavendish, J. Phys. Chem., (1960), 64, pp. 1328.

(3) N M Adamskii, S M Karpacheva, I V Mel'nikov, A M Rozen, Report AEC-tr-4852, (1960).

(4) W Davis (Jr), Nucl. Sci. and Eng., (1962), 14, pp. 159-178 (3 articles).

(5) P Leroy, Report CEA-R.3207, March 1967.

(6) J C Mailen, Nucl. Techn., (1981), 52, pp. 310.

(7) J Ly, Rev. Gen. Nucl., (1985), pp. 221.

(8) D F Peppard, J R Ferraro, J. Inorg. Nucl. Chem., (1960), 15, pp. 365.

(9) P J Kinney, M Smutz, Report IS-728, August 1963.

(10) L G Sillen, A E Martell, "Stability Constants of Metal-ion Complexes", The Chemical Society, Special Publication No. 17, London, (1964), pp. 166.

(11) J M Schaekers, et al., Results to be published.

Extraction of Iodine From Irradiated Uranyl Nitrate Samples

Muayed G.Jalhoom
Department of Analytical Chemistry, IAEC, Tuwaitha,Baghdad,Iraq

In early works [1,2] it have been shown that $^{99}TcO_4^-$ ions in basic as well as H_2SO_4 solutions can be separated from irradiated U_3O_8 samples. The distribution coefficient D of the tracers $NH_4{}^{99}TcO_4$ and $H^{99}TcO_4$ varies with the crown cavity size, substitutions, type of the donor atoms, size and charge (charge density) of the cation of the base used and the structure of the organic solvent. From NaOH and H_2SO_4 solutions the extracted complex was suggested to be as $(Na^+DB18C6)(TcO_4^-)$ and $(H^+DB18C6)(TcO_4^-)nH_2SO_4$ respectively. It was hypothesized recently that a complex such as $(H^+DCH18C6)(AuCl_4^-)$ could also be extracted [3].

In this work, extraction experiments were performed on irradiated $UO_2(NO_3)_2.6H_2O$ samples dissolved in HF, HCl, HI and HNO_3 sclutions by using the system dibenzo-18-crown-6-o-dichlorobenzene. A comparison experiments on the tracer $Na^{125}I$ were done using the crowns, 12-crown-4(12C4), 15-crown-5 (15C5), 18-crown-6(18C6), dibenzo-18-crown-6(DB18-C6), kryptofix-22 (K22) and dibenzo-24-crown-8 (DB24C8), dicyclohexyl-18-crown-6 (DCH18C6).

Samples ($\simeq$ 5mg) of $UO_2(NO_3).6H_2O$ were irradiated for 72 hrs, in the Iraqi reactor IRT-5000 in a flux around $2x10^{13}$ cm^{-2}. sec^{-1}. The samples then dissolved in 0.01M HNO_3 after few days of cooling. Aliquots from the dissolved samples were dried and redissolved by the medium of extraction. Equal volumes of the organic phase and the aqueous phase were mechanically shaken for 20 minutes after spiking by the tracer $Na^{125}I$. The activity was assayedusing NaI(Tl) well-type crystal detector connected with a single channel analyzer. In case of extraction of irradiated uranium samples, the Ge(Li) detector connected with a multichannel analyzer was used. The u.v.-vis. spectra were recorded on the PYE UNICAM SP8-400 u.v.-vis. spectrophotometer.

Negligible extraction from nitric acid solutions has been shown by ^{95}Zr, ^{95}Nb, ^{99}Mo, ^{99m}Tc, ^{103}Ru, ^{131}I, ^{140}Ba, ^{140}La, ^{141}Ce, ^{147}Nd, and ^{239}Np(Table-1). Extraction from 0.5-6M HI was accompanied by a precipitate formation. Some extraction ($D \simeq 0.05$) was observed for Ru,I,Ba,La and Nd. On the other hand appreciable extraction of ^{131}I was obtained from HCl and HF solutions. The distribution coefficient D increases with the initial HCl concentration in the aqueous phase up to 6M where after a precipitate was formed. Trace amounts of ^{95}Zr, ^{95}Nb, ^{99m}Tc and ^{103}Ru were extracted together with ^{131}I. However, minimum separation factor around 168 at 6M HCl was obtained for ^{99m}Tc.

Hydroflouric acid has also shown to be a good medium for the selective separation of ^{131}I fission product. In comparison with HCl solutions higher extraction could be obtained at the lower concentrations of HF. Only trace amount of ^{103}Ru could be detected in the organic phase . The separation factor of ^{131}I from ^{103}Ru was determined to be about 670 at 0.5M HF.

Acomparison study on the tracer $Na^{125}I$, similar results to that of the irradiated $UO_2(NO_3)_2.6H_2O$ were obtained. The extraction of iodine species increases with the increase of HCl concentration and a sharp increase was noticed after about 4M HCl (Fig.1). The appearance of a scattered D values on Fig.1 may suggests the presence of more than one extractable species. The behaviour is almost identical when o-dichlorobenzene (o-DCB) and 1,2-dichloroethane (1,2-DCE)were used as the organic solvents for the crown DB18C6. The effect of the extraction shaking time on the distribution coefficient at 4M HCl has been shown to be rather small.

Table I. The Solvent Extraction Data Of The Irradiated Uranyl Nitrate, (Distribution Coefficients), 0.025 M DBI8C6-o-Dichlorobenzene

Isotopes	[HF]M					[HCl]M					
	6	4	2	1	0.5	8	7	6	3	1.5	0.5
Zr-95	N.E	N.E	N.E	N.E	N.E	P	P	0.003			
Nb-95	N.E	N.E	N.E	N.E	N.E	P	P	0.015	0.004	0.0061	
Mo-99	N.E	N.E	N.E	N.E	N.E			N.E	N.E	N.E	
Tc-99m	N.E	N.E	N.E	N.E	N.E	P	P	0.028	0.005	0.012	
Ru-103	N.E	N.E	N.E	N.E	N.E	P	P	0.023	0.019	0.049	0.024
I-131	0.12	0.59	0.3	0.5	1.2	P	P	4.72	2.92	0.96	0.13
Ba-140	N.E	N.E	N.E	N.E	N.E	P	P	N.E	N.E	N.E	N.E
La-140	N.E	N.E	N.E	N.E	N.E	P	P	N.E	N.E	N.E	N.E
Ce-141	N.E	N.E	N.E	N.E	N.E	P	P	N.E	N.E	N.E	N.E
Nd-147	N.E	N.E	N.E	N.E	N.E	P	P	N.E	N.E	N.E	N.E
NP-239	N.E	N.E	N.E	N.E	N.E	P	P	N.E	N.E	N.E	N.E

* N.E Practically total activity in the aqueous phase

P Precipitate formation

The ultraviolate spectra of KI in different molarities of HCl are shown in Fig.2. The two peaks at 192 and 225 nm are attributed to I^- species [4]. The absorption at 192 nm almost disappeared after the addition of HCl, meanwhile the absorption at 225 nm decreases gradually, accompanied with a growth of a peak at 248nm. Very weak absorptions could also be recongnized around 343nm and 437nm. However, the decrease and increase at 225 and 248 nm absorptions are not regular which might be accounted to the formation of a new species. Depending on the spectroscopic methods Cason and Neumann [5] have proposed the following disproptionation reaction in the aqueous solutions

$$I_2Cl^- + Cl^- \rightleftharpoons ICl_2^- + I^- \quad \ldots\ldots\ldots (1)$$

The I_2Cl^- species were characterized by the strong absorption at 248nm (ϵ = 55000), 437nm (ϵ = 1100) and ICl_2^- species, 224nm (ϵ = 47000), 343 (ϵ = 243).

Negligible extraction is shown for the I^- species which are characterized by the absorption at 225nm (Fig.3). However, the absorptions at 248nm disappeared after extraction over the whole range of HCl concentrations used (1-8M). Meanwhile, almost complete extraction at 7 and 8M HCl can be attained for the species characterized by the absorption around 225 and 248 nm. At higher HCl molarities it seems that the major species exist as I_2Cl^- and ICl_2^- as shown in equation (1).

The spectra of the extracted species in 1,2-DCE are shown in Fig.4. The peaks around 364 nm and 294 nm are similar to that of I_3^- in 1,2-DCE [6]. However the absorptions of I_3^- in the aqueous phase (352 nm and 288 nm [4]) could not be observed. The increase in the absorbance with HCl concentrations (1-7N) indicates an increase in the extraction of the species although a different behaviour was observed at 8M HCl. The absorption at 364 nm diminishes and became broader, while the absorption at 294 nm becomes smaller with a tendency for a lower wavelength which could not be recorded. Probably this is due to the extraction of ICl_2^- species which were characterized by the absorptions at 336 nm (ϵ = 310) and 227 nm (ϵ = 54500) in acetonitrile [6]. It is not excluded that the broad peaks at 364 nm are due to both I_2Cl^- and ICl_2^- species. However it was also assumed the presence of the following time depending disproportionation reaction in the organic phase [6] :

$$2I_2Cl^- \rightleftharpoons I_3^- + ICl_2^- \quad \ldots\ldots\ldots (2)$$

Further confirmations for the fact that I^- species are less extractable when lower D values were obtained in the presence of small amount of NaI as carrier or a reducing agent like $Na_2S_2O_3$. Morover, the presence of oxidizing agent like KIO_3 could enhance the extraction in comparison with KI. The fittness of K^+ ions in the crown cavity size and the competition of IO_3^- ions in the extraction should also be considered. Another evidence for the higher extraction of the polyhalogen species is represented by Fig.5, which shows the effect of HF and HI on the D values. The higher extraction obtained in presence of HF might be due to the formation of I_2F^- and (or) IF_2^- species.

In conclusion ion-pair extraction by the crown compounds prefers the polyhalogen ions probably because they are more polar which might enduce further dipole-dipole and ion-dipole interactions.

A slop around unity was obtained for the relation of log.D and log[DB-18C6] at 5M HCl (Fig.6) which suggests the extraction of one crown molecule. So from HCl medium it can be suggested that the ion pair extracted complex may be as $(H^+DB18C6)$ (I_2Cl^-) and or $(H^+DB18C6)(ICl_2^-)$.

Polar organic solvent give better extraction . Almost a linear relationship was attained with the dielectric constant of the organic solvent in the order benzene < chloroform < chlorobenzene < o-dichlorobenzene < 1,2-dichloroethane < nitrobenzene.

The effect of the crown cavity size and substitutions is shown in Fig.7. From 4MHCl the order of extraction is DCH18C6 > 18C6 > DB24C8> DB18C6 > 15C5 > K22 > 12C4 . Obviosly the distribution coefficient increases with the cavity size. The presence of cyclohexyl group almost always enhances the extraction. This is may be due to the greater flexibility gained by the crown molecule. The nature of the counter ion is also important. The order of extraction of TcO_4^- ions from 6M H_2SO_4 [2] was DCH18C6 > DB24C8 > 18C6 > DB18C6 > 15C5 > 12C4 > K22 .

References

1. JALHOOM, M.G., AL-DELLAL, M.J.A. SHIHAB, K.M. to be published
2. JALHOOM, M.G.AL-DELLAL. M.J.A., SHIHAB, K.M, NRC 6130-P07-84,IAEC.
3. TSALON, S.I., KRYLOV, Yu.S: Sov. Radiochem., 24, 413 (1984).
4. KATZIN, I.L.: J.Chem.Phys., 23,2055 (1955).
5. CASON, D.L.NEUMANN, H.M.: J.Am. Chem. Soc. 83, 1822 (1961) .
6. GUTMANN, V.Halogen Chemistry, Academic Press London & New york 1967, V1 .

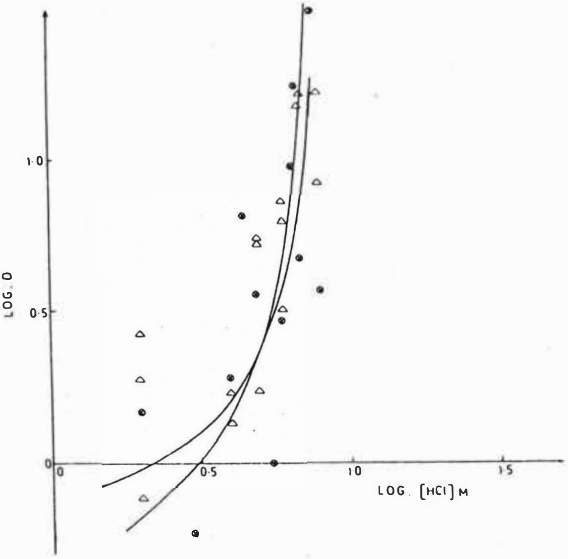

FIG. 1 EXTRACTION OF Na^{125}I

ORG. PH. ● 0·01M DB18C6- 1,2-DICHLOROETHANE

△ 0·025M DB18C6 -o- DICHLOROBENZENE

AQ. PH. : HCl SOLUTIONS

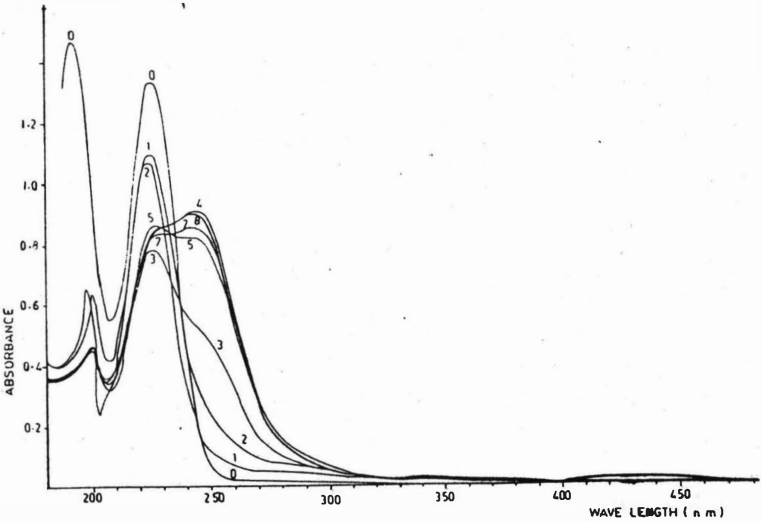

FIG. 2 ABSORPTION SPECTRA OF 0·001M KI IN HCl SOLUTIONS (0-8M)
PATH LENGTH 0·1 cm

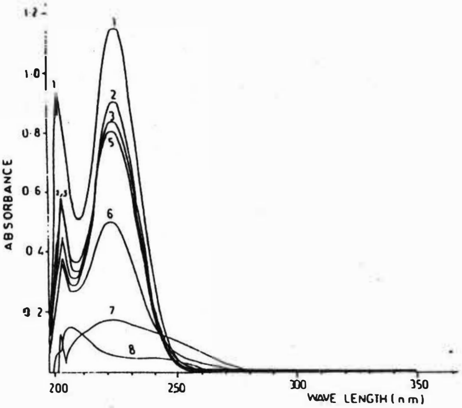

FIG.3 ABSORPTION SPECTRA OF THE AQUEOUS PHASE FOR
THE EXTRACTION SYSTEM:
AQUEOUS PHASE : 0·001 M KI-HCl SOLUTION (1-8 M).
ORGANIC PHASE : 0·01M DB18C6-1,2-DICHLOROETHANE
PATH LENGTH 0·1 Cm.

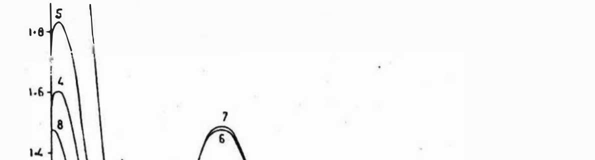

FIG.4 ABSORPTION SPECTRA OF THE ORGANIC PHASE FOR THE EXTRACTION SYSTEM:
AQUEOUS PHASE : 0·001M KI-HCl [0-8M]
ORGANIC PHASE : 0.01M DB18C6 1,2-DICHLOROETHANE,
PATH LENGTH 0·5 Cm

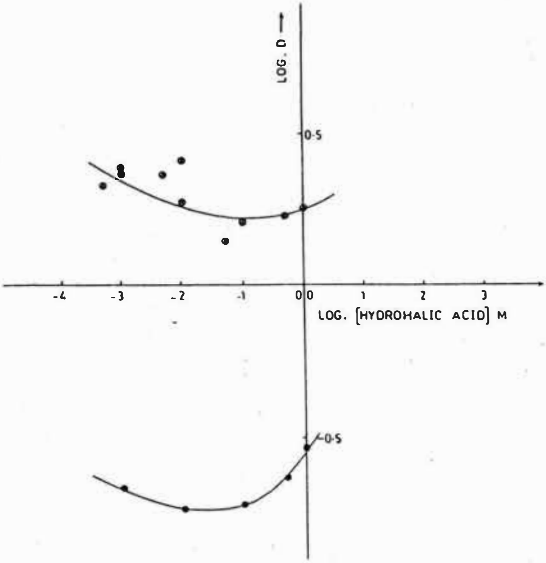

FIG. 5 EXTRACTION OF Na^{125}I

● 0.05M DB18C6 - 1,2 - DICLOROETHANE+HF SOLUTIONS

● 0.1 M DB18C6 - NITROBENZENE - HI SOLUTIONS

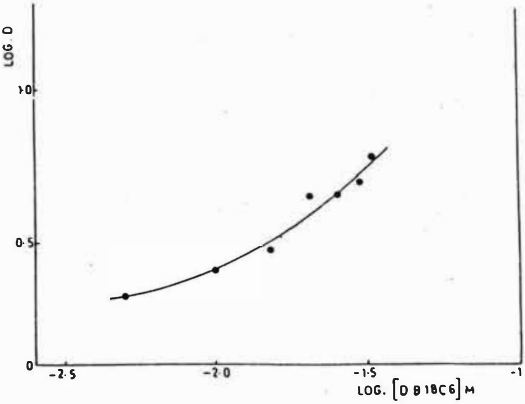

FIG. 6 EXTRACTION OF Na^{125}I

AQ. PH. : 5 M HCl

ORG.PH : DIFFERENT CONCENTRATIONS OF DB18C 6

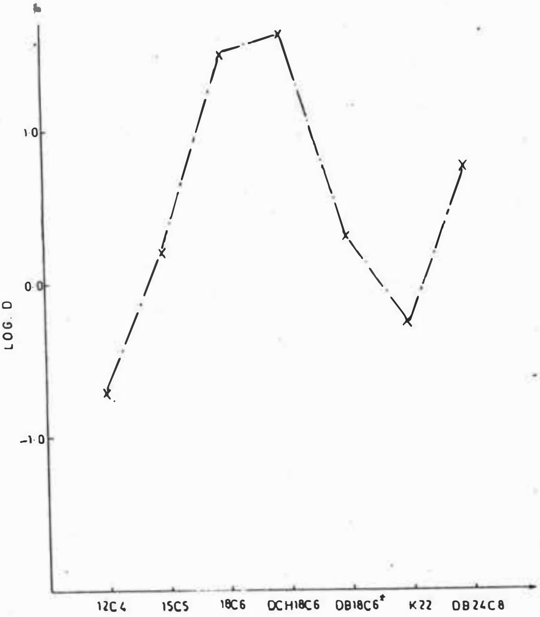

FIG.7 DISTRIBUTION COEFFICIENTS
ORG. PH. : 0·1M CROWN COMPOUND - 1,2 - DICHLOROETHANE
AQ. PH : 4M HCl
* 0·05M

Boundaries of third-phase formation by uranium (IV) and plutonium (IV) in TBP/diluent systems.

P D Wilson & J K Smith, British Nuclear Fuels plc, Sellafield, Cumbria, UK.

It is well known that tetravalent actinide nitrates, when extracted at high concentrations into tri-n-butyl phosphate (TBP) diluted with aliphatic hydrocarbons, can cause the organic phase to split into heavy and light fractions. There have been many studies of the minimum concentrations of actinide in the solvent at which this occurs; these limits depend on the metal ion, the acidity of the equilibrium aqueous phase, the temperature and the nature of the diluent.

The reprocessing of nuclear fuels by solvent extraction can involve relatively high concentrations of plutonium (IV) and sometimes of uranium (IV). The formation of third phases within industrial solvent-extraction equipment would gravely impair its operation, and cannot be tolerated: it is therefore essential to establish the concentration boundaries within which there is no such risk. For control purposes it is probably more important to determine the composition of the equilibrium aqueous phase at the boundary, rather than the loading of the solvent as has hitherto been studied, but it is desirable to know both.

The boundaries of third-phase formation as functions of acidity have been determined for Pu(IV) and U(IV) at various temperatures from 5 to 60°C, although the coverage is not yet complete; the diluents are odourless kerosene, Hyfrane-120 (understood to be a mixture of hydrogenated propylene tetramers) and n-dodecane. For Pu(IV), the boundary has been extended above acidities of immediate reprocessing interest to the point at which solvent and nitric acid alone form a third phase, thus setting a natural limit to the investigation. In general the tendency to formation of third phases increases in the diluent order Hyfrane $<$ kerosene $<$ n-dodecane, and declines with rising temperature: indeed, in kerosene at temperatures above about 30°C, plutonium has so far been found to form only a single organic phase, except where nitric acid is primarily responsible for splitting it. U(IV) continues to form third phases even up to 60°C, although data here are incomplete.

For U(IV) and dodecane, the boundaries in the solvent closely resemble those determined by Kolarik(1) at comparable temperatures. With plutonium there is commonly a minimum in the solvent-phase limit at about 2M aqueous acid and a more or less pronounced peak at about 7M, roughly coinciding with the acidity of maximum distribution ratio: a corresponding peak in the aqueous-phase boundary is shifted, with declining extractability, to 10-12M. At acidities from about 1 to 7M, the boundaries for U(IV) in the solvent or for Pu(IV) in the aqueous phase are relatively flat, showing only shallow minima: slopes in the opposite phase are steeper, reflecting changes in distribution ratio, and for the same reason are steeply negative in the aqueous phase at the lowest acidities. At acidities of 13-17 M, depending upon the temperature and diluent, a third phase can be formed in the absence of U or Pu.

As with most solubility effects, the boundary is very sensitive to temperature, which accounts for much of the difficulty in obtaining consistent results, particularly with Pu(IV) in the region of 20-30°C; it would probably be wise to avoid processing high concentrations at lower temperatures. This is especially true when the diluent is dodecane, which has a remarkably low capacity for the extracted complex at acidities above 2M and temperatures of 5 or 10°C; indeed, where avoidance of third phases is the paramount consideration, the choice of such a diluent would clearly be disadvantageous.

REFERENCE

(1) Z Kolarik, CIM Special Volume 21, p 178.

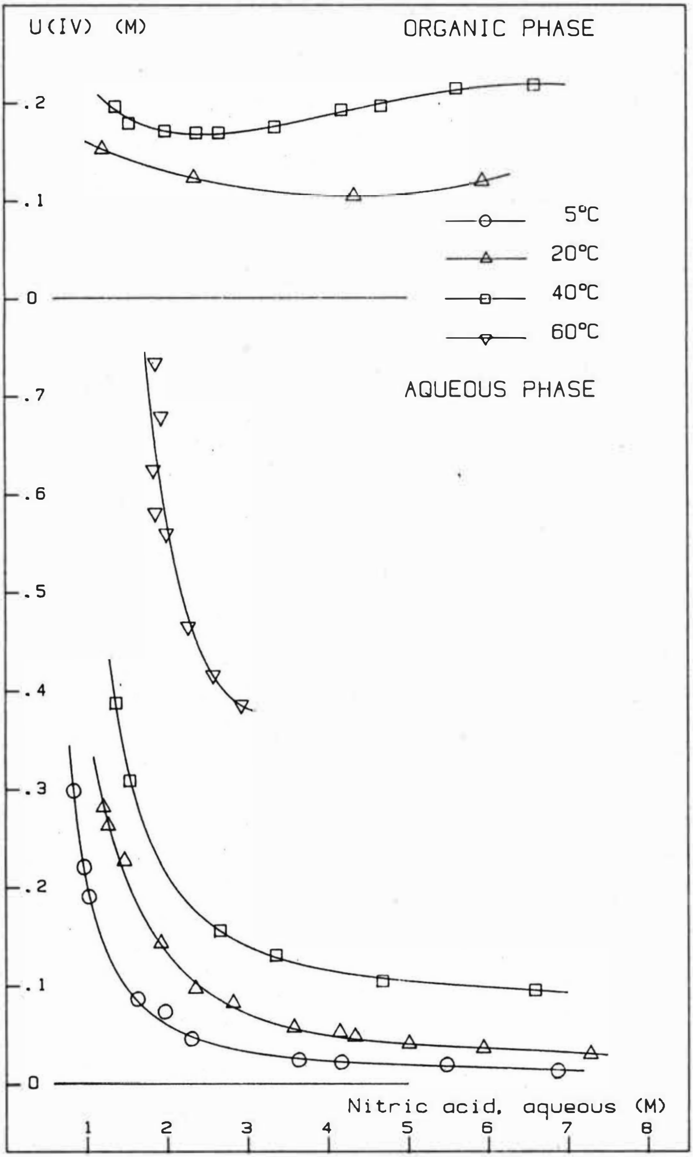

FIG. 1: URANIUM(IV) AND 30% TBP/KEROSENE.

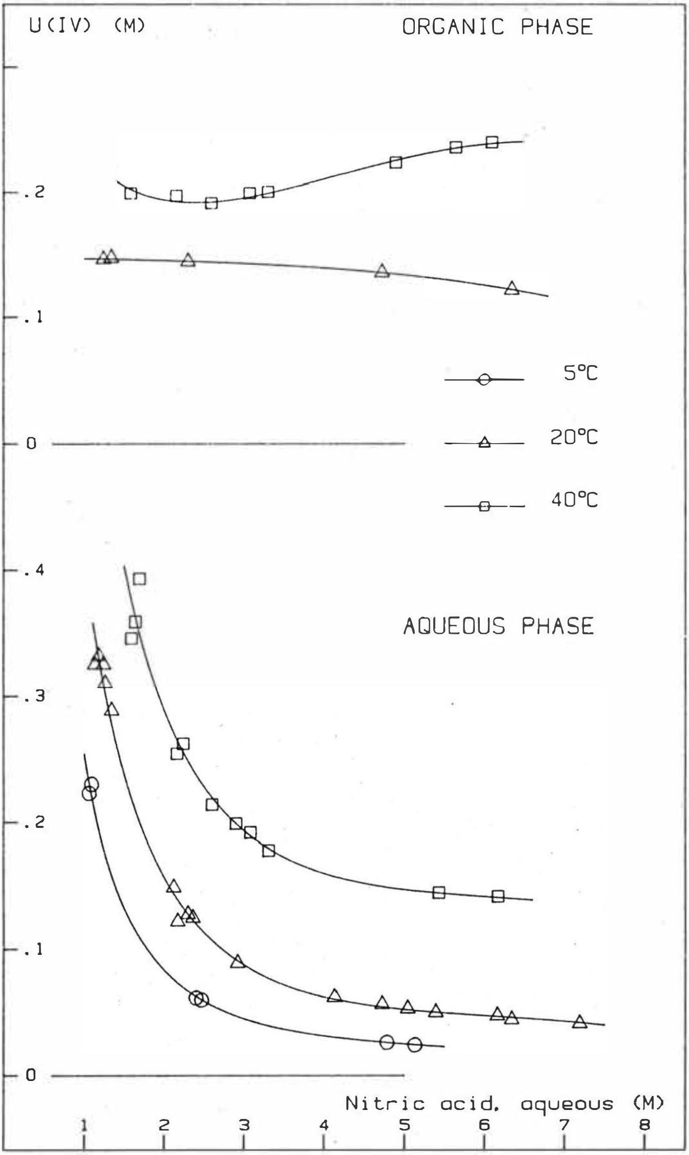

FIG. 2: URANIUM(IV) AND 30% TBP/HYFRANE.

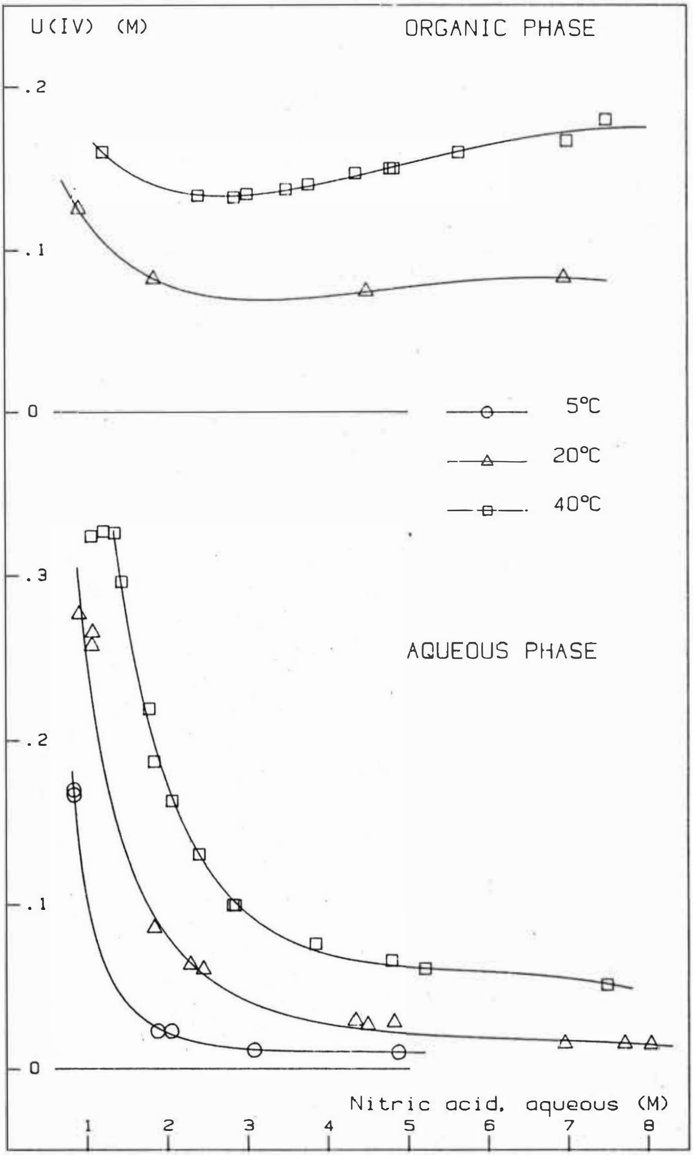

FIG. 3: URANIUM(IV) AND 30% TBP/DODECANE.

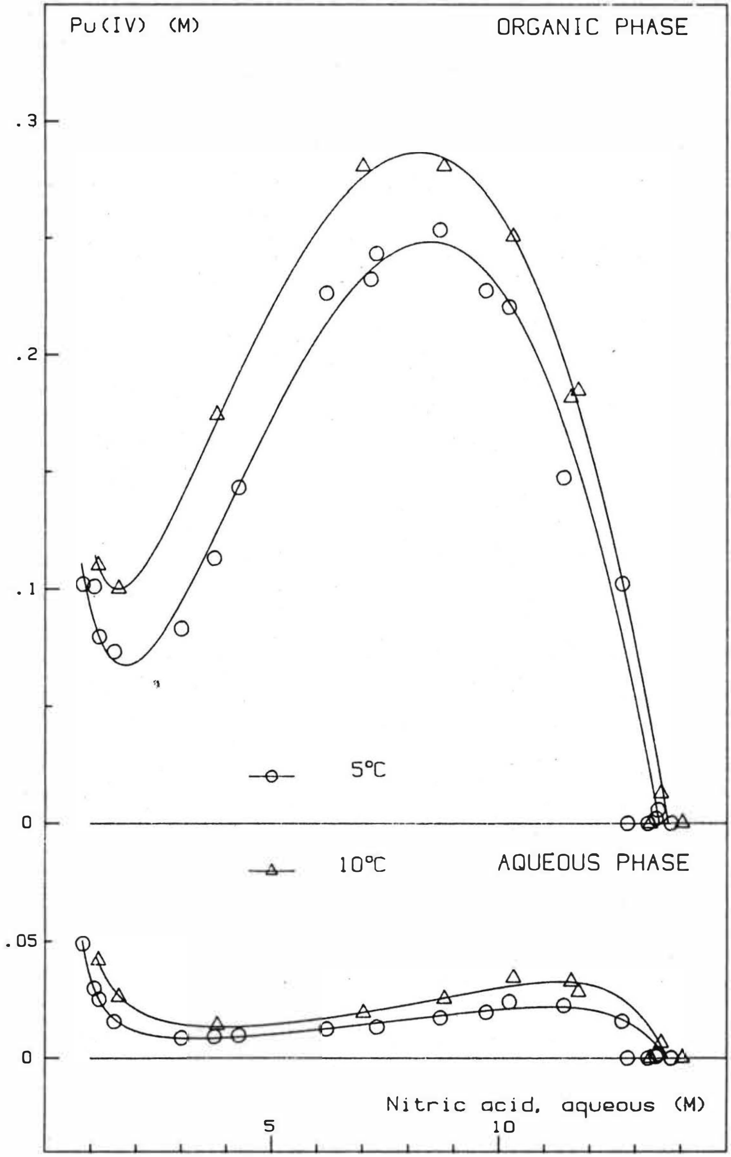

FIG. 4: PLUTONIUN(IV) AND 30% TBP/KEROSENE.

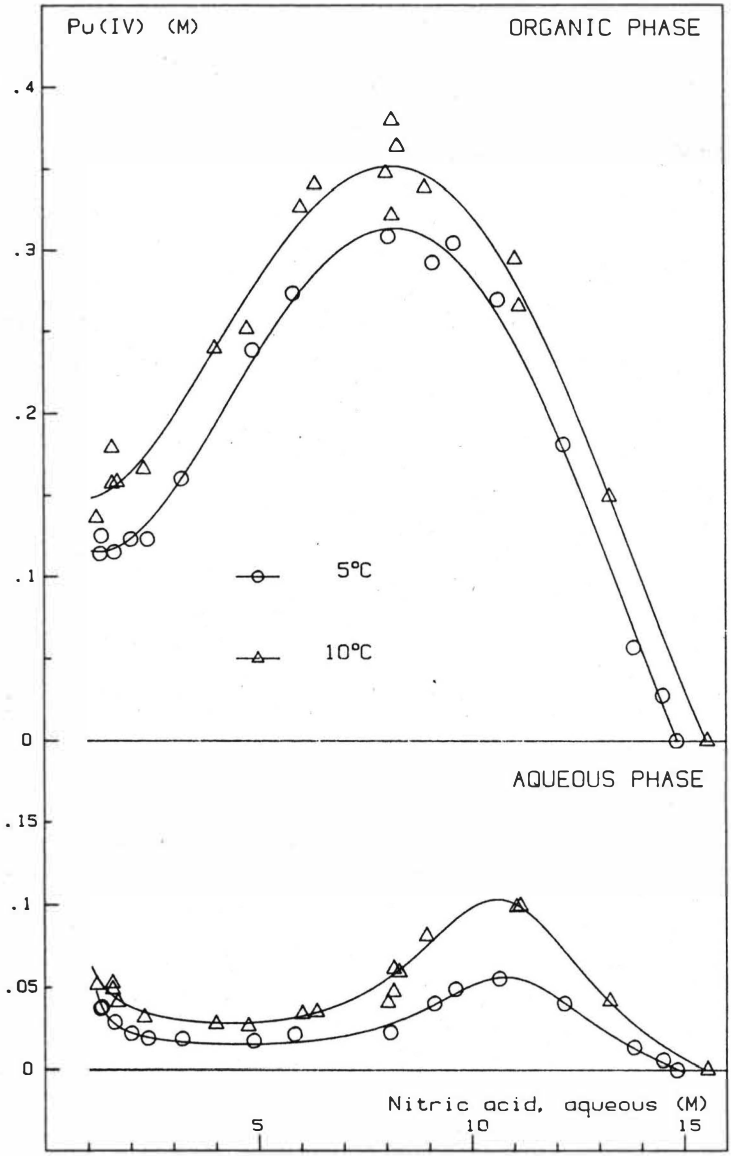

FIG. 5: PLUTONIUN(IV) AND 30% TBP/HYFRANE.

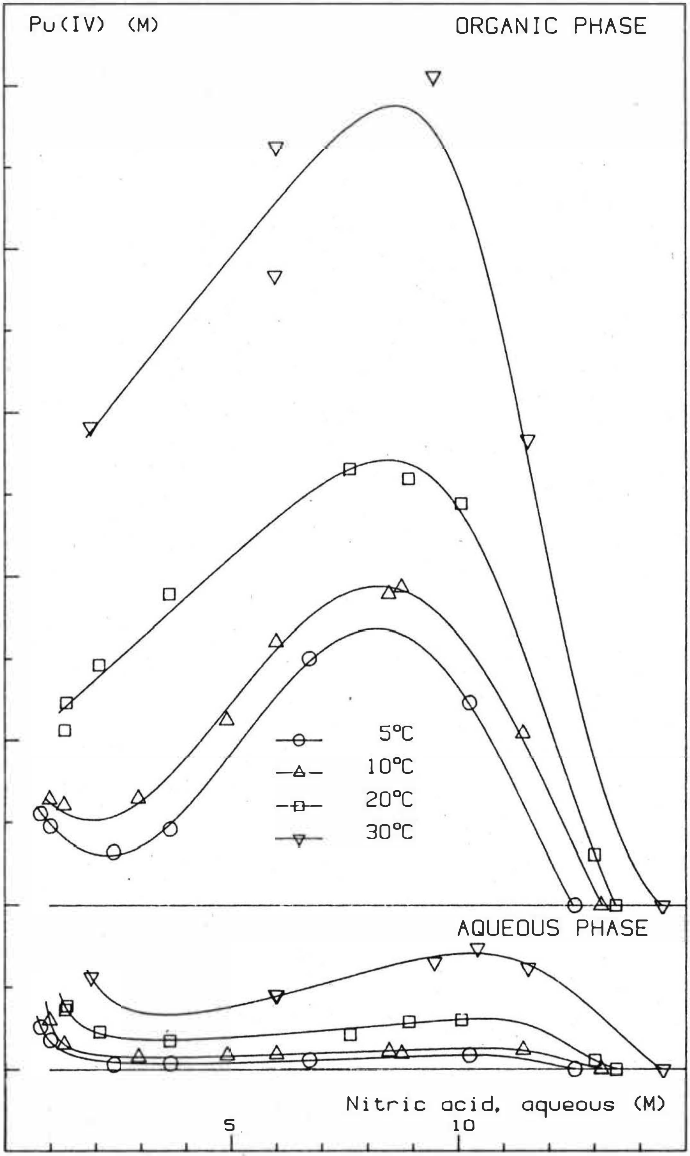

FIG. 6: PLUTONIUN(IV) AND 30% TBP/DODECANE.

Kinetics of Uranium Extraction and Stripping in DEHPA-TOPO Process of Uranium Recovery from Phosphoric Acid

R. Stevanović, Z. Ilić, S. Milonjić and V. Pavasović

Boris Kidrič Institute, P.O. Box 522, 11001 Beograd, Yugoslavia

Introduction

Due to decrease in uranium price on the market and increase in costs of raw materials and energy, uranium from phosphoric acid recovery processes are not economical for small phosphoric acid plants. Therefore, a number of countries have started research work on either development of new processes or improvement of the existing ones.

The most commercially used uranium recovery process is extraction by synergetic mixture of DEHPA (di-2-ethyl hexyl) phosphoric acid) plus TOPO (trioctylphosphine oxide) extractants in kerosene developed by the Oak Ridge National Laboratory (ORNL) /1/. Hurst and coworkers /2, 3/ gave a critical look at the unit operations and steps involved in uranium recovery process and pointed out some of the possibilities and ways for improving the process efficiency.

It is necessary to know the kinetics of extraction process to make an economical design of an extractor and an analysis of the use of pulsating or vibrating plate extractors for smaller plant capacities. The objective of this study was to find the rate determining step of extraction and stripping kinetics. At the time of preparing the paper the authors received two articles by Hurst /4,5/ where kinetic studies of uranium stripping and extraction have been done in more details.

Experimental

Phosphoric acid solutions were prepared from phosphoric acid samples produced from Togo (Africa) phosphate ores by the dihydrate process at the Zorka Company, Šabac, Yugoslavia. Barren phosphoric acid (concentration 5 M) after extraction of uranium, reagent grades of UO_2SO_4, iron(II) sulfate, and elementary iron were used to prepare the aqueous solutions. Commercial grades of DEHPA, TOPO, and purified from aromates kerosene, were used to prepare the organic solutions.

The experiments were carried out in a Lewis cell, jacketed for temperature control (Fig. 1.). The organic and aqueous phases were individually mixed by four flat-blade paddles at 60 and 120 rev/min. At these speeds, the interface is not appreciably disturbed and the interfacial area is known. A stainless steel baffle-arrangement was

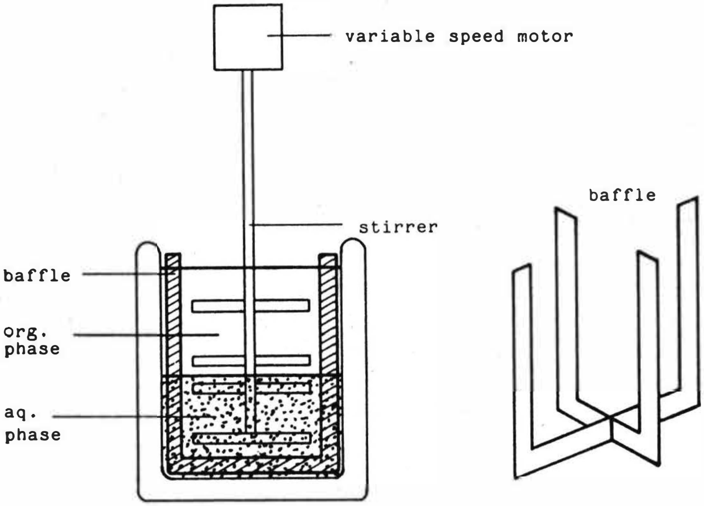

Fig. 1. A Lewis cell for uranium extraction kinetics studies.

added to improve mixing. Only aqueous-to-organic transfer was studied. Barren phases were introduced into the cell and mixed. When temperature and concentration equilibria were reached aqueous solution of uranium was injected, through a hollow leg of stainless steel baffle, into the aqueous phase near the interface. 2 ml samples of organic phase were taken just above the interface through the hollow leg by a syringe after short time periods. Analyses of uranium in organic samples were made by stripping of uranium by 8.5 M phosphoric acid containing 10 g/dm^3 of Fe(II) at 65°C. Uranium concentration in a stripped solution was measured spectrophotometrically at wave length of 665 nm developing colour by Arsenazo III /7,8/.

For the aqueous-to-organic transfer, near time = 0 where $c' \sim c'_0$ Horner and Mailen /6/ developed the equation:

$$k' = -\frac{V.E}{a\Delta\tau}\ln\frac{1 - c/(c'_o E)}{1 - c_o/(c'_o E)} \qquad (1)$$

where k' - rate constant of organic complex formation (cm/s); V - organic phase volume (cm^3); E - distribution coefficient; $\Delta\tau$ - time (s); c - uranium concentration in org. phase after time $\Delta\tau$ (g/dm^3); c'_o - uranium initial concentration in the aqueous phase (g/dm^3); c_o - uranium initial concentration in the organic phase at $\Delta\tau = 0$ (g/dm^3). The uranium initial concentration was varied from 0.5 - 2.0 (g/dm^3). Dependence of the rate constant, k', on time at temperatures 30, 40, and 50°C is illustrated in Fig. 2. Extrapolating data points back to time $\Delta\tau = 0$, when no concentration gradient and mass transfer are present, the true values of rate constants were obtained:

at $t = 30^oC$, $k' = 0.6.10^{-3}$ (cm/s)

$t = 40^oC$, $k' = 1.0.10^{-3}$ (cm/s)

$t = 50^oC$, $k' = 1.6.10^{-3}$ (cm/s).

The slope of Arrhenius plot of ln k' vs. 1/T shows activation energy of 40 kJ/mol (15.5 kJ/mol, Hurst /5/).

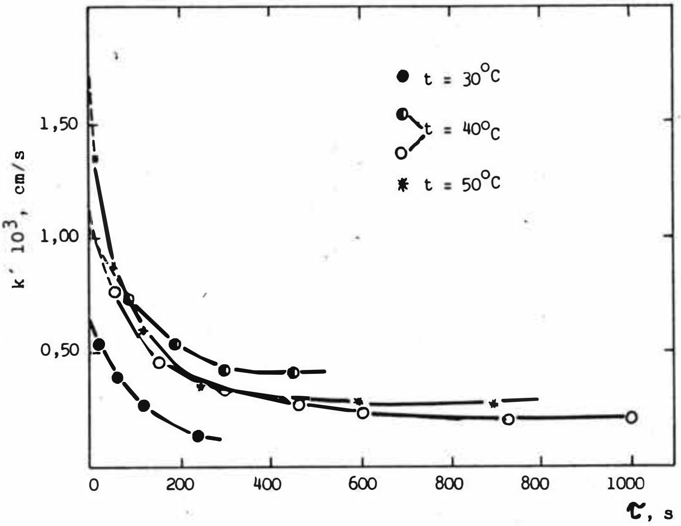

Fig. 2. Dependence of kinetic constant on time at different temperatures.

The obtained transfer rate constants are higher than the ones reported by Hurst /5/ (for example: at $t=50^{o}C$ and 5.0 M H_3PO_4, k' was $1.6.10^{-3}$ (cm/s) which is much higher than $k'=0.6.10^{-3}$ (cm/s) /5/).

The testing of aqueous-to-organic transfer kinetics for the second extraction cycle (0.3 M DEHPA + 0.075 M TOPO) gave the rate constant of $k'=0.38.10^{-3}$ (cm/s) at $t=30^{o}C$, the value lower than in the first extraction cycle. Probably the reaction constant is linearly dependent on the extractants concentrations.

Our preliminary experiments on the uranium stripping indicated that the reduction of U(VI) by Fe(II) to U(IV) was the rate determining step because the time required for reaching equilibria during stripping was much longer than during extraction under similar conditions.

The stripping experiments were carried out in the same cell as the extraction experiments only without the baffle. The equal volumes of barren organic phase and aqueous stripping solution (consisting of 5 M rafinate + 0.5 gU/dm^3 + 15 g $Fe(II)/dm^3$) were mixed in the stirred cell until concentration and temperature equilibria were reached. The mixing was stopped and a sample of aqueous phase was taken. The concentrated organic solution of uranium was injected at time $\tau=0$ and mixing with chosen number of stirrer rotation started. Samples were taken at short time intervals, the phases were quickly separated, and the uranium concentration in the aqueous phase was measured. The concentration of uranium(IV) was determined spectrophotometrically directly by reading the absorbance at 622 nm and 660 nm (the latter one used for lower uranium concentrations). The calibration curve was made by adding known amounts of uranium in barren phosphoric acid, also used as a reference solution, with the same Fe(II) concentration. In such a way, the influences of some uranium complexing agents were eliminated.

Assuming that the reaction of dissociation of uranium organic complex is the rate determining step and that uranium in the aqueous phase is in U(IV) state the following equation is obtained:

$$\ln \frac{c_o - (V'/V)(c'_T - c'_o)}{c_o} = - \frac{k.a}{V}\tau \tag{2}$$

where: a - interfacial area (cm^2); k - constant of organic-to-aqueous interphase transfer (cm/s); V - volume of organic phase (cm^3); V' - volume of aqueous phase (cm^3); c'_T - total uranium concentration in the aqueous phase (g/dm^3) at time τ; c_o - initial uranium concentration in the organic phase; c'_o - initial uranium concentration in the aqueous phase; τ- time (s).

Dependences of concentration change on time according to eq. (2) are presented in Fig. 3. The straight lines were obtained. The experiments were carried out at temperatures 30 and 50°C at stirring speed of 1.2 (m/s) (n=650 rev/min), and at 30°C at stirring speed of 0.6 (m/s). The straight lines proved that the interphase reaction is the rate controlling step and that the reduction of U(VI) to U(IV) by Fe(II) was very fast under experimental conditions.

From the obtained slopes and from the known forward rate constants (aqueous to organic), and extraction coefficients, E, the interfacial areas were calculated:

at $t = 30^{\circ}C$, $n = 320$ rev/min, $a = 162.5$ cm^2
$t = 30^{\circ}C$, $n = 650$ rev/min, $a = 3453$ cm^2
$t = 50^{\circ}C$, $n = 650$ rev/min, $a = 2938$ cm^2.

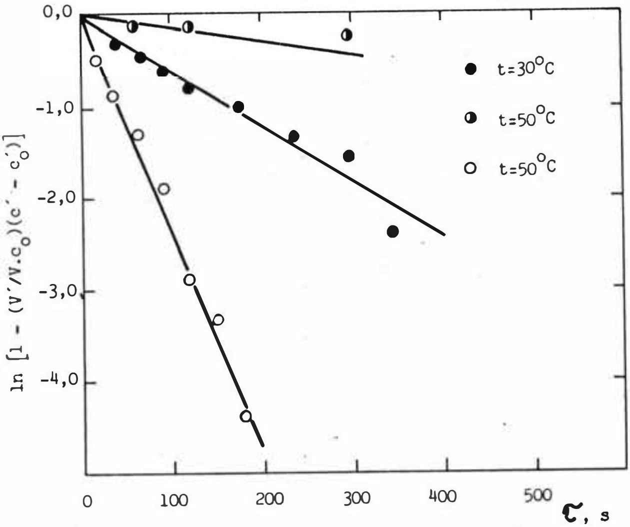

Fig. 3. Stripping transfer kinetic data.

References

1. Hurst F.J., Crouse D.J., Brown K.B., Ind. Eng. Chem. Process Des. Develop., 11, 122 (1972).
2. Hurst F.J., Posey F.A., Sulfuric/Phosphoric Acid Plant Operations, CEP Tech. Manual, 1982, pp. 184-194.
3. Hurst F.J., Crouse D.J., in: Actinide Recovery from Waste and Low Grade Sources, Eds Navratil J.D., Schulz W.W., Hardwood Academic Press, New York, 1982, pp. 201-224.
4. Hurst F.J. and Crouse D.J., Hydrometallurgy, 13, 15 (1984).
5. Hurst F.J., Interphase Transfer of Uranium Between Phosphoric Acid and DEHPA-TOPO Reagent, ORNL-6152 Chemistry Division Annual Progress Report, 106-109, Jan. 13, 1985.
6. Horner D., Mailen J., Thiel S., Scott T., Yates R., Ind. Eng. Chem. Fundam. 19, 103 (1980).
7. Savin S.B., Talanta, 8, 673 (1961).
8. Bunus F.T., Talanta, 24, 117 (1977).

Study of Extraction Rate for Uranyl Nitrate-TBP/n-Dodecane in a Single Drop Column

K.W. Kim, Y.J. Shin, J.H. Yoo, H.S. Park
Korea Advanced Energy Research Institute
Dae-Duk Science Town, Chung-Nam,300-31,Korea

The rate of mass transfer of uranyl nitrate from the aqueous phase of 2N HNO_3 to the organic phase of tributyl phosphate/n-dodecane mixture has been determined in a single drop column without external force, and the motion of the single droplet rising through the aqueous phase has been also observed as preliminary experiment. The mass transfer rate was increased with an increase of uranyl nitrate concentration in the aqueous phase. The effect of the drop size on mass transfer rate was significant at high uranyl nitrate concentration in the aqueous phase but not significant at low uranyl nitrate concentration. The correlations for terminal velocities of droplets with drop size and physical properties of both phases were also presented.

1. INTRODUCTION

Even if there are many effects on extraction efficiency in the various solvent extraction equipment as mixer-settler, pulsed perforated-plate extraction column, and others, the prime importance is to understand mass transfer rate between a dispersed phase and a continuous phase. It is well known that a study of an extraction rate using a single droplet should provide basic information to understand of the performance of solvent extractors.

Accordance with the earlier studies for rate of falling and rising of single liquid droplets, motion of a droplet as a drop deformation, oscillation, and tubulent circulation inside a droplet are usually occured in a single droplet rising through another liquid.[1-6] These phenomena give an effect on mass transfer rate of heavy metal from an aqueous phase to an organic phase, therfore, a hydrodynamic study of a single organic droplet in a stagnent aqueous phase must be carried out as a preliminary work.

Interfacial tubulence between two phases due to steep concentration gradient near the interface and physical properties of both phases such as viscosity and interfacial tension, etc is also important on extraction rate.[7]

In the preliminary work of this investigation to understand the motion of the single droplet rising through another stagnent liquid, 2N HNO_3 solution and the single droplet of tributyl phosphate (TBP)/n-dodecane were used as a continuous phase and a dispersed phase, respectively. The mass transfer experiment was carried out in uranyl nitrate solution having free acidity of 2N HNO_3 and 30% TBP/n-dodecane system.

The objectives of the current study are to experimentally observe the motion of the single droplet rising through another liquid, and to determine the extraction rate at various drop size and uranyl nitrate concentration in the continuous phase, using the single drop extraction column without external force.

2. THEORY

2.1 Motion of Droplet through Fluid without External Force

Considering a droplet rising through a fluid without external force, the force balance on the droplet can be represented as follows :

$$\frac{d}{dt}\left(\frac{\pi}{6} D_e^3 \rho_d U_d\right) = \frac{\pi}{6} D_e^3 g \left(\rho_c - \rho_d\right) - \pi D_e^2 \rho_c \frac{U_d^2}{2} C_D \qquad (1)$$

The droplet quickly reaches a terminal velocity, and then equation (1) is changed as follows :

$$C_D = \frac{4}{3}\,\frac{(\rho_c - \rho_d)\ g\ D_e}{\rho_c\ U_{\infty}^2} \tag{2}$$

Otherwise, if the mass transfer continuously occurs between both phases during drop life time, a concept of a terminal velocity will be disappeared, and the equation(1) is changed again as follows :

$$\rho_d \frac{dU_d}{dt} + U_d \frac{d\rho_d}{dt} = g\ (\rho_c - \rho_d) - \frac{3}{D_e}\rho_c C_D U_d^{\ 2} \tag{3}$$

Because the solution of this equation is not simple, approximately establish the empirical equation like as equation (4) under the assumption that the rising velocity of the droplet accompanying mass transfer at arbitrary time and location in a single drop column is identical with a terminal velocity of a droplet in no mass transfer system getting the same density difference with the droplet accompanying mass transfer.

$$U_d\Big|_t \simeq U_{\infty} = f\ (D_e, \Delta\rho,\ \ldots\ldots\ldots..) \tag{4}$$

2.2 Mass Transfer Rate

A mass transfer rate can be represented in a single droplet column as follows :

$$\frac{\pi}{6} D_e^3\ \frac{dC_d}{dt} = \pi D_e^2\ K_o\ (C_d^* - C_d) \tag{5}$$

In order to minimize the experimental error for the transfer occured by drop formation and coalescence, the shortest reference column must be used. In this case, the drop concentration after withdrawal from the reference column approximately equals that after the same length of rising in any longer column. The corresponding time of contact was the diffenence between the total rising times in the reference column and any longer column. With these boundary conditions, equation (5) is integrated to give the following expression for overall mass transfer coefficient, Ko :

$$K_o = -\frac{D_e}{6t} \ln\left[\frac{C_d^* - C_d}{C_d^* - C_{d,r}}\right] \tag{6}$$

The relation between the overall resistance and individual resistance in two film throry is :

$$\frac{1}{K_o} = \frac{1}{k_d} + \frac{m}{k_c} \tag{7}$$

The individual mass transfer coefficient in the aqueous phase, k_c can be calculated from Higbie penetration theory [8] and West theory [9] as follows :

$$k_c = 2\left[\frac{D_c U_d}{\pi D_e}\right] \tag{8}$$

In equation (8), diffusivity, D_c is also calculated by the following equation used usually in electrolyte.

$$D_c = \frac{2RT}{F^2}\ \frac{\lambda_+ \lambda_-}{(\lambda_+ + \lambda_-)}\left[1 + \frac{d\ln \gamma_{\pm}}{d\ln C}\right] \tag{9}$$

3. EXPERIMENTAL

3.1 Physical Properties

To search the effects of physical properties of the aqueous and organic phases on the motion of the single droplet and the extraction rate, densities and viscosities of the each phase and interfacial tension have been selected, and those values were determined by changing of volumetric fraction of TBP in the organic phase. The selected physical properties were measured as follows :

density by'DMA45 Density Meter' (accuracy;$\pm 10^{-4}$g/ml), interfacial tension by 'Drop Weight Method', and viscosity by 'Falling Ball Viscometer'.

All organic phases and the aqueous phase of 2N HNO_3 were mutually saturated before the main experiment was carried out. The measured physical properties are shown in Figure 1 and 2. From the current data, the correlations for the interfacial tensions and densities of organic phase with volumetric fraction of TBP in organic mixture takes the following.

$$\sigma = \frac{25.4220}{0.3738 + \log 3x} \tag{10}$$

$$\rho_d = 0.7602 + 0.0025\,x \tag{11}$$

where

$$x = \frac{\text{volume of TBP}}{\text{total volume of organic mixture}}$$

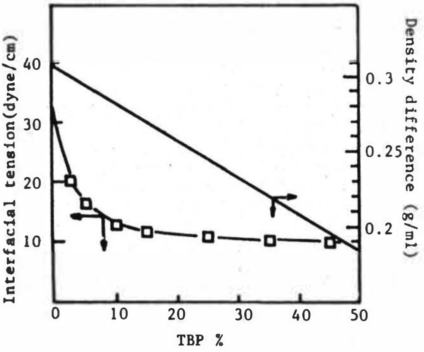

Fig.1. Interfacial tension and density difference between 2N HNO_3 and organic phase vs. volumetric percentage of TBP in organic phase at 25°C.

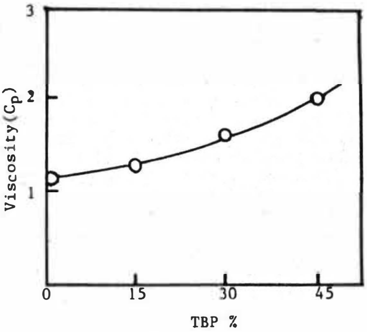

Fig.2. Effect of volumetric fraction of TBP in organic phase on viscosity of organic phase at 25°C.

3.2 Equipment and Procedure

The single drop column of annular type was constructed of two 150 cm-long glass tubes with inside diameters of 2.5cm and 4cm. 2.5cm I.D. glass tube was used as extraction column and annular chamber between 2.5cm I.D. glass tube and 4cm I.D. glass tube was used as water jacket to maintain operation temperature of 25°C. Hypodermic needles were used to form the liquid droplets at their tips. The oblique cut on the end of the needle was removed and the tip rounded off with a file to give a sharp-edged circular tip. The inside diameters of the selected needles were 0.278, 0.366, 0.431, 0.525, 0.644, 0.811, 1.029, 1.35, and 1.55mm. The size of each needle was measured by light projection method.

The drop size was obtained from the number of droplets and the volume of the organic phase passed. The passed organic volume was also measured by burette. To regulate the flowrate of the organic phase and to maintain a steady production rate of single droplet, the pressurized feeding system (35mmHg as Gauge pressure)was adapted in this investigation. In preliminary work, it was found that droplets attained terminal velocities after an initial height of rising of 30cm from nozzle tip . All terminal velocities of droplets were measured by free rising period of a droplet from 30cm above of the nozzle tip.

Extraction rate was determined by detection of uranium concentration extracted from the continuous phase to the single droplet and its contact time. The reference column of 30cm-long glass tube was used to eliminate the error occured by mass transfer during formation and breakup of droplet at tips. The extracted uranium concentration was measured by 'DMA 45 density meter'.

4. RESULT and DISCUSSION

4.1 Motion of Single Droplet without Mass Transfer

The effect of drop size on a terminal velocity of a rising droplet is shown in Figure 3, using 2N HNO_3 and TBP/n-dodecane mixture. As drop size was increased, the rising velocities of the droplets increased gradually, reached a maximum, and then slightly decreased again. These effects are in good agreement with the observations reported earlier. It was also found that the droplets rising through the continuous phase were nearly spherical in small sizes, and their deformation increased with an increase of drop size.

The terminal velocities of droplets were increased with an increase of TBP content in low volumetric fraction range of TBP($<$5%), but those values were decreased with an increase of TBP content in high fraction ($>$15%). Accordance with the result of physical property change in section 3.1, interfacial tension was steeply decreased with an increase of volumetric fraction of TBP in organic mixture until about 10% TBP but almost constant in volumetric fraction range of TBP of 20% above.
The difference of density between two phases was monotonouslly decreased with an increase of volumetric fraction of TBP in organic mixture. From above trend for physical properties, it was suspected that the dominant effect on the terminal velocity was interfacial tension at low volumetric fraction of TBP, and the difference of the density at high volumetric fraction of TBP.
When the terminal velocities from observed values were considered with respect to drop size and physical properties as forming two separate regions, region I($D_e \le D_{e,c}$) where the velocity increased with drop size and region II ($D_e > D_{e,c}$) where the velocity decreased with drop size, the following correlations are obtained:

$$o < D_e \le D_{e,c} \quad : U_\infty = 124.07\, D_e^{0.623} \Delta\rho^{0.636} \sigma^{-0.225} \qquad (12)$$

$$D_e > D_{e,c} \quad : U_\infty = 14.946\, D_e^{-0.069} \Delta\rho^{0.225} \sigma^{0.036} \qquad (13)$$

$$D_{e,c} = 0.0054\, \Delta\rho^{-1.121} \sigma^{0.948} \qquad (14)$$

The multifle regression coefficients of equation(12) and (13) are 0.88 and 0.94, respectively, and the standard deviations of the data from these equations are 1.73% and 1.09%, respectively.

4.2 Motion of Single Droplet Accompanying Mass Transfer

When the mass transfer continuously occurs from the continuous phase to rising droplets of 30% TBP/70% n-dodecane, concept of a terminal velocity cannot be applied to this system. However, under the assumption that the rising velocity of the droplet accompanying mass transfer at arbitrary time and lication in a single drop column is identical with a terminal velocity of a droplet in no mass transfer system getting the same density difference with the droplet accompanying mass transfer, the empirical equation of equation (4) could be approximately obtained from the terminal velocities of single droplets using 30% TBP/n-dodecane having various uranyl nitrate concentrations and 2N HNO_3 system. This system almost prevents back-extraction of uranyl nitrate from an organic phase to an aqueous phase because of high distribution coefficient.

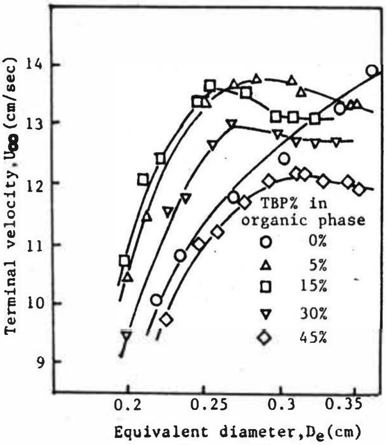

Fig.3. Terminal velocity vs. drop diameter at 25°C.

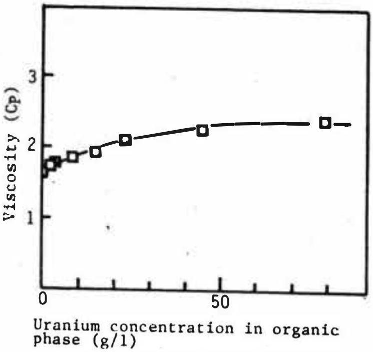

Fig.4. Effect of uranium concentration in organic phase on viscosity of organic phase at 25°C.

The effect of uranium concentration in the droplet on physical properties was observed and shown in Figure 4 and 5. The effect of drop size on the terminal velocity of rising droplet is also shown in Figure 6, using 2N HNO_3 and 30% TBP/n-dodecane having various uranium concentrations. From the current data, the following correlations are obtained.

$$0 < D_e \le D_{e,c} \quad : U_\infty = -7.924 + 23.295\, D_e + 60.353\, \Delta\rho \tag{15}$$

$$D_e > D_{e,c} \quad : U_\infty = 7.095 - 5.455\, D_e + 31.279\, \Delta\rho \tag{16}$$

$$D_{e,c} = 0.583 - 1.667\Delta\rho \tag{17}$$

$$\Delta\rho = \rho_c - 0.8351 - 0.0012\, C_d \tag{18}$$

The multifle regression coefficients of equation (15) and (16) are 0.96 and 0.97, respectively, and the standard deviations are 2.44% and 1.56%, respectively.

4.3 Extraction Rate

All experiments for extraction rate were carried out in uranyl nitrate/2N HNO_3-30% TBP/n-dodecane system. There are end-effects of the formation and coalescence of the droplets in the single drop column. These effects can be eliminated by comparing with reference column. The mass transfer rate observed is shown in Figure 7 and the overall mass transfer coefficients calculated by equation (6) are shown in Figure 8.

In case of low uranyl nitrate concentration in a continuous phase, the effect of the drop size on the overall mass transfer coefficient was not significant, but the overall mass transfer coefficient was increased with an increase of drop size due to increasing interfacial turbulence and turbulent circulation inside the organic droplet in case of high uranyl nitrate concentration in a continuous phase.

The resistance of each phase has been calculated from the equation (7) and (8). Here, the values of λ_+, λ_- and $\partial \ln \gamma_\pm / \partial \ln C$ used 349.8cm^2/ohm.mole, 71.4cm^2/ohm.mole, and 0.0886, respectively. The portion of resistance inside the droplet was about 60-80% of total resistance, and this portion was decreased with an increase of uranyl nitrate concentration in a continuous phase, especially at large droplets. (Figure 9).

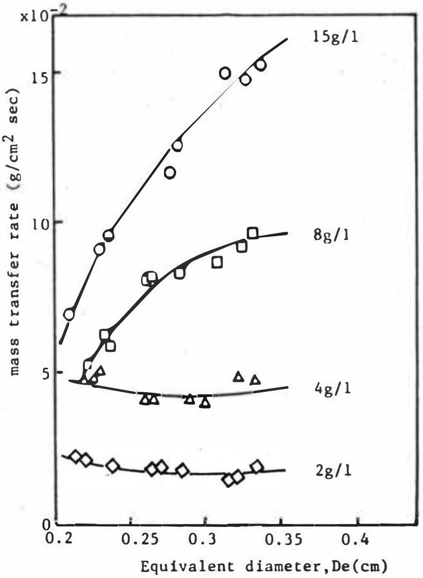

Fig.7. Effect of drop diameter on mass transfer rate at different uranium concentrations in aqueous phase.

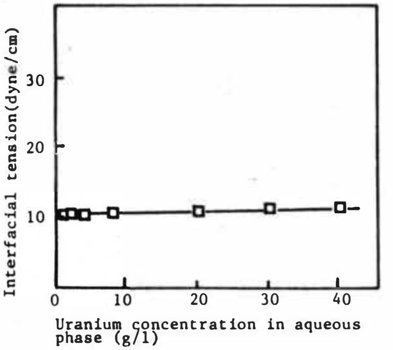

Fig.5. Effect of uranium concentration in 2N HNO_3 on interfacial tension at 25°C.

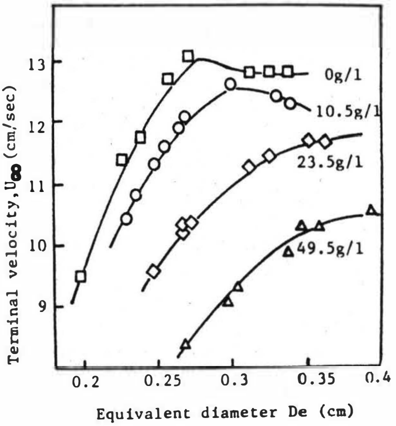

Fig.6. Effect of drop diameter on terminal velocity of droplet rising through continuous phase of 2N HNO_3 at different uranium concentration of droplet.

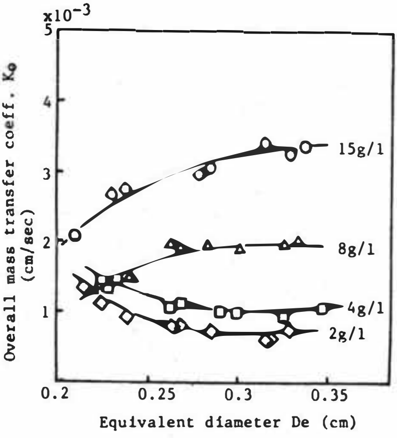

Fig.8. Overall mass transfer coefficient vs. drop diameter at different uranium concentrations in aqueous phase.

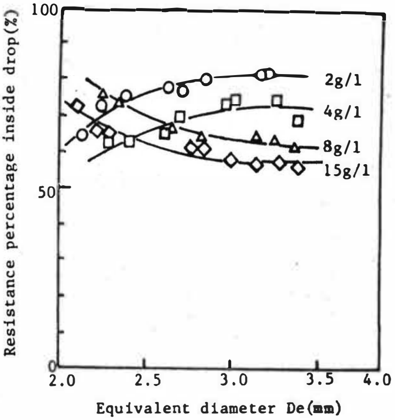

Fig.9. Resistance percentage inside drop vs. drop diameter at different uranium concentrations in aqueous phase.

5. CONCLUSIONS

Spherical shape of a droplet becomes more stable with an increase of uranyl nitrate concentration in a droplet. The mass transfer rate is increased with an increase of uranyl nitrate concentration in an aqueous phase. The effect of drop size on mass transfer rate is significant at high uranyl nitrate concentration in an aqueous phase, and the mass transfer rate is increased with an increase of drop size due to interfacial turbulence and turbulent circulation inside the droplet. In uranyl nitrate-30%TBP/n-dodecane extraction system, the portion of resistance inside the droplet for mass transfer was about 60-80% of total resistance.

NOMENCLATURE

C_D : drag coefficient
C_d : uranium concentration in organic phase, g/l
C_d^* : uranium concentration in organic phase at equilibrium, g/l
D_c : diffusivity of solute in aqueous film, cm^2/sec
D_e : equivalent diameter of droplet, cm
$D_{e,c}$: equivalent diameter of droplet at peak terminal velocity, cm
F : Faraday constant
k_c : individual mass transfer coefficient in aqueous phase, cm/sec
k_d : individual mass transfer coefficient in organic phase, cm/sec
K_o : overall mass transfer coefficient, cm/sec
g : gravitational constant, cm/sec^2
m : distribution coefficient of solute at given free acidity
R : gas constant,
t : time, sec
T : temperature, ^ok
U_d : rising velocity of droplet, cm/sec

$U_{d\infty}$: rising terminal velocity of droplet, cm/sec
x : volumetric fraction of TBP in TBP/n-dodecane mixture
ρ_c : density of continuous phase, g/cm^3
ρ_d : density of droplet, g/cm^3
σ : interfacial tension, dyne/cm
λ : equivalent ion conductivity, cm^2/ohm.mole

LITERATURE CITED

(1) Hu, Shengen and R.C.Kintner, A.I.Ch.E., 1(1), 42 (1952)
(2) Klee, A.J. and R.E. Tregbal, A.I.Ch.E., 2(4), 444 (1956)
(3) Lehrer, I.S., A.I.Ch.E., 26(1), 170 (1980)
(4) Elzinga, E.R. and J.T.Banchero, A.I.Ch.E., 7(3), 394 (1961)
(5) Handlos, A.E. and T.Baron, A.I.Ch.E., 3(1), 127 (1957)
(6) Inoue, K. and F. Nakashio, Chem.Eng. Sci., 34, 191 (1979)
(7) Sterning, C.V. and L.E. Scriven, A.I.Ch.E., 5(4), 514 (1959)
(8) Higbie, R., Trans. American Inst. Chem. Eng., 44, 621 (1952)
(9) West, F.B., A.J. Herrman, A.T. Chong, and L.E.K. Thomas, I.&E.C., 44, 621 (1952)

Interphase Transfer Kinetics of Plutonium and Nitric Acid in the System Nitric Acid - Tributylphosphate, Dodecane

C. Mas, G. Knittel, R. von Ammon

Institut für Heiße Chemie, Kernforschungszentrum Karlsruhe,
Federal Republic of Germany

1. Introduction

The interphase transfer kinetics of HNO_3 and of metal ions, e.g. U(VI) and Pu(IV) in the system U, Pu, HNO_3/tributylphosphate (TBP), dodecane have been studied by several authors using various techniques (1 - 6). The results have been interpreted either solely in terms of a diffusionally controlled mechanism (2, 3), or a mechanism where both diffusion and the chemical reactions 1 and 2 at the interface participate in the total mass transfer (5, 6).

$$HNO_3 + TBP \rightleftharpoons HNO_3\,TBP \qquad (1)$$
$$Pu(NO_3)_4 + 2\,TBP \rightleftharpoons Pu(NO_3)_4\,2TBP \qquad (2)$$

In the course of our efforts to model the extraction steps of the PUREX process (7) we have taken up interphase transfer studies in order to gain knowledge of the individual transport coefficients β_i of all species participating in the process.

In this contribution, some experimental results are communicated on the interphase transport of Pu(IV). The data were obtained in a Lewis-type stirred cell.

The data were interpreted following the model of Nitsch (2, 3).

In addition, we developed a new model based on the theory of irreversible thermodynamics (8). This model will be briefly outlined and applied to the reextraction of HNO_3 from TBP (equation 1).

2. Interphase Transfer of Pu(IV)

2.1 Experimental

2.1.1 Apparatus

A Lewis-type stirred cell was used similar to the cell described by Nitsch (9). Smaller dimensions, however, were chosen in order to reduce the amount of plutonium necessary: the volume of each phase was 97 cm³, the specific area of the interface (area/volume) was 0.2023 cm^{-1}.

The data obtained with this cell were standardized by a larger cell, in which the transport coefficients in the coextraction system (U(VI), HNO_3/TBP, dodecane given by Nitsch and van Schoor (2) could be reproduced satisfactorily well.

The organic and aqueous phases were stirred separately with a stirrer frequency in the aqueous phase (n_W) varying between 75 and 200 min^{-1}. In the organic phase it was adjusted according to the viscosities to obtain equal Reynold numbers (e.g. at n_W = 100 min^{-1}, n_O = 228 min^{-1}).

2.1.2 Solutions

In two series of experiments Pu(IV) concentrations were kept constant at 2.3 mmol/l and 0.020 mol/l, respectively. The stock solutions had been freshly separated from uranium and adjusted to the +4 oxidation state by established methods (10).

The HNO_3 concentration in n-dodecane (purum quality, Schuchardt) was either 1.1. mol/l (30% by volume) or 0.37 mol/l (10% by volume). The TBP (Fluka or Merck) was cleaned by washing with 10% Na_2CO_3 solution and water, drying over Al_2O_3 and filtering.

Temperature was kept constant at 25° C.

2.1.3 Analysis

Plutonium was analyzed either by α-spectrometry (10% TBP solutions) or by γ-spectrometry (30% TBP solutions).

HNO_3 was titrated potentiometrically with NaOH after complexation of plutonium with NaF + oxalate.

All data of extraction experiments are the average of three runs, all data of reextraction experiments of two runs.

2.2 Results

From the experimental kinetic data the initial reaction rates $\dot{n}_0$ (mmol/cm²·s) and the individual transport coefficients β_i (cm/s) of all species were evaluated according to the method of Nitsch et al. (2,3). β_{Pu} was obtained from extraction experiments, whereas the transport coefficients for the TBP complexes of Pu (β_{Ko}) and HNO_3 (β_{Kx}) were obtained from reextraction experiments.

The results of the series with 0.020 mol/l Pu and 30% TBP are plotted in fig.1 in dependence on stirrer frequency. The results of the series with the more dilute plutonium solution are very similar and therefore not shown here.

2.3 Discussion

Both figures show that the stirrer frequency has a pronounced effect on the transport coefficients. This seems to indicate that in this system under the specified conditions, transport takes place in a diffusionally controlled regime, as was deduced for uranium in the same system (2,3). The absolute values of the β-coefficients of Pu(IV) also compare well with those of U(VI).

Coextraction of HNO_3 is not influenced significantly by the presence of plutonium. An enhanced extraction of HNO_3, as it is observed in coextraction experiments with highly concentrated U(VI) solutions ($\gtrsim$ 0.5 mol/l) (2), is to be expected only at much higher Pu concentrations than those studied here.

3. Theory of Interphase Transfer Kinetics in the System HNO_3/TBP, Dodecane

3.1 Fundamentals

First, we evaluated our data following the model of Danesi (5), where both diffusion and chemical reaction at the interface play a comparable role, in order to determine the thickness of the diffusion layer.

The essential assumptions of this model are:

- The chemical reaction takes place in the aqueous phase close to the interface in a zone small compared to the diffusion film,

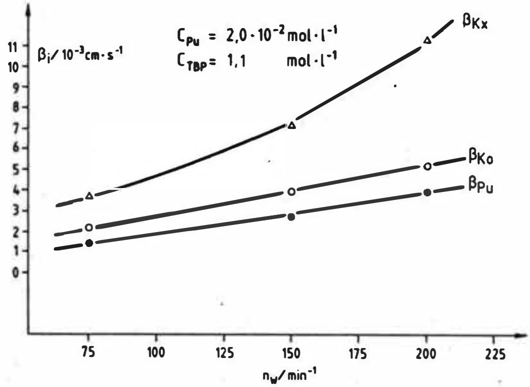

Fig.1: Dependence of transport coefficients β_i on stirrer frequency; Pu concentration of aqueous phase in extraction experiments: $2.0 \cdot 10^{-2}$ mol/l; TBP concentration in dodecane: 1.1 mol/l (30% by volume); Kx = $HNO_3 \cdot TBP$, Pu = $Pu(NO_3)_4$. Ko= $Pu(NO_3)_4 \cdot 2TBP$.

- concentration gradients in the aqueous and organic films (δ_a and δ_o) are linear, and

- steady state is prevailing.

The kinetic equation for the extraction flux density J is given by equation 3:

$$J = k_f\left[(Kx)_{bo} - J \cdot \Phi_{Kx}\right] - k_r\left[(T)_{bo} + J \cdot \Phi_T\right] \cdot \left[(H)_{ba} + J \cdot \Phi_H\right] \tag{3}$$

Here $\Phi_i = \delta_j/D_i$, where D is the diffusion coefficient and δ the thickness of the diffusion film. The indices i and j denote species and phases. respectively, and bo and ba the organic and aqueous bulk.

Further is:

$k_f = k_1^*/K_{p(Kx)}$ and $k_r = k_{-1}^*/K_{p(T)}$, where Kp_i are the partition coefficients and k_1^* and k_{-1}^* the rate constants of the forward and backward reactions at the interface.

This equation, solved by numerical methods (11) fits satisfactorily well with our experimental data (fig.2).

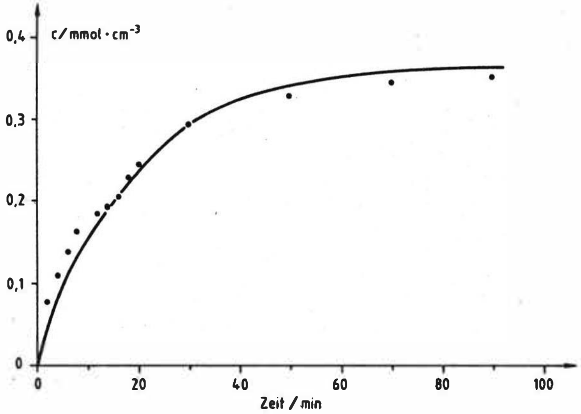

Fig.2: Backextraction of $HNO_3 \cdot TBP$ from the organic phase; fit of experimental data (x) with equation based on conventional model.

In this model the contributions of chemical reaction and diffusion to the total flux are still unknown. We tried to approach the problem of determining these contributions by applying the principles of irreversible thermodynamics (12).

The main idea is that the chemical reaction at the interface is vectorized, and that the resulting flux is coupled to the diffusional flux. Three assumptions are made:

- The chemical reaction at the interface is in thermodynamical equilibrium.
- the chemical potentials are independent of each other, and
- the concentrations at the interface are proportional to the bulk concentrations.

At first the interface concentrations of the participating species (marked by an asterix) are estimated by adopting proportionality constants c^i between bulk and interface concentrations. e.g.:

$$(Kx^*) = c^1/F_s \cdot (Kx) \qquad (4)$$

where F_s is the specific interface area.

The flux due to chemical reaction is:

$$J_r = k_f \cdot c^1 \cdot (Kx)^{\alpha(Kx)} - k_r \cdot c^2 \cdot (H)^{\alpha(H)} \cdot c^3 \cdot (T)^{\alpha(T)} \qquad (5)$$

Here α are stoichiometric coefficients.
The constants c^i turn out to be of appreciable magnitude. For instance, in the case of Kx ($HNO_3 \cdot TBP$) c^1 amounts to approximately 1/3.

Now an expression for the coupling of diffusion and chemical reaction is formulated. The fundamental equations for linear coupling of two processes, e.g. diffusion and reaction are:

$$L_{11} \cdot X_r + L_{12} \cdot X_d = J_r \qquad (6)$$
$$L_{21} \cdot X_r + L_{22} \cdot X_d = J_d \qquad (7)$$

Her $X_{r,d}$ are the driving forces of reaction and diffusion, respectively. The three unknowns (J_r, J_d, and the coupling constant $L_{12} = L_{21}$) can be evaluated, if the overlap of J_r and J_d is set equal to the flux J in equation 3. So, solution of the linear matrix 8 bx a numerical method (11) will give the desired results.

$$\begin{array}{cccl} X_d/F_s \cdot L_{12} & -J_r & 0 & = -L_{11} \cdot X_r \\ X_r \cdot L_{12} & 0 & -J_d & = -L_{22} \cdot X_d/F_s \\ (X_r + X_d/F_s) \cdot L_{12} & 0 & 0 & = J - L_{11} \cdot X_r - L_{22} \cdot X_d/F_s \end{array} \qquad (8)$$

J in the last line of the matrix is substituted by equation 3.

3.2 Results and Discussion

3.2.1 Thickness of Diffusion Film

If the diffusion coefficients D in equation 3 are substituted by experimental values, the film thickness δ is accessible. We adopted the following values for the diffusion coefficients:

$$D_{Kx} = 1.3 \cdot 10^{-6} \text{ cm}^2/\text{s}$$
$$D_H = 2.739 \cdot 10^{-5} \text{ cm}^2/\text{s}$$
$$D_T = 3 \cdot 10^{-6} \text{ cm}^2/\text{s}$$

D_{Kx} and D_H were taken from Marx et al. (13,14), D_T was estimated in lack of an experimental value.

Then a δ-value of $1.7 \cdot 10^{-4}$ cm was obtained.

For the sake of simplicity the film thickness on both sides of the interface was assumed to be equal. Furthermore. the diffusion coefficients were taken constant over the entire concentration range. As the data of Marx et al. indicate for $HNO_3 \cdot TBP$ (14). this may be an over-simplification. especially at very low concentrations (< 0.01 mol/l). However, a δ of $1.7 \cdot 10^{-4}$ cm corresponds well to values for the "diffusion film" obtained by interferometric measurements (15). Under the assumption that the interface is occupied completely by molecules of TBP which is a highly surface active substance. the film thickness would amount to approximately 2000 molecular layers.

3.2.2 Transport Coefficients

By definition, the transport coefficients β_i are given by the diffusion coefficients and the film thickness:

$$\beta_{Kx} = D_{Kx}/\delta_o = 7.63 \cdot 10^{-3} \text{ cm/s}$$
$$\beta_H = D_H/\delta_a = 0.16 \text{ cm/s}$$
$$\beta_T = D_T/\delta_o = 1.76 \cdot 10^{-2} \text{ cm/s}$$

Th β_{Kx}- and β_T-values are in satisfactory agreement with earlier determinations (16). β_H, however, is larger by an order of magnitude.

3.2.3 Mechanism of Interphase Mass Transfer

The most important result of this study is that during interphase transfer in the system HNO_3/TBP, dodecane both diffusion and chemical reaction are of comparable importance, and that they are coupled with each other. At the beginning of the process, the fluxes resulting from both mechanisms are very large, but of opposite sign (fig.3). As equilibrium is approached, they decrease until their sum eventually vanishes.

This means that from the start of an extraction process, reextraction also takes place immediately.

It is no longer possible to consider the mechanism of interface mass transport in this system to be solely diffusionally controlled. The large fluxes of opposing sign at the beginning of interphase mass transport also provide a plausible explanation for the familar phenomenon of "Marangoni instabilities".

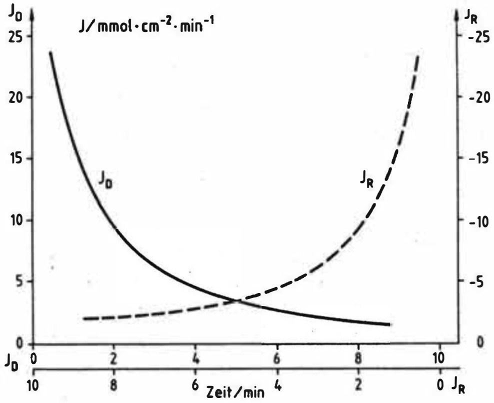

Fig.3: Flux through the interface (mmol/cm²·min) resulting from diffusion (J_D, left ordinate) and from chemical reaction (J_R, right ordinate) during backextraction of HNO_3·TBP from the organic phase.

Literature

1. Baumgärtner, F., Finsterwalder, L., J.phys.Chem. 74 (1970), 108.
2. Nitsch, W., van Schoor, A., Chem. Eng. Sci, 38 (1983), 1947.
3. Nitsch, W., Schuster U., Sep. Sci. Tech. 18 (1983), 1509.
4. Nitsch. W., Dillberger, M., personal communication 1984.
5. Danesi. P.R., Vandegrift. G.F., Horwitz. E.P., Chiarizia. R., J. phys. Chem. 84 (1980), 3582.
6. Horner. D.E., Mailen, J.C., Trans. Am. Nucl. Soc. 27 (1977), 484.
7. Petrich, G., Proceed. Int. Solv. Extr. Conf., Liège 1980.
8. Kammer. H.-W., K. Schwabe: "Thermodynamik irreversibler Prozesse". Weinheim: Physik-Verlag 1985.
9. Nitsch. W., Ber. Bunsenges. Phys. Chem. 83 (1979), 1171.
10. Schmieder H., Kuhn, E., Ochsenfeld. W., Kernforschungszentrum Karlsruhe. Report KfK 1306 (1970); Ochsenfeld. W., Schmieder H., Theiss, S., KfK 911 (1970).
11. Ebert. K., Ederer, H.: "Computeranwendungen in der Chemie", 2. Aufl., Verlag Chemie. Weinheim 1985
12. Keller, U.: "Thermodynamik der irreversiblen Prozesse", Teil I; Berlin, New York: de Gruyter 1976.
13. Feldner. K.H., Dissertation FU Berlin 1985.
14. Marx, G., et al., personal communication 1985.
15. Yagodin. G.A., V.V. Tarasov, S. Ivakhno. Hydrometallurgy 8 (1982), 293.
16. Nitsch, W., Ihle, E., Chem.-Ing.-Tech. 57 (1985), 141.

Kinetics of the extraction of uranium (VI) by synergistic mixtures: di-2-ethylhexyl-phosphoric acid (HDEHP) / neutral organophosphorus extractants (TBP and TOPO)

A. Maher, D. Pareau (Ecole Centrale de Paris, France)

The synergistic effect observed during the extraction of uranium (VI) from phosphoric acid by mixtures of HDEHP-TOPO and HDEHP-TBP is well known [1,2]. This phenomenon is commonly interpretated as a formation of mixed compounds between the two extractants and the metal species. One generally tries to explain the synergistic phenomena by studying the distribution ratio of the metal.

This method cannot alone explain the mechanism of the extraction with synergism. So we studied the mass transfer of uranium (VI) between phosphoric acid and the two synergistic mixtures to get more informations about this problem.

In a previous paper [3] we studied the interfacial transfer during the extraction of U(VI) by the HDEHP-TOPO system and ascertained the nature of the limiting step of the transfer:

- for HDEHP alone, the transfer limiting step is a diffusion with an interfacial resistance
- for TOPO alone, the transfer limiting step is an interfacial resistance
- for the mixture HDEHP-TOPO, our results could be interpretated by the West model [4].

MATHEMATICAL MODEL

Let us consider the extraction of a metallic cation M^{n+} by an acidic extractant HL:

$$M^{n+}_{(a)} \quad + \quad n\,HL_{(o)} \quad \rightleftarrows \quad ML_{n\,(o)} \quad + \quad n\,H^{+}_{(a)}$$

(a): aqueous phase (o): organic phase

If the rate is first order with respect to the metal concentration the material balance of an organic drop is:

$v'\ dC' = k\ a\ C\ dt - k'\ a\ C'\ dt$ (1)

C: metal concentration in the aqueous phase (= C initial concentration)

C' : average metal concentration in the organic drop

a: interfacial area

v' : drop volume

k and k' : rate constants

In this case the organic phase does not contain metal at t=0, so we can assume that $k' << k$.

The equation (1) becomes: $v'\ dC' = k\ a\ C\ dt$

By integrating this equation during the rising time of the drop we obtain, if k a and v' are constant: $v'\ C' = k\ a\ C\ \ t$

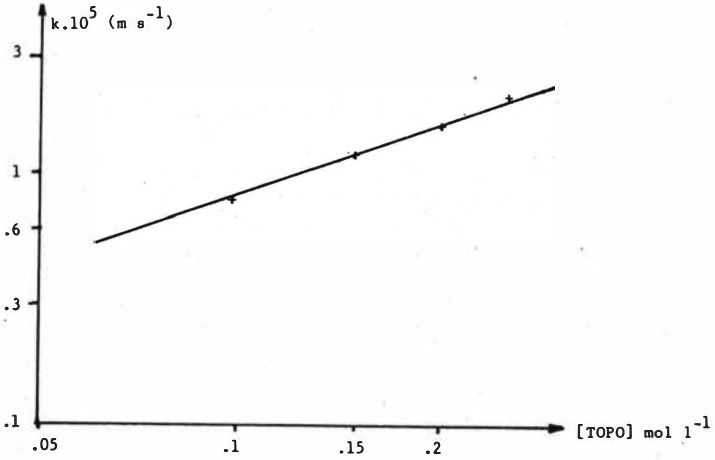

Figure 2: Variation of the transfer rate with the TOPO concentration

IV) Uranium extraction by HDEHP-TOPO

The influence of different parameters on the transfer rate was studied:

IV-1 Influence of metal concentration

The k values are listed in table 1: k only slightly varies with uranium concentration.

Table 1: Influence of the aqueous metal concentration on k

$[U]_{(a)}$ (mg l^{-1})	72	265	500	1000
k.10^5 (m s^{-1})	2.1	2.3	2.4	2.6

So the transfer rate is first order with respect to the metal concentration in the aqueous phase as we assumed before.

IV-2) Influence of TOPO concentration

The slope of the straight line C' = f (t) does not depend on the TOPO concentration (figure 3); C' is the uranium concentration in the drops after their rising time.

IV-3) Influence of the HDEHP concentration

The slope of the straight line C' = f (t) does not depend on the HDEHP concentration (figure 4).

EXPERIMENTAL

The interfacial transfer is studied by the single drop method. All the experimental techniques are described in a previous paper [3].

RESULTS

I) Uranium extraction by HDEHP

The influence of HDEHP concentration on the transfer kinetics was studied. We determine the variations of the metal concentration in the drops vs their rising time and calculated the value of the rate constant k from these results. The straight line log k = f (log [HDEHP]) has a slope of 1.3 (figure 1); [HDEHP] is the HDEHP concentration.

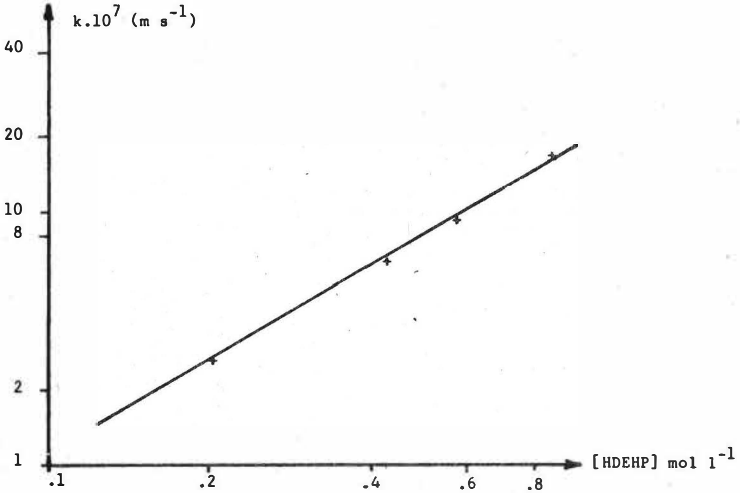

Figure 1: Variation of the transfer rate with the HDEHP concentration

II) Uranium extraction by TOPO

The straight line log k = f (log [TOPO]) has a slope of 1 (figure 2).

III) Uranium extraction by TBP

The straight line log k = f (log [TBP]) has a slope of 1

Table 2: Influence of TBP concentration in the organic phase on k

$[TBP]_{(o)}$ (mol l^{-1})	.1	.4	.6	.8	1	1.5
$k.10^5$ (m s^{-1})	.22	.32	.44	.56	.64	.94

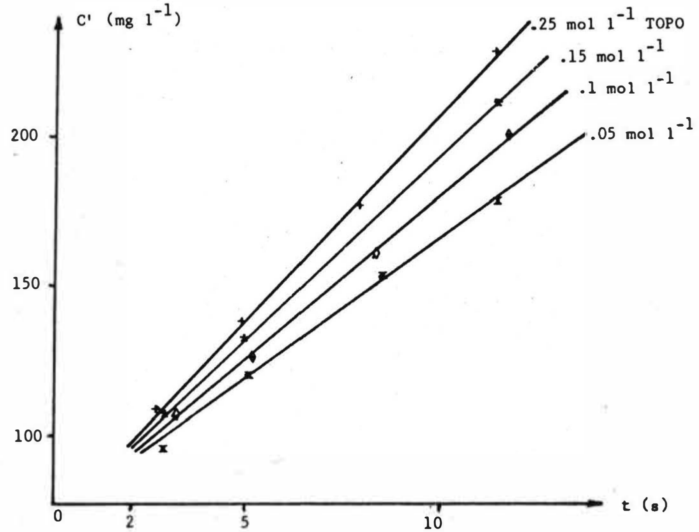

Figure 3: Uranium concentration in the drops vs their rising time HDEHP-TOPO system

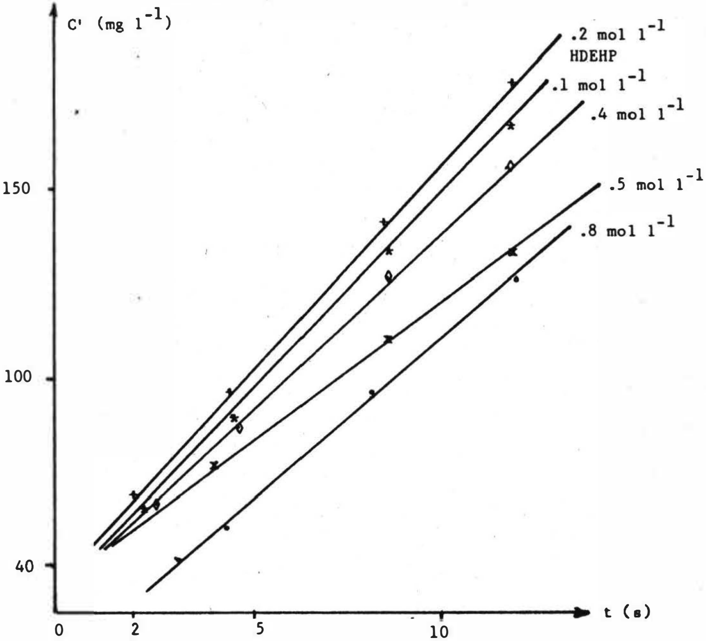

Figure 4: Uranium concentration in the drops vs their rising time HDEHP-TOPO system

V) Uranium extraction by HDEHP-TBP

V-1) Influence of the TBP concentration

The logarithm of the rate constant k vs the logarithm of the TBP concentration is a straight line of slope -0.5 (figure 5).

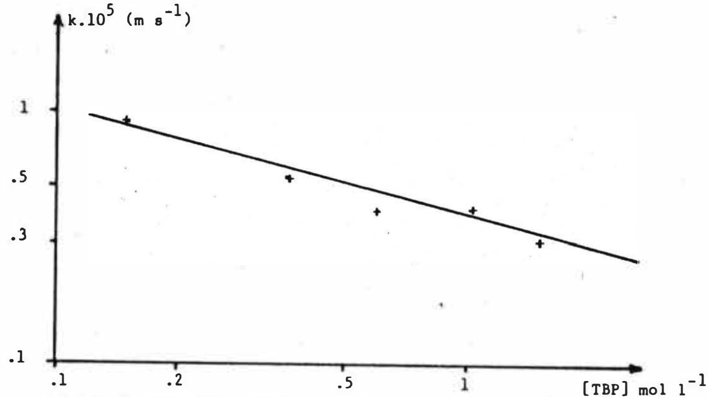

Figure 5: **Variation of the transfer rate with the TBP concentration**

V-2) Influence of the HDEHP concentration

The straight line log k = f (log [HDEHP]) has a slope of 1.3 (figure 6).

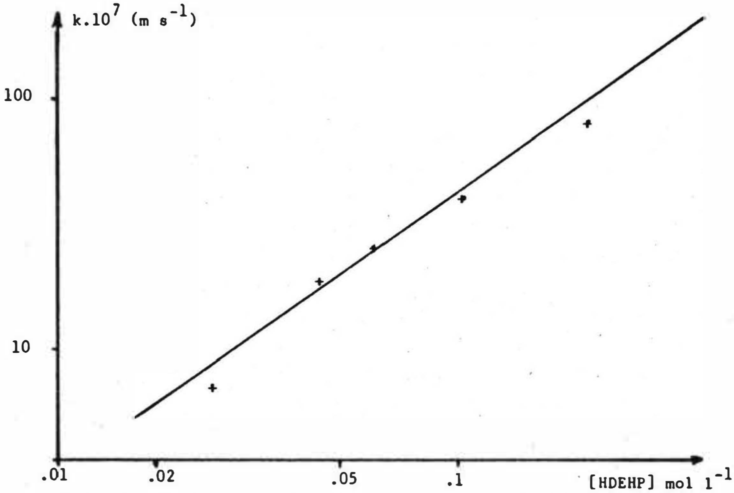

Figure 6: **Variation of the transfer rate with the HDEHP concentration**

INTERPRETATIONS

I) Uranium extraction by HDEHP

We suggest the following interpretation: the formation reaction of the metallic organic species takes place in the aqueous phase in an area very close to the interface. The different steps are the following:

- HDEHP transfer from organic to aqueous phase

$$H_2L_{2\,(o)} \rightleftarrows H_2L_{2\,(a)}$$

- dissociation in the aqueous phase

$$H_2L_2 \rightleftarrows H^+ + HL_2^-$$

- metal complexing in the aqueous phase
  - . 1-1 complex formation: $M^{2+} + HL_2^- \rightleftarrows MHL_2^+$
  - . 1-2 complex formation: $MHL_2^+ + HL_2^- \rightleftarrows ML_2H_2L_2$
- transfer of $ML_2H_2L_2$ from aqueous to organic phase

$$M_2L_2H_2L_{2\,(a)} \rightleftarrows M_2L_2H_2L_{2\,(o)}$$

We assumed that the limiting step is the formation of the 1-2 complex. A mathematical treatment of the transfer rate finally gives a relation between k and [HDEHP] , approximately first order with respect to the extractant concentration, what is in good agreement with our experimental results. So the proposed mechanisms are probable. The interfacial resistance is identified to be the formation of the 1-2 complex.

II) Uranium extraction by TOPO and TBP

The extraction mechanisms are the following:

$$UO_2(H_2PO_4)_2 + 2\,S \rightleftarrows UO_2(H_2PO_4)_2S_2$$

$$UO_2(H_2PO_4)_2H_3PO_4 + S \rightleftarrows UO_2(H_2PO_4)H_3PO_4.S$$

S = TBP or TOPO

In the case of these two neutral extractants the limiting step in the mass transfer was found to be an interfacial resistance of chemical or physical nature.

Nakashio et al [5] reported a mathematical treatment to determine the nature of this resistance. We used this model by taking into account the transfer in a drop [6]. So we suggest that the nature of this resistance is chemical for TOPO as well as for TBP.

In conclusion for these two neutral extractants we ascertained the following mechanisms:

- diffusion of the metallic species in the aqueous phase to the interface
- complexation by the neutral extractant
- diffusion of the formed species into the organic phase

III) **Uranium extraction by HDEHP-TOPO**

Our experimental results show that the transfer rate only slightly depends on the extractants concentrations. On the contrary with HDEHP or TOPO alone it varies with these concentrations.

Baes et al [7] in an equilibrium study show that the distribution ratio of uranium vs the extractant concentration curve exhibits a maximum. The general interpretation of this result is that the free HDEHP concentration is lowered because of the interactions between the two extractants:

$H_2L_2 \quad + \quad S \qquad H_2L_2S \quad \rightleftarrows \qquad \log K_{12} = 2.3$ [8]

$\frac{1}{2} H_2L_2 \quad + \quad S \qquad HLS \quad \rightleftarrows \qquad \log K_{11} = 4$ [8]

The formation of the mixed complexes are quantitative and the HLS complex is predominant with respect to H_2L_2S.

If S_0 and L_0 are the initial concentrations of TOPO and HDEHP, there are two possible cases:

- $L_0 < S_0$: $HLS = L_0 \quad H_2L_2S \simeq 0 \quad H_2L_2 \simeq 0 \quad S = S_0 - L_0$
- $S_0 < L_0$: $HLS = S_0 \quad H_2L_2S \simeq 0 \quad H_2L_2 = L_0 - \frac{1}{2} S_0 \quad S \simeq 0$

The only concentration being constant in both cases is the concentration of HLS; it is limited by the initial concentration of HDEHP or TOPO.

So we can suggest that the extracting species is the HLS one, what is in agreement with the fact that the transfer rate depends neither on HDEHP nor TOPO concentration.

IV) **Uranium extraction by HDEHP-TBP**

Our experimental results show that the transfer rate of the synergistic system is first order with respect to the HDEHP concentration, as well as for the HDEHP alone, but is reduced when increasing the TBP concentration (with TBP alone the transfer rate is first order with respect to the TBP concentration). So we can suggest that the extraction mechanism with the synergistic system is probably the same as for the HDEHP alone.

DISCUSSION

The dependence of the masa transfer rate on the organic phase composition and ita value are different for the two synergistic mixtures.

The observed rate for HDEHP alone is greater than those measured for both extractant mixtures. For example if the value of the transfer rate is 1 (arbitrary unit) for HDEHP alone, it becomes 0.8 for HDEHP-TOPO and 0.4 for HDEHP-TBP. The synergistic effect is therefore not related to an improvment of the transfer rate. In the case of HDEHP-TOPO the rate ia only slightly lower than that of the HDEHP. For the HDEHP-TBP the rate is much lowered. On the other hand the rate dependence for both synergiatic mixtures on the HDEHP concentration is the same as for the HDEHP alone. So the maas transfer rate seems to be related to the neutral reagent rather than the acidic. We ascribe this fact to the strength of the organic interactions between acidic and neutral extractants.

Two cases are possible:
- The species formed between the two extractants have a relatively high concentration and they can extract the metallic aqueous complexes. The transfer rate is only slightly reduced: the free HDEHP concentration is lowered but this diminution is compensated because the formed species are able to extract the metal.
- The concentration of the formed species is relatively low. There is no compensation. The transfer rate is reduced because of the diminution of the free HDEHP concentration.

In conclusion the basicity of the neutral reagent seems to have a great influence on the mass transfer rate. The synergistic effect depends on this basicity and therefore on the ability of the mixed species between both extractants to extract the aqueous metal species.

REFERENCES

[1] D. DYRSSEN, L.D. HAY Acta Chem. Scand. 14,9,1960
[2] F.T. BUNUS Talanta 94, 117 (1977)
[3] A. MAHER, D. PAREAU Bull. Soc Chim. France 1985, n°5, 718-724
[4] F.B. WEST Ind. Eng. Chem. 43, 234 (1951)
[5] F. NAKASHIO Kagaku Kogaku 38, 41 (1974)
[6] A. MAHER Thèse Docteur Ingénieur Ecole Centrale de Paris 5/12/1985
[7] J.C. BAES, H. T. BAKER ONRL 2443 (1957)
[8] R. G. BATES J. Res. Natl. Bur. Std. 47, 127 (1951)

Properties of Heavy Organic Phases and their Formation in the Purex Process

L. Stieglitz, R. Becker, H. Bautz, R. Will
Institute for Hot Chemistry
Nuclear Research Center Karlsruhe, FRG

Introduction

Heavy organic phases have been observed in the Purex process on some occasions. They have been associated in the past with products which sometimes could lead to exothermic reactions especially in evaporators and denitrators. These products, described as red oils, were considered as the main cause for operational failures /1-4/. For an explanation of these interferences the thermal behavior of uranylnitrate-tributylphosphate-nitric acid mixtures was studied in detail by G.S. Nichols /5/. The results of these investigations showed that in this system exothermic reactions are observed only at temperatures above 150°C, i.e. at temperatures not characteristic for the Purex process. Future operational trouble was avoided by a modified and controled flow sheet (maximum temperature limit below 130°C, removal of TBP from aqueous streams). No detailed information, however, is available about the chemical identity of the compounds as really present in the evaporators, their formation conditions and their thermo-chemical behavior. In view of the safety aspects of these issues an investigation was started in order to provide additional informations on these points.

Results

Concentration Experiments

Feed solutions of uranium (70g/l) in 0.1M HNO_3 (UNH) with varying amounts of tributylphosphate (TBP) were concentrated in a laboratory circulation evaporator up to uranium concentrations of 480 g/l. The experimental set up is shown in Figure 1. The evaporator (6), volume 2 l, is supplied with two heaters (4) with a power of total 1500 watts. The feed solution is transferred from the reservoir (1) by a piston pump corresponding to an evaporation rate of 500 ml/hr. After the experiments the TBP concentration in the distillate and the concentrations of TBP and HDBP (dibutylphosphoric acid) in the sump were determined by gas chromatography. The following experiments were performed:

A) Concentration of TBP-saturated UNH solutions.
In the first series the solution was prepared by dissolving 738.5g $UO_2(NO_3)_2 \cdot 6H_2O$ in 5l 0.1 M HNO_3 which had been previously equilibrated with TBP to contain 180-200 mg/l TBP. After the first run, the concentrate was diluted by water (equilibrated

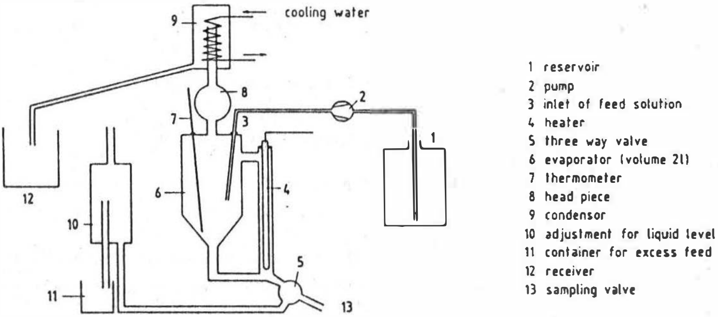
cooling water
9
8
7
3
2
1
12
6
4
10
5
11
13
1 reservoir
2 pump
3 inlet of feed solution
4 heater
5 three way valve
6 evaporator (volume 2l)
7 thermometer
8 head piece
9 condensor
10 adjustment for liquid level
11 container for excess feed
12 receiver
13 sampling valve

Fig. 1: Evaporator for the Study of Heavy Phase Formation

with TBP) to the original uranium concentration (70g/l). In total 7 runs were performed. The recovery of TBP was in all experiments 98-100%. 1-2% were left in the distillation sump, practically all TBP had been transferred by steam stripping to the distillate. No formation of heavy organic phases could be observed. In a second series small amounts of HDBP were added to the feed to give HDBP concentration between 15 and 30 mg/l. Five runs were made. The TBP recovery was again nearly 100%. In these experiments, however, 0.1ml of heavy organic phase was recovered. The molar ratio of TBP/HDBP in this compound was 1:1.01. Due to the small amount of material no further investigations could be carried out.

B) Behavior of TBP-saturated Solutions with 0.2 vol% Entrainment
In the reservoir 0.2 vol% solvent (30 vol% TBP-n Alkan) was added to the feed. The two phases were continuously mixed by a magnetic stirrer. Two series (no. 3 and 4) of experiments were made under these conditions. In series No.3 5l batches of feed were recycled ten times corresponding to a processed volume of 50l. In series no.4 the recycling of the feed was only four times, corresponding to a total volume of 20l. In both experiments a heavy organic phase was formed and could be isolated. The data are shown in Table 1. The total volume of heavy organic phase formed was 6 and 3 ml respectively. The yield relative to the entrained solvent volume is 6-7.5%, the corresponding fraction relative to the entrained TBP being 20% and 25% respectively. From the ratios of uranium, TBP, HDBP it is apparent that the heavy phases are mixtures of the complexes of $UO_2(NO_3)_2 \cdot 2TBP$ and $UO_2(DBP)_2$.

C) Behavior of $UO_2(NO_3)_2 \cdot 2TBP$ in TBP-saturated UNH Solutions.
For the study of this complex 20 ml of the compound were introduced into the evaporator. Feed solutions of UNH were concentrated as described above. Since from previous results it was concluded that HDBP has a stabilizing effect to the heavy

Table 1: Properties of Heavy Organic Phases (HOP)

Properties		Experiment	
		Ser. No.3	Ser. No.4
volume (HOP) recovered	(ml)	6	3
volume of entrainment processed	(ml)	100	40
fraction of HOP formed	(%)	6	7.5
density	(g/cm^3)	n.d.	1.4877
concentrations			
TBP	(g/l)	669	579
HDBP	(g/l)	85.8	237
H_2MBP	(g/l)	n.d.	1
H_3PO_4	(g/l)	n.d.	3
uranium	(g/l)	n.d.	396
nitric acid	(g/l)	n.d.	0.01

n.d. not determined

organic phase, the experiments were performed without HDBP (exper. ser. no.5) and with solutions containing 20 mg/l HDBP (exp. ser. no. 6) and 300 mg/l HDBP (exp. ser. no.7). The volume change of the organic phase and the chemical composition was investigated after each run. The aqueous concentrates were diluted after each run and reused. The data are shown in Table 2. In experiment no.5 without HDBP and in experiment no.6 with low HDBP concentrations a continuous decrease of the volume of

Table 2: Characterization of Heavy Organic Phases from the Evaporator

Run No.		Experiment		
		Ser. no.5	Ser. no.6	Ser. no.7
	HDBP	--	20 mg/l	300 mg/l
1	volume	-	-	13.2 ml
	TBP	-	-	678 g/l
	HDBP	-	-	196 g/l
	density	-	-	-
2	volume	-	6 ml	10 ml
	TBP	-	599 g/l	582 g/l
	HDBP	-	287 g/l	295 g/l
	density	-	-	-
3	volume	5 ml	4.4 ml	8.4 ml
	TBP	557 g/l	495 g/l	493 g/l
	HDBP	352 g/l	376 g/l	378 g/l
	density	1.5088 gcm^{-3}	1.5167 gcm^{-3}	-
4	volume	-	-	7.6 ml
	TBP	-	-	478 g/l
	HDBP	-	-	388 g/l
	density	-	-	-
5	volume	-	-	7.2 ml
	TBP	-	-	492 g/l
	HDBP	-	-	389 g/l
	density	-	-	1.5211 gcm^{-3}

the organic heavy phase is observed indicating a noticeable decomposition and TBP removal by steam stripping. In three runs the volume has decreased from 20ml to 4-5ml. The molar ratio of TBP:HDBP is 1:0.8 and 1:0.95. In experiment no.7 with 300 mg/l HDBP after three runs 8.4 ml of the organic phase are still present, during additional runs this compound remains relatively stable at a volume of 7-8ml. The molar ratio of TBP:HDBP after run 3 is 1:0.97 and remains practically at a value of 1:1 during runs 4 and 5. The uranium content of the residue after run 5 is 419 g/l (=1.76 M). From this value a composition such as $UO_2(NO_3)\cdot DBP\cdot$ TBP is derived.

Thermochemical Studies

The thermochemical behavior of the material isolated from the above described experiments was investigated using an instrument, mod. STA 409 (Fa. Netsch), which allows simultaneous thermogravimetric and differentialthermoanalytical measurements. The temperature range studied was from 30°C to 500°C. The data were compared with results obtained from model compounds such as $UO_2(NO_2)\cdot$ 2TBP, uranium dibutylphosphate and uranium monobutylphosphate. (Table 3)

$UO_2(NO_3)_2$ 2TBP: The thermal decomposition proceeds in two steps. At 225°C (peak maximum) a strong exothermic reaction takes place followed by an endothermic reaction at 289°C. From the thermogravimetric data it is concluded:

a) in the first step an oxidative degradation of two butylgroups by the nitrate anions,

b) in the second step a desalkylation of four butylgroups with the release of butene.

Table 3: Thermochemical Data of Heavy Organic Phases and Model Compounds

Compound	Reaction 1		Reaction 2	
	Peak maximum °C	Enthalpy J/g	Peak maximum °C	Enthalpy J/g
$UO_2(NO_3)_2\cdot$ 2TBP	225	- 390	289	255
$UO_2(HMBP)_2$	180	25	290	•
$UO_2(DBP)_2$	192	20	290	183
organic phase (series no.4) o.2 % entrainment	225	- 248	282	147
organic phase (series no.5) U-TBP complex w/o HDBP	229	- 188	282	150
organic phase (series no.6)	230	- 200	281	181
organic phase (series no.7)	230	- 160	283	136

The enthalpies as mean values from nine measurements are:

H1 (225°C) = - 331 KJ/M ± 15%

H2 (289°C) = + 216 KJ/M ± 14%.

Furtheron, we applied a technique as developed by J.Harris /7/ for the evaluation of the self ignition temperature. Here the sample is heated with different rates. With low heating rates the on set temperature is shifted towards lower temperatures. By extrapolating this shift to a heating rate close to zero a self ignition temperature can be estimated. From experiments with heating rates of 2.5°, 5°, 7.5° and 10°C/min a temperature for self ignition of 176°C is calculated. This value is more than 40°C above the temperatures set in the Purex process.

Uranium monobutylphosphate/dibutylphosphate: The thermal degradation consists of a desalkylation (endothermic) with the release of butene between 180 and 192°C (monobutylphosphate); besides that additionally at temperatures of 285-305°C dehydration occurs. The reactions are endothermic.

Heavy organic phases: The thermochemical data from the residues as obtained in the evaporation experiments correspond qualitatively with that of the $UO_2(NO_3)_2 \cdot 2TBP$ complex. Also here two decomposition steps are observed: an exothermic reaction between 225-230°C, and an endothermic one between 280-283°C. With the evaporator residues the reaction enthalpy of the exothermic degradation is distinctly lower. This is explained by the substitution of nitrate by dibutylphosphate. The decomposition temperatures remain practically unchanged at 225-230°C and 280-283°C.

Conclusions

From the evaporator experiments with different additions of organics (solvent entrainment, dibutylphosphate) so far no formation of "red oil" phase could be observed. The heavy organic phases which were isolated showed a composition with a molar metal-TBP-HDBP ratio of 1:1:1. Apparently under the experimental conditions this compound type is stabilized. The thermochemical degradations of these phases proceeds at similar temperatures (225° and 280°) as the $UO_2(NO_3)_2 \cdot 2TBP$ with lower enthalpies. From these laboratory studies it is concluded that even with medium entrainment of solvent into the evaporator no operational problems such as exothermal excursions should be expected.

References

/1/ J.T. Colven Jr, G.N. Nichols, T.H. Siddall,
Savannah River Laboratory Report DP-25, May 1953

/2/ J.J. Shefcik, Hanford Atomic Products Operation
Report HW 40556m Dec. 1955

/3/ J.M. Mc Kibben,
Savannah River Plant Report DPSPU 76-11-1, Oct. 1976

/4/ H.D. Harmon, M.L. Hyder, B. Tiffany, L.W. Gray, P.A. Soltys,
Savannah River Laboratory Report DP-1418, Aug. 1976

/5/ G.S. Nichols, Savannah River Laboratory
Report DP 526, Nov. 1960

/6/ L. Stieglitz, R. Becker, H. Bautz, A. Wünschel,
KfK-Report KfK-2613 (978)

/7/ J. Harris, Thermochim. Acta 14, 183-199, (1976)

Extraction of Cr, Nd, Ru and U in Purex-Media monitored by an analytical ultracentrifuge

V. Friehmelt, Ch. Frydrych, R. Gauglitz, S. Kriegel and G. Marx

Freie Universität Berlin
Institut für anorganische und analytische Chemie
Forschungsgruppe Radiochemie
Fabeckstr. 34-36
1000 Berlin 33
B. R. Deutschland

Abstract

The extraction of Cr, Nd, Ru and Zr was investigated in presence of high concentrations of $UO_2(NO_3)_2$ in order to provide data for optimizing the Purex-Process. For these elements the distribution coefficients between aqueous nitric acid solution and Tributyphosphate/dodecan = 30/70 were obtained, under varying concentrations of nitric acid, uranium and one of those elements aforementioned. By use of an analytical ultracentrifuge the local concentration profiles of the constituents being under investigation were obtained also for regions near to the boundary. Right from the beginning of the extraction the transport phenomena were monitored applying different optical systems of the analytical ultracentrifuge in order to find out in which cases diffusion processes were the speed determining step of the extraction. In previous experiments therefore the diffusion coefficients were measured not only in aqueous but also in organic systems.

Introduction

In the processing of spent nuclear fuel it was the aim to find a chemically and technically feasible method to remove uranium and plutonium from the high level waste. Due to this fact the knowledge of the distribution behaviour of actinides and fission products between aqueous nitric acid and the organic phase was of high importance for modelling extraction operations performed in the Purex-Process. For these calculations detailed information about the kinetics and the distribution data were needed for those elements the extraction should be simulated by.

Since the elucidation of the extraction behaviour of all fission productcs was not required, several elements of major interest were chosen: While investigations on neodymium represented the behaviour of the lanthanides, chromium and ruthenium were known to present a good deal of troubles because of entering the organic phase and accompanying uranium. Last not least zirconium was considered to be responsible for any crud formation.

As there was a significant interaction between the different components of the solutions, the kinetical measurements were performed by use of the analytical ultracentrifuge and the determination of the distribution coefficients were carried out for three different concentration of each element, the concentration of the nitric acid in the aqueous solutions varying from 0.02 M up to 3.00 M. $UO_2(NO_3)_2$ was added to these solutions, this parameter varying from 0 M to 1.0 M. Finally from these experiments a matrix resulted, which other points may be extrapolated from.

Experimental

In the aqueous and the organic phase the determination of the concentrations required efficient analytical methods for the different elements. Since all solutions were prepared gravimetrically by weighing definite quantities of stock solutions, concentrations could be precisely determined by density measurements. These were carried out by a digital densitometer, which was accurate within the 4th decimal place, air and bidestilled water being used for calibration. This procedure, for example, was used to check the titrated nitric acid concentrations by comparing these data with values found in literature. For the extraction measurements the aqueous nitric acid concentrations were adjusted to 0.02 M, 0.5 M, 1.5 M and 3.0 M. At first the organic mixtures were equilibrated with each of the nitric acids, which were used in the extraction experiments, in order to prevent the transport of this substance.

The initial uranium concentration in the four different acid concentrations was set to 0 M, 0.3 M, 0.7 M, and 1.0 M. For the detection of the amounts of uranium being present in both phases after the extraction, several analytical methods were applied: For γ-spectroscopy the peak from the radionuclid U-235 was registered at 186 keV. Aqueous solutions were titrated using either standard EDTA-solution or acidity titration (1). Also UV-spectroscopy proved to be very sensitive, especially after adding ascorbic acid to enhance the absorption by complex formation. All of these methods were tested by a lot of calibration measurements.

The concentrations of chromium and ruthenium were determined by atomic-absorption spectroscopy using a wavelength of $\lambda = 357.9$ nm for Cr and $\lambda = 372.8$ nm for Ru.

Problems arose from the diversity of existing ruthenium nitrosyl compounds and the sensitive equilibria between all these complexes. In order to achieve a stable composition the solutions, were heated to 70°C and stored for several days at 25°C (2).

For neodymium there was used titration with standard EDTA solution. After calibration with standard solutions of neodymiumnitrate quantitative measurements were performed by UV-spectroscopy at $\lambda = 521$ nm and $\lambda = 576$ nm. The determination of zirconium was carried out gravimetrically.

A Beckman Instruments Ltd. Model E analytical ultracentrifuge was employed to monitor the transport phenomena. All measurements were carried out at 25.0°C using a capillary-typ centerpiece consisting of two compartments which could be filled separately. For the extraction measurements 0.12 ml of the aqueous solution, containing the species to be extracted, were filled into one of the compartments and 0.12 ml aqueous solvent together with 0.24 ml equilibrated organic solution into the other one (fig. 1). The cell was fitted into a titanium rotor and accelerated to a final measurement velocity of 5.200 r.p.m., whereby half of the the organic layer was pressed through the capillary into the other compartment, overlaying the test solution there.

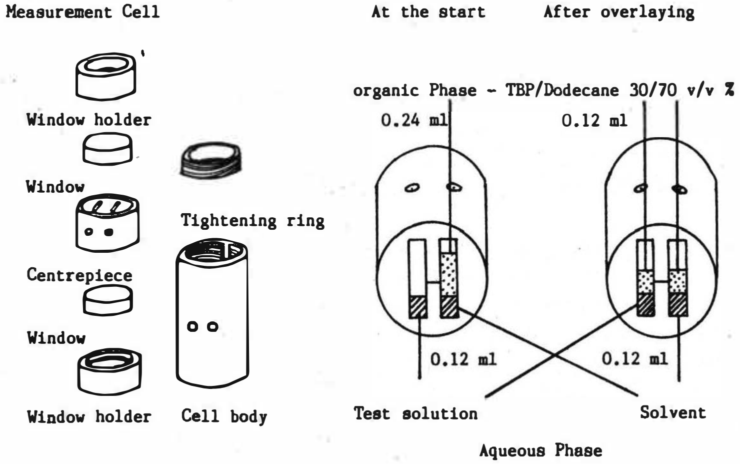
Measurement Cell
Window holder
Window
Centrepiece
Window
Window holder
Tightening ring
Cell body
At the start
After overlaying
organic Phase - TBP/Dodecane 30/70 v/v %
0.24 ml
0.12 ml
0.12 ml
0.12 ml
Test solution
Solvent
Aqueous Phase

Fig. 1

Right from the beginning the concentration profiles were obtained in a close distance to the boundary by simultaneus use of both the Schlieren and the absorption optical system of the analytical ultracentrifuge (fig. 2). The diffusion measurements were carried out in a similary way using one phase only and overlaying the solution with the same solvent or a dilute solution respectively (3,4).

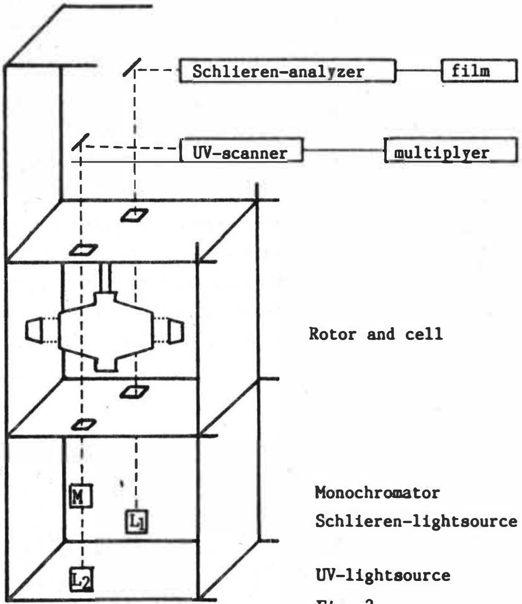

Fig. 2

Results and discussion

The well known extraction of uranium and plutonium from nitric acid solutions, depends on a fast reaction of the metal nitrates with tributylphosphate (TBP) (5,6). By this reaction stable neutral complexes are formed. On the other hand the nitrates of fission- and corrosion products and the pure nitric acid also form complexes of these kind, which have a definite composition as for example $HNO_3 \cdot TBP$, $UO_2(NO_3)_2 \cdot 2TBP$ or $Nd(NO_3)_3 \cdot 3TBP$. Even degradationproducts of the TBP, as for instance dibutylphosphate (DBP), form complexes and lead to troublesome precipitates especially in the case of zirconium, which the main part of the crud consists of. Besides the known Zr-DBP products a new complex could be isolated by our investigations. The product was identified to be $Zr(NO_3)_2 \cdot 2DBP$, being insoluble in the organic solvent. Since the extraction measurements were performed at 25°C the absence of this DBP-complex could be guaranteed and only $Zr(NO_3)_4 \cdot 2TBP$ had to be taken into account.

The extend of extraction of each element is characterized by the distribution coefficient K_D which is given by the ratio of the concentration in the organic phase after the extraction to that remaining in the aqueous solution. The value of the distribution coefficients is influenced by two important parameters, the aqueous nitrate concentration and the concentration of free TBP in the organic solution. Since the metalions have to combine with the nitrates at the boundary to get the extractable species, forming the neutral complex with TBP, the extraction in enhanced by raising the aqueous nitrate concentration. On the other hand the extraction ratio will be reduced by competing reactions, if already a lot of salts or nitric acid is extracted and only a small concentration of free TBP left behind.

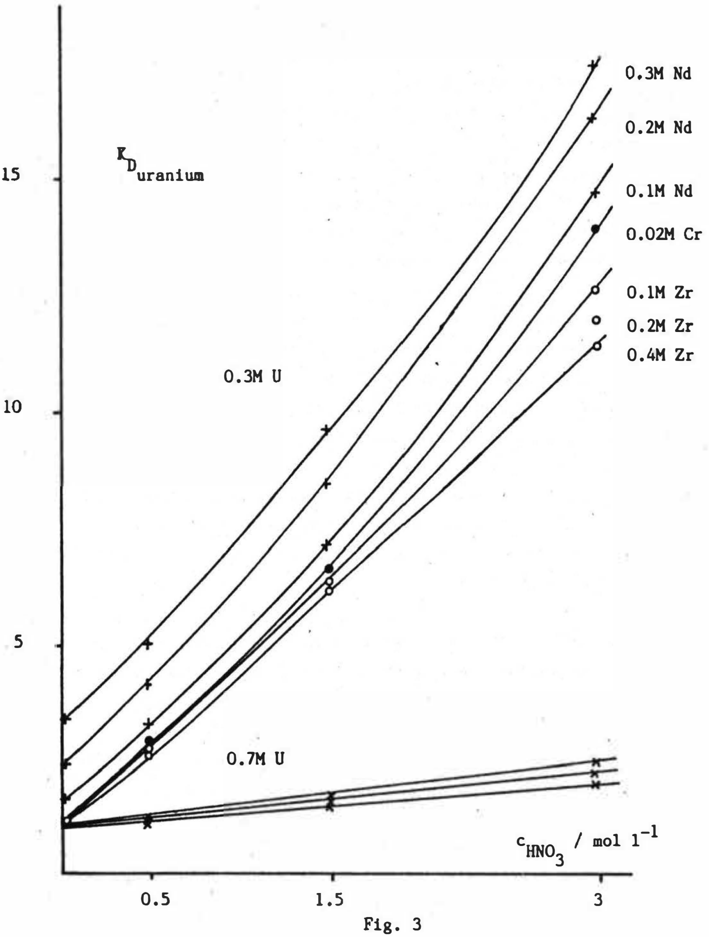

Fig. 3

As can be seen from the results the concentration of uranium is a very important parameter, because uranylnitrate forms very stable complexes with TBP and, so reduces drastically the possibility of fission-products to enter the organic phase. The distribution coefficients for uranium itself are rather low due to the highly concentrated aqueous uraniumsolutions of 0.7 M and 1.0 M (fig. 3), because in this case the organic solvent being nearly saturated with this speciall uraniumcomplex. So any raise of the nitrateconcentration caused by higher amounts of nitric acid, leads only to a slight increase of the distribution coefficients of uranium. For the low initial aqueous concentration of 0.3 M, however, the K_D-values of uranium are significantly influenced by the addition of nitric acid, because of raising the amount of the extractable species.

If the uraniumconcentration is 0.7 M or even 1.0 M the addition of the nitrates of Nd, Cr or Zr to the uranium systems will not have any detectable influence upon the uranium distribution. As can be seen from the diagram (fig. 3), there will be a slight change in the K_D-values of uranium, if the amounts of added salts are drastically increased. Those high concentrations are irrelevant for the Purex-process. Of course they only were chosen in order to get a detectable quantity of Zr or Nd into the organic solution. The concentrations of Cr can be kept at a lower level because of its extrability and perceptivity being better. Nevertheless this doesn't lead to any detectable change in the uranium distribution.

In the case of neodymiumnitrate the addition of this salt leads to an increase of the distribution coefficients of uranium. This observation may be explained by a salting-out-effect since the increase in the total nitrate concentration enhances the formation of the extractable species of uranylnitrate. A different behaviour can obviously be registered for Zr, which leads to a decrease of the K_D-values of uranium. This effect will be even more intensive, if the nitric acid concentration is raised, and may be due to a change in the zirconium species, which varies from zirconylnitrate to zirconiumnitrate by the influence of strong acids. Since this reaction withdraws nitrate from the solution, it results in a weakening of the extrability of uranium.

The distribution coefficients of the fission- and corrosion products are significantly lower than those measured for uranium. For Zr the values are even in the range of 10^{-3}. This low extractability causes analytical problems due to the marked increase in the errorlimit. In spite of this problems it can clearly be shown, that there will be a significant decrease in the K_D-values for Cr, if on the one hand the uranium concentration is increased and on the other hand also the nitric acid concentration. The reason is to be seen in a competing reaktion in the organic phase, which is nearly saturated with the uranium complex. At high nitric acid concentration there is left less free TBP for the formation of a chromium complex, which even is less stable. This observation is supported by the decline of the distribution values, when the Cr-concentration is raised. Some different results were obtained for Nd and Ru. In order to get extractable species of these elements the nitrate complexes had to be formed. Therefore nitric acid was necessary to support the extraction of these substances. The distribution values in 0.3 M uranium solutions reached a maximum of 0.4 M in the case of Ru and 0.01 M for Nd, when the nitric acid concentration was raised up to 3.0 M. In all systems there were found smaller values for Nd, which were caused by the small amount of extractable species formed by the competing reaction. In order to transfer Nd into the organic phase the Nd ion had to combine with three nitrates and three molecules of TBP. Again the addition of uranium again caused a drastical decrease of the extraction of both elements indicating the advantage of using high uranium concentrations in the Purex-process to prevent those fission products from entering the organic solution.

Measurering the kinetics by use of the analytical centrifuge, the centrifugal force supports the formation of a sharp boundary, which can be investigated by the optical systems. Because of this force the aqueous solution of higher density is to be found at higher values of distance r, as can be seen in the diagram (fig. 4). After a short time of contact already the decrease of Cr-concentration in the aqueous layer near to the boundary becomes obvious from the concentration profiles. On the other side there is an increase of concentration in the organic phase, indicating that there is a fast reaction, transfering the molecules through the boundary. With the time measurement proceeding a change in the concentration profiles also becomes obvious within in a greater distance, this distance, hovever, being somewhat greater in the aqueous layer. This effect may be explained by a slower transport within the organic mixture, as there are lower values of the diffusion coefficients to be found in that solvent. From the endpoint of the measurements at infinite time, the distribution coefficients can be calculated from the ratio of the absorption values of the components in the organic and aqueous layer.

In order to evaluate those measurements a lot of calibration work had to be done. For the calculation of the concentration profiles from the absorption data solutions of known concentrations were investigated by diffusion experiments. In the aqueous systems the diffusion coefficients showed a maximum at low concentration. Although this effect was slight, it was found in all investigated salt-solutions of the elements aforementioned. Numerous investigations are in progress to elucidate the reasons for this behaviour.

Contrary to the results obtained from aqueous solutions, the diffusion measurements in the organic solvent showed a linear relationship between diffusion coefficients and concentrations. Since in these non electrolyte solutions no coulombic forces were to be expected, there should be no interactions of the

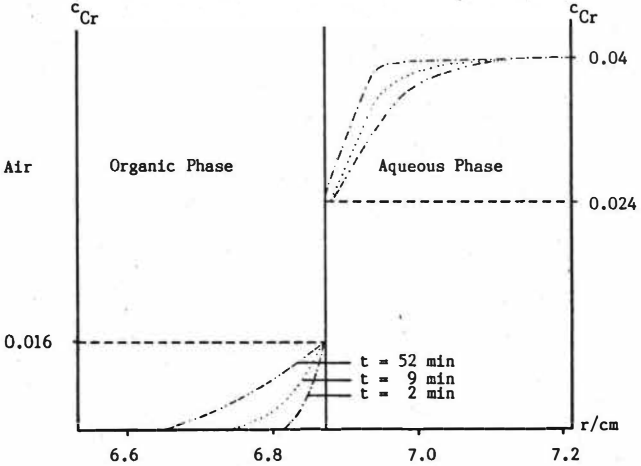

Fig. 4

molecules with each other. For example in the case of the uranylnitrate TBP complex it was shown, that this molecule had sufficient stability to diffuse as a distinct unit (7). Calculations using the diffusion coefficients to simulate the observed transport phenomena were in good agreement with the concentration profiles measured, proving the extraction to be controlled by transport phenomena.

References

1. G. Koch, Fresenius Z. f. Anal. Chemie, 214 (1965)
2. E. Blasius, J.P. Glatz, W. Neumann, Radiochim. Acta 29, 159 (1981)
3. C.H. Chervenka, A Manual of Methods for the Analytical Ultracentrifuge, Beckman Instruments Ltd., Palo Alto, U.S.A., 1973
4. V. Friehmelt, A. He, Z. Yang, G. Marx, Inorg. Chim. Acta, 109, L 25 (1985)
5. K. Alcock, F.C. Bedford, W.H. Hardwick, H.A.C. McKay, J. Inorg. Nucl. Chem., 4, 100 (1957)
6. G. Koch, Chemiker Zeitung, 101, 64 (1977)
7. V. Friehmelt, A. He, Z. Yang, G. Marx, Inorg. Chim. Acta, 111, 1 (1986)

Studies on Interfacial Precipitation of the First PUREX Extraction Cycle

F.Baumgärtner, A. Huber, Institut für Radiochemie, TU München, W. Germany

Solids at the interface of mixer-settlers may disturb the extraction of U and Pu in the first extraction cycle of the Purex process. These solids consist of particles with very small sizes in the nanometer range and are of colloidal nature. The opacity and dark colour of nuclear fuel solutions immediately after dissolution already indicates the presence of colloidal particles. In the course of time an increase of the number of colloidal particles is observed, which lasts for some weeks (1). It is to be expected, that these particles gather at the interfaces of the first extraction steps.

Beside the particles already present in the feed solution, additional solids can be produced at the interface through the contact with the organic phase. Especially Zr is known to form stable compounds with DBP, a hydrolysis product of TBP, which can lead to voluminous emulsions under the mixing action of the stirrers (2).

Nuclear fuels with medium burnup of 3 %, which is reached presently in nuclear power plants, contain tolerable amounts of solids for reprocessing. Experiences with high burnup fuel do not exist in large scale. Small scale dissolution experiments suggest however, that the amount of solids increases with burnup and the extraction process consequently can be severely disturbed. It is therefore necessary to remove the solids with suitable methods like filtration, centrifugation or flocculation. As the removal of small colloidal particles under process conditions of a reprocessing plant is not easy and laborious, the composition and behaviour of the solids have to be investigated closer, especially with respect to high burnups.

For the study of solids in nuclear fuel solutions 14 g of LWR-fuel with a burnup of 45 000 MWd/tU have been dissolved in 7M HNO_3. The fuel has been irradiated for 4 years and cooled down for 2.4 years. The solids in the solution were removed by 4 consecutive filtration steps with nuclepore-filters of 1 µm poresize after 2.5, 20, 68 and 164 hours. The filter residues were characterized by x-ray microanalysis in a scanning electron microscope, equipped for the analysis of highly radioactive material.

The first filtration step yields dissolver residues containing all particles greater than 1 µm. The following 3 filters show only the remaining particles smaller than 1 µm and solids, which formed after the first filtration. This type of solids we call postprecipitation, although the formation process is not believed to be a chemical precipitation than rather an agglomeration of particles (1). The two filters at 20 and 68 hours show Pd as the main constituent of their filter layer. No other fission products can be analyzed in appreciable concentrations. As Pd is known to precipitate as metallic colloids under intense γ-radiation (3), these two filters do not yield additional information about postprecipitations. Since the Pd-content and also the irradiation dose increases linearly with burnup, the amount of Pd-colloids can be estimated in dependence of the burnup from measurements of the mass concentration of Pd-colloids.

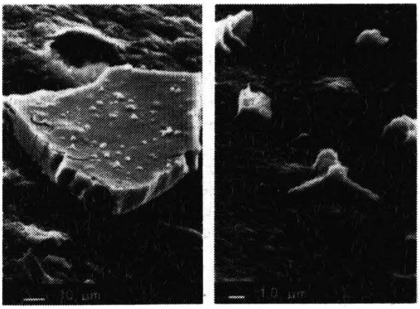

Figure 1: Secondary electron images of a piece of the filter layer from the last filtration of the fuel solution after 164 hours

An entirely different material is observed on the last filter, which represents postprecipitations formed between 3 and 7 days after dissolution. Figure 1 shows the secondary electron image of a piece of the filter layer. The filter is uniformly covered by this material with a thickness of 13 µm. The matrix material consists of the elements Mo,Tc,Ru,Rh and Pd and originates undoubtedly from colloidal particles, although the matrix material exhi-

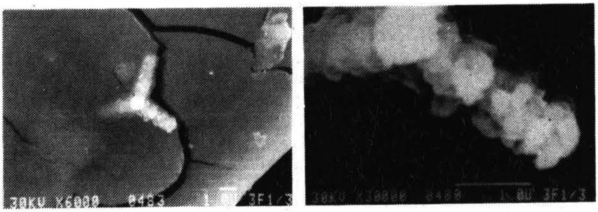

Figure 2: Fine structure of silver-halogenide crystals

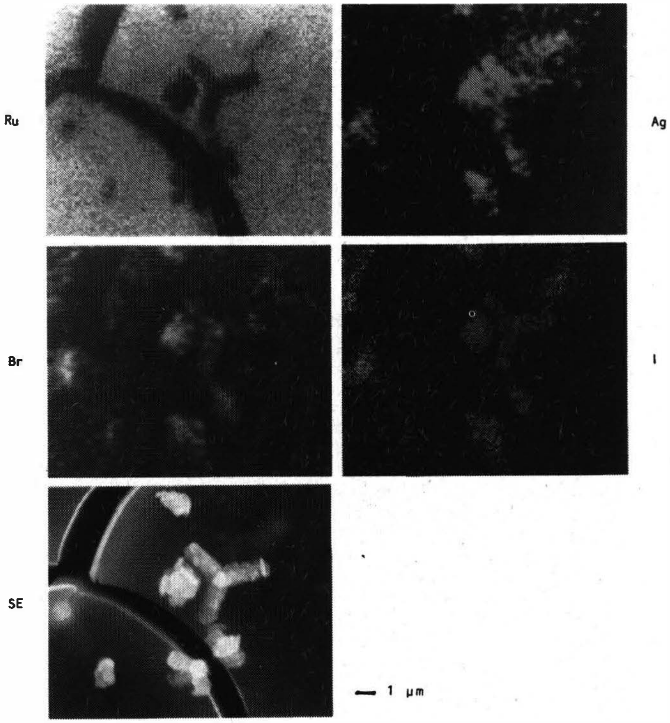

Figure 3: Elemental distribution maps of Ru, Ag, Br and I

bits no primary structure. In contrast to this smooth layer figure 1 also shows obvious crystallization products in form of trigonal AgBr- and AgI-particles with dimensions of some micrometers. The fine structure of these crystals, as shown in figure 2, points out that a rapid crystallization process took place. The elemental distribution maps of Ru,Ag,Br and I in figure 3 demonstrate that Ru is homogenously distributed over the filter layer and is clearly separated from the crystals. X-ray microanalysis of 91 points on the layer yields that this is also true for the other 4 elements Mo,Tc,Rh and Pd. The frequency distributions of the relative concentrations of the five elements in figure 4 are very sharp and indicate that the composition of the matrix material is constant throughout the filter layer. From these distributions a mean composition of 9% Mo, 7% Tc, 66% Ru, 11% Rh and 7% Pd is derived.

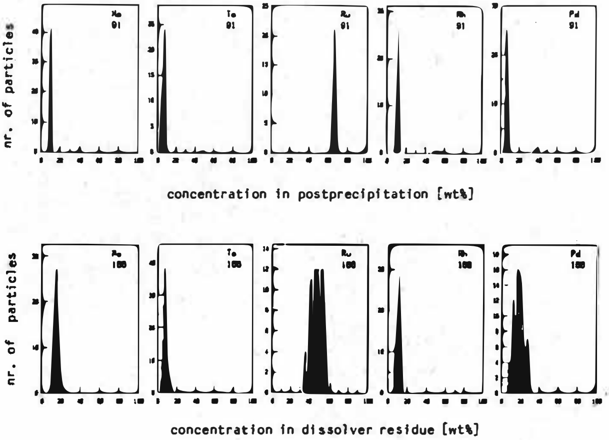

Figure 4: Frequency distributions of the alloy of Mo, Tc, Ru, Rh and Pd in the postprecipitation and in the dissolver residue

The five fission products Mo,Tc,Ru,Rh and Pd can already be identified in spent nuclear fuel material as a separate phase, known as "white inclusions". X-ray diffraction revealed that this phase is an alloy of the five metals with a hexagonal structure (4, 5, 6), which is insoluble in nitric acid. Most of this material therefore appears in the dissolver residue as particles with diameters in the micrometer-range. The composition of these particles originating from inclusions in the fuel is quite different from the colloidal particles observed. Analysis of 166 particles on the first filter after 2.5 hours yields a mean composition of 16% Mo, 8% Tc, 47% Ru, 11% Rh and 18% Pd. In addition the frequency distributions of the residue in figure 4 are broader. Postprecipitation and inclusions are similar, but not identical. Certainly the alloy-colloids are related to the same process which produces the alloy-inclusions in the nuclear fuel, but the origin and formation of the colloidal particles is not exactly known. A production of this type of colloids from simulated nuclear fuel solutions and alloys was not possible.

Solids in the organic phase were studied by filtrating tributyl-phosphate dissolved in kerosene, which has been used in a commercial reprocessing plant. A sample of 23 ml was drawn after scrubbing with sodium carbonate and filtrated through a cascade of 4 nuclepore filters with decreasing pore sizes of 4, 1, 0.1 and 0.03 µm. 90 % of the activity has been deposited on the first filter, the remaining activity is found on the second filter. The last two filters only had neglegible amounts of activity.

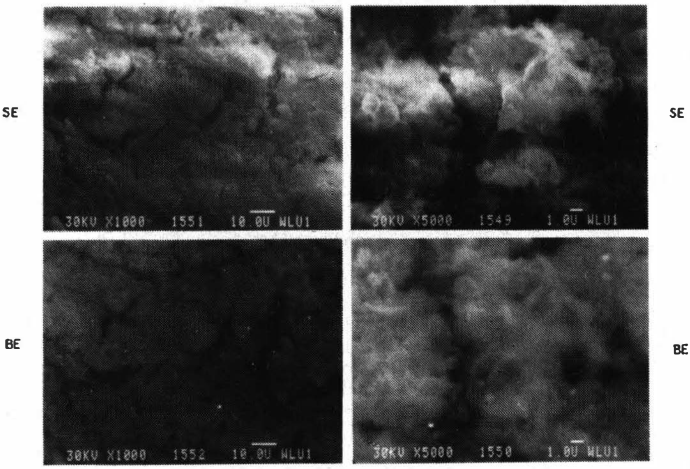
SE
SE
BE
BE
30KV X1000 1551 10.0U WLU1
30KV X5000 1549 1.0U WLU1
30KV X1000 1552 10.0U WLU1
30KV X5000 1550 1.0U WLU1

Figure 5: Secondary and backscatter electron images of the first filter from filtration of the organic phase with a poresize of 4 µm at two magnifications

The solids on the first filter form a dense filter layer, but no details of the constituents of this layer can be distinguished at higher magnifications in figure 5. The particles seem to have no clear contours. The elemental analysis shows Zr and Pd as main components, Mo and Ru are present in low concentrations. Zr and Pd exhibit a remarkable difference in their elemental distribution as is shown in figure 6. Pd is quite uniformly distributed, whereas Zr is subject to concentration variations. This means that the two elements form different chemical compounds in the organic phase. The concentrations of Mo and Ru are too low to be mapped.

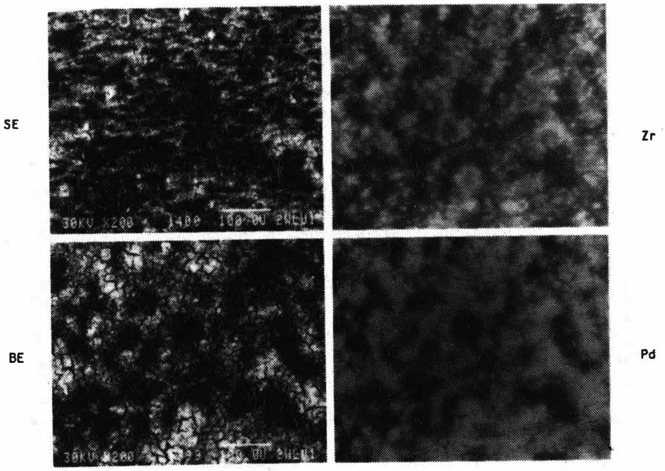

Figure 6: Elemental distribution maps of Zr and Pd (right) together with the corresponding secondary and backscatter electron image (left) from filtration of the organic phase

Although there had been no quantitative separation by the last two filtrations, some particles can be seen at high magnifications in figure 7. These particles are presumably the primary constituents of the layer on the first filter. Two major types of particles can be distinguished: spherical particles in the size range of 10 to 100 nm and rod-shaped particles with diameters of about 100 nm and lengths of about 300 nm. A third type can be seen in the upper right picture of figure 5, namely hollow spheres with diameters of up to 5 µm. These spheres are micels, which originate from emulsions at the interface of mixer-settlers. Due to the small size of the primary particles and the low content of Zr and Pd an elemental analysis of single particles is not possible. Also the tendency of these particles to agglomerate does not allow a further characterization of the solids on the first filter.

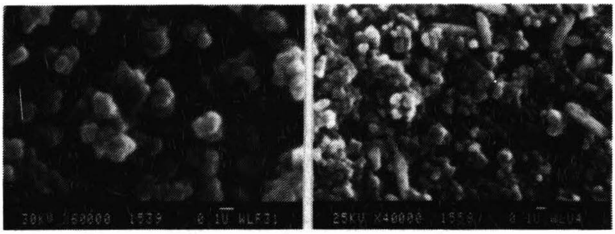

Figure 7: Spherical and rod-shaped particles on the last two filters from filtration of the organic phase

Summarizing the results of the investigations on solids at the interface three types can be distinguished due to their origin and formation:

1. metallic Pd-colloids arising from γ-radiolysis in the feed solution,
2. metalliic colloids of an alloy of Mo, Tc, Ru, Rh and Pd, presumably preshaped in the spent nuclear fuel,
3. a mixture of organic compounds of Zr and Pd and, to a lesser content, of Mo and Ru.

The formation of Pd-colloids depends, unter normal reprocessing conditions, on the Pd-concentration and the radiation dose of the fuel solution. The alloy colloids on the other hand are believed to have their origin in small inclusions in the fuel material. The amount of inclusions should increase with burnup, but an estimation of the amount of alloy colloids in the fuel solution is not possible due to lack of experience with high burnup fuel. The material used here yielded comparably high colloid concentrations as can be derived from an estimation of the mass deposition on the last filter after 164 hours. Another basic difference between the two colloids lies in its formation rate. Pd-colloids have been observed only up to 3 days after dissolution. The filtration after 68 hours removed all Pd-particles and no further formation took place. In contrast to this alloy colloids were found not until 68 hours after dissolution. Perhaps the formation of alloy colloids continued after the last filtration at 164 hours as has been reported by other investigators (1).

The feed solution naturally represents the primary source for solids gathering at interfaces. Perhaps these solids cause the formation of the Pd-, Mo- and Ru-compounds observed in the organic phase. Under this assumption Mo and Ru originate from the alloy colloids in the aqueous phase and Tc and Rh also should be present. The concentration of these two elements is probably too low to be detected. The solids at the interface under the process conditions of a reprocessing plant therefore consist mainly of Pd-colloids with small amounts of alloy colloids.

The Zr-solids on the other hand are certainly products of chemical reactions at the interface and in the organic phase, as has been shown by other investigations (2). No Zr-colloids have been observed in feed solutions. The results presented here are in agreement with these findings. Especially the existence of emulsions at the interface is confirmed by the observation of emulsion bubbles in the filter layer of figure 5.

Since early days of civil nuclear fuel reprozessing it is clear that with higher burnup the solids gathering at interfaces will increase. However not only the feed solution has to be clarified effectively but also the organic phase in order to prohibit recycling and accumulation of colloids at the aqueous-organic interface.

Literature:

1. D.O.Campbell, CONF-780308, III-23 (1978)
2. U.Bauder, Thesis, University of Heidelberg, 1978
3. M.Schmidt, Thesis, Technical University of Munich, 1986
4. J.I.Bramman, R.M.Sharpe, D.Thom, C.Gates, J.Nucl.Mat. 25(1968)21
5. D.R.O=Boyle, F.L.Brown, A.E.Dwight, J.Nucl.Mat. 35(1970)257
6. H.Kleykamp, R.Pejsa, J.Nucl.Mat. 124(1984)56

Extraction of actinides and fission products ions by non-chelating N,N'-tetraalkyldiamides

M.C. Charbonnel, C. Musikas, IRDI/DERDCA/DGR/SEP/SCPR - CEN/FAR -
Fontenay-Aux-Roses, BP n° 6 -92265 Cedex (France)

Introduction :

N,N-dialkylmonoamides [1],[2] are good extractants of metallic ions. They were considered as alternative to TBP in nuclear fuels reprocessing [3],[4]. The present paper deals with the extractive properties of N,N'-tetrabutylglutaramide

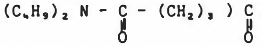

$$(C_4H_9)_2\ N - \underset{\substack{\| \\ O}}{C} - (CH_2)_3\ )\ \underset{\substack{\| \\ O}}{C} - N(C_4H_9)_2.$$

N,N'-tetraalkyldiamides of dicarboxylic acids except malonamides do not extract the trivalent actinides and lanthanides from aqueous HNO_3 solutions probably because there is no favorable ligand conformation to chelate the metallic ions. This feature is interesting for the nuclear fuel reprocessing since the presence of a second amide group could lead to new selectivities and to radiolytic and solvolytic degradation products easier to handle. We will present the investigation results of HNO_3, U(VI), Pu(IV) and fission products extraction by TBGA in toluene from HNO_3 aqueous solution.

Extraction of HNO_3 by TBGA

HNO_3 extraction isotherm by 0.5M TBGA in toluene is plotted figure 1. It can be seen that the ratio HNO_3/TBGA can be superior to one.

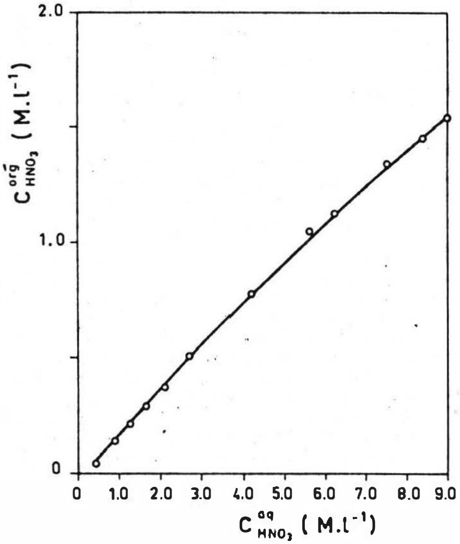

FIGURE 1 : HNO_3 EXTRACTION BY 0.5 M TBGA IN TOLUENE

Fairly good fits of experimental and calculated HNO_3 distribution curves are obtained by assuming that HNO_3 species in the organic phase are $(TBGA)_2HNO_3$, TBGA HNO_3 and $TBGA(HNO_3)_2$. FT IR spectroscopy has been carried out in order to check the validity of these assumptions. Main features are contained Table 1. The C = 0 stretching band is shifted to lower energies,

Table 1 : Influence of organic C_{HNO_3} upon C = 0 stretching energy (TBGA 0.76M in toluene)

$C^{ORG}_{H_2O}$ (M.l^{-1})	$C^{ORG}_{HNO_3}$ (M.l^{-1})	$\nu^{1645\ cm^{-1}}_{C\,=\,0}$	$\nu^{1635cm^{-1}}_{C\,=\,0}$	$\nu^{1595cm^{-1}}_{C\,=\,0}$	$\nu^{1530cm^{-1}}_{C\,=\,0}$
0.31	0	+			
0.32	0.081	+			
0.34	0.2	+	+		
	0.44	+	+		
0.35	0.78	+		+	
	1.16	+		+	+
0.4	1.6	+		+	+

(+ if the band is clearly observable).

but even for a HNO_3/TBGA ratio greater than 2,0 about 50 % of the band at 1645 cm^{-1}, attributable to the free C = O, is observed. This feature indicates that only one C = O is bonded to the HNO_3. The new bands which appeared at 1635 cm^{-1}, 1595 cm^{-1} and 1530 cm^{-1} can be attributed to the species : $(TBGA)_2HNO_3$, $TBGA(HNO_3)$, $TBGA(HNO_3)_2$. Increasing shifts can be attributed to a strengthening of the C = O....HNO_3 bonds. For the 1635, 1595 cm^{-1} band hydrogen bonding is probably involved, but for the 1530 cm^{-1} band there is probably an H^+ transfer from HNO_3 to the C = O. The 1530 cm^{-1} band is observed in $TBGA(HClO_4)x$ whereas the 1635 and 1595 cm^{-1} bands are not. The H^+ transfer in $TBGA(HNO_3)_2$ and not in $TBGA(HNO_3)$ can be explained by the competition between the two bases NO_3^- and TBGA for the proton. In $TBGA(HNO_3)_2$ it must be a weakening of one of the OH(in HNO_3)bond due to the binding of the NO_3^- to the second H^+. These assumptions are represented in figure 2.

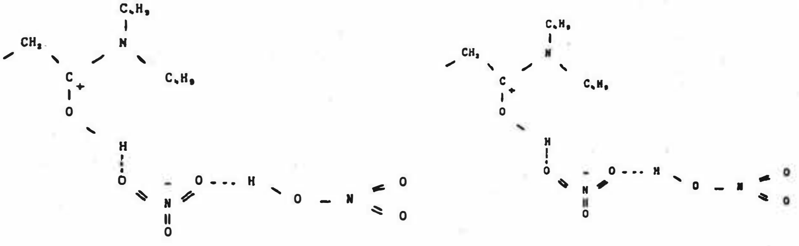

TBGA(HNO_3)$_2$ TBGA(HNO_3)

I. SCHEMATIC REPRESENTATION OF HNO_3 _ TBGA SPECIES IN TOLUENE

The organic water concentration is independent of HNO_3 organic concentration, so it seems that H_2O and HNO_3 extraction are independent.

Metallic ions extraction

The distribution ratios of several metallic ions present in the irradiated nuclear fuels, as a function of aqueous nitric acid concentration are plotted figure 3.

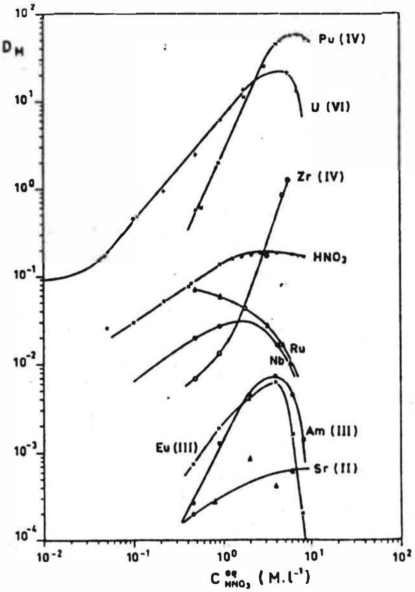

FIGURE 3 :
METALLIC IONS EXTRACTION
FROM HNO_3

It can be seen that TBGA is a good extractant for U(VI), Pu(IV) recovery from HNO_3 solutions. The fission products Ru, Zr, Sr, and trivalent lanthanides are poorly extracted. Extraction mechanism of U(VI) was investigated in more details. U(VI) distribution ratios were measured as a function of TBGA concentration for a low acidity in the aqueous phase (figure 4).

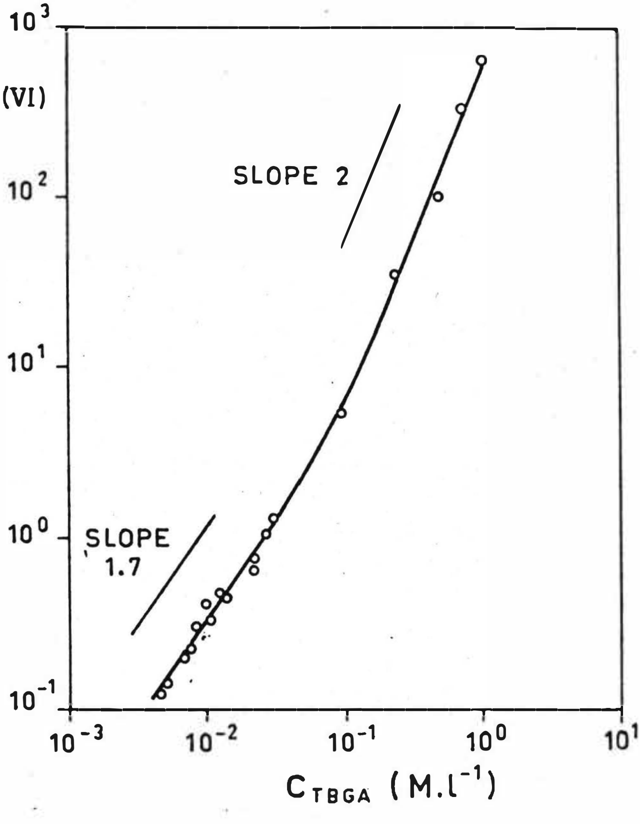

FIGURE 4 : U(VI) NITRATE EXTRACTION FROM AQUEOUS SOLUTIONS BY TBGA IN TOLUENE AS A FUNCTION OF TBGA (ACIDITY = 0, $LiNO_3$ = 0.2M)

It can be seen that the extraction curve has a variable slope between 1.5 and 2.0. At U(VI) saturation (precipitation of $UO_2(NO_3)_2TBGA$) the organic phase contains an uranyle complexe with UO_2^{2+}/TBGA mole ratio of one. There is no important changes in UV-visible spectra of organic U(VI) complexes with U(VI) concentrations increasing. These facts are in favor of the following extraction mechanism.

$$UO_2^{2+}\ 2NO_3^- + (1 + x)\overline{TBGA} \rightleftarrows \overline{[UO_2(NO_3)_2TBGA]}\ \overline{TBGAx}$$

x TBGA molecules are in the second uranyle coordination sphere, x can reach the value of 1.

At high nitric acidities there is a change in the organic uranyle complex UV-visible spectra. The extrem spectra are shown figure 5. The spectrum obtained at high acidities is typical of $UO_2(NO_3)_3^-$ anion [5], so the extraction mechanism is then :

$$UO_2^{2+} + 3NO_3^- + H^+ + \overline{TBGA} \rightarrow \overline{UO_2(NO_3)_3\ HTBGA}$$

This kind of mechanism was also found for the U(VI) extraction by monoamides [6].

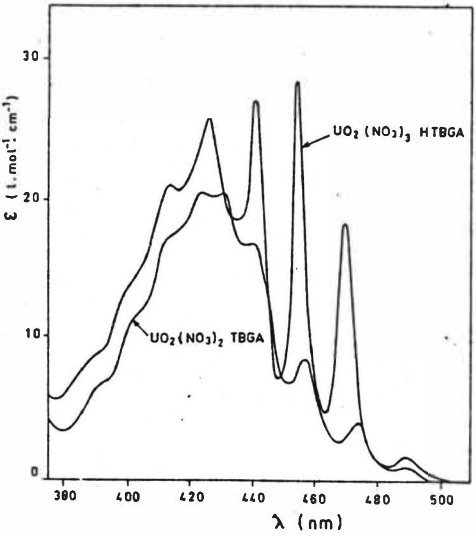

FIGURE 5 :
ABSORPTION SPECTRA OF THE
TWO ORGANIC SPECIES :
$UO_2\ (NO_3)_2$ TBGA ; $UO_2\ (NO_3)_3$ H TBGA

Conclusions :

The results of the investigations presented here showed that tetraalkyledicarboxylic acids diamides are better extractants than the carboxylic acids monoamides for U - Pu separations from fission products.

New advance in this field will be the synthesis of diamides extractants of which nitrato-uranyle complexes are sufficiently soluble in hydrocarbons diluents. Radiolytic behavior must be investigated. Finally the influence of N radicals upon U(VI) - Pu(IV) separation must be precised.

References

1. Fritz J.S., Orf G.M.
   Anal. Chem. 47, 12, 2043 (1975)

2. Siddall III Th.
   J. Phys. Chem. 64, 1863 (1960)

3. Siddall III, Th. Fulda M.O., Nichols G.S.
   DP 541 (1961)

4. Gasparini G.M., Grossi G.
   Sep. Sc. and Techn. 15, 825 (1980)

5. Rabinowitch E., Belford R.L.
   Spectroscopy and photochemistry of Uranyl compounds
   (Oxford : Pergamon Press) (1964)

6. Descouls N., Musikas C.
   Proceedings 14èmes journées des Actinides - Davos - April 1984
   Ed. J. Schoenes, p. 153.

Extraction of lanthanides and actinides (III) by di-2 ethyl hexyl dithiophosphoric acid and di-2 ethyl hexyl monothiophosphoric acid.

Structure of the complexes in the organic phase.

D. Pattée*, C. Musikas*, A. Faure**, C. Chachaty**

CEA-IRDI- * DERDCA-DGR-SEP-SCPR - CEN/FAR
** DESICP-DPC-SCM-CEN/SACLAY

To operate a trivalent actinide-lanthanide (III) group chemical separation from low pH nitric solutions we studied the extractive properties of the di-2 ethyl hexyl dithiophosphoric acid (HDEHDTP) ; this bidentate ligand which possesses a sulfur donor atom is a good extractant of soft acids [1]. We so expect a better selectivity for the actinides(III) extraction : 5f electrons have a better ability to delocalization than 4f electrons and form more covalent bounds as it has already been demonstrated by previous works in this laboratory [2].

As the di-2 ethyl hexyl monothiophosphoric acid (HDEHTP) is the main by-product of the synthesis of HDEHDTP and is also the main degradation product of HDEHDTP by a phenomenon of hydolysis [3] we also have investigated its extractive properties for trivalent actinides and lanthanides ; HDEHDTP is a bidentate ligand with one oxygen donor atom and so is a better extractant for hard acids like actinides and lanthanides (III) ; but its selectivity is weak.

The addition of TBP (tri-n butyl phosphate) to HDEHDTP deals to strong synergistic organic complexes with a great selectivity for Am(III). We explicited this phenomenon. When the metal is macroconcentrated the organic complexes aggregate and form inverted micelles.

1. Extraction of Am(III) and Eu(III) trace concentrations by HDEHDTP and HDEHTP

a - extraction by the purified acid HDEHDTP

We first plotted the distribution ratio of the metals versus the pH of the aqueous phase (fig. 1) at constant concentration of the extractant. The slope is very close to 3. Then we plotted the distribution ratio of the metals versus the concentration of the extractant at constant pH. The slope is also 3 (figure 2). So the mechanism of extraction is :

$$\overline{\mathrm{Am^{3+} + 3\ HDEHDTP}} + x\mathrm{H_2O} \rightleftarrows \overline{\mathrm{Am(DEHDTP)_3\ xH_2O}} + 3\mathrm{H^+} \qquad (1)$$

$$\mathrm{Eu^{3+}} + 3\ \overline{\mathrm{HDEHDTP}} + x\mathrm{H_2O} \rightleftarrows \overline{\mathrm{Eu(DEHDTP)_3\ xH_2O}} + 3\mathrm{H^+} \qquad (2)$$

$$\mathrm{Log}\ K_{ex}\ \mathrm{Am(III)} = -\ 7{,}87 \pm 0{,}52$$
$$\mathrm{Log}\ K_{ex}\ \mathrm{Eu(III)} = -\ 8{,}28 \pm 0{,}4$$

The constants of extraction are weak and it confirms the lack of affinity of trivalent actinides and lanthanides for a soft base like DEHDTP $^{\ominus}$. But the weak selectivity is in favour of Am(III)

$$\frac{D\ Am(III)}{D\ Eu(III)} = 2.55$$

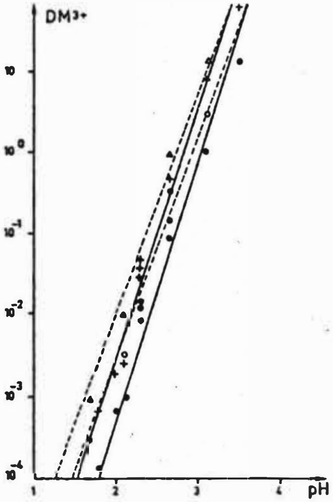

FIGURE 1 : VARIATIONS OF THE DISTRIBUTION RATIO DM³⁺ VERSUS pH.
- Aqueous phase : $[KNO_3] + [HNO_3]$ at I = 1.
  Eu(III) : 5 % of $[HDEHDTP]_i$
- Organic phase :
  + Am^{3+} ● Eu^{3+} $|HDEHDTP|_i$ = 0,5 M
  △ Am^{3+} ○ Eu^{3+} $|HDEHDTP|_i$ = 0,75 M

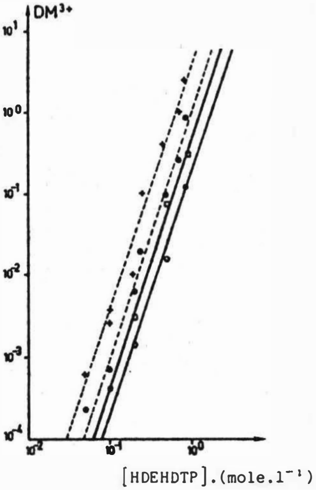

FIGURE 2 : VARIATIONS OF THE DISTRIBUTION RATIO OF DM³⁺ VERSUS THE CONCENTRATION OF THE EXTRACTANT HDEHDTP
- Aqueous phase : $[KNO_3] + [HNO_3]$ at I . Eu(III) : 5 % of $[HDEHDTP]_i$
- Organic phase : diluent : dodecane
  ● Eu^{3+} + Am^{3+} pH = 2,8
  ○ Eu^{3+} □ Am^{3+} pH = 2,5

b - Extraction by the purified acid HDEHTP (metals as traces).

The distribution ratio of the metals versus pH at constant concentration of the extractant are plotted. Figure 3, we also plotted the distribution ratio of the metals versus the concentration of HDEHTP at constant pH, figure 4.

As the extractant is dimerized [3] the slope analysis of these curves indicates the following extraction mechanism :

$$Am^{3+} + 1.5\ \overline{(HDEHTP)_2} + yH_2O \rightleftarrows \overline{Am(DEHTP)_3\ yH_2O} + 3H^+ \qquad (3)$$

$$Eu^{3+} + 1.5\ \overline{(HDEHTP)_2} + yH_2O \rightleftarrows \overline{Eu(DEHTP)_3\ yH_2O} + 3H^+ \qquad (4)$$

$$\text{Log Kex Am(III)} = -\,2{,}32 \pm 0.05$$
$$\text{Log Kex Eu(III)} = -\,2{,}27 \pm 0.05$$

The constants are stronger than those obtained with HDEHDTP because the hard acids Am(III) and Eu(III) have a better affinity for $\overline{\text{DEHTP}}^{\ominus}$ which possesses a hard oxygen donor atom. But there is no selectivity

$$\frac{D_{\text{Am (III)}}}{D_{\text{Eu (III)}}} = 0.89$$

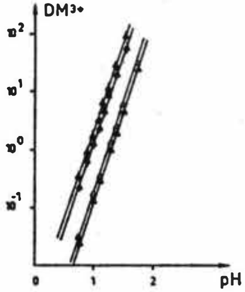

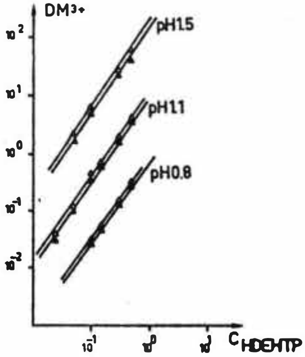

FIGURE 3 : VARIATIONS OF THE DISTRIBUTION RATIO OF DM^{3+} VERSUS pH.
- Aqueous phase : $KNO_3 + HNO_3$ at I = 1
Eu(III) : 5 % of $[\text{HDEHTP}]_i$

- Organic phase : diluent : dodecane
△ Eu^{3+}
▲ Am^{3+} $|\text{HDEHTP}|_i$ = 0,1 M.
▲ Eu^{3+}
▲ Am^{3+} $|\text{HDEHTP}|_i$ = 0,5 M.

FIGURE 4 : VARIATIONS OF THE DISTRIBUTION RATIO OF DM^{3+}
VERSUS THE CONCENTRATION OF THE EXTRACTANT
- Aqueous phase : $[KNO_3] + [HNO_3]$ at I = 1
Eu(III) : 5 % of $[\text{HDEHTP}]_i$

- Organic phase : diluent : dodecane
▲ Am^{3+}
△ Eu^{3+}

2. Extraction of Nd(III) in macro concentrations by raw HDEHDTP

This raw material contained at least 10 % of HDEHTP. So we plotted log D - 3 log $([\overline{\text{HDEHDTP}}]_o - 3\,[\overline{\text{Nd(DEHDTP)}_3}])$ versus pH (figure 5). The slope indicates the number of exchanged protons[3].

The first part of the curve is the extraction of Nd(III) by HDEHTP (figure 6). The second part of the curve is the extraction of Nd(III) by HDEHDTP (figure 7). The last part of the curve is the extraction by KDEHDTP which does not depend on the pH.

The slope of the intermediate part of the curve very close to 3.5 (figure 5) indicates that another phenomenon takes place during the extraction. We supposed and verified that it is the aggregation of $Nd(DEHDTP)_3$, according to :

$$Nd^{3+} + 3\ \overline{(HDEHDTP)} + mH_2O \rightleftarrows \frac{1}{j}\overline{(Nd(DEHDTP)_3,\ mH_2O)}_j + 3H^+ \qquad (5)$$

$$\text{with } \log D = \log K_{ex} + 3\log([HL]_i - 3[Nd]_{org}) + \frac{1}{j}\log j + \frac{j-1}{j}\log[Nd]_{org} + 3pH \qquad (6)$$

We determined $j \geq 5$ $\log Kex \geq -7$ and $m = 25$

The aggregation of the organic complex stabilizes it.

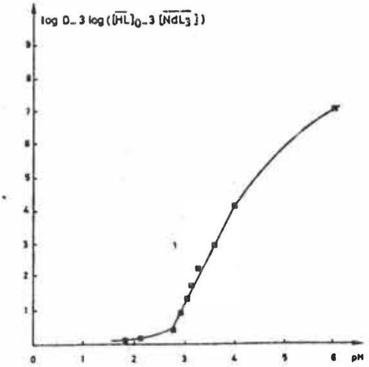

FIGURE 5 : VARIATION OF LOG D VERSUS pH
- Aqueous phase : $[Nd(III)]_i$ = 0,27 M

- Organic phase : raw $[HDEHDTP]_i$ = 0,585 M/dodecane

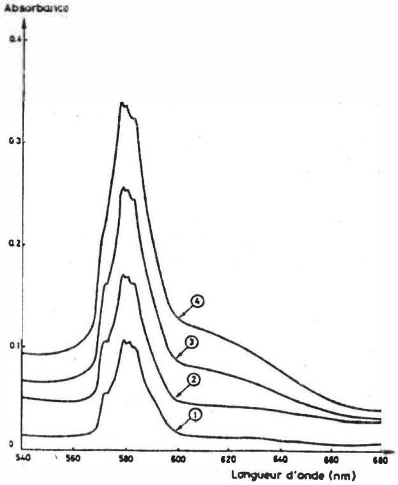

FIGURE 6 : U.V-visible spectrum of the organic phase after extraction (pH aq.< 3)
before extraction : aqueous phase : [Nd(III)] = 0,27 $M.l^{-1}$

organic phase : raw [HDEHDTP] = 0,585 $M.l^{-1}$ / dodecane

after extraction : aqueous phase : pH = 1,45 ①, 1,82 ②, 2,15 ③, 2,95 ④.

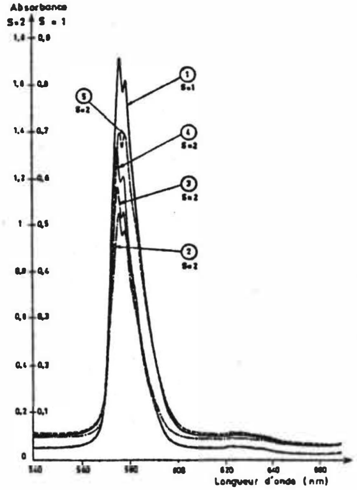

FIGURE 7 : U.V. VISIBLE SPECTRUM OF THE ORGANIC PHASE AFTER Nd(III)EXTRACTION (pH aq > 3)

before extraction : aqueous phase : $[\mathrm{Nd(III)}] = 0,27\ \mathrm{M.l^{-1}}$
organic phase : raw $[\mathrm{HDEHDTP}] = 0,585\ \mathrm{M.l^{-1}}$ / dodecane

after extraction : aqueous phase : pH 3,1 ①, 3,3 ②, 3,6 ③, 4 ④, 5,6 ⑤.

3. Extraction of 4f and 5f ions by a synergistic mixture

When the complex $[\overline{\mathrm{Nd(DEHDTP)_3}}]$j is formed we add one equivalent of TBP to the organic phase. We can observe two phenomena (see also figure 8).

- no NO_3^- ion is extracted
- water is expelled from the organic phase
- the U V-visible spectrum shows a fine electronic structure with a strong nephelauxetic effect and a strong enhancement of the molar absorption coefficient (ε_M = 5 (575 nm) → ε_M = 22,5 (585 nm)).

This phenomenon has already been observed with the charge transfer complex of Eu(III) with HDEHDTP [4] it is well explained by the substitution and the elimination of water molecules from the inner coordination sphere of Nd(III) ; this induces a shortening of the S-metal bound ; this shortening [5] [6] reveals the better ability of 5f electrons to form covalent bounds ; consequently we can observe the higher stability of the organic complex Am(DEHDTP)$_3$TBP compared to Eu, complex (see figure 9) $\frac{D_{Am(III)}}{D_{Eu(III)}} = 25$

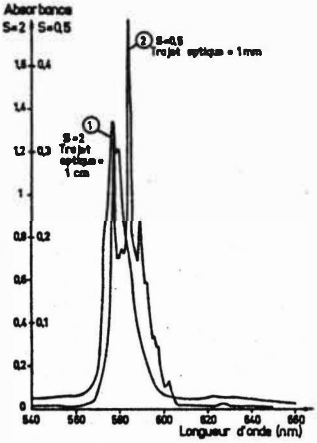

FIGURE 8 : U.V-VISIBLE SPECTRUM OF THE ORGANIC PHASE AFTER EXTRACTION.

before extraction Aqueous phase : Nd(III) = 0,27 $M.l^{-1}$
Organic phase : [HDEHDTP] = 0,585 $M.l^{-1}$ + TBP = 0,2 $M.l^{-1}$

after extraction Aqueous phase : pH = 5,6

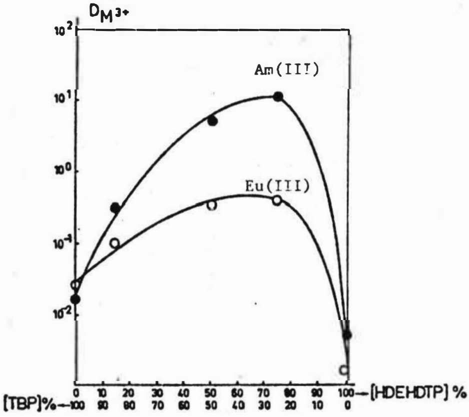

FIGURE 9 : VARIATIONS OF THE DISTRIBUTION RATIO OF DM^{3+} VERSUS THE PERCENTAGE OF HDEHDTP

Aqueous phase : $[HNO_3] + [KNO_3]$ / I = 1
[Eu(III)] + 10 % of [HDEHDTP]$_i$

Organic phase : diluent : dodecane $[\mathrm{HDEHDTP}]_i + [\mathrm{TBP}]_i = 1M$

4. Structure of the organic complexes

The evidence of the micellisation of the organic complexes has been provided by (H_2O ^1H NMR) and low angle X_Ray diffraction.

a _ NMR results :

In our previous work [3] [7] we demonstrated that NaDEHDTP forms inverted micelles in benzene and cyclohexane ; we used the mass action law model and applied the hypothesis that the chemical shift of the proton δ is a level-headed average between the chemical shift of water bound to the monomere δi and the chemical shift of the water bound to the n-mere δn (see fig. 9 and 10). This leads to the following equation :

$$\log c\,(\delta - \delta 1) = n \;\log c\,(\delta n - \delta) + \log nK - (n-1) \log (\delta n - \delta 1) \qquad (6)$$

$$\text{with } c = c1 + cn \qquad \text{and } \delta = \frac{c1}{c}\,\delta 1 + \frac{cn}{c}\,\delta n$$

$$\text{and} \quad nM1 \overset{K}{\rightleftarrows} Mn \qquad \text{and} \quad K = \frac{Cn}{n(c1)^n}$$

We can determine n and K by a linear regression on the equation (6) where $x = \log c(\delta n - \delta)$ and $y = \log c(\delta - \delta 1)$.

With this model we determined for $\overline{\mathrm{La(DEHDTP)_3TBP}}$ n = 2 and K = 188,3 before the c.m.c. (critical micellar concentration) and n = 8,4 and K 5,29 10^{15} after the c.m.c.

c.m.c. = 7.5 10^{-3}M.

For $\overline{\mathrm{La(DEHDTP)_3}}$ the c.m.c. was determined on the plot because the experimental points cannot be interpreted by the previous model. We determined c.m.c. = 1.5 10^{-3}M. (see figure 10).

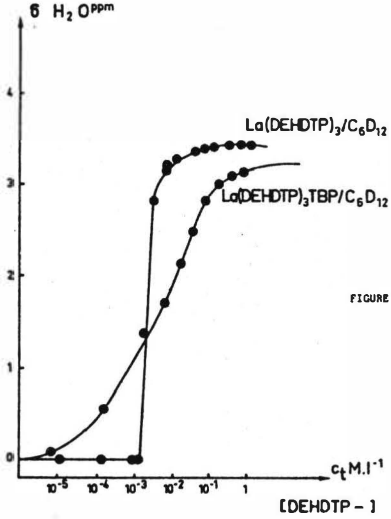

FIGURE 10 : VARIATIONS OF 1H WATER THE CHEMICAL SHIFT VERSUS THE CONCENTRATION OF [DEHDTP$^-$] DILUENT C_6D_{12} (CYCLOHEXANE).

b - low angle X ray diffraction :

The experiments confirmed the aggregation of $\overline{La(DEHDTP)_3}$ and $\overline{La(DEHDTP)_3TBP}$. The inverted micelles have the form of hollow shells where the La^{3+} ions are strongly tied to the ligands. For $La(DEHDTP)_3$ the pool is filled with water (m = 25 molecules of water by molecule of salt). For $La(DEHDTP)_3TBP$ the quantity of water is weak (m < 5).

Conclusion

We investigated the extractive properties of HDEHDTP and HDEHTP for trivalent actinides and lanthanides. We found that HDEHDTP is able to operate lanthanide/actinide group separation in presence of TBP. TBP expells water from the complex so that the S-metal bound is shortened and the selectivity Am(III)/Eu(III) is enhanced.

The organic complexes form inverted micelles with high metal concentrations.

References

[1] J.L. Sabot and D. Bauer, J. Inorg. Nucl. Chem., 40, (1978) 1129

[2] C. Musikas, P. Vitorge, R. Fitoussi, M. Bonnin, D. Pattée in "Actinides recovery from wastes and low grade sources" (J.D. Navratil, and W.W. Schulz Ed) Harwood. Academic Publishers, Chur, London, New-York (1982) 255

[3] D. Pattée, Thesis to be published as CEA-R.

[4] C. Musikas, P. Vitorge, D. Pattée, Proceed. ISEC 83 6 (1983)

[5] C.K. Jórgensen, Prog. Inorg. Chem., 1962, 4, 73

[6] P. Caro, J. Derouet, Bull. Soc. Chem. Fr., 1972, 1 46

[7] D. Pattée, A. Faure, C. Musikas, C. Chachaty Journ. Less. Common. Metal to be published.

The Reciprocical Effect of Iron (III) and Uranium (VI) Extraction by Synergistic Mixture Di-2(-ethylhexyl)phosphoric Acid and Trioctylphosphine Oxide from Phosphoric Acid Solutions

S. Meleš, I. Fatović, M.V.Proštenik and J.Romano
INA-Research and Development, Zagreb, Yugoslavia

Di(2-ethylhexyl)phosphoric acid (abbreviated as HDEHP) is widely used in hydrometallurgical process for the separation and purification of a number of metals such as uranium, rare earth, copper, cobalt and nickel. Iron is a very common impurity in raw industrial acid metal solutions in either the divalent or trivalent states. So, it is associated with uranium in the wet - process phosphoric acid, and it is coextracted during the uranium recovery by HDEHP-TOPO (1-2) (TOPO = trioctylphosphine oxide). Therefore, it is of a great importance to know the extraction properties of iron in the given system (3). Our earlier investigation gave us some information on the behaviour of Fe(III) extraction with HDEHP from phosphoric acid solutions (4). The purpose of the present investigation was to define the mutual influence of U(VI) and Fe(III) extraction from phosphoric acid solutions, with HDEHP-TOPO in kerosene.

Experimental

All chemical reagents were of analytical grade. HDEHP and TOPO were provided as a high purity product by Mobil Co. Aqueous solutions of selected concentrations were prepared from the real wet process acid (industrial plant-green grade) by dissolving Fe(III) chloride and uranyl nitrate. Organic solutions were prepared with HDEHP and TOPO in nonaromatic hydrocarbon diluent Mobil 190/210. Distribution ratio measurements were performed in the thermostated bath. Equal volumes of aqueous and organic solutions were mixed mechanically for

20 min to ensure thermal and chemical equilibrium. The uranium and iron concentration in the aqueous and organic phases were determined by spectrophotometry (5).

Results and discussion

Typical isotherms for coextraction of Fe(III) and U(VI) from real 5,1M H_3PO_4 with 0,3M HDEHP + 0,075M TOPO in kerosene at 25°C are presented in Fig. 1. The results show significant influence of U(VI) concentration on the extraction of Fe(III). Moreover this influence is very marked at higher concentration of U(VI). It means that at higher concentration of uranium, extraction of Fe(III) is lower. A slight positive effect on the extraction of U(VI), caused by the presence of Fe(III), is also evident.

The values of distribution ratios of Fe(III), with the initial U(VI) concentration of 4,9g U/L, as a function of real H_3PO_4 concentration are presented in Fig. 2. The same values for U(VI) extraction, starting with 3,50 - 32,30g Fe/L as initial aqueous concentration, are shown in Fig 3. It is observed that the distribution ratio of U(VI) decreases in all cases with increasing H_3PO_4 concentration. However, the values of distribution ratios for Fe(III) extraction slightly increase for the concentrations above 5,1M H_3PO_4 and 20g Fe/L in aqueous phase, which is in good agreement with Fig. 1. The distribution ratios of Fe(III) extraction (Fig. 4), at constant concentration of U(VI), decrease with the increase of temperature for the concentration of Fe(III) in aqueous phase up to 20g Fe/L. The same influence of distribution ratio U(VI) extraction is less evident in the used concentration range of Fe(III) (Fig.5). The effect of increasing distribution ratio Fe(III) above the initial concentration of 20g Fe/L, at constant U(VI) concentration in 5,1M H_3PO_4, is evident with increasing molarity of extractant (Fig.6).

The iron has been reextracted from the obtained organic phases (phase ratio O/A = 1,33 - 6) with real 5M H_3PO_4 at 25-50°C. The content of Fe in H_3PO_4 has been 1,90g Fe/L. It is found that about 88 - 92% of Fe(III) has been removed (O/A = 3 - 4) from 0,5M HDEHP + 0,125M TOPO at 25°C. Simulaneously about 7 - 10% of U(VI) has been reextracted. The same results have been obtained from 0,3M HDEHP + 0,075M TOPO (O/A = 4 - 6). The organic phases have been treated with water to remove phosphate and then have been stripped, at initial pH values 9,3 - 9,45, with 0,35 - 0,55M $(NH_4)_2CO_3$ (O/A = 2). The stripping efficiency in three stages has been about 96 - 99,5%, depending on the concentration of $(NH_4)_2CO_3$ used. The precipitation of $Fe(OH)_3$ in the solutions of ammonium uranyl tricarbonate has not been noticed at all.

Very good results have been obtained in the experiments of Fe(III) reectraction with 5M H_3PO_4 containing 5g Fe/L. However, these experiments are still in course.

All results are confirmed by countercurrent extraction on mixer-settler units.

References

1. F.J. Hurst and D.J. Crouse, Ind.Eng.Chem.Proc.Des.Develop., 13, 3, 286 (1974)
2. W.W. Berry and A.V. Henrickon, US.Pat. 4, 302, 427 (1981)
3. F.T.Bunus, V.C. Domocos and P. Dimitresen, J.Inorg.Nucl. Chem. 40, 117 (1978)
4. S. Meleš, M.V.Proštenik, Polyhedron 3, 615 (1984)
5. I. Brčić, E.Polla and M.Radošević, Analyst, 110, 1249, 1463 (1985)

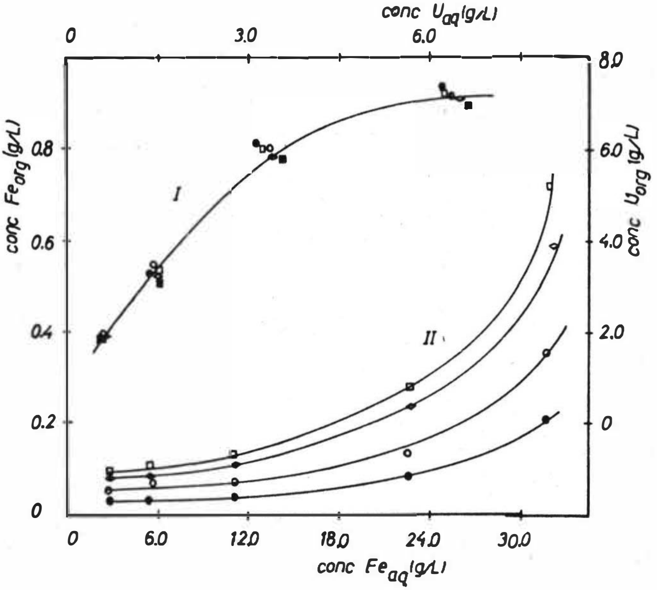

Figure 1. Isotherms for Fe(III) and U(VI) coextraction from 5,1M H_3PO_4 with 0,3M HDEHP + 0,75M TOPO at 25°C:
I initial conc. U(g/L): □ 2,65 ◐ 4,85 ○ 9,38 ● 13,92
II initial conc. Fe(g/L): ■ 3,47 ◐ 5,42 ○ 12,30 □ 22,40 ● 32,42

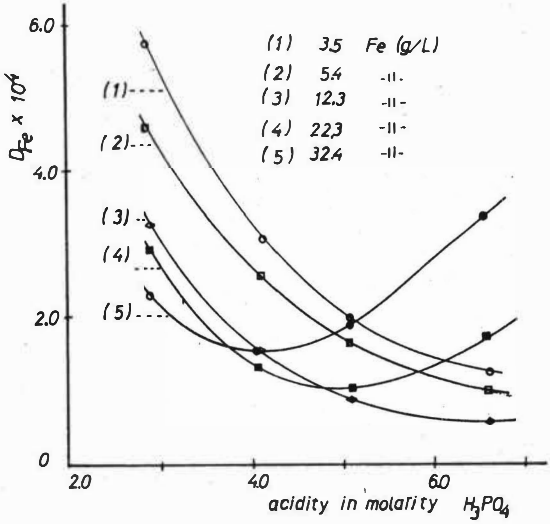

Figure 2. Distribution ratios of Fe(III) as a function of acidity: 0,3M HDEHP + 0,075M TOPO at 25°C, initial conc. U(g/L) = 4,85

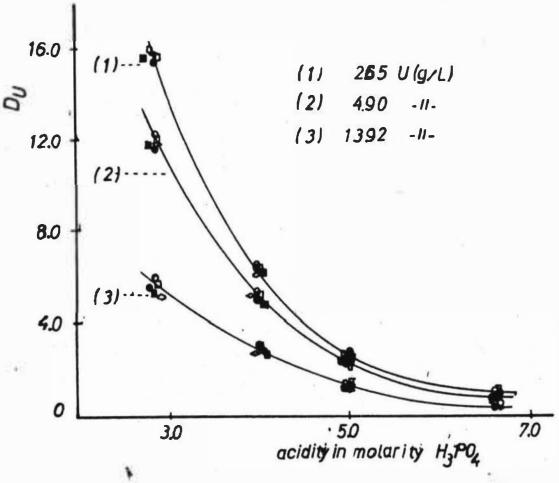

Figure 3. Distribution ratios of U(VI) as a function of acidity: 0,3M HDEHP + 0,075M TOPO at 25°C, initial conc. Fe(g/L) ○ 3,47 □ 5,42 ● 22,30 ◆ 32,42

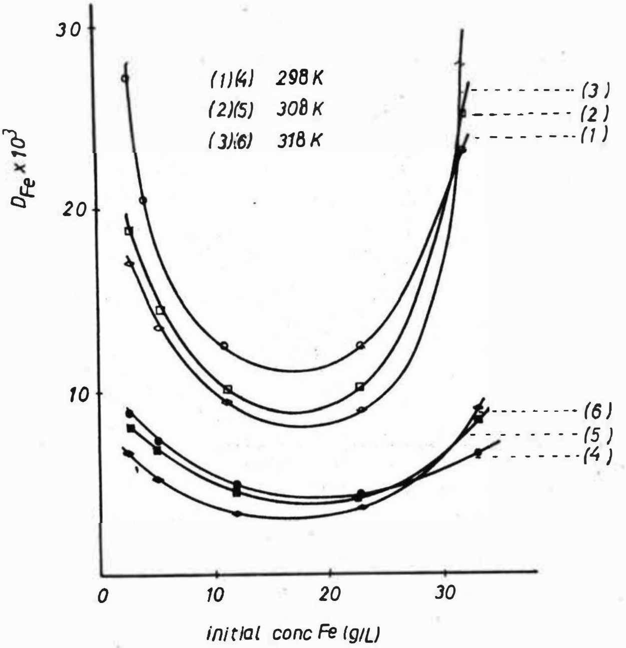

Figure 4. Effect of initial Fe(III) concentration on the extraction of Fe(III) from 5,1M H_3PO_4: 0,3M HDEHP + 0,075M TOPO, initial conc. U(g/L) ○ □ ◇ 2,65 ● ■ ◆ 13,92

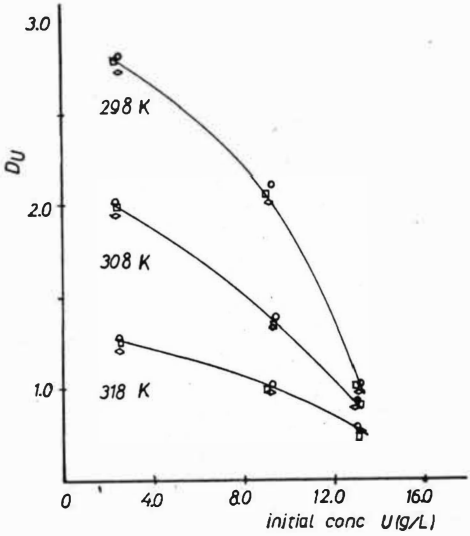

Figure 5. Effect of initial U(VI) concentration on the extraction of U(VI) from 5,1M H_3PO_4:0,3M HDEHP + 0,075M TOPO, initial conc. Fe(g/L) ○ 3,47 □ 5,42 ◇ 12,30

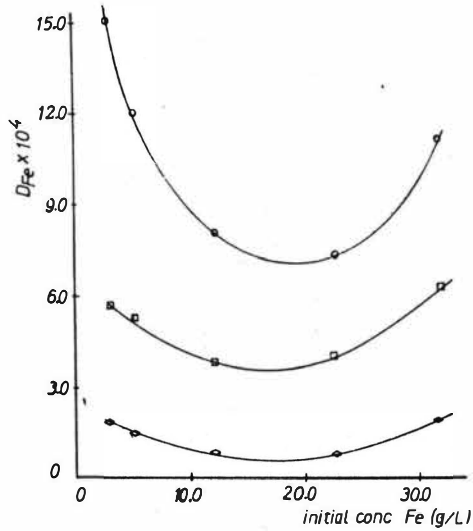

Figure 6. Effect of initial Fe(III) concentration on the extraction of Fe(III) from 5,1M H_3PO_4 at 25°C: o 1M HDEHP + 0,250M TOPO ☐ 0,5M HDEHP + 0,125M TOPO ◇ 0,3M HDEHP + + 0,075M TOPO, initial conc. U(g/L) = 4,90

Improved Urphos Process to Extract Uranium from Phosphoric Acid Using New Organo-Phosphorous Solvents.

A. Bathelier, FAR ; G. Lyaudet, A. Textoris, Bessines ; P. Michel, Velizy, France.

Many processes have been designed and operated to recover uranium from the phosphoric acid, most of the time by solvent extraction. Uranium can be extracted either as tetravalent uranium, or as hexavalent uranium.

COGEMA has in a first step developped a process called URPHOS [1] using a conventional solvent mixture (D_2EHPA-TOPO) with a single cycle. The CEA (French Atomic Energy Commission) and IRCHA (French Institute for Applied Chemistry) have developped a synergistic mixture of the same family [2] . The first component is a phosphine oxide called DinHMOPO (Di n Hexyl Octyl Methoxy Phosphine Oxide) with the following formula :

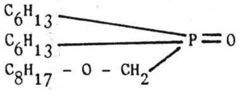

The second component is a dialkyl phosphoric acid called BIDIBOPP (Bis Dibutoxy 1.3 Propyl 2 Phosphoric Acid) with the following formula :

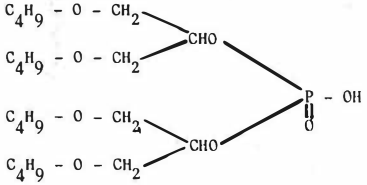

COGEMA has tested that mixture on a laboratory, then on a pilot scale [3] . Some specific new problems arose, the solution of which is dealt with in the present paper.

1. Recall of the new solvents characteristics

Distribution coefficient and solvent load have been measured for uranium and ferric iron. For that purpose, two different acids were used. Tests conditions are summed up in the table 1.

Table 1
Laboratory test conditions

		Acid n° 1	Acid n° 2
Origin		Morocco	Jordan
Content in :			
P_2O_5	%	32.2	28.3
U	mg/l	103	118
Fe	g/l	2.2	8.2
Solvent		Synergistic mixtures	
Phosphine oxide	M	0.125	0.125
Dialkyl phos.acid	M	0.5	0.5

The results achieved for the distribution coefficient are given in the table 2.

Table 2
Distribution coefficients

Synergistic mixture	Acid n° 1				Acid n° 2			
	kd U	Ratio n/1	kd Fe	Ratio n/1	kd U	Ratio n/1	kd Fe	Ratio n/1
1. TOPO-D_2EHPA	4.5	1	0.04	1	6.9	1	0.03	1
2. TOPO-BIDIBOPP	13.6	3	0.36	9	14.2	2.05	0.39	13
3. DinHMOPPO-D_2EHPA	6.5	1.45	0.07	1.75	8.1	1.15	0.08	2.65
4. DinHMOPPO-BIDIBOPP	21.3	4.75	0.77	19.25	26.5	3.85	0.51	17

From table 2, it can be noticed that the influence of changing the dialkyl phosphoric acid is larger than the same with phosphine oxide. By selecting the mixture DinHMOPPO-BIDIBOPP,distribution coefficient is multiplied by a factor in the margin 3.5 - 5. The influence is more sensitive with a more concentrated acid.

In the same time, iron distribution coefficient is enhanced in a much larger extent than it is for uranium. The influence of the nature of the dialkyl phosphoric acid is very important on the iron extraction. For instance, the respective content of uranium and iron in the various stages of the extraction section would be as shown in table 3.

Table 3
Extraction section Uranium and Iron solvent content (mg/l)

	Stage 1		Stage 2		Stage 3		Stage 4		Stage 5	
	U	Fe	U	Fe	U	Fe	U	Fe	U	Fe
Acid n° 1	1 400	1 090	697	1 230	365	1 220	215	1 340	174	1 240
Acid n° 2	1 297	2 950	1 226	3 110	1 015	3 410	725	3 370	337	2 610

Preliminary bench scale tests have shown that such amounts of iron would give lot of trouble in the stripping operation. Therefore some investigations had to be carried out to overcome these difficulties.

2. Selective stripping of iron

The SEPA (COGEMA's Service of process studies and analysis) has carried out investigations in three different ways :

- To find a specific stripping reagent for iron,
- To achieve a new steady state for uranium and iron using a scrubbing with a flow of free iron phosphoric acid,
- To achieve the same state using a scrubbing with an acid mixture which could be recycled to the phosphate attack section.

The basic flowsheet of the URPHOS bis process is on the figure 1.

2.1. Iron removal with oxalic acid

Many acids have been tested such as hydrochloric and tartric acid, but the best results were achieved with the oxalic acid. No reaction occurs between oxalic acid and uranium in the organic phase. On the contrary iron forms very strong complexes with oxalic ions.

That way iron can be stripped from the organic phase and it comes into the aqueous phase. Bench scale test runs yielded the results shown in table 4.

Table 4
Iron stripping by oxalic acid

Stage number	Iron content of the organic phase (mg/l)		
	Run 1	Run 2	Run 3
1	1 353	1 482	1 275
2	858	1 073	965
3	345	637	627
4	151	347	431
5	97	210	253

No uranium is stripped during that operation and the uranium concentration in the organic phase remains constant.

The operating conditions were as follows :

- Content in $H_2C_2O_4$, 2 H_2O...........................	23 g/l
- Stages number	5
- Ratio organic/aqueous..............................	1/2.7
- Run duration.......................................	62 h
- Iron removal rate	80-85 %
- Oxalic acid consumption............................	8-10 kg/kg Fe

The oxalic scrubbing is technically very efficient , but very expensive : it needs 3 to 5 stages and requires 8 to 10 kg of oxalic acid per kilogram of iron. Oxalic acid regeneration would be possible using successively a base and an acid but does not make that way profitable.

2.2. Iron removal with 7 M phosphoric acid

The purpose of that way is to use iron free phosphoric acid to scrub loaded solvent. The preparation of such an acid is carried out in five stages on a part of the flow of uranium free phosphoric acid with a blank solvent. The 7 M phosphoric acid is obtained by evaporation. In a first step iron is removed from barren phosphoric acid, which in a second step is concentrated.

From a 4.6 M barren acid, containing 1 290 mg/l of iron and less than 3 mg/l of uranium, the kinetics appears to be slow : 72 % of the maximum concentration achieved within 10 minutes.

A continuous test run has been carried out under the following conditions :

. Iron free acid :

P_2O_5(7 M) : 493 g/l Fe : 80 mg/l
Contact time in each stage : 5 min

. Loaded solvent :

U : 1 375 g/l Température : 30 °C
Fe : 2 125 g/l Org/Aq ratio: 1/1

The results achieved are read in the table 5.

Table 5
Iron removal with concentrated phosphoric acid

Stage number	Iron stripped (%)		Uranium stripped (%)	
	In the stage	Cumulative	In the stage	Cumulative
1	60.6	60.6	16.7	16.7
2	19.5	80.1	13.2	29.9
3	6.1	86.2	10.9	40.8
4	4.6	90.8	9.1	49.9
5	4.1	94.9	7.3	57.2

The complete flowsheet is given in the figure 2.

The efficiency of the operations of differential stripping of iron and uranium is shown on figure 3.

The results so achieved show that two stages would be enough to strip 80 % iron carrying away 30 % uranium. It requires 7 M iron free phosphoric acid obtained through at least 3 stages and an evaporation.

The advantages of that process are :

- No new reagent, use of only phosphoric acid,
- Technical efficiency.

The disadvantages are large :

- 5 to 6 additional stages to prepare the reagent (iron free phosphoric acid),
- An evaporation is required to concentrate the iron free acid.

The whole process is uneconomical.

2.3. Iron removal with a sulphuric phosphoric mixture

Sulphuric acid being used to convert phosphate into phosphoric acid, it was obvious that it had to be tested as a reagent to remove iron from loaded solvent. By adding some sulphuric acid to a barren phosphoric acid it is possible to prepare a reagent rich in acid which might be efficient.

The corresponding flowsheet is on the figure 4.

Preliminary tests have been effected under the following operating conditions :

- Contact time : 10 min
- Temperature : 40 °C
- Org/Aq ratio : 1/1
- Overall acid content : 12 N.

Results are given in the table 6.

Table 6

Distribution coefficient for iron and uranium with sulphuric-phosphoric mixtures

Test Number	Scrubbing solution Composition (M)		Kd Fe	Kd U	Metal stripped (%)	
	H_3PO_4	H_2SO_4			Fe	U
1	1.67	3.5	0.71	1.92	58.3	34.1
2	2.00	3.0	0.53	2.63	65.5	27.4
3	2.30	2.5	0.42	4.17	71.4	19.0
4	2.67	2.0	0.44	5.55	69.0	15.6
5	3.00	1.5	0.33	4.76	75.3	17.0
6	2.33	1.5	1.28	12.50	48.6	

The best conditions are achieved in the number 5 test.

From those figures, the bench scale continuous test was carried out under the following conditions :

- Contact time in the mixers : 5 min
- Temperature : 40 °C
- Org/Aq ratio : 1/1
- Number of stages : 1, 2 or 3

and with a phosphoric acid showing the following characteristics :

- U content .... 0.136 g/l
- Fe content .... 11.9 g/l
- P_2O_5 .... 408 g/l

Scrubbing reagent composition :

- H_3PO_4 .... 293.5 g/l
- H_2SO_4 .... 147 g/l

The results achieved are gathered in the table 7.

Table 7
Bench scale test runs results

Number of mixers settlers	Loaded solvent ingoing		Fe content of scrubbing reagent	Loaded solvent outgoing		Metal stripped (%)	
	U g/l	Fe g/l	g/l	U g/l	Fe g/l	Fe	U
1	1.35	1.38	1.04	1.21	0.65	53.0	10.4
1	1.28	2.41	1.05	1.19	1.03	57.2	7.0
1	1.30	3.17	1.12	1.18	1.06	66.6	9.2
2	1.32	2.14	1.19	1.22	0.35	83.5	7.6
2	1.38	2.76	1.04	1.22	0.37	86.5	11.6
2	1.40	2.43	0.97	1.24	0.46	81.1	11.4
3	1.37	3.01	1.16	1.15	0.33	89.1	15.8
3	1.43	2.38	1.11	1.25	0.29	87.7	12.5
3	1.35	2.33	0.99	1.18	0.30	87.3	12.8

It can be seen from those results that 2 stages could allow to strip between 80 and 85 % of iron versus only 8 to 11 % of uranium. Such a liquid effluent rich in sulphuric and phosphoric acid can be recycled to the attack of phosphates.

3. Conclusions

Iron removal with sulphuric phosphoric mixtures has been shown as the most efficient way. It does not require iron free phosporic acid and acid concentration, and yields good iron removal and satisfactory selectivity Fe/U.

From a capital cost viewpoint, the process requires only two stages of mixer-settlers and a solvent removal device which allows recycling of the aqueous acid phase in the phosphoric plant as a small part of the attack reagent.

REFERENCES

[1] P. Michel, G. Ranger, P. Corompt, P. Bon

New process for the recovery of uranium from phosphoric acid
I.S.E.C. Liège Belgium, September 1980.

[2] C. Ginisty

Improved dialkyl phosphoric acid-phosphine oxide synergistic systems for uranium recovery from phorphoric liquors.
I.S.E.C. Denver USA, August 1983.

[3] G. Lyaudet, A. Textoris

Nouveaux solvants pour l'extraction de l'uranium de l'acide phosphorique
Symposium sur l'extraction par solvants et l'échange d'ions. Paris Avril 1984.

BASIC FLOWSHEET OF URPHOS BIS PROCESS

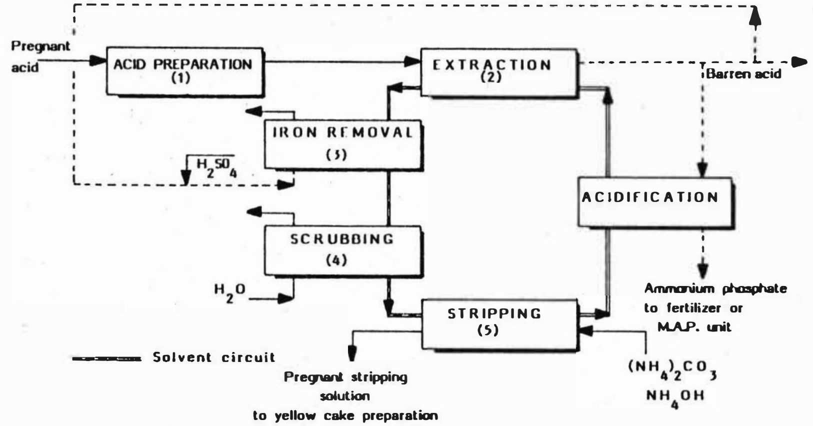
Pregnant acid
ACID PREPARATION (1)
EXTRACTION (2)
Barren acid
IRON REMOVAL (3)
H_2SO_4
ACIDIFICATION
SCRUBBING (4)
H_2O
STRIPPING (5)
Ammonium phosphate to fertilizer or M.A.P. unit
Solvent circuit
Pregnant stripping solution to yellow cake preparation
$(NH_4)_2CO_3$
NH_4OH

Figure n° 1

IRON REMOVAL BY SCRUBBING WITH 7 M PHOSPHORIC ACID

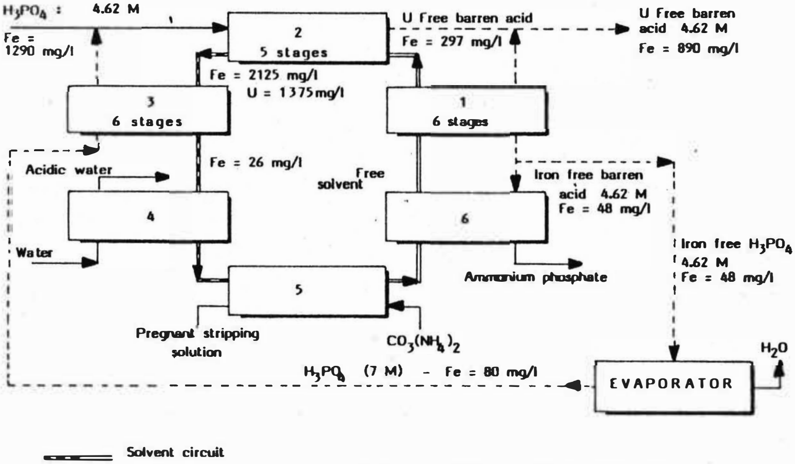
H_3PO_4 : 4.62 M
Fe = 1290 mg/l
2
5 stages
U Free barren acid
Fe = 297 mg/l
U Free barren acid 4.62 M
Fe = 890 mg/l
Fe = 2125 mg/l
U = 1375 mg/l
3
6 stages
1
6 stages
Fe = 26 mg/l
Free solvent
Acidic water
4
Iron free barren acid 4.62 M
Fe = 48 mg/l
6
Water
Iron free H_3PO_4
4.62 M
Fe = 48 mg/l
Ammonium phosphate
5
Pregnant stripping solution
$CO_3(NH_4)_2$
H_2O
H_3PO_4 (7 M) - Fe = 80 mg/l
EVAPORATOR
Solvent circuit

1. Iron removal from barren phosphoric acid
2. Uranium extraction
3. Iron removal from solvent
4. Water scrubbing of iron free solvent
5. Uranium stripping
6. Solvent acidification with iron free acid

Figure n° 2

IRON REMOVAL BY SCRUBBING WITH SULFURIC PHOSPHORIC MIXTURES

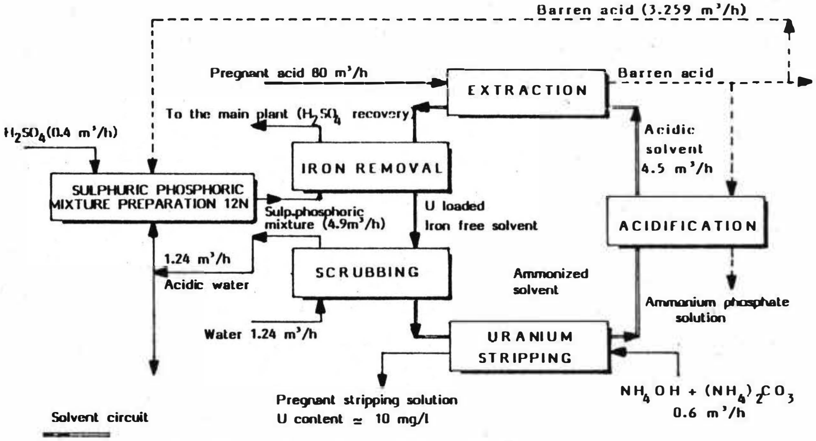
Barren acid (3.259 m³/h)
Pregnant acid 80 m³/h
EXTRACTION
Barren acid
To the main plant (H2SO4 recovery)
H2SO4 (0.4 m³/h)
IRON REMOVAL
Acidic solvent 4.5 m³/h
SULPHURIC PHOSPHORIC MIXTURE PREPARATION 12N
Sulp-phosphoric mixture (4.9m³/h)
U loaded Iron free solvent
ACIDIFICATION
1.24 m³/h
Acidic water
SCRUBBING
Ammonized solvent
Ammonium phosphate solution
Water 1.24 m³/h
URANIUM STRIPPING
Pregnant stripping solution
U content ≃ 10 mg/l
NH4OH + (NH4)2CO3
0.6 m³/h
Solvent circuit

Pregnant acid : U = 0.08 g/l - Fe = 1.31 g/l - H_3PO_4 = 442 g/l

Figure n° 4

IRON REMOVAL AND CO-STRIPPING OF U BY SCRUBBING WITH PHOSPHORIC ACID

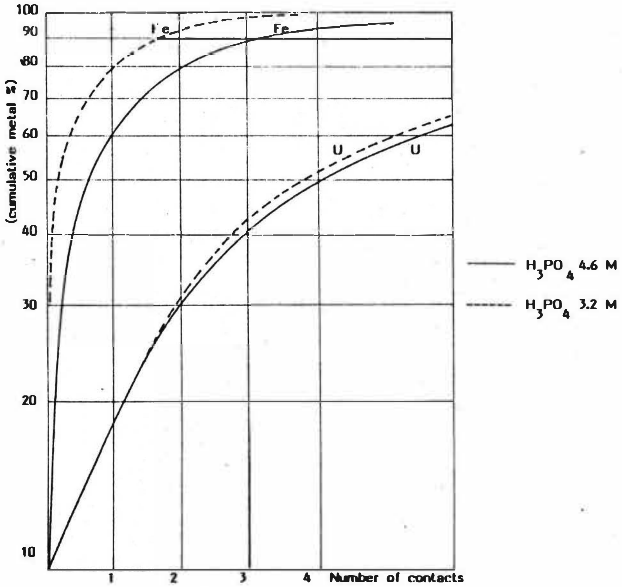

Figure n° 3

Analysis of the Extraction Tailing in Purex Process

F. Baumgärtner, K. Stephan, B. Kanellakopulos*, J.I. Kim

Institut für Radiochemie, TU München, 8046 Garching, FRG
*Institut für Heiße Chemie, Kernforschungszentrum Karlsruhe,
7500 Karlsruhe, FRG

Abstract

A so called extraction tailing in the Purex process has been investigated in pure HNO_3 systems by consecutive multi-stage extractions as well as by batch extractions with different initial Pu concentrations. The Pu species in aqueous phases from multi-stage extractions and in diluted acid are characterized by laser-induced photoacoustic spectroscopy. In multi-stage extractions, no tailing effect is observed, whereas the change in distribution coefficients is found in batch extractions at pu-conc. < 10^{-5} mol/L. The observed phenomena are briefly discussed.

1 Introduction

The plutonium extraction by a multiscale-countercurrent technique is known to be quantitative (> 99.9 %) [1-4]. However, a very low-level plutonium loss (< 0.04 %) can take place in the extraction process, as demonstrated by Ochsenfeld et al. [1,3], Baumgärtner [2] and Lloyd [4]. This is ascribed to disturbances arising in the multi-stage phase distribution [2,4], i.e. a decrease in plutonium distribution coefficients along with successive extraction stages [4]. A plutonium feed solution of 3 M HNO_3 shows a small but significant amount being inextractable into 30 % TBP-dodecane [4]. Distribution coefficients are observed to decrease from 17 to 0.2 in seven consecutive extraction stages and the tailing in the aqueous phase involves <0.01 % of the plutonium feed concentration. The study of various possible reasons made by Lloyd [4], for example, redox reaction or disproportionation reaction of Pu(IV), plutonium polymer formation and organic impurities in the extractant, does not lead to any conclusive explanation for the observed extraction tailing.

This effect is not only of scientific interest to have an insight into the plutonium behaviour in its extraction process but also of technical importance for managing the nuclear waste today. For these reasons, we have undertaken experiments to explain whether the tailing effect exists really and, if so, what can be the major reasons for such an effect. The present study is, therefore, confined to pure plutonium solutions without including nuclear fuel components, such as, actinides, fission products and other component elements. The main objective is to comprehend the tailing effect, at first, in non-technical systems.

2 Experimental

Two different plutonium charges are used: ^{239}Pu-charge (0.044 % ^{238}Pu, 90.405 % ^{239}Pu, 8.871 % ^{240}Pu, 0.568 % ^{241}Pu, 0.112 % ^{242}Pu) and ^{238}Pu-charge (94.84 % ^{238}Pu, 4.89 % ^{239}Pu, 0.241 % ^{240}Pu, 0.024 % ^{241}Pu, 0.004 % ^{242}Pu. The starting Pu solution (^{238}Pu and ^{239}Pu) is prepared by extracting Pu(IV) in 5 M HNO_3 into 30 % TBP-dodecane, back-extracting into 1 M HNO_3 and adjusting to 5 M HNO_3 by addition of conc. HNO_3. The absorption spectrum of this solution verifies the pure Pu(IV) ion. This solution is used as a starting solution for the major part of experiment. Another ^{238}Pu solution is prepared by dissolving the Pu(IV) hydroxide precipitate in 5 M HNO_3. The spectroscopic analysis shows that this solution contains ca. 4 % Pu(VI) and 96 % Pu(IV). For extraction experiments, analytical grade HNO_3, dodecane and TBP are used and TBP is further purified by an alkaline-treatment in order to separate the HDBP impurity. 30 % TBP-dodecane is used for all experiments throughout, except the first experiment with 20 % TBP (cf. Fig. 1). The phase separation is made by centrifugation at 40 000 g in order to ensure a clear separation. Activity measurements are made by liquid scintillation counting, α-spectrometry and low-energy gamma spectrometry. The speciation of Pu in solution is made by absorption spectroscopy for relatively high concentrations and laser-induced photoacoustic spectroscopy (LPAS) [5,6] for lower concentrations.

3 Results and discussion

3.1 Consecutive extractions from 5 M HNO_3

Starting from 1.16×10^{-3} mol/L ^{238}Pu(IV) in 5 M HNO_3, 6 stages consecutive extraction has been conducted and the results are shown in Fig. 1 (curve a). Distribution coefficients (DC) are scattering somewhat from one stage to another but remain constant at DC (Pu(IV)) = 8.7 ± 0.9 as

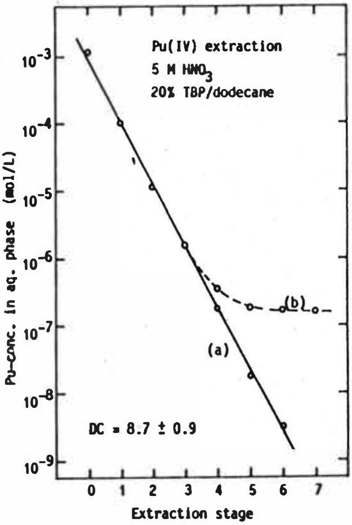

Fig. 1: Consecutive multi-stage extractions of the Pu(IV) ion in 5 M HNO_3 with 20 % TBP/dodecane: the Pu concentration in the aqueous solution as a function of the extraction stage. (a) and (b) belong to the solutions without and with Am contamination, respectively.

an average for 6 stages of extraction. No extraction tailing can be confirmed from this experiment for the Pu concentrations down to 10^{-9} mol/L. This observation does not corroborate the Lloyd's result, which demonstrates a decrease of DC from 12 to 0.9 in one experiment with 3 stages of extraction and from 17 to 0.2 in another experiment with 7 stages of extraction [4]. Both experimental results from Lloyd have shown clearly extraction tailings.

In another experiment, as shown in Fig. 1 (curve b), we have observed an extraction tailing, which starts from the 4th stage extraction and finally gives rise to DC ∼ 0.5. Measurements are at first based on liquid scintillation countings alone. A close examination of all solutions by low-energy gamma spectrometry demonstrates that there is a contamination of ^{241}Am during the experiment. The contaminated Am concentration is equivalent to 1.7×10^{-7} mol/L Pu in the solution, which amounts 0.005 % of the starting Pu concentration. Such an accidental contamination and the resulting consequence reflect that even a few ppm impurity can lead to the observation of a "pseudo" extraction tailing. Since the tailing may occur only in the lower Pu concentration range ($< 10^{-5}$ mol/L), any impurity effect in a given solution can be a reason for the appearence of extraction tailing. The impurity ions of chemical homology to Pu(IV), also Pu itself with oxidation states other than Pu(IV) and its realcolloids or pseudocolloids, all in microconcentrations, can be accountable for the tailing generation. To verify the possible existence of the Pu extraction tailing, experiments are further conducted in lower HNO_3 concentrations, in which impurity effects can be better distinguished.

3.2 Concentration dependent distribution coefficients

A number of batch extractions are carried out in two different HNO_3 concentrations (1 M and 2 M), while varying the Pu concentration in each acid medium. The results are given in Figs. 2 and 3. The DC values are decreasing with lowering the Pu concentration in both acid media, starting with the Pu concentration between 10^{-4} and 10^{-5} mol/L. From extractions carried out along with different aging times of the Pu solution, e.g. 1, 2, 3, 9 and 13 days (Fig. 2), no distinctive difference in DC values can be observed but they are all scattering within experimental fluctuations. However, the DC change at lower Pu concentrations ($< 10^{-5}$ mol/L) appears clearly evident. Efforts are further directed to search the underlying mechanisms that are responsible for such concentration dependent DC changes.

From the Pu(IV) solution of 1 M HNO_3 containing 1.26×10^{-4} mol/L Pu, consecutive extractions are performed and the remaining Pu in aqueous phase from each extraction stage is examined spectroscopically. Since the Pu concentration in the aqueous phase becomes lowered in each successive stage, we applied laser-induced photoacoustic spectroscopy (LPAS) [5,6], which has a speciation sensitivity about 10^3 times higher than attainable by normal absorption spectroscopy. The results of consecutive extractions are shown in Fig. 4. The Pu concentration in the aqueous phase decreases systematically, illustrating a constant DC value in 6 stages of extraction. An average DC value of 1.11 ± 0.04 is determined. At each stage, a portion of the aqueous solution is taken for spectroscopy. The two absorption band regions: 460 - 490 nm and 595 - 620 nm are chosen, because in the former area the absorption peak of the

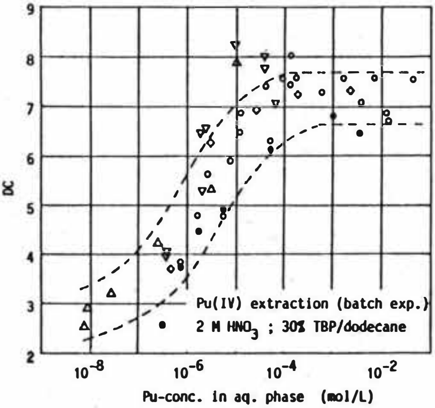

Fig. 2: Batch extractions of the Pu(IV) ion (^{238}Pu and ^{239}Pu) in 2 M HNO_3 with 30 % TBP/dodecane for different initial Pu concentrations. The distribution coefficient (DC) as a function of the equilibrium Pu concentration in the aqueous phase. Symbols: (○) for the freshly prepared Pu solution; (▽) after 1 d, (◇) after 3 d, (△) after 9 d and (●) after 13 d storage of the Pu solution.

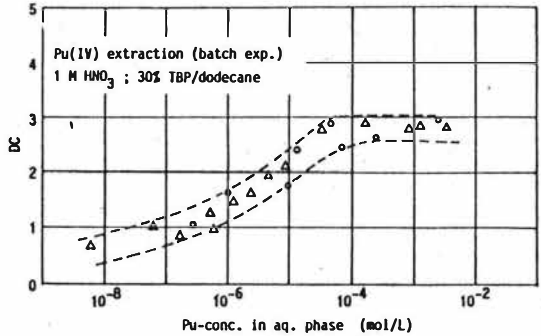

Fig. 3: Batch extractions of the Pu(IV) ion (^{238}Pu and ^{239}Pu) in 1 M HNO_3 with 30 % TBP/dodecane for different initial Pu concentrations. The distribution coefficient (DC) as a function of the equilibrium Pu concentration in the aqueous phase. Symbols: (△) for extraction and (○) for back-extraction.

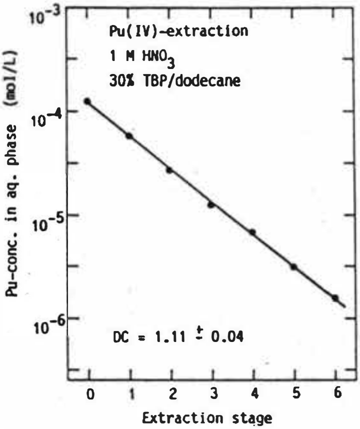

Fig. 4: Consecutive multi-stage extractions of the Pu(IV) ion in 1 M HNO_3 with 30 % TBP/dodecane: the Pu concentration in the aqueous solution as a function of the extraction stage (cf. Figs. 5 and 6).

Pu(IV) ion (476 nm) and in the latter area the absorption bands of the Pu(III) ion (605 nm) as well as the Pu(IV) polymer species (610 nm) can be detected [7]. In Fig. 5, the spectra of the Pu(IV) ion in the aqueous solution after 1st, 2nd, 5th and 6th stage extractions are shown. All spectra indicate the Pu(IV) ion and the concentration decrease appears systematical as the extraction stage progresses. Fig. 6 demonstrates the absorption charasteristics of the 1st and last stage aqueous solutions for the region where absorptions of the Pu(III) ion and Pu(IV) polymer species are expected. The spectra illustrate neither of these species being present in detectable amounts (> 10^{-7} mol/L). The extraction process shown in Fig. 4 is found to involve mainly the Pu(IV) ion. From these consecutive extractions, we cannot find any evidence that explains the DC decrease observed in batch extractions as shown in Figs. 2 and 3.

3.3 Spectroscopic investigation of the Pu solution in low acidity.

The Pu(IV) solution (1.26 x 10^{-4} mol/L) of 1 M HNO_3 is further diluted with H_2O to an acidity of 0.1 M HNO_3, in which the Pu concentration becomes 1.26 x 10^{-5} mol/L. After 2 and 5 days of storage, the spectroscopic investigation of the solution reveals that only a small amount of Pu appears as ionic species comprising Pu(III), Pu(IV) and Pu(VI) and the rest becomes colloidal species, which can be detectable spectroscopically by an overlapping effect (610 nm) on the Pu(III) absorption (605 nm). Fig. 7 shows the absorption peak of the Pu(IV) ion (spectrum b), whereas in Fig. 8 one of the twin peaks of the Pu(III) ion at 605 nm can be distinguished (spectrum a). At 5 days after preparation, the generation of the Pu(IV) polymer species can be detected (peak shift from 605 nm to 610 nm and peak broadening: spectrum b). By acidification of the solution to 3 M HNO_3, it is observed that the Pu(IV) peak at 476 nm increases due to the dissolution of the colloidal species present in the solution (Fig. 7: spectrum a). At the same time, the absorption bands of

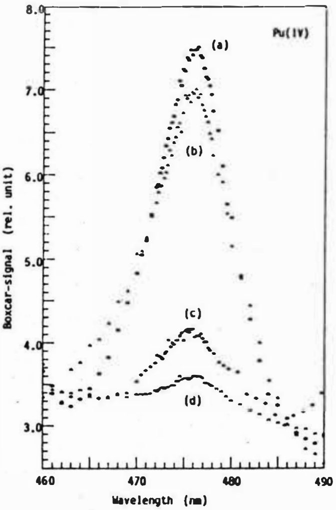

Fig. 5: Absorption spectra of the Pu(IV) ion taken by the LPAS [5,6] for the aqueous solution (1 M HNO_3) after consecutive multi-stage extractions as shown in Fig. 4: (a) after 1st stage, (b) after 2nd stage, (c) after 5th stage and (d) after 6th stage of extraction.

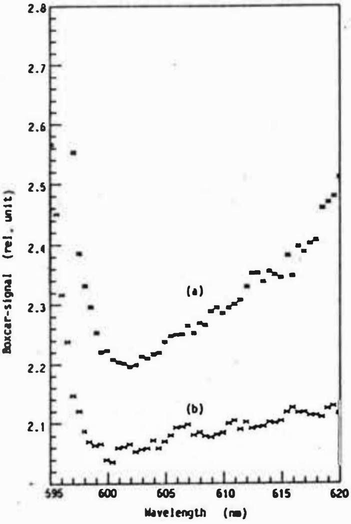

Fig. 6: Absorption spectra taken by the LPAS [5,6] for the aqueous solution (1 M HNO_3) after consecutive multi-stage extractions as shown in Fig. 4 in the region where the absorption bands of the Pu(III) ion (605 nm) and Pu(IV) polymers (610 nm) [7] are expected. These species are not detectable.

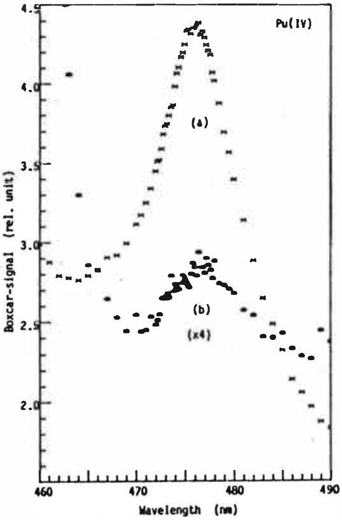

Fig. 7: Absorption spectra of the Pu(IV) ion (1.16×10^{-5} mol/L) in 0.1 M HNO_3 (spectrum b) taken by the LPAS [5,6] after dilution from 5 M HNO_3 and in 3 M HNO_3 after acidification with conc. HNO_3 (spectrum a: Pu-conc. = 1×10^{-5} mol/L).

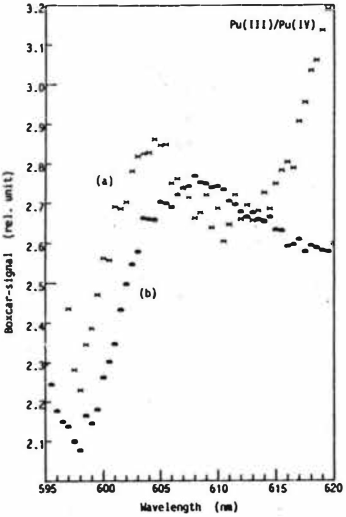

Fig. 8: Absorption spectra of the Pu(III) ion (spectrum a: 605 nm) and a mixture of the Pu(III) ion and Pu(IV) polymers (610 nm) (spectrum b) taken by the LPAS [5,6] at 2 d and 5 d after the solution preparation (0.1 M HNO_3).

the Pu(III) ion and Pu(IV) polymer species (Fig. 8: spectra a and b) disappear, suggesting that the former oxidizes and the latter dissolves. The experimental results indicate that the effects of redox reaction or disproportionation reaction of Pu(IV) or its polymerization in a given extraction process can only be significant in lower HNO_3 concentrations (< 1 M) and shall not be the major disturbing factor that may cause an extraction tailing in higher HNO_3 concentrations (> 1 M).

3.4 Conclusions

The Pu extraction tailing as observed by Lloyd [4] can not be verified by consecutive multi-stage extractions in pure HNO_3 systems (> 1 M HNO_3). However, in batch extractions, we observed the DC decrease at lower Pu concentrations (< 10^{-5} mol/L). The main difference between the batch extraction and the consecutive extraction is, first of all, the Pu concentration in each experiment: in the former, diluted Pu concentrations are introduced at the beginning, while, in the latter, the Pu concentration is diluted at consecutive extraction stages. Therefore, the surrounding condition for the dilution of the Pu concentration in the two systems may differ considerably. In a given solution system composed of multicomponents, micro concentrations of impurities are always present and their chemical influences on very diluted Pu concentrations (< 10^{-5} mol/L) can always be expected. This might be the reason why the microchemical behaviour of Pu is not often reproducible in different laboratories. Experiments are still in progress for the explanation of the DC decrease in batch extractions in lower Pu concentrations (cf. Figs. 2 and 3).

References

1. W. Ochsenfeld, H. Schmieder and S. Theiss, Report KfK 911 (EUR 4167d) (1970).
2. F. Baumgärtner, Kerntechnik, 6, 245 (1976).
3. W. Ochsenfeld, F. Baumgärtner, U. Bauer, H.J. Bleyl, D. Ertel and G. Koch, Report KfK 2558 (1977).
4. M.H. Lloyd, in Proc. Am. Nucl. Soc. National Topical Meeting: The Plutonium Fuel Cycle, May 2-4, Bal Harbour, Florida (1977).
5. R. Stumpe, J.I. Kim, W. Schrepp and H. Walther, Appl. Phys. B 34, 203 (1984).
6. R. Stumpe and J.I. Kim, Report RCM-02084 (1984).
7. D.A. Costanzo, B.E. Biggers and J.T. Bell, Inorg. Nucl. Chem., 35, 609 (1973).

Non Reductive Partitioning of Uranium and Plutonium in the PUREX Process

D. O. Campbell (Oak Ridge National Laboratory, Oak Ridge, Tennessee, 37831, USA)

A. L. Mills (AERE, Harwell, Oxon OX11 ORA, England)

Introduction

Irradiated nuclear fuel from power reactors is reprocessed on an industrial scale in order to recover the fertile uranium and fissile plutonium for re-use in the nuclear fuel cycle.

Virtually all the reprocessing schemes in use world-wide today are based on the PUREX process, that is, a liquid-liquid extraction process using tri-n-butyl-phosphate in an inert organic diluent as the extractant. In addition to separating uranium and plutonium from each other, it is necessary to separate them both from the fission products and higher actinides that are present in irradiated nuclear fuel. Thus a third 'product' of the PUREX process is the various fission product waste streams. These may require further treatment subject to requirements for the storage or disposal of such streams.

The percentage of plutonium with respect to uranium in irradiated nuclear fuels varies from about 1% for light water reactor fuels to about 20% for fast reactor fuels.

Product specifications for plutonium and uranium from the PUREX process vary widely but 1E-05 gm Pu/gm U and 1E-02 gm U/gm Pu are illustrative of likely specifications. (In this paper it is assumed that the specification with respect to fission products and the higher actinides is achieved.)

For some purposes the Pu in U and U in Pu levels might be more restrictive than the examples quoted above, but accepting the figures quoted then a separation of uranium from plutonium and plutonium from uranium of about 1E03 and 1E05 is implied.

Uranium-Plutonium Separation Techniques

There are two main techniques used for separating or partitioning plutonium and uranium from each other by liquid-liquid extraction. The technique selected depends to some extent on the liquid-liquid extraction equipment to be used - some partition schemes are kinetically controlled thus a short residence time contactor might be inappropriate to a given scheme. Some schemes employ chemical reagents that could pose subsequent waste management problems, whilst other schemes could have process control implications.

Noting these comments, for thermal reactor fuels the partition is usually accomplished by reducing the plutonium to the (essentially) non extractable trivalent state whilst leaving the uranium in the extractable hexavalent state.

Ferrous ion, hydroxylamine, U(IV) and other reductants are used. Because of possible reoxidation of Pu(III) to Pu(IV) by nitrous acid a nitrite destroyer such as sulphamate or hydrazine is also used in the partition.

With fast reactor fuels where the plutonium content is much greater than in thermal reactor fuels a reduction process is often of limited use due to the quantity of reductant required. An alternative partitioning technique is to preferentially complex say the plutonium to an inextractable form leaving the uranium uncomplexed. This can be achieved with sulphuric acid.

A non 'chemical' technique that appears to be applicable to both thermal and fast reactor fuel reprocessing is electrolytic reduction of Pu(IV) to Pu(III) in situ in a special liquid-liquid contactor.

Whichever technique is used and accepting any implications on equipment design or waste handling the objective for any partitioning method must be to obtain conditions such that the separation factor β ($\beta = K_{d(U)}/K_{d(Pu)}$, where $K_{d(U)}$ is the partition coefficient for U etc.) is as large as possible. This will enable the partition to be accomplished in an acceptable number of stages in the reprocessing plant.

In considering the relationship between β and the number of stages required for partition, the required levels of U in Pu and Pu in U should not be overlooked. If the plutonium product is to be converted to oxide for use in mixed oxide fuels then a fraction of a percent of uranium in the product is probably of no consequence. However if the uranium product is for re-enrichment or for conversion in a 'hands on' plant, very low levels of plutonium in this product will be required. The possibility of adjusting the partition process to bias one product against the other is generally desirable.

The Partition Flowsheet

Figure 1 shows a typical partition contactor flow diagram, a mixer settler contactor has been shown but other contactors may be substituted.

The diagram shows a compound contactor having both a plutonium strip section and a uranium backscrub section. The uranium and plutonium are introduced into the centre of the contactor in the organic phase and the partition reagent is fed into one end of the contactor in the aqueous phase. Plutonium is stripped from the organic phase in this section of the contactor say as the reduced Pu(III) or as an inextractable complex. Some uranium is inevitably stripped into the aqueous phase and this is scrubbed out, back into the organic phase, in the scrub section of the contactor.

In addition to the values of $K_{d(U)}$ and $K_{d(Pu)}$ the flowsheet designer can also manipulate the solvent-aqueous flow ratios in the contactor and the relative number of stages used for the plutonium strip and uranium backscrub to optimise the process. The use of reductants and complexants to effect the partition have already been noted. A further alternative is to carry out the partition with the use of nitric acid alone. This can be done in the same process layout as in Figure 1 where the partition reagent is nitric acid only.

U-Pu Partitioning by Nitric Acid

It has been noticed that the distribution coefficients for Pu(IV) and U(VI) between aqueous nitric acid and TBP-diluent vary with such parameters as: aqueous metal and nitric acid concentration, temperature, TBP concentration, organic phase solute concentration, organic diluent composition etc.

There is a paucity of distribution data for U(VI) and Pu(IV) for the conditions of interest here but recently obtained data in the United Kingdom and in the United States (unpublished) demonstrate that with the appropriate choice of conditions a practical flowsheet for partition is possible without the use of reductants. The following general observations may be made:

- the distribution coefficients for Pu(IV) and U(VI) vary in opposite directions as a direct function of temperature,
- as T decreases $K_{d(Pu)}$ decreases and $K_{d(U)}$ increases,
- as the TBP concentration in the organic phase decreases, then at a given aqueous acidity $K_{d(Pu)}$ and $K_{d(U)}$ decrease but at different rates.

Given the distribution coefficients determined from laboratory measurements, calculations have been made using both the SEPHIS (US) and QUANTEX (UK) codes which indicate that in theory a practical flowsheet is possible.

The sensitivity of the process to parameters such as input flowrates and concentrations has been examined theoretically and it was found that although the process might not be as easy to control as the more traditional partition processes, by controlling both solvent feeds simultaneously to give a constant flow in the partition section of the contactor, control could be readily achieved.

One aspect of the solvent extraction of plutonium that should not be overlooked and might be of particular consequence in the nitric acid partition is the retention in the organic phase of plutonium by ligands formed as a result of extractant or diluent degradation. Given such circumstances it is unlikely that nitric acid alone will remove all the plutonium from the organic phase. Some reductant in the nitric acid partitioning feed might therefore be unavoidable. However the quantity of reductant required should be small and any kinetic problems should be trivial.

A partition process using minimal amounts of reductant could be particularly useful in fast reactor fuel reprocessing.

Summary of Theoretical Work

The assessment of control problems has been referred to above. Further calculations have been made using SEPHIS to investigate the effects of temperature and TBP concentration on hypothetical flowsheets. A typical Fast Breeder Reactor fuel reprocessing flowsheet has been assumed, the fuel having a high Pu/U ratio. The UK and US experimental distribution coefficient data have been taken into account but the calculations which are somewhat inexact at this time because the distribution coefficient algorithms have not yet been fully optimised to fit the experimental data. Nonetheless it is believed that the results of the present calculation are reasonably correct and indicate trends quite well.

In commercial nuclear fuel reprocessing it is usual to employ a TBP concentration between about 0.7 and 1.0 M. Experimental data show that the separation factor β increases as the TBP concentration decreases. The relationship between β and TBP concentration has not yet been fully determined. Also β increases as the operating temperature decreases.

Changes in TBP concentration and/or operating temperature have implications for plant and process design. Lower TBP concentrations result in higher organic phase volumetric throughputs, lower operating temperatures may change process liquor physical properties adversely. A combination of both may result in plutonium third phase formation.

A further variable studied was the influence of the aqueous phase nitric acid concentration on β. Lower acidities favour a high β value but low nitric acid concentrations tend to enhance the possibility of plutonium polymer formation. This is mitigated by low temperature operation but insufficient data are presently available for 'rules' to be formulated.

It can be seen that there are a large number of variables to be considered, their interdependances have not yet been fully ascertained. Both the theoretical and experimental work to date (see below) indicate the feasibility of the process but the question of whether to 'bias' the process to give a very low Pu in U level at the expense of U in the Pu product, or whether to remove the residual Pu from the U product by reduction has yet to be resolved.

The calculations (using SEPHIS) have been used to ascertain the best combination of conditions to give an approximately linear 'trade off' of U in Pu and Pu in U (Figure 2). The lines with a slope of 135°, represent for a given temperature, concentration of Pu product and TBP concentration approximately the best products available given the correct choice of feed stage and organic U backscrub flow. The calculations indicate the very wide range of product purities (about a factor of 1000) that can be achieved by varying the operating conditions over a given range of values. For say a product specification of 1% U in the Pu product, the calculations indicate a Pu contamination of the U product of from 0.01 to 5 ppm, changing the feed plate position will increase the Pu in U for approximately the same U in Pu value. An improvement in the Pu in U levels may be possible by decreasing the process temperature, TBP concentration or product concentration.

Experimental Work

Some essentially ad hoc trials of the acid partition carried out in miniature mixer settlers in the UK demonstrated the possibility of the process. It was this early work that led to the subsequent more detailed study reported above and the experimental work performed at ORNL of which the following is illustrative.

Figure 3 shows the (ORNL) flowsheet used.

Figure 4 presents one set of concentration profiles for U, Pu and acid as determined experimentally using the flowsheet in Figure 3.

The TBP concentration was 10% TBP and the operating temperature about 15°C. After flowrate adjustments the U content of the Pu product was approximately 1.7% and the Pu content of the U product was about 100 ppm. This level of Pu in U is too high for most purposes, further optimisation of the process as indicated by the theoretical work might decrease this level but it is not clear that say < 1 ppm Pu in U can be obtained without the use of some reductant. (Solvent degradation effects might require the use of some reductant.)

It should be noted however that > 99% of the total Pu was obtained in the Pu product stream without the use of reductant.

Conclusion

The theoretical work which is generally supported by (as yet uncompleted) small scale experimental trials indicate that the 'acid split' approach to U-Pu partitioning offers the possibility of a partitioning system with no chemical additions. At the least it appears to offer, even for the most stringent product specifications, a partitioning technique requiring small amounts of reductant rather than the gross amounts used in present flowsheets.

Acknowledgement

The authors would like to acknowledge the work done by colleagues at ORNL and at Harwell and Dounreay in determining some of the distribution data and for carrying out the experimental solvent extraction trials.

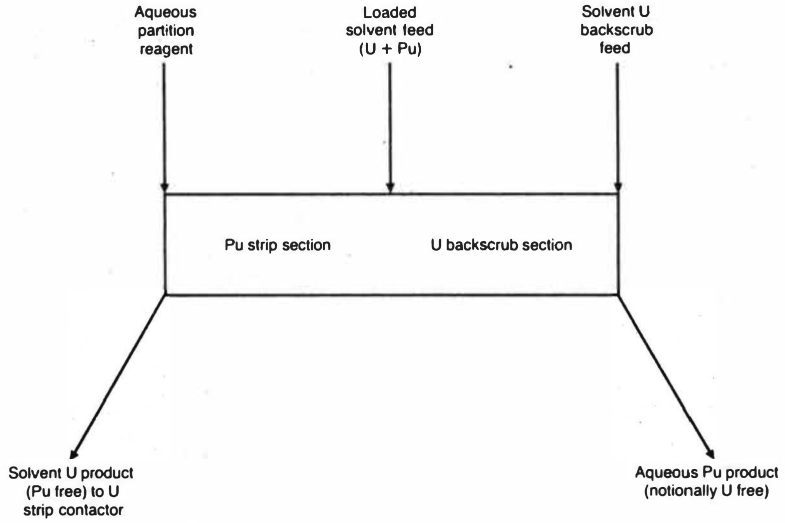
Aqueous partition reagent
Loaded solvent feed (U + Pu)
Solvent U backscrub feed
Pu strip section
U backscrub section
Solvent U product (Pu free) to U strip contactor
Aqueous Pu product (notionally U free)

Figure 1. The partition contractor, flow diagram

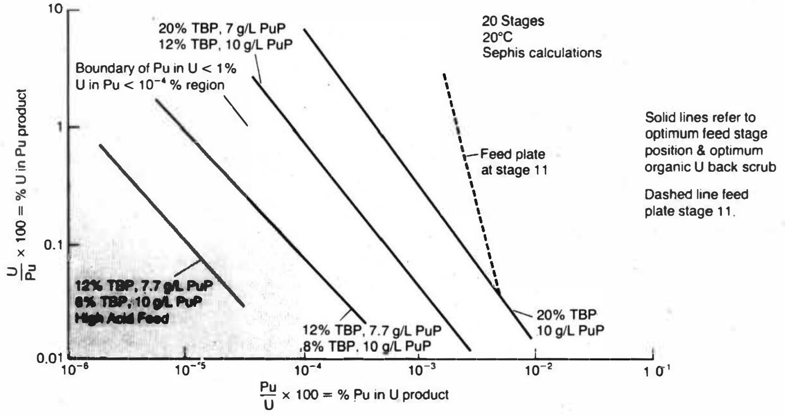

Figure 2. Effect of % TBP and Pu product (PuP) concentration on Pu in U product and U in Pu product

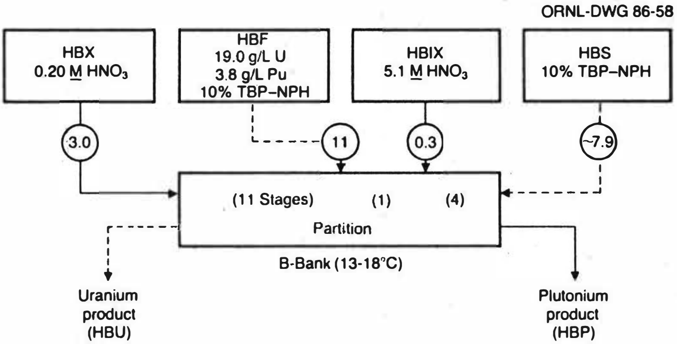
ORNL-DWG 86-58
HBX
0.20 M HNO3
HBF
19.0 g/L U
3.8 g/L Pu
10% TBP–NPH
HBIX
5.1 M HNO3
HBS
10% TBP–NPH
3.0
11
0.3
~7.9
(11 Stages)
(1)
(4)
Partition
B-Bank (13-18°C)
Uranium
product
(HBU)
Plutonium
product
(HBP)

Figure 3. Illustrative acid-split flowsheet at ORNL

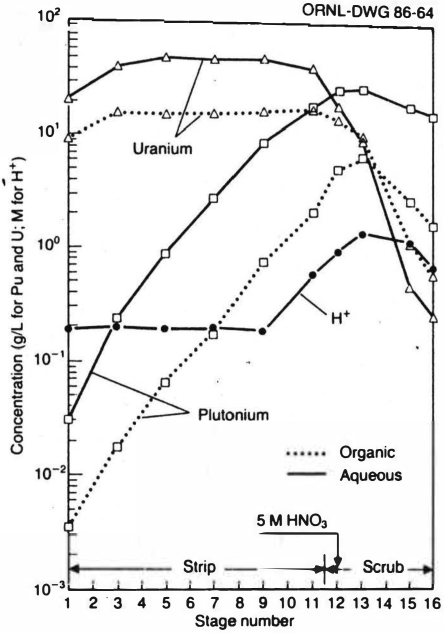

Figure 4. Observed concentration profile for uranium, plutonium, and nitric acid in partition contactor for flowsheet of Fig. 3.

Demonstration of the Electrochemical Reduction of Pu(IV) in the Purex-Process in the Absence of Hydrazine

M. Heilgeist, K. Flory, U. Galla, H. Schmieder
Kernforschungszentrum Karlsruhe, FRG

Separation of plutonium (Pu) from uranium (U) in the Purex process for spent nuclear fuel is normally carried out by reduction of Pu(IV) to the Pu(III) valency. By this way the Pu, which is well soluble as Pu(IV) together with U(VI) in an organic 30 % Tributylphosphate (TBP)/Dodecane solvent, but almost insoluble as Pu(III), passes over to the aqueous, nitric acid containing phase in a counter current extractor. The reducing agents commonly used are Fe(II), U(IV), hydroxylammoniumnitrate (HAN) or, the most modern one, the electron, by way of electrodes.
Common practice for all reducing agents is the necessity to add a nitrite scavenger to the solution, for example hydrazine, to stabilize the trivalent Pu against re-oxidation by nitrous acid, which is usually present in 1 M nitric acid solutions. This scavenging of nitrous acid is very important, as the HNO_2 else acts in an autocatalytic way upon Pu(III) by means of the solvent, nitric acid:

$$2\ Pu^{3+} + 2\ HNO_2 + HNO_3 + H^+ = 2\ Pu^{4+} + 3\ HNO_2 + H_2O \qquad (1)$$

According to pH/potential-diagrams (fig.1) nitrous acid loses its oxidizing capabilities and furthermore acts as a reducing agent relative to Pu(IV), if the pH of the solution is raised.

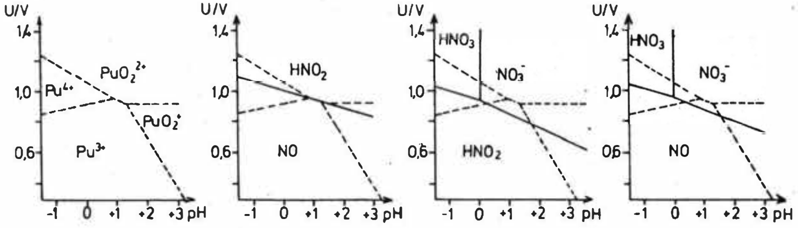

fig.1 Pourbaix-diagrams for Plutonium and $NO/HNO_2/HNO_3$

Taking as reference the pH-dependent values for the formal potential of Pu(III)/Pu(IV) according to (1) one can see that the reducing effect of HNO_2 on Pu(IV) will start at an acid concentration equal to or less 0.5 M nitric acid:

$$2\ Pu^{4+} + HNO_2 + H_2O = 2\ Pu^{3+} + NO_3^- + 3\ H^+ \qquad (2)$$

Consequently HNO_2, or NO, which is in equilibrium with HNO_2, were used successfully as a reducing means for the backextraction of Pu^{4+} in the purification cycle (2,3,4). As the redox-behaviour of the system Pu/HNO_2 is not only pH-dependent but also dependent on the concentration of the counteracting substances there are some difficulties to overcome. On the one hand, high concentrations of HNO_2, about 0.01 to 0.1 M, are required and on the other hand, low nitric acid concentrations, down to 0.1 M, in order to insure a sufficiently fast reduction.
As HNO_2 is extracted easily into the organic phase (distribution coefficient (org/aq.) for HNO_2 = 10) it expells U(VI) from the organic phase, thus lowering the U/Pu seperation efficiency. This means that the process is not suitable for the first cycle. Other disadvantages of HNO_2 as a reducing agent are its inability to reduce U(VI) and the fact that in the organic phase it still has an oxidizing effect upon Pu(III), even with low acid concentrations (5,6).

Taking into account all arguments in favour of HNO_2, it almost lies at hand that working in the low acid region, thus avoiding the oxidizing effects of HNO_2, and using a suitable reducing means like the electrochemical one, would be a proper way for the Pu(III)-valence adjustment und for the U/Pu-separation.

Experimental Results

1. Laboratory Scale

Experimental set up and procedure:
The experiments in the laboratory scale were all run without the influence of the organic phase. The experimental setup was a simple electrolytic cell without diaphragm (fig.2): Cathode and case: Titanium, A = 90 cm^2 / anode: platinum, A = 3.7 cm^2 / electrolyte volume: 90 cm^3.

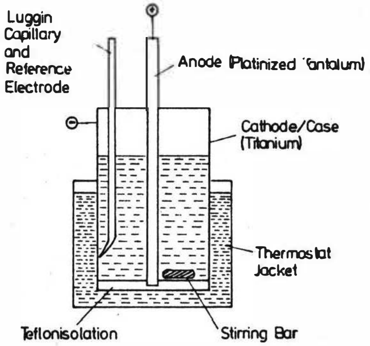
Luggin Capillary and Reference Electrode
Anode (Platinized Tantalum)
Cathode/Case (Titanium)
Thermostat Jacket
Teflonisolation
Stirring Bar

Fig.2: experimental setup

The cell design was fitted to the parameters of an electrolytic pulse column where the possibly successfull experiments were to be run in a counter current process. The experiments were run at constant current and the potential of the titanium cathode was measured versus the Standard Calomel Elecrode (SCE).
The experiments were run batchwise. The cell was filled with the Pu-containing nitric acid solution and after switching on the current, concentrations of the different Pu and U valencies were determined by their typical absorption spectra with a spectrophotometer (7).

1.1 Dependence of the electrochemical Pu^{4+}-reduction on the nitric acid concentration

Experimental parameters:
Electrolyte: 5 g/l Pu(IV), 20 g/l U(VI), 0.1 to 0.5 M HNO_3 /
cathodic current density: 1 mA/cm^2 / Temperature: 30 °C

As fig.3a shows, Pu(III) build-up takes place during electrolysis. Depending on the concentration of nitric acid, there are three different types of redox behaviour. Reoxidation before reaching 100 % Pu(III) as in the case of 0.5 M HNO_3. Reoxidation just after reaching 100 % Pu(III) as for 0.4 M HNO_3. Build-up of 100 % Pu(III) and its stability until the end of the experiment (0.1 to 0.3 M HNO_3). The comparison between the Pu(III) course and the build-up of nitrous acid (fig.3b) and U(IV) (fig.3c) in the same solution explains the reoxidation behavior of Pu(III): The nitrite concentration goes down and the U(IV)-concentration goes up when the acid concentration is lowered. The dependence of the nitrite build-up on the acid concentration can be explained by the diminishing current efficiency of the direct electrochemical nitric acid reduction and by the Pu(IV)/HNO_2-reaction at low acidities. As to the course of U(IV) the following explanation could be given: The onset of a measurable amount of U(VI)-reduction is only to be seen on completion of the Pu(IV) reduction. As long as the nitrous acid concentration does not exceed 2.10^{-3} M, the reoxidation of U(IV) and Pu(III) does not occur.

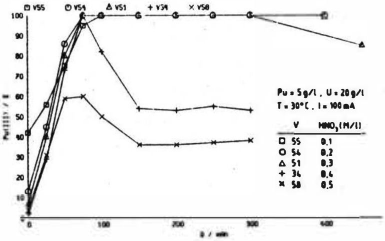

fig.3a: Influence of nitric acid concentration

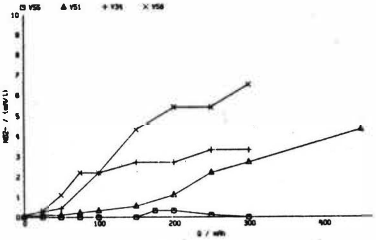

fig.3b: Course of nitrous acid (legend s. fig.3a)

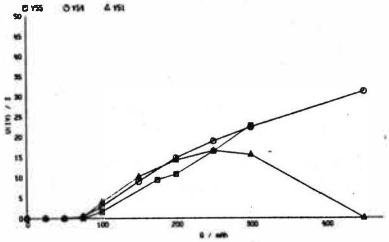

fig.3c: Course of Uranium(IV) (legend s. fig.3a)

1.2 Dependence of the electrochemical Pu^{4+}-reduction on the cathodic current density

Experimental parameters:
Electrolyte: 5 g/l Pu(IV), 20 g/l U(VI), 0.7 M HNO_3 /
cathodic current density: 0.5 to 5 mA/cm^2 / Temperature: 20 °C

The experiments in 0.7 M HNO_3 (fig.4). have been chosen to illustrate the influence of the current density.
There must be a minimum cathodic current density of 2 mA/cm^2 to have a 100 % reduction of Pu(IV). Parallel to the effect of potential change with current density, the higher current flow per time unit makes the Pu(IV) reduction without hydrazine possible, even at higher nitric acid concentrations.

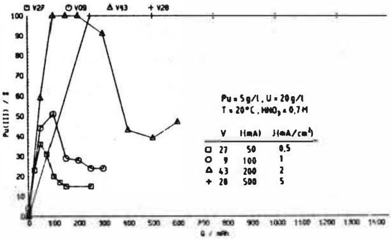

fig.4 Influence of current density

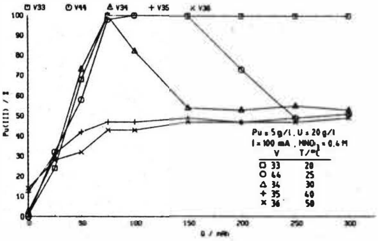

fig.5 Influence of temperature

1.3 Dependence of the electrochemical Pu^{4+}-reduction on the temperature

Experimental parameters:
Electrolyte: 5 g/l Pu(IV), 20 g/l U(VI), 0.4 M HNO_3 /
cathodic current density: 1 mA/cm^2 / Temperature: 20 °C to 50 °C

The course of Pu(III) is to be seen in fig.5. The temperature turns out to be a very important factor. Under the given experimental conditions, one gets a 100 % reduction of Pu(IV) at temperatures up to 30 °C, whereas the U(IV) build-up only occurs at 20 °C and 25 °C. As the electrochemical reduction itself is not very sensitive to a temperature rise, the HNO_2/Pu(III) reaction seems to predominate over the electrochemical Pu(IV) reduction at higher temperatures.

1.4 Influence of the U/Pu ratio on the electrochemical reduction of Pu without hydrazine

Experimental parameters:
Electrolyte: 1.) U/Pu = 4:1: 5 g/l Pu(IV), 20 g/l U(VI), 0.3 M HNO_3 /
2.) U/Pu = 344 : 1: 58.1 mg/l Pu(IV), 20 g/l U(VI), 0.3 M HNO_3 /
T = 40 °C / cathodic current density = 1 mA/cm^2.

Fig.6 shows the different reduction efficiencies. In spite of the rather high temperature at which, with the normally used Pu(IV) concentration, a 100 % Pu(III) production could not be achieved, the changed U/Pu ratio now makes it possible to have the Pu(IV) reduced completely. A reason of this different behaviour seems to be the current-to-Pu ratio (Ampere/Mol) which was raised at the same time by factor 86 by reducing the Pu concentration and keeping the U concentration constant. Thus the U(IV) production increases as the reoxidizing effect decreases with the lower Pu concentration.

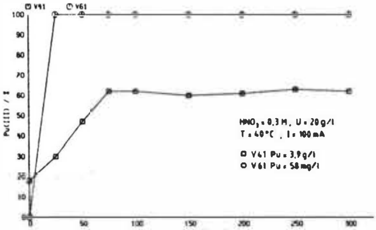

fig.6 Influence of U/Pu ratio

1.5 Influence of very low concentrations of hydrazine on the electrochemical reduction of Pu

Experimental parameters:
Electrolyte: 5 g/l Pu(IV), 20 g/l U(VI), j = 1 mA/cm^2.

The influence of very low concentrations of hydrazine was checked for those nitric acid concentration and temperature ranges where it was difficult to achieve or to maintain a 100 % Pu(III) build-up. The different runs are listed in table 1.

A comparison of the runs with and without addition of hydrazine shows that hydrazine has a striking effect on the Pu(III) reduction efficiency even at very low concentrations (fig.7). In all runs (table 1) a 100 % Pu(III) production with strong build-up of about 30 % U(IV) was observed.

Run	HNO_3 M	$N_2H_5NO_3$ M	T °C
14	0,5	10^{-4}	20
45	0,4	10^{-3}	30
46	0,5	10^{-3}	30
56	0,4	10^{-4}	30
47	0,4	10^{-3}	40

table 1: Experiments with very low hydrazine concentrations

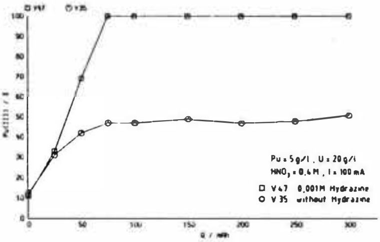

fig.7: Influence of hydrazine

One would expect that the hydrazine is oxidized at the anode within 1 to 10 minutes, the faradaic value for the anodic hydrazine oxidation being 107.2 Ah/mol.

As the reoxidation does not occur during the electrolysis, one must assume, that

1. the current efficiency for the oxidation of hydrazine at such a low concentration is much lower than 100 %
2. this small amount of hydrazine is sufficient, to suppress the autocatalytic reaction of Pu(III) with HNO_2
3. parallel to the anodic water oxidation, Pu(III) is oxidized at the anode faster than hydrazine ($c_{Pu(III)}/c_{Hy}$ = 20 : 1 bis 200 : 1)
4. the content of U(IV) in the solution ensures a fast Pu(IV)-reduction
5. cathodic formation of HNO_2 ist suppressed under these conditions

2. Technical Scale

On the basis of the promising results of the aqueous laboratory experiments, the aim of using a reductive separation process without hydrazine was transferred to the 2-phase counter current process in a pulse column (8). The column was run under continuously aqueous conditions. Organic feed solution: 30 % TBP/dodecane, U ca. 95 g/l, Pu ca. 1 g/l, HNO_3 ca. 0.1 M / Q ca. 24.5 l/h. Aqueous solution: HNO_3 ca. 0.1 M / I = 31 - 44 Amp. / T ca. 30 °C.

The total flowrate was about 1/4 of the flooding flow of the column. During the runs, the hydrazine concentration was reduced successively from 0.1 M to zero in the aqueous strip solution (table 2). The values of the Pu-concentration of the organic solvent leaving the extractor (U-product) were between 0.5 to 3.2 mg/l, whether hydrazine was contained or not contained in the BX-stream. The concentration of nitric acid in the aqueous phase in the pulse column was between 0.25 and 0.45 M HNO_3. The results show that it is possible to run the U/Pu-separation process without hydrazine if the most important conditions like HNO_3 and temperature are kept within the process limits.

run	$(N_2H_5^+)$ aqu. M	flow ratio org/aqu	(Pu) org. mg/l	separation effect Pu_{in}/Pu_{out}
1	0.1	4	2.0	363
2	0.04	4	2.6	288
3	0.02	4	2.2	314
4	0.008	4	2.5	320
5	0.002	4	3.0	267
6	0.0	4	2.0	350
7	0.002	2.4	0.8	1300
8	0.0	2.4	0.5	2083
9	0.1	6	3.0	195
10	0.0	6	3.2	219

table 2: Influence of hydrazine on the organic Pu-concentration and the separation efficiency

Conclusions:

On the basis of the laboratory experiments with aqueous solutions and the runs in the pulse column with the organic and aqueous system, it is demonstrated that the U/Pu separation in the Purex-process can be run without hydrazine by using the electrochemical Pu reduction in the low nitric acid region.
The advantage of such a process would be

1. no production of hydrazoic acid which is created by the reaction of hydrazine with HNO_2

2. no production of ammonia which is created by the direct reduction of Pu(IV) by hydrazine (9)
3. avoiding of handling with cancerogene hydrazine
4. no need to take care of a special reoxidation step of hydrazine and Pu(III) because Pu(III) is reoxidized in an unstabilized solution by simply raising the concentration of nitric acid.

The only disadvantage is the necessity to keep the nitric acid concentration and the temperature below the limit values. This means, that constant pumping rates are needed in order to ensure constant org./aqu. flow ratios.

1. P.I. Artiukhin, A.D. Gel'man, V.I. Medvedovskii, Doklady AN, SSSR 120 (1958) 269
2. A. Bathellier, Conf. "Solvent Extraction Chemistry of Metals", Harwell, 27. - 30. Sept. 1965
3. T. Tsujino, T. Aochi, J. Nucl. Sci.Techn. 13 (1976) 321
4. E.D. Collins, D.E. Benker, J.E. Bigelow, F.R. Chattin, L.J. King, M.H. Lloyd, R.G. Ross, R.G. STacy, H.C. Savage, TANSAO, 40 (1982) 120
5. P. Biddle, H.A.C. McCay, J.H. Miles, Conf. "Solvent Extraction Chemistry of Metals", Harwell, 27. - 30. Sept. 1965
6. V.V. Revyakin, V.I. Marchenko, E.S. Gitkovich, N.A. Korableva, V.P. Varykhanov, Radiokhimiya, 25 (1983) 317
7. H. Schmieder, E. Kuhn, W. Ochsenfeld, KfK-report 1306 (1970)
8. U. Galla, H. Schmieder, KfK-Nachrichten 2 (1986)
9. M. Heilgeist, KfK-report 3517 (1983)

Investigations Concerning Lay-out of Industrial Extraction Columns for the PUREX-Process: Influence of mixing Effects on Mass Transfer Parameters

K. Eiben; K.Haberland; Wiederaufarbeitungsanlage Karlsruhe Betriebsgesellschaft mbH, Leopoldshafen, West Germany

P.Feucht; A.Merz; R.Walter, Kernforschungszentrum Karlsruhe GmbH, West Germany

I. Introduction

Mass transfer in pulse columns is influenced by axial and radial mixing effects which should be considered for the purpose of the design and layout of industrial extraction columms. The origin of insufficient mixing behavior may be related either to special physical properties of the involved liquid systems, certain geometrical as well as apparative needs of the layout or of operational conditions applied during the extraction procedure.

Earlier investigations for instance have shown this for a HA-pulse column designed and tested in industrial size for a PUREX-reprocessing plant /1,2/. During the course of scale up the extraction length was calculated according to the Logsdail-Thornton equation considering the axial but not radial mixing effects. It was shown that the insufficient radial mixing influenced mass transfer remarkably. The investigated HA-system included on the one side a high gradient of density ($\Delta\delta$ = o,5 g/cm) between the aqueous and organic phase.

On the other side it was demanded by operating conditions to disperse the smaller and aqueous phase (o:a= 2.3) which implied the introduction of nozzle instead of sieve plates to avoid wetting problems. It was found that the nozzle plates probably supported channelling effects over the entire active length of the column as well as the dispersion of the aqueous phase at the inlet of the column needed a special designed ringtyp distributor to avoid inhomogenous maldistribution over the cross section of the column. The radial mixing could be improved by introducing LOUVER plates or systematic packings at certain sections of the cartridge.

The investigations on dispersion and mixing phenomena have now been extended to the

BX-pulse column for the uranium-/plutonium separation and the
C-pulse column used for the backextraction of the uranium
from organic into aqueous phase.

The extraction columns with an internal diameter of 380 and 430 mm resp.are installed in an industrial testrig for extraction equipment. The test facility (TEKO) is operated by WAK under contract of DWK (Deutsche Gesellschaft für Wiederaufarbeitung von Kernbrennstoffen, Hannover) at the side of the Nuclear Resarch Centre at Karlsruhe.

II. Experimental set up

II. 1. C-Pulse column

The uranium which is bound as a complex to the tributylphosphate (30 Vol% in dodecane)is reextracted by means of an aqueous acid solution ($<0,05$ mol HNO_3) at a temperature of 60°C and implying a phase ratio a:o of one. The total throughput is approximatly 4,5 m^3/h. The extraction column is equipped with sieve plates mounted in a distance of 50 mm, providing a free area of 23 %. The feeding lines of the organic and aqueous phases are halfring shaped, each having three lanceolate pipes, radial entering the column between the first two sieve plates of the upper and lower catridge section. The pulsation is generated with a mechanical operated pulsator capable of setting the frequencies between 1 and 1,5 Hz. Amplitudes were adjusted to 10 and 15 mm. As can be seen from figure 2, eight sampling positions are available alongside the extraction column for taking concentration profiles of the aqueous and organic phases.

To realize the radionuclide-measurements szintallation-detectors are mounted on four levels on the outside of the columns (1-16), near the outlet- and inletpositions (17-22) and in the height of the interphase outside of the bottom decanter (23). The detectors were connected with a computer controlled data aquisition system /3/. The organic phase was tracered with approx. 5 ml of F-18-labeled hexafluorobenzene while approx. 5 ml of an acid In-113-solution was used to tracer the aqueous phase in separate experiments.

II.2. BX-pulse column

For separating the plutonium from uranium the loaded organic phase /BXF, 70-90 (gU/l); 1900 (l/h)/ is treated at room temperature with an aqueous acid solution /BXX; 100 (g UIV/l); 1 m HNO_3; 45 (l/h)/. plutonium-IV is reduced by means of the uranium IV to yield plutonium-III which is extracted into the aqueous phase (BXP).
The column tested was equipped with sieve plates, which are arranged in distances of 50 mm providing a free axial space of 32 %. The air-pulsator was set to a frequency of 1 Hz and an amplitude of 10 mm. The organic dispersed phase (BXF) entered the column radial by six lancolate pipes as discribed for the C-column. The aqueous hydrazine stabilized uranium-IV-solution (BXX) is devided in two side streams of 20 and 80% at the positions marked on figure 3. The scrub solution (BXS, 0,1 m/l HNO; 215 l/h) was added between the first two sieve plates. All aqueous solutions are distributed via single lances equipped with few 2 mm Ø holes. Because of the side streams the phase ratio o:a deviates from 7.3 to 8.8 over the length of the column.
All experiments are performed with uranium containing solutions. The concentration profile of both uranium-IV and the total uranium content was taken from 13 sampling positions (I-XIII). The arrangement of the 24 detectors for the radionuclide measurements are shown in figure 3. As specific tracer for the organic phase F-18 labeled hexafluorbenzene was injected at the organic feeding point.

III Results und Discussion

III. 1 C-Pulse column

Figure 1 shows the concentration/time functions of the tracered organic and aqueous phases measured at the marked locations of the detectors. The mean values of the statistical moments (μ_1*) and their standard deviation (σ*) are shown in fig.2 for the dispersed and the continous phases. The hold-up ($\bar{\varepsilon}$) was calculated for the sections between the detector levels. In addition the hold up was directly measured by taking a sample of the mixed phases in the upper section of the column. However at this position mass transfer has already occured. It can be deduced from the concentration profil for the organic and aqueous phases (fig. 2) that the mass transfer takes place in the lower section of the pulse column.

The mean coefficient of dispersion ($\overline{D}$) and the velocity of convection were calculated considering that the active length and the decanter contribute to the mass transfer in the column /4/. The calculated values are compiled in table 1.

The concentration/time function of the aqueous phase (fig. 1) compraises that distribution at the feeding point it not uniform. The signals of the detectors 14 and 16 show a delay in distribution and amount of activity compared to the positions 13 and 15. This delay is propagated into the lower section of the column, thus demonstrating that radial mixing is insufficient over a long distance, even in a system with a low gradient of density between the two phases and a balanced phase ratio (hold up). It also shows that sieve plates which, compared to nozzle plates, are assumed not to propagate channeling effects, seem not to improve radial mixing. However the insufficient radial mixing in the C-column seems not to influence the mass transfer sufficently. This is completed almost in the lower half of the column. With respect to the radial mixing it is concluded for the C-column that the distribution of the dispersed phase at the feeding point could be improved.

For the axial mixing the results at detector 23(fig.1) are instructive. Part of the organic continuous phase is forced downstream by the dispersed phase into the bottom decanter. The radioactive tracered organic phase gives rise to a concentration vs. time function at the interphase. The relatively long residence time of the organic phase in the settling zone can be related to an nearly ideal agitating vessel. It considerably contributes to the mass transfer, thus lowering remarkably the active length of the extraction column. This important effect of back mixing could even be increased by applying a higher amplitude. In this case partial or local hold-up increased as well and worked like a plug respectively to the phase velocities, increasing the intensity of axial mixing in this zone even further.

III. 2. BX-pulse column

Figure 4 shows the concentration vs. time functions for the organic disperserd phase in the BX-column. In case of complete mixing within a cross section, the tracer concentration vs. time plots should show identical signals in a given plane of measurement. The same holds true for the total number of pulses (I_{ges}) from each probe. However caused by the inhomogeneous radial distribution of the dispersed organic phase, different signal amplitudes appear, which are even shifted in time relative to each other.

The axial dispersion is superposed by channeling routes, which in turn can initiate displacement effects. These effects may influence the decontamination factors (DF) especially for the separation of plutonium.

Figure 3 represents on the one side the concentration profil for uranium in the organic phase in absence of plutonium, which was not used during the course of these experiments. On the other side the statistical moments ($\overset{*}{\mu}(1)$) and their standard deviations (σ^*) are displayed according to the positions of measurement. The hold up ($\bar{\epsilon}$) was calculated for the sections between the detectors. In comparison the measured hold up of two positions are added. The agreement is resonable between both the calculated and measured values.

The local hold up shows distinct deviations in the areas where the aqueous continous phases are added to the system. The increased range of deviation results from the inhomogeneous feeding.

Since the experiments of the BX-pulse column were conducted together with the four columns of the extraction cycle, feed backs of process deviations influenced the hydraulic stability of the BX-column, especially the aqueous phase with the small flow rate and the long residence time. The flow velocity of the aqueous continous phase was varied between 1 and 7 m/h. Thus the interpretation of the residence functions and coefficients of dispersion for the aqueous phase was not possible.

From these results it is concluded that single tests of a apparatus without disturbing influences of connected process lines may be of theoretical interest but need to be confirmed under realistical and improved conditions of interconnected plant operation. These experiments are planed for the future.

LITERATUR

/1/ A Merz, H. Zimmermann
Axial Convective Phasetransport and radial Mixing Effects in Pulsed Plate Columns
Proceed. Fuel Reprocessing and Waste Management
ISBN 0-89448-118-S; Jackson Wy/USA (1984) Vol I p 189-198

/2/ H. Zimmermann, K. Haberland, A. Merz, R. Walter
Untersuchungen an mit Düsenböden ausgerüsteten pulsierten Extraktionskolonnen im industriellen Maßstab einer WAA
Chem. Ing. Techn. 57 (1985) p 540

/3/ A. Merz, J.J. Porta, R. Walter
On the Modelling of the Twophase Flow in Solvent Extraction Columns; ISEC, Munich (1986), Poster Nr. 247

/4/ A. Merz, Radiotracertechnische Diagnose der Zweiphasenströmung in industriellen Extraktionsapparaten.
KfK-Bericht (in preparation)

Tabelle 1

					Results				
		A(mm)	f(min^{-1})	T (°C)	$\bar{V}$ (cm/s)	$\bar{D}$(cm^2/s)	$\bar{V}/\bar{D}$(m^{-1})	$\bar{\epsilon}$(%)	ϵ_{TEKO}(%)
C-pulsecolumn organ. continuous	a_d	10	90	60	4,5	86	5,2	8,5	9,6
	o_c	10	90	60	0,4	10	4,1	-	-
BX-pulsecolumn aqu.continuous	o_d	10	60	25	4,0	85	4,7	13	10,5

A = Amplitude

f = Frequency

T = Temperature

$\bar{V}$ = mean value of the convective velocity

$\bar{D}$ = mean value of the coefficient of dispersion

$\bar{\epsilon}$ = hold up (calculated)

ϵ_{TEKO} = hold up (measured)

a_d = aqueous disperse

o_c = organic continuous

o_d = organic disperse

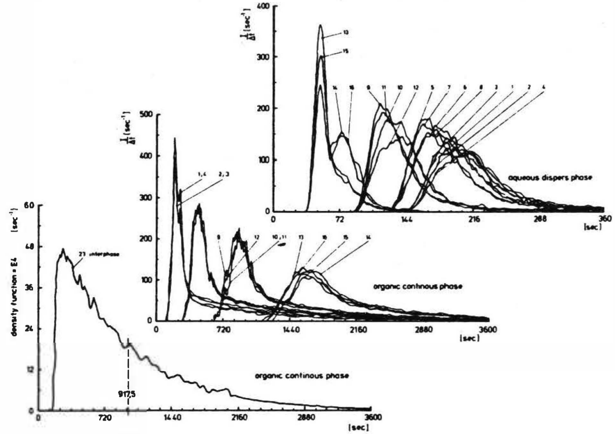

Fig.1 C-column: concentration/time-functions of the radiotracer experiments

(The numbers refer to the detector arrangements outside of the column according to Fig.2)

04.86 GK

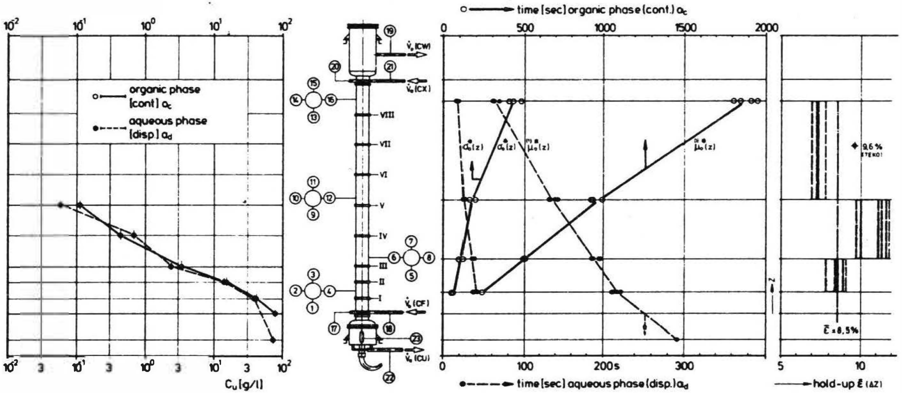

Fig.2 C-column: Uranium concentration profile; statistical moment $\binom{(1)}{\mu}*$); standard deviation (σ^*) and hold-up ($\bar{\varepsilon}$)

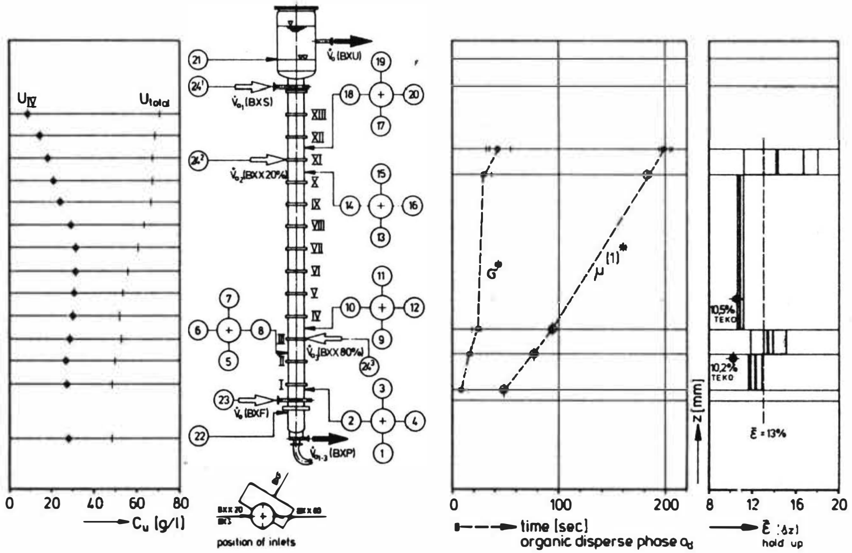

Fig.3 BX-column:
Uranium concentration profile; statistical moment ($\overset{(1)}{\mu}{}^*$); standard deviation (σ^*); and hold-up($\bar{\varepsilon}$)

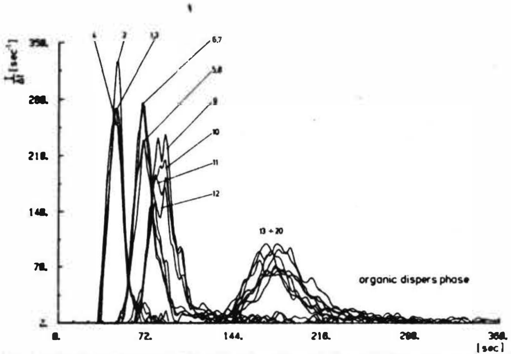

Fig.4 BX-column: concentration/time-functions of the radiotracer experiments
(The numbers refer to the detector arrangements outside of the column according to Fig.3)

THOREX Process Studies

E. Zimmer and J. Borchardt, KFA Jülich, Federal Republic of Germany

1. Scope of the Investigations

The utilization of thorium is very attractive in nuclear power reactors with a thermal neutron spectrum since U-233, bred from thorium, has the highest neutron yield of all fissile materials under these conditions. The use of thorium as a fertile material offers the greatest advantages in the heavy water moderated reactor where high conversion ratios are reached and even genuine breeding might be expected. The use of thorium is also promising in a second reactor system, viz. in the graphite-moderated high-temperature reactor (HTR). Heavy water reactors may use $(Th,U)O_2$ with a U-235 content of about 5 w/o, or an equivalent amount of Pu-239 (1). HTR fuel may consist of either pure UO_2 (or UC_2) and pure ThO_2, or of $(Th,U)O_2$. The U-235 content is usually 10 w/o. As a basis for the present "cold" study, a uranium content of 5 w/o in the fuel was adopted.

The THOREX processes for reprocessing thorium bearing fuel is carried out in a nitrate medium with tributyl phosphate as an extractant. In the first THOREX processes $Al(NO_3)_3$ was used as a salting-out agent (2). These flowsheets were originally developed for feed solutions which already contained this salt anyway after dissolution of aluminium containing fuel. In contrast, thorium fuel from power reactors do not contain aluminium so that the volume of the radioactive waste can be considerably reduced by using nitric acid as a salting out agent. Nitric acid can be recycled or destroyed whereas $Al(NO_3)_3$ can practically not be separated from the fission products.

Processes using nitric acid as a salting-out agent are called "acid" THOREX processes. The first acid THOREX process was developed by the ORNL for the reprocessing of slightly irradiated thorium (3). In this process an acid deficient feed solution was used, i.e. the Th/NO_3 ratio was lower than 4. In other words, nitric acid formed by hydrolysis was removed from solution, for example, by steam stripping (4). The reason for this treatment is to increase the hydrolysis of some fission products, particularly zirconium. These species are less extractable than non-hydrolyzed salts present in a solution with free acid.

However, the acid deficient feed solution has a drawback. Precipitates are formed during the adjustment of the acid defiency if high burn-up fuel is reprocessed. KÜCHLER et al. have developed the Dual Cycle THOREX Process (5). They used a feed solution with free acid in the first cycle, thus avoiding the formation of precipitates in the feed adjustment step. For the second cycle an acid deficient feed solution is prepared.

The objective of our study with natural Th and U was the reprocessing of spent thorium fuel from power reactors. Therefore, the Dual Dycle THOREX Process was the basis of the investigations. For extraction, the main efforts were directed towards the effects of feed solutions with either free nitric acid or acid deficiency. Since there is no choice for the first cycle the main question to be answered is whether the relatively complicated preparation of an acid deficient feed solution is necessary for the second cycle. Since this cycle was the main objective of the investigations our feed solutions contained neither fluoride nor aluminium. These elements are present in considerable concentrations in feed solutions prepared with the so-called THOREX solution (6). However, both elements mainly accompany the fission products and do not reach the second cycle in amounts which would cause process disturbances. During the investigations, the two different re-extraction modes, either combined re-extraction or partition of thorium and uranium, became also a point of major interest. Unexpected process interferences in the re-extraction step required modifications of the flow-sheet.

2. Investigations on the Dual Cycle THOREX Process

2.1 Extraction

2.1.1 Acidity profiles and process performance

Like the PUREX process, the Dual Cycle THOREX Process uses a 30 v/o solution of tributyl phosphate (TBP) in a paraffinic diluent (preferably n-dodecane) as an extractant and nitric acid as salting out agent. The extraction procedures of both cycles need almost the same amount of nitric acid. However, the nitric acid supply via feed solution and scrub differs very much in the two extracting variants. Fig. 1 shows a generalized flow-sheet of the Dual Cycle Process.

In case (a) the feed solution contains 1 mole/l free nitric acid (first cycle). In this case the acidity of the scrub must be relatively low (0.1 mole/l HNO_3). Otherwise the nitric acid concentration will become so high in the vicinity of the feed point that a second organic phase ("third phase") occurs. In case (b), the feed solution contains no free acid, or is even acid deficient whereas the scrub has a nitric acid concentration of 1 mole/l (second cycle). Apart from the acid fed by the feed and scrub solutions, both process variants provide a supply of concentrated nitric acid near the aqueous outlet. The high acidity present in this section of the extraction apparatus reduces the Th loss and a third phase cannot be generated here since the Th concentration is too low.

As can be seen in Fig. 1, the total nitric acid supply is very similar for both variants. This is not surprising since it was the aim of KÜCHLER et al. to accomplish a similar acidity profile in the first cycle as in the already proven second cycle. However, the authors conceded that they had only partially reached this goal (5). In any case, the low HNO_3 concentration of the incoming scrub solution in case (a) suggests that there is a substantially lower nitric acid concentration in the whole scrubbing section.

Our analysis of the HNO_3 profiles in a 16-stages mixer-settler provided the results illustrated in Fig. 2. Although the acid concentration in the vicinity of the scrub inlet is lower in the "acid" THOREX variant, it quickly rises to higher values in subsequent stages than in the acid deficient variant. HNO_3 is obviously transported into the scrub section via the organic phase. In the extraction sections, the nitric acid concentrations are more or less equal.

McCabe-Thiele diagram interpretations of the two variants can be carried out by means of the evaluated acidity profiles and available distribution data (7,8). The diagrams do not reveal significant differences between both extracting sections nor between both scrubbing sections. Extraction is completed in a few stages. Consequently, Th losses were regularly less than 0.05 % in our mixer-settler runs, while uranium losses were below the detection limit of the analysis method used ($\leq$ 0.1 %). The diagrams also show that a pinch point is reached in both variants after a few steps in the scrubbing sections. In view of the rather different acid concentrations in the scrubbing sections, this similarity is surprising at first glance. However, at Th concentrations of 0.1 - 0.2 mole/l (as observed in the scrubbing section) the Th distribution coefficient is not strongly influenced by varying the HNO_3 concentrations from 1.5 to 3 moles/l (7,8). In good agreement with the theoretical stability of the flow sheets, constant organic effluent concentrations were always attained for both extracting variants. Generally, it can be concluded from these results that none of the process variants has essential advantages with regard to heavy metal recovery and process performance.

2.1.2 Zirconium Decontamination

An argument in favour of the acid deficient process is usually its better Zr-decontamination. The zirconium extraction with TBP is, as commonly known, strongly affected by the acidity of the aqueous phase, since only the non-hydrolyzed Zr^{4+} seems to be the extractable species (9). The question arises whether the better decontamination achieved by the acid deficient process is due to the lower acidity in its scrubbing section or due to the higher degree of Zr-hydrolysis in its feed solution. The lower acidity in the scrubbing section can only produce a minor effect because the acidity in the "acid" process is similar. The higher degree of hydrolysis in the acid deficient feed solution, however, could play a very important role, provided that the hydrolyzed species are metastable during the time of extraction in the highly acidic medium of extracting and scrubbing. We have studied this problem by means of mixer-settler runs and batchwise extraction experiments.

For the mixer-settler experiments, acid as well as acid deficient feed solutions were prepared containing the same concentrations of Zr (0.1 g/l) with Zr-95 as a tracer (260 μCi/l). The relatively low Zr concentration was chosen since at higher concentrations Zr is precipitated if acid deficient solutions are prepared. The Zr containing solutions were boiled for at least one hour in order to reach equilibrium conditions. After 11, 12 and 13 hours of mixer-settler operation (steady state is reached after approx. 6 hours) samples were taken and measured by γ-spectrometry to determine the amount of Zr-95. The decontamination factors found in several runs were 30 ± 3 for the acid feed solution and 77 ± 5 for the acid deficient one. Thus, the decontamination factors differ only by a factor of approximately 2, and both are much lower than those reported for the PUREX process. The explanation for the difference may be found in the higher loading of the organic phase with heavy metals under PUREX scrubbing conditions.

The slightly different decontamination factors are presumably only caused by the different acidities in the scrubbing sections and not by the metastability of the hydrolyzed species present in the acid deficient feed solution. Equilibrium between zirconium species seems to be established quickly (with respect to the residence time in mixer-settlers) at the high acidity of extracting and scrubbing. Therefore, batchwise extraction experiments were carried out to study how fast the equilibrium between zirconium species is achieved under these conditions. Starting solutions were again acid and acid deficient feed solutions with the same zirconium and Zr-95 concentrations as given above. These solutions were diluted with nitric acid and then immediately extracted with 30 v/o TBP in n-dodecane (phase ratio 1:1; temperature 22°C). After an extraction time of 15 minutes, the equilibrium concentrations of thorium and nitric acid were as follows:

	thorium [mole/l]	nitric acid [mole/l]
aqueous phase	0.09	2.1
organic phase	0.11	0.37

Thus, the thorium concentrations were similar to those observed in the scrubbing sections, the nitric acid concentrations were even lower. For the extraction batches prepared with an acid feed solution, the zirconium fractions extracted were 2.0, 2.8, and 1.8 % (mean value 2.2 %). For the three batches prepared with an acid deficient feed solution the fractions extracted were 2.9, 2.2, and 1.9 % (average 2.3 %). It can be concluded from these results that the species present in an acid deficient feed solution are not metastable for more than some minutes at this acid concentration.

This conclusion is supported by "multiple extraction" experiments. For this batchwise extraction technique the equilibrated aqueous phase (same composition as above) was again contacted with a zirconium free organic TBP phase which, however, had been already pre-equilibrated with thorium and nitric acid. Extraction time was again 15 minutes and the temperature 22°C. The time between the end of first extraction and the start of the next one was 10 minutes. Zr-95 was used as a tracer (520 µCi/l). For an aqueous phase prepared with an acid feed solution the first extraction yielded 2.3 %, the second one 2.2 % Zr extraction. The corresponding values for an aqueous phase prepared with an acid deficient feed solution were 3.0, 2.9, and 2.9 %.

These results again confirm the assumption that the equilibrium between zirconium species is established within approximately 15 minutes or, probably, much faster under the highly acidic conditions of extraction and scrubbing in the THOREX process. Thus, the pretreatment of zirconium does not play a role if mixer settlers with their comparatively long residence time ($\leq$ 1 hour) are used as extraction apparatus. The history of the zirconium could only be of importance if an extraction apparatus with a shorter contact time is employed, e.g. pulse columns or even centrifugal extractors. A similar behavior of the zirconium was also found by D.A. ORTH et al. for PUREX process conditions (10).

2.2 Re-extraction

The flow-sheet of the Dual THOREX Process provides a joint re-extraction (co-stripping) of thorium and uranium with 0.01 $\underline{M}$ HNO_3 in the first cycle. After a further decontamination in the second cycle thorium and uranium are separated by subsequent re-extraction. Thorium is re-extracted by a 0.01 $\underline{M}$ HNO_3 solution and uranium is kept in the organic phase by a scrub of fresh organic solvent (7). Uranium is stripped with 0.01 $\underline{M}$ HNO_3 in the last step of the process.

Our studies have revealed serious problems if re-extraction is carried out with such a dilute nitric acid. In both mixer-settlers and pulse columns, a process perturbing crud formation was observed. In the co-stripping step, the crud is initially formed in the vicinity of the inlet of the aqueous phase by interaction with the almost unloaded organic phase. In-depth investigations have shown that a precipitate of thorium and dibutyl phosphate (DBP) causes emulsification. The disturbances due to emulsification propagate from the place of origin along the entire extraction apparatus. The crud does not only impair material separation but it also blocks the extraction apparatus due to its viscosity. RATHVON et al. already observed process flow difficulties due to formation of a crud during thorium stripping (3). This crud problem appeared after several weeks of trouble-free operation. In our experiments, crud formation sometimes occured after days or even weeks of undisturbed operation. Then, both mixer-settlers and pulse columns became blocked within hours by crud. On separation and analysis the chemical formula of the precipitate was exactly $Th(DBP)_4$ as already found by RATHVON et al.. An elementary analysis showed a Th:P ratio of 1:4 (less than 1 % deviation) and IR and NMR spectra confirmed the presence of DBP.

The mechanism of the formation of Th(DBP)$_4$ is evident. DBP is produced in the extraction step by hydrolysis of TBP. Due to the high acidity present there, the DBP formed is transported via the organic phase to the re-extraction step. In our cold experiments, we have found a DBP concentration of 25 ppm in the organic phase leaving the extracting/scrubbing mixer-settler. At the low acidity of the re-extraction, the DBP is stripped together with the thorium into the aqueous phase and Th(DBP)$_4$ is precipitated. Even more serious crud problems can be expected in hot runs where much more DBP is produced by radiolysis.

Our investigations have shown that the precipitation of Th(DBP)$_4$ can be avoided if the HNO$_3$ concentration of the strip solution is increased to 0.5 mole/l. The actual aqueous HNO$_3$ concentration in the extraction apparatus will increase to about 0.7 mole/l due to HNO$_3$ re-extraction. It is evident that a joint re-extraction of uranium and thorium cannot be accomplished at this acidity since uranium is practically not stripped under these conditions. A separate thorium re-extraction, however, can be achieved. With flow rates of 3.2 ml/min for the organic feed solution (0.11 $\underline{M}$ Th; 0.005 $\underline{M}$ U; 0,15 $\underline{M}$ HNO$_3$), 4 ml/min for the aqueous strip solution (0.5 $\underline{M}$ HNO$_3$) and 0.8 ml/min for the scrub (fresh TBP solution) and acceptable separation of thorium and uranium was obtained. The experiments were again carried out in a 16-stages mixer-settler with the feed point in stage 8. Only 0.2 % of the thorium accompanied the uranium but there was a 2 % loss of uranium to the aqueous (thorium containing) stream. Nevertheless, these results can probably be improved by optimization of the flow sheet; in addition, the mixer-settler used here had only a stage efficiency of approx. 50 %. Thus, better extraction apparatus could also improve partitioning.

After thorium re-extraction with a 0.5 $\underline{M}$ HNO$_3$ solution, uranium stripping is easily accomplished by a 0.01 $\underline{M}$ HNO$_3$ if thorium is adequately separated in the previous step. Otherwise, Th(DBP)$_4$ is precipitated and a crud is formed during uranium stripping. The reason for this is that DBP is not re-extracted in the thorium stripping step but accompanies the uranium in the organic phase. The precipitate is formed if the uranium is contaminated with too much thorium. The degree of separation described above was sufficient to avoid this problem.

3. Conclusions

The Dual Cycle THOREX Process was developed for the reprocessing of high burn-up fuel from power reactors. The process consists of a first cycle with an acid feed solution and a second cycle with an acid deficient feed solution. The latter cycle is similar to the single cycle THOREX process developed for the reprocessing of thorium with low fission product content. The combination of both cycles appears to be reasonable since precipitates are avoided in the first cycle and a better zirconium decontamination is allegedly achieved by the second cycle.

Our experiments have revealed that only a slightly better decontamination is obtained with the acid deficient process but this minor improvement is only due the lower nitric acid concentration in the second cycle scrub section. The hydrolyzed and, in principle, less extractable Zr species produced during adjustment of the acid deficiency are not metastable in the highly acidic medium of extraction and scrubbing. Therefore, the complicated preparation of an acid deficient feed solution is not necessary. Further efforts should be directed towards a reduction of the acid concentration in the scrubbing section if an acid feed solution is used. This could be done by modifying the nitric acid supply via feed solution and scrub. For instance, the nitric acid concentration of the feed solution can be reduced to approx. 0.5 mole/l without the formation of zirconium precipitates. A dual cycle process with only acid feed solutions - but with a modified supply of nitric acid - could provide the same decontamination factors as the "Dual Cycle THOREX Process". However, in view of the fact that a remote refabrication of U-233 and possibly of thorium as well is necessary anyway, the question arises whether a dual cycle process is actually required. Furthermore, prior to reprocessing very long cooling times of the fuel ($\geq$ 5 years) are common today. Thus, a high decontamination of Zr-95 with its half life of 64 days should not be an important point of thorium reprocessing. An optimized single cycle process could probably provide the necessary decontamination factors.

Co-stripping of uranium and thorium should be avoided since $Th(DBP)_4$ is precipitated at the low acidity necessary for this step. The crud produced by this salt causes serious flow problems in the extraction apparatus. On the other hand, uranium/thorium partitioning can be carried-out at such an acidity (0.7 $\underline{M}$ HNO_3) that the formation of $Th(DBP)_4$ is avoided. After proper separation of thorium, uranium can be re-extracted by dilute nitric acid (0.01 $\underline{M}$ HNO_3) without problems. Therefore, separation of heavy metals should already be done after the first extraction and further decontamination, if necessary at all, should be carried out separately as is the preferred procedure in the PUREX process.

References

(1) McLean, D.R.: Trans. Act. Nucl. Soc. 40 [1982] 124

(2) Haas, W.O.; Smith, D.J.: Report KAPL-1306 [1956]

(3) Rathvon, H.C. et al.: USAEC-CONF-660542 [1966] 765-824

(4) Rainey, R.H. and Moore, J.G.: Nucl. Sci. Eng. 10 [1961] 367-371

(5) Küchler, L. et al.: Kerntechnik, 13 [1971] 319-322

(6) Bond, W.D.: Report ORNL 2519 [1958]

(7) Nakashima, T. et al.: Solvent Extraction and Ion Exchange, 2(4&5) [1984] 635-65

(8) Nakashima, T. and Zimmer, E.: Report Jül-1920 [1984] ISSN 0366 0885

(9) McKibben, M.: Radiochimica Acta, 36 [1984] 3-15

(10) Orth, D.A. et al.: Proc. Intern. Solvent Extraction Conf. 1971, Soc. Chem. Ind., London 1971

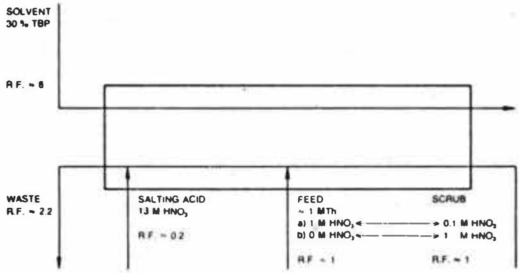
SOLVENT
30 % TBP
R.F. ≈ 6
WASTE
R.F. ≈ 2.2
SALTING ACID
13 M HNO$_3$
R.F. ≈ 0.2
FEED
≈ 1 M Th
a) 1 M HNO$_3$ ↔ 0.1 M HNO$_3$
b) 0 M HNO$_3$ ↔ 1 M HNO$_3$
R.F. ≈ 1
SCRUB
R.F. ≈ 1

Fig. 1: Generalized Flow-sheet of the DUAL CYCLE THOREX PROCESS

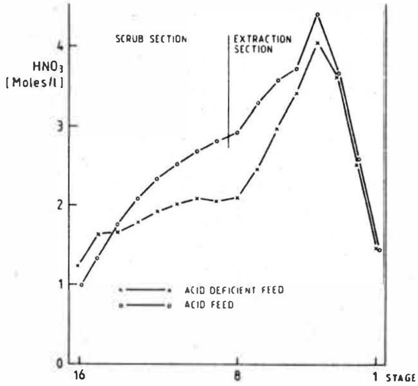

Fig. 2: Acidity Profiles Found in a 16-stage Mixer-Settler

SEPARATION OF FISSION PRODUCTS FROM U AND PU IN THE HIGHLY RADIOACTIVE CYCLE OF THE PUREX PROCESS

Z. Kolarik, H.-J. Bleyl and H. Schmieder

Institut für Heisse Chemie, Kernforschungszentrum Karlsruhe,
75 Karlsruhe 1, P. O. Box 3640, Federal Republic of Germany

INTRODUCTION

The Purex process can be simplified and its costs can be reduced, if the efficiency of the decontamination of uranium and plutonium from fission products in the highly radioactive extraction cycle of the process (the first Purex cycle) is increased. Valuable information for realizing this intention were obtained from results of experimental work done in a heavily shielded, laboratory scale extraction facility (MILLI). With its small throughput (1 kg U+Pu/d, i.e. 1 milliton/d) the facility was very versatile and made it possible to perform at hot counter-current experiments with true irradiated fuels reasonable costs (a survey of the experiments is given in [1]). Conclusions drawn from the results and suggestions for improvements of the Purex process are summarized in this paper.

EXPERIMENTAL

The MILLI facility, described in detail in [2,3], is equipped with mixer-settlers. The arrangement of the first Purex cycle, as applied in the hot experiments, is shown in Fig. 1. The type of the reprocessed fuel as well as the composition and flow rates of some process streams are gathered in Table 1. The solvent, in all experiments fresh, nonrecycled 30 vol.% TBP in n-alkanes (C_{10} - C_{13}), was pretreated by a carbonate wash. The HBXX and HBXS streams contained U(IV) and hydrazine nitrates, the HBSX stream was fresh solvent, and the HCX stream was 0.01 or 0.02M nitric acid. The irradiated fuel was dissolved in hot nitric acid and fines were removed by a sintered metal filter and, additionally in the runs 20 - 22, by a bed of diatomaceous earth. U, Pu, nitric acid, and fission products were determined as surveyed in [4]. Dibutyl phosphoric acid was determined by gas chromatography [5]. Decontamination factors (DF) were calculated as the radioactivity of a nuclide per g U in the feed solution divided by the radioactivity of the nuclide per g U in the respective process stream.

RESULTS AND DISCUSSION

The Behaviour of Zirconium-95 and Ruthenium-106

Decontamination factors of both nuclides in the organic outlet stages of the HA/HS1 and HS2 banks increase with the sum of the concentrations of U and Pu in the loaded solvent. The response of the DF values to changes of the solvent loading is rather fast: e.g. a decrease of the loading from 91 to 61 g (U+Pu)/l and a subsequent increase to 84 g (U+Pu)/l are each followed by corresponding variations of the

DF_{Ru-106} value within two hours. An example of a DF_{Ru-106} vs. loading dependence is given in Fig. 2. Similar dependences were found also for the DF_{Zr-95} value. The essential importance of the solvent loading for the decontamination efficiency is illustrated by the fact that the DF_{Zr-95} and DF_{Ru-106} values tended to unity in those periods of the run 14, in which the solvent loading decreased (due to disturbances) to process-irrelevant values of <20 g (U+Pu)/l. To compare the decontamination efficiency for ^{95}Zr and ^{106}Ru in different runs, we estimated DF values achieved at the organic outlets of the HA/HS1 and HS2 banks at a process relevant solvent loading of 90 g (U+Pu)/l (Table 2). Different DF values are found in various runs in spite of the defined solvent loading and of comparable process parameters. Moreover, log DF vs. solvent loading dependences obtained in various runs exhibit different steepness and a strongly variable scattering of the experimental points.

^{95}Zr tends to accumulate in the extraction part (HA) of the HA/HS1 bank (see the upper part of Fig. 3). No tendency to any accumulation is exhibited by ^{106}Ru (see the lower part of Fig. 3), which is less extractable than Zr(IV) at nitric acid concentrations typical of the extraction part of the HA/HS1 bank (4 - 5M). Distribution ratios of Zr(IV) and nitrosyl Ru (D_{Zr-95} and D_{Ru-106} respectively) were calculated from concentration profiles for those stages of the HA/HS1 bank, in which the solvent was loaded with U and Pu to <10% of its capacity. The D_{Zr-95} values have no truly equilibrium character (the stage efficiency of the MILLI mixer-settlers is <100%), but plotted vs. the nitric acid concentration they mostly lie near an equilibrium dependence taken from [6,7]. However, some values lie below the curve and are up to ~10 times lower than expected. D_{Ru-106} values from the MILLI runs are by a factor of 2.5 - 10 lower than allegedly equilibruim D_{Ru-106} values taken from [8]. On the other side, the D_{Ru-106} values from the MILLI runs are markedly higher than time dependent values reported in [9] for stirring times of 1 min - 4h. The differences between the D_{Ru-106} values from the MILLI runs and the published values are not surprising, because the distribution behaviour of nitrosyl Ru species is strongly dependent on the history of the stock Ru solution taken for the distribution experiments. We also calculated D_{Ru-106} values in the scrub section of the HA/HS1 bank and in the HS2 bank, where nitrosyl Ru is reextracted. Since extracted nitrosyl Ru species are in the solvent changed into slowly reextractable species, namely by a transition of solvating TBP molecules from the outer coordination sphere of the central Ru ion into the inner sphere [10], a reextraction equilibrium is at room temperature established after a long contact time only. In spite of this, the results are rather reproducible and illustrate the extent to which the D_{Ru-106} value is suppressed by an increase of the solvent loading and the acid concentration. D_{Zr-95} values at a solvent loading of >10% are too scattered for showing any definite coherence with these variables.

Due to the distribution behaviour of Zr(IV) and nitrosyl Ru, the efficiency of the decontamination from ^{95}Zr becomes higher and that of ^{106}Ru becomes lower, if the nitric acid concentration in the HS1S scrub stream is reduced (see data of run 21 in Table 2). The effect is also visible in the organic outlet stage of the HS2 bank, because at a higher acid concentration in the HS1S scrub stream larger amounts of acid are brought with the solvent into the HS2 bank. The opposite effect on the DF_{Ru-106} and DF_{Zr-95} values at the change of the nitric acid concentration in the HS1S scrub stream demonstrates that a simple lining up of two scrub sections with different nitric acid concentrations need not improve the general decontamination efficiency of the whole 1st Purex cycle, if the sections are mutually coupled (in this case by directing the aqueous stream from the HS2 bank into the scrub part of the HA/HS1 bank).

The contribution of the HS2 bank to the decontamination of the loaded solvent from ^{106}Ru and ^{95}Zr can be considerable, even at a rather unfavourable organic to aqueous flow ratio of ~9 (Table 2). Unfortunately, the contribution changes from run to run and exhibits no clear coherence with process parameters. Quite unambiguous is the more effective scrubbing of ^{106}Ru at elevated temperature in the HS2 bank: At a solvent loading of 65 - 90 g (U+Pu)/l and an organic to aqueous flow ratio of 6.0 the decontamination efficiency for ^{106}Ru in the HS2 bank is improved by a factor of 13 - 20, if the bank is operated at 55 - 60°C (Fig. 2). The effect is still visible at a rather unfavourable organic to aqueous flow ratio of 19.4 (see data on the run 12 in Table 2). The HB and HC banks also contribute to the decontamination of the loaded organic phase. During the pass through the 9th to 16th stages of the HB bank, the loaded solvent is decontaminated from ^{95}Zr and ^{106}Ru by a factor of ~10 at organic to aqueous flow ratios of 4.9 (run 14) and 4.4 (run 21). However, the decontamination is as low as by a factor of ~2, if the flow ratio is 8.7 (run 15). The distribution ratios of ^{95}Zr and ^{106}Ru in the HB bank are low and, consequently, the aqueous Pu product stream (HBP) contains about ten times higher contamination than the organic uranium product stream (HBU). Fractions of ^{95}Zr and ^{106}Ru accompanying U during its stripping in the HC bank vary between ~10 and ~90%.

The particular circumstance must be emphasized that the solvent was never recycled in the MILLI experiments. It turned out in comparative batch distribution experiments that the behaviour of coextracted ^{106}Ru and ^{95}Zr in a highly recycled industrial solvent is different from that in the MILLI solvent. First, a ^{106}Ru fraction of 50 - 70% (but a negligible fraction of ^{95}Zr) can be removed from the industrial loaded solvent (HS2P) by filtration through membrane filters with a pore size of 0.2 and 1 μ [11]. Second, ^{106}Ru and ^{95}Zr are scrubbed with an aqueous solution of uranyl nitrate and nitric acid more effectively from the HS2P stream originated in a MILLI experiment than from the industrial HS2P stream. Distribution ratios of ^{106}Ru in batch experiments with the industrial HS2P sample are unexpectedly high. This can be ascribed to the fact that compounds like didodecyl phosphoric acids are formed radiolytically in the highly recycled industrial solvent. These compounds are not removed in a conventional carbonate wash, and accumulate at a radiation dose of ~12 Wh/l to concentrations as high as 1.7×10^{-4}M. In the nonrecycled solvent in the MILLI experiments, at a radiation dose of ~0.1 Wh/l, their concentration was $\leq2\times10^{-5}$M [12]. Samples of HS2P streams, both industrial and from MILLI runs, were in the batch experiments consecutively contacted with two or three fresh portions of an aqueous scrub solution. In most cases the distribution ratios of ^{95}Zr and ^{106}Ru increased from contact to contact. Obviously, traces of nitrosyl Ru and Zr(IV) can be retained in the HS2P solution by dibutyl and higher dialkyl phosphoric acids so strongly, that they practically cannot be scrubbed.

The Behaviour of Cesium-137, Cerium-144 and Europium-154

Concentration profiles of ^{144}Ce in the extraction part of the HA/HS1 bank show that cerium is present in the feed solution predominantly as the weakly extractable Ce(III). Cs(I) is extremely weakly extractable. In contradiction to these facts, the radioactivity level of ^{144}Ce and ^{137}Cs in the loaded solvent is reduced less than expected in the scrub part (HS1) of the HA/HS1 bank, and is litlle changed when the solvent passes the HS2, HB and HC banks. Both fission products are then found in the U and Pu aqueous product streams (HCP and HBP respectively). Distribution ratios of both ^{144}Ce and ^{137}Cs are regularly low in the extraction part of the HA/HS1 bank only. In the scrub part of the bank (HS1) and in all following banks the distribution ratios of the nuclides are unrealistically high, sometimes even $D_{Cs-137}>1$. Irregularly high distribution ratios of ^{144}Ce and ^{137}Cs are also observed in the U and Pu purification cycles, which then yield only a low or even no additional decontamination of U and Pu from ^{137}Cs and ^{144}Ce. In the first Purex cycle the decontamination factors for ^{144}Ce and ^{137}Cs are extremely irreproducible and fail to exhibit any correlation with the solvent loading.

The behaviour of ^{144}Ce and ^{137}Cs in the process part following the scrubbing in the HA/HS1 bank implies that both nuclides are present in the corresponding process streams in a heterogenous form and cannot be removed from the solvent in liquid-liquid contact operations. It is an interesting phenomenon that there is a correlation between the radioactivities of ^{144}Ce and ^{137}Cs observed in a majority of the MILLI runs irrespective of the mode of the fines removal from the feed solution. A mathematical evaluation of the correlation between the ^{144}Ce and ^{137}Cs radioactivities (made for the runs 13, 17, 19, 20 and 21) shows that the heterogenously contaminating radioactivity of ^{137}Cs is present in the process streams in two separate fractions. One of them is dependent on the radioactivity of ^{144}Ce (henceforth bound ^{137}Cs radioactivity), while the other does not depend on the radioactivity of ^{144}Ce (henceforth independent ^{137}Cs radioactivity). The correlation between the radioactivities of ^{137}Cs and ^{144}Ce can thus be described as

$$A_{Cs-137} = {}^{0}A_{Cs-137} + rA_{Ce-144}$$

with ${}^{0}A_{Cs-137}$ denoting the independent radioactivity of ^{137}Cs and with r denoting a constant ratio between the bound radioactivity of ^{137}Cs and the total radioactivity of ^{144}Ce. In the separation of Pu from U, a predominant part of the independent radioactivity but a small part of the bound radioactivity of ^{137}Cs accompanies Pu. On the other hand the organic U product stream contains prevailably bound radioactivity of ^{137}Cs. A similar fractionation proceeds in the strip of U or Pu with a very dilute solution of nitric acid. Then the aqueous product stream contains again a mixture of both fractions of the radioactivity of ^{137}Cs, while prevailably bound radioactivity remains in the barren solvent. The constant ratios of the bound ^{137}Cs to the total ^{144}Ce radioactivities, obtained for various runs as the r value from the above equation, corresponds to Cs/Ce atomic mass ratios ranging from 0.8 to 2.4 (calculated according to [13]).

The behaviour of the ^{144}Ce and ^{137}Cs radioactivities implies that they both are components of colloidal solids. It is not probable that Cs and Ce are constituents of a slightly soluble stoichiometric compound forming an unsupported colloid, because radioactivities plotted in Fig. 4 correspond to concentrations as low as 4×10^{-9} to 6×10^{-6} g-atom Cs/l and 9×10^{-10} to 2.5×10^{-6} g-atom Ce/l. It is more probable that Cs and Ce form secondary colloids, being adsorbed on solid impurities which frequently exist in Purex process solutions. Such impurities can be formed by corrosion products like Fe(III), Ti(IV) and Cr(III), fission products like Mo or Pd, silica, or perhaps heteropolyacids of phosphorus. A solid containing Pd and Zr at a constant stoichiometric ratio and also carrying Mo, Ru and Ti is dispersed in an industrial, highly recycled solvent [14]. However, a Zr compound is probably not the supposed carrier for ^{144}Ce and ^{137}Cs in the MILLI runs, because there is no correlation between the radioactivities of ^{95}Zr and ^{137}Cs. No reliable data are yet available about the filterability of the heterogenous contamination of the solvent by ^{144}Ce and ^{137}Cs. In some cases it could simply be removed by paper filter (blue ribbon) but, in other cases, not by a membrane filter.

Concentration profiles of ^{154}Eu are in the extraction part of the HA/HS1 bank very similar to those of ^{144}Ce. Distribution ratios of ^{144}Ce and ^{154}Eu at a low solvent loading with U and Pu give a reasonable picture as functions of the nitric acid concentration. There is a fairly good agreement between the D_{Eu-154} values found in the MILLI runs and a published equilibrium curve [6].

The Behaviour of Antimony-125

DF_{Sb-125} values of several hundreds to several thousands were mostly found at the organic outlets of the HA/HS1 and HS2 banks and were not coherent with the solvent loading. Also ^{125}Sb appears to be present in the loaded solvent in the form of a heterogenous contamination. A correlation between the radioactivities of ^{137}Cs and ^{125}Sb was found in some runs, representing a simple proportionality with a constant ^{137}Cs/^{125}Sb ratio of ~14. This corresponds to an atomic mass ratio of ~150 [13], which implies that ^{125}Sb is adsorbed on or coprecipitated with a Cs containing solid. A part of ^{125}Sb is present as a solid also in an industrial loaded solvent, from which ~70% ^{125}Sb can be removed by a membrane filter with a pore size of 0.2 μ [11].

CONCLUDING REMARKS

Further development of the Purex process, which up to now has predominantly been concentrated on improved removal of the homogenous contamination from the loaded solvent, must necessarily be extended to the removal of the heterogenous contamination. The homogenous contamination of the loaded solvent can be suppressed by optimizing conventional process parameters. Let us mention the improved scrubbing of ^{106}Ru at elevated temperature and the enhanced DF_{Zr-95} and DF_{Ru-106} values at an appropriately high loading of the solvent with U and Pu. It also is very desirable to disconnect partially the HS2 bank from the scrub section of the HA/HS1 bank by directing the aqueous stream from the first stage of the HS2 bank not into the last stage but into the feed inlet of the HA/HS1 bank. The stream from the HS2 bank can be intermediately treated before the introduction into the feed stage of the HA/HS1 bank, e.g. by heating to ~100°C, in order to suppress the extractability of the scrubbed ^{95}Zr and ^{106}Ru species. Our preliminary experiments showed that at least the extractability of ^{106}Ru could be lowered in this manner. The purification of the barren solvent from the HC bank before its recycling into the HA/HS1 bank should also remove long chain dialkyl phosphoric acids, which are not washed out in the conventional carbonate wash. Removal of the heterogenous contamination from the loaded solvent by filtration could be slow and, thus, incompatible with the process performance. Forced coagulation of colloid solids and coalescence of entrainment droplets e.g. by electric field, eventually followed by filtration, proved in our preliminary experiments to be potentially feasible.

REFERENCES

1. W.Ochsenfeld and H.-J. Bleyl, Report KfK 3740, 258-273 (1984).
2. W. Ochsenfeld, W. Diefenbacher and H. O. Leichsenring, Report IAEA-SM-209/25 (1976), p. 87.
3. W. Ochsenfeld and H.-J. Bleyl, Atomkernenergie-Kerntechnik, 33, 251 (1979).
4. D. Ertel and G. Horn, Atomkernenergie-Kerntechnik 46, 89 (1985).
5. L. Stieglitz, R. Becker, H. Bautz and A. Wünschel, Report KfK 2613 (1978).
6. Z. Kolarik and K. Grudpan, Solvent Extr. Ion Exch. 3, 61 (1986).
7. U. Bauder, Thesis, University of Heidelberg (1978).
8. E. Hallaba and R. A. I. Azzam, Z. Anorg. Allg. Chem. 314, 53 (1962).
9. D. J. Pruett, Radiochim. Acta 27, 115 (1980).
10. L. Maya, J. Inorg. Nucl. Chem. 43, 385 (1981).
11. G. Horn and D. Ertel, unpublished results.
12. L. Stieglitz and R. Becker, Proc. ACS Internat. Topical Meeting Fuel Reprocessing Waste Management, August 26 -29, 1984, Jackson, Wyoming, USA, Vol. 1, p. 451.
13. H. W. Wiese, in Report KfK 3775 (1984), p. 109; personal communication.
14. F. Baumgärtner, Report RCM 02185 (1985).

TABLE 1

Composition and flow rates of some process streams in the MILLI runs. Fuel type: LWR - uranium oxide from light water reactor; MOX: mixed oxides from light water reactor; FBR: fast breeder reactor fuel. N.D.: not detectable;

Process stream, its composition and flow rate		Run 7	8	9	10	11	12	13	14
fuel type		LWR	LWR	LWR	LWR	MOX	LWR	MOX	FBR
HAF	U(VI), g/l	220	245	240	250	230	230	260	210
	Pu(IV), g/l	2.3	2.3	2.7	2.5	4.9	3.2	6.8	21.0
	nitric acid, mol/l	3.2	3.1	3.1	3.1	4.2	3.3	3.2	3.2
	^{95}Zr (Ci/l)	0.03	0.65	0.1	16	0.3	N.D.	5	0.2
	^{106}Ru (Ci/l)	4.8	21	12	41	25	5	36	3
	^{137}Cs (Ci/l)	18	26	24	30	15	24	32	10
	^{144}Ce (Ci/l)	8.4	52	21	100	26	25	100	11
	flow rate, ml/h	250 to 400							
HAX	flow, ml/h	700 to 1000							
HS1S	nitric acid, mol/l	3.0 to 6.0							
	flow rate, ml/h	35 to 80							
HS2S	nitric acid, mol/l	1.0 to 1.5							
	flow rate, ml/h	36 to 125							

Table 1 (continued)

Process stream, its composition and flow rate		Run 15	16	17	19	20	21	22
fuel type		LWR	FBR	FBR	LWR	LWR	FBR	FBR
HAF	U(VI), g/l	250	160	205	220	220	175	90
	Pu(IV), g/l	3.1	33.0	33.0	3.5	2.8	27.0	21.6
	nitric acid, mol/l	3.2	3.3	3.4	3.7	3.3	4.3	5.2
	^{95}Zr (Ci/l)	0.1	N.D.	0.1	0.1	N.D.	19	0.2
	^{106}Ru (Ci/l)	17	0.6	1.3	3	11	20	5
	^{137}Cs (Ci/l)	34	16	8	7	45	42	16
	^{144}Ce (Ci/l)	43	2	23	6	17	200	150
	flow rate, ml/h	225 to 400						
HAX	flow, ml/h	400 to 900						
HS1S	nitric acid, mol/l	1.5 to 10						
	flow rate, ml/h	35 to 40						
HS2S	nitric acid, mol/l	0.8 to 3.0						
	flow rate, ml/h	37 to 180						

TABLE 2

Decontamination factors for ^{95}Zr and ^{106}Ru in the organic outlet stages of the HA/HS1 and HS2 banks (runs 7 to 21) or in the 14th stage of the HA/HS1 bank (run 22) at a solvent loading of 90 g (U+Pu)/l. HDBP: dibutyl phosphoric acid; N.M.: not measured; N.D.: no ^{95}Zr detectable.

Run	DF for ^{95}Zr		DF for ^{106}Ru		HDBP concn. mg/l	Flow ratio HAX to	
	HA/HS1	HS2	HA/HS1	HS2		HS1S+HS2S	HS2S
7	170	~3000	~100	~200	70-240	4.0 to 6.7	5.0 to 19.4
8	27	400	70	500	10-120		
9	N.M.	58	N.M.	90	10- 50		
10	N.M.	240	240	90	<10- 30		
11	20	100	230	700	14- 26		
12	N.D.	N.D.	210	4900*	N.M.		
13	14	160	120	600	<10- 40		
14	160	1100	~160	500	40- 60		
15	3.4	8	130	220	60-210		
16	N.D.	N.D.	~80	300	40-180		
17	110	1000	120	500	14- 30		
19	~150	~600	~1000	~1700	<15- 40		
20	N.D.	N.D.	80	400	N.M.		
20	N.D.	N.D.	80	10000*	N.M.		
21	35**	400**	750**	2200**	10- 43		
21	210***	1000***	300***	~800***	24		
22	75	N.M.	750	N.M.	80-110		

* The HS2 bank was operated at 55 - 60°C.
** With 5.0M nitric acid taken as the HS1S stream.
*** With 1.5M nitric acid taken as the HS1S stream.

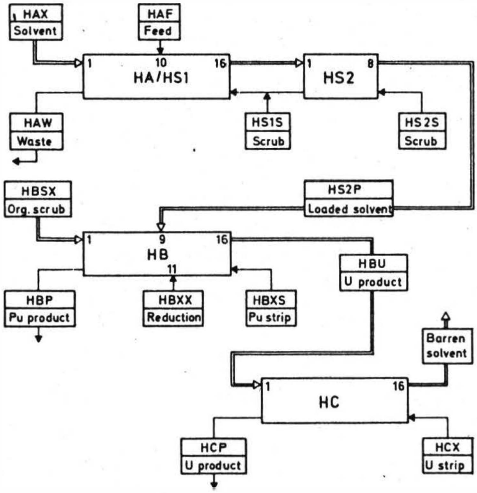
HAX
Solvent
HAF
Feed
1
10
16
HA/HS1
1
8
HS2
HAW
Waste
HS1S
Scrub
HS2S
Scrub
HBSX
Org. scrub
HS2P
Loaded solvent
1
9
16
HB
11
HBU
U product
HBP
Pu product
HBXX
Reduction
HBXS
Pu strip
Barren
solvent
1
16
HC
HCP
U product
HCX
U strip

FIG. 1. The flowsheet of the 1st Purex cycle in the MILLI runs (see Table 1 for the composition and flow rates of some streams).

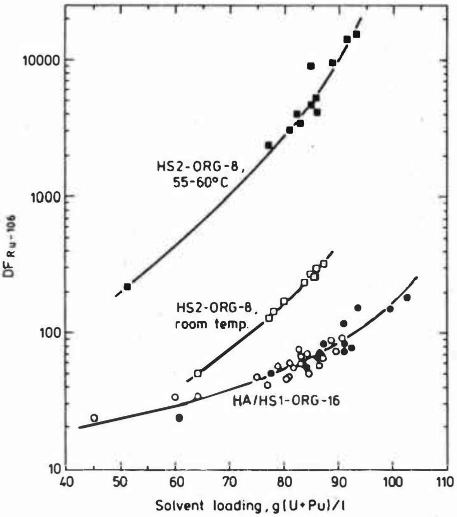

FIG. 2.

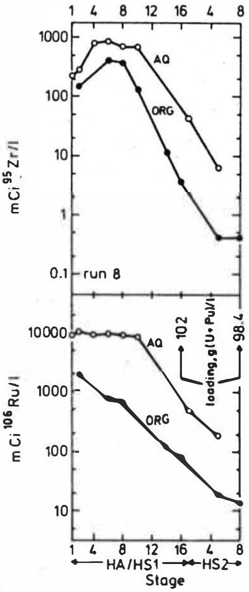

FIG. 3.

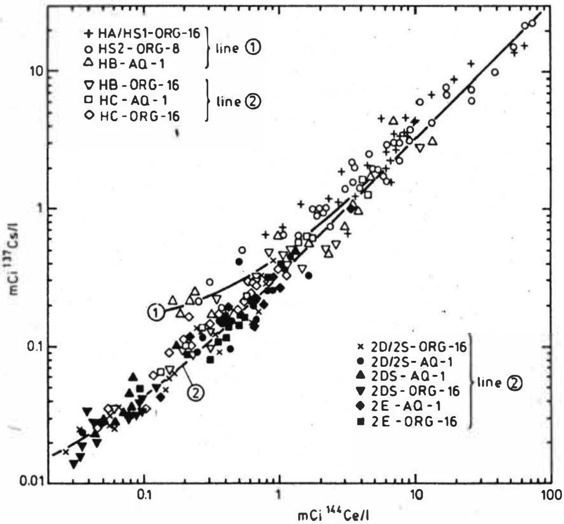

FIG. 4.

FIG. 2. The decontamination factor for ^{106}Ru in the organic outlet stages of the HA/HS1 and HS2 banks as a function of the solvent loading with U+Pu in the run 20.
FIG. 3. Examples of concentration profiles of ^{95}Zr (upper part) and ^{106}Ru (lower part) in the HA/HS1 and HS2 banks.
FIG. 4. Correlation between the radioactivities of ^{137}Cs and ^{144}Ce in various process streams of the 1st and 2nd cycle in the run 21. The solid lines were calculated from the equation on p. 4. 2D and 2E are the extraction and strip banks respectively in the 2nd uranium cycle.

Plutonium and Americium Extraction Studies with Bifunctional Organophosphorus Extractants

J. D. Navratil, Rockwell International, Rocky Flats Plant, Golden, CO/USA

Chemical processing activities at the Rocky Flats Plant (RFP) involve the recovery of plutonium from RFP scrap and residues (1). Nitric acid (7M) waste streams from aqueous plutonium processing operations contain 1-10 mg/l concentrations of plutonium and americium. The acid waste is sent through a secondary anion exchange process, and then to waste treatment where it is first neutralized with caustic and then processed through three stages of ferric hydroxide carrier precipitation (2). The resulting sludges are dried and drummed for off-site shipment and storage. The americium in the waste often times causes excessive radiation exposure to waste treatment operators. Furthermore, by reducing the actinide content of the waste and recovering additional amounts of plutonium, the stream might be able to by-pass waste treatment and go directly to a spray dryer for conversion to non-TRU nitrate salts. Therefore, processes to selectively remove and concentrate plutonium and amercium separately prior to waste treatment are being investigated. (The isolated americium could be placed in special casks for storage and the plutonium recycled in the process.)

Neutral bifunctional organophosphorus extractants, such as octylphenyl-N,N-diisobutylcarbamoylmethylphosphine oxide (CMPO) and dihexyl-N,N-diethylcarbamoylmethylphosphonate (CMP), are under study at RFP to remove plutonium and americium from the 7M nitric acid waste (3). These compounds extract trivalent actinides from strong nitric acid, a property which distinguishes them from monofunctional organophosphorus reagents. Furthermore the reagents extract hydroytic plutonium (IV) polymer which is present in the acid waste stream (4).

The compounds extract trivalent actinides with a 3:1 stoichiometry whereas tetra- and hexavalent actinides extract with a stoichiometry of 2:1. Preliminary studies indicate that the extracted plutonium polymer complex contains one to two molecules of CMP per plutonium ion and the plutonium(IV) maintains a polmeric structure (4). Recent studies by Horwitz and co-workers (5) conclude that the CMPO and CMP reagents behave as monodentate ligands.

At RFP, three techniques are being tested for using CMP and CMPO to remove plutonium and americium from nitric acid waste streams. The different techniques are liquid-liquid extraction, extraction chromatography, and solid-supported liquid membranes. Recent tests of the last two techniques will be briefly described. In all the experiments, CMP was an 84 percent pure material from Bray Oil Co. and CMPO was 98 percent pure from M & T Chemicals.

In the extraction chromatography tests, CMP was loaded onto the Amberlite XAD-4 as described previously (6), and the CMPO was loaded by melting it in the presence of the resin, mixing, and cooling. Fifty milliliter columns were used and feed was passed at 10 ml/min. to determine breakthrough capacities.

Preliminary studies indicated that CMP was not adequate to remove americium from nitric acid waste using an extraction chromatography mode; however, CMPO did an excellent job with the effluent americium concentration remaining below 10^{-4} g/l for 120 BV (bed volumns). For plutonium removal, both CMP and CMPO performed very well; 10 percent breakthrough was observed after 560 BV. However difficulties still remain in the elution of plutonium.

Solid-supported liquid membranes hold great promise for solving actinide removal and concentration problems. Consequently, amercium and plutonium transfer behavior was studied using laboratory-built hollow-fiber membrane modules. Two different hollow-fiber materials were used: Celanese Celgard and Armak Accurel. The Celgard fibers (10 per module) were 11.5 cm long, 0.04 cm I.D., with a 0.0025 cm wall thickness and 45 percent void volume.

Because of continuing problems with leaks, the Celgard fibers were replaced with thicker Accurel fibers (2 per module), also 11.5 cm long, 0.15 cm I.D., with a 0.1 cm wall thickness and 75 percent void volume.

The activity of americium as a function of time was followed by an on-line NaI(TI) gamma detector in conjunction with a multichannel analyzer operating in the multi-scalar mode.

The feed and strip solutions were recirculated through the membrane module until no further change in feed americium concentration was observed. The initial and final actinide concentrations were determinded radiometrically.

Preliminary studies indicated incomplete transfer of americium from 7.0 M $HNO3$ to 0.25 M $H_2C_2O_4$ at equilibrium through a membrane of undiluted CMP. The reason for 100 percent transfer is the co-transfer and build-up of nitric acid in the strip solution and consequent back-transfer of americium. The transfer of nitric acid was demonstrated in a separate experiment. Therefore, the transfer of americium(III) was studied as a function of nitric acid concentration at a total nitrate concentration of 7.0 M. Sodium nitrate was used to make up the balance of the nitrate. This procedure simulates a partial neutralization of a 7.0 M HNO_3 feed stream.

Table 1 summarizes the percent americium transferred as a function of nitric acid concentration. The greatest transfer is observed at the lowest concentrations of nitric acid, as expected.

Table 1. Percentage Transfer of Americium(III) through a Hollow Fiber Membrane of CMP as a Function of Feed Nitric Acid Concentration

$[HNO_3]$,M	$[NaNO_3]$,M	CELGARD	ACCUREL
7.0	0.0	46.8	60.9
5.0	2.0	55.2	64.0
3.0	4.0	75.5	75.9
2.0	5.0	87.2	--
1.0	6.0	96.8	90.2
0.1	6.9	92.8	94.0

The forward permeabilities were calculated and the results for the two modules agree well, showing an increase in permeability with decreasing acid concentration. The maximum permeabilities (1×10^{-3} cm/sec) are about the same as those determined for other metal ions in other systems using flatsheet membranes (7,8). These studies indicate the best conditions for americium transfer are 0.1 M HNO_3 plus 6.9 M $NaNO_3$. Actual waste streams may be brought to these conditions by adding the correct amount of sodium hydroxide. Studies of plutonium(IV) transfer under the same conditions indicate similar permeabilities, but a lower fraction transferred (70 percent).

Other experiments investigated changing the feed:strip (F:S) ratio using CMP on Accurel fibers with a 7.0 M HNO_3 feed and 0.25 M $H_2C_2O_4$ strip. Table 2 summarizes the results. A roughly linear relation between the F:S ratio and the concentration factor is shown. The concentration factor is less than the F:S ratio because some americium remains in the membrane at the conclusion of the experiment. A roughly inverse relationship between the ratio and the percent americium transferred is also observed, because of the increased concentration of acid in the strip solution.

Table 2. Effect of Feed:Strip Volume Ratio on the Transfer of Americium from 7.0M HNO_3 to 0.25M $H_2C_2O_4$ Through an Accurel supported CMP membrane.

FEED:STRIP	% TRANSFER
3:1	61
5:1	52
10:1	44

These studies have defined some of the operating conditions for using the promising new technology of solid-supported liquid membranes for the recovery and concentration of plutonium and americium from nitric acid feeds. Using CMP and CMPO in the extraction chromatography mode appears to have definite disadvantages over the use of conventional liquid-liquid solvent extraction contactors.

References

1. C. E. Baldwin and J. D. Navratil in Actinide/Lanthanide Separations, G. R. Choppin, J. D. Navratil and W. W. Schulz (Eds.) World Scientific Pub. Co., Singapore, 1985, p.226.

2. T. E. Boyd, R. L. Kochen, J. D. Navratil and M. Y. Price, Radioact. Waste Manag. Nucl. Fuel Cycle, 4, 195 (1983).

3. W. W. Schulz and J. D. Navratil, Sep. Sci. Technol., 19, 927 (1984-85).

4. A. C. Muscatello, J. D. Navratil and M. E. Killion, Sep. Sci. Technol., 18, 1731 (1983).

5. E. P. Horwitz, A. C. Muscatello, D. G. Kalina and L. Kaplan, Sep. Sci. Technol., 16, 417 (1981).

6. L. L. Martella, J. D. Navratil and M. T. Saba, in Actinide Recovery from Waste and Low Grade Sources, J. D. Navratil and W. W. Schulz (Eds.), Harwood Academic Pub., New York, 1982, p.27.

7. P. R. Danesi, E. P. Horwitz, G. F. Vandgrift, and R. Chiarizia, Sep. Sci. Technol., 16, 201 (1981).

8. P. R. Danesi, E. P. Horwitz, and P. Richert, Sep. Sci. Technol., 17, 1183 (1982).

The extraction of uranium (IV) from wet-process phosphoric acid in a centrifugal extractor

K.Grabas, Institute of Inorganic Technology and Mineral Fertilizers
Technical University of Wrocław, Poland

Uranium recovery process from the solution of wet-process phosphoric acid obtained by dihydrate method, according to the technology developed in the Institute (1), is based, at the first stage, on its isolation by the extraction method from the acid solution, initially utilized by adsorptive clarification. An extractant was applied, selectively extracting uranium on +4 oxidation state, because utilization of the crude acid, despite removing fine- crystalline suspension and the organic compounds contained in it, aims at correcting simultaneously the oxidation state of uranium present in the solution.
Correction of oxidation state is carried out with introduction of $FeSO_4$ $7H_2O$ to the solution, in the amount enabling total reduction of uranium.
The equimolar mixture of mono- and dinonylphenylphosphoric acids (NPPA) in kerosene solution is the extractant of U(IV) used in the process.

The aim of investigations

The aim of investigations was estimating usefulness of the centrifugal extractors of chamber type, for uranium (IV) extraction from wet-process phosphoric acid by kerosene solution of NPPA.
Uranium extraction in the technological system producing wet-process phosphoric acid is set between acid filtration and concentration. Thus the cubic capacity of the installation for uranium extraction is very important for the works being run. Application of the centrifugal extractors, distributing the emulsified solutions with centrifugal force, enables carrying out the extraction with great unit yield. Usefulness of this apparatus was tested, taking into account phase disengagement and mass exchange.

Experimental apparatus

In the investigations, two types of the extractors, based on the same construction and overall dimensions of the mixer and centrifuge, were used:

a) an apparatus in which the mixer agitator, the centrifuge and pump rotors removing solutions from the apparatus, are driven by a common shaft - this type was elaborated for the use of "Purex" process (2)

b) an apparatus in which both the agitator and the centrifuge have independent drives (3)

Flow-sheet of the research installation is presented in Fig. 1.
Feeding the extractor on wet-process phosphoric acid was carried out by a centrifugal pump of smoothly regulated flow intensity. Extractant solution was fed from the gravity tank (3). Indications of the rotameters (4) controlled flow intensities of the solutions.

The mixer

- internal diameter	40 mm
- maximum rotational speed	6000 turns/min
- total volume	35,6 cm^3
- volume of the upper chamber	14,0 cm^3
- turbine mixer	30mmx5mmx3mm

The separator

- internal diameter	75 mm
- maximum rotational speed	6000 turns/min
- volume	75 cm^3
- flow radius of the organic phase	16 mm
- flow radius of the aqueous phase	21 mm

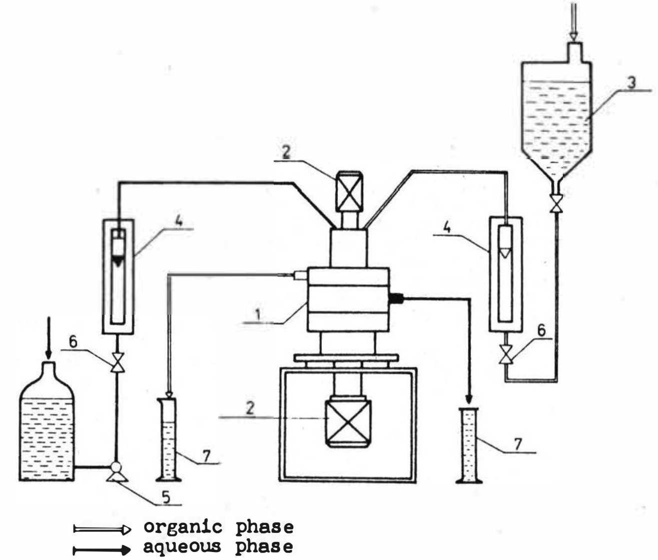

Fig. 1. Flow-sheet of the research installation
1-centrifugal extractor, 2-electric engine, 3-gravitative tank, 4-rotameter, 5-pump, 6-valve, 7-volume measurement

Methodology of conducting the investigations

The experiments were based on industrial solutions obtained from Marocco and Florida phosphorites. Crude acids were utilized by clarifying with mineral-carbon adsorbent, and correcting oxidation state of the uranium contained in them, by ferrous sulphate. The run of experiments was evaluated considering phase disengagement (purity of phases obtained at the apparatus output) and mass exchange estimating uranium extraction efficiency.

$$\psi = \frac{x_s - x_R}{x_s} \tag{1}$$

Uranium determination was performed by the spectrophotometric method - using colour reaction of U(IV) with Arsenazo III (4).
Equilibrium distribution coefficient D defined in the earlier experiments, is contained in the interval 24-95 (5), for the phosphoric acid of 26-32% P_2O_5 concentration. On the grounds of carried out investigations (6) the equilibrium distribution coefficient was presented in the form of a mathematical dependence (7)

$$D = b_o + \sum_{i=1}^{k} b_i z_i + \sum_{i=1}^{k} b_{ii} z_i^2 + \sum_{i=1}^{k} b_{ij} z_i z_j \tag{2}$$

where particular variables are:

z_1- wet-process phosphoric acid concentration (% P_2O_5)

z_2-NPPA concentration (M)
z_3-temperature (^oC)
z_4-introduced Fe(II) concentration (%)

A list of coefficients from the equation (2) is presented below:

TABLE 1. Coefficients of the equation (2)

b_i	b_o	b_1	b_2	b_3	b_4
	-372,94	-13,46	11238	-10,94	651,2
b_{ii}		b_{11}	b_{22}	b_{33}	b_{44}
		0,771	666,6	-0,0648	-985,9
b_{ij}		b_{12}	b_{13}	b_{23}	b_{34}
		-397,9	0,541	10,58	-2,72

Application of the above equation to the system being investigated, with the value of coefficient D calculated makes it possible to search for a theoretical number of stages and to settle the relationship between the extraction efficiency ψ, the extraction coefficient and the number of stages n.
The extraction coefficient ε is defined by the equation:

$$\varepsilon = D \frac{\vartheta_E}{\vartheta_R} \tag{3}$$

Dependence of thb extraction efficiency coefficient ψ in a single-stage is defined by the equation:

$$\psi = \frac{\varepsilon}{\varepsilon + 1} \tag{4}$$

and in a counter-current battery by the equation:

$$\psi = \frac{\varepsilon^{n+1} - \varepsilon}{\varepsilon^{n+1} - 1} \tag{5}$$

The run of experiments

Having settled the hydrodynamic equilibrium in the centrifugal extractor, the samples of both phases were collected in measuring cylinders, in which phase disengagement and uranium concentration were determined. General efficiency η was calculated as the ratio of extracted uranium to the amount theoretically possible. Table 2 presents the results of investigations conducted in the apparatus in which the agitator and the centrifuge are fixed on a common shaft. The experiments were carried out in a single apparatus as well as in a two-stage counter-current battery. Extraction of uranium was accomplished from phosphoric acid obtained from Marocco phosphorite.
Incomplete phase disengagement is a crucial disadvantage of the apparatus. The aqueous phase constituted the contaminated phase. In the collected samples the phase disengagement efficiency was defined as voluminal ratio of the aqueous phase to the total volume of the sample. Particular investigations on the phase disengagement in this apparatus and the battery are presented in the paper (8).

TABLE 2. Results of uranium extraction from wet-process phosphoric acid 0,16M NPPA at the temperature $20 \pm 2\,^{\circ}C$

Number of stages n	Phase ratio ϕ	Average retention time τ	Amount of introduced Fe(II)	Revolutions frequency ω	Equilibrium distribution coefficient D	Extraction efficiency ψ		Separation efficiency of the aqueous phase φ	General efficiency η
						analytical	equilibrium		
		s	%	s^{-1}				%	%
1	0,166	3,55	0,19	40	106,3	0,89	0,95	99,6	93,7
	0,164	5,8				0,92	0,94	99,9	97,9
	0,066	3,56				0,69	0,88	99,5	78,4
	0,06	5,95				0,74	0,86	99,8	86,0
2	0,169	5,83	0,04	40	88,3	0,343	0,937	97,3	36,6
	0,084	6,26		40		0,422	0,88	99,8	48,8
	0,173	5,88		30		0,365	0,939	97,6	38,9
	0,116	4,15		30		0,28	0,911	99,4	30,7

TABLE 3. Results of uranium extraction from wet-process phosphoric acid 0,16 M NPPA

Ordinal	Phase ratio ϕ	Average retention time τ	Temperature t	Amount of introduced Fe(II)	Revolutions frequency of the agitator ω_m	Revolutions frequency of the centrifuge ω_s	Equilibrium distribution coefficient D	Extraction efficiency ψ analytical	Extraction efficiency ψ equilibrium	General efficiency η
		s	°C	%	s^{-1}	s^{-1}				%
1.	0,153	1,95	29,0	0,66	28,8	76,6	53,0	0,325	0,89	36,5
2.	0,152	1,87			55,8	77,5		0,341	0,89	36,3
3.	0,078	0,94			56,6	91,7		0,204	0,81	25,2
4.	0,162	1,92	28,5	0,1	29,0	76,6	66,15	0,118	0,91	13,0
5.	0,163	2,0			56,6	76,6		0,274	0,91	30,1
6.	0,059	0,91			56,6	91,7		0,137	0,80	17,1
7.	0,156	1,99	27,0	0,13	29,2	76,6	74,31	0,230	0,92	25,0
8.	0,16	1,96			55,0	76,6		0,377	0,92	41,0
9.	0,077	0,91			56,6	91,7		0,211	0,85	24,8
10.	0,086	1,01			33,3	93,3		0,135	0,865	15,6
11.	0,151	1,87	35,0	0,2	30,0	76,6	99,1	0,303	0,937	32,3
12.	0,155	1,89			56,6	76,6		0,364	0,939	38,8
13.	0,071	0,92			46,6	98,3		0,154	0,876	17,6
14.	0,149	1,79	40,5	0,33	29,3	76,6	101,6	0,466	0,938	49,8
15.	0,147	1,83			61,6	76,6		0,525	0,937	56,0
16.	0,055	0,92			58,3	91,7		0,230	0,848	27,1

Results of investigations conducted in the apparatus with independent drive of the agitator and the mixer are presented in Table 3. Uranium extraction was carried out basing on the acid obrained from Florida phosphorite. Over the entire range of parameters used in the process, full phase disengagement was observed.

Discussion of the results

The centrifugal extractor with independent drive of the centrifuge and the agitator affords possibilities for complete phase disengagement of the extraction system used in the experiments over the investigated range of parameters. The apparatus of this type, thanks to the ability of intensifying the centrifuge run, is more advantageous than the type in which the centrifuge and the agitator are fixed on a common shaft. In the first type, conditions of the apparatus operation, optimum for the phase disengagement, were to be found (obtainment of definite emulsification of the dispersed phase considering the distributive ability of the centrifuge). General efficiency of the extraction results from the efficiency of three processes: mixing, phase disengagement, and mass exchange. The applied mixing system enables intensification of the stirring processes and the time of retention in the mixer should be chosen according to the kinetics of mass transfer. The presented results show that contact time of phases in the mixer lesser than 3,5 s, and emulsion dispersion, are insufficient for the extraction to be run in the proximity of equilibrium, with the assumption that the calculated equilibrium distribution coefficients are close to real ones. Over the range of parameters investigated in the experiments, mass transfer of uranium in the complex with NPPA, occurred from the compact phase (phosphoric acid) to drops and no inversion of emulsion was observed. The following parameters have a crucial influence on the uranium extraction yield:

- reduction potential of the solution - concentration of the introduced Fe(II)
- the period between introduction of Fe(II) and completion of the attempts
- phase ratio.

The carried out investigations proved the possibility of using the centrifugal extractors for the process of uranium recovery from wet-process phosphoric acid.
The kinetics of extraction conducted in the centrifugal apparatus requires, however, further investigation.

Denotations

b - coefficient
D - equilibrium distribution coefficient
n - number of stages
t - temperature
x - component concentration
ν - flow intensity
z - variable, parameter
ε - extraction coefficient
η - general efficiency
ψ - extraction efficiency, equation (1)
φ - separation efficiency of the aqueous phase
ϕ - phase ratio (of the organic to aqueous phase)

Indexes

c - concerns the centrifuge
E - concerns the extract
i, j, u - the number of index

m - concerns the mixer
R - concerns the raffinate

Literature

1. Pat. PL 127814 (1981)
2. Pat. PL 99080 (1978)
3. Pat.App.PL 248469)1984)
4. Górecki H., Górecka H., Talanta 31 (1984) 459
5. Górecki H., IAEA Conference "Advances in uranium are processing and recovery from non-conventional resources" IAEA-TC-491/11 Vienna, 1985
6. Górecka H., Badania nad odzyskiem uranu z ekstrakcyjnego kwasu fos - forowego, Ph.D.thesis, Wrocław 1982
7. Górecki H., Sielicki A., Wójcik T., Raport SPR 40/85 Instytutu Technologii Nieorganicznej i Nawozów Mineralnych Politechniki Wrocławskiej, Wrocław 1985 (unpublished)
8. Górecki H., Grabas K., Hoffmann P., Rogoziński W., Inż.Chem.i Proc. (in press).

SEPARATION OF LONG ALPHA EMITTERS FROM MEDIUM ACTIVITY LIQUID WASTES BY SOLVENT EXTRACTION WITH TRI BUTYL ACETO HYDROXAMIC ACID (TBAH)*.

Maurizio Casarci, Dino Carlini, GiulioMaria Gasparini, Giuseppe Grossi, and Giancarlo Torri.

ENEA - Fuel Cycle Dept. C.R.E. Casaccia P.O. Box 2400 00100 Rome (Italy).

* Work performed in the frame of the 2nd Five Years Plan of European Community on "Management and Disposal of Radioactive Wastes", under contract n°WAS 175-81-31-(S).

The elimination of long lived highly radiotoxic nuclides (essentially TRU elements) from radioactive wastes is of great interest, since it would make their management easier and safer.

Among different possible techniques only chemical precipitation and ion exchange have found more diffused industrial applications.

In spite of these applications, the problem is far from being solved and considerable improvements have to be reached in order to obtain higher decontamination factors and volume reductions.

During recent years researches have been addressed in this direction with the aim to improve the performance of inorganic ion exchangers (1) or to couple the chemical precipitation with some more sophisticated liquid-solid separation technique such as the ultrafiltration (2) with sometimes interesting results. But separations due mainly to physical effects, like coprecipitation or to chemical reactions, like ion exchange, appear not to be furtherly improved.

In our opinion it is possible to obtain a substantial improvement, by taking advantage of the strong complexing capacity of special chelating substances. These substances can capture selectively the radioactive nuclides and form a nonpolar complex soluble into organic diluents, or simply insoluble in water.

As a consequence, liquid extraction, selective precipitation and, in special cases, extraction chromatography could give a valid contribution to the problem of waste treatment, as they have the potential capacity to reach very elevated decontamination factors ($> 10^4$).

Studies on complexing substances expecially prepared for actinides are in progress in many laboratories.

In the past years we have investigated some Tri alkyl aceto hydroxamic acids:

$$(Alkyl)_3C-C(O)NHOH.$$

These compounds are powerful complexing agents of Plutonium in acidic conditions (0.1-1 M HNO3) and, in these conditions, exhibit an elevated selectivity, because only Vanadium, Iron, Molybdenum, Zirconium and Niobium are complexed.As an example of the performances of typical hydroxamic acid(Tri n Butyl Aceto Hydroxamic Acid,TBHA), **Table 1** shows its extracting behavior at different acidities..

Unfortunately the hydroxamic acids show a poor stability in presence of nitrous acid (which is always in equilibrium in a nitric solution of radioactive ions) and a practical separative application requires the use of large amounts of nitrous acid scavengers (urea,hydrazine etc).

These shortcomings are avoided when the nitric acid is absent.

We have proposed the employ of these compounds to treat the alkaline wastes coming from the regeneration of the solvent utilized in a reprocessing plant using a classical Purex flow-sheet.

These radioactive effluents,responsible for important losses of Plutonium, have the average chemical composition reported in **Table 2.**

As extractant we have utilized the Tri Butyl Aceto Hydroxamic Acid (TBHA):

$$(C_4H_9)_3-C-C(O)NHOH$$

This is a solid compound, prepared by an Italian producer (3), very stable at room temperature.Its characteristics are given in **Table 3.** Its chemical and extractive properties have been deeply investigated and reported elsewhere(4).

A 0.1M Tri Butyl Aceto Hydroxamic Acid solution in Di Ethyl Benzene (isomers mixture) and 10% of 1 Octanol has been choosen as extracting organic solution.

The stripping solution is a 0.35M Oxalic Acid buffered at pH 2.2.

The flow-sheet proposed is illustrated in **Fig 1.**

This flow-sheet is based on the following considerations:

- From these alkaline liquid wastes, hydroxamic acids extract only TRU elements and the couple Zr95-Nb95. Frequently, with aged solutions, this couple is not present and the extraction with an hydroxamic acid permits the selective separation of the alpha emitters Plutonium ,Americium and Neptunium.

- In these conditions Uranium is not extracted in account of the antagonistic action of the carbonate ions.
- Sr^{90}, Ru^{106}, Cs^{134}, Cs^{137}, Sb^{125}, usually present in these effluents, are not extracted by the hydroxamic acid.
- A stripping section with a concentrated Oxalic Acid solution, permits the quantitative reextraction of these elements and the utilization of the organic solution for a new extraction cycle.
- With a suitable adjustement of the two phases ratios both in the extraction and in reextraction sections and from the calcination of the oxalic solution, it is possible to foresee a substantial volume reduction.

The main uncertainties of this procedure have been:

- The presence of TBP and of its degradation products in the aqueous wastes could interfere with the extraction procedure and could generate antagonistic effects and, as a consequence, lower decontamination factors.
- In carbonate solutions,Plutonium might be present in a hardly extractable chemical status(polymerized species).
- The extraction kinetics,in a carbonate solution,could be too slow to permit practical applications.

Discontinuous tests using alkaline wastes, produced in the La Hague plant, have been carried out.(5)For these tests 15 ml of the aqueous solution, having the composition given in **Table 4**, have ben shaken with the same volume of the organic solution; after the centrifugation and the separation of the two phases, the distribution coefficients for Plutonium, Ruthenium, and Antimony have been determined.The aqueous phases have been extracted a second time with a fresh organic solution, in order to verify the overall decontamination factors;at the same time the reextraction step has been tested on the charged organic solution, which has been shaken with the oxalic acid solution.

The results of these tests,given in **Table 5**, show that the decontamination factors after two extractions are high and demonstrate the potential advantages of these techniques,involving the formation of strong complexes,compared to other methods, based mainly on a physical mechanism or on a weak and not specific chemical bond.

On the other side, the reextraction tests permitted to verify the complete recovery of the alpha activity in the stripping solution.
During these tests the two phases remained clear and no formation of a solid or liquid third phase has been observed.

Discontinuous and continuous tests have been carried out with simulated traced solutions in order to observe the effect of the TBP degradation products on the decontamination factors and to verify the overall flow-sheet in mini scale mixer settlers.

The results of these tests (**Table 6**)have shown that:

- An elevated decontamination factor can be reached both for alpha and for beta-gamma emitters.
- The Plutonium traced solutions prepared in our laboratory,contain variable amounts of unextractable nuclide,which decreases the extraction performances at these experimental conditions.
- Amounts, greater than 500 mg/l of the TBP degradation products, can affect the decontamination coefficients. The extraction kinetics is sufficiently fast also in a carbonate medium.
- The volume reduction reached with mini mixer settlers has been at least 10. This is only a demonstrative value, as, with larger mixer settlers, this value can be considerably increased; the real limitation to a very elevated reduction of the volume,is the saturation of the oxalic solution with other metal impurities.
  To obtain a further volume reduction it is convenient to envisage a calcination section permitting to destroy the oxalate complexes and to obtain the radionuclides in an oxide form.
- The organic phase, before reutilization, must be washed with water to eliminate little amounts of oxalic acid equilibrated in the reextraction section.

A simple equipment is necessary for the treatment,which can be contained in a hot cell.Mixer settlers for the extraction,reextraction and solvent regeneration are foreseen,following the general setup illustrated in **Fig.1**.

References

1) R.G.GUTMAN et al."Radioactive Waste Management and Disposal"2th European Community Conference 22-26 April 1985;and private communications.

2) J.F.DOZOL,S.EYMARD,R.GAMBADE,G.LA ROSA;CEA RT DRDD n°56 (1985)(Private communications)

3) PROCHIMICA s.r.l. via Baini 57; 27020 Trivulzio (Parma).

4) a)G.M.GASPARINI, Proc.of the Inter. Solvent Extraction Conf. (ISEC 77) Toronto p 654 (1977). b) G.M.GASPARINI,Gazz.Chim;Ital. 109 237 (1979).

5) These experiments are carried out under contract CEE at the" Service des Effluents et des Dechets de Faible et Moyenne Activité" at the CEN de Cadarache (France)

Aknowledgments:

The authors are indebted for the helpful contribution of M G.Puzzuoli and A.Tieri

Tab 1. Extraction behaviour of hydroxamic Acids.
100 % Extraction with 0.1 M TBHA in Di ethyl benzene

(metal ions in trace at the stable valence state)

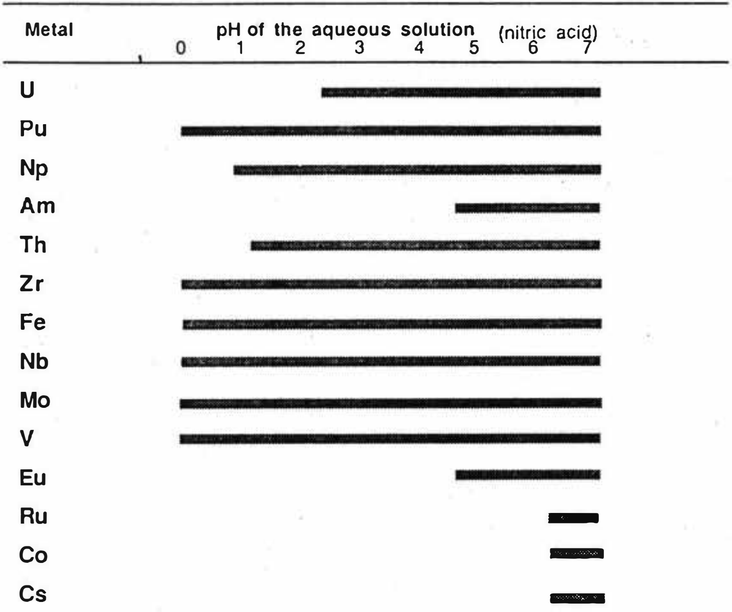

Table 2. Reference composition of an alkaline solution obtained by the regeneration section of a reprocessing plant using TBP.

Na_2CO_3	0.2 M
$NaNO_3$	0.1 M
DBP + MBP	100 mg/l
Uranium	0.5-2 g/l
TRU elements	0.5-2mCi (8-30 mg Pu^{239}/l)
Fission Products. (Ru/Rh-Zr/Nb-Sb)	1-5 mCi/l (ß activity)

Tab 3. Characteristics and solubility of the Tri n Butyl Aceto Hydroxamic Acid (TBHA).

Formula	MW	MP (°C)	Colorimetric Purity
$(nC_4H_9)_3C(O)NHOH$	243.4	132-3	98%

Solvent	mmmoles/l	Solvent	mmoles/l
ethyl alcohol	10^3	mesitylene	32
chloroform	440	n heptane	2.1
carbon tetrachlor.	43	water	0.07
benzene	76	1M nitric ac.	insoluble
xylene	62		

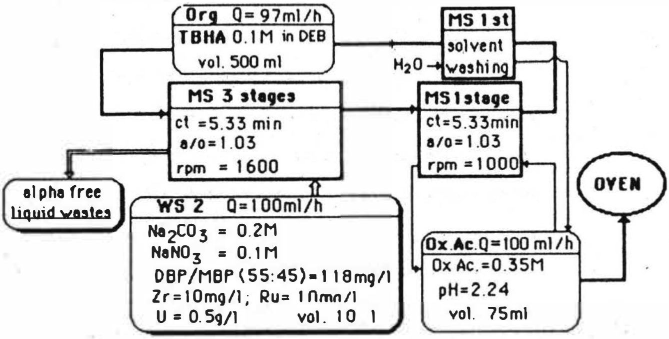
Org Q= 97ml/h
TBHA 0.1M in DEB
vol. 500 ml
MS 1st
solvent washing
H_2O
MS 3 stages
ct =5.33 min
a/o=1.03
rpm = 1600
MS 1 stage
ct=5.33min
a/o=1.03
rpm =1000
alpha free liquid wastes
WS 2 Q=100ml/h
Na_2CO_3 = 0.2M
$NaNO_3$ = 0.1M
DBP/MBP (55:45)=118mg/l
Zr=10mg/l; Ru= 10mg/l
U = 0.5g/l vol. 10 l
OVEN
Ox.Ac.Q=100 ml/h
Ox Ac.=0.35M
pH=2.24
vol. 75ml

Fig 1. Flow-sheet and experimental conditions

Q=flow rate; ct= contact time; o/a=phase ratio; rpm= mixer speed; MS mixer settler

Tab 5. **Results of experiments with an alkaline solution of the La Hague plant** (discontinuous tests).

	DF	Residual Activity
Extraction		
	$Pu^{239+240}$	
First extraction	= 100-136 (*)	0.045-0.06 KBq/ml
Second extraction	= 1300(*)	0.006 KBq/ml
	Pu^{238}	
First extraction	= 93(*)	0.024 KBq/ml
Second extraction	= 104(*)	0.008 KBq/ml
Reextraction		
Complete	(no alpha activity into the organic phase)	

(*) These values are dependent on the initial activity

Table 6. Results of the experiments with simulated traced solutions.

Extraction in batch		Extraction in a 6 stages mixer settler	
DF		gross alpha DF	Residual activity
Pu^{239}	> 100	First cycle = 12	variable (depends on the preparation method)
$Zr^{95}(Nb^{95})$	> 100		
Rare Earths	> 100	Second cycle = 21	
Reextraction		Reextraction	
Complete for Pu and Zr 20% for Nb		Complete for gross alpha	
		Volume reduction	
		> 10	(depends on the total ions extracted and on the equipment size)

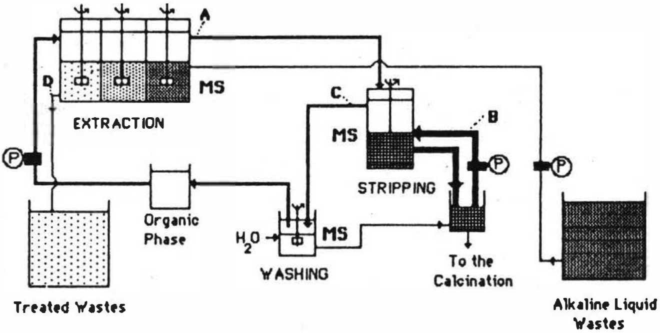
A
D
MS
EXTRACTION
C
B
MS
STRIPPING
P
P
P
Organic Phase
H_2O
MS
WASHING
To the Calcination
Treated Wastes
Alkaline Liquid Wastes

Fig 2. Experimental setup

P=pump; A,B,C,D = sampling points; MS= mixer settler.

Preconcentration of Uranium by Membrane Extraction with Di-2-ethylhexylphosphoric Acid

F.Macášek, P.Rajec, Vu Ngoc Anh, V.Řeháček, Department of Nuclear Chemistry,
Comenius University, 842 15 Bratislava, Czechoslovakia

The separation of uarnium by liquid membranes was developed both for supported [1-3] and emulsion [4-12] membranes containing a complexing carrier for uranium species. As the carrier various solvating and chelating agents were used : di-2-ethylhexylphosphoric acid, DEHPA [3-6,9,10,12,13] ,trioctylphosphine oxide, TOPO [12] and their mixtures [4, 6,7] , tertiary amines, TOA [1] , KELEX ^{R}100 [5,8-10,12] , 8-hydroxyquinoline [8,11] and LIX ^{R} 63 [7].

In our previous works [8-10] we demonstrated that the emulsion liquid membranes would be efficient, if such the composition of membrane and internal (stripping) solution is chosen, when a solute is obtained mainly in the inner solution and the membrane extraction is equivalent to several (N) stages of extraction with the membrane solvent alone. In this respect the membrane extraction by the emulsion of 0.18-0.36 M DEHPA and 0.05-0.09 M TOPO with 5-8 M H_3PO_4 and $FeCl_2$ [4,6] or by 0.015-0.18 M DEHPA with 0.1-2 M HNO_3 [13] gives multiplication factor N about 3.5 in the first case and hardly exceeds unity in the last systems. It was obtained that the emulsions with TOPO and TOA do not suit well for membrane extraction because of rapid proton transfer between the internal and feed solutions [8-10] which occurs even in absence of the solvating carrier [12] . As the most perspective for uranium pertraction, there were substantiated the systems with DEHPA carrier in dodecane and 1-2.5 M H_2SO_4 or H_3PO_4 as the encapsulated stripping agents [12]. The emulsions with sulfuric acid, as the less diffunding strippant, were preferred for uranium leach solutions [5] while those with phosphoric acid were chosen and examined for treatment of large-volume analytical samples. Our goal consisted in a rapid, single-step preconcentration of 20-50 l samples with a factor about 100-500.

Experimental

The advantages of membrane extraction as a preconcentration technique were investigated in the three-phase systems : acidic water solutions (phase I, feed) - DEHPA in dodecane (phase M, membrane) - H_3PO_4 solution (phase II, strippant). The preparation of the emulsions and extraction in double emulsion systems, as well as other experimental details have been reported elsewhere [8,10,13,14]. Kinetic measurements were made in a 1000 ml cylindre provided with a four-blade agitator, modeling a head of pilot preconcentration column [14]. At appropriate time intervals the agitation was stopped and after a short-time settling the samples were withdrawn and analysed for uranium content spectrophotometrically by Arsenazo III. To establish uranium distribution , when necessary, the emulsion was broken in external field of electric spark of a vacuum tester.

Results and Discussion

The pertraction of phosphoric acid from 0.1 M inner solution to 0.1 M NaCl outer solution, at a volume ratios $V_{II} : V_M : V_I = 5 : 5 : 100$, through the membrane consisting from n-dodecane and 3 % SPAN 80 and SPAN 85 (2:1) emulgator, proceeded with a half-time about 115 min, i.e. it is close to that of perchloric acid in the series [12] : $HNO_3 < H_3PO_4$, $HClO_4 < HCl \ll H_2SO_4$. Though the permeation may become a source of trouble at technological applications, we believed that it would not be a problem in the analytical preconcentration, with a part of phosphoric acid going to raffinate. Hence, all the results were obtained with 2.5 M H_3PO_4 as a strip acid in internal solution. No advantage was found in application of DEHPA + TOPO synergestic mixtures used earlier [4,6] because TOPO increases the proton transfer dramatically.

A summary of the data taken from batch experiments is given in Table 1. A comparison of the yields obtained at relatively low DEHPA concentrations shows that the membrane extraction is sufficient to meet the efficiency demands at various and typical composition of feed solutions (salinity, pH) and DEHPA concentration in membrane.

At the first approximation, the kinetics of the process, expressed as a function of the yield of recovery (R) vs. time follows, at a large pertraction factor, the equation [9]:

$$V_I \log (1-R) = -k' t \qquad (1)$$

where V_I is the volume of outer solution and k' is an apparent rate constant. Varying V_I within the ratio $r_I^{-1} = V_I / V_M = 20 : 1$ to $200 : 1$, the value $k' = 1.33 \pm 0.30\ s^{-1}$ was obtained for the systems with 0.005 M DEHPA and 6.7×10^{-3} M uranium in feed of batch experiments (Fig.1). At the low carrier concentrations, however, the pertraction proceeds, at least from the start, in a regime of saturation of the outer interface with uranium, which can be approximated by a Langmuir type isotherm [15] and instead of Eq.(1) there is a mixed first- and zero-order kinetics given by a Langmuir-Hinshelwood type equation [15]

$$(1/D_o) \log(1-R) - 0.43\, q_o r_I R = -\, k_h t \qquad (2)$$

where k_h is a hydrodynamically dependent rate constant, D_o is a maximal distribution ratio of uranium at the outer boundary and q_o is the molar ratio of uranium and DEHPA ($q_o = 2\, c_U V_I / c_{DEHPA} V_M$, $r_I = V_M / V_I$) . This change of first-order kinetics, indicated by Fig.2, should be obvious for a stoichiometrically low (substoichiometric) carrier concentrations when the capacity of emulsion is ensured by the internal stripping solution.

Because the systems met both static, economic and dynamic demands [15] for a successful performance in column conditions, the emulsions were applied for preconcentration of uranium spiked water solutions . For the samples of 10 - 50 litres, passed through a pilot column [14] the desired results were obtained - Table 2. The fact that uranium can be concentroted with about 98 % yield from 50 l volumes within 4 hours and by a preconcentration factor about 300, is of a great importance for radiochemical analysis and encouraging for uranium recovery from low-grade sources.

It confirms therefore that the membrane extraction has tremendous potential as a rapid technique for preconcentration of uranium and other elements, and theoretical preconditions of the first-approximation models of the process pseudo-equilibrium and dynamics were verified at the carrier con centrations where no solvent extraction would occur to a considerable extent. The only practical limitations of the process ensue from interfacial phenomena and rheological properties of the emulsions applied.

References

1. W.C.Babcock, R.W.Bakes, E.D.La Chapelle, K.L.Smith, J.Membr.Sci. 7, 71 (1980).
2. T.J.Hardwick, P.O.Drower, In: Proc. Int. Solv. Extraction Conf. ISEC'83, p.297, Am.Inst.Chem.Eng., Denver 1983.
3. K.Akiba, T.Kanno, Talanta 32, 824 (1985).
4. J.W.Frankenfeld, N.N.Li, R.L.Bruncati, U.S.Patent 1 596 410 (Cl.27.12.1976).
5. F.Macášek, P.Rajec, V.Řeháček, Czechoslov. Pat. 231 779 (Cl.20.9.1982).
6. H.C.Hayworth, W.S.Ho, W.A.Burns,Jr., N.N.Li, Sep.Sci.Technol. 18, 493 (1983).
7. K.Akiba, T.Takahashi, T.Kanno, Bull.Chem.Soc.Japan 57, 2618 (1984).
8. F.Macášek, V.Mikulaj, P.Rajec, R.Kopunec, A.Švec, Final Report IAEA Contract 2662/RB, Comenius University, Bratislava 1984.
9. F.Macášek, P.Rajec, R.Kopunec, V.Mikulaj, J.Mišianik, In: Proc. Int. Solv. Extraction Conf. ISEC'83, p.62, Am.Inst.Chem.Eng., Denver 1983.
10. F.Macášek, P.Rajec, R.Kopunec, V.Mikulaj, Solv.Extr.Ion.Exch. 2, 227 (1984).
11. F.Macášek, R.Kopunec, J.Radioanal.Nucl.Chem.Lett. 86, 347 (1984).
12. F.Macášek, P.Rajec, V.Řeháček, Vu Ngoc Anh, T.Popovňáková, J.Radioanal.Nucl.Chem. Lett. 96, 529 (1985).
13. S.Weiss, A.Castaneda, In: Proc. 5th Summer School Model. Heat and Mass Transfer Processes and Chem.Reactors, p.149, Bourgas 1985.
14. V.Mikulaj, P.Rajec, A.Švec, Chem.listy, in press
15. F.Macášek , First Intern. Conf. on Separation Science and Technology, New York, April 15-17, 1986.

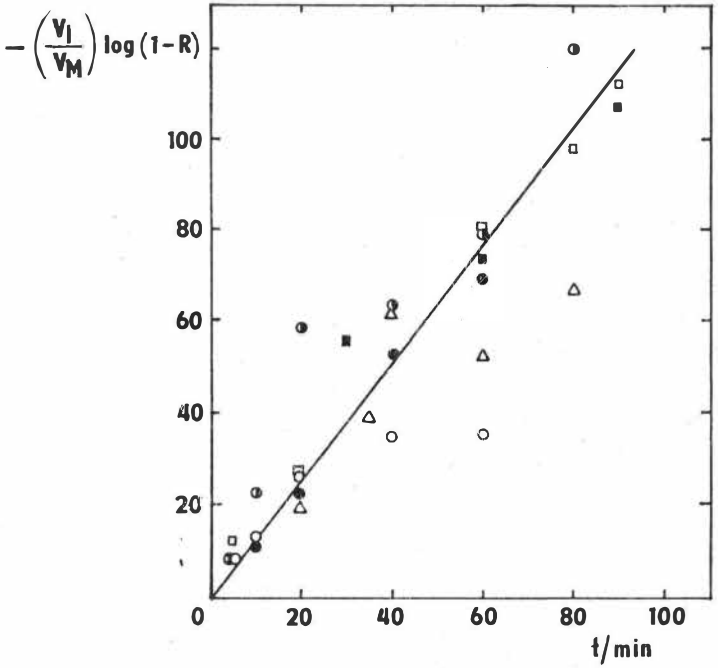

FIGURE 1.

Emulsion membrane extraction of uranium with 0.005 M DEHPA in n-dodecane from various volumes (V_I) of feed solution (6.7×10^{-3} M uranium in 0.01 M HNO_3)

	$V_I : V_M$
○	1 : 20
●	1 : 40
◐	1 : 60
□	1 : 80
△	1 : 100
■	1 : 200

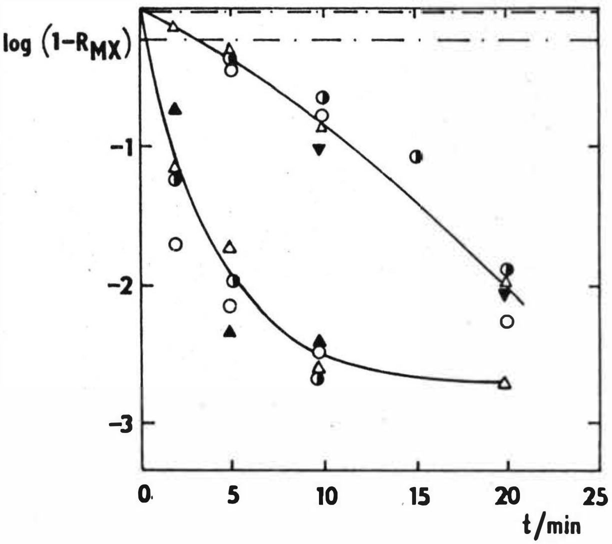

FIGURE 2.

Emulsion membrane extraction of uranium

Outer solution : 6.7×10^{-3} M uranium in 0.01 M HNO_3

Membrane : 0.005 M DEHPA (upper curve) or 0.05 M DEHPA (lower curve) in n-dodecane, stabilized by 3 % SPAN 80

Internal solution : 2.5 M H_3PO_4

Volume ratios : $r_I = V_M/V_I = 0.1$; $r_{II} = V_M/V_{II} = 1.0$

Concentration of NaCl in outer solution :

△ 0

● 0.5 M

○ 2.0 M

▼ 2.5 M

TABLE 1. Membrane extraction of uranium in batch conditions (volume ratio feed to membrane = 10 : 1)

Liquid membrane : di-2-ethylhexyl-phosphoric acid (DEHPA) + 3 % SPAN 80 in n-dodecane

Internal solution : 2.5 M H_3PO_4 , volume ratio $r_{II} = 1$

Feed solution : 6.7×10^{-3} M uranium in 0.01 M HNO_3 and various concentration of NaCl

No	NaCl in feed ($mol.dm^{-3}$)	DEHPA in membrane ($mol.dm^{-3}$)	Time (min)	log (1-R)	uranium content in membrane (%)	in stripping (%)
1	0.0	0.100	10	-2.39	17.6	82.1
2	0.5	0.1	10	-2.44	19.2	80.1
3	1.0	0.1	10	-2.54	18.7	80.0
4	2.0	0.1	10	-2.53	15.2	84.1
5	1.0 Na_2SO_4	0.1	10	-1.20	-	-
6	0.0	0.05	10	-2.41	8.7	90.9
7	0.5	0.05	10	-2.66	8.7	91.0
8	1.0	0.05	10	-2.61	9.9	89.6
9	0.05	0.05	10	-2.45	8.6	91.0
10	0.0	0.01	10	-2.69	1.8	98.0
11	0.5	0.01	10	-2.34	3.5	96.2
12	1.0	0.01	10	-2.31	4.3	95.2
13	2.0	0.01	10	-2.53	3.7	95.7
14	2.5 $NaNO_3$	0.01	10	-2.34	5.5	94.0
15	0.0	0.005	10 (20)	-0.86 (-1.93)	0.9	98.8
16	0.5	0.005	10 (20)	-0.65 (-1.69)	0.9	98.9
17	2.0	0.005	10 (20)	-0.83 (-2.27)	1.2	98.5
18	2.5	0.005	10 (20)	-1.39 (-1.99)	1.5	98.2

TABLE 2. Membrane extraction of uranium in dynamic conditions of a pilot preconcentration column.

Liquid membrane : 0.01 M DEHPA + 4 % SPAN 80 in n-dodecane
(a) 103 ml , (b) 52 ml
Internal solution : 2.5 M H_3PO_4 , volume ratio $r_{II} = 1$
Feed solution : 1 M NaCl solution spiked with uranium, flow rate 12 dm^3/hour

No	Feed volume (dm^3)	Uranium ($mol.dm^{-3}$)	Time (min)	Final volume of internal solution (ml)	Final concentration of H_3PO_4 (M)	Material balance of H_3PO_4 (%)	Concentration factor of uranium	Yield (%)
1	5	7.56×10^{-6}	25	133 [a]	1.87	-3.4	38	82.3
2	15	2.52×10^{-6}	75	152 [a]	1.59	-6.2	99	87.0
3	25	1.52×10^{-6}	125	170 [a]	1.46	-3.6	147	103
4	35	1.08×10^{-6}	175	220 [a]	1.10	-6.0	159	102
5	45	0.94×10^{-6}	225	152 [a]	1.66	-2.0	300	97.6
6	25	7.56×10^{-7}	125	70 [b]	-	-	357	93.0

The Influence of Plate Surfaces on the Hydrodynamics of Pulsed Plate Columns

W Batey, S J Lonie, P J Thompson, J D Thornton, Caithness/UK

Introduction

Pulsed plate liquid-liquid extraction columns are being used increasingly in the nuclear industry for the reprocessing of irradiated nuclear fuels. The growing interest in this field has led to a study being carried out at the Dounreay Nuclear Establishment (DNE) into the hydrodynamic behaviour of two immiscible liquids in a pulsed column in the absence of mass transfer. Many factors influence the hydrodynamic characteristics of a pulsed column. Surface effects at liquid-liquid interfaces and liquid-solid boundaries influence the behaviour of the equipment. Variations in column geometry, materials of construction, and operating conditions can dramatically change column performance. In order to obtain a full understanding of the behaviour of droplets in a pulsed column it was decided to examine at DNE both the motion of the droplets in a second immiscible liquid phase and to study the effects of changing flowrates, pulse velocities and surface properties. Furthermore, an attempt has been made to obtain non-empirical correlations between the various measured parameters. (1, 2).

Equipment

The column consisted of three 3 ft sections of 3 in diameter precision bore borosilicate glass pipeline fitted with 3 ft settling sections at each end. The sieve or nozzle plates were spaced at 2 in intervals in each of the three main column sections and were manufactured from ⅛ in stainless steel sheet; each sieve plate was drilled with ⅛ in holes set in a triangular pitch to give a free area of 25% whereas in the nozzle plates, with the same diameter, free area and perforation size, each perforation came from a nozzle of base 0.23 in at an angle of 54.2° to the plate surface.

The column was air-pulsed in the usual way by applying a fluctuating air pressure to a 1 in diameter leg connected to the bottom of the column. The pulse waveform was monitored over a range of frequencies and amplitudes by means of an electrical conductivity probe located in the top liquid-liquid interface. The pressure drop across the pulse leg was adjusted until the waveforms were sinusoidal.

Droplet sizes were recorded photographically for a range of flowrates, pulse frequencies and amplitudes both below and at the flooding-point. Several hundred droplets were measured during each run and the mean volumn-surface diameter, d_{vs}, computed. In all instances the droplet size distribution approximated closely to a Gaussian form.

The extraction system employed was either 3M aqueous nitric acid with 20% TBP/OK as the dispersed phase or, in the reverse mode, with an aqueous 3M nitric acid dispersed phase. The two phases were equilibrated before use.

The pulse column was operated using sieve plates under two sets of wetting conditions. Initially the column packing was constructed from stainless steel plates which had been degreased and washed in water. When the column was run under these conditions the plates were termed "clean" and there was very little plate wetting by the organic solvent. With time, however, if not cleaned, the plates accumulated organic material on to their surfaces so that the wetting properties changed and then the plates were considered to be in the "aged" condition.

In order to operate the column under solvent phase continuous conditions, it was necessary to install nozzle plates, with the nozzles pointing downwards in the direction of the dispersed aqueous phase flow. Under these conditions a certain amount of plate wetting by the dispersed aqueous phase was unavoidable. When the nozzle plates were used in the same configuration but under aqueous phase continuous operation it became apparent that a layer of solvent, trapped below each plate by the protruding nozzles, affected the drops as they rose through the column: the undersides of the plates behaved as though they were wetted to some extent by the dispersed phase.

Droplet Behaviour

For a pulsed column of given geometry, employing feed liquors of constant physical properties with no mass transfer occurring, the mean droplet size is governed by a dynamic equilibrium between the various mechanisms of droplet formation and droplet coalescence. Thus hold-ups, pulse velocity and the surface properties of the perforated plates and column walls will determine the mean droplet size and droplet characteristic velocity. These factors are discussed in turn below:

Variation of Droplet Size with Holdup

The variation of the mean droplet size with holdup at selected pulse velocities and plate surface conditions was plotted graphically and it was found that there was no relationship between droplet size and holdup when (fA) 20 mm/s under aqueous phase continuous conditions. When, however, (fA) 20 mm/s a straight line relationship of the form

$$d_{vs} = c + mx \quad .... \quad 1$$

was obtained where c and m are constants. The constant m is a measure of the rate of change of droplet size with hold-up and the constant c is in the intercept of this line with the ordinate in the limiting condition $x \rightarrow 0$. For $x \rightarrow 0$, coalescence between droplets may be neglected so that the constant c represents the mean droplet size in the absence of coalescence, that is, the characteristic droplet size, d°_{vs}. Thus equation 1 can be written as:

$$d_{vs} = d^{\circ}_{vs} + mx \text{ .... } 2$$

where d°_{vs} is the value obtained at the intercept of the line as $x \to 0$. The absolute values of d°_{vs} and m will be dependent upon the pulse characteristics, the physical properties of the system employed, column geometry and plate wetting characteristics (see Table 1).

Variation of Droplet Size with Pulse Velocity

On physical grounds it may be expected that as the mathematical limit $(fA) \to \infty$ is approached, d_{vs} will tend to a small but finite value. The other limit as $(fA) \to 0$ cannot be achieved as a small pulse energy must be present before a pulse column can operate. If the lower limit is taken to be the point where the value of (fA) is just sufficient to maintain column operation, the droplet size would approach a maximum value. If the shape of the curve between these two limits is assumed to be exponential, a logarithmic plot of d°_{vs} versus (fA) should give a straight line of negative gradient. Figure 1 shows such a plot and it may be seen that the values of d°_{vs} fit well on the line under aqueous continuous conditions apart from those obtained at low pulse velocities using clean plates. A similar exponential dependence of column HTU values on (fA) has been reported previously (3).

Droplet Characteristic Velocity and Droplet Size

If a link can be established between the droplet characteristic velocity $\bar{V}_o$ and the mean droplet size d_{vs}, dispersed phase holdup and hence specific interfacial area could then be estimated from a knowledge of the droplet size. Conversely, the droplet size could be calculated from measurements of the characterisitic velocity. Thus since holdup and droplet characteristic velocity are related through the holdup equation

$$\frac{V_d}{x} + \frac{V_c}{1 - x} = (1 - \int) \bar{V}_o (1 - x) \text{ .... } 3$$

and

$$d_{vs} = d^{\circ}_{vs} + mx \text{ .... } 2$$

it is only necessary to establish the form of the function

$$\bar{V}_o = f(d_{vs}) \text{ .... } 4$$

This has been the subject of a separate study at DNE and will be published elsewhere. The argument, however, may be summarised as follows: a single droplet in infinite media will travel under the influence of gravity with a velocity U so that

$$U = f'(d^{\circ}_{vs}) \text{ .... } 5$$

The form of this function will depend upon a number of factors including the physical properties of the system and the droplet size. If it is assumed that the droplets are small and approximate in behaviour to solid spheres, the functional dependence of U upon d^{o}_{vs} will be given by the usual drag co-efficient - Reynolds number relationships for solid particles.

In the present work, when the column operated in the dispersion regime, the droplets were small and had Reynolds number generally below 50 so that droplet motion can be approximated by the Intermediate Law, so that

$$U \propto (d^{o}_{vs})^{1.14} \quad \ldots\ldots\ldots\ldots\ldots\ldots\ldots\ldots \quad 6$$

The velocity U is thus the velocity that a droplet would have if it travelled in an unimpeded manner as in a spray column. In a plate column, however, the droplet motion is hindered to a certain extent by impact with the plates and so the observed droplet velocity, $\overline{V}_o$, is somewhat less than U. It has been found that the ratio $(\overline{V}_o/U)$ is substantially constant over a wide range of operating conditions at a value of approximately 0.94 so that

$$\overline{V}_o = 0.94U$$

$$\text{that is, } \overline{V}_o \propto U \propto (d^{o}_{vs})^{1.14} \quad \ldots\ldots\ldots\ldots \quad 7$$

$\overline{V}_o$ is plotted versus d^{o}_{vs} in Fig 2 for the case where the solvent was the dispersed phase and the data lie well on a straight line through the origin with the exception of the measurements for cleaned plates where anomalous droplet sizes were encountered. The fact that the curve is linear indicates that, within experimental accuracy, the exponent on d^{o}_{vs} is 1.00 as opposed to 1.14 predicted by the Intermediate Law. Thus the latter represents a close approximation to droplet motion in this Reynolds number range.

The above discussion is restricted to the situation where no appreciable droplet coalescence occurs due to plate wetting or to interfacial turbulence accompanying mass transfer. In the latter case, a more sophisticated treatment is called for and the reader is referred to a later publication (4).

Droplet Characteristic Velocity

A logarithmic plot of $\overline{V}_o$ versus (fA) for aqueous phase continuous conditions (Fig 3) indicated that much larger values of $\overline{V}_o$ were achieved when using clean sieve plates than when using aged sieve plates or nozzle plates at a given pulse velocity. This was attributed to larger mean droplet sizes associated with enhanced coalescence.

Conclusions

Under comparable pulsing conditions, the mean droplet sizes produced by clean sieve plates were significantly larger than those obtained with aged plates, an effect which is associated with the different surface characteristics of the two types of plate. The corresponding values of the droplet characteristic velocity were also larger in the case of clean plates indicating that the column had a higher limiting throughput in this instance. These findings may well account for the progressive deterioration in column performance with time which has been observed previously by numerous workers.

When clean nozzle plates were installed in the column with the nozzles downwards, that is, pointing towards the dispersed phase entry point, the column performance approximated closely to that observed with aged sieve plates. This is thought to be due to the masking of the underside of the trays by a thin layer of coalesced solvent so that the contact angles of the upstream plate surfaces no longer played a significant role in determining the mean droplet size of the column.

The variation of droplet size with pulse velocities greater than 20 mm/s was attributed to the fact that at lower pulse velocities a high proportion of the droplets coalesce and reform at the plate surface whereas at higher values interdroplet coalescence governs droplet size, with large holdups leading to a higher probability of droplet interactions.

Under aqueous phase continuous conditions, a negative exponential relationship was found to relate droplet characteristic velocity ($\overline{V}_o$) to pulse velocity (fA). Futhermore, a plot of droplet characteristic diameter against droplet characteristic velocity gave a straight line through the origin. The droplets were estimated to have Reynolds numbers corresponding to those in the intermediate law range and thus the relationship between droplet size and droplet velocity involves an exponent on d^o_{vs} of 1.14. Within the errors involved in calculating $\overline{V}_o$ and d^o_{vs} from the experimental data, the experimental exponent of 1.0 is in good agreement with the theoretical result.

References

(1) Batey W, Lonie S J, Thompson P J and Thornton J D.
The Dynamics of Pulsed Plate Columns. Part I Dispersed Phase Holdup in the Absence of Mass Transfer. In press Trans Instn Chem Engrs 1986.

(2) Batey W, Lonie S J, Thompson P J and Thornton J D.
The Dynamics of Pulsed Plate Columns. Part II Droplet Size Studies in the Absence of Mass Transfer. To be published in Trans Instn Chem Engrs.

(3) Batey W, Lonie S J, Thompson P J and Thornton J D.
Uranium Mass Transfer in a Pulsed Column. Extraction '84 pp 57-68 Instn Chem Engrs Symposium Series No 88 1984.

(4) Batey W, Thompson P J and Thornton J D.
To be published.

Acknowledgements

Thanks are due to the Director, Dounreay Nuclear Power Development Establishment, for permission to publish the paper.

Table 1

Values of d°_{vs} obtained for 3M nitric acid/20% TBP/OK.

Plate Condition	Continuous Phase	fA mm/s	d°_{vs} mm
Clean sieve	Aqueous	11.22	2.75
		12.66	2.75
		18.36	0.89
		22.44	0.96
Aged sieve	Aqueous	11.22	1.34
		12.66	1.38
		18.36	1.07
		22.44	0.73
Nozzle	Aqueous	12.80	1.36
		24.00	0.60
Nozzle	Solvent	25.00	1.19

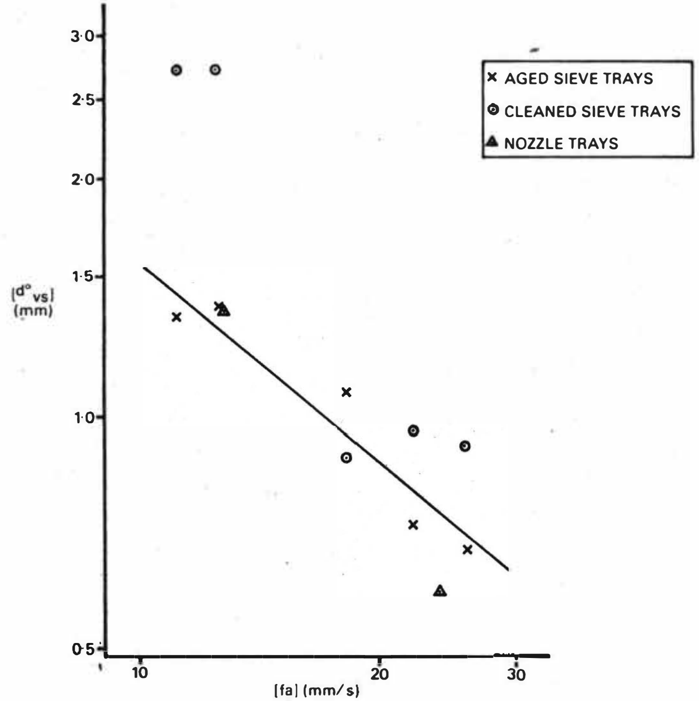

FIG 1 LOGARITHMIC PLOT OF DROPLET CHARACTERISTIC DIAMETER VS PULSE VELOCITY - AQUEOUS CONTINUOUS DATA

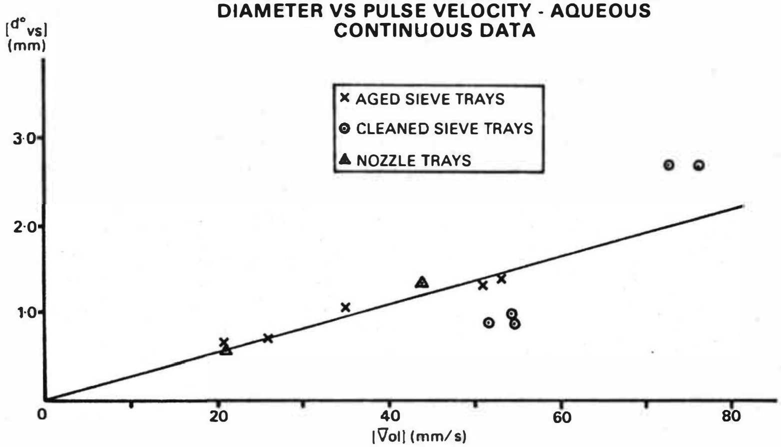

FIG 2 PLOT OF DROPLET CHARACTERISTIC DIAMETER VS DROPLET CHARACTERISTIC VELOCITY-AQUEOUS CONTINUOUS DATA.

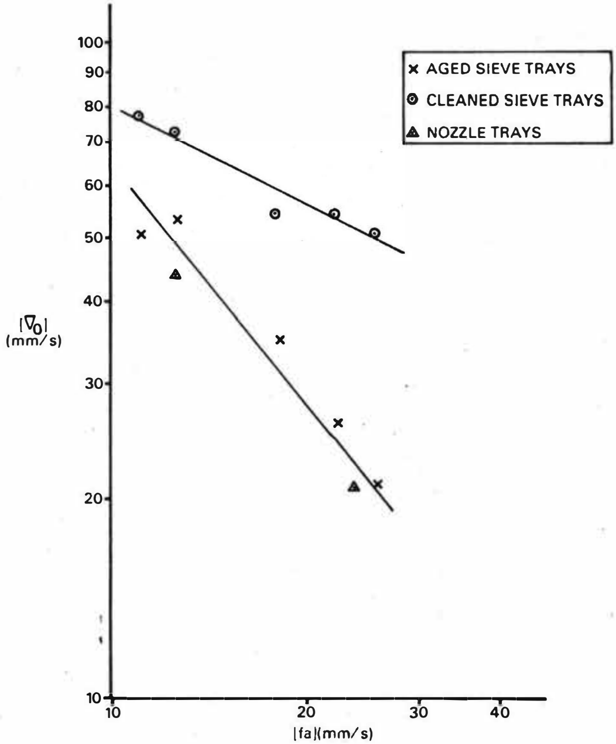

FIG 3 LOGARITHMIC PLOT OF DROPLET CHARACTERISTIC VELOCITY VS PULSE VELOCITY-AQUEOUS CONTINUOUS DATA.

The Design, Operation and Performance of a Pulsed Column Pilot Plant for Fast Reactor Fuel Reprocessing

J.A. Jenkins*, D.H. Logsdail, E. Lyall, P.E. Myers

A pilot plant is being operated to study the performance of pulsed columns for the system uranyl nitrate/nitric acid (UN/HNO_3)-20% tri-n-butyl phosphate in odourless kerosene (TBP/OK). It is part of a development programme on pulsed columns leading to the detailed specification of the equipment required for reprocessing fast reactor type fuels. The objectives are to measure the throughput capacity of the columns for a variety of flowsheet conditions, to study the effect of scaling up column diameter on U mass transfer performance and to provide the hydraulic and mass transfer data required to develop and validate a dynamic simulation model of pulsed columns.

The pilot plant can accommodate up to four air-pulsed columns, each with plated heights of 10m and internal diameters ranging from 25 to 200mm. In the present arrangement there are 25 and 50mm diameter columns for compound extraction and scrub, and 50 and 100mm diameter columns for stripping. Uranium product solutions are recycled via a kerosene wash and concentration in an evaporator. The TBP/OK is washed with alkali and dilute nitric acid solutions prior to recycling.

Samples of the aqueous and organic phases, and measurements of liquid pressure and temperature, can be taken at regular intervals along each column. Optical cells are fitted at intervals to the outside of the columns to facilitate photography of the liquid-liquid dipersion.

The paper describes in detail the plant design and operation, particularly the experimental methods to measure the performance of the columns. Illustrative data on the profiles of U and HNO_3, temperature, dispersed-phase hold-up and drop size are given, and the ways in which they are used to fulfil the experimental objectives are explained.

* **Address**

Mr. J.A. Jenkins
Chemical Engineering Division
B.351.15, AERE
Harwell, Oxfordshire OX11 0RA
United Kingdom

As the manuscript was not available at the 28th May 1986, the deadline for printing this book, we only print the short abstract of the paper.

EFFICIENCY OF CONTACTORS*

D. A. Orth, F. R. Graham, and D. L. Holt, E. I. du Pont de Nemoura and Company,
Savannah River Laboratory, Aiken, South Carolina 29808

INTRODUCTION

The efficiency of any type of solvent extraction equipment, in terms of losses, purity of products, and throughput, depends on the effectiveness of contact and disengagement of the two phases, and on kinetic exchange rates. Many studies on mixer-settlers, including a large number reported at ISEC's, have considered the relations of mixer configuration and other mixing parameters to droplet size, phase coalescence, and transfer of solute between phases. The droplet sizes determine interfacial area, which is a paramount factor in determining the transfer of solute between phases and the efficiency of the contact. The droplet size also determines the coalescence characteristics and the degree of entrainment from a given settling system. Kinetic factors for equilibration of extractable species both between and within the aqueous and organic phases can cause substantial differences between the performance of rapid contactors and other types.

Information on these factors and their application is the expected result from current studies on Savannah River Plant (SRP) contactors. The Savannah River Plant has reported on the operation of mixer-settlers and a centrifugal contactor for the Purex process and several other tributylphosphate-based processes.[1,2,3] The mixer-settlers were developed in the 1950's at SRP and have been operated with no modifications since that time. Because of time constraints during the initial development, the units were not fully optimized for maximum efficiency or flexibility. After an acceptable design was established to meet the requirements, further development was curtailed.

In 1966, short-residence centrifugal contactors replaced the Purex 1A mixer-settler bank. The desirability of improved decontamination of product streams and increased capacity has led to the present studies on impeller effects in mixer-settlers, and kinetic effects in the centrifugal contactors.

SUMMARY

The Savannah River Plant has two separations plants that began Purex operations in 1954 and 1955 with pump-mix mixer-settlers as contactors to process nuclear fuels. The only changes to the extraction equipment were replacement of most of the mixer-settlers in one plant with larger units in 1959, and the further replacement of the large 1A bank with a bank of rapid-contact centrifugal contactors in 1966. Improved performance of the old units has become highly desirable, and an experimental program is underway.

Good contact between the phases, and adequate settling without entrainment of the opposite phase are required for high efficiency operation of the mixer-settlers. Factors that determine efficiency are mixer design, drop size generated, and phase coalescence properties. The original development work and accumulated plant data confirm that the tip speed of a given impeller design determines the throughput capacity and extraction performance. An experimental unit with three full-scale stages has been constructed and is being utilized to test different impeller designs; reduced pumping and better mixing with lower speeds appear to be the key factors for improvement.

Decontamination performance of the rapid-contact centrifugal contactors is limited by the number of scrub contacts and the time of contact because of slowly equilibrating fission product species. Where solvent degradation is not a factor, the longer scrub contact of mixer-settlers gives better decontamination than the centrifugals. This kinetic effect can be overcome with long scrub contacts that follow the initial short extraction and short scrub contacts in the centrifugal contactors. A hybrid experimental unit with both rapid contact sections and longer contact acrub sections is under development to establish the degree of improvement that might be attained.

---

* The information contained in this article was developed during the course of work under Contract No. DE-AC09-76SR00001 with the U.S. Department of Energy.

DISCUSSION

Mixing Relationships

The relations between mixing conditions, approach to equilibrium, and entrainment have received extensive study. The two most significant correlations proposed are N^3D^2 and tip speed, Π ND, where N is rotation rate and D is impeller diameter. Constant N^3D^2 is considered to give constant power per unit mass of solution and to be the proper relation to use in scaling similar configurations for equivalent mixing intensity. Tip speed has been suggested as a primary determinant of drop size, through the effect on turbulence around the impeller. Drop size in turn affects the settling time and degree of entrainment in a given system.

ISEC '71 has several related studies on mixing conditions, drop size, emulsion properties, and settling characteristics, with a variety of correlations between these variables and impeller rotation rate and diameter.[4,5,6,7] A few of the many other studies also can be cited.[8,9,10] The differences really are small, with drop size or settling rate correlations with N and D in the range of $N^{1.0}$ to $N^{1.5}$ and $D^{0.8}$ to $D^{1.0}$, with some other relations also proposed. Additionally, coalescence rate in some correlations is cited as dependent only on the flow rate of the dispersed phase per unit area of coalescing surface. However, drainage of the continuous phase from the emulsion band also is cited as a flow counter to the settling path of the dispersed phase droplets that also must affect emulsion band characteristics.

A more recent, very pertinent study, which includes a review of much other work, is on the interfacial area generated under different mixing conditions with water and several organic materials.[11] Experimental variables included the volume fraction of dispersed phase, tank size, impeller size, impeller speed, and fluid properties of the phases. The simple results of the tests were that the interfacial area was primarily dependent upon the tip speed among the mechanical mixing variables, with little separate influence of power per unit volume. The dependence is nearly linear. The Sauter mean diameter of drops in a distribution is equivalent to a drop that has the same surface to volume ratio as the dispersed phase as a whole and is inversely proportional to the interfacial area. Hence, the mean drop size also is nearly linearly (inversely) dependent on the tip speed.

The relation to mixer-settler operation is straightforward. The interfacial area will determine the approach to equilibrium in an extraction operation, and the interfacial area depends on the tip speed. Further, drop size will determine the settling time and the degree of entrainment with a given settler design, and drop size again depends on tip speed.

SRP Mixer-Settlers and Mixing Variables

Three sizes of mixer-settlers were involved in the original SRP development work. The banks for the original Purex installations that started operating in 1954 and 1955 were pump-mix units with impeller diameters of 12.7 and 17.8 cm.[12,13] The impellers act as centrifugal pumps to move the aqueous phase. In 1959, so-called "Jumbo" banks with 22.9 cm impellers replaced the original banks in one of the Purex plants.[13] The other Purex plant was converted to processing enriched uranium normally and also was utilized for processing thorium, uranium-233, irradiated plutonium, and other special feed materials.

The development work confirmed by plant operation was that the pump-mix design gave good operation for losses and entrainment over a limited range of solution throughput rates. Higher impeller speeds necessary to pump the heavy aqueous phase at higher rates generate finer drops that do not settle in the reduced time, and that result in increased entrainment and lower efficiency. Substantially lower than normal impeller speeds give inadequate phase contact, hence low efficiency again. At high throughput rates, the upper and lower limits on impeller speed converge. Near the throughput limit, the operable impeller speed range is relatively few revolutions per minute.

Plant data showed early that decontamination and losses are affected differently by impeller speed. In the scrub section of a bank, for example, impurities in the bulk organic phase are to be back-extracted into a small volume of dispersed droplets of aqueous phase, an unfavorable geometric arrangement for transfer. The dispersion conditions in the scrub section that give adequate contact without excessive mixing, with the consequent entrainment of the scrub solution, are likely to be different from the conditions in the extraction section that give good efficiency and low losses of product. Analogous conditions may exist where the organic phase is the scrubbing section. The result is that the same impeller speed and impeller design generally are not good where different flow ratios exist in the same bank.

The total flow of both phases appears to be a significant measure of coalescence rate per unit area for the SRP units. The original development work showed that the defined cutoff of 3% entrainment of aqueous in organic was reached at the same impeller speed for the same total flow for a wide range of flow ratios.[12,13] This would give a constant total disengaging rate per unit area at a given impeller speed, but a large variation in disengaging rate if based on the dispersed phase only. Additionally, the experimental data discussed in the next paragraph also presents a reasonable grouping based on total flow of the mixed phase, but a wider spread when considered on the bases of the separate phases. Logically the continuous phase must have some effect on the settling rate of the dispersed phase since it must drain from the emulsion counter to the movement of the dispersed drops, as noted previously.

Experience in entrainment and efficiency with three different sized banks and impellers in Purex, enriched uranium processing, Thorex, and other programs can be examined in terms of disengaging rate per unit settling area and impeller speed. Limits on performance can be based on both excess entrainment or on serious loss of efficiency, as measured by losses or contamination of end streams. Given in Table 1 are the specific areal flows of the combined phases, the tip speeds of the different sized impellers, and the observed result. A graph (Figure 1) of the data compares the different limiting flows and the tip speeds. These data cover wide variations in solution properties that influence mixing and settling in the different processing systems. These varying properties include densities and viscosities as well as substantial differences in observed interfacial tensions between the aqueous and organic phases as a result of solvent degradation products and different tributylphosphate (TBP) strengths. The data spread is large, but much smaller than when based on dispersed phase settling only.

The general relations provide some guidance for the experimental work. Flow capacity, as set by entrainment or efficiency with the present centrifugal impellers, increases as the impeller speed decreases. The obvious approach is to modify the impellers so that they mix better at slower speeds and still pump adequately. Some of the early development work, after startup and too late for implementation, showed that appreciable improvement might be made with relatively simple modifications.[14] To explore impeller effects, a three-stage plant-scale experimental unit has been constructed with transparent walls and top to allow observation of the mixing and settling zones. The results of the test work in progress will be presented at the conference.

Kinetic Effects on Performance

The rate of exchange of solutes between phases is influential in losses of valuable products and in purity of the products. In Purex and related tributylphosphate processes, the extraction rates of uranium, plutonium, and other actinide products are quite rapid. Hence, short contact times with reasonable contacting efficiency can attain low losses in the extraction banks at times as short as 10 to 15 seconds per stage, as in the SRP centrifugal contactors.

The fission products that limit decontamination are ruthenium and zirconium. Ruthenium specifically has many different ionic species in both aqueous and organic phase, including a whole family of nitrato-nitrosyl ruthenium compounds, with slow equilibration between these species, as attested to by many studies. Zirconium also appears to have slower extraction rates than plutonium and uranium. It is proposed that slow conversion of hydrolyzed and polymeric zirconium species are responsible for the rates.[15]

TABLE 1. Limiting Settling Conditions

Mixer-Settler Service	Observation	Emulsion Disengaging Rate ml/min/cm^2	Impeller Tip Speed, cm/sec
1. 1A, Large Purex, Extraction	Emulsions, 1AW losses	14.7	383
2. 1B, Large Purex, Partition	Pu loss to organic U stream.	13.9-12.7	419-407
3. 1C, Large Purex, U Strip	Gross entrainment, both aqueous and organic end streams.	28.2 21.2 22.2 19.5	287 263 293 287
4. 1E, Large Purex, U Strip	Aqueous entrainment in 1EW organic.	17.2	275
5. 2A Small Purex, 2nd Pu Extraction	High losses, low decontamination.	27.1	226
	Entrainment, scrub section only.	14.0	249
6. 2B, Small Purex, 2nd Pu Strip	Aqueous entrainment in 2BW organic.	9.1	139
7. 1E, Small Purex, 2nd U Strip	Aqueous entrainment in 1EW organic.	6.9 8.6	363 353
8. 1A, Small Enriched U, Extraction	1AW losses increased, decontamination decreased.	9.4	422
9. 2A, Small Np, Extraction	2AW losses	11.3	226
10. 1A, Small Thorex, Extraction	Emulsions	17.8	266
11. 1B, Small Thorex, Partition	Aqueous entrainment in organic.	17.2 19.3	283 266
12. 2B, Small Thorex, Th Strip	End stream entrainment.	19.8	233

Note: Impeller diameters are 22.9 cm on large banks, 17.8 cm on small 1E bank, and 12.7 cm on all other small banks.

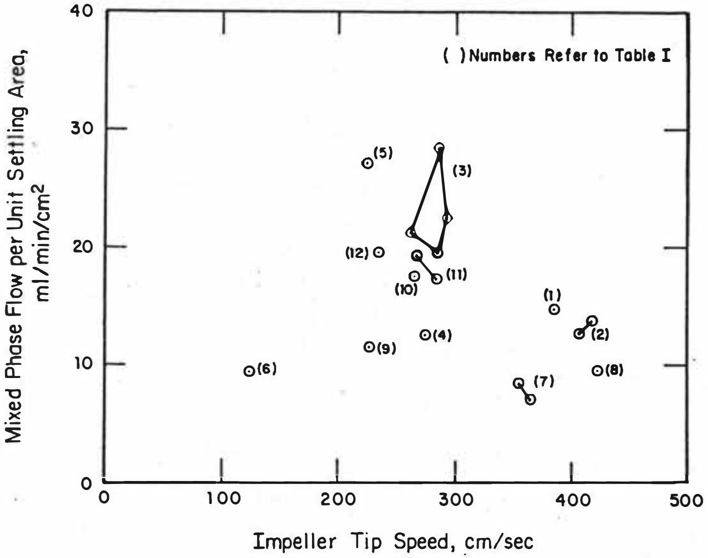

FIGURE 1. Limiting Settling Rates

Short-residence centrifugal contactors replaced the large Purex mixer-settlers in 1966 as part of a program to reduce solvent degradation effects. The units solved the degradation problem, but brought a new fission product extraction pattern that was assigned to kinetic effects.[3] It was proposed that decontamination performance might be improved by combining rapid extraction and scrubbing, followed by slow scrubbing. The rapid contact would recover the uranium and plutonium produced and separate the bulk of the fission products; the slow scrubbing would allow equilibration and back extraction of the small amount of ruthenium and zirconium carried through the centrifugal scrub stages. The results of an experimental program are expected to be equally applicable to high TBP Purex flowsheets and low TBP flowsheets for recovery of enriched uranium.

Separate tests with laboratory-scale centrifugal contactors and mixer-settlers were made as a preliminary step to the testing of hybrid extraction equipment. Decontamination factors for zirconium were determined in center-fed 16-stage centrifugal contactors and mixer-settler units with an enriched uranium recovery flowsheet utilizing 7.5% TBP. The feed solution was chemically the same as plant feed, with a one-thousandth aliquot of plant feed to provide zirconium tracer. In one pair of runs, a portion of the regular plant solvent with its accompanying degradation products was added to the laboratory solvent. The results are shown in Table 2. The longer scrubbing time of the mixer-settlers gave distinctly better decontamination in series 1 and 2. Increased temperatures gave better decontamination with both mixer-settlers and centrifugals; the benefits of increased temperature have long been noted. Decontamination decreased markedly when plant solvent was added; more in the mixer-settler run than in the centrifugal run, but the mixer-settler still was the better of the two.

More experimental facilities have been constructed with both short and long contact stages. The system should resolve the combined effect of short contact during extraction and initial scrubbing, which should reduce the formation of solvent-bound zirconium species, and long contact in additional scrub stages. The equipment has a mini-centrifugal bank of 16 extraction stages that can be divided between extraction and scrub stages as desired and 12 mini-mixer-settler scrub stages. The residence times are 5-30 seconds per stage in the centrifugal bank and 3-5 minutes per stage in the mixer-settlers. The results of the test work in progress will be reported at the conference.

TABLE 2. Scrubbing Time and Decontamination

Feed Solution: 5 g/L U, 1.4 M HNO_3, 1.5 M $Al(NO_3)_3$

Radioactive Spike: 1/1000 volume addition of plant feed solution;

	Zr-95 Decontamination Factor	
Temperature	Centrifugal Contactor	Mixer-Settler
33^0C	70	370
50^0C	130	820
50^0C (With Plant Solvent spike)	110-140	180

REFERENCES

1. D. A. Orth and T. W. Olcott, Nucl. Sci. and Eng., 17 593, (1963).
2. D. A. Orth, Solvent Extraction Chemistry of Metals, 47 MacMillan & Co. (1963).
3. D. A. Orth, J. M. McKibben, and W. C. Scotten, Proceedings ISEC '71, 514, (1971).
4. J. W. van Heuvan and W. J. Beck, Proceedings ISEC '71, 70, (1971).
5. J. W. Giles, C. Hanson, J. G. Marsland, Proceedings ISEC '71, 94, (1971).
6. F. P. Pike and S. C. Wadhawan, Proceedings ISEC '71, 112, (1971).
7. R. W. Luhning and H. Sawistowski, Proceedings ISEC '71, 873, (1971).
8. H. T. Chen and S. Middleman, AIChE J., 13 989, (1967).
9. J. B. Fernandes and M. M. Sharma, Chem. Eng. Sci., 22 1267, (1967).
10. C. A. Coulaloglou and L. L. Tavlarides, AIChE J., 22 289, (1976).
11. R. E. Eckert, C. M. McLaughlin, and J. H. Rushton, AIChE J., 31 1811, (1985).
12. T. J. Colven, Jr., UASEC Report DP-140, (1956).
13. A. A. Kishbaugh, UASEC Report DP-289, (1958).
14. A. T. Davis and T. J. Colven, Jr., AIChE J., 7 72, (1961).
15. G. A. Yagodin and V. V. Tarasov, Proceedings ISEC '71, 888, (1971).

01DA0002:ksr

The Effect of Phase Ratio on Pulse Column Capacity for a High Volume/Low Uranium Concentration System

T. A. Todd, A. L. Olson, Westinghouse Idaho Nuclear Company, Inc., Idaho Falls, ID USA

INTRODUCTION

The Idaho Chemical Processing Plant (ICPP) is a reactor fuel reprocessing facility which uses a variation of the PUREX solvent extraction process for the recovery of fissionable material from spent reactor fuel elements. Total dissolution of spent reactor fuel elements at ICPP results in large dissolver product solution volumes with very low heavy metal concentrations. Heavy metal is extracted from the aqueous dissolution product using 6 to 30 volume percent tri-n-butyl phosphate (TBP) in a n-dodecane diluent. Pulse columns are used to contact the aqueous dissolution product with solvent.

An upgrade of solvent extraction systems at ICPP required that pulse column capacities for given solution pairs be known to assure that projected spent fuel processing goals could be achieved. The column capacity was essential because of large volumes of dissolver product to be processed and equipment size constraints imposed by criticality safety requirements. Futhermore, a 50% decrease in the uranium distribution coefficient is realized due to the spent fuel dissolution chemistry. This decrease is relative to a standard nitric acid-uranyl nitrate-TBP system and is caused by uranium complexes of fluoride and sulfate.

The above mentioned items required a non-typical aqueous/organic (A/O) flow ratio, relative to the standard PUREX flowsheet, to meet uranium recovery requirements. Typically, high A/O ratios would be utilized to process the large aqueous solution volumes. However, because of the decreased uranium distribution coefficient, the A/O flow ratio must be reduced.

Column capacity is known to be a function of the A/O ratio.(1,2,3) The effect on column capacity realized when the A/O ratio is changed must be evaluated (the system is operated in an organic continuous mode). Pilot plant tests were performed to quantitatively evaluate the effect of phase ratio on pulse column capacity for a system with relatively no heavy metal mass transfer.

THEORY

Pulse column capacity is a function of many variables, however, most are fixed by process chemistry and equipment design. These variables include the physical properties of the solutions, mass transfer, plate wetting characteristics, plate geometry, and to a certain extent, operating temperature. Once these variables are fixed, column capacity becomes a function only of pulse frequency and amplitude, and A/O ratio. It is desired to predict flooding capacity for a given process as a function of the A/O ratio.

An expression for the dispersed phase holdup (x) in a spray column was given by Thornton(4) and has been shown to apply to pulse columns also.

$$V_d + \left(\frac{x}{1-x}\right) V_c = \bar{\nu}_o\, x\, (1-x) \tag{1}$$

where $\bar{\nu}_o$ is the characteristic, or limiting droplet velocity and V_c and V_d are the superficial phase velocities for the continuous and dispersed phases. The dispersed phase holdup at flooding ($x=x_f$) can be determined by differentiating this equation twice with respect to x with the following constraints applied:

$$\frac{dV_d}{dx} = 0 \quad \text{and} \quad \frac{dV_c}{dx} = 0$$

The following expression for dispersed phase holdup at flooding can then be obtained

$$X_f = \frac{2}{3 + (1+8/R)^{0.5}} \tag{2}$$

where $R=V_d/V_c$. Equations (1) and (2) can be combined to give an expression for flooding capacity as a function of A/O ratio.(5)

$$\frac{\bar{\nu}_o}{(V_d+V_c)_f} = 3.375 + 1.225 \log R - 0.41 (\log R)^2 - 0.22 (\log R)^3 \tag{3}$$

If process chemistry and equipment variables are fixed, and the flooding capacity of the column is known for one flow ratio, flooding capacity for other A/O flow ratios may be estimated by an equation of the form

$$\frac{(V_d+V_c)_{f1}}{(V_d+V_c)_{f2}} \cong \left[\frac{(V_d/V_c)_1}{(V_d/V_c)_2}\right]^n \tag{4}$$

EXPERIMENTAL

The experimental equipment consists of a single glass extraction column, air pulser mechanism, tankage, pumps, and interface control equipment. A schematic diagram of the system is shown in Figure 1. Specific column dimensional parameters are shown in Table 1.

Table 1. Column Design Parameters

Active height:	6.25 m
Diameter:	0.051 m ID
Plate specifications:	Stainless steel nozzle plates - 23% free area - 0.00475 m orifice size - 0.051 m plate spacing
Pulse leg:	0.0125 m ID glass tubing

A simulated dissolver product solution consisting of 3 M nitric acid and 0.6 M aluminum nitrate was used. This aqueous solution consisted of the same viscosity and density as the dissolver product. The solvent was a mixture of 30 volume percent TBP in a n-dodecane diluent. A summary of the physical properties of each solution at 25°C is shown in Table 2.

Table 2. Physical Properties of Solutions

	30% TBP	AQUEOUS FEED
Specific gravity:	0.82	1.15
Viscosity (Pa-s):	1.80 E-03	1.50 E-03

The aqueous and organic flowrates were incrementally increased, after initial column operation was established, at a constant A/O ratio and pulse energy. Column operation between flowrate changes was visually observed for a time period of 30-45 minutes. This procedure was followed until visual observation of flooding was observed. Dispersed phase holdup was measured at each flowrate.

DISCUSSION

Equation (4) is based on open, spray column operation but appears to apply to pulse column operation within reasonable data scatter. Evaluation of unpublished data from Gronier(6) suggests the exponent of equation (4) is equal to 1/6. Data from experiments at ICPP show reasonable agreement with this value in the range of A/O ratios from 0.2 to 10. A plot of the estimated flooding curves using equation (4) with $n = 1/6$, and calculated from experimental flooding data with an A/O ratio of 0.5, is shown in Figure 2.

This equation has been successfully used at ICPP for predicting maximum pulse column flooding capacity since maximum values for different A/O ratios may not occur at the same pulse energy. Pulse energy is defined as the frequency-amplitude product (f x a). The equation is valid only for a system in which the flooding capacity at one A/O ratio is known and all other system parameters are similar (equipment, process chemistry, etc.). Use of the equation has assisted in estimating throughputs for ICPP systems in which adjustments in the A/O ratio are routinely made.

NOMENCLATURE

a	Pulse amplitude (m)
A	Aqueous phase flowrate (L/h)
f	Pulse frequency (counts per minute)
O	Organic phase flowrate (L/h)
V	Superficial phase velocity (m/h)
$\bar{v}_o$	Characteristic or limiting droplet velocity (m/h)
x	Dispersed phase holdup
R	Phase ratio, V_d/V_c

subscripts

c	Continuous phase
d	Dispersed phase
f	Flooding

REFERENCES

1. G. Sege and F. W. Woodfield, Chemical Engineering Progress, Vol. 50, No. 8, August 1954.

2. L. D. Smoot, B. W. Mar, and A. L. Babb, Industrial Engineering and Chemistry, 51, 1005-1010, (1959).

3. R. Berger and K. Walter, Chemical Engineering Science, Vol. 40, No. 12, 1985.

4. J. D. Thorton, Chemical Engineering Science, Vol. 5., No. 5, 1956.

5. J. T. Long, Engineering for Nuclear Fuel Reprocessing, Gordon and Breech, New York, 1967.

6. W. S. Groenier, Oak Ridge National Laboratory, unpublished data, 1966.

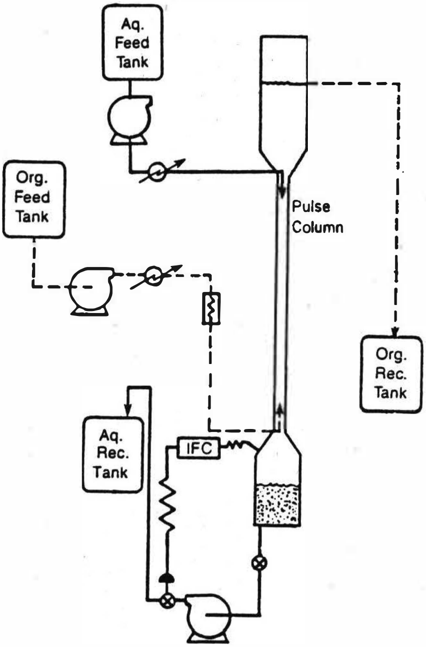
Aq.
Feed
Tank
Org.
Feed
Tank
Pulse
Column
Org.
Rec.
Tank
Aq.
Rec.
Tank
IFC

Figure 1. Schematic Diagram of Experimental Equipment.

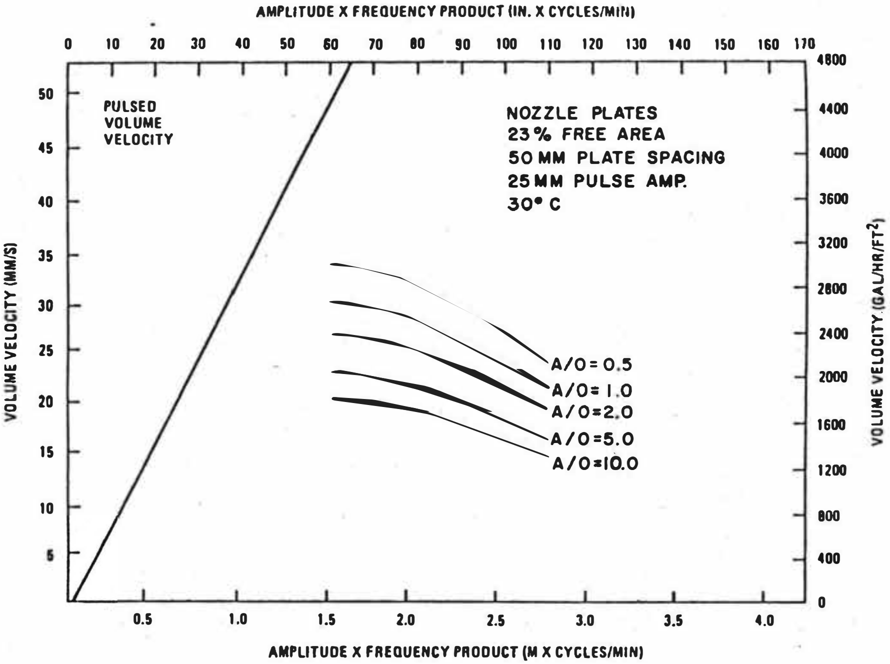

Figure 2. Estimated Pulse Column Flooding Capacity as a Function of A/O Ratio.

Tritium Separation from PUREX-Solution

P.Feucht; G.Petrich; Kernforschungszentrum Karlsruhe GmbH,
Karlsruhe; West-Germany
K.Eiben; H.Evers; Wiederaufarbeitungsanlage Karlsruhe
Betriebsgesellschaft mbH, Leopoldshafen
West Germany

I. Introduction

The major amount of tritium in LWR-reactors is produced by ternary fission of the nuclear fuel. The fuel with a burn up of 33 GWd/t uranium contains approximately 26 TBq tritium per ton uranium. About 50% of the tritium is trapped in the nuclear fuel while the rest is fixed as hydrid to the zircaloy cladding. Under PUREX-Process conditions i.e. low temperature treatment and no chemical decladding this tritium remains in the hulls.

The fuel trapped tritium is released during the dissolution with nitric acid and is distributed as tritiated water (HTO) or acid (TNO_3) in the feed solution for the extraction. The concept of the German industrial reprocessing plant to be built in Wackersdorf/Bavaria deals with an annual amount of 9,1 PBq tritium to be handled with 350 tons of burned fuel.

While the major amount of the dissolved tritium follows the aqueous streams a small part is extracted in or entrained by the organic solvent (30 Vol% tributylphosphate in dodecane) which is loaded with uranium and plutonium. In order to prevent spreading of this tritium beyond the extended head end area, thus avoiding tritium contamination of all product and waste effluents of the plant, a special second scrub section has been added to the first high active scrub (HS1). Consequently the layout of this second scrub should not increase drastically the waste volume of the plant and the apparative needs with respect to operational size and reliability of plant operation.

A tritium scrubber is introduced therefore in the first highly active extraction cycle which is fed with a small stream of tritium free acid (0,8 molar). The scrub solution (HS2S) is contacted with the tritium containing HS1P,applying a phase ratio o:a of 20 or 40. The tritium loaded scrub solution of the HS2-extractor is added to the scrub solution of the HS1-column (HS1S) and ends up via the HA-column in the high active waste concentrate. A fraction of the tritium contaminated water is recycled with the recovered acid, and is used again in the head end of the reprocessing plant. The design and operational behavior of a multistage mixer settler with internal recycling of the scrub phase and a pulsed sieve plate column, both in the scale of an industrial plant, are investigated as alternatives and are described in this paper.

II. Experimental set-up

II. 1. Mixer settler

A five stage mixer settler /1/ based on a modified multistage Holley Mott mixer settler (fig. 1) was installed in a testrig which comprises a full scale first extraction cycle for the reprocessing plant. /2/. For criticality reasons a flat box construction was chosen, which in addition can be equipped with sheets of hafnium for heterogenious poisoning. As a typical feature the apparatus is designed to have the mixing-chamber strictly separated from the settling compartment. The weirs for the organic and aqueous phases are adjusted to fixed positions, also implying a stable position of the interphase. In addition a bottom centred outlet is connected via a pipe to the bottom inlet of the mixing chamber, providing the internal recycle of the mixing chamber by means of a pump mixing impeller, whose speed can be adjusted within certain limits.
Thus the amount of recycled aqueous solution and the dispersion of the two phases in the mixing chamber can be regulated. The operational mode is aqueous continous. The dispersed phases are directed by a special device toward the bottom of the mixing chamber inducing a torus shaped flow pattern as indicated in figure 2.

The mixer settler can be operated with an external phase ratio of up to 40 while the internal phase ratio is approximately one. To demonstrate this hold up measurements were made. The results are shown in fig.2. It was found that for a wide speed range of the impeller the mixing efficiency and the hold up profil in the vertical as well as diagonal direction of the mixing chamber is quite constant (40-60 %). The residence time of the dispersed phase in the mixing chamber is approximately one minute. The mean residence time of the organic phase in the settling compartment amounts to five minutes, which was confirmed by radiotracer experiments /3/.

The overall residence time of the aqueous scrub solution is approximately 1,5 days. Because of the stable aqueous continous operational mode over the whole battery,the aqueous entrainment in the organic phase was low (<0,02 vol %).

The hydraulic stability of the battery was proven during several longterm runs. Start-up and shut-down behavior were tested extensively. As a typical malfunction the failure of an impeller was simulated over a period of eight hours.The overall countercurrent transfer of the two phases remained constant and hydraulic stability could be proven, but the loss of one extraction stage in total efficiency has to be accepted.

II. 2. Pulse column

Comparative investigations on the tritium scrub were conducted in a pulsed sieve plate column which is installed in the testrig PUSTA /4/. Apparative details are shown in fig. 3. The column was operated with depleted uranium and D_2O to simulate the tritium. Valve operated air pulsation with a frequency of 1 Hz and an amplitude of 15 mm was applied. The pulse energy is transfered to the bottom decanter via a pulse leg. The D_2O concentration profile was obtained sampling the organic and aqueous phase at eight positions along the active column.

Because of the high phase ratio (o:a=20 or 40) and the organic dispersed operational mode the flow velocity of the aqueous phase was very low. Therefore it was thought that backmixing effects may influence the required separation factors.

III. Results and discussion

The results shown in fig.4 for the mixer settler comprise lab size exchange experiments by shaking HTO or D_2O containing organic solutions in a shaking funnel.

These results can be compared with the D_2O experiments in the single stage operation of the mixer settler which showed a stage efficency of up to 96 %. Assuming a mean stage efficency of 80% for the tritium scrub in the five stage mixer settler, an overall separation factor (DF) of 120 can be guaranteed. In the case of a failure of one pump mixing aggregate the overall efficency of the battery will be lowered but still gives a sufficently high DF. The required separation factor in the reprocessing plant is set to DF $\geq$ 40.

The experiments in the pulse column were made applying an areal loading of 250 l/d m^2 h. The separation factors obtained are 70 applying a phase ratio o:a = 20. Using a phase ratio o:a = 40 the DF was 36. The concentration profiles for D_2O are measured during the start-up period and after the system reached stationary conditions. The measured values are compared with the VISCO-Program simulating the dynamic process /5/ . Figure 5 shows the good relation of measured and calculated values for the start-up period applying a phase ratio o:a = 40. It can be concluded from the values, which were obtained 490 min after start up that the calculated values of the steady state process are almost reached. This means that an almost stable profile is built up in the column within the time of experiment (8 hours).

Conclusion

Tritium separation from the U-and Pu-loaded organic solvent could be demonstrated with a sufficiently high DF by applying a second scrub in the highly active extraction cycle, using either a five stage mixer settler or a pulse column both operated at phase ratios o:a up to 40.

The good agreement between the values calculated with the VISCO program and the experimental data allowed a correlation of throughput, hold up, mixing as well as mass transfer parameters.
For the conceptional design of the German reprocessing plant a HS2-mixer settler was originally chosen, but the option to install a HS2-pulse column is still discussed. Advantages are seen for the pulse column because of size, heterogeneous poisoning and shorter residence time for the organic phase. Reliability of operation -even if the failure of a stirrer is considered- seems to be in favor of the mixer settler. The final decision will be made after a longterm testrun where the HS2-pulse column is operated together with all columns and equipment of the first extraction cycle.

LITERATUR

/1/ H. Bauer, et. al.
Versuche zum Stoffaustausch und zur hydraulischen Optimierung eines Originalmischabsetzers für die Tritiumabtrennung in einer WAA.
KfK-Bericht 3290

/2/ K.Eiben, H.Zimmermann
Uraniumextraction cycle in the TEKO facility
Atomkerntechnik, Kerntechnik Vol.47 (1985) No. 2 pp 83

/3/ A.Merz
Radiotracertechnische Diagnose der Zweiphasenströmung in industriellen Extraktionsapparaten
KfK-Bericht (in Preparation)

/4/ P.Feucht
Pulskolonnenteststand PUSTA,
KfK-Bericht 3835

/5/ G. Petrich
The PUREX-Process computer modul VISCO and its applications
ISEC, Munich (1986)

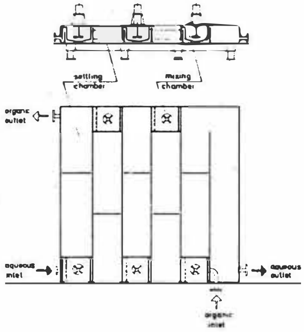
settling chamber
mixing chamber
organic outlet
aqueous inlet
aqueous outlet
organic inlet

Fig 1 Five staged Mixer Settler for the Tritium Scrub

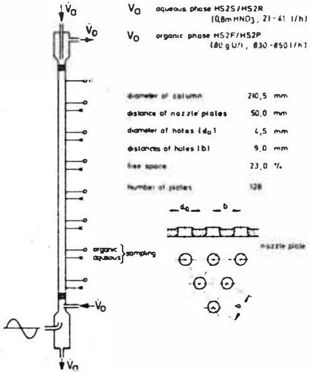
$\dot{V}_a$
$\dot{V}_o$
V_a aqueous phase HS2S/HS2R (0,8m HNO_3, 21-41 l/h)
V_o organic phase HS2F/HS2P (80 g U/l, 830-850 l/h)
organic
aqueous
sampling
d_o
b
nozzle plate

diameter of column	210,5	mm
distance of nozzle plates	50,0	mm
diameter of holes (d_o)	4,5	mm
distances of holes (b)	9,0	mm
free space	23,0	%
Number of plates	128	

Fig 3 HS2 - Pulse column

Number of Extraction Stages	DF for Deuterium	DF for Tritium
1	4,25	4,47
2	3,20	2,97
3	3,86	4,12
4	3,95	3,85
total DF	207	210

Fig 4 Comparison of DF's for Deuterium and Tritium

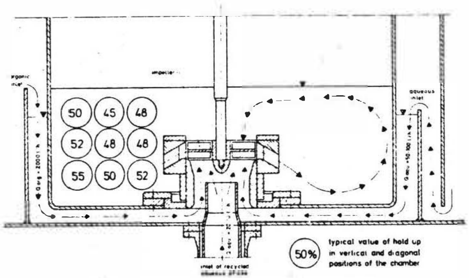
impeller
organic inlet
aqueous inlet
Q org = 200 l/h
Q aqu = 50-100 l/h
Q aqu = 20 l/h
50
45
48
52
48
48
55
50
52
inlet of recycled aqueous phase
50%
typical value of hold up in vertical and diagonal positions of the chamber

Fig. 2 Cross section through the mixing chamber with hold up - profile

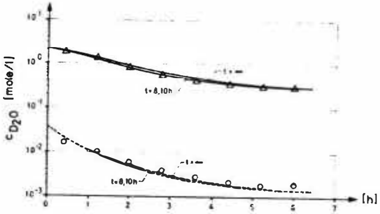

Fig 5 Build up of the D_2O - concentration profile in the HS 2 Pulse column
Aqueous (Δ) and organic (o) phase (measured values) lines are calculated values according to the VISCO - program

Transient Behaviour of Purex Pulsed Columns

J. Schön, H. J. Bleyl, D. Ertel, E. Hamburger, M. Kluth, G. Petrich
and W. Riffel
Institut für Heiße Chemie
Kernforschungszentrum Karlsruhe
P.O.B. 3640, D-7500 Karlsruhe,
Federal Republic of Germany

Introduction

Industrial-scale reprocessing of irradiated nuclear fuels is presently performed by the Purex process /1/, which is suited for processing nuclear fuel from light water reactors (LWR) and fast breeder reactors (FBR) /2/. The contactors preferably used are pulsed sieve plate columns /1/. A computer code for the dynamic simulation of Purex multicomponent extraction has been developed at KfK in order to be capable of calculating Purex flowsheets and of evaluating experiments performed in a countercurrent mode on LWR and FBR fuel reprocessing /3/.

This so-called VISCO computer code, originally conceived for mixer-settlers, has become applicable meanwhile to pulsed columns as well /4/. For uranium the transfer of results on extraction from test columns with small diameters to columns designed on an industrial scale has already been demonstrated with the VISCO code /5/.

A miniature pulsed column facility (MINKA) has been built at the Institut für Heiße Chemie with a view to investigating experimentally flowsheets and courses of malfunctions in Purex pulsed columns. The facility allows to study the development with time for concentration and temperature profiles.

One of the major objectives is the verification of the VISCO code with the help of the experimental data obtained from MINKA, especially under conditions of Pu accumulations. Starting from the experiments and VISCO based computations it shuld be possible to make reliable predictions of the behaviour of plutonium in pulsed columns installed in industrial-scale reprocessing facilities.

Experimental

The miniature pulsed column facility (MINKA) is installed in a glovebox of 30 m^3 volume (length x height x width = 6 x 5 x 1 m). The facility comprises an extraction cycle equipped with four pulsed sieve plate columns and two Holleymott mixer-settlers for solvent washing.

Besides, MINKA accommodates the electrochemical apparatuses ELKE for U/Pu separation, and ROXI and REXI for Pu(III) oxidation and Pu(VI) reduction, respectively /6/. Immediately after they have left the contactor, the aqueous product solutions are freed from TBP in a column with sorption resins /7/.

The MINKA pulsed columns can be interconnected in such a way that they can be operated according to the flowsheet of a codecontamination cycle, a separation cycle or a purification cycle.

All columns have an active height of 3.5 m. One column each is available for extraction and scrubbing. It is 26 mm in diameter and operated in an organic continuous mode. U/Pu separation and U re-extraction take place in columns of 35 mm diameter which are run in an aqueous continuous mode. U/Pu separation can be achieved electrochemically (ELKE) or by U(IV) feed. The scrubbing and re-extraction columns can be heated to 60 °C.

Two continuously operated alpha monitors /8/ are used to monitor the raffinate stream from the extraction column (A-column) and the organic runoff from the separation and re-extraction columns, respectively (B- and C-columns). The raffinate from the scrubbing column (S-column), prior to being fed into the extraction column, is analysed continuously for uranium and plutonium by an optical fiber/laser photometer /9/.

All columns are equipped over the entire length with 50 cm spaced temperature measuring points and sampling points for the pure organic and aqueous phases and for the mixed phase.

The MINKA process solutions are metered in with remote-head membrane pumps. Meanwhile, an accuracy of metering is feasible with a deviation from the theoretical value of $\leq \pm 1\%$. The process streams are monitored by mass flowmeters operating on the Coriolis principle with an accuracy of measurement of ±0.4%.

The pulse for operating the MINKA columns is generated by reciprocating pumps installed outside the box. The pulse is transferred directly to the column through a hydraulic system. With this configuration pulse frequencies of 15 - 150 [1/min] and pulse amplitudes of 5 - 25 mm can be variably set. Pulsation in the column and its holdup are monitored continuously by pressure cells.

The flooding points in Table 1 indicate the range of operation of the MINKA columns. For each column the pulse amplitude was fixed at a constant value and only the frequency was varied. The flooding points were measured in the presence of uranium.

During the function tests of MINKA a number of uranium extraction and re-extraction experiments were performed. Besides metering, pulsation and thermostatic control of the columns, the sampling system and the measurement of holdup were examined. In addition, the droplet sizes were determined by taking photographs.

The VISCO code was verified with the help of the analytically determined uranium and acid concentration profiles. A good agreement was found to exist between the measured and the calculated data.

Results

The first U/Pu experiment was performed in MINKA in December 1985. A codecontamination cycle was run. The flowsheet is given in Table 2. The columns were operated at 60 to 70% of their flooding capacity.

During the experiment of 8 days duration no hydraulically induced disturbances occurred in the MINKA columns. At the interface of the A-column about 100 ml of black, flaky crud accumulated. The interfaces of the S- and C-columns remained free from crud. The equilibrium of extraction in the combined columns was attained after about 5 hours.

The plutonium loss in the raffinate of the A-column was 0.9 to 1.1 mg Pu/l for an extraction length of 3 m. This value confirms the good extraction properties of the miniature column.

Re-extraction of uranium and plutonium at room temperature using 0.12 M HNO_3 proceeded unsatisfactorily. In the CW 1.0 to 1.5 g U/l and 40 to 50 mg Pu/l were entrained. Increasing the temperature of the C-column resulted in an improvement of uranium re-extraction. The CW content dropped to < 0.06 g U/l. The Pu value remained unchanged. The DBP content of CW was 15 to 20 mg/l so that a satisfactory explanation cannot yet be given for the plutonium losses.

The measured U, Pu and H^+ concentration profiles and the temperature profile of the A +S column are given in Fig. 1 together with the data calculated with VISCO. The temperature and the concentration values have been plotted versus the total length of the A + S column.

The total length of the column arrangement plotted on the abscissa of Fig. 1 is a computational quantity derived from the geometric length of the extraction part (0 - 3 m) and the scrubbing part (4.2 to 7.7 m). The 3.0 to 4.2 m levels correspond to the top part of the A-column, the top decanter and the bottom S-decanter. These sections are approximated by VISCO as constituting nearly ideal agitator vessels.

The 0 m level corresponds to the AX point and the AW outlet. The feed and SR enter at the 3 m level. The AS inlet and the SP outlet points are at 7.7 m column height.

As appears from the figure, the VISCO computation agrees well with the measured values also for U/Pu coextraction. The figure exhibits for the center of the S-column (4 to 6 m) an accumulation of uranium and plutonium in the aqueous phase. The maximum concentrations are 55 g U/l and ~2 g Pu/l. A raffinate containing 2 M HNO_3, 0.7 g Pu/l and 14 g U/l is extracted from the S-column and returned into the A-column. The amount recycled is equivalent to 14% and 4%, respectively, of the Pu and U supplied with the feed.

In the first malfunction simulating experiment all flows and concentrations were kept constant, except for the AS-stream whose acid concentration was abruptly lowered from 0.78 M HNO_3 to 0.40 M HNO_3.

Uranium and plutonium accumulation in the S-column slightly increased. Together with the SR-stream 28% and 6%, respectively, of the Pu and U supply were recycled in the state of equilibrium. The plutonium losses in the AW remain constant at about 1 mg/l.

It is envisaged to study in further experiments the influence exerted by variations of flows and concentrations on the extraction behavior of uranium and plutonium under conditions typical of LWR and FBR fuel element reprocessing.

Literature

/1/ G. Koch, Atomkernenergie-Kerntechnik 33 (1979) 241.

/2/ W. Ochsenfeld et. al., KfK 2558 (1977).

/3/ G. Petrich, Proc. IASTED Symp. on Modelling, Identification and Control, Davos, March 2 - 5 (1982) 49.

/4/ G. Petrich et. al., I. Chem. E. Symposium Series No. 88 (1985) 247.

/5/ Anon, KfK 3884 (1985) 2 - 6.

/6/ H. Schmieder et. al., this conference.

/7/ I. Schön et. al., ISEC 1983, pp. 92 -93.

/8/ P. Groll et. al., KfK 3231 (1982).

/9/ J. Römer et. al., KfK 3844 (1984).

Table 1: Flooding points of the MINKA columns

Flowsheet: AF 3 M HNO_3 245 g U/l
AX 30% TBP-kerosene
AS 0.8 M HNO_3
CX 0.1 M HNO_3

Column	A	S	C
Flow ratio /O/A/	2.5	7.0	0.46
Column diameter /mm/	26	26	35
Pulse amplitude /mm/	15	15	25
Flooding point /l/dm² h / at frequency /l/min/			
50	-	285	325
60	365	265	300
70	350	210	-
80	265	-	250

Table 2: Flowsheet of the codecontamination cycle

Stream	Rel. flow rate	Composition			
		M HNO_3	g U/l	g Pu/l	%TBP
AX	100	0.2	<0.06	$<5\times10^{-3}$	30
AF	34	2.83	247	2.07	
AS	14.5	0.78			
CX	217	0.12			

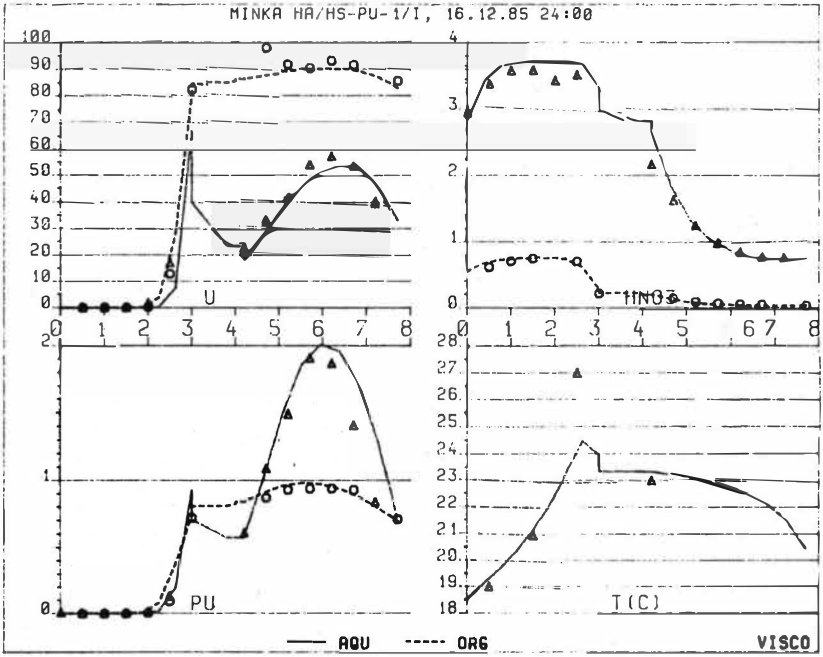

Hydrodynamics in Pulsed Perforated Plate Extraction Columns of Annular and Circular Cross Section

Hans Schmidt, Kernforschungszentrum Karlsruhe, Institut für Reaktorbauelemente

In irradiated fuel reprocessing especially in Fast Breeder reprocessing the use of columns having an annular cross section can be required for reasons of safety against criticality. This configuration in space is realized by a central tube located in the vertical axis of the column containing a neutron absorber. Such columns are not well known today. The small amount of available informations outlines the scope of reduction in volumetric throughput and, to a smaller extent, in efficiency in comparison to cylindrical columns of similar cross section [1].

In this paper experimental investigations concerning the fluid dynamic behavior of an annular pulsed column are reported. The results are compared with those of a column of similar but circular cross section.

The experiments are carried out in the aqueous nitric acid/organic 30 vol. % tributyl phosphate, 70 vol. % dodecan PUREX system. The columns run in the aqueous phase continuous, organic phase dispersed mode of operation. The volumetric flow rates are varied up to high flow rate ratios, i.e. large differences between dispersed phase and continuous phase throughput. Also the sinusoidal pulsation is varied in frequency of pulsation and partly also in the amplitude of pulse stroke.

The experimental set-up and the geometry of the internals are given in Fig. 1. The column length is 4 meters, the length of the cartridge is 3.55 meters. The perforation of plates consists of cylindrical holes with 4 mm diameter and a hexagonal spacing of 7 mm, thus the fractional free area of the plates is 29 %. The plate spacing is 50 mm. The right hand side of Fig. 1 shows the annular configuration of plates as well as the circular configuration. In Fig. 2 the methods and the position of measurements for determination of the fluid dynamic quantities are shown. The dispersed phase holdup is measured by sampling and phase separation at seven points equidistantly spaced along the column. The distribution of drop sizes encountered inside the columns is obtained by evaluation of photographs taken at the two places of observation indicated in Fig. 2.

The determination of longitudinal mixing is carried out by taking into account the dispersion model [2,3]. In the continuous phase, low flow velocities are observed, leading to residence times in the order of hours. Under these conditions the longitudinal mixing is determined using the steady-state tracering technique [4]. The dye tracer enters the column at a constant small flow rate, and the dye concentration profil is measured in the backward direction along the column. The non-steady-state dye tracer method is used to determine the mixing in the drop phase [5]. An impulse injection marks the phase in the continuous state just before entering the column. Inside the column a cloud of dyed drops among uncolored drops is produced by dispersion, the residence time of which is measured in two planes α and ω indicated in Fig. 2 using laser photometry [6].

Operating Characteristics

In Fig. 3 the upper solid line shows the so called flooding curve, experimentally determined by varistion of pulsation frequency and the overall volumetric flow rate. Beyond this curve the column is overloaded and operation is not possible. Below this line there are different types of column operation to be observed. The mixer-settler region occurs at low frequencies of pulsation and low flow rates respectively. By raising frequency or throughput, the dispersion type operation is reached, characterized by a uniform drop distribution in terms of time and location. This mode of operation is achieved in practical application. If pulsation or volumetric flow rates are further increased, an unstable type of operation is reached. The population of drops is very dense and drop coalescence into large clusters of dispersed phase occurs locally, causing an unstable mode of operation with respect to dispersed phase holdup and drop size [7].

The dashed lines are associated with the column of circular cross section. It can be recognized that the individual modes of operation do not differ significantly. In the region of maximum throughput the flooding curves have a difference of about 10 %. A possible explanation of this is given in the discussion of holdup measurements.

Drop Size

The distribution of drop sizes is determined by semi-automatic optical evaluation of photographs. From the spectrum of drop sizes, a mean diameter is calculated. In Fig. 4 the Sauter mean diameter d_{32} is plotted versus the pulsation frequency.

The drop size decreases with increasing intensity of pulsation. In the dispersion zone a minimum is reached, while an increase of drop size is to be observed in the unstable mode of operation as a result of a higher rate of drop coalescence due to very dense packing of drops. The slopes of the drop size curves are not very much different for the two types of columns, but the numerical values are separate. The place of observation is the same in both experiments located in the upper part of the columns (Fig. 2).

The larger mean drop diameter of the cylindrical column, however, is found in the lower part of the annular column. While the drop size passing a length of 10-20 equidistantly spaced perforated circular plates practically remains constant [9] inside the annular column, a further continuous decrease of drop size is observed, leading to the significantly smaller mean diameter of drops, shown in Fig. 4, in the upper part of column.

Holdup

In Fig. 5 the holdup is plotted as a function of column height. The flow rate ratio is shown as a parameter while the total volumetric flow rate and the pulsation remain constant. This means an increase in dispersed phase flow rate results in a continual rise of dispersed phase holdup. The solid lines indicate a continuous increase of holdup values in flow direction of the drop phase inside the annular column. This corresponds to an observation concerning the drop size: larger drops are less influenced by pulsation than smaller drops. This means that the residence time of smaller drops is increased, causing a rise in holdup values. The decrease of drop size therefore results in higher holdup values, leading to the observed growth in holdup with increasing column height.

The column of circular cross section, according to the drop size observations, shows an almost constant slope of holdup profiles [8]. The mean values of holdup are about 10 % higher than the corresponding values measured in the annular configuration.

In Fig. 6 the holdup is plotted versus the pulsation frequency. A continuous rise in holdup with increasing frequency is observed. In the range of 0.5 to 1.5 [s^{-1}] the values of the annular column are below the dashed curve [10]. The flooding point however, is reached at similar holdups of about 75 % and frequencies of pulsation of about 2.7 [s^{-1}] in both columns (Figs. 3 and 6) with the same throughput.

Investigations discussed in [11] point out that the holdup on the flooding curve reaches approximately identical values in the case of constant physical properties of the system, pulsation as well as geometry. Hence increased maximum throughput measured of the annular column in the frequency range of about 1[s^{-1}] (Fig. 3) possibly could be caused by the fact that the improvement in capacity of about 10 % causes holdup values of about 75 % affecting flooding.

Specific Interfacial Area

The specific interfacial area [a] formed by holdup and mean drop diameter, is defined as transfer interfaces per unit volume inside columns and an important quantity for mass transfer calculations [10]. These investigations show, as a main result, that in the achieved dispersion mode of operation the numerical value of "a" is similar in both types of columns. This is due to the fact that 10 % higher holdup values in the case of a circular cross section is compensated by 10 % smaller drop sizes in the annular cross section.

Longitudinal Mixing

The counter current flow of the two immiscible liquids is influenced by pulsation and internals inside the columns. The result is the achieved dispersion of one of the two phases into drops. On the other hand, timely and locally considerably different flow velocities are produced. There are two effects: deterministic factors, causing fluid elements of different velocities and direction and stochastic factors, as a result of turbulent fluctuation intensities. In this way, flow patterns are produced which deviate to a high degree from plug flow conditions. The concentration differences in the two phases as a result of material transfer are mixed up in flow direction, resulting in a possibly large reduction of separation power.

The dispersion model makes the assumption that the convective transport in flow direction is superimposed by a dissipative transport of mixing. The ratio of transport by convective and dissipated flow rates is defined as the Peclet number. This mixing parameter is measured by tracer experiments. Taking into account the measured values of Pe-number and continuous phase flow velocity v_c or the residence time of drops inside the column section limited by the two planes α and ω respectively, the coefficient of transport by dissipation E can be calculated [12].

Continuous Phase Mixing:

In Fig. 7 the mixing parameter Pe_c and the transport coefficient E_c are plotted versus the mean flow velocity v_c of the continuous phase on a double logarithmic scale. The very low velocities result from small flow rates of the continuous phase in relation to the column cross section and to the dispersed phase holdup F_K $(1-\varepsilon)$.

High Pe numbers indicate less mixing. This means that the coefficient of mixing is small. In the limiting case of plug flow conditions, E_c becomes zero, i.e. no mixing exists, and Pe_c approaches infinity. Therefore, decreasing Pe_c-numbers in Fig. 7 indicate an increase in mixing when the continuous phase flow velocity decreases. The two upper lines show the continuous phase mixing inside both columns of different cross section, in the absence of the drop phase; i.e. mixing caused by pulsation and cartridges only. In the presence of the dispersed phase longitudinal mixing increases as the measured lowered slopes of Pe-number and the elevated slopes of E_c indicate.

The comparison of both columns show that continuous phase mixing in the annular column is increased by a factor of 2.

Dispersed Phase Mixing:

The results of longitudinal mixing in the drop phase are plotted in Fig. 8 on a double logarithmic scale. It can be noticed that longitudinal mixing in the dispersed phase is not influenced significantly by the volumetric flow rate ratio. However, fairly high differences are observed by variation of the pulsation.

The pulsation of A x f = 15 x 1 mm/s causes the drop phase to move batchwise by pulsation from one to the next reaction zone each limited by a 50 mm equidistantly spaced perforated plate. In this case high Pe-numbers and low dispersed phase mixing coefficients are measured. Setting the intensity of pulsation (A x f) at a constant value by increasing the frequency of pulsation and decreasing the pulse stroke at the same time the residence time of drops and, consequently, the dispersed phase holdup are increased, leading to higher mixing values. This causes the content of drops to be pushed only partly from one to another reaction zone, resulting in an increase of longitudinal mixing of one order of magnitude.

The longitudinal mixing in the drop phase is increased, similar to continuous phase mixing, in the annular column by a factor of 2; the tendencies caused by variation of pulsation observed in the column of circular cross section are roughly the same.

Conclusion

The experimental investigation shows that the fluid dynamic behavior of pulsed perforated plate columns of annular cross section is not significantly different from those of circular cross section.

The change in geometry from a circular to an annular cross section increases the wall effects resulting in obviously increased shear stresses. By this, the drop size distribution is shifted to smaller drops within a long distance of annular column hight.

At the same time the transport in the transverse direction of the deterministic and stochastic flow pattern is diminished and by this the mixing transport in the axial direction is favored, resulting in an increase in longitudinal mixing.

The specific transfer area being similar inside both columns, this can affect the decrease in efficiency of the annular column, as noted at the beginning of this report. However in order to make a final statement in this case, further investigations are necessary. In particular measured and calculated concentration profiles must be compared.

Literature:

[1] G.E. BENEDICT et. al.: Consolidated Fuel Recycle Program Annular Pulsed Column Development Studies. General Atomic - A 15452; UC-77, July 1979.

[2] T. Miyauchi: USAEC Report, UCRL-3911, 1957.

[3] F. Widmer: Vermischungseffekte bei Gegenstromverfahren. Chem. Rundschau 26, Nr. 14 (1973).

[4] J.E. Mecklenburgh, S. Hartland:The Theory of Backmixing. John Wiley + Sons, Ltd., London 1975.

[5] R. Bauer: Berechnung von Diapersionskoeffizienten nach der instationären Tracermethode. Chem. Rundschau Nr. 26 (1975) 5.

[6] H. Schmidt, E. Eggert: Laserphotometrie zur Bestimmung von Strömungsvorgängen und Stoffübertragung in Pulskolonnen; KfK-Bericht 3630, Feb. 1984, pp. 227-234.

[7] H. Schmidt: Operating Characteristics of Pulsed Plate Columns; Separation Science and Technology, 18 (1983), pp. 1595-1616.

[8] H. Schmidt, H. Miller: Betriebsbereiche, Holdup, Tropfengröße und axiale Vermischung gepulster Bodenkolonnen bei hohen dispersen und geringen kontinuierlichen Volumenströmen; KfK-Nachrichten, Jahrgang 14, 3/82, pp. 154-165.

[9] H. Schmidt: Holdup, Drop Size and Axial Mixing of Pulsed Extraction Columns. Int. Solvent Extraction Conf., Denver U.S.A., 1983, pp. 164-165

[10] H. Schmidt: Das Betriebsverhalten von Pulskolonnen bei großen dispersen und kleinen kontinuierlichen Volumenströmen. KfK-Bericht 3740, 1984, pp. 288-310.

[11] H. Miller: Fluten von pulsierten Boldenkolonnen - gegenwärtiger Stand der Kenntnisse. KfK-Bericht 3771, 1986.

[12] H. Schmidt: The Effect of Operating Variables on Longitudinal Mixing in Pulsed, Perforated Plate Extraction Columns. Extraction Par Solvant Et Exchange D'ions. Inst. Du Genie Chimique, Toulouse, Juin 1985, pp. II-E-1-9.

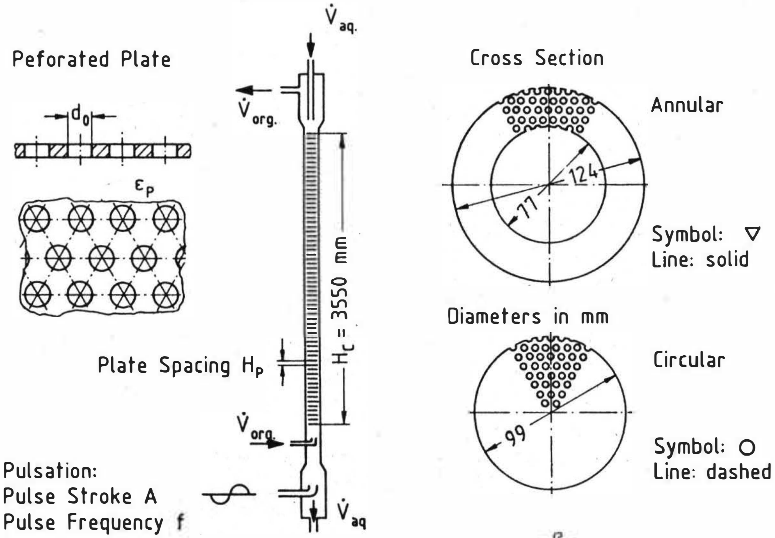
$\dot{V}_{aq.}$
Peforated Plate
d_0
ε_P
$\dot{V}_{org.}$
$H_c = 3550$ mm
Plate Spacing H_P
$\dot{V}_{org.}$
Pulsation:
Pulse Stroke A
Pulse Frequency f
$\dot{V}_{aq}$
Cross Section
Annular
124
77
Symbol: ▽
Line: solid
Diameters in mm
Circular
99
Symbol: ○
Line: dashed

Fig. 1 Experimental Set-up, Geometry Investigated

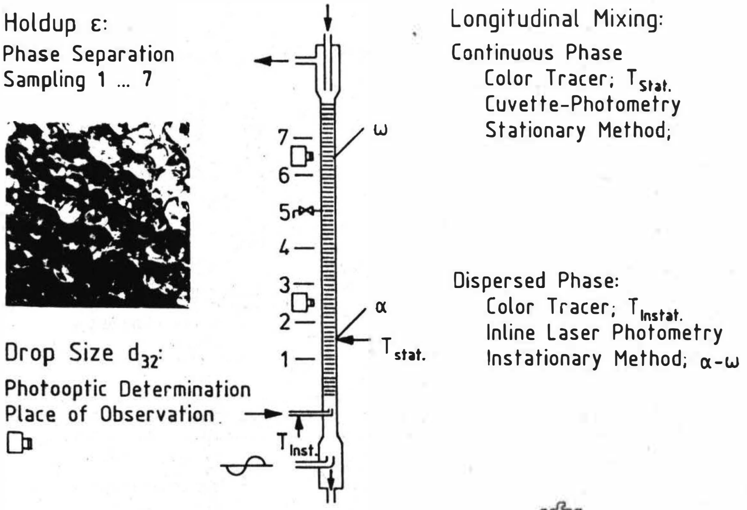
Holdup ε:
Phase Separation
Sampling 1 ... 7
7
6
5
4
3
2
1
ω
α
$T_{stat.}$
$T_{Inst.}$
Drop Size d_{32}:
Photooptic Determination
Place of Observation
Longitudinal Mixing:
Continuous Phase
Color Tracer; $T_{Stat.}$
Cuvette-Photometry
Stationary Method;
Dispersed Phase:
Color Tracer; $T_{Instat.}$
Inline Laser Photometry
Instationary Method; α-ω

Fig. 2 Experimental Set-up, Technique and Location of Measurements

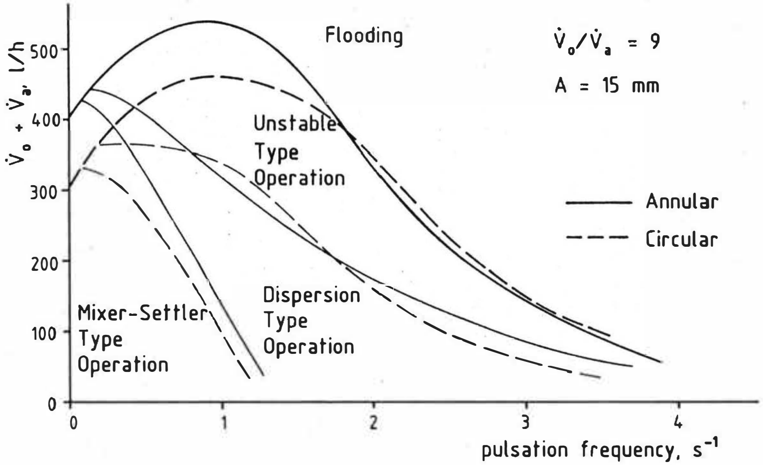

Fig. 3 Operating Characteristics, Aqueous Continuous Phase Mode of Operation

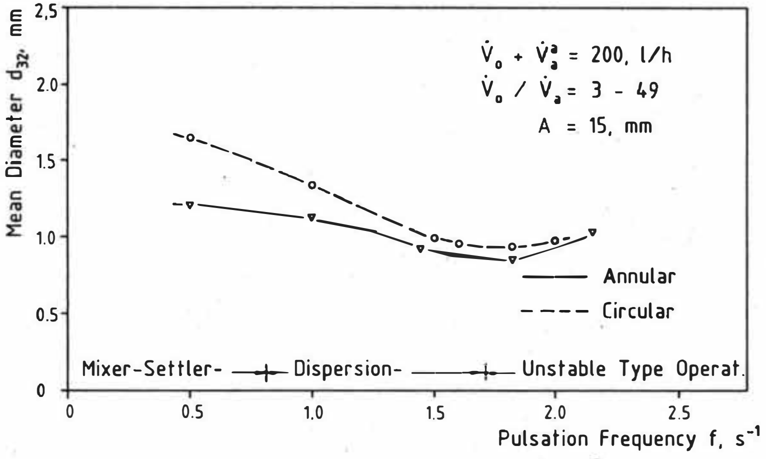

Fig. 4 Sauter Mean Diameter vs Pulsation Frequency

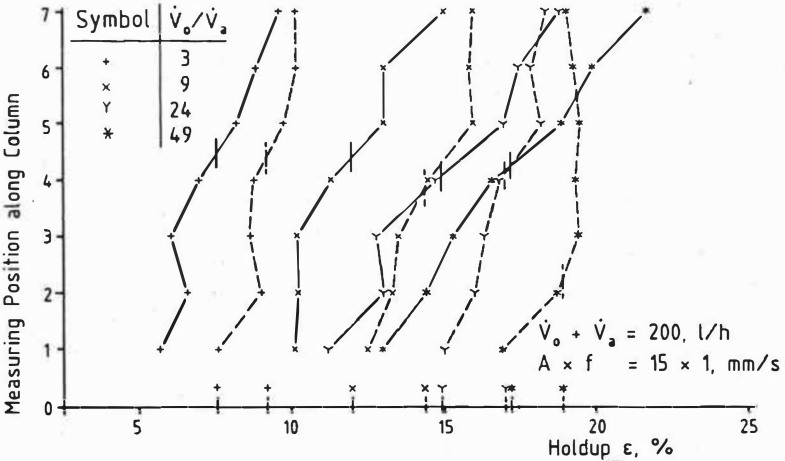

Fig. 5 Holdup vs Column Hight

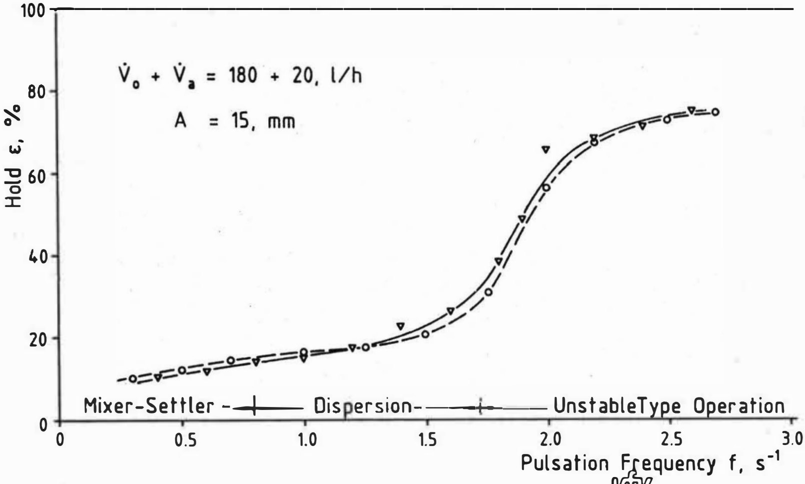

Fig. 6 Holdup vs Pulsation Frequency

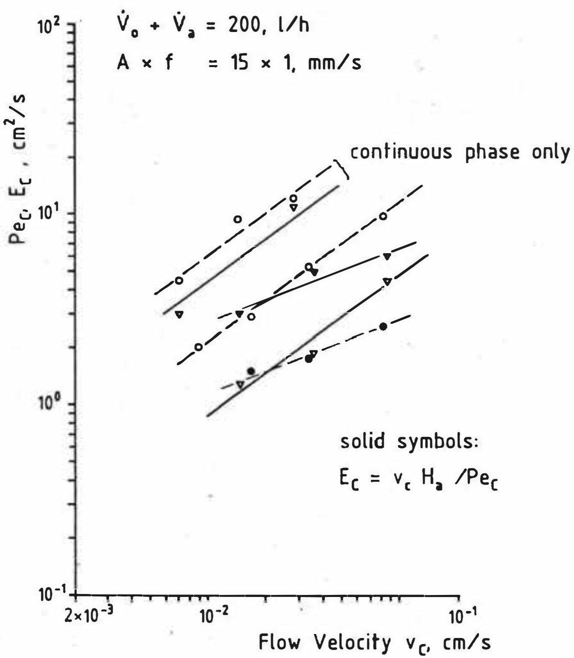

Fig. 7 Continuous Phase Longitudinal Mixing vs Flow Velocity

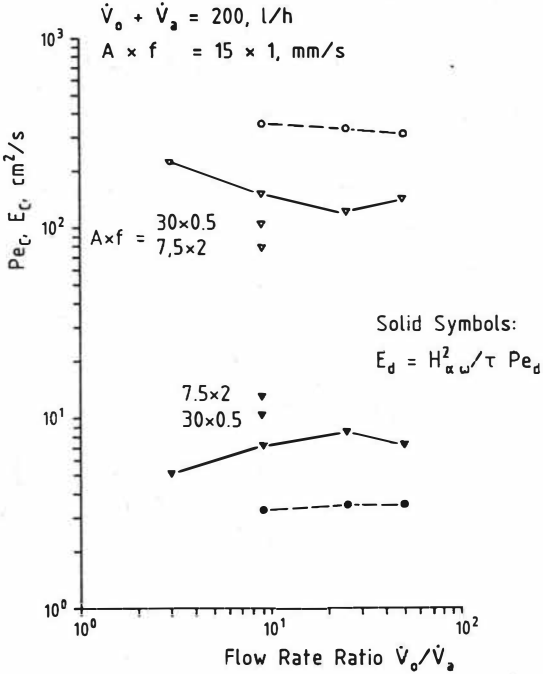

Fig. 8 Dispersed Phase Longitudinal Mixing vs Flow Rate Ratio

Development Of Low Capacity Centrifugal Extractors For Small Scale Reprocessing Facilities

S.B. Koganti, V. Sreedharan, G.R. Balasubramanian, Reprocessing Programme, Indira Gandhi Centre For Atomic Research, Kalpakkam, India .

Introduction

Aqueous reprocessing of fast reactor fuel will lead to high plutonium content and high fission product activity which present many problems, the main being the radiolytic decay of solvent Tri-n-Butyl Phosphate(TBP) leading to loss in extraction efficiency and reduced decontamination of fission products. The main advantages of using centrifugal extractors in fuel reprocessing are; (a) low residence time (5-10 secs), (b) less radiolytic damage to solvent, (c) less volume and hence reduced requirement of solvent inventory, (d) critically safe equipment even for high throughputs, (e) high extraction efficiency, (f) possibility of extracting selective fission products in processes like civex etc, (g) rapid attainment of steady state operating conditions.

Centrifugal contactors with rotor diameter as large as 25 cms and a separating zone length of 35 cms have been in operation at Savannah River Laboratory(1)(SRL) for more than 15 years and their performance was reported satisfactory. Argonne National Laboratory(2)(ANL) had undertaken the modification of SRL design to make a critically safe unit for the reprocessing of liquid metal fast breeder reactor(LMFBR) fuels. Similar units have been reported by various laboratories(3-5), based on SRL design. Later ANL has reported a simplified design, an annular centrifugal extractor(6), where in the mixing chamber, mixing paddle and injection nozzle that are characteristic of SRL design, have been eliminated. French workers(7)have developed a multistage centrifugal extractor wherein 8-10 stages are housed in a rotating cylinder. This design gives the least volume to capacity ratio of centrifugal extractors reported.

Low Holdup Centrifugal Extractors

Low capacity centrifugal extractors find place in pilot plants and small scale reprocessing facilities. These units are also more useful for flowsheet studies. For the fast breeder test reactor under operation at Kalpakkam, a reprocessing rate of 2 Kg/day of irradiated fuel of mixed carbide is planned. With the envisaged 70 gm/lit concentration of fuel after dissolution and make up, the total throughput for the first cycle solvent extraction will be of the order of 5 lit/hr. Assuming a residence time of 10 seconds, the holdup for each stage will be of the order of 15 ml. Low capacity centrifugal extractors developed by American(8) and Russian workers(4), are of the cylindrical bowl type, similar to original SRL design. These units operate at speeds of 6000 rpm and above, primarily due to reduced bowl radius. The high operating speeds compensate the small radius of the bowl, for effective separation. In order to obviate the problem of high speed and the associated problems of vibration and maintenance, two types of low capacity centrifugal extractors viz. (a) multistage unit with 3 physical stages, operating at 1000-1500 rpm and (b) Individual stage unit operating at 2000 - 3000 rpm were developed.

Description of the units

(a) Multistage unit: It is a three stage unit, based on the tubular settler section developed at our laboratory(9). Mixing in each stage is due to the fluid friction by a stationary disk within the rotating compartment and settling is achieved in four small volumetric segments milled symmetrically around the axis of rotation at a larger radius to improve the centrifugal force. Radius of the mixing compartment is larger than the radii of aqueous and organic weirs and hence the mixed phase from the mixer is pumped by a small centripetal pump wheel attached underneath the stationary disk. Once the liquids are pumped into the settler, the settled phases flow to the subsequent mixers due to centrifugal force to achieve counter current operation. Finally the aqueous and organic product streams flow out of the unit through two centripetal pump wheels. Physically the stages are stacked one over the other and the unit is driven by a motor from the top. Since the height of each stage is very small (approx.1.65 cms), stages upto 12 can be stacked in one unit. The main disadvantage of this unit is the requirement of interstage seals, a feature not encouraged in reprocessing industry. The schematic of the unit is shown in Figure 1.

(b) Individual stage unit: This unit is similar to ANL's modified design,except for a small volume of the rotating bowl that is utilised for settling. Mixing is achieved through couette flow between the rotating bowl and the stationary outer bowl. The effective settling volume is confined to two 10 mm wide rectangular slots 180°apart along the length of the bowl. Both the phases are mixed in the annulus as they flow down. Radial vanes at the bottom of the stationary housing inhibit the rotation of the fluid and also aids in mixing. The mixed phase enters the bottom of the rotating bowl and is pumped up through the rectangular slots. The dispersed phase separates out during the travel up the slots and both the phases flow over their respective weirs to the collection chambers. Vertical baffles placed along the inside surface of the stationary bowl were helpful in reducing the liquid build up in the annulus, thereby preventing the flow of liquid directly to the organic collection chamber. A thin disk placed on the radial baffles also reduced the liquid build up in the annulus drastically, but the mass transfer efficiency is found to be less due to reduced mixing and hence is discarded in the final unit. The design details of the unit are presented in Figure 2.

The rotating bowl, aqueous and organic weirs,air control arrangement for controlling the interface etc. are housed in a single welded unit which can be driven by a shaft from the top. The only maintenance expected here is the bearing housing that supports the drive shaft. A bank consisting of 8 individual stages has been fabricated in such a way that all the stages can be remotely dismantled and reassembled using master slave manipulators(MSM). All the eight stages are arranged in a serpentine fashion and are driven by a common air motor. A liquid seal is used at the top of the drive pulley for interface control.

Performance tests

(a) Multistage unit: Separating capacity tests were conducted using dilute HNO_3 as aqueous phase and 30% n-TBP/Shell Sol T as the organic phase. Drive speeds were varied from 800 to 1500 rpm using a d.c motor. Table 1. shows the hydraulic capacity data obtained in a three stage unit at speeds of 1250 and 1500 rpm.

Table 1. Hydraulic capacity data

Operating speed: 1250 rpm			Operating speed: 1500 rpm		
Aq. flow cc/min	Org. flow cc/min	Entrainment Aq in Org %	Aq. flow cc/min	Org. flow cc/min	Entrainment Aq in Org %
105	180	nil	105	180	nil
130	160	0.5	60	184	0.2
160	155	0.5	133	176	nil
190	125	0.5	208	180	nil
207	119	0.5	215	108	nil

At 1500 rpm maximum capacity is not realised due to the limitation of pump capacity. The contact time per stage is about 3 sec at a throughput of 400 cc/min. Figure 3. shows the plot of mass transfer performance of the 3 stage unit for HNO_3-30% TBP in Shell Sol T. The performance of the unit approaches that of a theoretical stage.

(b) Individual stage unit: Figures 4 & 5. show the flooding capacity curves for HNO_3 - 30% TBP in Dodecane and Uranyl Nitrate- 30% TBP in Dodecane systems. The points indicate 1% entrainment of aqueous in organic. Throughout the flooding capacity runs, no entrainment of organic in aqueous was observed. The experiments were conducted without any interface control. The capacity curves would have been different if interface control were used. With an annular gap of less than 5 mm it was found that liquid build up was more and overflow of the mixed phase to organic collection chamber was observed. Increasing the gap may reduce the build up, but increases the mixer volume enormously. According to Leonard etal.,(10) the dispersion number which essentially indicates the mixing effectiveness, is independent of the annular gap width and therefore a value of 5 mm was chosen for the design.

Holdup measurements are important for the calculation of radiation damage to the solvent. In an annular contactor, the volume of liquid in the mixer is more or at par with that of the settler unlike the centrifugal extractors with impeller mixing, wherein the mixer volume is around 1/3 to 1/5 that of settler. Most of the radiation damage will occur in the mixing zone and hence the need to measure the holdup. Figures 6 & 7. show the plot of fraction of dispersed phase vs dispersed phase flow rate with continuous phase flow rate as the parameter for both the systems. The flow rates were such that aqueous was dispersed in organic. The dispersed phase holdup increases with dispersed phase flow rate for a fixed continuous phase flow rate. For a given dispersed phase flow rate, the fraction of dispersed phase decreases as the continuous phase flow rate increases. The same trend was observed by changing the dispersion to organic. Table 2. presents the mass transfer efficiencies for both the systems at 3000 rpm for different A/O and total throughput. Mass transfer efficiencies of over 90% were achieved.

Conclusions

Centrifugal extractors are superior compared to pulsed columns and mixer settlers in their performance and also are cost effective for large size reprocessing plants. Small capacity annular centrifugal extractors operating at low speeds can be designed for small scale production facilities or pilot plant applications. The multistage unit may not be suitable for handling liquids with solid particles and need elaborate feed clarification system. The individual stage unit is easy to fabricate and provision for remote maintenance can be incorporated easily at the design stage.

References

(1) Webster, D.B., et al., Report DP-MS-67-71, SRL (1967)

(2) Bernstein, G.J., et al., Report ANL-7968 (1973)

(3) Roth, B.F., Report KFK-862, May (1969)

(4) Kuznetsov, G.I., et al., Report SRARI (1973)

(5) Nagarajan, S,. et al., IIChE 30th annual session, Chandigarh (1977)

(6) Bernstein, G.J., et al.,Report ANL-7969 (1973)

(7) Dollfus, J., Communication in solvent extraction conference, Imperial college, London (1969)

(8) Jennings, A.S., DP-680, SRL (1962)

(9) Koganti, S.B., et al., National Symposium on solvent extraction of metals, Bombay (1979)

(10) Leonard, R.A., et al., AIChE J., 27(3),495 (1981)

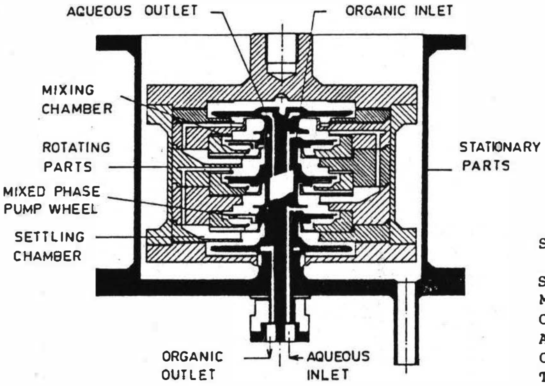
AQUEOUS OUTLET
ORGANIC INLET
MIXING CHAMBER
ROTATING PARTS
MIXED PHASE PUMP WHEEL
SETTLING CHAMBER
STATIONARY PARTS
ORGANIC OUTLET
AQUEOUS INLET

THREE STAGE LOW HOLD UP CENTRIFUGAL EXTRACTOR

Fig. 1

Salient features:

Settler volume/stage =15 cc
Mixer volume =5cc
Organic weir radius =2.75cm
Aqueous weir radius =3.35cm
Overall bowl diameter =15.6cm
Typical acceleration
(volume average) 145.00g

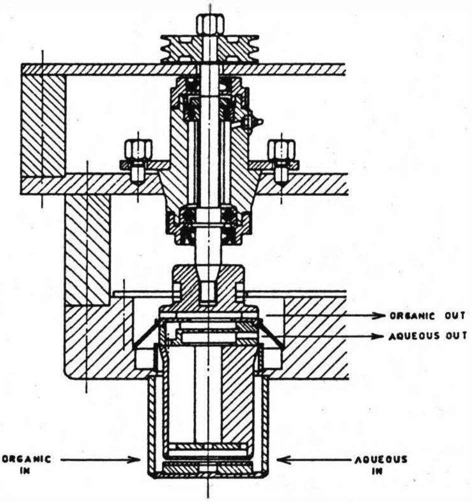
ORGANIC OUT
AQUEOUS OUT
ORGANIC IN
AQUEOUS IN

ANNULAR CENTRIFUGAL CONTACTOR

One stage of a bank of 8 contactors

Fig. 2

Salient features:

Diameter of the
rotating bowl =4.5cm
Settler chamber
dimensions =1.5 x0.8x5.55cm
Settler volume =15cc
Mixer volume =20-40cc
depending on
rpm, A/O and
throughpout
Organic weir
radius =1.25cm
Aqueous weir
radius =1.35cm
Typical accelration
(volume average) 180g

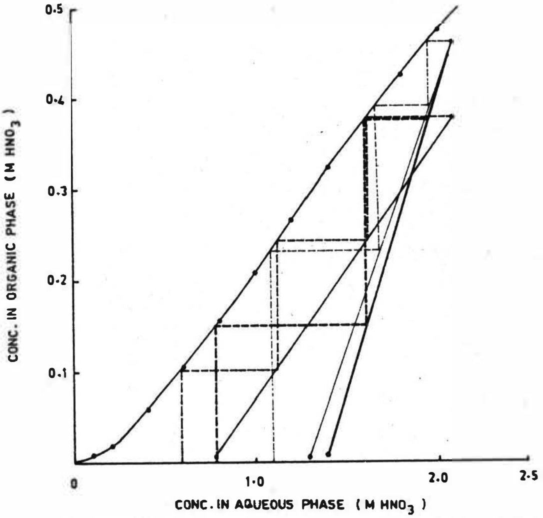

FIG.3. MULTISTAGE UNIT MASS TRANSFER PERFORMANCE (HNO_3 -30% TBP / IN SHELL SOL.T)

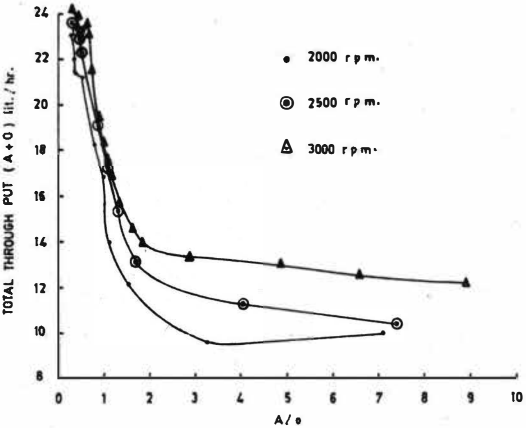

FIG.4. FLOODING CAPACITY CURVE (INDIVIDUAL STAGE UNIT) FOR HNO_3 -30% TBP / IN DODECANE SYSTEM.

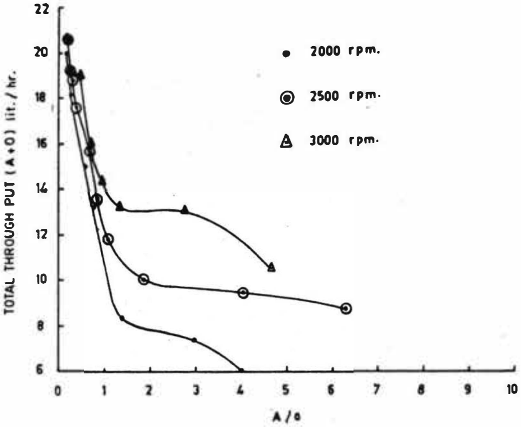

FIG.5. FLOODING CAPACITY CURVE (INDIVIDUAL STAGE UNIT) FOR URANYL NITRATE -30% TBP/ IN DODECANE.

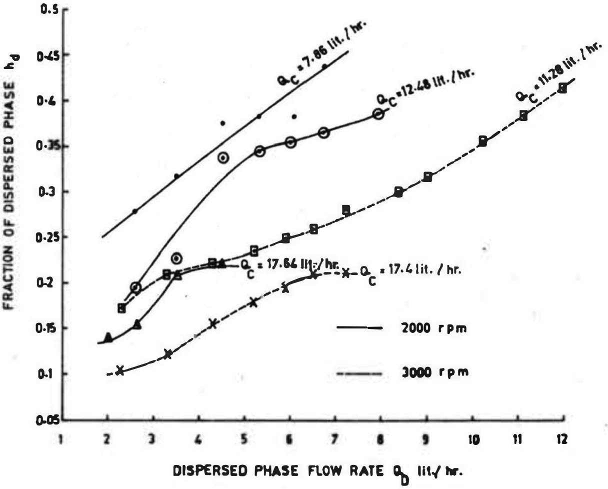

FIG. 6. DISPERSED PHASE HOLDUP (INDIVIDUAL STAGE UNIT) FOR HNO_3 -30% TBP/ IN DODECANE SYSTEM

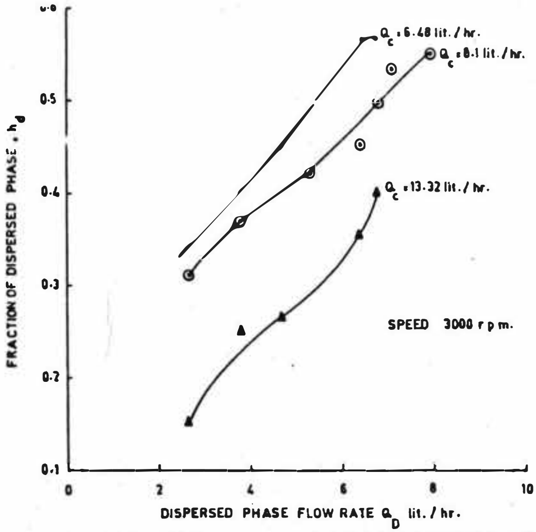

FIG. 7. DISPERSED PHASE HOLD UP (INDIVIDUAL STAGE UNIT) FOR URANYL NITRATE -30% TBP/ IN DODECANE

Table. 2 Mass transfer performance of a individual stage unit

Nitric acid-30% TBP/Dodecane				Uranyl nitrate-30% TBP/Dodecane			
A/O	Throughput lit/hr	E_O %	E_A %	A/O	throughput lit/hr	E_O %	E_A %
0.322	12.06	92.98	91.62	0.373	14.58	88.78	95.99
0.485	9.00	92.53	90.35	0.510	9.06	101.50	93.38
0.705	13.50	95.99	92.23	0.780	6.84	100.57	91.17
1.063	5.94	92.29	100.00	0.931	6.72	96.05	89.26
2.200	5.76	94.10	116.79	1.818	11.16	102.62	89.91
3.167	7.50	93.46	96.06	3.282	10.02	90.52	98.54
5.367	11.46	97.26	108.85	5.184	11.52	99.08	92.18

where

E_O & E_A are mass transfer efficiencies based on organic and aqueous respectively.

DISCOSEARCH - a computerised storage and retrieval system for PUREX distribution data

A. L. Mills, Chemistry Division, UKAEA, Harwell
Mrs. R. Ross, Department of Computing, The Polytechnic, Oxford

Introduction

The basis for all solvent extraction process flowsheets is a collection of suitable distribution data for the solutes involved.

The PUREX process which is in general use in nuclear fuel reprocessing is concerned with uranium, plutonium and nitric acid as solutes and tri(n)butylphosphate as the extractant.

There are a number of variants of the basic PUREX process where the extractant concentration, operating temperature or other features may differ but in general terms a good fundamental data base is a necessary requirement to the process designer.

There are many distribution data for the PUREX process in both the classified and unclassified literature, but with perhaps one notable exception (1) there are no readily available collections of such data.

A preliminary literature search has revealed over 7000 distribution coefficient data sets for U, Pu and HNO_3 in the PUREX process and with more data sets being determined it was felt appropriate that a more organised method of recording such data should be considered.

It is thought that a computerised storage and retrieval system would be of value particularly if at a later date information retrieved from the system could be tested statistically. The data storage and retrieval system, DISCOSEARCH and work to date on the statistical assessment of retrieved data DISCOSTATS is discussed in this paper.

DISCOSEARCH

DIS(tribution) CO(efficient) SEARCH has been written for a CBM PET and an Apple IIe computer. The program can be readily adapted for use on other micro computers and it could also be modified for use on a main frame machine if required.

Access to DISCOSEARCH is via a menu system where the user is asked to respond to questions displayed on the computer VDU screen. Given a set of acceptable responses the computer will then search for the requested data and print it out in a tabulated form.

At present some 7000 distribution coefficient data sets for the PUREX process have been recorded and are stored. Storage of additional data is straightforward.

A distribution coefficient data set contains the following information.

Total U (aqueous plus organic) gm l^{-1} default zero
Total Pu (aqueous plus organic) gm l^{-1} default zero
Percent Pu(VI) in system, default value zero
All Pu assumed Pu(IV)
Aqueous HNO_3 M default zero
Aqueous H_2SO_4 M default zero
TBP (as volume percent), diluent not specified
Temperature ^{o}C where known
For the system above,
Aqueous U g/l, organic U g/l, D_u ($= \frac{\text{org U}}{\text{aqu U}}$)
Aqueous Pu(IV) g/l, $D_{Pu(IV)}$ ($= \frac{\text{org Pu}}{\text{aqu Pu}}$)
Aqueous Pu(VI) g/l, organic Pu(VI) g/l, $D_{Pu(VI)}$ ($= \frac{\text{org Pu(VI)}}{\text{aqu Pu(VI)}}$) if appropriate
Aqueous HNO_3 M, organic HNO_3 M, D_{HNO_3} ($= \frac{\text{org } HNO_3}{\text{aqu } HNO_3}$)
Together with the reference from which the data have been taken.

Some built-in checks are included in the program; mass balances for U, Pu, HNO_3 are checked, and errors > 10% for U and Pu are noted, as are errors > 25% for HNO_3, similarly D values are checked, and any deviation noted.

The system is used in the following way. After the program has been loaded into memory the 8 key fields and the data ranges stored for each key field are displayed. To access the data the user is prompted to input the key field(s) and data ranges in which he is interested (Figure 1). The system performs a search of the data on the data disc and displays the number of data sets which satisfy the requested data range for each key field input. A cross search is then carried out and the number of data sets are displayed for each key field which satisfy the data range requested for it and for all the requested key fields to its left on the table (see Figure 2 DISCOSEARCH screen display).

At each stage the user may change the key fields and data ranges. When satisfied with the outcome of the search a printed copy may be obtained (see figure 3), this consists of:

1. A copy of the screen display
2. The data values for each dataset retrieved
3. A list of references

The retrieved data are stored on disc for use with DISCOSTATS is required

DISCOSTATS

DIS(tribution) CO(efficient) STAT(istic)S has been written specifically for a CBM PET computer, but like DISCOSEARCH it could be adapted for other machines.

The data stored in DISCOSEARCH has not been assessed other than to check mass balances and the arithmetic associated with the calculation of distribution coefficients. It is realised that this might detract from the value of the information stored but it is felt that it is better to have as complete a compilation of data as possible as a data bank and then have the ability to abstract data and test it. Thus acceptance or rejection of data is a matter for the individual user of the data rather than the compiler.

DIStribution COefficient STATisticS requires the DISCOSEARCH data discs and, in its present form enables the user to search and find data from DISCOSEARCH and to correlate statistically any two variables from the data found, i.e. any two from: Total U, Total Pu, Total HNO_3, aqueous U, organic U, D_U, aqueous Pu (or Pu(VI)), organic Pu (or Pu(VI)), D_{Pu} (or Pu(VI)), aqueous HNO_3, organic HNO_3, D_{HNO_3}. Clearly some combinations of variables, two at a time, are not meaningful.)

Upon selecting data (up to 200 sets), the scales for the X and the Y axis are chosen by the program and a plot of the data from DISCOSEARCH is displayed. On request, DISCOSTATS will perform a least squares fit to the data using a polynomial form to describe the dependence of the two variables. The order of the polynomial (up to fourth order) may be specified by the user or may be determined by searching for the optimal fit. The fitted polynomial is then displayed on the same plot as the data and a hard copy is provided if desired.

A statistical analysis of the fit is given, if required, showing the significance of the parameters in the polynomial and the fit itself. The polynomial may be used for interpolation or extrapolation and a statistical estimate of the associated error is given.

A feature of DISCOSTATS is that it offers the possibility to remove data supplied by DISCOSEARCH either on the basis of a statistical comparison of the different data sets or at the request of the user. The modified data set may then be re-fitted as described above.

Implementation

DISCOSTATS is a menu-driven program which may be automatically run from DISCOSEARCH. The user is initially requested to select the two variables for which the statistical correlation is required. A plot of the data is then displayed (Figure 3). When the user wishes to proceed MENU 1 is displayed (Figure 4). If the user selects a fit routine (options 1 and 2) the fit is performed and displayed (Figure 5). If the user selects the data change option (option 5) then MENU 2 is displayed (Figure 6) detailing the various possibilities. Once the user has chosen a modified data set, return can be made to MENU 1 (option 8) and the data may be refitted.

At the present time DISCOSTATS will only deal with two dimensional statistics. Further work is planned to extend the scope of the statistics.

General Comment

Although in the form presented above DISCOSEARCH and DISCOSTATS are used in conjunction with data specific to the PUREX process, the 'shells' of the programs can be used for the storage and examination of any sets of related data i.e. for other solvent extraction programs, distillation data etc.

Reference 1   G. Petrich KfK 2536

Acknowledgement

One of the authors (RR) would like to acknowledge the financial assistance given by the Harwell Laboratory of the UKAEA in supporting this work.

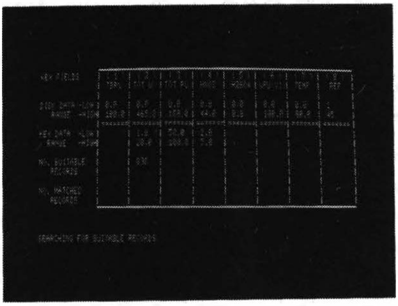

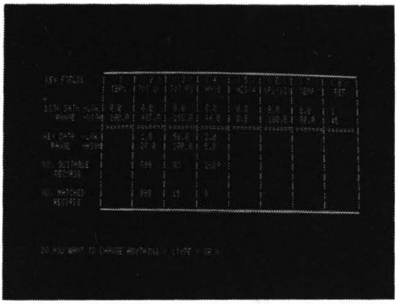

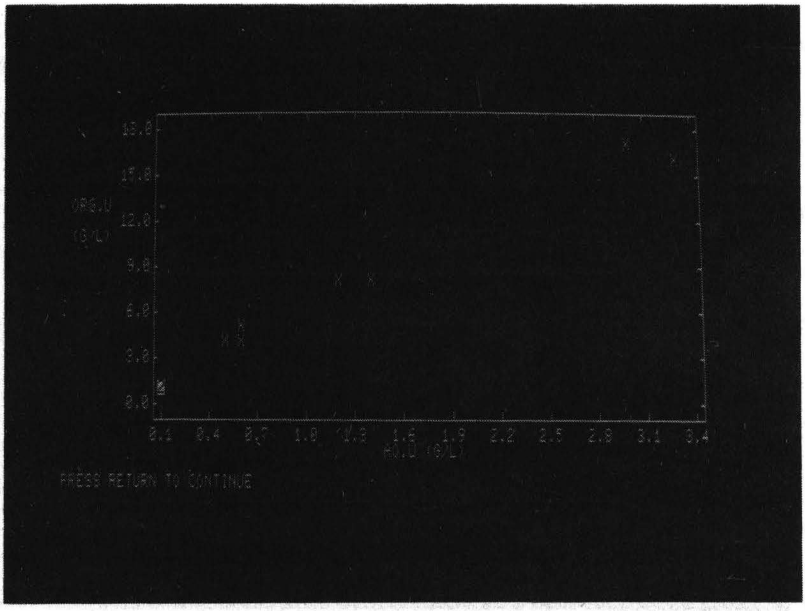
18.0
15.0
ORG.U
(G/L)
12.0
9.0
6.0
3.0
0.0
0.1
0.4
0.7
1.0
1.3
1.6
1.9
2.2
2.5
2.8
3.1
3.4
HO.U (G/L)

```
PRESS RETURN TO CONTINUE
```

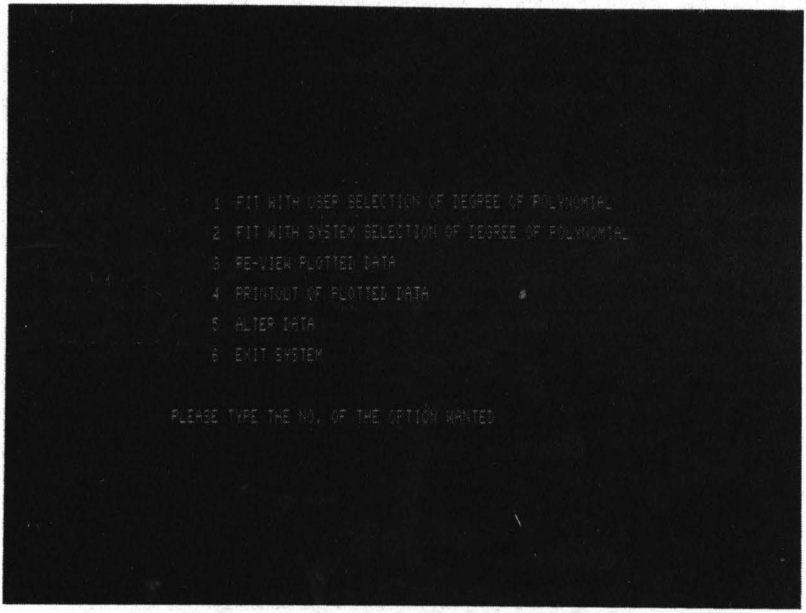

```
1  FIT WITH USER SELECTION OF DEGREE OF POLYNOMIAL
2  FIT WITH SYSTEM SELECTION OF DEGREE OF POLYNOMIAL
3  RE-VIEW PLOTTED DATA
4  PRINTOUT OF PLOTTED DATA
5  ALTER DATA
6  EXIT SYSTEM

PLEASE TYPE THE NO. OF THE OPTION WANTED
```

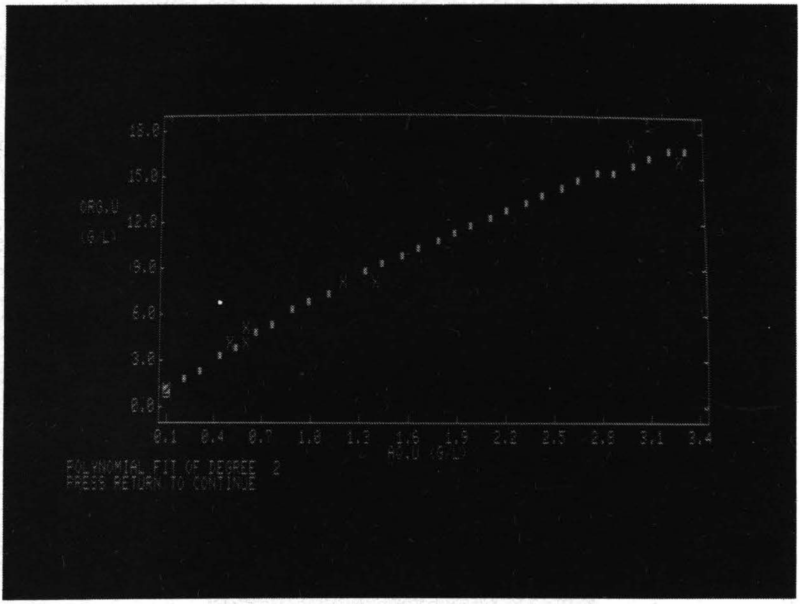
18.0
15.0
12.0
9.0
6.0
3.0
0.0
ORG.U
(G/L)
0.1
0.4
0.7
1.0
1.3
1.6
1.9
2.2
2.5
2.8
3.1
3.4
AS.U (G/L)

```
POLYNOMIAL FIT OF DEGREE  2
PRESS RETURN TO CONTINUE
```

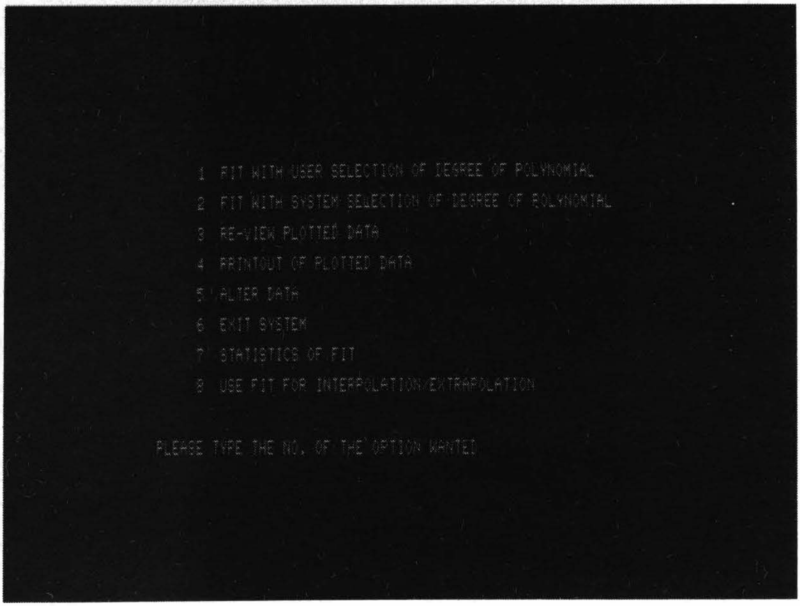

```
  1  FIT WITH USER SELECTION OF DEGREE OF POLYNOMIAL

  2  FIT WITH SYSTEM SELECTION OF DEGREE OF POLYNOMIAL

  3  RE-VIEW PLOTTED DATA

  4  PRINTOUT OF PLOTTED DATA

  5  ALTER DATA

  6  EXIT SYSTEM

  7  STATISTICS OF FIT

  8  USE FIT FOR INTERPOLATION/EXTRAPOLATION


PLEASE TYPE THE NO. OF THE OPTION WANTED
```

Application of the Code PULCO for the Simulation of Pulsed Column Behaviour in the 1. Extraction Cycle of the PUREX-Process

E. Gelfort, B. Heits, Deutsche Gesellschaft für Wiederaufarbeitung
von Kernbrennstoffen mbH
Hamburger Allee 4, D 3ooo Hannover 1 / FRG

H. Kühl, W. Weyer, Wissenschaftlich-Technische
Ingenieurberatung GmbH
Mozartstr. 13, D 5177 Titz-Rödingen / FRG

The calculation code PULCO /1/ has been developed to simulate the PUREX extraction process in pulsed column extractors. PULCO includes model equations for

- mass transfer from liquid drop to continuous phase
- drop diameter and drop velocity in the pulsed column
- relative hold-up of dispersed and continuous phase
- longitudinal eddy dispersion coefficients

The equations are derived from Japanese experiments for small columns (⌀ 5 cm, height 2oo cm). Eight components of PUREX-process medium can be simulated simultaneously. The code is written in FORTRAN and has been implemented on an IBM-mainframe computer in a slightly modified form.

PULCO has been applied to the 1o m-columns of the Uranium Extraction Cycle (UEZ) at the test facility (TEKO) of the reprocessing plant (WAK) at KfK Karlsruhe.

First results for extraction and reductive separation are encouraging. The computed stationary uranium profiles are in good agreement with experimental results.

1. Introduction

The PUREX extraction process is a major step in the reprocessing of spent nuclear fuel. The recyclable uranium and plutonium is separated and purified of radioactive fission products. The PUREX extraction can be realized in mixer-settlers or in pulsed columns with sieve plates, which have in common a nitric acid aqueous phase being counter-currently contacted with an organic phase of 3o % Tri-n-Butyl-Phosphate (TBP) in e.g. n-dodecane.

Codes for the simulation of pulsed columns at different operational conditions are appropriate e.g. for the design and the determination of the inventory of columns and may be employed in systems control. The calculation code PULCO has been developed for these applications at Tokai Mura in Japan. The theoretical model is based on an extensive evaluation of literature. Its implementation in a computer program and its verification by measurements on 2 m-columns is documented in the publication /1/ (1982). On behalf of DWK the code has been revised and implemented on an IBM-computer 3o81 based on the published listing.

2. Problem

For the calculation of the separation efficacies of pulsed columns the concentration profiles for all relevant substances must be determined accurately. Our objective was to verify the calculation code on the basis of experimental data obtained under realistic operation conditions and to establish good agreement between calculated and measured concentration profiles. In UEZ/TEKO the first extraction cycle of a major reprocessing plant is tested at full size with depleted uranium used as feed. Experimental data from tests run at UEZ/TEKO have been used to validate the PULCO code.

The computer program PULCO has been developed on the basis of Japanese laboratory experiments for 2 m-columns. The modelling of drop formation, kinetics of mass transfer, and fluid dynamics have been tested in these experiments. The extension of the numerical model to true scale columns of an industrial reprocessing plant is problematic. In /1/ no explicit extension of the code to scaled-up columns is demonstrated.

Only a comparison of calculated results with data obtained under realistic conditions, as e.g.

- dimensions of extraction apparatus
- fluid dynamics
- pertubations

can qualify a numerical program for practical usage. Work to that end is in progness.

3. Theory

The PULCO code is based on a dispersion model for the PUREX process.

The behavior and interaction of up to eight components in aqueous and organic phase can be simulated simultaneously by PULCO. All the required physical and chemical constants are built into the code for

HNO_3	(nitric acid)
$UO_2(NO_3)_2$	(uranylnitrate U(VI)
$Pu(NO_3)_4$	(plutonium nitrate Pu(IV))
$Pu(NO_3)_3$	(plutonium nitrate PU(III))
$U(NO_3)_4$	(uranium nitrate U(IV))
NH_2OH	(hydroxylamine)
HNO_2	(nitrous acid).

The axial concentration distribution in the column is calculated from one-dimensional mass bilance equations:

$$\varphi_a(z) \cdot \frac{\partial x_j(z)}{\partial t} = E_x \cdot \frac{\partial^2 x_j(z)}{\partial z^2} + u_x \cdot \frac{\partial x_j(z)}{\partial z} - K_{od,j} \cdot a(z) \cdot \left\{x_j(z) - x_j^*(z)\right\} + \sum_r R_{arj}(z) \cdot \varphi_a(z)$$

$$\varphi_o(z) \cdot \frac{\partial y_j(z)}{\partial t} = E_y \cdot \frac{\partial^2 y_j(z)}{\partial z^2} - u_y \cdot \frac{\partial y_j(z)}{\partial z} + K_{od,j} \cdot a(z) \cdot \left\{x_j(z) - x_j^*(z)\right\} + \sum_r R_{orj}(z) \cdot \varphi_o(z)$$

$$y_j(z) = m(x_j(z) \text{ or } y_j(z)) \cdot x_j^*(z)$$

The following physical-chemical processes are taken into account:

- backmixing due to the imposed pulsation in the column
- mass transfer by convection
- mass transfer between liquid drop and continuous phase
- redox reactions in organic and aqueous phases.

z is the axial coordinate in the column and t the time. x_j and y_j are the concentrations of component j in aqueous and organic phase, respectively. E_x and E_y are the dispersion (or turbulent diffusion) coefficients and take account of backmixing. u is the velocity of the phase in the column and its fractional hold-up. K_j is the mass transfer coefficient of component j, m_j its distribution coefficient. A is the drop surface area per volume. R_{arj} is the reaction rate for component j due to the r-th redox reaction, which may take place in some of the columns of the PUREX extraction cycle.

The distribution coefficients m_j (i.e. the ratios of the equilibrium concentrations of organic and aqueous phase) are essential input data, which must be known as function of temperature, composition, and concentrations. A relation based on Richardson /2/ is built into PULCO for the distribution coefficients of HNO_3, U(VI), Pu(IV), Pu(III), U(IV), and HNO_2.

Each component contributes two equations for the system of coupled non-linear partial differential equations (due to the concentration dependence of distribution- and mass transfer coefficients, and reaction rates).

To some extent the z-dependence of the paramters is taken into account. Heat balance is not considered in PULCO, but the temperature gradient in the column may be specified, and the temperature-dependence of mass transfer- and distribution coefficients is allowed for.

Hold-up, dispersion coefficient, velocity, mass transfer coefficient, and drop surface area are calculated by PULCO from the geometry and the operational conditions of the pulsed column, but they can also be specified by input.

In /1/ good agreement has been obtained between PULCO results and measurements for small columns for Pu, U, and H^+. In contrast, we had to compromise in our efforts to simulate the pulsed columns of UEZ/TEKO. The hold-up calculated from the PULCO-formula is wrong up to an order of magnitude. Therefore we had to fix the hold-up by input according to measurements.

4. Results

PULCO-calculations of stationary concentration profiles have been performed for the pulsed columns HA, BS, and 1C of the test facility UEZ/TEKO. The results are presented in Fig. 1-3. Evaluations of the calculated results show a good agreement with the experimental data.

Further PULCO-calculations are planned to simulate the complete process in UEZ/TEKO. Additionally the dynamical behaviour of e.g. disturbance of PUREX-process, start-up, or shut-down of a pulsed column will be taken into consideration during future developement.

Literature:

/1/ Gonda, K., Matsuda, K., PNCT 841-82-19 (1982)

/2/ Gonda, K., Okamatsu, I., Fukuda, Y., PNCT 841-79-26 (1979)

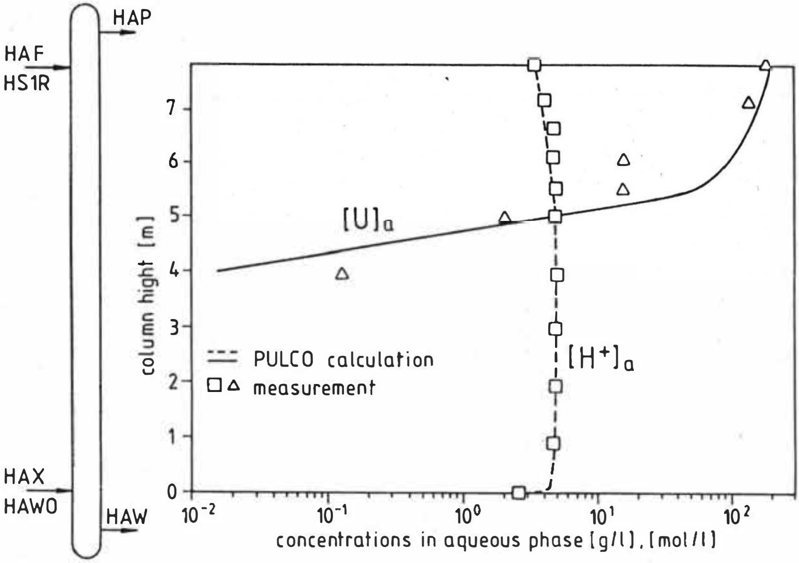

Fig. 1: concentration profiles in HA-column of UEZ/TEKO

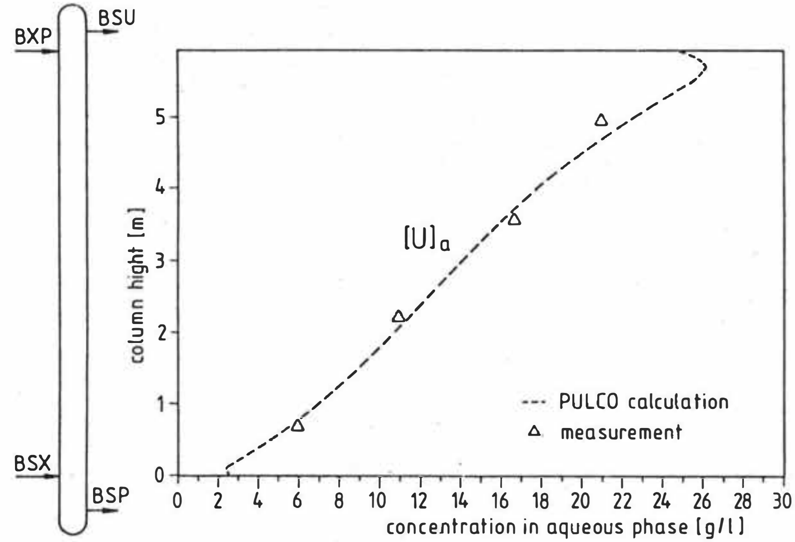

Fig. 2: concentration profile in BS-column of UEZ/TEKO

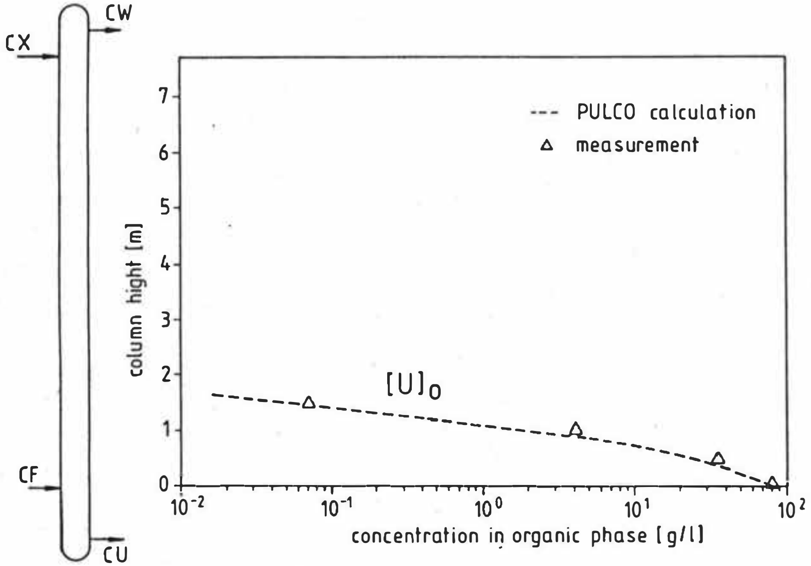

Fig. 3: concentration profile in 1C-column of UEZ/TEKO

The Tri-n-butylphosphate (TBP) Distruction owing to Nitric Acid, Zirconium and Hafnium

O.A.Sinegribova, G.A.Yagodin, A.A.Varnek, R.P.Ozerov, A.H.Kuznetsov.
The Mendeleev Institute of Chemical Technology, Moscow, USSR.

TBP (tri-n-butylphosphate) suffers the acidic hydrolysis owing to nitric acid and water. The hydrolysis of TBP was earlier studied (1) but the mechanism of hydrolysis has not been determined in detail and the data concerning the effect of metals in TBP upon its hydrolysis were discrepant. For instance, in (2) it was shown that zirconium promoted the TBP hydrolysis by increasing its rate however in (3) it was pointed out that the rate of hydrolysis didn't change in presence of zirconium. The effect of hafnium upon the hydrolysis of TBP was not studied yet.

This work is the attempt to determine the mechnism of TBP acidic hydrolysis and to predict the effect of zirconium and hafnium upon it on the basis of quantum chemical calculations. We tried also to confirm the conclusions drown from the calculations by the experimental data.

The quantum chemical calculations were carried out in 2 stages by CNDO/2 method. At the first stage the calculation of electron structure was realized for some neutral organophosphoric compounds, at the second - for their protonated species. In the calculations of the first stage the lengths of bonds P = O(1.42Å) and C - H(1.09Å) in alcylphosphates have been fixed and the other geometrical parameters have been optimized. These calculations resulted in the information about the charge distribution and the structure of molecular orbitals (MO) in studied molecules. The higher occupied MO is lokalizing at the ether oxygen atoms and corresponds to the electrons of undivided pairs, the other high lied MO are considerably delocalized that indicates the conjugation of all P - O bonds in studied systems. The calculated values of charges at the atoms are shown in Table 1.

The analysis of these data leads to a fact that lengthening of alcyl chain does not result in the considerable change of charge values of mentioned atoms. It allows to use in the following calculations the simplest of examined molecules - trimethylphosphate (TMP) as a model object. For analysis of the protonation process is expedient to use the distribution of molecular electrostatic potential (MEP) in alcylphosphats that describes the energy of electrostatic interaction between proton and reagent in any point of space (4). MEP distribution in TMP (Fig.1) has been constructed on the basis of quantum chemical calculation and with regard for the pecularities of electron structure of molecule. Two distinct MEP minimums are observed: near the phosphoryl and ether oxygen atoms. The comparison of their values (-0.050a.u. and -0.036a.u.) indicates that a primary protonation of phosphoryl oxygen atom takes place. This fact is confirmed by well known experimental data. The analysis of the surface of polarization term for the protonation energy leads to the similar conclusion: it has more negative values near the phosphoryl oxygen atom.

Table 1

CHARGES AT THE ATOMS IN NEUTRAL AND PROTONATED SPECIES OF TRIALCYLPHOSPHATES

	$(CH_3O)_3PO$	$(C_2H_5O)_3PO$	$(C_3H_7O)_3PO$	$(CH_3O)_3PO\ H^+_{(Ph)}$	$(CH_3O)_3PO\ H^+_{(eth)}$
C	0.160	0.201	0.199	0.149	0.114
O_{eth}	-0.224	-0.244	-0.247	-0.170	-0.067
O_{Ph}	-0.323	-0.329	-0.329	-0.229	-0.226
P	0.561	0.558	0.555	0.774	0.541
H^+	-	-	-	0.318	0.333

The comparison of charges at the atoms of neutral and protonated TMP species (Table 1) indicates that the protonation of the phosphoryl oxygen atom results in an increase in positive charge at a phosphorus atom and decrease at a carbon atom and besides that a decrease in negative charge at the oxygen atoms too. In the case of the ether oxygen protonation the value of positive charge at the phosphorus and carbon atoms decreases and the value of negative charge at the oxygen atoms decreases as well. Such charge redestribution is explained in the terms of valence-bond method: a phosphorus atom forms three single bonds with the ether oxygen atoms, it gives a pair of electrons on the free orbitals of an oxygen atom and an oxygen atom also gives its pair of electrons on the free d-orbitals of a phosphorus atom. These donor-acceptor interactions $P^+ \rightarrow O^-$(I) and $P^- \leftarrow O^+$(II) realize the double bond. The protonation of phosphoryl oxygen atom leads to the destabilization of process (II) and the stabilization of process (I), the electrons of ether oxygen atom move to a phosphorus atom. This phenomenon is confirmed by the calculation of bond energies (Table 2): the $P-O_{Ph}$ bond is destabilized and the $P-O_{eth}$ bond is intensificated. The protonation of the ether oxygen atom improves the process (II). In this situation the change of $P-O_{Ph}$ bond energy is negligible but the C-O_{eth} bond is greatly destabilized because of the charge transfer at a proton.

Table 2

ENERGY OF BONDS IN NEUTRAL AND PROTONATED SPECIES OF TMP (a.u.)

	$P = O_{Ph}$	$P - O_{eth}$	$C_\alpha - O$
Neutral	-1.28	-0.89	-1.04
O_{Ph} protonated	-1.04	-0.95	-1.00
O_{eth} protonated	-1.27	-0.62	-0.94
" - "	-1.27	-0.92	-1.00

Independence of a charge decrease at a carbon atom on a type of oxygen atom protonated is an important result of our calculation. The cause of this phenomenon is the destabilization of C-O_{eth} bond. It means that the electrostatic control of nucleophil (water) attack to a carbon atom decreases. At the same time the protonation considerably changes an energy and a structure of free MO on which the electrons of nucleophil are given: the energy of MO with great contribution of atomic orbitals of the carbon atoms becomes lower ($\Delta \sim 5$ eV) and the contribution of the carbon atoms orbitals into these MO noticeably enhances because of destabilization of C-O_{eth} bond. So the catalytic action of a proton is an improvement of orbital control of the attack of H_2O molecules to TBP protonated. The analysis carried out results in the supposition that multicharged cations such as Zr^{4+} and Hf^{4+} are able to effect upon the trialcylphosphate hydrolysis as catalists. The metal cation is coordinated by the phosphoryl oxygen atom and influences over trialcylphosphate in the similar way as a proton. In this case the energy of an interaction between the cation and the reagent (TAA) is apparently higher than the energy of protonation because the electrostatic term of energy enhances proportionally to the cation charge but the polarization term - proportionally to the second power of charge. It is confirmed by the comparison of stability constants of complexes TBP with HNO_3 and $Zr(NO_3)_4$. Besides that at high acidity zirconium and hafnium compounds with HNO_3 are able to pass into TBP (5). The activity of these acids is higher than the activity of only nitric acid. Because of 4 first vertical ionization potentials of hafnium are higher than of zirconium (6) the levels corresponding to free atomic orbilals of 4-charged cations are situated deeper in a hafnium atom than in a zirconium atom. That is why the term of energy corresponding to transfer of the charge from a reagent to a cation must be higher for hafnium. It is known (7) that Hf complexes are more stable. Therefore hafnium catalytic effect upon TBP hydrolysis must be greater than zirconium effect.

In experimental part of work the dependence of the concentration of TBP hydrolysis products (mainly HDBP - dibutylphosphoric acid) on the concentration of HNO_3, zirconium, hafnium and on the temperature was studied. The experiments were carried out with the system "TBP - aqueous solution of HNO_3 (Zr, Hf)" with the ratio A:O = 1:1. The system was agitated during 3 hr. The analysis of hydrolisis acidic products was multistepped and was based on the difference in the solubility of alcylphosphoric acids and their Na-salts in water and in inert organic diluents with final destruction of organic part by H_2SO_4 and analysis of PO_4^{3-} concentration at the last step.

The dependence of HDBP formation kinetic (mc $mol \cdot l^{-1} \cdot hr^{-1}$) on the concentration of HNO_3 in TBP (Fig.2) is different for systems without zirconium (curve 1) and in its presence (curve 2). The experimental data of HNO_3 influence upon TBP hydrolysis correlate the data of other authors for the lower acidity (8). The comparison of 1 and 2 curves indicates that in the extraction system containing zirconium the hydrolysis is considerably intensificated inspite of decrease in H_2O concentration in the organic phase when HNO_3 and zirconium concentrations increase. For the curve 3 the data of (9) were used. These data have been obtained without zirconium but zirconium nitrate replaces water in TBP therefore after the extraction of zirconium the concentration of H_2O in the organic phase will be lower. The concentrations of zirconium and nitric acid in the equilibrium phases in the experiment corresponding to curve 2 (in Fig.2) are shown in Table 3.

Table 3

CONCENTRATIONS OF ZIRCONIUM AND NITRIC ACID IN EQUILIBRIUM PHASES ($mol \cdot l^{-1}$) 8

№№:	Component:	Aq.phase:	Org.phase:	Component:	Aq.phase :	Org.phase
1	HNO_3	2.50	1.76	Zr	0.14	0.07
2	HNO_3	5.50	2.79	Zr	0.06	0.15
3	HNO_2	8.80	3.31	Zr	0.03	0.18

It can be noted that if nearly equal amounts of zirconium are extracted from various solutions (5.5 and 8.8 $mol \cdot l^{-1}$ HNO_3) the more intensive hydrolysis is observed in the system with 8.8 $mol \cdot l^{-1}$ HNO_3 (Fig.2, curve 2). The calculation of rate constants for the first step of hydrolysis (the interaction with HNO_3) confirms this fact: $4.8 \cdot 10^{-6}$ $mol^{-1} \cdot l \cdot hr^{-1}$ in the first case and $4.6 \cdot 10^{-5} mol^{-1} \cdot l \cdot hr^{-1}$ in the second case. These data show the increasing activity of proton in the compound $HZr(NO_3)_5 \cdot 2TBP$ (or $H_2Zr(NO_3)_6 \cdot 2TBP$) extracted from the strong acid solutions. A great amount of HDBP is accumulated in the extraction system containing zirconium after a long duration: up to 2 $g \cdot l^{-1}$ after 20 days if the initial Zr concentration in the aqueous phase was 30 $g \cdot l^{-1}$. The effect of hafnium upon the TBP hydrolysis is greater (Table 4).

Table 4

EFFECT OF Zr AND Hf ON HDBP FORMATION[a]

№№	Zr(Hf) $mol \cdot l^{-1}$, aq.	Zr(Hf) $mol \cdot l^{-1}$, org	HDBP $mcmol \cdot l^{-1} \cdot hr^{-1}$
1	0.13 (Zr)	0.20 (Zr)	14.6
2	0.123(Hf)	0.045(Hf)	122.1
3	0.256(Hf)	0.054(Hf)	1842.3

[a] $[HNO_3]_{aq.}$ = 5.5 $mol \cdot l^{-1}$, $[HNO_3]_{org.}$ = 2.8 $mol \cdot l^{-1}$

The experiments carried out in the presence of hafnium (№№ 2-3 in Table 4) indicate that the aqueous phase takes a big part in TBP hydrolysis. Inspite of alike values of Hf concentrations in the organic phase in the experiments 2 and 3 the amounts of HDBP formed are considerably different. In these experiments Hf concentrations in the aqueous phase were various: in the experiment 3 the concentration of hafnium in the aqueous phase is twice as much. The hydrolysis is apparently intensificated at the interface. The TBP hydrolysis increases at higher temperature but not so greatly than without zirconium or hafnium.

Without zirconium and hafnium HDBP formed as the result of TBP hydrolysis was distributed between the organic and aqueous phases with the coefficients D_{HDBP} = 1 - 1.5. In the presence of metals (Zr, Hf) the distribution coefficient of HDBP was equal to 1.5 - 4. Monobutylphosphoric acid (HMBP) was not found in the experiments with zirconium. But it must be noted that the presence of zirconium and hafnium in the system is able to enter a mistake in the determination of HDBP and HMBP concentrations due to the interaction of these elements and organophosphoric acids during the experiment and analysis. It means that the real values of HDBP and HMBP concentrations have to be higher.

The decrease in TBP stability owing to zirconium is also observed when heating the solvate $ZrCl_4 \cdot 2TBP$. The destruction of TBP molecule takes place in the bond "alcyl-oxygen" as well as in the hydrolysis process. Butylchloride and polymerized butylphosphate of zirconium are formed. Alcylphosphonate is destroyed in the same way. Phospine-oxide has no O_{eth} and it is not distructed due to $ZrCl_4$.

References

1. A.S.Solovkin, M.V.Vladimirova, I.A.Kulikov. Ekstraksia ionov metallov mono- i di-n-butilphocphornimi kislotami, produktami gidrolyza i radiolyza tri-n-butilphosphata, Itogi nauki i techniki, ser. "Neorgan.chimia", t.12, VINITI, Moskva, 1985, 136 s.
2. R.G.Wilbourn, G.E.Benedict, - Trans.Amer.Nucl.Soc., 35 (11), 114 (1980).
3. E.Scrocco, J.Tomasi, - Adv.Quant.Chem.,11,115 (1978).
4. Z.N.Tsvetkova, A.S.Solovkin, N.S.Povitski, et al., Zhurn.neorgan. khimii, 6(2), 489 (1961).
5. A.M.Chekmarev,- Koord.khimia, 7(6), 819 (1981).
6. H.A.Plesskaja, O.A.Sinegribova, I.K.Shvetsov, E.G.Chudinov in "Tez.dokl. 5 Vsesojuznoi konf. po chimii ekstraksii", Novosibirsk, 1978, p.199.
7. M.V.Vladimirova, D.A.Fedoseev, I.A.Kulikov et al. in "Tez.dokl. 2 Vsesojuznoi konf. po chimii neptunia i plutonia", Leningrad, "Nauka", 1982, p.14.

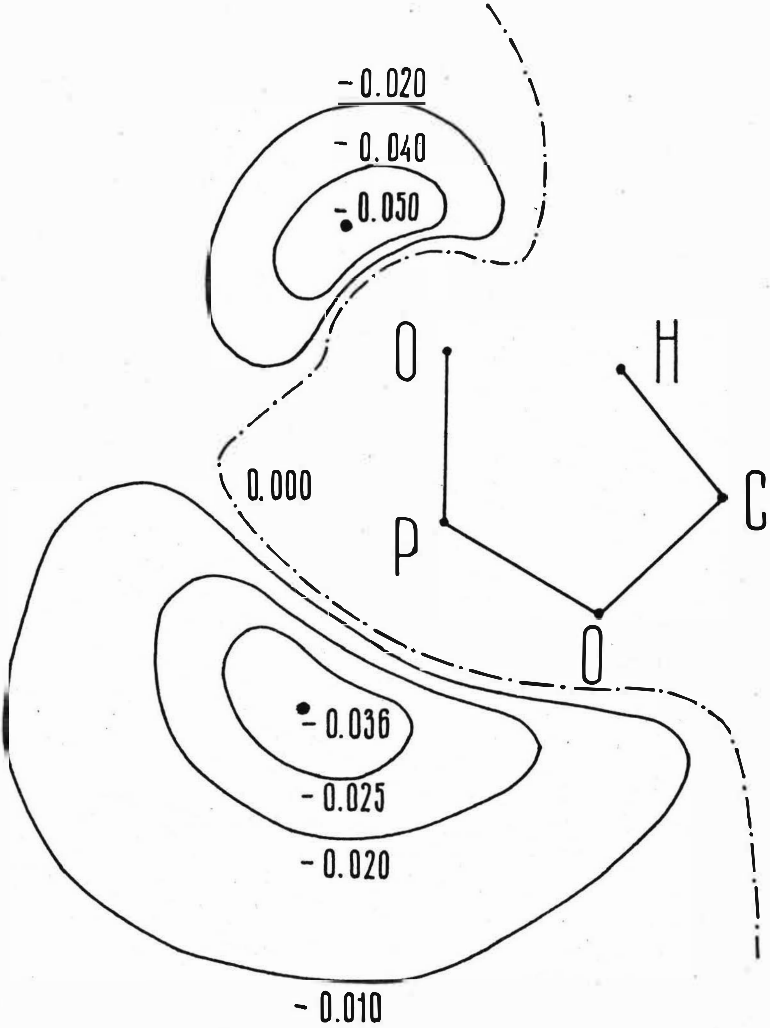
- 0.020
- 0.040
- 0.050
0.000
O
H
P
C
O
- 0.036
- 0.025
- 0.020
- 0.010

Fig.1.Distribution of molecular electrostatic potential in the molecule of trimetylphosphate.

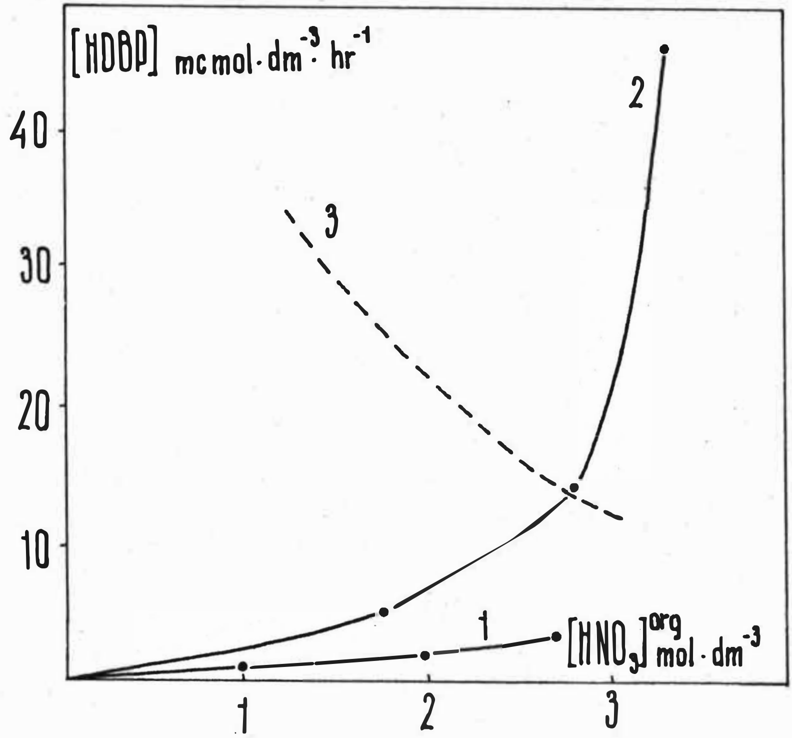

Fig.2.Plot of HDBP formation rate as a function of HNO_3 concentration in TBP.

Curve1 - without zirconium.

Curve2 - in the presence of zirconium.

Curve3 - concentration of water in TBP(9).

Chemical Degradation of Amine Solvents

Y. Sze, D.P. Archambault, C.G. Martin, T.E. McDougall and D.G. Boase
Atomic Energy of Canada Limited, Whiteshell Nuclear Research Establishment
Pinawa, Manitoba, Canada

1. INTRODUCTION

The properties of an amine solvent, 20% trilaurylamine (TLA) in a branched dodecane, were studied extensively by the Commisariat a l'Energie Atomique (CEA) in France [1-8]. These studies led to the industrial-scale application of an amine solvent extraction process for plutonium purification in reprocessing irradiated fuel [6]. During the above studies, it was found that TLA in contact with nitric acid solutions was susceptible to degradation by the nitrous acid that was used to adjust the plutonium valence [7]. The accumulation of the degradation products caused precipitates to form [5,9] and/or phase separation difficulties [2,7] in the alkaline-wash mixer-settlers used for solvent recovery, thereby disturbing the normal functioning of the process.

At the Whiteshell Nuclear Research Establishment (WNRE), an amine process was tested for the recovery of plutonium from CANDU^{TM} fuel [10]. The amine used was Alamine 336*, which is a mixture of tertiary amines (ca. 97%) with the octyl group predominating, and the diluent was diethylbenzene (DEB). The WNRE amine process was also tested recently by the Comitato Nazionale per L'Energia Nucleare (CNEN) at the EUREX plant in Italy [11]. However, in neither of these tests were the solvents subjected to an extended period of use with solvent washing and recycling. Thus, the viability of the WNRE amine process under adverse conditions was not established by these tests. This report describes a comparative study of the degradation behaviour of the WNRE solvent and a TLA solvent similar to that used in the CEA studies [1]. The properties of secondary amines formed by degradation were also investigated.

2. EXPERIMENTAL

The principal solvents used in this study were 0.32 mol/L (20% v/v) TLA in Isopar L** and 0.15 mol/L (7.5% v/v) Alamine 336 in DEB. They are generally referred to as TLA/Isopar and Alamine/DEB in this paper. The TLA/Isopar solvent had essentially the same composition as that used by the CEA [1] and the Alamine/DEB solvent was identical to that used at WNRE [10].

---

* Product of Henkel Corporation, Minneapolis, U.S.A.

** Supplied by Esso Chemical Canada. Ninety-five percent of this petroleum product is branched alkanes. Boiling point, flash point and density of Isopar L listed below are very close to those of tetramethyloctane used by the CEA [1] (in parentheses): 188-207°C (187-212°C), 62°C (63°C) and 0.767 (0.76).

The commercial tertiary-amine solvents (TLA and Alamine 336) used in this study and previously by others [2,10,12] invariably contain some secondary amines. In TLA, the major secondary amine is dilauryl amine (DLA), and in Alamine 336, dioctyl (DOA), octyldecyl (ODA) and didecyl (DDA) amines are present. The TLA/Isopar and Alamine/DEB solvents were purified by passing through an alumina column and subsequently washed twice with an aqueous solution of 1 mol/L Na_2CO_3, or 1 mol/L K_2CO_3 and 0.5 mol/L KOH.

The solvents (800 mL) were exposed in a two-stage mixer-settler (Model AT-1 of CEA, which had a mixer volume of 60 mL and a settler volume of 143 mL) to an aqueous solution of 0.04 mol/L HNO_2 in 2 mol/L HNO_3 that flowed counter-currently. The flowrate of the two streams was 2 mL/min. In most of the runs, the outlet solvent was washed with an alkaline solution in a second mixer-settler. The solvent was then passed into a reservoir from which it was recirculated (see Figure 1). The stages in the mixer-settlers are referred to as follows: MS-I-1 (mixer-settler I, stage 1), MS-II-1 (mixer- settler II, stage 1), etc. The duration of each run was about 10 days.

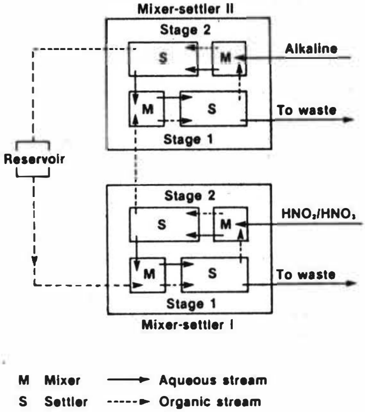
Mixer-settler II
Stage 2
S
M
Alkaline
M
S
To waste
Stage 1
Reservoir
Stage 2
S
M
HNO₂/HNO₃
M
S
To waste
Stage 1
Mixer-settler I
M Mixer
S Settler
Aqueous stream
Organic stream

FIGURE 1. Schematic outline for amine solvent degradation in mixer-settlers.

3. RESULTS AND DISCUSSION

3.1 Amine Solvent Preconditioning

The alumina column was effective in removing 40 to 70% of the secondary amines, depending on the flowrate. The alkaline washes did not remove secondary amines to any significant extent from the fresh undegraded solvents.

3.2 Properties of Secondary Amines in the Amine Solvent

3.2.1 Precipitation

The studies by the CEA showed that DLA and lauric acid were the main degradation products produced in the TLA/branched dodecane solvent contacted with the HNO_2/HNO_3 mixture [6,13]. While lauric acid was easily removed in the alkaline wash during solvent regeneration [2,5,9,13], removal of DLA was not straightforward and the formation of precipitates was attributed to DLA nitrate [8]. For this reason, we studied the properties of DLA in more detail.

We studied the following two solutions of DLA:

Solution I - 0.020 mol/L DLA in 20% TLA/Isopar L
Solution II - 0.020 mol/L DLA in 20% TLA/DEB.

When solution I was contacted with aqueous 0.1 mol/L HNO_3, a considerable amount of precipitate was formed. Germain and Bathellier reported that, in the presence of a small quantity of HNO_3, the secondary amine (DLA) nitrate salt is formed preferentially because the secondary amine (DLA) is a stronger base than the tertiary amine (TLA) [12]. The DLA nitrate precipitates because of its low solubility in 20% TLA/branched dodecane ($< 3 \times 10^{-4}$ mol/L) [12]. No precipitate was formed when solution II was contacted with the 0.1 mol/L HNO_3 aqueous solution. This indicates that the DLA nitrate is more soluble in the aromatic system.

Similar experiments were performed with the Alamine/DEB solvent to which DDA or DOA was added to form a 0.020 mol/L DDA or DOA solution. With aqueous 0.1 mol/L HNO_3, phase disengagement into clear phases was achieved immediately.

These results show that significant differences exist between the amine/aliphatic and amine/aromatic diluent systems. In terms of phase disengagement and solubility of the secondary amine salts, the solvents with DEB as diluent are definitely better than with Isopar L. The stronger solvent power of aromatic than aliphatic diluents has been reported in a number of previous studies [7,14,15].

3.2.2 Reactions of Secondary Amines with HNO_2/HNO_3

Secondary amines are known to react with HNO_2 [16]. In the TLA/Isopar and Alamine/DEB systems degraded by HNO_2/HNO_3, the amount of a secondary amine (DLA, DOA, ODA or DDA) at any specific time is, thus, the sum of the initial amount (as an impurity in the tertiary amine) and the amount formed by degradation of the tertiary amine minus the amount destroyed by reaction with HNO_2/HNO_3. The rate of the reaction between a secondary amine and HNO_2/HNO_3, under conditions similar to those of the TLA/Isopar or Alamine/DEB system, can nevertheless be studied if the secondary amine (e.g., dioctylamine) is added to a solvent in which the tertiary amine (e.g., trilaurylamine) cannot be degraded to that particular secondary amine.

Experiments were, therefore, conducted with a solution of 0.15 mol/L tertiary amine in a diluent containing additions of secondary amines. The solutions were agitated with equal volumes of aqueous solutions containing either 0.04 mol/L HNO_2 and 2 mol/L HNO_3 or 2 mol/L HNO_3. Figure 2 shows the results. On contact with HNO_2/HNO_3, the concentration of DOA decreased with time (curve 1). In contrast, the concentration of DLA increased with time (curve 2), because TLA, which yields DLA on decomposition, degrades more quickly than DLA. It is expected that the DLA concentration would eventually level off. In the absence of HNO_2, the concentrations of DOA (curve 3) and DLA (curve 4) remained constant.

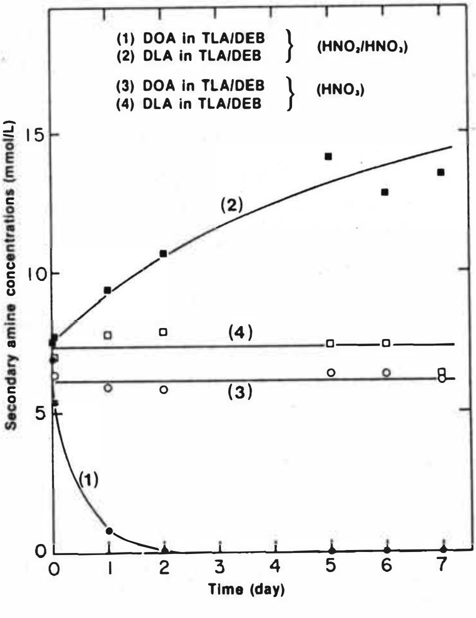

FIGURE 2. The behaviour of DOA and DLA in TLA/DEB.

Figure 3 shows the rate of degradation of two secondary amines, DOA (curve 1) and DLA (curve 2), in tridecylamine (TDA/DEB) on contact with HNO_2/HNO_3. The alkyl chain length in the secondary amine (C_8 in DOA and C_{12} in DLA) seems to have little effect on the rate of the reaction. The concentration of DDA increased steadily with time and is expected to level off (curve 3).

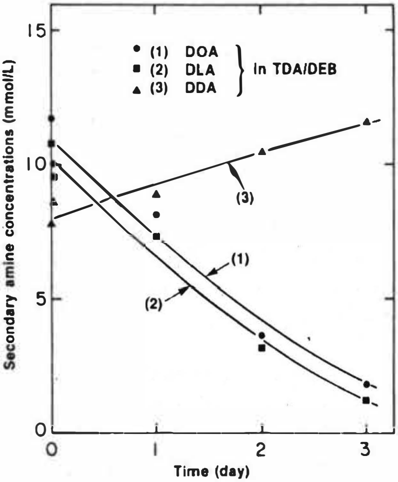

FIGURE 3. Effect of chain length of the secondary amine on its degradation by HNO_2/HNO_3

3.3 Degradation of the TLA/Isopar and Alamine/DEB solvents by HNO_2/HNO_3 in mixer-settlers

Twelve runs were completed with the two solvents. The observations are described briefly below.

In Run #1, the alkaline wash was not used so that information on the rate of degradation could be obtained under these particular experimental conditions. The concentration of DLA in TLA/Isopar increased steadily from 4.5 mmol/L to 15 mmol/L in an eight-day run. The solvent phase remained clear throughout the run.

In Run #2, the TLA/Isopar solvent, after passing through the HNO_2/HNO_3 contactor (MS-I), was washed with a mixed solution of 0.5 mol/L KOH and 1.0 mol/L K_2CO_3 in MS-II. Very serious operational problems were encountered in this run. Interfacial crud was formed in MS-II and accumulated with time. On the fourth day of the run, MS-II was completely filled with crud, and the crud flowed into the solvent reservoir and the alkaline waste container. This caused intolerable solvent loss and, therefore, the run was terminated.

The concentration of DLA in the solvent decreased with time, from an initial concentration of 4.5 mmol/L to 3.4 mmol/L on the second day and 1.7 mmol/L on the third day, instead of the increase observed in Run #1 where no alkaline wash was used. These results and the earlier observation that the alkaline wash was unable to remove secondary amines from fresh solvent can be explained as follows. As discussed earlier, dilaurylammonium nitrate (DLA nitrate) has a very low solubility in TLA/branched dodecane solvent [12]. However, the solubility of this salt in the acidified solvent, i.e., trilaurylammonium nitrate (TLA nitrate)/ branched dodecane, and the solubility of DLA in TLA/branched dodecane are much higher [12]. Furthermore, the reaction of the alkaline wash with DLA nitrate is considerably slower than that with TLA nitrate [17]. For this reason, the DLA nitrate can conceivably precipitate out when a significant amount of the TLA nitrate has been converted into TLA. This precipitate stabilized the crud and being a solid, its reaction with the alkaline wash was slow [9]. Complete reaction between the DLA nitrate and the alkaline wash should lead to complete redissolution of the precipitate. Apparently this was not achieved, due to the slow kinetics.

In Run #3, in an attempt to improve the performance of the TLA/Isopar solvent, we used TLA of higher purity (98% min. from Kodak Laboratory Chemicals). After further purification with an alumina column, the concentration of DLA was only 0.65 mmol/L. Despite the considerably lower DLA concentrations in this run, compared with Run #2, interfacial crud was formed and accumulated, and by the eighth day, the system could not function.

Nine runs were completed with the Alamine/DEB solvent. All the runs were basically successful. In some of the runs, a small amount of interfacial crud was formed in MS-II-2. This was identified as a hydroxo-amine-iron compound [18], the iron originating from corrosion of an equipment component. The quantity of the crud was small, and it did not affect the hydrodynamic performance of the contactor. In no case was solvent lost to the alkaline waste stream.

The difference in the performance of the TLA/Isopar and Alamine 336/DEB solvents is attributed to the difference in the solubilities of dialkylammonium nitrates in the two solvent systems. In Section 3.2.1, we have shown that TLA/DEB and Alamine/DEB are much better solvents for dialkylammonium nitrates than TLA/Isopar. The higher solubilities of dialkylammonium nitrates in the Alamine/DEB solvent retards their precipitation in this solvent and, thereby, reduces crud formation.

In the degradation runs with the Alamine/DEB solvent, the concentrations of each of the secondary amines reached a constant value after some time. For DOA and ODA, the constant concentration values are about 8 mmol/L, and for DDA, about 2 to 2.5 mmol/L. Figure 4 shows typical results for these runs. For each of the

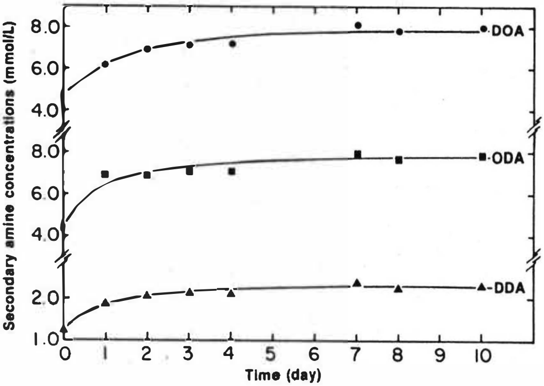

FIGURE 4. Secondary amine concentrations in mixer-settler Run #8.

secondary amines, a steady state was reached on the third to fourth day of the run. The steady-state concentration represents the upper limit of the concentration of this secondary amine in a mixer-settler run. Extensive tests performed in this study showed that, even at these upper concentration limits, the solvent performs well without any operational problems.

4. SUMMARY AND CONCLUSIONS

TLA/Isopar and Alamine/DEB solvents are degraded by HNO_2/HNO_3 to form secondary amines. The basic difference in the performance of the two degraded solvents was revealed when the two solvents were washed with an alkaline wash. In the case of the TLA/Isopar solvent, precipitation of DLA nitrate occurred and caused extensive crud formation and insurmountable operational problems in the mixer-settler experiments. In extensive tests with the Alamine/DEB solvent under identical experimental conditions, no such difficulties were encountered, even at the highest achievable dialkylammonium nitrate concentrations. The difference in the behaviour of the two solvents was attributed to the better solvent power of the aromatic diluent, DEB.

REFERENCES

1. A. Chesne, G. Koehly and A. Bathellier, Nucl. Sci. Engineering 17, 557 (1963).

2. A. Bathellier, G. Koehly, J.-J. Perez and A. Chesne, CEA-R 2594 (1964).
3. M. Lucas and A. Bathellier, CEA-N-856 (1967); ANL-trans-619, p. 90.
4. A. Bathellier and G. Faudot, CEA-N-969 (1967), AEC-tr-7028, p. 75.
5. A. Bathellier, Bull. Inform. Sci. Tech. (Paris), 127, 35 (1968).
6. A. Bathellier, A. Grieneisen and L. Plessy, Energ. Nucl. (Paris), 10, 186 (1968).
7. M. Germain and A. Bathellier, in Proc. Int. Conf. Solvent Extraction, The Hague, Netherlands, 1971 April 19-23, p. 1161, J.G. Gregory, B. Evans and P.C. Weston, Eds., Society of Chemical Industry, London (1971).
8. J. LeBouhellec, and J. Berthaud, CEA-N-856 (1967); ANL-trans-626, p. 26.
9. A. Bathellier, CEA-N-856 (1967); ANL-trans-619, p. 94.
10. L.J. Clegg, J.K. Close, J.R. Coady, D.R. Greig, W.W. Morgan and L. Pollard, Unpublished information, Whiteshell Nuclear Research Establishment (1976).
11. G.R. Grant, D.G. Boase, D.R. McLean, F. Pozzi, A. Hall, V. Pagliai and G. Alonzo, in Proc. Int. Conf. Solvent Extraction, Denver, U.S.A., 1983 August 26 - September 2, p. 325. R.B. Akell et al., Chairmen, American Institute of Chemical Engineers (1983).
12. M. Germain and A. Bathellier, CEA-N-856 (1967); ANL-trans-619,p 96.
13. M. Germain, CEA-N-1044 (1968), AEC-tr-7076, p. 65.
14. A.V. Hultgren, KR-126 (1967), p. 201.
15. M. Zifferers, in Aqueous Reprocessing Chemistry for Irradiated Fuels Symposiu Brussels, 1963, European Nuclear Energy Agency, p. 107.
16. J.D. Roberts and M.C. Carserio, Basic Principles of Organic Chemistry, W.A. Benjamin, Inc., New York, 1965, p. 666.
17. M. Germain and A. Bathellier, CEA-N-856 (1967); ANL-trans-619, p. 94.
18. Y. Sze, D.P. Archambault, C.G. Martin, T.S. McDougall and D.G. Boase, Unpublished information, Whiteshell Nuclear Research Establishment (1986).

Fundamental Studies

Measurement of Liquid-Liquid Interfacial Kinetics: Where Do We Stand?

Richard D. Noble
National Bureau of Standards
Center for Chemical Engineering
Chemical Engineering Science Division
Boulder, Colorado 80303

Introduction

Liquid-liquid interfacial kinetics has become an increasingly important subject over the last 15 years. Researchers from diverse fields such as nuclear engineering, hydrometallurgy, pharmaceutical chemistry, and biotechnology have realized the need to better understand interfacial mass transfer. Investigations of different systems have proliferated in the literature, and several authors have proposed general reaction schemes or models. In spite of the wealth of information which has been generated, there is still no general agreement on the mechanisms and the rate-determining role of interfacial reactions or on the experimental technique most suitable to measure them. In the review, I will summarize the different measurement techniques which have been applied. The emphasis will be on the theory and application of the techniques rather than a detailed discussion of interfacial reaction mechanisms for different systems.

There are two distinct types of systems which are industrially important. The simplest system involves transfer of a mutually soluble solute from the oil phase to the aqueous phase or vice versa. These systems typically appear in biological applications such as drug transfer across a lipid membrane. Carboxylic acid transfer is another example of the "purely diffusive" systems. The second type of system is more complex. The solute is typically soluble only in the aqueous phase, and transfer to the oil phase is accomplished by an oil-soluble complexing agent. Metal-ion transfer is the most typical example of an "interfacial reaction" system. A hybrid of these two systems can occur if a complexing agent is present when a mutually soluble species is being transferred. An example of this process would be carboxylic acid transfer with an amine carrier present.

There are several problems with true interfacial kinetics measurement. In all real processes, the total mass-transfer rate is determined not only by the interfacial kinetics, but also by diffusion of the reactant to the interface and diffusion of the products away from the interface. In some cases, the process may be diffusion-limited and in others, kinetically limited. The most complicated situations arise when a system operates in a regime in which both diffusion and kinetics affect the transport rate. It is essential, therefore, to develop a measurement technique which can measure kinetics free from the influence of diffusion. Typically, the apparatus is designed to operate either in a kinetically limited regime, or to allow calculation of the diffusional component of the overall mass-transfer rate. The second problem is contamination of the interface by impurities which are more surface-active than the solute or the complexing agent. Special care must be exercised to insure that all equipment and reagents are free from any potential contaminants. Cleanliness is a particular problem when studies are done using complexing agents "as received" from the manufacturer. Accurate determination of the interfacial area is an additional problem. Direct liquid contact methods often have slightly rippled interfaces, and methods using membranes must account for the pore structure in calculating the contact area.

In this review, I will summarize the measurement techniques which have been applied to various interfacial systems. Space limitations do not allow for discussion of some measurement methods. The reader is referred to Hanna and Noble (1) for a more thorough discussion.

Finally, where is interfacial-kinetics research heading? What advances can be made in understanding diffusion, interfacial kinetics, and surface contamination? Can a better measurement method for hydrodynamics and interfacial area be developed? I will examine these questions as I summarize the review.

The Stirred Cell

Lewis (2,3) was the first to recognize the need for better interfacial measurement systems and proposed an apparatus to address the problems. The Lewis cell apparatus provided direct liquid-liquid contact with a well-defined interfacial area and agitation of both phases without breakup of the interface. The cell was completely full of liquid to prevent vortexing at the upper surface. The baffles were placed at the center to eliminate vortexing and at the edges to eliminate wall effects. The baffles were beveled to allow droplets of the opposite phase which were accidentally entrained to roll to the interface. Interfacial transfer took place in the annular region. The upper and lower phases were stirred in the same direction and at the same rate. The degree of interfacial turbulence varied from system to system, but the interfacial region generally remained flat.

The first major set of modifications was made by Nitsch and Hillekamp (4). The screens situated on either side of the interface are the most important addition to the Lewis cell. Each phase was stirred separately and in the opposite direction, and the stirring rates were adjusted so that the Reynolds number in each phase was equal. The geometry of the system allowed a high degree of turbulence within each phase but maintained a quiescent interface. In previous Lewis cells, the stirrer blades were very low-pitch to avoid breakup at the interface. The low-pitch blades were not as efficient for bulk mixing as the higher-pitch which can be used with the Nitsch cell. Nitsch (5) recently summarized some of the problems associated with studying interfacial kinetics for liquid-liquid systems. He then discussed this type of stirred cell and recommended calibration measurements to insure that stirred cells were operating in the proper regime.

A second major modification was made by Danesi et al (6). The ARMOLLEX (Argonne Modified Lewis cell for Liquid-liquid Extraction) was designed to accomplish efficient interfacial contact without requiring large volumes or intermittent sampling. The Nitsch cell has a capacity of approximately 1L, but the ARMOLLEX requires only 100 mL. The ARMOLLEX allowed continuous sample analysis by incorporating a flow loop. The flow loop also eliminated problems associated with volume change due to sampling during a run.

An alternative mixing design for the stirred cell was demonstrated by Stowe and Shaiewitz (7) who used rotating discs on each side of the interface instead of stirring paddles. They solved the equation of motion for flow far from the disc to characterize the flow field at the interface. They presented their data in terms of calculated vs. observed Sherwood numbers, and direct comparison to other studies is difficult.

Other investigators have used Lewis cells of different types (8-12), but all the devices are either similar to Lewis's original model (2) or the Nitsch (4) or Danesi (6) modified types.

Other contacting cells have been developed. Bhaduri et al. (13) developed the gauze cell. The cylindrical contacting chamber had a platinum gauze, which was approx. 40% porous, positioned at the interface. Stirrers in each interface attempted to minimize diffusional effects. The Kreevoy contactor was reported by Ulrick et al. (14). The cell consisted of a sandwich made up of a membrane between two static mixers and two silicone rubber gaskets. An organic layer was contained in the membrane pores and aqueous phases were pumped through static mixers on each side of the cell.

Highly agitated contactors have also been reported. The AKUFVE apparatus has been reviewed previously (15,16). Carter and Freiser (17) developed a highly stirred contacting cell. Two phases were intimately mixed at 5,000 - 20,000 rpm and samples were periodically withdrawn. The interfacial area for this system was unknown and not necessarily reproducible.

The Rotating Diffusion Cell

Following the successful adaptation of a Stokes diffusion cell for interfacial kinetics measurements (18), Albery et al. (19) created the rotating-diffusion cell (RDC) and successfully combined the hydrodynamics of the rotating disc with interfacial mass transfer. A thin membrane attached to a hollow cylinder was rotated which created rotating-disc hydrodynamics on both sides of the filter depending on the procedure and solutions used. Mass transfer occurred from the inner chamber, through the membrane, and into the outer chamber. The RDC can therefore be considered a type of immobilized liquid membrane cell with known hydrodynamics.

In the rotating diffusion cell, the overall mass transfer can encounter up to five resistances in series. On each side of the membrane, there is a diffusive boundary layer and an interfacial reaction. In addition to these resistances, the species must also diffuse through the liquid held in the membrane. The overall transfer rate will depend on all these resistances if the cell is set up in "sandwich" form with aqueous solutions on each side of the membrane and an organic liquid in the membrane. One of the interfacial reaction terms can be eliminated if the cell is set up with only two phases present rather than the "sandwich" configuration. If the solutions in the inner and outer chambers are identical, then the diffusive boundary layer contributions on each side are equal. If the reactions occurring on each side of the membrane are the same, then the kinetic contributions are equal. The exact mathematical formulation for the resistances depends on the system being studied.

Most other investigators (20-22) have used RDC's which are nearly identical with the one reported by Albery et al. (18), Huang et al. (23) constructed a "spinning liquid disc" and made flux measurements as a function of Reynolds number. The liquid was contained in a cylindrical chamber with a membrane on the end, which was exposed to the other fluid. The resistances to mass transfer are the same for the liquid disc system and the RDC, and the data from the liquid disc produced conclusions similar to those which could be drawn from the RDC. Stowe and Shaewitz (7) conducted experiments in a cell which resembles a Lewis cell, but the propeller stirrers were replaced with rotating discs.

Other measurement methods have been developed. The liquid jet recycle reactor (LJRR) was reported by Freeman and Tavlarides (24). An aqueous liquid jet flows downward through a cocurrent, coaxially flowing organic fluid. The contact time is short and the organic phase is continuously recycled through a spectrophotometric loop. Single drop methods have recently been summarized (16). Nitsch and Schuster (25) presented an experimental method whereby an array of capillaries at the bottom of a tank produced uniformly sized droplet swarms which coalesced at the tank top. Single drop analysis was used to determine mass transfer coefficients. Guy et al. (26) recently presented a measurement method for solute transfer kinetics based on the capillary tube procedure for self diffusion.

Modeling

In order to understand the basic physical and chemical processes occurring at the liquid-liquid interface, it is necessary to develop a mathematical description which accurately depicts the interfacial processes. The resulting model needs to be sufficiently detailed and free to empirical parameters so that the physical properties, kinetics, and operating conditions which affect the interface can be correctly identified and quantified.

A critical feature of any model is the ability to properly account for diffusional boundary layers adjacent to the interface. Danesi et al. (27) demonstrated that diffusional resistances in the boundary layers adjacent to the interface can mimic interfacial two-step consecutive reactions. If one cannot accurately separate the different contributions to transport across the interface, the proposed reaction mechanisms and corresponding coefficients will be in doubt.

An accurate and complete model needs to be based on experimentally measurable quantities. Use of quantities which are very difficult or impossible to independently measure would make the usefulness of any model very limited.

Models based on mass action begin with the balanced stoichiometric equation for the reaction under study. The rate of the chemical reaction is then assumed to be proportional to the concentrations of the reactant raised to the powers equal to their coefficients in the balanced reaction. At equilibrium, the forward and reverse reaction are equal.

There are several difficulties with the mass-action approach. Nonidealities in either phase cause deviations which would require accurate activity measurements to correct. In addition, only the rate-limiting step in the reaction can be determined. Consequently, conclusions from mass-action models can be misleading. Despite these shortcomings, models for interfacial kinetics based on mass action are the most prevalent. Some examples of kinetic models based on mass-action principles include Hughes and Rod (28), Nitsch and van Schoor (29), and Kondo et al.(8).

There have been various attempts (30,31) to model the liquid-liquid interface by modeling the "interfacial resistance" to mass transfer. The interfacial resistance is associated with the interface itself and is separate from any diffusional resistance to mass transfer.

One method to determine the kinetic rate expression for an interfacial reaction is to use statistical analysis to accept or reject certain proposed reaction mechanisms or models. Freeman and Tavlarides (32) used statistical methods to develop an expression for copper chelation kinetics. They proposed various possible models based on different combinations of diffusion, absorption/desorption, and rate-limiting reaction steps at the interface. They collected data and tested the validity of each model with an F ratio between the experimental variance and the regression variance. The F test can determine the statistical-significance level of a model.

The results of Freeman and Tavlarides (32) indicated that several mechanisms all successfully modeled the copper extraction process. Therefore, postulating a mechanism solely on its ability to fit the data is not necessarily an acceptable approach. They suggested that rate data can be used to reject specific rate models if the model has a low confidence level in the F-ratio test.

Areas of Continuing Research

In order to advance our understanding of interfacial kinetics for liquid-liquid systems, several areas of research will have to be developed. The definition of the liquid-liquid interface (mathematical or physical) is still the subject of some debate. Some researchers believe the thickness of the interfacial region is on the order of 1 nm, which could allow the interface to be defined (mathematically) as a phase boundary. The transition between phases would occur on the order of tens of molecules. Other researchers assert than an interfacial reaction zone exists on the order of 1 μm (28). In the reaction zone concept, "interfacial" reactions are really occurring in a bulk region which has properties that are different from either of the individual phases. A resolution of these divergent views is essential in order to move forward with our knowledge of interfacial reaction mechanisms.

A second critical area of research is the role and the accurate determination of boundary layers adjacent to the interface. The experimental methods which are presently in use do not allow for a detailed analysis of the boundary layers. The rotating diffusion cell does allow a comparison between theoretical and observed boundary layer thickness, but the device is not designed to study the role of the boundary layer per se. In order to perform this research, it will be necessary to use a measurement method which has well-characterized hydrodynamics and an interfacial area which remains constant (these requirements are usually satisfied only in laminar-flow conditions).

Accurate determination of the effect of impurities absorbed at the interface is crucial to measurement of interfacial kinetics. In addition, the role of surfactants needs to be clarified and refined. Most studies on this subject have centered on retardation of kinetics by absorbed layers. More fundamental work on the mechanism of retardation (or enhancement) by surface active agents needs to be performed.

A confusion exists in the literature for systems we have described as "purely diffusive" or "solute-transfer". Chemical engineers have traditionally approached solute-transfer systems empirically using a mass-transfer coefficient k. The flux of solute from phase 1 to phase 2 is typically given by

$$J = k\Delta C \tag{1}$$

where J is the flux, (mass per unit area per time) and ΔC is the concentration driving force. Equation 1 models the transfer process as diffusion across the interface, but the mass transfer coefficient k often includes diffusive boundary layer effects and can be considered a lumped parameter. The flux (or transfer rate) is first order in concentration and also depends on the available area.

Chemists, on the other hand, have often treated these systems as chemical reactions. Typically, the reaction is written

$$A_{(aq)} \rightarrow A_{(org)} \tag{2}$$

where the rate of transfer at the interface is given by

$$\text{rate} = k_1[A]_{(aq)} - k_{-1}[A]_{(org)} \tag{3}$$

The total transfer rate must also include contributions from diffusion on each side of the interface. The free energy changes associated with eq 2 are typically small (<10kJ/mol) and there is no reaction per se; that is, A is still A after the "reaction" has occurred.

Many of the discrepancies between measurements and philosophies have arisen because of the diverse backgrounds of the investigators. Interfacial kinetics has emerged as its own field in recent years, but most the experienced researchers have approached the problem with their specific application in mind (as opposed to evaluating the general problem of liquid-liquid interfacial kinetics).

At present, there are no generally established criteria for proper interfacial-kinetics measurement. The important criteria such as hydrodynamics, surface cleanliness, contribution of diffusion, purity of reagents, accuracy of accompanying physical properties, and surface area need to be defined and detailed so that all investigators can accept them. Once accepted, researchers should make every effort to abide by the criteria so that all research will be on the same basis.

REFERENCES

(1) Hanna, G. J. and R. D. Noble, Chem. Rev., 85, 583-598, 1985.

(2) Lewis, J. B., Chem. Eng. Sci., 3, 218-259, 1954

(3) Lewis, J. B., Chem. Eng. Sci., 3, 260-278, 1954.

(4) Nitsch, W. and K. Hillekamp, Chem Ztg., 96, 254-261, 1972.

(5) Nitsch, W., Faraday Discuss. Chem. Soc., No. 77, Paper 77/8, 1984.

(6) Danesi, P. R., C. Cianetti, E. P. Horowitz and H. Diamond, Sep. Sci. Tech., 17 (7), 961-968, 1982.

(7) Stowe, L. R. and J. A. Shaeiwitz, Chem. Eng. Commun., 11, 17-26, 1981.

(8) Kondo, K., K. Kita and F. Nakashio, J. Chem. Eng. Jpn., 14 (1), 20-25, 1981.

(9) Asai, S., J. Hatanaka and Y. Uekawa, J. Chem. Eng. Jpn., 16 (6), 463-469, 1983.

(10) Shanbag, V. P., Biochim. Biophys. Acta., 320, 517-527, 1973.

(11) Byron, P. R., R. T. Guest and R. E. Notari, J. Pharm. Sci., 70 (11), 1265-1269, 1981.

(12) Scholtens, B. J. R., S. Bruin and B. H. Bijsterbosch, CIM Spec., 21, 256-259, 1979.

(13) Bhaduri, M, C. Hanson, M. A. Hughes and R. Whewell, Int. Solv. Extr. Conf. [Proc.], 293-294, 1983.

(14) Ulrick, L. A., K. D. Lokkesmoe and M. M. Kreevoy, J. Phys. Chem., 86, 3651-3657, 1982.

(15) Rydberg, J., H. Reinhardt and J. O. Liljenzin, Ion Exch. Solvent Extr., 3, 111-135, 1973.

(16) Danesi, P. R. and R. Chiarizia, CRC Crit. Rev. Anal. Chem., 10 (1), 1-126, 1980.

(17) Carter, S. P. and H. Freiser, Anal. Chem., 51 (7), 1100-1101, 1979.

(18) Albery, W. S., A. M. Cooper, J. Hadgraft and C. Ryan, J. Chem. Soc. Faraday Trans. 1, 70, 1124-1131, 1974.

(19) Albery. W. J., J. F. Burke, E. B. Leffler and J. Hadgraft, J. Chem. Soc. Faraday Trans. 1, 72, (7), 1618-1626, 1976.

(20) Guy. R. H. and R. Fleming, Int. J. Pharm, 3, 143-149, 1979.

(21) Sagert, N. H., M. J. Quinn and R. S. Dixon, Can J. Chem., 59, 1096-1100, 1981.

(22) Amidon, G. E., W. I. Higuchi and N. F. H. Ho., J. Pharm. Sci., 71 (1), 77-84, 1982.

(23) Huang, C., D. F. Evans and E. L. Cussler, J. Colloid Interface Sci., 82 (2), 499-506, 1981.

(24) Freeman. R. W. and L. L. Tavlarides, Chem. Eng. Sci., 35, 559-566, 1980.

(25) Nitsch, W. and U. Schuster, Sep. Sci Technol., 18 (14,15), 1509-33, 1983.

(26) Guy, R. H., R. S. Hinz and M. Amantea, Faraday Discuss. Chem. Soc., No. 77, Paper 77/14, 1984.

(27) Danesi, P. R., G. F. Vandegrift, E. P. Horwitz and R. Chiarizia, J. Phys. Chem., 84, 3582-3587, 1980.

(28) Hughes, M. A. and V. Rod, Faraday Discuss. Chem. Soc., No. 77, Paper 77/7, 1984.

(29) Nitsch, W. and A. van Schoor, Chem. Eng. Sci., 38, 1947-1957, 1983.

(30) Brenner, H. and L. G. Leal, AIChE J., 24 (2), 246-254, 1978.

(31) Shaiewtiz, J. A. and K. T. Raterman, Ind. Eng. Chem. Fundam., 21, 154-161, 1982.

Reactions in Monolayers Between Liquid Phases

Michel Th., Matt K., Hamza A. and Nitsch W.
Technical University of Munich, Garching/Germany

Even for a longer time surfactant effects on mass transfer processes are known, meanwhile numerous publications concerning this matter have been compiled (1;2). But until today it has not been possible to draw a complete picture of surfactant actions on mass transfer. Especially at reactive mass transfer on the one hand this is due to the mostly complicate reaction itself, on the other hand in particular the reason will be the difficulty in relating results of measurements to physicochemical aspects of the system.

Mass transfer between two liquid phases, therefore heterogeneous systems, is distinguished by coupling of transport and reaction processes. Hence the effect of surface active substances can be subdivided into two fundamental different domains

- effect on transport processes
- influences on the mass transfer reaction itself.

At examinations of surfactant action already this classification requires the use of experimental techniques, which easily and unequivocally allow to distinguish between transport and reaction limitation. According to our opinion this is excellently possible by means of flow calibrated stirred cells. Here transport limitation turns out as an linear dependence of transfer rate from stirring speed, on the contrary reaction limitation appears as a more or less distinct marked plateau rate independent on stirring speed.

Comparatively detailed knowledge could be collected concerning the influence of surfactants on transport processes. In this case it is only possible, that surfactants act on the liquid flow adjacent to the interface. This consequently hydrodynamic inhibition is caused by gradients of interfacial tensions damping the crucial flow near the interface. Particularly by measurements in stirred cells it was possible to aquire the typical phenomenas of hydrodynamic surfactant action (fig.1).

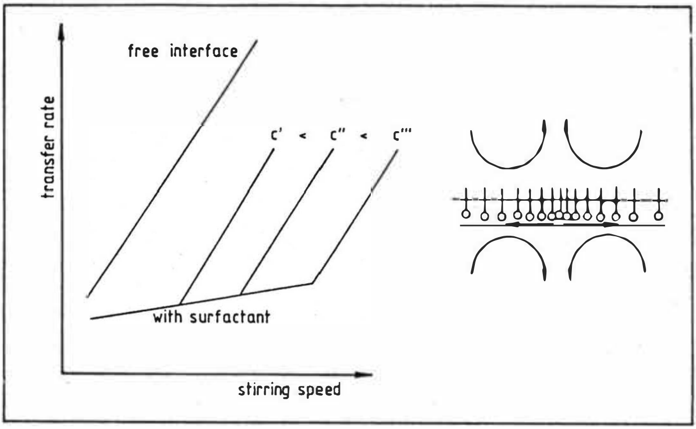

Fig. 1 The effect of surfactants on transport limited mass transfer
The inhibition is illustrated by different surfactant concentrations
In the right the microscopic model of the surfactant influence on
hydrodynamics is demonstrated.

This characteristic influence could be demonstrated using soluble and insoluble surfactants with heat transfer measurements, physical mass transfer and as well with transport limited metal extraction (3;4).
Furthermore by means of laser doppler anemometry (LDA)at a liquid/liquid flow through a channel, it was possible by measuring the flow adjacent to the interface or even the interfacial flow itself to verify the model of flow induced gradients of interfacial pressure (5).
An interesting effect of surface active substances on transport limited mass transfer is, that for surfactant concentrations above the critical micelle concentration (cmc) all inhibiting gradients of interfacial pressure were neutralized and the undisturbed liquid/liquid flow pattern turns up (3).
Consequently one succeeds in simulating the free interface by deliberate addition of surfactants, a condition otherwise is only very difficult to realize.

Of fundamental different character as described above surfactant effects are on mass transfer processes limited by reactions. Despite of their significance almost none systematic investigations concerning this matter are known till today, in contrast to hydrodynamic surfactant effects.

In the following part of paper several aspects of our results will be presented. At this it is absolutly necessary to secure definitely that the mass transfer considered is governed by reaction.
Methodically we use as a model reaction the extraction of zinc from buffered water solution to toluene with dithizone (HDz) according to the stoichiometric equation

$$Zn^{2+}_{aq.} + 2\ HDz_{org.} \text{---->}\ ZnDz_{2_{org.}} + 2\ H^{+}_{aq.}$$

By former detailed work the kinetic of this reaction was cleared up (6). An interfacial reation occurs, distinguished by the interesting attribute of being reaction limited by proceeding to sufficient low metal concentrations, recognizable by plateau rates independent on stirring speeds. Without such a clear-cut probe reaction it would be impossible to state anything concerning effects of surfactant matrices at interfaces.
At plateau rates and equilibrium far on the solvent side, in this case back reaction can be neglected, the kinetic equation

$$r = k\ K\ \frac{(\ Zn^{2+})\ (\ HDz\ )}{(\ H^{+})}$$

holds with k = rate constant and K = dissociation constant of dithizone.
At an interface a monomolecular film is formed by surfactant molecules, soluble ones by adsorption and insoluble ones as a spread film. Certainly these layers will affect the reaction occuring at this interface.
It must be emphasized here, that at examinations concerning effects of different surfactants it seems less in meaning to neglect questions related to the interfacial behaviour of these surfactants. Only by measuring the dependence of interfacial tension upon concentration and following calculation of surface excess, applying the Gibbs equation, it is possible to consider and to compare interfaces with the same amount of adsorbed molecules, instead of calling on nearly the same bulk concentrations for comparison.
Nevertheless, on the other side enhanced attention must be paid to the frequent exceptional sensitivity of the interfacial behaviour of surfactants to contaminations. In this case it is necessary to criticize the usefulness of the substances via time dependences of the measurements of surface tension, in order to decide wether the surfactant must be subjected to thorough purification procedures.

In our experiments the concentration of zinc and dithizone were kept constant (10^{-4}m and $1{,}25 \cdot 10^{-4}$m respectively) at a buffer pH of 5,01. Chemically controlled mass transfer was compared by adjusting the same surface excess of surfactants .In cases of mass transfer still superimposed by transport dependencies the pure reaction limited rate is evaluated by applying a method, which extrapolates the dependence upon stirring to infinite stirring speeds.

The experiments prove that adsorption layers at interfaces can influence the reaction in different manners.

1. effect of the state of charge at the interface, that means potential effects
2. dense aggregates of particles present at the interface
3. influences of substance specific interactions of the monolayer with the interfacial reaction.

Ad 1. Potential effects

Caused by the ionic character of e.g. sodium dodecylsulfate there exists a potential at the interface as against the bulk phase, depending on the surface excess and the amount of electrolyte present in the water phase.

Fig. 2 demonstrates how the reaction can be influenced by potentials. The direction of the influence is of opposite sign, according as wether the layer is charged positively or negatively. There is the matter of a sign effect only explicable by influences of potentials. Adding an 1-1 electrolyte into the waterphase the potential at the interface can increasingly be reduced. As a result the reaction rate in the presence of an anionic layer is decreased further,however in the case of a cationic layer it is increased.

The results show, that here it is the question of a phenomenon which cannot be explained by applying the classical Gouy- Chapman- Stern treatment of the diffuse double layer in the water phase, like it is known from the stability of colloidal dispersions. It is not possible to relate the changes of the reaction rates with an enrichment of zinc or hydrogen ions near the interface caused by electrostatic attraction, till today such effects could only be demonstrated by e.g. hydrolysis of special monomolecular films at air/liquid interfaces (7).

Indeed the influence of potential on dissociation of the dithizone molecule can be brought into line with the sign effect, but on the other hand by this it is not possible to explain the effects of added electrolytes.

Fig. 2 The effect of potentials on transfer rate
abscissa: stirring speed
ordinate: transfer rate
nadds = sodium dodecylsulfate
dtmab = dodecyltrimethylammonium bromide

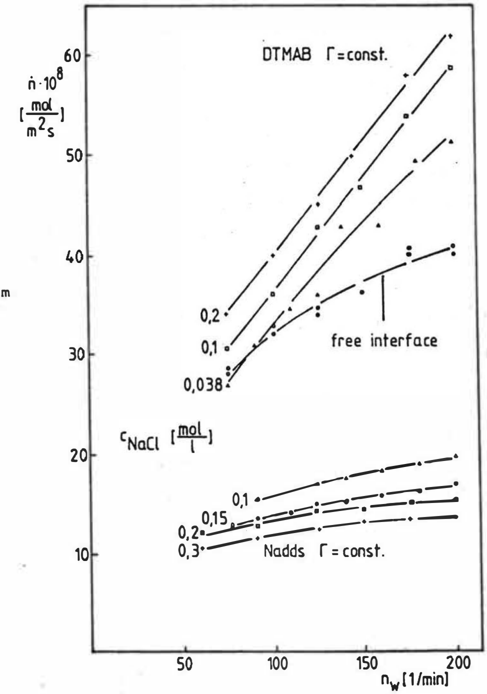

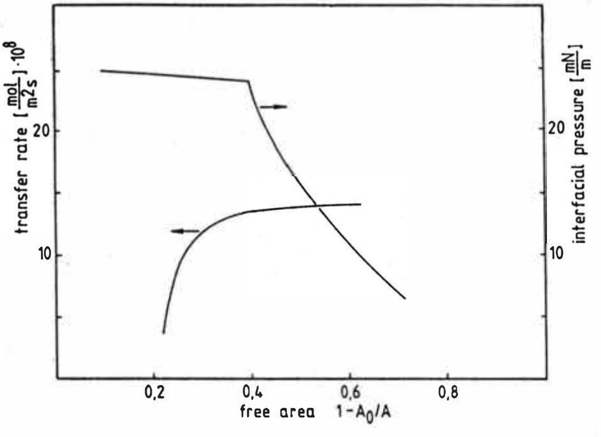

Fig. 3 The correlation between state of compression of the cephalin layer and transfer rate
the free area is related to A_0 = 36 Å^2

Ad 2. Aggregation

By means of a special technique of preparation of unsoluble films at liquid/liquid interface in stirred cells, it was possible to demonstrate by measurements of zinc transfer through interfaces covered with cephalin layers of different states of compression that then this interface can be made nearly impermeable. At a state of compression of the cephalin film on which a phase transition occurs at liquid/liquid interface (that means the single molecules begin to cohere), the reaction rate decreases steeply (fig.3). With this a striking example is presented demonstrating that the coverage of the interface with single molecules is not the decisive parameter, but the presence of dense aggregates determines the permeability of an interfacial adsorption layer.

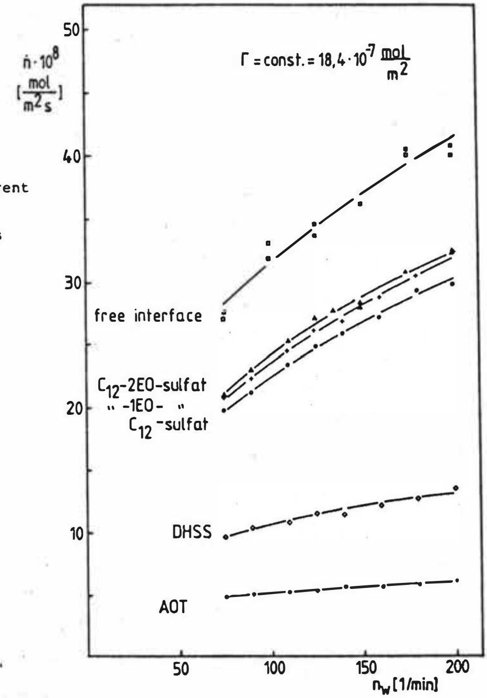

Fig. 4 The influence of different surfactants on transfer rate "-EO-" represents ethoxy groups DHSS = dihexylsulfosuccinate sodium salt, AOT = aerosil-OT

Ad 3. Specific effects of the adsorption layer

Like it can be seen in fig. 4 some surfactant layers are able to reduce extraordinarily the reaction rate compared with transfer across the free interface. Here it is the matter of an effect clearly far exceeding pure potential influences. A bulk effect within the meaning of complex formation of zinc ions by the sulfosuccinate cannot be hold responsible for such a decrease of the reaction, if only the concentration speaks against it. The same holds at the interface because in the case of reaction limitation virtually no concentration gradient exists between bulk and interface.

At present no certain statements are possible concerning probable explanations of these special influences of adsorption layers. It would be thinkable that, caused by the transfer component zinc itself, similar effects of coherence of the surfactant molecules could appear like described above.

Finally it is the question to accent that characterisation of influences of surfactants on reactions at liquid/liquid interfaces only is certain if one takes into account all partial aspects of the whole surfactant influence. For that reason it must be proceeded in this way that one can exclude or separate single effects (e.g. the hydrodynamic one) and that a well known and as much as possible simple reaction is used, in order to draw a certain picture of the very complicated problem of surfactant action on reactive mass transfer.

Under the viewpoint of possible specific effects at multi component metal extraction these examinations seem to be of pronounced interest and of great promise, also on account of understanding of several processes occuring at membranes that means ion exchange, liquid membrane and at least biomembrane permeation.

Literature:

1. J. T. Davies, Turbulence Phenomena, New York, London 1972
2. V. G. Levich, Physicochemical Hydrodynamics, Prentic Hall Inc., New York 1962.
3. W. Nitsch and L. Navazio, Proceedings International Solvent Extraction Conference ISEC 1980.
4. W. Nitsch and K. Roth, Coll. Polym. Sci. 256 (1978), 1182.
5. R. Ollenik and W. Nitsch, Ber. Bunsenges. Phys. Chem. 85 (1981),900.
6. W. Nitsch and B. Kruis, J. Inorg. Nucl. Chem. 40 (1978), 857.

7. J. T. Davies and E. K. Rideal, Interfacial Phenomena, New York, Academic Press 1963.

Laser Light-Scattering and Laser Fluorescence Studies of Solvent Extraction Systems

Ronald D. Neuman, Department of Chemical Engineering, Auburn University,
Auburn, AL 36849/USA

The solvent extraction of metal ions from an aqueous solution to a nonpolar organic phase is a separation operation of major technological significance in the hydrometallurgical and nuclear industries. It is now recognized that the interface plays a key role in the extraction process. However, the interfacial chemistry which occurs in the solvent extraction of metal ions is still very incompletely understood.

Although investigations of the interfacial behavior of extraction reagents, in the past, have provided valuable information, progress is becoming more difficult in obtaining new fundamental information from classical surface-chemical approaches. The application of more sophisticated and recently developed techniques, such as laser techniques, holds promise for significant advances in understanding the molecular principles underlying the interfacial behavior of extractant molecules and their interactions with metal ions. This paper will discuss recent advances in laser light-scattering and laser fluorescence techniques and their application to liquid/liquid interfacial systems.

Laser Light Scattering

If a light beam is made to impinge on a liquid/vapor interface such as the air/water interface, most of the light is reflected or refracted. However, a very small amount is scattered in all directions. This surface light scattering is caused by the liquid surface being not flat but slightly rough or corrugated due to thermal fluctuations (1). The early light-scattering studies on liquid surfaces were limited to the scattered intensity and polarization. But it became possible with the development of coherent light (laser) sources to study the frequency distribution of the light scattered from the thermally excited surface capillary waves. Whereas spectral analysis permits one to determine values of the surface tension and viscosity of liquids, the power spectrum of the light scattered from monomolecular films on liquids, however, depends additionally on the viscoelastic parameters of the film (2).

McQueen and Lundström (3) were the first to study capillary waves on water covered by monomolecular films using laser light-scattering (LLS) techniques. Their measurements, however, suffered from poor resolution and sensitivity as well as the lack of a quantitative analysis of instrumental effects. Hård et al. (4) developed an improved laser heterodyne apparatus for measuring properties of liquid surfaces where these limitations were overcome. Hård and Löfgren (5) determined for the first time the interfacial elasticity and interfacial viscosity of a monolayer by LLS measurements. Byrne and Earnshaw (6) reported LLS measurements on fatty acid monomolecular films. Langevin (7) also examined a fatty acid monolayer but, in contrast to Byrne and Earnshaw (6), concluded that a transverse interfacial viscosity also plays an important role in the motion of the monolayer. Similar studies in our laboratory led Hård and Neuman (8) to conclude that the transverse viscosity was negligible for the monomolecular films studied.

The LLS technique also has been used to measure interfacial tensions of simple liquid/liquid systems (9) and more complex two-phase and three-phase microemulsion systems (10). Furthermore, we have shown recently that it should be possible to obtain quantitative information on the interfacial viscoelastic properties of some solvent extraction systems if high resolution LLS measurements are made, especially so if n-hexane and water are employed as the two bulk phases (11).

However, before we could undertake measurements on solvent extraction systems, it was first necessary to re-examine the propagation and damping of thermally excited capillary waves at pure liquid/vapor interfaces. This was required because there were still unresolved questions concerning the validity of various theoretical models used to describe the motion of capillary waves even for the basic reference liquid, i.e., water (12,13). Such a study was also needed for correctly interpreting LLS measurements of monolayer-covered liquid surfaces since there was also disagreement concerning which viscoelastic properties are significant constitutive coefficients. High resolution measurements clearly are required for providing the high-quality experimental data to determine whether the present theoretical models are adequate or whether improved models which more accurately describe the behavior of fluid/fluid interfaces -- both in the absence or presence of surface-active substances -- are needed.

An advanced interfacial laser heterodyne light-scattering apparatus was constructed for the purpose of obtaining high resolution LLS measurements. The LLS measurements were performed in a similar manner to that described earlier by Hård and Neuman (8) but differed in the following respects: A spatial filter/beam expander replaced lens L_1 in front of the grating. The cabinet was made of double-walled stainless steel which allows thermostatted water to flow between the walls. The use of stainless steel instead of Lucite for the inner wall material reduces surface contamination. A sandblasted glass Wilhelmy plate which wets better than platinum was used for the surface tension measurements. The photomultiplier anode current was fed directly into a simple current-to-voltage converter after which the signal was input to a broadband amplifier/filter unit with upper and lower cut-off frequencies set at 250 and 3.15 kHz, respectively. Next, the signal was analyzed in a 256 live channel correlator (LFI, Model 1096) operating in duplexing mode, producing 528-channel correlograms. Prior to being fed to the correlator (analog input), the signal level was matched to the internal voltage-to-frequency converter of the correlator by an adapter (LFI, AM-01).

In the data fitting procedure, the correlogram was first (digitally) Fourier transformed, and the Lorentzian fit was accomplished by a least-square minimization procedure which yields two parameters of interest: the peak frequency and the half-width at half-height of the power spectrum. The measured power spectrum, after correcting for instrumental effects, was interpreted by comparison with the following theoretical power spectrum which takes into account the presence of the second bulk phase (14):

$$P(\omega) = \frac{k_B T}{\pi\omega} \cdot \mathrm{Im}\left(\frac{1}{i\omega} \cdot \frac{X_1}{X_1 \cdot X_3 - X_2^2} \right) \qquad [1]$$

where

$$X_1 = \eta_1(k+m_1) + \eta_2(k+m_2) - \frac{\varepsilon^* k^2}{i\omega}, \qquad [2]$$

$$X_2 = \eta_1(k-m_1) - \eta_2(k-m_2), \qquad [3]$$

$$X_3 = \eta_1 \frac{m_1}{k}(k+m_1) + \eta_2 \frac{m_2}{k}(k+m_2) - \frac{\sigma k^2}{i\omega} \text{ and} \qquad [4]$$

k_B = Boltzmann constant, T = absolute temperature, $k = \frac{2\pi}{\Lambda}$ = measured wavenumber, Λ = wavelength of the measured surface waves, σ = surface tension, ρ_1 = bulk liquid density, η_1 = bulk liquid shear viscosity, ρ_2 = air density, η_2 = air shear viscosity, $m_1 = [k^2 - i(\omega\rho_1/\eta_1)]^{1/2}$ $\mathrm{Re}[m_1] > 0$, $m_2 = [k^2 - i(\omega\rho_2/\eta_2)]^{1/2}$ $\mathrm{Re}[m_2] > 0$, $\varepsilon^* = \varepsilon - i\omega\kappa$, ε = sum of interfacial shear elasticity and interfacial dilational elasticity and κ = sum of interfacial shear viscosity and interfacial dilational viscosity.

Absolute, accurate and high resolution laser light-scattering measurements of capillary waves of water were successfully performed at three wavenumbers -- 834, 1114, and 1394 cm^{-1} -- in order to investigate the propagation and damping of capillary waves (15). The wavenumbers were directly measured using a new reference grating technique to within ± 0.2%. With the carefully designed LLS apparatus used in this study, low instrumental broadening of the capillary wave spectra (9, 4, and 2%, respectively) was achieved. Our results show that the capillary wavemotion follows hydrodynamic theory using standard bulk property values within the experimental inaccuracies which are ± 0.3 and ± 3% in frequency and damping, respectively. This makes these measurements the most accurate in the field to date.

The excellent agreement between experiment and theory then permitted us to extend LLS measurements to monolayer-covered aqueous subsolutions (16). The film-forming compounds studied were octanoic acid, myristic acid, stearic acid, tetradecanol, PMMA, and PDMS. We convincingly found that the wavemotion is determined, apart from static surface tension, only by a horizontal interfacial elasticity, ϵ, and a horizontal interfacial viscosity, κ. This result is in contrast with Langevin (7) who found transverse viscoelastic properties are significant for myristic acid, stearic acid, and PMMA. The measured ϵ is equal to or larger than the static elasticity which is in agreement with our earlier study (8). Our κ values are consistently smaller than surface viscosities found in other studies, most pronounced for octanoic acid, where κ differed at least by four orders of magnitude when compared with a mechanical wave generating rheometer.

We feel the low κ values are a consequence of the nondisturbing character of LLS measurements of thermal waves, and this makes our values likely to be correct. In contrast, our results indicate that mechanical devices used to measure interfacial viscoelastic properties can seriously perturb the interface. The LLS technique, therefore, should be used rather than mechanical viscometers to obtain reliable interfacial viscoelastic properties.

Presently, we are optimizing the apparatus optics for LLS measurements of liquid/liquid interfaces. The geometry selected should minimize the deleterious effects of background scattered light which can also beat with the light scattered from the capillary waves in most practical cells. Once the optimization is completed, we will be able to obtain high resolution LLS measurements and, hence, obtain reliable information on the interfacial rheological properties of solvent extraction systems.

Interfacial rheological studies are very important because investigations of the interfacial behavior of extractants should not just be limited to interfacial activity or tension measurements. Other interfacial properties may also influence the rate at which metal ions are transferred from one phase to another (17). Furthermore, the enhanced stability often observed during the coalescence of dispersed droplets in an emulsion has been attributed to the formation of coherent interfacial films by virtue of their dilational viscoelastic properties (18). Thus, LLS measurements of the interfacial elasticity and interfacial viscosity are most relevant to an understanding of not only the interfacial mass transfer process but also the coalescence behavior of droplets during solvent extraction.

Laser Fluorescence

Another laser technique under further development in our laboratory is that of a laser fluorescence grating technique. Fluorescence techniques have been especially useful in biological membrane (19) and model membrane (20) studies to measure the lateral or translational diffusion of molecules parallel to the membrane surface. Fluorescence photobleaching recovery (FPR) is the most commonly used technique. It should be possible to extend FPR to interfacial studies of model extractants, i.e., surface or interfacial films of long-chain phosphoric acids or phosphate esters that are less soluble and yet expose the same functional groups to the two bulk phases. Indeed, Peters and Beck (21) recently reported experiments on phospholipid monolayers at the air/water interface using fluorescent probes.

The basic idea of FPR is simple: An intense light pulse from a CW-laser, the pulse being short compared with the characteristic diffusion time of the system of interest, is made to impinge on the film under study. The energy of the pulse is chosen high enough to irreversibly bleach the fluorescent probe molecules which should be uniformly distributed within the host film. With the intensity of the laser beam attenuated 10^3-10^4 times, the temporal fluorescence recovery of the bleached region is then measured. The recovery is due to diffusion of probe molecules into the bleached area from surrounding, non-bleached regions. The characteristic diffusion recovery time, τ_D, is related to the lateral diffusion coefficient of the probe molecules, D, through the relation

$$\tau_D \approx \frac{a^2}{D} \qquad [5]$$

where a is a characteristic spatial width of the bleached region.

When the film substrate is a liquid, surface flow also transports non-bleached probe molecules into (and bleached molecules out of) the bleached region with a characteristic time

$$\tau_F \approx \frac{a}{v} \qquad [6]$$

where v is the flow velocity. The measured recovery time, τ, is therefore dependent on both τ_D and τ_F, which in practice can seriously hamper accurate diffusion coefficient determinations.

Particularly vulnerable to flow are measurements whereby a single, stationary circular spot is used both for bleaching and monitoring. which is the common way of measurement. In order to determine τ_D from τ one then has to rely on the detailed shape of the recovery curve which is not very accurate. Another major problem with all single spot FPR measurements is to determine a accurately.

Instead of using a single spot, a simple Moiré technique will be employed for measuring lateral film diffusion using FPR, where the film is bleached in a periodic pattern of parallel light and dark stripes. During fluorescence recovery the imprinted pattern will be compared with an identical translated reference mask. This allows the use of only one detector, gives simple data analysis, and provides high signal-to-noise ratio. The periodic pattern increases the spatial resolution relative to the conventional single spot technique and results in more accurate diffusion constant determinations. This technique also allows separation between diffusion and flow which is important when liquid substrates are used.

This relatively new technique should permit us to probe the nature of the microenvironment about the polar head groups of extractant molecules since translational diffusion should be a sensitive indicator of changes occurring in the vicinal water adjacent to the interfacial film. As such, we will then be better able to analyze the effect of the water structure in the interfacial region (22). It will be desirable also to evaluate the influence of anions to determine whether a structure-breaking action of chaotropic anions on water is observed which may be helpful in interpreting the extraction rates determined for solvent extraction systems.

Acknowledgments

Financial support from the Office of Basic Energy Sciences, Division of Chemical Sciences, Department of Energy under Grant No. DE-FG05-85ER13357 is gratefully acknowledged.

References

1. M. von Smoluchowski, Ann. Physik, 25, 225 (1908).
2. D. Langevin and M.A. Bouchiat, C.R. Acad. Sci. B, 272, 1422 (1971).
3. D. McQueen and I. Lundström, J. Chem. Soc. Faraday Trans. I, 69, 694 (1973).
4. S. Hård, Y. Hamnerius and O. Nilsson, J. Appl. Phys., 47, 2433 (1976).
5. S. Hård and H. Löfgren, J. Colloid Interface Sci., 60, 529 (1977).
6. D. Byrne and J.C. Earnshaw, J. Phys. D., 12, 1145 (1979).
7. D. Langevin, J. Colloid Interface Sci., 80, 412 (1981).
8. S. Hård and R.D. Neuman, J. Colloid Interface Sci., 83, 315 (1981).
9. H. Löfgren, R.D. Neuman, L.E. Scriven and H.T. Davis, J. Colloid Interface Sci., 98, 175 (1984).

10. A. Pouchelon, J. Meunier, D. Langevin and A.M. Cazabat, J. Phys. Lett., 41, 239 (1980).

11. R.D. Neuman and A.G. Gaonkar, Proc. Int. Solvent. Extraction Conf., ISEC '83, p. 16 (1983).

12. J.A. Stone and W.J. Rice, J. Colloid Interface Sci., 61, 160 (1977).

13. D. Byrne and J.C. Earnshaw, J. Colloid Interface Sci., 74, 467 (1980).

14. J. Kramer, J. Chem. Phys., 55, 2097 (1971).

15. S. Hård and R.D. Neuman, J. Colloid Interface Sci., in press.

16. S. Hård and R.D. Neuman, submitted for publication.

17. J.T. Davies and E.K. Rideal, "Interfacial Phenomena." Academic Press, New York, 1963.

18. Th. F. Tadros, Colloids Surfaces, 1, 3 (1980).

19. R. Peters, J. Peters, K.H. Tews and W. Bähr, Biochim. Biophys. Acta, 367, 282 (1974).

20. D.E. Koppel, D. Axelrod, J. Schlessinger, E.L. Elson and W.W. Webb, Biophys. J., 16, 1315 (1976).

21. R. Peters and K. Beck, Proc. Natl. Acad. Sci, USA, 80, 7183 (1983).

22. G.F. Vandegrift and E.P. Horwitz, J. Inorg. Nucl. Chem., 39, 1425 (1977).

Effect of Dissolved Salts on the Binary Vapour-Liquid Equilibria and Binary and Ternary Liquid-Liquid Equilibria

V.K. Srinivas and D. Srinivasan

Department of Chemical Engineering, A.C. College of Technology,
Anna University, Madras 600 025, India.

Abstract

As a part of our continuing research programme on the study of the salting out effects of dissolved salts in distillation and solvent extraction systems we took up for investigation the ternary system ethyl acetate - isopropanol - water which tends to exhibit a solutropic behaviour with two of its constituent binaries forming azeotropes. The idea behind such an exercise was to ascertain whether the presence of an inorganic salt like NaCl at some concentration could break azeotropes and avoid formation of a solutrope.

We have studied experimentally the effect of dissolved NaCl at various concentrations - 5, 10 etc. upto 25% by weight (within the saturation limit) on (i) the relative volatility (α) of the azeotropic binary system isopropanol - water (ii) the mutual solubility of the partially miscible binary system ethyl acetate - water and (iii) the selectivity (β) of the solutropic ternary system ethyl acetate - isopropanol - water. It has been observed that in the case of the system isopropanol - water the azetrope gets shifted but is not broken even at high concentrations of the salt NaCl. As for its effect on the ternary LLE the region

of heterogenity increases with increase in its concentration. Both α and β get enhanced with increase in salt concentration. The binary experimental VLE data have been correlated well by Wilson equation. Similarly the experimental ternary tie-line data have been successfully fitted by Ishida's model which has been suggested for ternary solutropic systems. The results are presented and discussed in the text of the paper.

As the manuscript was not available at the 28th May 1986, the deadline for printing this book, we only print the short abstract of the paper.

Selectivity and Equilibria in Extraction with Macrocycles in Synergistic Combination with Organophilic Acids

W.J. McDowell, B.A. Moyer, S.A. Bryan, R.B. Chadwick, and G.N. Case
Oak Ridge National Laboratory, Oak Ridge, Tennessee, USA

ABSTRACT

Reported here is the behavior of several organophilic macrocyclic polyethers (crown ethers) as coordinative extraction synergists in combination with 1) a long-chain neo carboxylic acid, 2) an alkyl phosphoric acid, and 3) an alkyl-aryl sulfonic acid. Selected combinations of these organophilic cation exchangers and macrocyclic coordinators were examined as extractants for alkali, alkaline earth, and first-row transition elements from nitrate systems. Both synergistic and antagonistic effects were produced. Macrocycles having a cavity size to fit the metal ion usually produced the largest synergistic effect; however, the nature of the substituents on the macrocyclic ring also has a strong effect on selectivity. In general, alkali metal ions prefer to bond to benzo-substituted crown ethers while alkaline earth ions prefer to bond to cyclohexano-substituted ones. Iron, cobalt, and nickel extractions are antagonized by the macrocycles while copper is synergized only slightly and manganese and zinc moderately strongly. Evidence indicates that the organic-phase complex consists of a single macrocycle ring per metal together with acid anions sufficient to neutralize the metal valence. Sometimes neutral acid molecules are also included. Complicating features of the chemistry of these systems include the tendency of the crown ethers to form strong intermolecular compounds with the organophilic acids and the tendency of these acids and their salts to form aggregates.

INTRODUCTION

The ability of crown ethers to form coordination complexes with alkali and alkaline earth ions in polar solvent systems (water, water-alcohol, alcohol, chloroform, and ethylene dichloride) is well known and documented.(1) Some of the earliest work with crown ethers was a demonstration of their complexation with alkali metal ions by extraction of picrate salt of the metal into a chloroform solution of crown ethers.(2-6) The phenomenon of size selectivity in complexation was thus demonstrated. The use of organophilic acids to serve as organic phase cation exchangers in combination with organophilic crown ethers has been shown to allow extraction of alkali, alkaline earth, and other ions into organic solvents of low polarity such as toluene.(7-10) The organophilic acids that have been used in systematic studies are shown in Fig. 1.

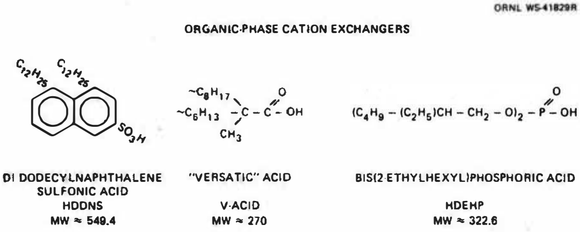
ORNL WS-41829R
ORGANIC-PHASE CATION EXCHANGERS
C12H25
C12H25
SO3H
~C8H17
~C6H13
C
C
O
OH
CH3
(C4H9 – (C2H5)CH – CH2 – O)2 – P – OH
O
DI DODECYLNAPHTHALENE SULFONIC ACID
HDDNS
MW ≈ 549.4
"VERSATIC" ACID
V-ACID
MW ≈ 270
BIS(2-ETHYLHEXYL)PHOSPHORIC ACID
HDEHP
MW ≈ 322.6

FIGURE 1. The Organic-Phase-Soluble Acids Reported in This Paper. All three compounds are liquids at room temperature.

The use of organic solvents (diluents) of low polarity allows the experimental system to more closely approximate the type of system that might be practical in a process where inexpensive diluents of low toxicity and high flash point are demanded. However, it also requires that macrocycles be chosen that are soluble in diluents of low polarity and that distribute to aqueous phases only slightly. The metal/salt adducts of these macrocycles should also be organophilic. A number of macrocycles have been found to fit these requirements. The ones used in this work are shown in Fig. 2.

The use of an organophilic acid (cation exchanger) in combination with an organophilic macrocycle in a diluent is believed to allow 1) the formation (perhaps at the organic/aqueous interface) of an organophilic salt of the metal ion, 2) the coordination of the metal ion by the macrocyclic compound accompanied by shedding of all or most of metal ion's water of hydration, and 3) transfer of the resulting organophilic complex to the organic phase.

Reported here are the results of, and conclusions from, several investigations using the reagents shown In Figs. 1 and 2.

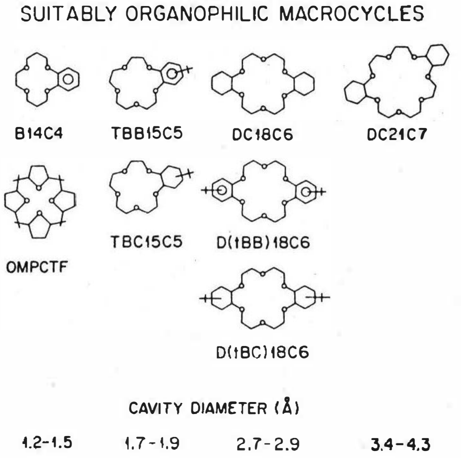

FIGURE 2. The Organic-Phase-Soluble Macrocycles Used as Synergists. B14C4 = benzo-14-crown-4, TBB15C5 and TBC15C5 = t-butylbenzo-15-crown-5 and t-butylcyclohexano-15-crown-5, DC18C6 = docyclohexano-18-crown-6 (tBB and tBC are t-butylbenzo and t-butylcyclohexano), DC21C7 = dicyclohexano-21-crown-7, ONPCTF = octamethylperhydrocyclotetrafurfurylene.

EXPERIMENTAL

Bis(2-ethylhexyl) phosphoric acid (HDEHP) was purified by Cu(II) precipitation and molecular distillation.(11,12) The neo carboxylic acid called "versatic acid 1519" (V-acid) was obtained from Shell Development Laboratories and purified by molecular distillation. The didodecylnaphthalene sulfonic acid (HDDNS) was obtained from King Industries of Norwalk Connecticut and purified by published ion-exchange procedures.(13) Crown ethers were obtained from Aldrich and Parish chemical companies. The macrocycles were stated to be 99% pure by infrared measurements by the supplier and were used as recieved.

The two-phase equilibrations were made in small separatory funnels or vials at room temperature, 23 to 25°C. Analyses of the equilibrated phases were usually by radiotracers, sometimes by atomic absorption spectrometry.

RESULTS AND DISCUSSION

HDEHP has considerable selectivity of its own for the alkalis and alkaline earths (See Fig. 3). For example, lithium is extracted more than the other alkali metals and beryllium more than the other alkaline earth metals. The addition of crown ethers to the system does, however, change the selectivity. Figure 3 illustrates synergism by two different concentrations of DC18C6.

Extractions with the carboxylic acid, V-acid, show a strong preference for the alkaline earth elements over the alkali metals and strong synergistic effects by crown ethers are seen in the extraction of the alkaline earths. At pH 8.5 strontium extraction is synergized by a factor of approximately 1000 by DC18C6 and barium and radium by a factor of approximately 100 by DC21C7. Although insufficient detailed studies have been made, it appears that excellent selective separations of the alkaline earths from each other and from the alkali metals are possible using carboxylic acids with crown ethers.

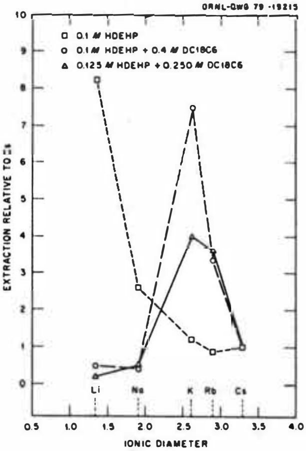

FIGURE 3. Synergistic Effects Produced by Two Different Concentrations of DC18C6 on Alkali Metal Extraction from a Solution 0.1 M in Each Alkali Metal Nitrate by 0.1 M HDEHP in Toluene.

Organophilic sulfonic acids used alone should be less selective than carboxylic or phosphoric acids because the sulfonic acid oxygens complex metals poorly. The data in Fig. 4 are consistent with this idea. Under these conditions we might expect most of the extraction selectivity shown by crown ether - sulfonic acid mixtures to be due largely to the crown ether. Strong size-selective synergism is seen in Fig. 4 where all the alkali elements were mixed in the same aqueous solutions

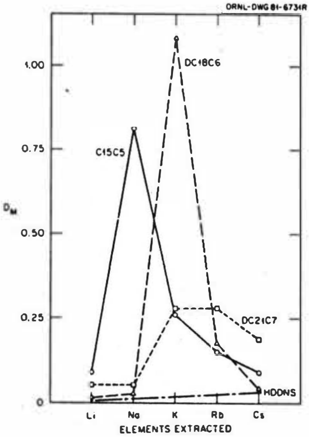

Size-Selective Synergism: Loading Conditions

FIGURE 4. The Effects of Three Crown Ethers (0.05 M) on the Extraction Selectivity of 0.1 M HDDNS in Toluene for Alkali Metals from an Aqueous Solution 0.1 M in Each Alkali Metal Nitrate. (Fig. from Ref. 8.)

(competitive extraction) and in Fig. 5 (from Ref. 10) where the metals were extracted separately at tracer level. But note also in Fig. 5 that there are significant differences between benzo- and cyclohexano-substituted crown ethers of the same size and that for potassium, rubidium, and cesium the benzo-substituted crowns produce the largest synergistic effect and thus, presumably, the strongest bond with the alkali metal.

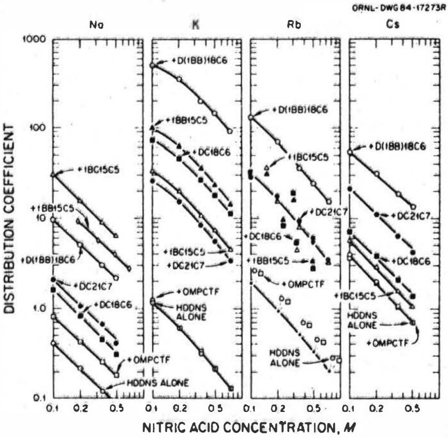

FIGURE 5. Extraction of Tracer-Level Sodium, Potassium, Rubidium, and Cesium from Nitric Acid by Toluene Solutions 0.1 M in HDDNS and 0.05 M in Macrocycle.

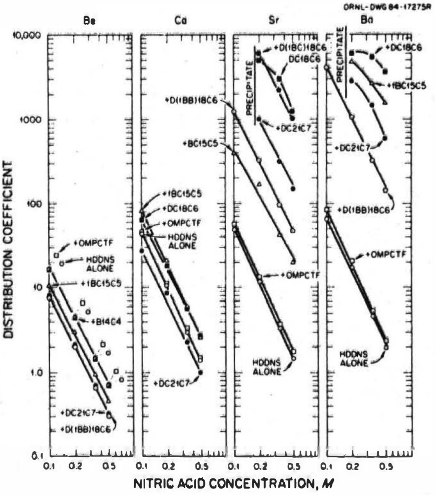

FIGURE 6. The Extraction of Tracer-Level Beryllium, Calcium, Strontium, and Barium from Nitric Acid by Toluene Solutions 0.1 M in HDDNS and 0.05 M in Macrocycles.

Figure 6 (from Ref. 10) shows the extraction of tracer-level alkaline earths with HDDNS and HDDNS plus crown ethers. Beryllium is not synergized, calcium only slightly, and strontium and barium very significantly. Note that here the benzo-substituted crowns are less effective synergists than the cyclohexano-substituted crowns. The benzo- and cyclohexano-substituted crown ethers reverse their selectivity between alkali and alkaline earth elements. For example, the extraction coefficient for potassium is 350 using the benzo-substituted crown but only 46 using the cyclohexano-substituted crown while for strontium the coefficients are 300 for the benzo- and 6000 for the cyclohexano-substituted compound. Rubidium and cesium both show stronger extraction with the benzo compound while, again, barium shows a strong preference for the cyclohexano-substutited compound. Inductive effects would be expected to reduce the electronegativity (basicity) of four of the six ether oxygens thus reducing their bonding strength and synergistic effect but would not explain an increase as in the case of potassium, rubidium and cesium. Further, ion/cavity size correspondence seems to have little to do with this phenomenon.

The cyclohexano-derivatives of crown ethers are known(14) to be more flexible than are the benzo-derivatives and this suggests the following speculation: 1) The more rigid benzo-substituted crown may maintain a cavity in solution thus allowing the alkali metal to profit in overall reaction energy from the fact that it is not necessary to rearrange the coordinating oxygens of the benzo-substituted compound into a cavity (entropy effect). 2) The doubly-charged alkaline earth ions may attempt to pull the bonding oxygens into some configuration not easily attained by the benzo-substituted crown ether (steric effect).

The 15C5 ring is the correct size to accept first-row transition metal ions; however, for the series of divalent elements manganese through zinc, only the end elements are synergized significantly. Copper is synergized very slightly and Fe(II), Co(II), and Ni(II) are antagonized (Fig. 7).

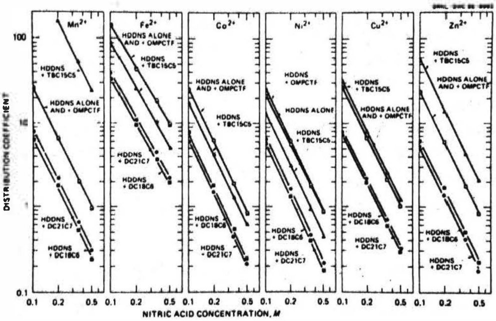

FIGURE 7. The Extraction of Tracer-Level Manganese(II), Iron(II), Cobalt(II), Nickel(II), Copper(II), and Zinc(II) from Nitric Acid by toluene solutions 0.1 M HDDNS + 0.05 M tBC15C5. (Data from Ref. 10.)

In order to explain the observed antagonistic effect, one must propose reactions between the macrocycle and the organic acid that compete with metal complexation. Such reactions have been confirmed using vapor pressure osmometric (VPO) and infrared methods. For HDDNS and tBC15C5 two intermolecular adducts are required to satisfy least-squares fitting of the VPO data, tBC15C5$_2$(HDDNS)$_5$ and tBC15C5(HDDNS)$_3$. Since VPO measurements show HDDNS alone in toluene to be aggregated, a range of combining ratios in the adducts between HDDNS and tBC15C5 is suggested. The differences in the effect of added tBC15C5 on extraction across the divalent transition elements Mn through Zn (See Fig. 8) suggest that the structural-preference energy or ligand-field stabilization energy (LFSE) that would allow Fe(II), Co(II), and Ni(II) to bond strongly with strong electron donors such as nitrogen is not available in the bond to the weak electron donor oxygens in the crown ether. Further, the fact that five bonding sites are offered by the crown ether and two by the sulfonic acid argues for pentagonal bipyramid geometry and this is not consistent with the usual pusedo-octahedral complex preference of Fe(II), Co(II), Ni(II), and Cu(II). In other words, the structural and bonding preferences of these elements are not satisfied by tBC15C5 plus 2DDNS^{-1}. The organic phase (extraction) complexes formed in these studies have not been completely characterized. Studies to do this are underway. However, we do know that the crown ethers form adducts or complexes with the sulfonic acid but in diferent (average) combining ratios with different crown ethers. Also, for those systems examined, 'the evidence thus far (slope analysis and least-squares fitting of equilibrium data and isolation and analysis of solid compounds) indicates one crown ether per metal atom in the organic-phase complex. Various amounts of the sulfonic acid appear to be bonded depending on the concentration of metal in the organic phase. Infrared, proton nuclear magnetic resonance, and vapor pressure osmometry studies indicate that for the complex of strontium with DC18C6 and $DDNS^{-1}$ the stoichiometry is $Sr(DDNS)_2 \cdot DC18C6 \cdot 2H_2O$ and that the strontium is within the DC18C6 ring. Studies of the extraction of very low concentrations of manganese (< 0.001 *M*) indicate the formation of the complex $Mn(DDNS)_2 \cdot 4HDDNS$. The macrocycle tBB15C5 does not form a complex with manganese.

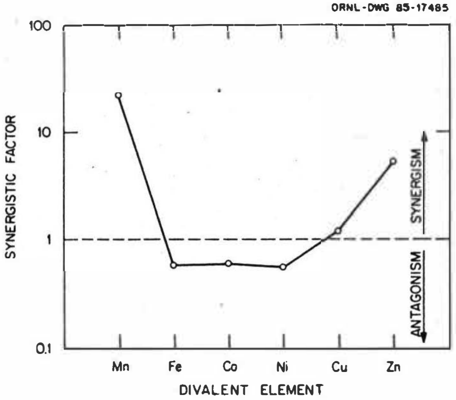

FIGURE 8. Synergistic Factors ($D_{mixture}/D_{HDDNS}$) for the First-Row Transition Elements Mn Through Zn due to the Addition of 0.05 M tBC15C5 to 0.1 M HDDNS in Toluene. The aqueous phase was 0.2 M nitric acid. (Fig from Ref. 10)

REFERENCES

1. R.M. Izatt, J.S. Bradshaw, S.A. Nielsen, J.D. Lamb, and J.J. Christensen, *Chem. Rev.*, 85, 271-339 (1985)
2. C.J. Pedersen, *J. Am. Chem. Soc.*, 89, 7017 (1967)
3. C.J. Pedersen, *J. Am. Chem. Soc.*, 89, 2498 (1967)
4. C.J. Pedersen, *J. Am. Chem. Soc.*, 92, 391 (1970)
5. C.J. Pedersen, *J. Am. Chem. Soc.*, 92, 386 (1970)
6. H.K. Frensdorff, *J. Am. Chem. Soc.*, 93, 4674 (1971)
7. W.F. Kinard, W.J. McDowell, and R.R. Shoun, *Sep. Sci. and Technol.*, 15 1013-1024 (1980)
8. W.J. McDowell, G.N. Case, and D.W. Aldrup, *Sep. Sci. and Technol.*, 18, 1483-1507 (1983)
9. W.F. Kinard and W.J. McDowell, *J. Inorg. Nucl. Chem.*, 43 2947 (1981)
10. W.J. McDowell, B.A. Moyer, G.N. Case, and F.I. Case, "Selectivity in Solvent Extraction of Metal Ions by Organic Cation Exchangers Synergized by Macrocycles: Factors relating to Macrocycle Size and Structure", *Solv. Ext. and Ion Exch.*, In Press.
11. W.J. McDowell, P.T. Perdue, and G.N. Case, *J. Inorg. Nucl. Chem.*, 38, 2127 (1976)
12. J.A. Partridge and R.C. Jensen, *J. Inorg. Chem.*, 31, 2597 (1969)
13. P.R. Danesi, R. Chiariza, and G. Scibona, *J. Inorg. Nucl. Chem.*, 35, 3926-3928 (1973)
14. W. Wallace, C. Chen, E.M. Eyring and S. Petrusccl, *J. Phys Chem.*, 89, 1357 (1985)

Modelling of Salting Out Effects and Solvent Extraction Equilibria

H. Pitsch, UNAM, Mexico/MEX. J. Ly, C. Poitrenaud, INSTN, Gif-sur-Yvette / F

Physico-chemical basis

In the equilibrium equations, activity coefficients in both phases represent salting-out effects. We adopted Sergievskii's hypothesis as regarding the non-ideality of the behaviour of species in the organic layer (1) : for a definite solvent (i.e. diluent + extractant at constant total concentration), the activity coefficient of any organic species only depends on the activity of water in the system :

$$\overline{y}_i = \overline{y}_{s,i}\ (a_w)$$

a_w is the activity of water.

On the other hand, aqueous solutions are supposed to obey Zdanovskii's rule (2), and therefore the expression proposed by Ryazanov-Vdovenko (3) describes exactly the activity coefficient of any species i present in the aqueous phase :

$$y_i = \frac{f_i(a_w)}{\sigma}$$

σ is the total concentration of species in the aqueous solution.

On this basis, it was previously shown (4) than any equilibrium in an aqueous solution or between two inmiscible phases may be characterized by a function of the water activity in the system, from which the apparent equilibrium constant K in any medium might be calculated. For example :

$$M + nL \rightleftharpoons MLn \qquad K = \frac{[MLn\ ]}{[M]\ .\ [L]^n} = G(a_w)\ .\ \sigma^{-n}$$

Distribution Equilibria

The general equation of the distribution equilibrium of a metallic element M between two non-miscible liquid phases may be written :

$$M + \sum_i e_i\, \overline{E}_i \rightleftharpoons \overline{M}' + \sum_j r_j\, R_j$$

and the corresponding expression of the distribution coefficient is :

$$D = K^{\circ}_{ext} \cdot \frac{y_M}{\prod_j y_{R_j}^{r_j}} \cdot \frac{\prod_i \overline{y}_{\overline{E}_i}^{e_i}}{\overline{y}_{M'}} \cdot \frac{\prod_i [\overline{E}_i]^{e_i}}{\prod_j [R_j]^{r_j}} \cdot \alpha^{-1}_{M(L_k)}$$

In the first place appears the thermodynamic constant, which depends on the temperature and pressure. The next two therms describe the medium effects in the aqueous and in the organic phase respectively, and may be reduced to functions of a_w and σ. Finally, the last two terms represent the chemical effects, due to the main reaction and possible interfering processes (complexation in the aqueous phase).

According to the previously developped considerations, it is then possible, at constant temperature and pressure and for a given solvent, to express D by a product of three terms, the salting-out one (function of a_w and σ), the mass action term (concentrations) and the complexation term (ligand concentration, a_w and r) :

$$D = G_{ext}(a_w) \cdot \sigma^{\Sigma r_j - 1} \cdot \frac{\prod_i [E_i]^{e_i}}{\prod_j [R_j]^{r_j}} \cdot \alpha^{-1}_{M(L_k)}$$

Here $G_{ext}(a_w)$ is the distribution function which characterize the peculiar equilibrium, and the general expression for the complexation coefficient is :

$$\alpha_{M(L_k)} = 1 + \sum_{k=1}^{n} \sum_{i=1}^{n_k} G_{k,i}(a_w) \cdot \left(\frac{[L_k]}{\sigma}\right)^i$$

(n ligands L_k, n_k complexes with L_k).

Results

1) Extraction of mineral acids : extraction of HCl by TBP (30 %) in dodecane.

* The distribution function was determinated by extraction experiments from different hydrochloric media (Fig. 1), according to the distribution mechanism generally admitted for the present experimental conditions :

$$H^+ + Cl^- + 2\,\overline{TBP} \rightleftharpoons \overline{HCl(TBP)_2}$$

* Deducing the corresponding value of the distribution function from this curve, it is possible to predict extraction coefficients even from aqueous phases containing other salts than those used in the previous study.

2) Extraction of a metal-chelate : distribution of uranium (VI) between aqueous solutions and thenoyltrifluoracetone (HTTA) in toluene.

x The distribution function corresponding to the equilibrium :

$$UO_2^{2+} + 2\,\overline{HTTA} \rightleftharpoons \overline{UO_2(TTA)_2} + 2H^+$$

was determined by extraction from non-complexing perchlorate media (Fig. 2).

x The characteristical functions of the complexation equilibria of UO_2^{2+} by nitrate ions in aqueous solution were determined in the range $.7 < a_w < 1$ by means of displacement of the previous distribution equilibrium under controlled media conditions (fixed water activity and known σ) (Fig. 3). These functions allow speciation calculation of any nitric solution of uranyle in the mentionned range of water activity.

3) Extraction of an element by combined mechanism : extraction of TcO_4^- by TBP (30 %) in dodecane from mixed chloride solutions.

x The distribution functions G^n_{ext} for the following distribution equilibria were determined :

$$M^+ + TcO_4^- + 4\,\overline{TBP} \rightleftharpoons \overline{MTcO_4(TBP)_4} \qquad M^+ = H^+,\ Na^+,\ Li^+$$

$$M^{2+} + TcO_4^- + Cl^- + 3\,\overline{TBP} \rightleftharpoons \overline{MTcO_4\,Cl(TBP)_3} \qquad M^{2+} = Ca^{2+},\ Mg^{2+}$$

as well as the water activity functions corresponding to the three identified interfering reactions :

$$H^+ + TcO_4^- \rightleftharpoons H\,TcO_4 \qquad G_H$$

$$Na^+ + TcO_4^- \rightleftharpoons Na\,TcO_4 \qquad G_{Na}$$

$$Ca^{2+} + TcO_4^- \rightleftharpoons Ca\,TcO_4^+ \qquad G_{Ca}$$

x It follows that the general expression of the distribution coefficient of Tc(VII) between chloride solutions containing the cations H^+, Na^+, Li^+, Ca^{2+}, Mg^{2+} and TBP (30 %) in dodecane is :

$$D = \frac{(G^H_{ext}.[H] + G^{Na}_{ext}.[Na] + G^{Li}_{ext}.[Li])\ .\ \dfrac{[\overline{TBP}]^4}{\sigma^2} + (G^{Mg}_{ext}.[Mg] + G^{Ca}_{ext}.[Ca]).\dfrac{[Cl]\,[\overline{TBP}]}{\sigma^3}}{1 + G_H.\dfrac{[H]}{\sigma} + G_{Na}.\dfrac{[Na]}{\sigma} + G_{Ca}.\dfrac{[Ca]}{\sigma}}$$

Further experiments involving complexe solutions (from two to four salting out agents) were used to check the validity of this equation. The excellent coincidence between calculated and experimental values is shown in Fig. 4.

Conclusion

It is shown that describing salting-out effects by means of the two parameters a_w and σ allows a simple and precise modelling of distribution equilibria. Prediction of distribution coefficients is therefore possible even in case of complexe solutions. This permits to identify unambiguously and characterize chemical reactions which may interfere with the extraction process.

Limits of application of the present way of modelling distribution equilibria are mainly determined by the simplicity of aqueous mixtures (i.e., their obedience to Zdanovskii's rule). Most systems involving electrolytes of industrial interest, especially in hydrometallurgy, are liable to be analysed by this method.

---

(1) V.V. Sergievskii, Dokl. Akad. Nauk. SSSR., 1976, 228, 160

(2) A.B. Zdanovskii, Trudy Solyanoi Laboratorii Akad. Nauk. SSSR., 1936, 6, 1

(3) V.M. Vdovenko, M.A. Ryazanov, Zh. Fiz. Khim., 1968, 42, 1936

(4) J. Ly, Thesis, University of Paris 6, 1984.

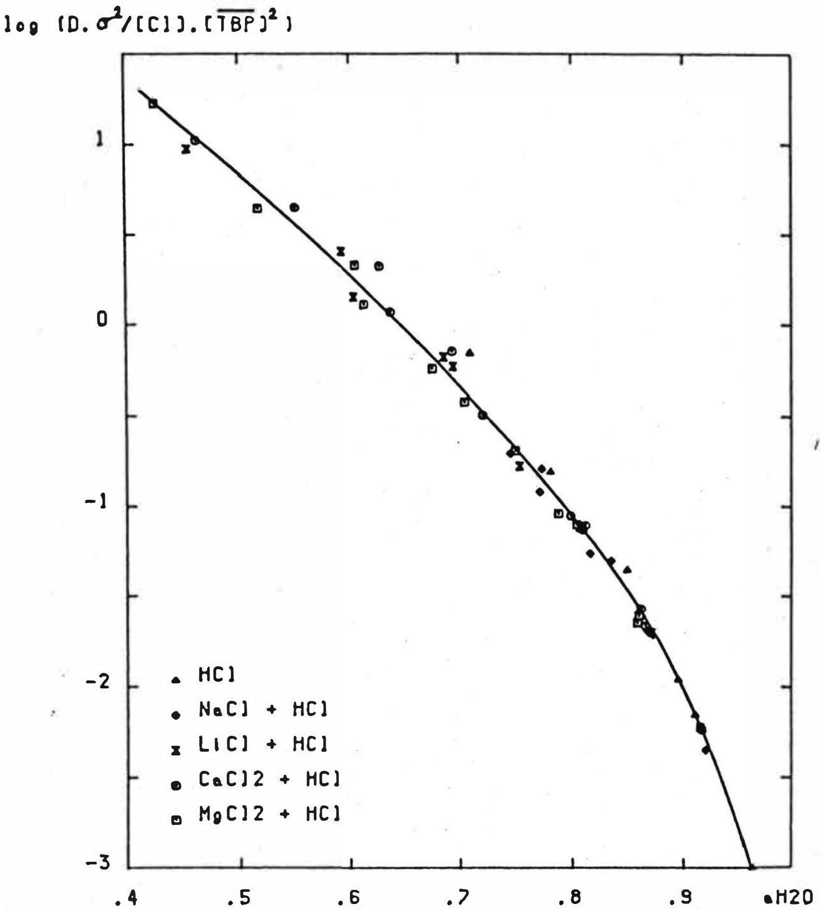

Figure 1 : Distribution function of HCl between aqueous chloride solutions and TBP (30 %) in dodecane.

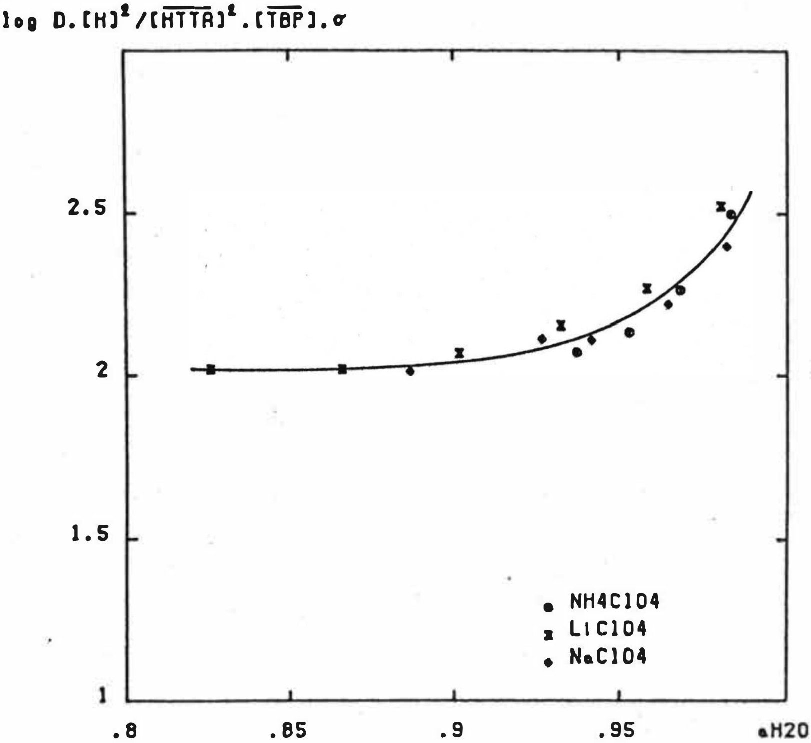

Figure 2 : Distribution function of uranyle between aqueous solutions and HTTA in toluene.

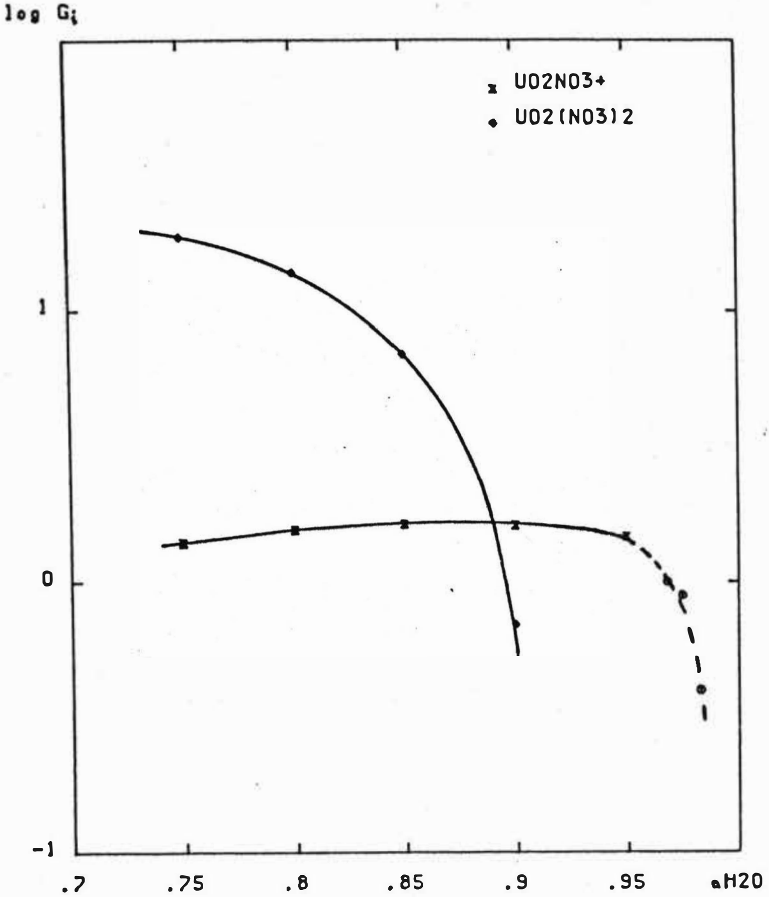

Figure 3 : Water activity functions for the complexation reactions :

$$UO_2^{2+} + NO_3^- \rightarrow UO_2NO_3^+$$

$$UO_2^{2+} + 2\ NO_3^- \rightarrow UO_2(NO_3)_2$$

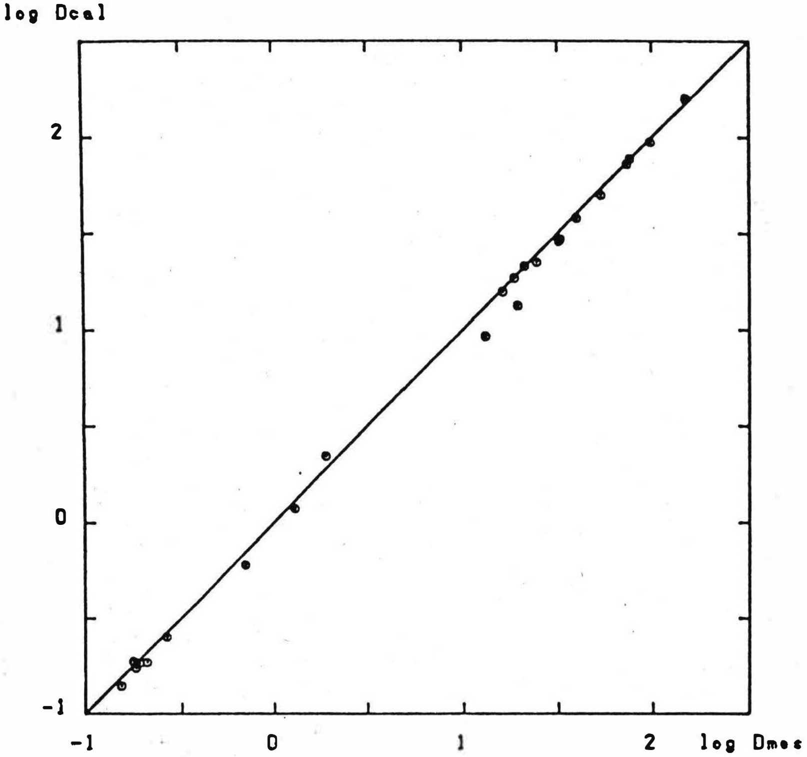

Figure 4 : Comparison of calculated and measured distribution coefficients of Tc(VII) between chloride solutions and TBP (30 %) in dodecane.

A general model for computing liquid-liquid equilibria. Application to the extraction of cobalt, copper and manganese by tri-iso-octylammonium chloride.

P.A. NOIROT, M. WOZNIAK
Ecole Nationale Supérieure de Chimie de Lille, 59652 VILLENEUVE D'ASCQ - France

The design of a solvent extraction process for metals starts with the determination of experimental equilibrium data. For multicomponent systems, which involve a competitive extraction, the distribution coefficient of one solute is a function of the concentrations of others and the winning of such data requires considerable work. Then the modelling is essential to reduce the experimental work and next to reach material balance flowsheets.
At present, if one except the empirical and semi-empirical models, the modelling of equilibrium data for the extraction of metals is essentially based on chemical interactions (1). Consequently, the physical interactions are overlooked and the introduced equilibrium constants are thus highly conditional, i.e. the model is only valid near the determination conditions and in a broad range of ionic composition for the aqueous phase.

This work therefore describes (i) a general model based on chemical and physical interactions and (ii) its application to the study of the extraction of cobalt, copper and manganese from lithium chloride and nickel chloride solutions by tri-iso-octylammonium chloride.

1. THE MODEL

The proposed model is based upon
- the stability constants of the species present in the aqueous and in the organic phases,
- the equations for the activity coefficients of the species (strong or weak electrolytes) which affect the "apparent" stability constants,
- the mass balance equations.

1.1. Equilibrium and species

As in conventional chemical models (2), it is first considered that the species in presence are derived from particular and independent species (A, X ... H) named the "components" of the system.
The general formation reaction of a species can thus be written :

$$aA + xX + \dots + hH \rightleftarrows A_aX_x \dots H_h + \omega H_2O$$

to which corresponds an overall thermodynamic formation constant:

[1] $$\beta_T = \frac{\{A_aX_x \ .... \ H_h\}\{H_2O\}^{\omega}}{\{A\}^a \ \{X\}^x \ ....\{H\}^h} \quad \text{where } \{\} \text{ denotes activity}$$

The number of components or species in only limited by the computer memory size and the stoichiometric coefficients a, x ... h, ω may be zero, positive or negative, integer or fractional.

As mass-balance equations require concentrations rather than activities, concentrational constants β are introduced. They are calculated by the relation :

[2] $$\beta = \frac{[A_aX_x\ldots H_h]}{[A]^a[X]^x \ldots[H]^h} = \frac{\gamma_A^a \ \gamma_X^x \cdots \gamma_H^h}{\gamma_{A_aX_x\ldots H_h}\{H_2O\}^{\omega}} \cdot \beta_T$$

where γ_J is the activity coefficient of J, the units being those of section 1.3. Moreover the definition phase of a component or of a species is to be specified. Afterwards, an organic species will be overlined and the corresponding stability constant noted $\overline{\beta}_T$. If a given species is present in the two phases, two constants $\overline{\beta}_T$ and β_T are introduced, whose ratio is the conventional partition constant.

1.2. Activity coefficients

Only the activity coefficients of the aqueous species have been taken into consideration. They are indeed highly variable due to the fact that the ionic composition of the aqueous phase is likely to change very strongly during an extraction process. At the moment, ideality is thus assumed for the organic species ($\overline{\gamma} = 1$) : in fact, their activity coefficients are included into the equilibrium constants. This approximation remains valid as long as the composition of the organic phase is not significantly altered.

Numerous theoretical or semi-empirical functions-reviewed recently by Renon (3)- have been proposed for the prediction of activity coefficients of electrolytes, even in concentrated solutions. Among them, we have chosen to adopt the Bromley representation. A single activity coefficients γ_J is given by the following equation (4), in the molality scale :

[3] $$\log \ \gamma_J = - \frac{A Z_J^2 \ I^{1/2}}{1 + I^{1/2}} + \Sigma \ \dot{B}_{KJ} \ \overline{Z}^2_{KJ} \ [K]$$

with $$\overline{Z}_{KJ} = \frac{(|Z_K| + |Z_J|)}{2} \qquad \dot{B}_{KJ} = \frac{(0.06 + 0.6 \ B_{KJ}) \ |Z_K Z_J|}{(1 + \frac{1.5}{|Z_K Z_J|} I)^2} + B_{KJ}$$

I = ionic strength of the solution $I = \frac{1}{2} \Sigma \ Z^2_K \ [K]$

[K]= molality of species K, moles/kg water

Z_K= charge of K

A = Debye-Hückel constant

B_{KJ} = interaction parameter between K and J

In Bromley's model, the index K refers only to ions of opposite sign to ion J existing in the multicomponent solution. So as to consider molecule-ion interactions, we will admit that species K may also be a molecule ($Z_K = 0$). Ternary or higher order interactions are ignored.

Water activity $\{H_2O\}$ is derived from the osmotic coefficient ϕ

[4] $\ln\{H_2O\} = -\dfrac{\Sigma[J]}{n_w}\phi$ where n_w represents the number of unbounded moles of water per 1000 g of total water.

[4a] $$\frac{1-\phi}{\ln 10} = A|Z_+Z_-|\frac{I^{1/2}}{3}\sigma - (0.06 + 0.6\,B)\,|Z_+Z_-|\,\frac{I}{2}\Psi - B\frac{I}{2}$$

[4b] $$\sigma = \frac{3}{I^{3/2}}\left\{1 + I^{1/2} - \frac{1}{1 + I^{1/2}} - 2\ln(1 + I^{1/2})\right\}$$

[4c] $$\Psi = \frac{2}{aI}\left\{\frac{1 + 2\,aI}{(1 + aI)^2} - \frac{\ln(1 + aI)}{aI}\right\}$$

with $B = 4(\sum_J\sum_K B_{JK}\,\overline{Z}^2_{JK}\,[J][K]) / (\Sigma[J]\,(\Sigma Z_J^2\,[J])$

$|Z_+Z_-| = \Sigma Z^2{}_J[J]/\Sigma[J]$ and $a = 1.5/|Z_+Z_-|$

It should be noted that Ψ (equation [4c]) is not rigorously correct. However, the effect of the approximation is negligible, the term involving Ψ being at most a few percent of the other terms.

The advantages of this model are (i) the reduced number of adjustable parameters B_{KJ} and (ii) the possibility for predicting untabulated values of B_{KJ} from individual parameters ($B_{KJ} = B_K + B_J + \delta_K + \delta_J$). Despite that, Bromley has observed good correlations, in the case of single electrolytes, for ionic strength up to 6 m.

1.3. Mass balance equations

The mass balance constraints are applied to the choosen components. For example, with component X we have the following expressions

[5] $$q_X = m[X](\text{or } \overline{v}\overline{[X]}) + m\Sigma x[A_aX_x\ldots H_h] + \overline{v}\Sigma x\,\overline{[A_aX_x\ldots H_h]}$$
$$q_X = m[X](\text{or } \overline{v}\overline{[X]}) + m\Sigma x\beta[A]^a[X]^x\ldots[H]^h + \overline{v}\Sigma x\overline{\beta}[A]^a[X]^x\ldots[H]^h$$

with m = mass of water, kg

$[J]$= molality of J, at equilibrium, moles/kg of water, replaced by $[\overline{J}]$ for organic components.

$\overline{v}$ = volume of the organic phase, dm^3

$[\overline{J}]$= concentration of the organic species J at equilibrium, moles/dm^3

q_X= moles of component X in feed, known from the compositions of the aqueous and organic phases.

The set of the equations [5] makes a non-linear system where [A], [X]...[H] are the unknowns. Its resolution is performed by the Newton method [5] .

THE PROGRAMS

Computer programs have been developed on the basis of equations [1]-[5]for the prediction of the composition of the equilibrated phases (GMODEX program) as well as for the refinement of the unknown parameters of the model (AFFINEX program).
The input data for GMODEX consists essentially in (i) the number of components for the system, the stoichiometric coefficients to define the species in presence and the related thermodynamic stability constants (ii) the interaction parameters B_{JK} which number is reduced by adopting common values and (iii) the mass-balance information (concentrations of the components, mass of water, volume of the organic phase, incrementations to be applied for a curve simulation).
Starting with the thermodynamic constants, GMODEX uses an iterative method : the free concentrations of the components are calculated from the set of equations [5] , and next the concentrational stability constants (equations [2] - [4]) which are returned to the previous step as long as a convergence tolerance is not attained.
AFFINEX program uses a least-squares technique for the refinement of the unknown parameters (β_T, B_{KJ}) from various experimental data. The error-square sum which is minimized is defined by $S = \Sigma (Y_c - Y_e)^2$ which Y_e represents an experimental measurement and Y_c a quantity depending on the unknown parameters. S is minimized with respect to the values of the parameters using an iterative method. The allowed refinement variables Y are (i) any concentration at equilibrium or linear combination of concentrations e.g. the total concentration of a metal in the organic phase (ii) the water activity (iii) the osmotic coefficient and (iv) the distribution coefficient of a component. Moreover their logarithm can also be selected.

EXPERIMENTAL

Tri-iso-octylamine - Sherex commercial compound, marketed as Adogen 381 - was used without further purification. The amine was diluted in an aromatic solvent (Solvesso 150) in the presence of a modifier as 3rd phase suppressor (6) . A 0,4 M amine solution was converted to the hydrochloride form by contacting it with hydrochloric acid

(7). The concentration was determined by potentiometric titration in a water/ethanol mixture.

Aqueous solutions of Co(II), Cu (II), Mn (II) were prepared by dissolving their chlorides in lithium chloride or nickel chloride solutions (analytical reagent grades). All solutions were made by weighing.

The phases of the desired composition were shaken for 30 min., at 25°C ± 0.2°C ; after centrifugation the metal in the organic phase was stripped with diluted perchloric acid. Metal analysis was performed by atomic spectrophotometry or by conventional volumetric analysis.

RESULTS

The model has been tested by means of the AFFINEX program (i) on the distribution data of the cobalt chlorocomplexes in aqueous solution (Fig.1) in order to obtain their stability constants and (ii) on the extraction isotherms of cobalt (Fig.2), copper (Fig.3) and manganese (Fig.4). The species found to give the best fits, their stability constants as the introduced interaction parameters are listed in Table I.

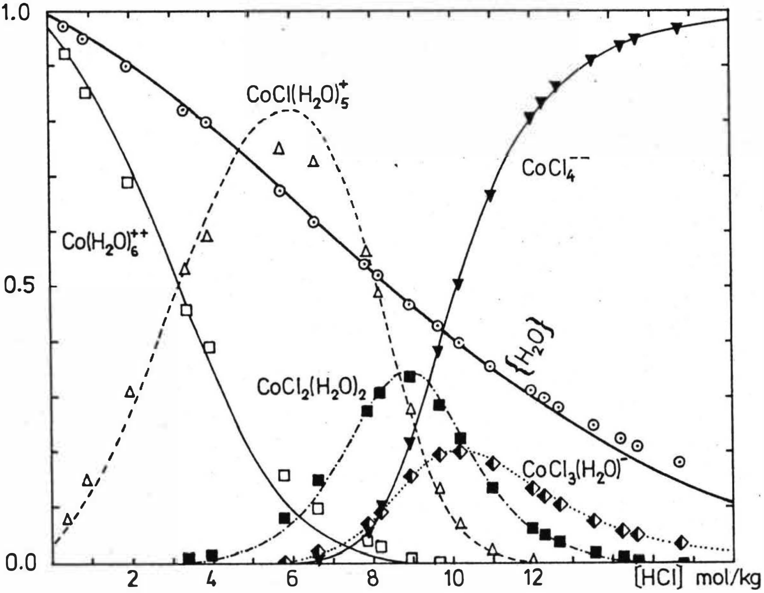

Fig. 1 - Distribution of the indicated cobalt species and water activity $\{H_2O\}$ as a function of HCl molality.

□ △ ■ ◆ ▼ ⊙ Experimental data, from Zeltmann et al. (8)

—— - - - —·—·— ······· Calculated curves, according to our model. Fixed parameters : $B_{H,Cl} = 0.1433$; $B_{Co,Cl} = 0.1016$; refined : $B_{H,CoCl_i} = 0.05$ and β_T (see table IA)

Table I - Parameters for cobalt, copper and manganese extraction by tri-iso-octylammonium chloride (R_3NHCl), at 25°C

Species	$\overline{R_3NHCl,H_2O}$	$M(H_2O)_6^{2+}$	Cl^-	Li^+ or Ni^{2+}	H_2O	log β_T(3 σ)^a		
						Ⓐ M = Co ^{b}	Ⓑ M=Cu ^{c}	Ⓒ M = Mn ^{c}
$M\ Cl(H_2O)_5^+$	0	1	1	0	-1	-0.34	1.20(0.17)	-0.42(0.27)
$M\ Cl_2(H_2O)_4$	0	1	2	0	-2		-0.28(2.3)	
$M\ Cl_2(H_2O)_2$	0	1	2	0	-4	-3.24		-1.95(0.14)
$M\ Cl_3(H_2O)_3^-$	0	1	3	0	-3		-2.29(from 9)	
$M\ Cl_3(H_2O)^-$	0	1	3	0	-5	-6.07		-6.43(from 10)
$M\ Cl_4(H_2O)_2^{--}$	0	1	4	0	-4		-4.5(from 9)	
$M\ Cl_4^{--}$	0	1	4	0	-6	-8.64		
$\overline{(R_3NHCl)M\ Cl_2}$	1	1	2	0	-7	-2.90(0.26)	-0.04(0.68)	
$\overline{(R_3NHCl)_2M\ Cl_2}$	2	1	2	0	-8	-0.87(0.09)	1.79(0.85)	-1.73(0.17)
$\overline{(R_3NHCl)_3M\ Cl_2}$	3	1	2	0	-9	-0.05(0.13)	2.27(0.70)	-0.88(0.14)
$B_{M,Cl}$ (Ref.4)						0.1016	0.0654	0.0869
$B_{Ni,Cl}$ (Ref.4)							0.1039	0.1039
$B_{Li,Cl}$ (Ref.4)						0.1283		
$B_{Ni,\ MCl_n}$ B_{Li,MCl_n}						0.01	0.01	0.01

(a) σ = standard deviation, only for the refined parameters ;(b) from data in LiCl media ; (c) from data in $NiCl_2$ media.

During the refinements, the interaction parameters were fixed at Bromley's values except for $B_{Li,MCln}$, $B_{Ni,MCln}$(M=Co, Cu, Mn), the influence of which is insignificant and which were thus arbitrarily fixed at 0.01. In all cases, it was assumed that interactions between chlorocomplexes and others ions were the same whatever the degree of formation e.g. $B_{Co,Cl} = B_{CoCl,Cl} = B_{CoCl_2,Cl} = B_{Co,CoCl_2} = B_{Co,CoCl_3} = B_{Co,CoCl_4}$. It should be noted that three extractable species are needed to describe the system. The consideration of $\overline{(R_3NHCl)_2MCl_2}$ alone leads to a poor fit (Fig.1). This model is not unreasonable since one could put forward the aggregation of the extractant for $\overline{(R_3NHCl)_3MCl_2}$ and the presence of the modifier for $\overline{(R_3NHCl)MCl_2}$.
The values of Table IB, IC are to be regarded as preliminary results since the β_T of the predominant chlorocomplexes, highly correlated with the $\overline{\beta}_T$ of the extractable species, have been determined simultaneously. The prediction of the extraction of cobalt in $NiCl_2$ media (Fig.2), directly from the LiCl determinations (Table IA) i.e. only by substituting $B_{Ni,Cl}$ = 0.1039 for $B_{Li,Cl}$, could be improved by considering a new value for $B_{Ni,Cl}$, determined in a wide range of ionic strength, i.e. up to 11 m (instead of 6 m).

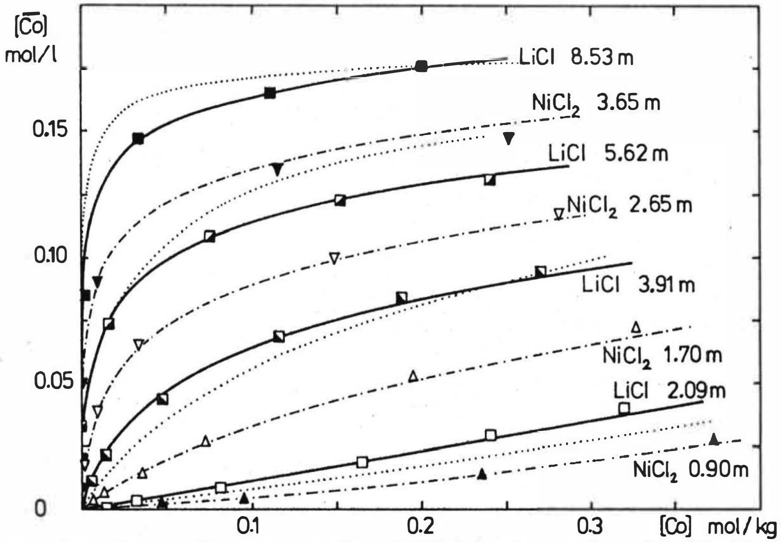

Fig.2 - Extraction isotherms for cobalt by 0.372 M tri-iso-octylammonium chloride LiCl media : ■ ◪ ◩ □ experimental data ——— calculated isotherms, parameters of Table IA ······· calculated isotherms assuming a single extracted species $\overline{(R_3NHCl)_2-CoCl_2}$; $NiCl_2$ media : ▼ ▽ △ ▲ experimental data —·—·—·— predicted isotherms, from the LiCl model of Table IA ($B_{Li,Cl}$ substituted by $B_{Ni,Cl}$ = 0.1039)

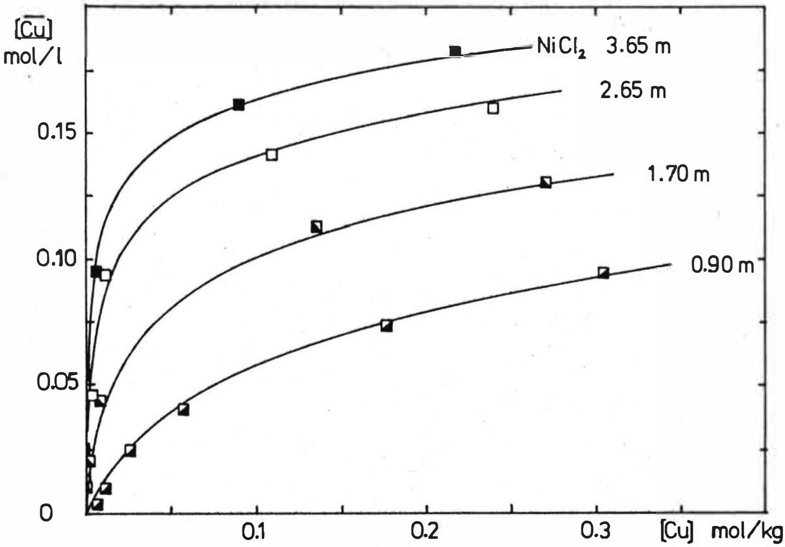

Fig.3 - Experimental and calculated extraction isotherms for copper, from $NiCl_2$ solutions, by 0.385 M tri-iso-octylammonium chloride (parameters of Table IB)

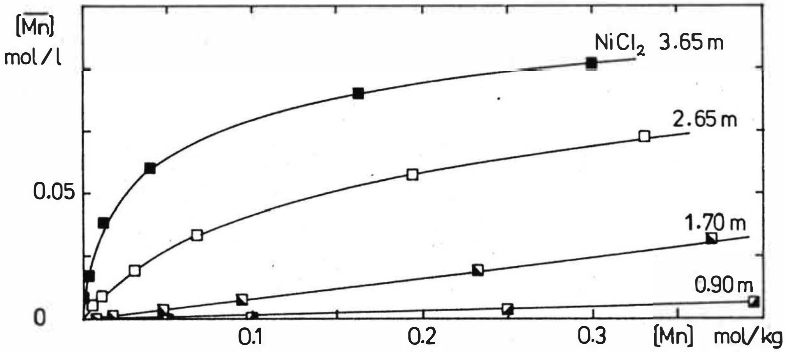

Fig.4 - Experimental and calculated extraction isotherms for manganese, from $NiCl_2$ solutions, by 0.386 M tri-iso-octylammonium chloride (parameters of table IC)

CONCLUSIONS

The proposed model, despite its simplicity, has proved to be quite satisfactory for the analysis and prediction of extraction data. It is planned to extend the activity model by accounting for molecule-molecule interactions. This model is already used for the design of extraction plants (INSTALLEX program, to be published).
As to the extraction mechanism, additional work is in progress in order to consider equilibria - such as the deprotonation, the aggregation or the hydration of the extractant - which have been omited.

ACKNOWLEDGEMENT - To the Agence Française pour la Maîtrise de l'Energie and to Minemet Recherche for financial support.

REFERENCES

(1) C. Forrest, M.A. Hughes, Hydrometallurgy, 1 (1975) 25
(2) D.H. Liem, Acta Chem. Scand., 25 (1971) 1521
D.H. Liem, Proc. Int. Solv. Extr. Conf., Liège, 1980, Vol.1, nbr. 80-142
(3) H. Renon, Found. Comput. Aided Chem. Proc. Des., Proc. Int. Conf., 2 (1980) 53
(4) L.A. Bromley, AIChE Journal, 19 (1973) 313
L.A. Bromley, D. Singh, S. Sridhar, S.M. Read, AIChE Journal, 20 (1974) 326
(5) P.A. Noirot, M. Wozniak, Hydrometallurgy, 13 (1985) 329
(6) C.J. Bouboulis, CIM Special Volume, 21 (1976) 32
(7) L. Newman, P. Klotz, J. Phys. Chem., 65 (1961) 796
(8) A.H. Zeltmann, N.A. Matwiyoff, L.O. Morgan, J. Phys. Chem., 72 (1968) 121
(9) H.C. Helgeson, Am. J. Sciences, 267 (1969) 729
(10) D.F.C. Morris, E.L. Short, J. Chem. Soc, (1961) 5148

To the Theory of the Mutual Influence of Metals in Extraction Systems with Aggregated Extractants

V.V.Bagreev, Yu.A.Zolotov, S.O.Popov, C.Fischer, V.I.Vernadsky Institute of Geochemistry and Analytical Chemistry, USSR Academy of Sciences, Moscow/USSR and The Central Institute of Solid State Physics and Material Research, GDR Academy of Sciences, Dresden/GDR

The salts of tertiary high molecular weight amines and quaternary ammonium bases (QAB) are efficient extractants for isolation of whole number of metals, e.g., of lanthanides and actinides. Normally, these metals are extracted simultaneously from solutions of complex composition. It is, therefore, very important to know how the extraction of one of the components in the aqueous phase affects the recovery of another one, i.e. to study the mutual influence of metals during extraction. In those cases when one of the extracted metals is present in solution in a much higher concentration (macroelement) than another one (microelement) their mutual influence often results in the suppression of the microelement extraction.

Extraction with such extractants as the salts of amines and QAB aggregated in the organic phase leaves an imprint on the individual and the simultaneous extraction of elements. It is clear that the study of the mechanism and the quantitative description of metals extraction supression in these systems required the knowledge of the aggregation and dissociation constants of the organic phase components. One of the most effective approaches, making it possible to solve this problem successfully, can lie in measuring the conductivity, the freezing point, the IR and NMR spectra of extracts.

The aforesaid predetermined the object of the present work, viz.:
- systematic investigation of the structure, stoichiometry, dissociation and aggregation of simple and metal-containing trioctyl- and trioctylalkylammonium (alkyl = CH_3 - C_8H_{17}) compounds in organic solvents, using the cryoscopic, conductometric, IR- and NMR-spectroscopic methods to investigate the extracts;
- using the obtained results to develop the theory of the elements extraction suppression in systems with aggregated extractants and to construct a mathematical model of this phenomenon.

The state of simple and metal-containing trioctyl- and trioctylalkylammonium salts in organic phases.

Solutions of simple nitrate and chloride, as well as lanthanide-, uranyl-, thorium-, iron (III)-, indium- and gallium-containing trioctylalkyl- and trioctylammonium compounds in benzene and nitrobenzene were studied using the methods of cryoscopy, conductometry, IR and NMR spectroscopy. From the data in literature it followed that the aggregation constants (ß) of alkylammonium salts in non polar diluents can be calculated most correctly with the help of the generalized theory of associative equilibriums (GTAE) (1), using experimental data on the thermodynamic activity of the diluent (a_s) in the studied solution. To process the experimental dependences between the equivalent conductivity of solution (Λ) and the concentration of dissolved compound (C_A) and calculate the dissociation constants (K_d) of alkylammonium salts in high-polar diluents the most suitable is the model based on the Fuoss-Onsager theory of electrolyte solutions (2), and in non polar media - various semiempirical relations. It is also fairly simple to calculate the aggregation and dissociation constants of QAB compounds from the data of NMR-spectroscopic study of the extracts.

Using all the above methods we calculated the aggregation constants for the extractants themselves, as well as metal-containing compounds of trioctyl-(TOA), trioctylmethyl- (TOMA), trioctylethyl- (TOEA), trioctylpropyl- (TOPA), trioctylamyl- (TOAA), tetraoctylammonium (TeOA), Aliquat-336, ($R^1_3CH_3N^+Cl^-$ with $R^1 = C_8H_{17} - C_{10}H_{21}$) and trialkylbenzylammonium chloride (TABACl, $R^2_3BzN^+Cl^-$ with $R^2 = C_7H_{15} - C_9H_{19}$ and Bz = benzyl) in benzene and nitrobenzene. Table 1 shows, as an example, the values of dissociation constants for some QAB chloride compounds, calculated with the help of Fuoss-Onsager theory from conductivities data. The conventional methods, however, did not make it possible to determine with sufficient accuracy the aggregation constants of QAB compounds in a high-polar organic solvent and their dissociation constants in a weakly polar one. As we see it, this is a consequence of the fact that correct values of aggregation and dissociation parameters can only be obtained when both these phenomena are simultaneously accounted for. Indeed, the overall concentration of all the forms of dissolved compound in organic phase ΣC_i (i.e. the overall concentration of monomers, dimers and higher multimers, as well as all their ionized forms) essentially depends both on the aggregation and the dissociation processes, this dependence being of the opposite nature. Aggregation decreases ΣC_i, and dissociation increases it. The ΣC_i value, directly or indirectly, enters into the equations of any aggregation or dissociation model. Therefore, if the corresponding constants are calculated without the mutual influence of the dissociative and the aggregative equilibriums being taken into account there is bound to be a systematic error in these calculations. The fact is that the overall concentration of all the forms of dissolved compound, actually existing in solution, is always higher than the ΣC_i value predicted by the aggregation model and is lower than the value predicted by the dissociation model. Therefore, calculations will produce underestimated values of aggregation and dissociation constants.

Table 1

Dissociation constants of QAB compounds in nitrobenzene, calculated with the help of Fuoss-Onsager theory

QAB	Extracted compound	K_d
Aliquat-336	$R_4N^+FeCl_4^-$	$(1.4\pm0.3)\cdot10^{-2}$
	$R_4N^+GaCl_4^-$	$(1.4\pm0.3)\cdot10^{-2}$
	$R_4N^+Cl^-$	$(1.6\pm0.6)\cdot10^{-2}$
TABACl	$R_4N^+FeCl_4^-$	$(8\pm2)\cdot10^{-2}$
	$R_4N^+Cl^-$	$(1.4\pm0.4)\cdot10^{-3}$

We tried to overcome this shortcoming of the GTAE and the Fuoss-Onsager theory models by the using of the common treatment of the data produced by the cryoscopic and the conductometric study of the extracts. Our model was developed with the following assumptions on the possible equilibriums of the organic phase components. Firstly, the stepwise aggregation constants of dissolved compound are equal to one another ($\beta_1 = \beta_2 = \ldots = \beta$). Secondly, all the alkylammonium compounds are dissociating in the organic phase mainly at the first stage with the dissociation constant K_d. And, thirdly, ionized forms of the dissolved compound molecules do not take part in aggregative equilibriums, in other words, the aggregates of QAB compounds can only dissociate according to equation

$$(R_4NB)_j \xrightarrow{K^1} R_4N^+ + B^- + (R_4NB)_{j-1}$$

with the dissociation constant $K^1 = K_\partial / \beta$.

In accordance with these assumptions, the equations of Fuoss-Onsager equations were reduced to the form of

$$\Lambda = \Lambda_0 - S_1(\alpha C_{A1})^{1/2} + E(\alpha C_{A1}) \ln(\alpha C_{A1}) + J_1(\alpha C_{A1}) - J_2(\alpha C_{A1})^{3/2} - \Lambda \alpha C_{A1}^2 f^2/(K_\partial \cdot C_A) \quad (1)$$

$$\log f = - A(\alpha C_{A1})^{1/2}/[1 + \mathring{a} B_1 (\alpha C_{A1})^{1/2}] \quad (2)$$

where Λ_0 is the equivalent conductivity at infinite dilution, C_{A1} is the concentration of the monomeric alkylammonium species present in the solution, α and K_∂ are the dissociation degree and the dissociation constant of the dissolved compound, $\mathring{a}$ is the interionic distance parameter in an ion pair, f is the mean ionic activity coefficient, and S_1, E, J_1, J_2, A and B_1 are numerical coefficients. In their turn, the equations of the GTAE model were transformed by the substitutions $m_A = m_A - \alpha m_{A1}$ and $m_S^1 = m_S + (R_A + 1)\alpha m_{A1}$, m_S, m_A and m_{Aj} are the concentrations of the diluent, alkylammonium salt and its j-meric aggregate, respectively, in molality units, and R_A is the ratio of the molar volumes of the dissolved compound and the solvent.

Thus, within the framework of the proposed aggregation and dissociation common model (ADCM), concentration of the monomeric molecules of alkylammonium salt in solution (C_{A1}) can be calculated in the case of high-polar media from equation

$$C_{A1} = [K_\partial + 2C_A - (K_\partial^2 + 4C_A K_\partial)^{1/2}]/2 \quad (3)$$

and in the case of non polar ones from equation

$$C_{A1} = [1 + 2\beta C_A - (1 + \beta C_A)^{1/2}]/(2\beta^2 C_A) \quad (4)$$

In our opinion, the principle of co-ordinating of the dissociation and aggregation constants of the compounds in organic solutions and the mathematical model developed on its basis make it possible to determine simultaneously these constants both in high- and non-polar solvents, where - as the initial models cannot provide this. The use of ADCM, on the one hand, makes it possible to describe aggregation in systems containing considerable concentrations of the dissociated forms of dissolved compound, and, on the other hand, expands the area of application of the conductivity theory to cover the media of lower polarity. The latter effect is caused by the use of a much smaller C_{A1} value instead of C_A in conductivity equations (1) and (2) making it possible to apply these equations even in the case of benzene solutions.

With the help of ADCM we have calculated the aggregation and dissociation constants for a number of trioctylalkylammonium species in benzene and nitrobenzene. The data obtained are listed in Table 2. Comparison of the β and K_∂ values given in this table with the data calculated using the GTAE and the Fuoss-Onsager models has shown ADCM to produce higher values of aggregation and dissociation constants. This is the very effect expected when the mutual influence of aggregation and dissociation processes was discussed.

Table 2

Aggregation constants (β , kg/mole) and dissociation constants (K_d , mole/l) for QAB compounds in benzene and nitrobenzene, calculated with the help of ADCM*

Cation QAB	Anion	Benzene		Nitrobenzene	
		β	$K_d \cdot 10^5$	β	$K_d \cdot 10^2$
TOMA	NO_3^-	37	5.9	1.8	3.2
TOMA	$Er(NO_3)_5^{2-}$	42	70	3.6	8.4
TOMA	$Th(NO_3)_6^{2-}$	119	87	5.2	0.63
TOMA	$UO_2(NO_3)_4^{2-}$	77	51	4.7	5.0
TOMA	Cl^-	26	0.05	0.7	0.03
TOMA	$FeCl_4^-$	134	226	7.1	120
TOMA	$ErCl_5^{2-}$	36	104	2.2	9.9
TOMA	$UO_2Cl_4^{2-}$	58	59	4.1	6.3
TOMA	$ThCl_6^{2-}$	93	81	5.0	4.4

* Relative error of K_d and β determination is 40%

As a result of calculations it was established that dissociation constants of trioctylalkylammonium compounds with the same anion increase with increasing length of the alkyl radical in the extractant molecule,and aggregation constants decrease in the same direction. It has also been found that dissociation constants of simple and metal-containing QAB compounds differ between one another in chloride systems to a much higher extent than in nitrate systems. Thus, in nitrobenzene the ratio between the dissociation constants of simple and uranium (VI)-containing TOMA compound is equal to 8.6 in the nitrate system and to $1.2 \cdot 10^3$ in the chloride system.

Investigation of the structure and stoichiometry of alkylammonium compounds in solution

The paramagnetic shifts of protons and ^{13}C nuclei of different atomic groups of the trioctylalkylammonium cation were measured in the NMR spectra of the compounds of europium, erbium and ytterbium nitrates and chlorides with TOMA, TOEA, TOBA, TOAA and TeOA nitrates and chlorides in nitrobenzene. The constancy of the ratios between these shifts in the series of the studied lanthanides testified to the absence of Fermi contact interaction contribution to the total nuclei paramagnetic shift value, as well as to the isostructurality of the compounds of different lanthanides with the same QAB cation and to a pseudoaxial symmetry of the investigated compounds in solution.

With the help of McConnel-Robertson equation the cation-anion distances were calculated for ion pairs formed by QAB cation and lanthanide pentanitrate or pentachloride. The main calculation results are summed up in Table 3.

Knowing the geometry of QAB compounds with the lanthanide-containing anion we estimated the possibility of the formation of extracted compounds with a different alkylammonium salt/metal ratio. For this purpose the mean length of the cation alkylchains was calculated using Eiring's equation for the polymethylene chain. The calculations have shown that, for a given geometry of ionic associates, not more that two QAB cations can be easily positioned in the

Table 3

Cation-anion distances in ion pairs formed by trioctylalkylammonium cations with lanthanide pentanitrates and pentachlorides in nitrobenzene

QAB cation	Cation-anion distance (Å)	
	Chloride system	Nitrate system
TOMA	7.3	7.8
TOEA	7.4	7.9
TOPA	7.7	8.1
TOBA	7.7	8.2
TOAA	7.8	8.2
TeOA	7.8	8.2

vicinity of the anion. The insertion of a third and subsequent cations is geometrically impossible. A conclusion can, therefore, be drawn that lanthanide nitrates and chlorides are extracted with OAB slats into the organic phase only in the form of 1:1 and 2:1 compounds.

A similar conclusion for the extraction of metals with TOA salts was made as a result of studying the IR spectra of extracts. It has been shown that iron (III), gallium (III) and indium (III) are extracted with TOA chloride into such solvents as benzene and carbon tetrachloride only as 1:1 and 2:1 compounds of $TOAH^+MeCl_4^-$ and $(TOAH \ldots Cl \ldots HTOA)^+MeCl_4^-$ composition.

Mathematical modelling of extraction suppression

The extraction of the microelements with alkylammonium salts was regarded as being represented by the following set of reactions in the aqueous and the organic phase:

$$R_4NB \xrightarrow{K_A} R_4N^+ + B^-$$

$$n_1 R_4NB + M \xrightarrow{K_{ex}} (R_4N)_{n_1}MB_{n_1}$$

$$R_4NB + (R_4N)_{n_1}MB_{n_1} \xrightarrow{K_S} R_4NB(R_4N)_{n_1}MB_{n_1}$$

.... (5)

$$(R_4NB)_j(R_4N)_{n_1}MB_{n_1} \xrightarrow{j \cdot K_A} R_4N^+ + [(R_4N)_{j-1}B_j(R_4N)_{n_1}MB_{n_1}]^-$$

$$(R_4NB)_j(R_4N)_{n_1}MB_{n_1} \xrightarrow{j \cdot K_A} [(R_4N)_jB_{j-1}(R_4N)_{n_1}MB_{n_1}]^+ + B^-$$

$$(R_4NB)_j(R_4N)_{n_1}MB_{n_1} \xrightarrow{K_M} R_4N^+ + [(R_4NB)_j(R_4N)_{n_1-1}MB_{n_1}]^-$$

where K_{ex} is the extraction constant, M is the extracted form of the metal in the aqueous phase, K_S are the stepwise **solvation** constants, K_A is the dissociation constant of the extractant, and K_M is the dissociation constant of the metal-containing compound of microelement in the organic phase. As it follows from the data of the NMR- and IR-spectroscopic study of the extracts, n_1 in equations (5) in all probability does not exceed two. Taking into account the fact that the dipole moment of 2:1 alkylammonium compounds is not large and is always smaller than that of the corresponding simple alkylammonium salt, one can take $K_S = \beta$, where β is the aggregation constant for the simple salt in the same organic solvent. Then, from the set of equations (5) the following expression can be obtained for the degree of extraction supression with respect to the trace of a metal:

$$S = \frac{[R_4NB]_1^{n_1}(1-\beta_2 C_{A1,2})\left[1+K_M[R_4N^+]_1^{-1}+K_A(1-\beta_1 C_{A1,1})^{-1}([R_4N^+]_1+[B^-]_1)\right]}{[R_4NB]_2^{n_1}(1-\beta_1 C_{A1,1})\left[1+K_M[R_4N^+]_2^{-1}+K_A(1-\beta_2 C_{A1,2})^{-1}([R_4N^+]_2+[B^-]_2)\right]} \qquad (6)$$

where $[R_4N^+]+[B^-] = (K_A[R_4NB]+[R_4N^+]^2)(K_A[R_4NB][R_4N^+])^{-1}$, and $[R_4N^+]$ can be calculated from equation

$$[R_4N^+]^4+2K_{M'}[R_4N^+]^3+(K_{M'}^2-K_{M'}C_{M',0}-C_AK_A+n_2C_{M',0}\cdot K_A)[R_4N^+]^2-$$

$$(C_{M',0}\cdot K_{M'}^2+2C_AK_AK_{M'}-(n_2+1)C_{M',0}K_AK_{M'})[R_4N^+]+K_AK_{M'}(C_{M',0}-C_A)=0 \qquad (7)$$

or, for K_A, $K_{M'} < 10^{-3}$, from equation

$$[R_4N^+] = (K_{M'}C_{M',0}+K_AC_A-n_2K_AC_{M',0})^{1/2} \qquad (8)$$

The value of C_{A1} in equation (6) was determined from the following relationship

$$C_{A1}^2(C'_A\beta^2-C'_{M',0}\beta^2)-C_{A1}(1+2\beta C'_A-3C'_{M',0}\beta)+C'_A-2C'_{M',0}=0 \qquad (9)$$

Here $C_{M',0}$ is the analytical concentration of the trace element in the organic phase and $[M'^-]$ is the concentration of its dissociated form n_2 is the stoichoimetric coefficient in the extraction equation for the macroelement,

$$C'_A = C_A[R_4N^+]+(n_2-1)[M'^-], \quad C'_{M',0} = C_{M',0}-[M'^-]$$

Analysis of equation (6) has shown that, in accordance with the previously studied regularities of the extraction suppression of microelements, the degree of this suppression increases with increasing alkylammonium "common ion" concentration and with increasing macroelement concentration and its dissociation constant in the organic phase ($K_{M'}$). Some results of calculating from this equation the degree of suppression for the extraction of erbium traces in the presence of uranium (VI) or thorium are shown in Table 4. A satisfactory correspondence between the theoretical and the experimental S values is seen to have been obtained.

Table 4

Theoretical calculation of the degree of erbium extraction suppression in the presence of thorium or uranium (VI) in the joint extraction of metals with 0.2 M TOMA chloride and nitrate solutions in benzene

$C_{M'}$, M	$[R_4N^+]$, M	C_{A1}, M	log S_{Er}	
			from eq.(6)	experiment
	Thorium nitrate			
0	0.00344	0.0187	0	0
0.01	0.00327	0.0179	0.13	0.14
0.05	0.00253	0.0132	0.81	0.82
	Uranyl nitrate			
0	0.00344	0.0187	0	0
0.01	0.00390	0.0179	0.14	0.14
0.05	0.00543	0.0135	0.83	0.84
	Thorium chloride			
0	0.00029	0.0249	0	0
0.01	0.00248	0.0239	0.63	0.69
0.05	0.00598	0.0178	1.37	1.40
	Uranyl chloride			
0.01	0.00217	0.0239	0.61	0.69
0.05	0.00515	0.0178	1.37	1.44

Equation (8) allows us to draw a very important conclusion on the possibility of the "common ion" mechanism existence itself in a concrete extraction system. According to this mechanism, the extraction suppression occurs because during the macroelement dissociation in the organic phase a "common ion" - alkylammonium cation is formed, which, in accordance with the mass action law, shifts the microelement extraction equilibrium and reduces its distribution coefficient. If expression C_M ($K_{M'} - K_A n_2$) in equation (8) is less than or equal to zero, i.e. $K_{M'} \leqslant n_2 K_A$, an increase in the macroelement concentration in the organic phase will not lead to the growth of the concentration of alkylammonium cations. Therefore, neither will there exist any precondition for the "common ion" mechanism to be actualized. For a more extended expression (7) this conclusion is not so obvious, but it was verified and proved by numerical methods to be valid in this case too.

It has been previously established by us (3) that in a nitrate extraction system with a **trialkylmethylammonium** salt the lanthanides extraction suppression occurs only as a result of a simple competition of the macro- and the microelement for the extractant, even in high-polarity organic solvents. This phenomenon has now found its explanation. Indeed, in nitrate systems (see Table 1) the difference between the K_A and $K_{M'}$ values is not sufficiently high to cause a noticeable change in the concentration of alkylammonium cations with the growing macroelement concentration. It is for this very reason that suppression of the extraction of lanthanides traces in a nitrate system is mainly determined by "extractant shortage" and in a chloride system - by a greater differentiation between the dissociation constants of compounds in the organic phase, i.e. the "common ion" mechanism.

References

1. Ye.V.Komarov, A.A.Kopyrin, V.V.Proyaev. Teor.i Eksperim. Khimiya, 14, 620(1981).

2. W.Linert, P.Rechberger. Comput. and Chem., 6,101(1982).

3. S.O.Popov, V.V.Bagreyev, Yu.A.Zolotov. Zh.Neorgan.Khimii, 27, 2628(1982).

Interfacial Phenomena of Liquid-Liquid Systems Under Electric, Magnetic and Gravitational Fields

V. Mohan*, P. Jayasankar and K. Padmanabhan**

*Department of Chemical Engineering,
A.C. College of Technology, Anna University, Madras 600 025, India.

**Central Instrumentation Laboratory, University of Madras,
Madras 600 025, India.

1. Interfacial electrostatic force: Let V' is the voltage applied to the electrodes in a cell shown in Figure 1. The electrostatic pressure acting on the interface [1] between the two liquids is equal to

$$P_e = \frac{1}{2} \frac{D^2}{\epsilon_0} \left(\frac{1}{\epsilon_2} - \frac{1}{\epsilon_1}\right) \qquad \ldots (1)$$

where $D = \epsilon_0 \epsilon_1 E_1 = \epsilon_0 \epsilon_2 E_2$ ... (2)

Here D denotes (the dielectric flux density) in coulomb/m^2,
ϵ_0 - permittivity of free space F/m,
ϵ - dielectric constant.

The pressure, P_e on the interface will be either positive or negative depending upon whether ϵ_1 is greater or less than ϵ_2. If the lower liquid, that is the denser one, has a higher dielectric constant, then P_e becomes positive. Hence there is an upward force and the interface appears to move down, that is, in the opposite direction. For example, in the mixing setup for benzene and nitrobenzene the interface moves down because the heavier liquid, namely, nitrobenzene, has a higher dielectric constant ($\epsilon_1 > \epsilon_2$). In the case of a denser liquid having a lower dielectric constant than its mixing counter-part the value of P_e becomes negative ($\epsilon_1 < \epsilon_2$) and the force is downwards or the interface appears to move upward.

2. Interfacial magnetic force: Let a vector magnetic potential, A, be applied to the fluids in a cell shown in Figure 1. The magnetic pressure on the interface [2] will be equal to

$$P_m = \frac{1}{2} \mu_0 [\mu_2 H_2^2 - \mu_1 H_1^2] \qquad \ldots (3)$$

where P_m - interfacial magnetic pressure in N/m^2

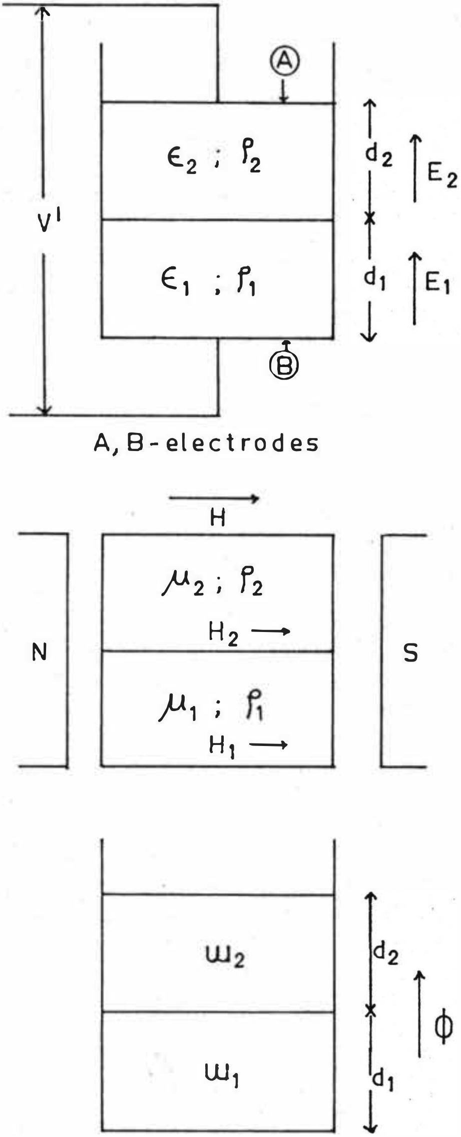
A
V'
ϵ_2 ; ρ_2
ϵ_1 ; ρ_1
d_2
d_1
E_2
E_1
B
A, B-electrodes
H
N
S
μ_2 ; ρ_2
H_2
μ_1 ; ρ_1
H_1
ω_2
ω_1
d_2
d_1
ϕ

Figure.1. Schematic diagram of the cell

μ_o - permeability of free space in rationalised system of units (the value of $\mu_o = 4\pi \times 10^{-7}$ web/amp.m)

μ_1, μ_2 - are the relative permeabilities of the phases 1 and 2 respectively

H_1, H_2 - are the magnetic field intensities of the phases 1 and 2 respectively (in amp/m).

The pressure, P_m on the interface will be either positive or negative depending upon whether μ_2 is greater or less than μ_1 (considering an hypothetical situation where $H_1 = H_2 = H$). If the lower liquid, that is the denser one, has a lower relative permeability (μ_1), then P_m becomes positive. Hence there is a downward force and the interface will appear to move up, that is, in the opposite direction. If the top liquid, that is, the lighter one has a lower relative permeability, (μ_2), then P_m becomes negative. Hence there is an upward force and the interface will appear to move downwards, that is, in opposite direction.

3. Interfacial gravitational force: Consider the two liquids in the cell shown in Figure 1, placed in a gravitational potential ϕ (J/kg). The gravitational pressure on the interface [3] is equal to

$$P_g = \phi(w_1 - w_2) \qquad \ldots \quad (4)$$

where w_1 , w_2 are mass per unit volume.

The pressure, P_g , on the interface will be either positive or negative depending upon whether w_2 is less or greater than w_1 . If the lower liquid has a higher mass per unit volume (w_1), then, P_g becomes positive. Hence there is an upward force and the interface will appear to move down, that is, in the opposite direction. In the case when w_1 is less than w_2 , then P_g becomes negative and the force is upwards or the interface will appear to move upward.

4. Comparison of forces: As an example, electrostatic pressure for the system benzene and nitrobenzene is calculated for an applied voltage of 5000 Volts for phase thickness of 0.01 m each, and found to be equal to 2.076 N/m^2. The interfacial magnetic pressure, P_m (N/m^2) is calculated at a particular field intensity H (H = 8×10^5 A/M) for the system Benzene - Nitrobenzene is found to be

- 0.12587 N/m^2 (negative indicates upward force). Similarly one can calculate interfacial gravitational pressure. The minimum pressure, P_{min}, required for bubble formation (for a gravitational field change from 0 to 9.81 m/sec^2) for benzene - water is found to be 7.65 $kg/m\ sec^2$.

Conclusion:

The contribution of a superimposed field to the mobility and to the orientation can result in altered transport rates. Interfacial force can be made use off for enhancement in mass transfer rates and for the super imposition of electric field, the enhancement of rates are found to be of the order of ten times for most systems and for viscous systems, sometimes, the order of enhancement was sixty times [4]. Similarly one can make use of magnetic and gravitational fields for enhancement of rates and better control of transport processes and in hydro-metallurgy and for unit operations in space-labs which can result in considerable reduction in size of contacting equipments.

References:

[1] V. Mohan, K. Padmanabhan and K. Chandrasekharan, Adv. Space. Res., 3, No. 5, 177, 1983.

[2] S. Ganeshmurthy, Thermodynamics of fluids under applied field conditions, M.Tech. Thesis, Anna University, 1984.

[3] K. Ravinder, Fluid systems under gravitational field, M.Tech. Thesis, Anna University, 1985.

[4] K. Chandrasekharan, P.R. Madhavan, K. Padmanabhan and V. Mohan, Paper No. H2-23, Microfilms, CHISA'78, Praha, Czechoslovakia.

- * -

Interfacial transfer under electrostatic field in solvent extraction

M. Hund, F. Lancelot, Saint-Etienne, France.

Abstract

Electric field may be applied to the realization of liquid-liquid contactors in which mixing and phase separation are caused by electrostatic effects. Thus changes in mass transfer coefficients are promoted by charged species orientation due to electrostatic forces or by interfacial turbulence motions.

We studied the mass transfer in a suitable device : a modified Lewis cell in which the electric field is applied perpendiculary to the plane interface between two immiscible fluids. We used different systems (ternary systems with or without reaction) and pointed out the result of electrostatic forces combined or not with hydrodynamic phenomena.

Introduction

When a liquid-liquid interface is submitted to an electrostatic field, droplets can desingrate if it is spherical and instabilities can appear if it is plane. We aimed to observe, particulary, transfer across plane interface. Many workers(1-4) were interested in the study of field-induced instabilities in small-size cell without stirring. They, thus, established an instability criteria dependent to phase density difference, to interfacial tension and to no-conducting fluid permittivity. Likewise, interfacial tension changes have been studied only for isolated drop(5,6). Mass transfer has not been yet considered.

We have, therefore, imagined a cell(7) to study the electric field action on mass transfer for ternary systems with and without reaction. We will see that electrostatic forces act, in the way, on interfacial hydrodynamic and on molecule orientation which increases or decreases interfacial reaction (8-10).

Experimental

To study electrostatic field influence on mass transfer, we had to modify the plane interface cell called as "Lewis cell"(11,12). This modified cell, described in fig. 1, allows :

- correct phase homogenization
- good hydrodynamic control
- possibility of kinetic control for a long time
- parameters regulation (pH, temperature, ...)

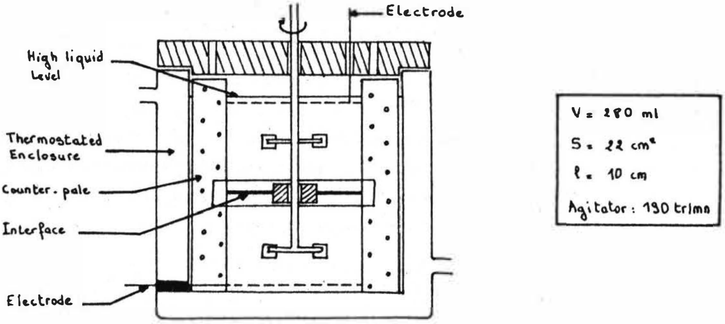
Electrode
High liquid Level
Thermostated Enclosure
Counter. pale
Interface
Electrode
V = 280 ml
S = 22 cm²
l = 10 cm
Agitator : 190 tr/mn

Figure 1 - *modified Lewis cell*(7) *for application of an electrostatic field.*

Electrodes are connected to an E.H.T. power supply (Brandenburg, 0.30 kV, 1mA).

In our study conditions, flux(7,13) can be expressed in terms of diffusion coefficient D, concentration at the interface c_i and in the phase c_b, and hydrodynamic layer depth L by :

$$N_A = \frac{D_A}{L} (c_i - c_b) = k_A (c_i - c_b) \qquad [1]$$

$$\text{as by } N_A = \frac{V}{S} \frac{dc_b}{dt} \qquad [2]$$

Arranging formula [1] and [2], we can calculate mass transfer flux and transfer coefficient for the applied voltages from molar concentration measurement in the phases.

Results

System I : Cu/LIX 65 N(7)

We, first, studied a ternary system with complexation reaction, where copper is transferred from aqueous to organic phase.

Aqueous phase : $CuCl_2$ 0.1N in NaCl 2M at pH = 1.5

Organic phase : LIX 65 N (called RH) at 30 % in ESCAID 110 (sort of kerosene).

The interfacial tension, without voltage, is about 13 dyn/cm. The involved reaction is :

$$Cu^{2+} + 2\,\overline{RH} \rightleftarrows \overline{CuR_2} + 2H^+$$

Copper concentration evolution in the organic phase was followed by sampling diluted with ethanol and titrated by atomic absorption spectroscopy and is shown in fig. 2.

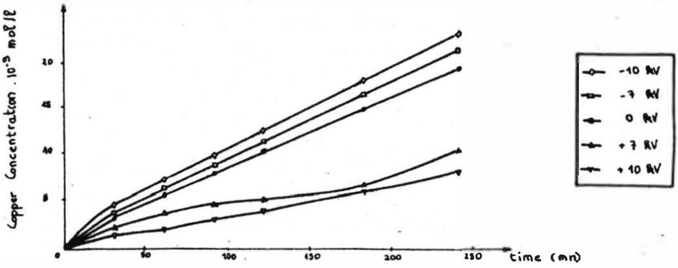

Figure 2 - organic phase copper concentration (.10^{-3} mol/l) versus time and voltage.

Results in terms of fluxes and transfer coefficients are given in tab. 1.

Voltage (kV)	Initial Flux x10^{-9}mol/cm.s		Transfer coefficient x10^{-5} cm/s
0	18.3	---	5.98
+ 7	16.0	- 14 %	2.42
- 7	20.4	+ 10 %	7.00
+10	11.4	- 61 %	2.04
-10	24,5	+ 25 %	7.89

Table 1 - Calculated fluxes and transfer coefficients for different applied voltages.

These curves show some differences according to the field polarity : for positive voltages, the evolution is slower than for zero or negative voltages. Thus transfer is increased by a negative electric field and decreased by a positive one.

More we have to remark that whatever the field intensity may be, no interfacial deformation occurs during experiments.

System II : nitric acid/rare earth

In a second time, we studied a ternary system with ion exchange, where a rare earth is transferredfrom organic to aqueous phase.
Aqueous phase : HNO_3, 6N
Organic phase : Kerosene + Organic Acid + Rare Earth (called S).
The value of interfacial tension, without electric field, is 18.4 dyn/cm. The involved reaction is :

$$\overline{R_3S} + 3H^+ \rightleftarrows 3\ \overline{RH} + S^{3+}$$

Rare earth concentration evolution in the aqueous phase was followed by sampling diluted with nitric acid and titrated in U.V. spectrophotometry and is presented on fig. 3.

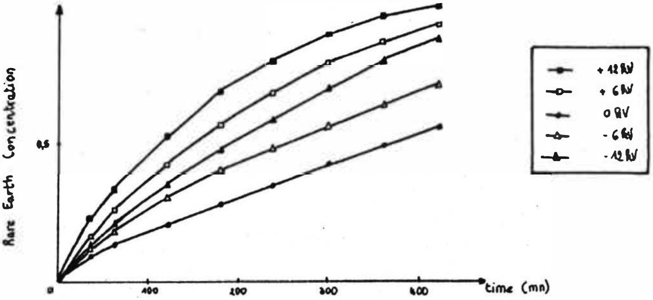

Figure 3 - aqueous phase rare earth concentration versus time and voltage.

Results in terms of fluxes and transfer coefficients are given in tab. 2.

Voltage (kV)	Initial Flux 10^{-9} mol/cm.s		Transfer Coefficient 10^{-5} cm/s
0	6.6	---	2.42
- 6	7.8	+ 15 %	3.82
+ 6	9.3	+ 29 %	5.35
-12	9.2	+ 28 %	4.33
+12	16.6	+ 60 %	8.40

Table 2 - Calculated fluxes and transfer coefficients for different applied voltages.

These curves show that transfer is enhanced by applying an electrid field and this better for positive voltage than for negative one, and, in each case, increasing with the intensity. More we had to notice some turbulence occurency when the voltage increases.

System III : Acetic Acid/TBP in dodecane

Finally we studied a ternary system without reaction. Acetic acid is transferred towards the organic phase, where tri-butyl-phosphate (TBP) can act as a Lewis base.

Aqueous phase : CH_3 COOH 0.5N

Organic phase : TBP in dodecane at different percentage (15, 20 and 25). The value of the interfacial tension, without electric field, is about 9.3 dyn/cm for 15 % TBP, 8.5 dyn/cm for 20 % TBP and 7.3 dyn/cm for 25 % TBP.

occurency and its influence is equivalent to the electrostatic one.

For the system III (CH_3 COOH/dodecane + TBP), we only needed electrohydrodynamic phenomena to explain transfer coefficient increasing, these turbulences are surely linked with field-induced changes to interfacial tension.

We sumed up the electrostatic effects on the studied systems in tab. 4

	Electrostatic Force	Electrohydrodynamic phenomena
System I (Cu/LIX 65N)	1	0
System II HNO_3/Rare Earth	1/2	1/2
System III CH_3COOH/dodecane + TBP	0	1

0 = no effect
1 = main effect
1/2 = combined effect

Table 4 - Action of an electric field on some systems

In the same way, results exponation in term of flux agrees entirely with previous interpretation as you can see it on fig. 5.

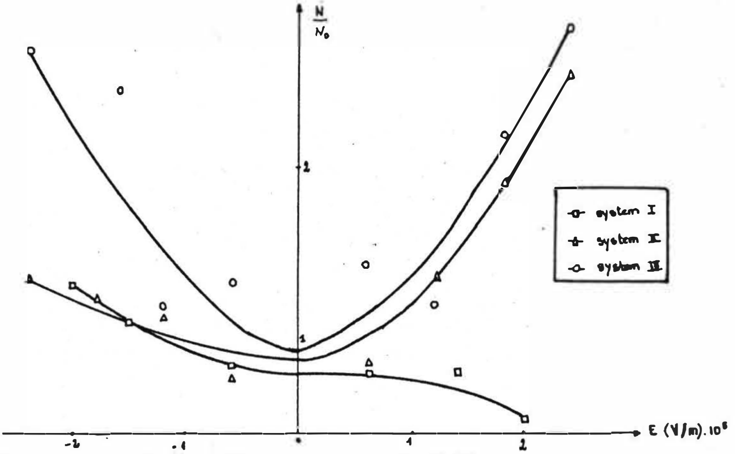

Figure 5 - Standardized Flux versus electric field.

For the system I, the curve is dissymmetrical and decreasing from negative polarities to positive ones. For the system III, the curve is rather symmetrical and increasing when the voltage increases in absolute value. On the other hand for the system II, it behaves as the system I for negative voltages (electrostatic effect :

Acid concentration evoluting in organic phase was followed by sampling analysed by acid-base titration and is shown on fig. 4.

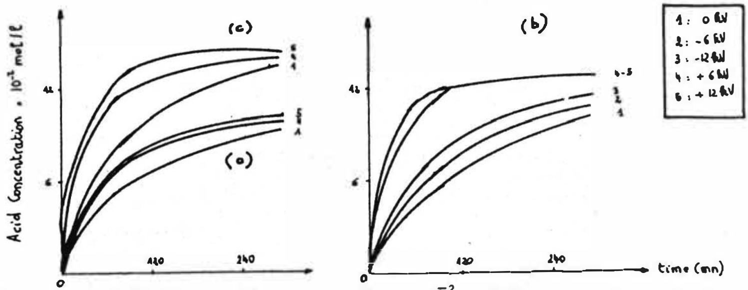

Figure 4 - organic phase acid concentration ($\times 10^{-2}$ mol/l) versus time and voltage:
(a) with 15 % TBP (b) with 20 % TBP (c) with 25 % TBP

Results in terms of fluxes and transfer coefficients are given in tab. 3.

Voltage (kV)	15 % TBP in dodecane			20 % TBP in dodecane			25 % TBP in dodecane		
	Initial Flux 10^{-9} mol/cm.s		Transfer Coef. 10^{-5} cm/s	Initial Flux 10^{-9} mol/cm.s		Transfer Coef. 10^{-5} cm/s	Initial Flux 10^{-9} mol/cm.s		Transfer Coef. 10^{-5} cm/s
0	3.61	---	13.2	3.45	---	6.9	4.98	---	18.9
- 6	....	....	....	4.19	+ 18 %	9.2	....	....	....
+ 6	4.46	+ 19 %	23.0	4.35	+ 21 %	20.4	7.69	+ 35%	26.5
-12	....	....	....	9.12	+ 62 %	34.5	....	....	....
+12	6.26	+ 42 %	23.7	9.50	+ 64 %	56.3	10.81	+ 54%	37.2

Table 3 - Calculated fluxes and transfer coefficients for different applied voltages

These curves show that transfer is electrically enhanced and dependent only to field intensity. For low voltages, we notice a weak increase and for higher ones, we see a strong increase, in the same time turbulences appear.

Discussion

If we consider the whole results dealing with the electric field effect on transfer across a plane interface, we point out electrostatic effect and/or electrohydrodynamic phenomena according to the system.

For the system I (Cu/LIX 65N), we supposed that charged molecules are oriented under the field influence (the involved ion during limiting stage acts as a dipole). Therefore, transfer is promoted by electrostatic forces. For the system II (HNO_3/rare earth), molecule orientation is unsufficient to explain mass transfer coefficient changes (the exchange stage is too quick to allow orientation). On the other hand, an electrohydrodynamic phenomena is added dealing with turbulence molecule orientation) and as the system III for positive voltages (electrohydrodynamic phenomenon : decreasing in interfacial tension).

A more complete study is in progress allowing to establish the electric field intensity at a liquid-liquid phase plane interface taking account of various parameters as density, interfacial tension, permittivity and so on.

As a conclusion, the fig. 5 sums up the transfer behavior under an electric field : predominance of electrostatic forces with polarity influence (charged species orientation) or of electrohydrodynamic phenomena with a symmetrical shape (changes in interfacial tension) and the intermediate case where the both previous effects are in competition.

Notation

c_i, c_b = molar concentration respectively at interface or in the bulk (mol/l).
D_A = diffusion coefficient of specy A (cm^2/s)
E = electric field (V/m)
k_A = transfer coefficient of A (cm/s)
L = hydrodynamic layer depth (m)
l = distance between the electrodes in the cell (m)
N_A = flux of A ($mol/cm^2.s$)
N_o = flux without voltage ($mol/cm^2.s$)
S = interfacial area of the cell (cm^2)
V = phase volume (cm^3)
ΔV = electric voltage (V)

References

(1) - J.R. Melcher and C.V. Smith, Phys. Fluids, 12 (4), 778, (1969)
(2) - G.I. Taylor and A.D. Mc Ewan, J. Fluid Mech., 22 (1), 1, (1965)
(3) - H. Terasawa, Y.H. Mori and K. Komotori, Chem. Eng. Sci., 38 (4), 567, (1983)
(4) - J.R. Melcher and G.I. Taylor, Ann. Rev. Fluid. Mech., 1, 111, (1969)
(5) - P.V.R. Iyer and H. Sawistowski, Proc. Intern. Solvent Ext. Conf., 2, 1029, (1974)
(6) - G. Poisson-Auffrere, Thesis, E.N.S.M., Saint-Etienne, (1980)
(7) - C. Fombarlet, Thesis, E.N.S.M., Saint-Etienne, (1984)
(8) - B.O. Holland, ISEC Funda, 5 (2), 204, (1966)
(9) - M. Kalbasi, Ph. D. Thesis, University of Newcastle upon Tyne, (1980)
(10)- P.J. Bailes and I. Wade, Proc. Intern. Solvent Ext. Conf., 1 (2B), 196,(1980)
(11)- L.J. Austin, L. Banczyk and H. Sawistowski, Chem. Eng. Sci., 26, 2120, (1977)
(12)- A. Kamen, Thesis, E.N.S.M., Paris, (1983)
(13)- T. Kikindai and J. Morel, C.E.A. Report, R-3718, (1969).

Amine Phase Partitioning Using Emulsion Liquid Membranes

A. Kirkkopru[1], R. D. Noble[1], and A. L. Bunge[2]

[1] National Bureau of Standards
Center for Chemical Engineering 773.1
Boulder, CO 80303, USA

[2] Colorado School of Mines
Chemical Engineering and Petroleum Refining Dept.
Golder, CO 80401, USA

Introduction

Emulsion liquid membranes (ELMs) have been studied as a method for organics removal from aqueous streams. Amines have been used as model compounds in these studies (1-3).

Accurate measurement of amine partitioning between the aqueous and organic phase is an important consideration in accurately determining the amine extraction rate. In some cases, the partition coefficients measured using ELMs appear to be different from those measured using the nonemulsion system. Some previous results have suggested that interfacial adsorption may occur in ELM sysems (1). A new measurement technique using ELMs was developed to accurately determine the partition coefficient under extraction conditions.

All the experiments that were performed can be divided into two parts:

1. Experiments which were performed to observe the change in decomposition of aromatic amine solutions due to mixing, lighting, and aeration effects. Aromatic amines are known to be easily oxidized by air.
2. Bulk phase partition coefficient (K_{bm}) experiments using emulsion liquid membranes. Amines are dissolved in the continuous aqueous phase and the partitioning is studied as a function of various amounts of internal phase volume in the emulsion liquid membrane.

Decomposition Experiments

One liter of amine solution (255-260 ppm) was placed in a two liter glass reaction vessel. Mixing was performed at 500 rpm using an electric mixer with a 5.08 cm (2 in.) diameter turbine impeller. To determine the effects of the various parameters on amine decomposition, the following experimental conditions were used:

Mixed vs. Unmixed: Stirring at 500 rpm vs. unstirred.
Uncovered vs. Covered: Exposure to light vs. light blocked by covering the vessel with aluminum foil.
Open vs. Closed: Exposure to air vs. covering vessel top to block air entry.

Figure 1 shows the results for aniline. The results indicate that it is critical to keep the system free of oxygen. The results also show the amine oxidation is catalyzed by light. Mixing can affect the decomposition by continuously supplying oxygen to the solution.

The reason that the above results are important is that typical partition experiments are mixed and exposed to light. The change in concentration is monitored until a equilibrium value is attained. For these systems, the traditional approach would produce a erroneous result due to the slow oxidation.

Bulk Phase Partition Experiments

It was decided to perform the partition experiments using the continuous phase and emulsion liquid membranes containing various amounts of internal phase. By varying the fraction of internal phase, any partitioning due to interfacial absorption could be observed. This variation is measured by

$$\frac{1-f_m}{f_m} = \frac{\text{internal volume fraction}}{\text{membrane volume fraction}} \tag{1}$$

Figure 2 shows a typical result for aniline. There is a rapid change in aniline concentration followed by a slow decline. This slow decline approximately parallels the decline due to decomposition. Therefore, the partitioning was measured using the rapid change value.

Table 1 shows the results for p-toluidine. These results show that K_{bm} is essentially constant and there is little or no effect of interfacial adsorption on partitioning for this system.

Conclusions

Accurate determination of organic extraction using emulsion liquid membranes requires measurement of partition coefficient under extraction conditions. Effects due to chemical reaction and/or interfacial adsorption have to be taken into account or the result can be in serious error.

REFERENCES

(1) Baird, R. S., A. L. Bunge and R. D. Noble, "Batch Extraction of Amines Using Emulsion Liquid Membranes: Importance of Reaction Reversibility," AIChE J., in press.

(2) Teramoto, M., H. Takihana, M. Shibutani, T. Yuasa, Y. Miyake and H. Teranishi, "Extraction of Amine by W/O/W Emulsion System," J. Chem. Eng. Jpn., 14, 122, 1981.

(3) Teramoto, M., H. Takihana, M. Shibutani, T. Yuasa, and N. Hara, "Extraction of Phenol and Cresol by Liquid Surfactant Membrane," Sep. Sci. Tech., 18, 397, 1983.

$\frac{1-f_m}{f_m}$	$K_{bm} = \frac{\text{organic phase con.}}{\text{aqueous phase con.}}$
0	2.454
	2.484
.25	2.675
	2.671
.50	2.478
	2.388
.75	2.518
	2.541
1.0	2.187
	2.369

Table 1: Partition coefficient for p-toluidine.

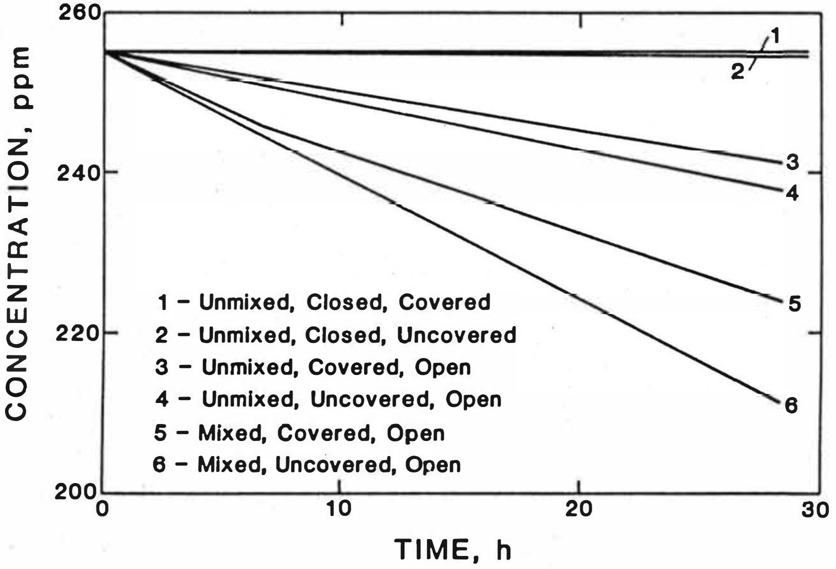

Fig. 1: Aniline concentration in reactor (no emulsion present).

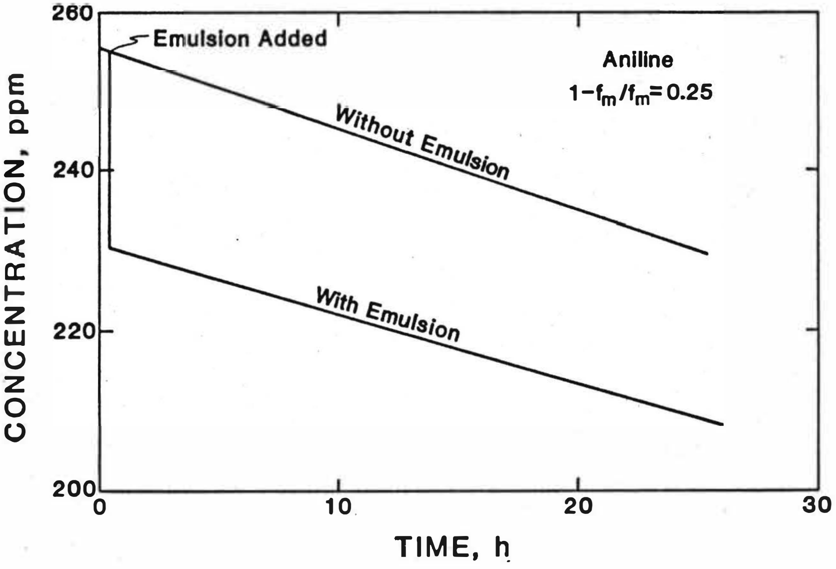

Fig. 2: Aniline concentration in reactor (with/without emulsion present).

Liquid Membranes

Challenges and Progress in Ion Selection and Transport Systems

O. Kedem, A. Warshawsky, Rehovot/IL

An ideal solubility membrane would combine separation principles of extraction and of membrane transport, achieving a synergisitc effect. It became apparent at a very early stage that it is impossible to combine even the basic advantages of membrane technology, viz. stability and a unified extraction/stripping step without substantially loosing either the specificity or the rate of extraction. The supported liquid membranes preserve the selectivity and fast diffusion characterizing the solvent. At the same time they impart to the process the compact transfer from one aqueous phase to the other, characteristic to membranes, sacrificing the mechanical and chemical stability of normal polymeric membranes. The liquid membranes, comprising double emulsions, are one more step closer to conventional extraction and require a step analogous to stripping. To take advantage of the small volume of solvent, highly specific and effective extraction agents, like crown-ethers are currently introduced.

In hydrometallurgic separation synergistic extractants are often effective. For incorporation into liquid membranes bifunctional extractants incorporating the elements of the synergistic structure must be designed and developed.

The principles of extraction can contribute to membrane technology by a different route: combine the selectivity of defined sites in the membrane with a selective solvation effect of the total polymer matrix. Such a case is an anion exchange membrane using preferred uptake of one ion to achieve discrimination between univalent anions.

Supported Liquid Membranes in 1986: New Technology or Scientific Curiosity?*

Pier Roberto Danesi[a]

Chemistry Division, Argonne National Laboratory, Argonne, IL 60439, U.S.A.

Thin layers of organic solutions of solvent extraction reagents (membrane carriers), immobilized on microporous inert supports and interposed between two aqueous solutions (feed and strip), were first proposed more than two decades ago as a new and promising technique for separating and concentrating metal species. Such immobilized layers, representing supported liquid membranes (SLM), have been extensively studied by our group during the last six years (1) mainly for their ability to separate and concentrate metal ions of critical and strategic importance and of relevance to the nuclear industry. In this presentation the major results obtained by our group up to 1986 in the field of SLM's are summarized. A brief indication of the major problems to be addressed to implement SLM's as a new separation technology is also given.

SLM's are an attractive alternative to traditional solvent extraction processes since, at least in principle, represent a simple approach to metal separation, purification and recovery. This is particularly true when dealing with dilute solutions. Figure 1A schematically shows a comparison between the two techniques. Although the combination of extraction, stripping and solvent regeneration in a single stage is one of the attractive features of SLM separations, the absence of a scrubbing section and difficulties in multistaging SLM processes represent a drawback for their utilization. The use of highly selective extractants as membrane carriers is therefore necessary to overcome these limitations. Hopefully, research efforts aimed at the synthesis of new, selective organic extractants will be beneficial for SLM's as well. As far as limitations in the overall membrane area available for the mass transfer process are concerned, they have been removed by the advent of hollow-fiber SLM modules. They can contain up to several thousand fibers, permitting membrane packaging densities as high as 1000 m^2/m^3. A schematic description of a hollow-fiber SLM module, operated in a recycling mode, is shown in Figure 1B. It has to be observed that with these modules feed to strip volume ratios as large as 100 can be easily used.

---

*Work performed under the auspices of the U.S. Department of Energy under contract number W-31-109-ENG-38.

[a] Present address: Seibersdorf Laboratory, International Atomic Energy Agency, Wagramerstrasse 5, P. O. Box 100, A-1400, Vienna, Austria.

The modelling of the transport properties of SLM's, both for the case of counter-transport and co-transport of metal species (Figure 2A), has been performed by us considering that diffusion through aqueous boundary layers and the liquid membrane, as well as interfacial chemical reactions (occurring between the metal species and the carrier), can be rate determining processes (3). The model, schematically shown in Figure 2B, assumes that at the steady state the concentration profiles are linear and the membrane flux, J, is only determined by the metal containing species. The solution of the flux equation has led to the simple relationships reported in Tables 1A and 1B, holding for the two limiting cases of metal species present at low concentrations ($\leq 10^{-3}$ $\underline{M}$, Table 1A) and at moderate and high concentrations ($\geq 10^{-2}$ $\underline{M}$, Table 1B). In the former case the rate of permeation is of the pseudo first order type (logarithmic dependence of C on t). In the latter case the rate of permeation is of the zeroth order type (linear dependence of C on t). The validity of the model and of the corresponding equations have been experimentally verified on several SLM systems, using various metal cations and membrane carriers. Some of the SLM systems we have investigated are reported in Table 2. Metals of critical and strategic importance, such as Co and Ni (4), as well as actinides (5) (Am, Pu, U, Np) and fission products, have been successfully separated and concentrated using appropriate carriers. The equations reported in the table also permit the quantitative prediction and control of the separation process. The necessary permeability coefficients, P, can be evaluated by independently measuring the distribution ratios (K_d) of the metal species to be separated between the organic liquid membrane and the adjacent aqueous feed solution. The diffusional parameters, Δ_a and Δ_o, are generally known by separate measurements. Different rate controlling processes (Figure 3, membrane diffusion or aqueous film diffusion) can be selected for the species to be separated by choosing the appropriate chemical, hydrodynamic and geometrical conditions, with the objective to maximize the ratios of the permeability coefficients and hence the extent of separation. The experimental studies have demonstrated that good separations of many metal species are indeed feasible at the laboratory level. An example of such a separation is shown in Figurea 4A and 4B. By using the selective extractant of Co(II) bis(2,4,4-trimethylpentyl)phosphinic acid (CYANEX 272) as membrane carrier (Figure 4A) a very good Co-Ni separation is obtained in a single stage. Figure 4B shows that the Co(II) content of the feed solution rapidly decreases (Co(II) permeates the SLM) while the Ni concentration stays practically unchanged. As a result of the efforts summarized above we believe that the transport properties of SLM's are now sufficiently well characterized from both the experimental and the theoretical point of view.

Although there are several advantages in the use of SLM's for metal separation and concentrations (Table 3), very few process applications have been reported so far. One of the main reasons which has limited the widespread use of SLM's has been the lack of information available on their life-time. Relatively long-living SLM's are needed in most practical processes in order to be cost effective. Moreover, even for those processes where periodical and frequent reimpregnation of the support is acceptable, predictable life-times are required. Recently we have experimentally and theoretically addressed the question of SLM stability and answers to the questions: (a) what are the factors controlling the SLM stability? (b) how can the life-time of a SLM be maximized?, (c) what is a reasonable estimate for the life-time of a SLM system having a given chemical composition?, have been given. By studying the correlations existing between the SLM life-time, the interfacial properties and contact angles of the SLM system, the solubilization of water into the SLM and the transport of water through the SLM, the following conclusions were reached: (i) stable SLM's can be obtained by minimizing the osmotic pressure gradient across the SLM and the water solubility into the organic layer, (ii) the life-time of the SLM can be predicted and monitored through the extent of water transported across it. At the same time the mechanism controlling the water transport through SLM's was elucidated. In Figure 5 the long-term performance of a SLM suitable for removing an acid from an aqueous stream is shown. Although not all problems in the field of SLM stability have been completely solved, we think that a much better understanding and control of the life-time of the membranes has been eventually gained.

During 1985, through cooperative efforts with an industrial partner, pilot scale evaluations of large SLM hollow-fiber modules were also initiated. This work has led to very encouraging results. For many applications the economics of SLM processes look very favourable and scale up effects appear to be minimal, indicating that significant part of the development work can be performed at the laboratory scale.

In conclusion we believe that as far as basic research is concerned major areas of interest at present lay in the stability of SLM's. In particular:

(a) the synthesis of new polymeric SLM's, possessing very long life-times without detrimental effects on the membrane selectivity and flux, and

(b) the synthesis of new polymeric microporous hollow-fiber supports for liquid membranes, with optimized pore size, pore shape and porosity and characterized by even higher hydrophobicity and, possibly, with controlled surface properties, appear as research areas which can lead to significant improvements of technological relevance. As far as the physical-chemistry and the transport properties of SLM's are concerned, they still represent an intellectually very stimulating research topic. Nevertheless, we do not think that major impediments for the practical development of the new technology can be removed by research in this area. On the other hand, major efforts must be directed into engineering work, aiming at evaluating the performance of large hollow-fiber SLM modules. These studies should be application-specific since different chemistries can result in completely different performances. Only in this way engineers will be able to assess to which extent the simple equipment and low energy consumption of SLM processes, as well as the advantages listed in Table 3, can be economically exploited in real industrial processes and if SLM's are going ro remain a scientific curiosity or a new separation technology.

References

1. P. R. Danesi, Sep. Sci. and Techn. 19, 857 (1984-85).
2. P. R. Danesi, Solvent Extr. Ion Exch. 4 (1) (1985).
3. P. R. Danesi, E. P. Horwitz, R. Chiarizia, and G. F. Vandegrift, Sep. Sci. and Techn. 16, 201 (1981).
4. P. R. Danesi, L. Reichley-Yinger, C. Cianetti, and P. G. Rickert, Solvent Extr. Ion Exch. 2, 781 (1984).
5. P. R. Danesi, R. Chiarizia, P. G. Rickert, and E. P. Horwitz, Solvent Extr. Ion Exch. 3, 111 (1985).

The submitted manuscript has been authored by a contractor of the U. S. Government under contract No. W-31-109-ENG-38. Accordingly, the U. S. Government retains a nonexclusive, royalty-free license to publish or reproduce the published form of this contribution, or allow others to do so, for U. S. Government purposes.

Fig. 1A

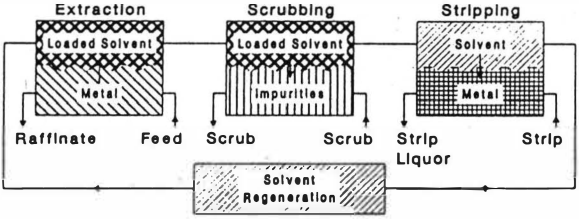
Extraction
Scrubbing
Stripping
Loaded Solvent
Loaded Solvent
Solvent
Metal
Impurities
Metal
Raffinate
Feed
Scrub
Scrub
Strip Liquor
Strip
Solvent Regeneration

Solvent Extraction

Strip
Strip Liquor
brane
Raffinate
Feed

Supported Liquid Membrane

Fig. 1B

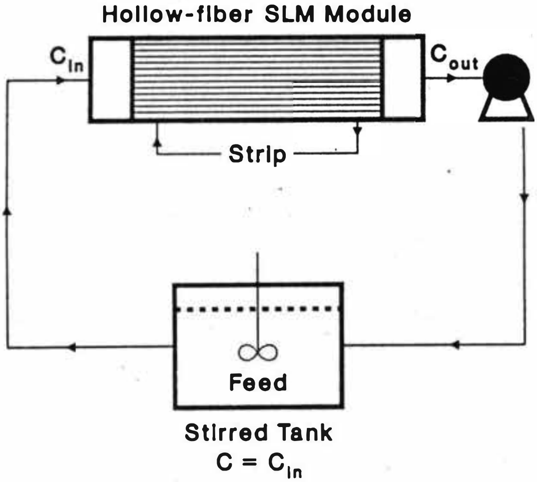
Hollow-fiber SLM Module
C_{in}
C_{out}
Strip
Feed
Stirred Tank
$C = C_{in}$

Table 1A

DILUTED FEEDS

$$J = P \cdot C$$

$$P = \frac{K_1}{K_1\Delta_a + K_{-1}\Delta_o + 1}$$

Fast Chemical Reactions

$$\boxed{P = \frac{K_d}{K_d\Delta_a + \Delta_o}}$$

P = Permeability coefficient
J = Flux
Δ_a = d_a/D_a
Δ_o = d_o/D_o
K_d = K_1/K_{-1} = Membrane/aqueous-feed distribution ratio

$$\boxed{\ln \frac{C}{C_o} = -\frac{Q}{V} \cdot P \cdot t}$$

C = Concentration at time t
C_o = Concentration at time zero
Q = Membrane area
V = Aqueous feed volume
P = Permeability coefficient
t = Time

Table 1B

CONCENTRATED FEEDS

$$P = \frac{J}{C} = \frac{[\bar{E}]/nC}{([\bar{E}]/nC)\Delta_a + \Delta_o}$$

$[\bar{E}]$ = Total carrier concentration

n = Number of carrier molecules per metal ion

$[\bar{E}]/n$ = Organic metal concentration

$$\boxed{J = \frac{[\bar{E}]}{n\,\Delta_o}}$$

$$M + n\,\bar{E} \rightleftharpoons \overline{ME_n}$$

$$\boxed{C = C_o - \frac{[\bar{E}]}{n\,\Delta_o} \cdot \frac{Q}{V} \cdot t}$$

$[\bar{E}]$ = Carrier concentration
n = Carrier molecules per permeating metal species
Δ_o = d_o/D_o
Q = Membrane area
V = Aqueous feed volume

Fig. 2A

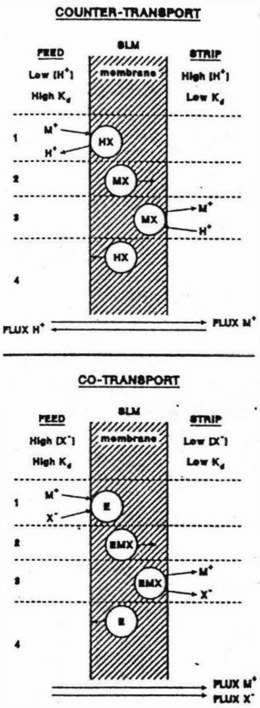
COUNTER-TRANSPORT
FEED
Low [H⁺]
High K_d
SLM
membrane
STRIP
High [H⁺]
Low K_d
1
2
3
4
M⁺
H⁺
HX
MX
MX
M⁺
H⁺
HX
FLUX H⁺
FLUX M⁺
CO-TRANSPORT
FEED
High [X⁻]
High K_d
SLM
membrane
STRIP
Low [X⁻]
Low K_d
1
2
3
4
M⁺
X⁻
E
EMX
EMX
M⁺
X⁻
E
FLUX M⁺
FLUX X⁻

Fig. 2B

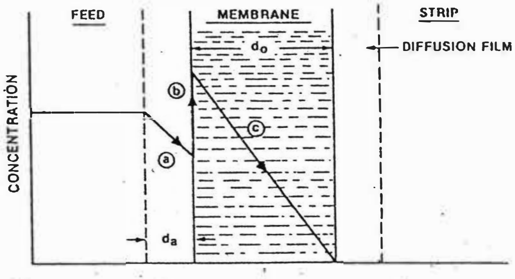
FEED
MEMBRANE
STRIP
DIFFUSION FILM
CONCENTRATION
d₀
dₐ
ⓐ
ⓑ
ⓒ

$$J = -\frac{dC}{dt} \cdot \frac{V}{Q}$$

J = Flux
C = Concentration at time t
t = Time
V = Aqueous feed volume
Q = Membrane area

$$J_a(\text{aqueous film}) = -D_a \frac{\partial c}{\partial x}$$

$$J_i(\text{interf. reaction}) = K_1 A^a B^b - K_{-1} C^c D^d$$

$$J_o(\text{membrane diffusion}) = -D_o \frac{\partial c}{\partial x}$$

$$J_a = J_i = J_o$$

Fig. 4A

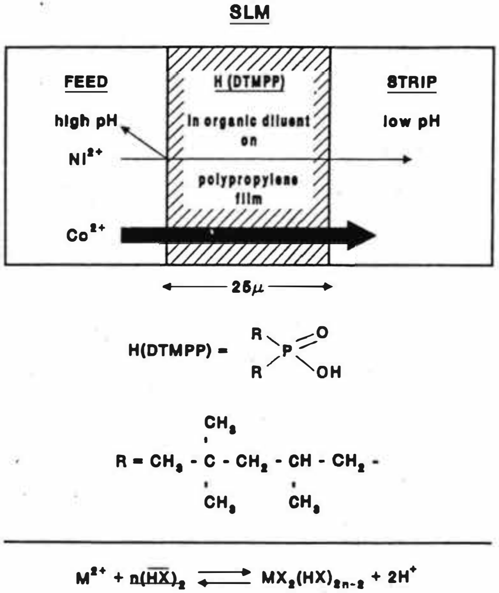
SLM
FEED
high pH
Ni²⁺
Co²⁺
H (DTMPP)
in organic diluent
on
polypropylene
film
STRIP
low pH
25μ
H(DTMPP) =
R
R
P
O
OH
R = CH₃ - C - CH₂ - CH - CH₂ -
CH₃
CH₃
CH₃
M²⁺ + n(HX)₂ ⇌ MX₂(HX)₂ₙ₋₂ + 2H⁺

Fig. 4B

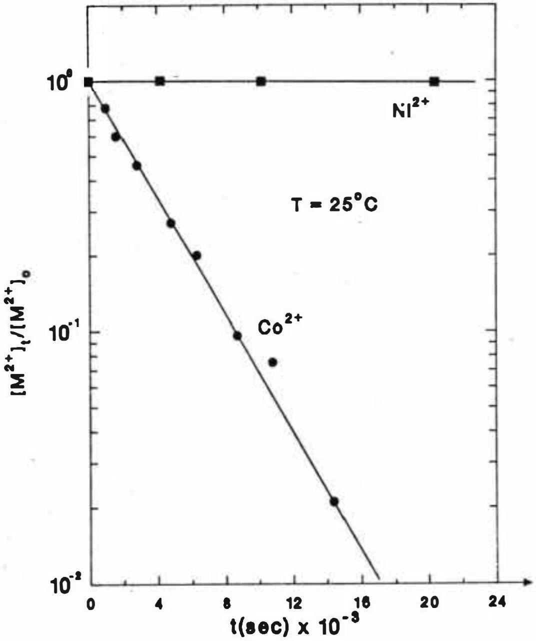
[M²⁺]ₜ/[M²⁺]₀
10⁰
10⁻¹
10⁻²
Ni²⁺
Co²⁺
T = 25°C
0
4
8
12
16
20
24
t(sec) x 10⁻³

Fig. 3

Rate Controlling Processes

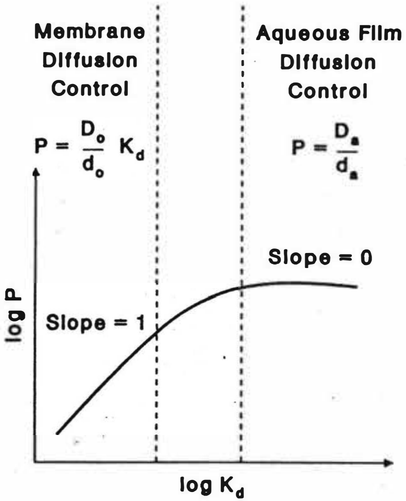
Membrane
Diffusion
Control
$P = \frac{D_o}{d_o} K_d$
Aqueous Film
Diffusion
Control
$P = \frac{D_a}{d_a}$
Slope = 0
Slope = 1
log P
log K_d

$$\boxed{P = \frac{K_d}{K_d \Delta_a + \Delta_o}} \qquad \Delta_a = \frac{d_a}{D_a} \qquad \Delta_o = \frac{d_o}{D_o}$$

Table 2

SLM - INVESTIGATED SYSTEMS

Ion	Feed	Strip	Carrier-Diluent	D_o (cm^2/sec)
Eu^{3+}	HCl	HCl	HDEHP-Dodecane	2×10^{-7}
Cu^{2+}	HCl	HCl	Oxime-Toluene	2.2×10^{-6}
Am^{3+}	$LiNO_3$	HCOOH	OφD(IB)CMPO-Diethylbenzene	2.4×10^{-6}
Zn^{2+} Cd^{2+}	HCl	CH_3COONH_4	TLA-Triethylbenzene	3.2×10^{-6}
Co^{2+} Ni^{2+}	CH_3COOK	HCl	Dialkylphosphinic acid Decalin-DIIPB	3×10^{-7}
H^+	$NaNO_3$	NaOH	TLA-Dodecane	4.4×10^{-7}
	$NaNO_3$	NaOH	TLA-Diethylbenzene	6.5×10^{-6}
	$NaNO_3$	NaOH	Primene JMT-Diethylbenzene	6.5×10^{-6}
	$NaNO_3$	NaOH	TOPO-Diethylbenzene	-
	$NaNO_3$	NaOH	OφD(IB)CMPO-Diethylbenzene	-
	$NaNO_3$	NaOH	DHDECMPO-Diethylbenzene	-

Support: microporous polypropylene

Fig. 5

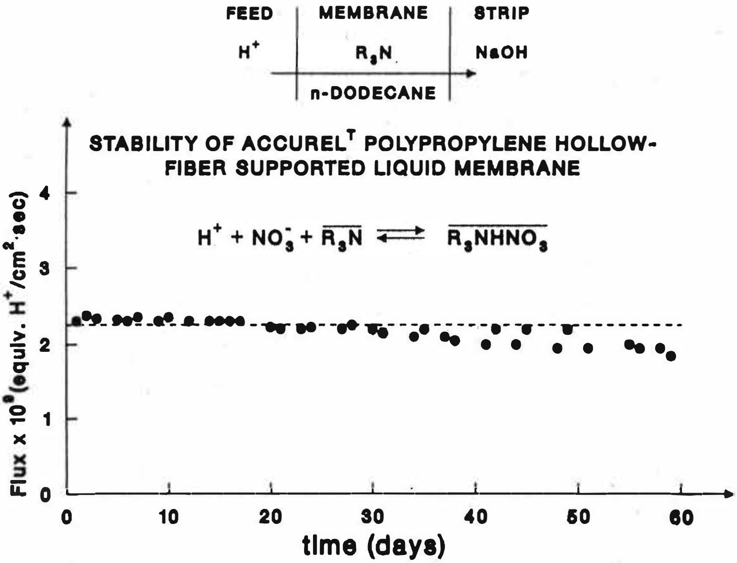

Table 3

ADVANTAGES OF SLM SEPARATIONS

- High selectivities
- Ions can be pumped "uphill"
- Fluxes are higher than with solid membranes
- Lower capital and operating cost
- Expensive extractants can be utilized
- High separation factors are achieved in a single stage
- High feed/strip volume ratios

The Extraction of Metals using Supported Liquid Membranes: the Copper/o-Hydroxyoxime System.

Dr Michael Cox and Darron A Mead, Division of Chemistry, The Hatfield Polytechnic,
Hatfield, Herts. UK.
John Melling, Warren Spring Laboratory, Department of Trade and Industry,
Stevenage, Herts. UK.

Introduction

Liquid membranes potentially offer an attractive alternative to liquid-liquid extraction processes in that they combine the operations of extraction and stripping. In addition the organic phase inventory is greatly reduced thereby reducing not only capital but also running costs. Two types of process are currently under development employing liquid membranes, these are described as (a) surfactant or emulsion membranes (1,2) and (b) supported membranes (3,4). The polymer supported membranes are considered to have the advantage of being able to adapt the established technologies of cross-flow filtration, reverse osmosis, etc. The surfactant membranes, although receiving a lot of commercial interest, do tend to suffer from the drawback of requiring emulsion breakdown to retrieve the strip solution and subsequent reformation of the emulsion phase for recycle. Current studies on both forms of liquid membranes have centered on the use of commercially available liquid extraction reagents as the transfer agent (5 - 8). However one of the significant advantages of both operations is the low solvent inventory and consequent possibility of using more expensive reagents. In addition consideration of the processes involved in the transfer of the metal from the feed to the strip solution suggests that the criteria for reagent selection might differ from liquid-liquid extraction. Thus the need for high metal loading capacity is probably less important than high interfacial activity and rapid kinetics, both chemical and diffusional. However it is still essential for the reagent to have low aqueous solubility to ensure in particular a long operating life for the process. The loss of the liquid membrane phase from the support is probably one of the more important factors in determining the commercial adoption of the technology, and because of this a research programme to investigate various aspects of membrane stability is being undertaken in our laboratories. As part of this study a comparison of the kinetic behaviour of a series of reagents was carried out and this work is reported here.

As mentioned above the majority of the reported work on supported liquid membranes (SLM) have used commercial reagents as carriers. These reagents may contain surface active impurities which could interfere with the transfer process and as the available surface area of membrane is limited it is advisable to use as pure a reagent as possible. For this study the system copper-hydroxyoxime was chosen as this allowed the comparison of commercial reagents, which have been extensively studied as liquid-liquid extractants, with a number of synthesised compounds with carefully defined alkyl side-chains.

Experimental

Membrane Equipment: The comparison of experimental studies of extraction by SLM from different laboratories is difficult because of possible variation in the characteristics of the membrane material. Indeed with some materials the pore distribution can be very erratic, and thus for comparative studies it is essential to use either a large surface area of membrane or reuse the same membrane for all the systems. In this work the same membrane module (working area 91 cm^2) was used for all the experiments. The membrane material chosen was Accurel Type II polypropylene fibres, marketed for cross-flow filtration by Enka AG. The walls are nominally 0.3 mm thick and have an internal diameter of 1.1 - 1.2 mm. These were formed into bundles of 10 fibres with a working length of 25 cm, and the ends sealed into a Perspex tube to provide a rigid sleeve which can act as a seal between the feed and strip solutions. The bundle was inserted into a glass sleeve to produce a shell construction where the feed solution was circulated through the lumens from a resevoir fitted with pH-stat facilities, while the strip solution circulated around the fibres (figure 1). The feed solution consisted of 2 dm^3 of 100 ppm solution of copper sulphate at pH 4, and the strip solution was 1 dm^3 of 10% v/v sulphuric acid. The extractant phase, normally 5% v/v purified reagent in MSB210 (Shell Chemical Co) was impregnated into the skein by filling the lumens with the solution and leaving to soak. Excess reagent was removed and water circulated around and through the skein for 8 - 16 hours to remove surface reagent from the polymer. The feed and strip solutions were then connected and the experimental run started using a flow rate of 100 cm^3 min^{-1}. Samples were taken over a 24 hour period and the copper content of the feed solution analysed by atomic absorption spectrophotometry. At least two experimental runs were carried out for each extractant and at the conclusion of each series the extractant phase was removed from the polymer by washing with diethyl ether. Following removal of the ether the amount of extractant in the polymer could be checked.

Extractants: The commercial reagents: LIX65, LIX860 (Henkel Corporation); SME529 (Shell Chemical Co); P17, P50 (Acorga Ltd) were purified by formation of the copper complex (9). Other aromatic compounds were kindly supplied by Dr J Ainscough and Professor J A Connor (University of Kent) as copper derivatives. The free reagent was obtained by stripping an organic solution of the copper complex with dilute sulphuric acid followed by washing the organic phase several times with water. LIX63 was synthesised as described by Swanson (10) and again purified via the copper derivative.

Results

The choice of flowrate (100 cm^3 min^{-1}) was equivalent to a linear feed velocity of 600 m h^{-1}, which had been shown in earlier work using similar equipment (8) to be appropriate for these feed concentrations. The earlier work also showed that little variation of copper flux occurred over the range pH 2 - 4. The experimental results were plotted as a concentration - time relationship and the data were found to follow best (correlation coefficient >0.997) a half-order relationship in accord with other studies at these feed concentrations (8). The membrane permeability was calculated from the rate coefficient and the volume/area relationship of the Accurel fibres (0.00029 m) using the following expression:

$$P_{0.5} \quad = \quad k_{0.5}\, V/a \qquad g^{0.5}\, m^{-0.5}\, h^{-1}$$

The experimental results are given in terms of the half-order permeability ($P_{0.5}$) and flux ($F_{0.5}$) in Tables 1 - 4.

$$F_{0.5} \quad = \quad k_{0.5}\, /a \qquad g^{0.5}\, m^{-3.5}\, h^{-1}$$

Discussion

The overall process of metal transport from the feed to the strip solution across the polymer support can be described in terms of a number of chemical and diffusional rates (figure 2). By suitable choice of experimental conditions the rate determining steps can be restricted to those processes occurring within the membrane, which will be dependant upon the extractant structure and the diluent. This project was devised to compare the behaviour of extractant systems used for liquid-liquid extraction with SLM performance and some preliminary results will be presented covering the areas of variation of extractant structure, effect of modifiers (nonyl phenol), and the system LIX65N/LIX63.

a. Variation of extractant structure

A series of aromatic hydroxyoximes, both commercial and laboratory synthesised were studied under identical experimental conditions. The results are presented in Tables 1 and 2. From extensive studies on liquid-liquid extraction (11) it has been widely accepted that the rate controlling processes involve chemical reaction between the extractant phase and aqueous solutions at, or close to, the aqueous/organic boundary. This implies that interfacial concentration, which is related to interfacial activity, will be important in the overall process. Further it has been shown that under conditions where these chemical reactions are fast, i.e. high pH and high reagent concentration, then diffusion of the metal complex in the organic phase becomes rate controlling (12). The experimental conditions used in this study, i.e. pH 4 and reagent concentrations 0.15 - 0.2 mol dm^{-3}, fall within this range giving fast kinetics and thus metal transport will reflect diffusion across the membrane. The results show that when R_2 = H or CH_3 the value of $P_{0.5}$ is generally within the range 1.7 - 2.0 $g^{0.5}\, m^{-0.5}\, h^{-1}$ but when R_2 is bulky, e.g C_6H_5 (LIX65N), or n-C_9H_{19} (reagent 5), the rate of diffusion is much slower. The result for P17 (R_2 = $CH_2C_6H_5$) seems abnormal and no easy explanation can be given. Another point of interest was the observation of brown specks, presumably the copper reagent complex, during extraction with reagent 4. Formation of such insoluble material was implied by Teramoto (13) for high concentrations of LIX64N and LIX65N with a consequent reduction in flux. Further studies are in progress under a slow kinetic regime where interfacial activity is expected to be more dominating. In addition the effect of variation in size and chain-branching of the substituent R_1 on the rate of leakage from the membrane phase is being studied to optimise the reagent structure.

b. Effect of modifiers (nonyl phenol)

Nonyl phenol is often found as an impurity in reagents where $R_1 = C_9H_{19}$, and is also deliberately added as a diluent modifier. However one of its more important functions is in the Acorga P5000 series of extractants where it is blended with the reagent P50 to modify the extraction performance of the latter. Studies have shown (14) that nonyl phenol increases the transfer capacity of the reagent by improving the performance of the strip cycle with little loss of extraction capability. Their excellent kinetic behaviour has led to the use of the P5000 series in SLM studies (8), so it was interesting to discover what effect nonyl phenol would have on SLM performance. Various mixtures of P50 and nonyl phenol were prepared and the transfer of copper studied under the same conditions as before. As results in Table 3 show the addition of nonyl phenol does produce a small increase in the transfer of copper with a maximum value about the 1:1 ratio, which is equivalent to the reagent P5100 (15). It seems likely that the reduction of permeability found with higher concentrations is a result of a number of factors, including reduction in the activity (concentration) of P50 caused by complex formation with the phenol (15) and replacement of P50 by nonyl phenol near the membrane surface.

c. Effect of LIX63 addition to LIX65N

Since 1963 it has been known that LIX63 will extract copper from aqueous solution above pH 2.0 and this compound is present at about 1% with LIX65N in the formulation of LIX64N. Its presence is desirable in the mixed extractant to improve the extraction kinetics, and a series of experiments were performed to see if this behaviour was extended to SLM applications. The results, Table 4, do show an increase in transfer up to a LIX63 concentration of 25% in the mixture. Above this value the permeability decreases until at 100% LIX63 no copper transfer is found. Instead the polymer support turns green signifying the formation of the polymeric 1:1 copper:LIX63 complex (16). This behaviour is completely different from the liquid-liquid system where kinetic enhancement tends to level off above 40% LIX63 (17) and extraction of copper by LIX63 alone results in the formation of the brown 1:2 copper:LIX63 complex. Further work using different diluents is in progress to see whether this is a general phenomenon or whether the decrease in permeability as LIX63 concentration is increased above 25% is a result of poor solubility of the 1:1 complex in the polymer support phase.

Conclusions

Although it is too early to provide definite conclusions the results presented above imply that supported liquid membranes will probably require development of compounds which exhibit different properties from those optimised for liquid-liquid extraction. Thus because of limited interfacial area available the interfacial activity and thus molecular arrangement are going to be critical. In addition it is unlikely that systems which display good performance in liquid-liquid processes will be as effective in SLM operations.

References

1. Davies G A Hydrometallurgy '81, Society of Chemical Industry. London 1981, paper D1
2. Li N N , Cahn R P , Naden D, and Lai R W W Hydrometallurgy 9 , 277 , (1983)
3. Babcock W C , Kelly D J , LaChapelle E D , Smith K L and Baker R W Hydrometallurgy '81, Society of Chemical Industry, London 1981, paper D2
4. Danesi P R Sepn. Sci. and Technol. 19 , 857 , (1984)
5. Danesi P R , Reichley-Yinger L , Ciaretti C and Reichert P G Solv. Extn. and Ion Exch. 2 , 781 , (1984)
6. Imoto T , Obawa H , Moroka S , and Kato J. J Chem. Eng. Japan 14 , 288 , (1981)
7. Flett D S , Melling J , and West D Proc. Oslo Symp.: Ion Exchange and Solvent Extraction, Society of Chemical Industry, London 1982 paper 1 - 16
8. Pearson D Ion Exchange Membranes, ed Flett D S , Ellis - Horwood, Chichester, 1983, pp 55
9. Fleming C A , Nicol M J , Hancock R D , and Finkelstein N P J Appl. Chem. Biotechnol. 28 , 443 , (1978)
10. Swanson R R US Patent 3 224 873 (1965)
11. Danesi P R and Chiarizia R CRC Critical Reviews in Analytical Chemistry, 10 , 1 , (1981)
12. Cox M , Hirons C G and Flett D S Proc. ISEC80, Liege, 1980, vol 1, paper 80 paper 80 - 48
13. Teramoto M and Tanimoto H Sepn. Sci. and Technol. 18 , 871 , (1983)
14. Tumilty J A , Dalton R F and Masson J P Adv. in Extn. Metall. Inst. Mining and Metall., London, 1977 pp 123.
15. Dalton R F and Seward G A Reagents for the Mining Industry , Rome , Inst. Mining and Metall. London, 1984 , pp 107
16. Fritz J S , Beuerman D R and Richard J J Talanta 18, 1095 , (1971)
17 Whewell R J , Hughes M A and Hanson C J inorg. nucl. Chem. 38 , 2071 , (1976)

Reagent	R_1 (figure 3)	R_2	$P_{0.5}$ ($g^{0.5}m^{-0.5}h^{-1}$)	$F_{0.5}$ ($g^{0.5}m^{-3.5}h^{-1}$)	%C
LIX65N	C_9	C_6H_5	1.2	0.74	99.5
LIX860	C_{12}	H	1.7	1.1	99.3
SME529	C_9	CH_3	1.9	1.2	97.2
P17	C_9	$CH_2C_6H_5$	1.8	1.1	99.7
P50	C_9	H	1.9	1.2	99.8

Table 1 Extraction of copper by commercial hydroxyoximes (5% v/v in MSB210) supported by Accurel fibres, feed solution 100 ppm copper sulphate at pH 4.0 at a flow rate of 600 m h^{-1}, strip solution 10% v/v sulphuric acid at a flow rate of 5 m h^{-1}.

Reagent	R_1	R_2	$P_{0.5}$	$F_{0.5}$	%C
1	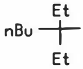 $\text{nBu}-\overset{\text{Et}}{\underset{\text{Et}}{\vert}}-$	H	1.8	1.1	99.8
2	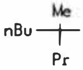 $\text{nBu}-\overset{\text{Me}}{\underset{\text{Pr}}{\vert}}-$	H	2.0	1.3	99.7
3	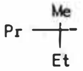 $\text{Pr}-\overset{\text{Me}}{\underset{\text{Et}}{\vert}}-$	H	1.7	1.1	99.5
4*	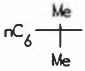 $\text{nC}_6-\overset{\text{Me}}{\underset{\text{Me}}{\vert}}-$	H	1.0	0.6	99.9
5**	H	nC_9	0.25	0.16	99.5

Table 2 Extraction of copper by pure aromatic hydroxyoximes (expl. conditions as Table 1 except * brown specks observed on polymer surface
** 3% w/v. solution ;

Ratio P50: Nonyl phenol	$P_{0.5}$	$F_{0.5}$	%C
1:0	1.8	1.1	99.7
1:0.5	1.8	1.1	99.8
1:1	2.0	1.25	99.0
1:2	1.8	1.15	99.7

Table 3 Extraction of copper by mixtures of P50 and nonyl phenol (expl. cond. as in Table 1)

%LIX63	$P_{0.5}$	$F_{0.5}$	%C
0	1.2	0.74	99.5
3	1.4	0.89	99.9
6	1.6	1.0	99.8
12	1.6	1.0	99.8
25	1.9	1.2	99.8
50	1.7	1.1	99.9
75	1.1	0.67	99.5
100	0	0	

Table 4 Extraction of copper by LIX63/LIX65N mixtures (experimental conditions as in Table 1)

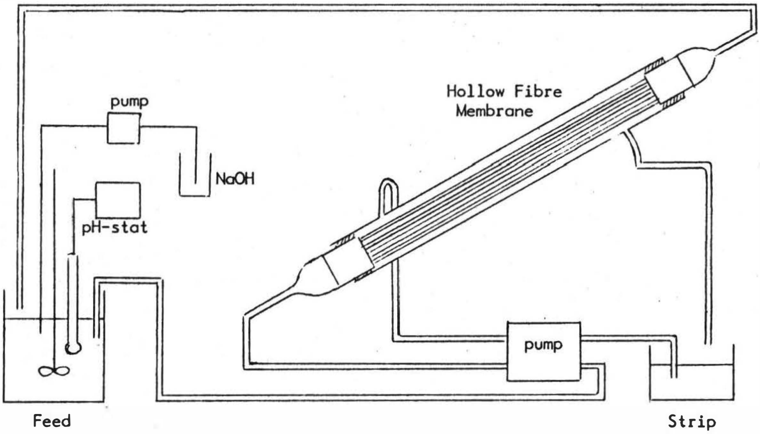
Hollow Fibre
Membrane
pump
NaOH
pH-stat
pump
Feed
Strip

Figure 1 Diagram of Experimental Equipment

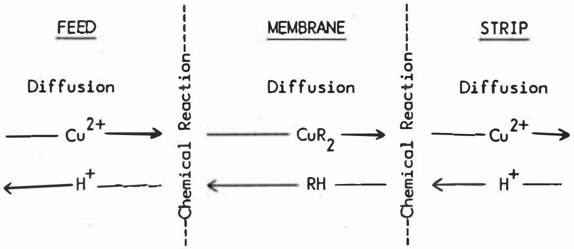
FEED
MEMBRANE
STRIP
Diffusion
Diffusion
Diffusion
Chemical Reaction
Chemical Reaction
Cu2+
CuR2
Cu2+
H+
RH
H+

Figure 2 Rate Processes in SLM Transfer

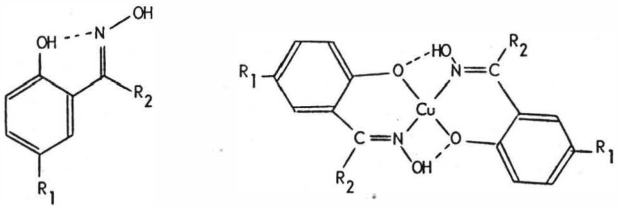
OH
N
OH
R2
R1
R1
O
HO
N
C
R2
Cu
C
N
O
R1
R2
OH

Figure 3 Structure of hydroxyoximes and copper complexes

Selectivity in the extraction of metals by liquid membranes

Masaaki Teramoto, Tadashi Sakuramoto, Hitoshi Takaya, Yuji Katayama, Atsushi Kojima, Yoshikazu Miyake and Hideto Matsuyama, Kyoto Institute of Technology, Kyoto, Japan

Liquid membrane technique has been attracting attention as a useful method for the separation and concentration of various solutes such as metal ions, acids and bases(1). Although a number of papers have been presented on the permeation mechanisms of single species through supported liquid membranes, few papers (2-6) have dealt with competitive permeation rates in multicomponent systems on the basis of the theory of mass transfer with chemical reactions. Danesi et al.(4) have analyzed the selectivity in the separation of Co and Ni by supported liquid membranes containing di(2,4,4-trimethylpentyl) phosphinic acid. However, their quantitative treatment has been limited to the condition of low metal loading at the feed-membrane interface. In the separation of Co and Ni using organophosphorus extractants, the selectivity under the condition of high metal loading is of practical importance and also of great interest because very high separation factor is obtained.

In the present paper, permeation rates of Co and Ni through supported liquid membranes containing 2-ethylhexylphosphonic acid mono-2-ethylhexyl ester(abbreviated as PC-88A or EHPNA) were measured over a wide range of loading ratio using a diffusion cell, and analyzed by a permeation model in which the formation of aggregates of metal-carrier complexes was considered when the loading ratio was high. A spiral-type supported liquid membrane module, which could remove and concentrate metal ions very effectively and could be used for selective permeation of metal ions, was developed. The stability of the membrane was found to be satisfactory. The design equations for predicting the degree of removal of each metal is presented.

1.Experimental

The diffusion cell used in the present work was similar to that used by Danesi et al.(2). The supported liquid membranes consisted of Floropore FP-010 microporous Teflon film(Sumitomo Electric Co., Ltd., mean pore diameter:0.1μm, porosity:0.57, thickness:60μm) on which a solution of PC-88A in dodecane was absorbed. The membrane area was 20cm^2, and the volumes of the feed and strip solutions were 0.250 and 0.045dm^3, respectively. Both solutions were stirred by magnetic stirring bars at 300rpm. The feed solution was prepared by dissolving

$Co(NO_3)_2$ and/or $Ni(NO_3)_2$ in deionized water, and pH was adjusted by 0.1 mol/L acetic acid-sodium acetate buffer solutions. 3 mol/dm^3 HCl solution was used as a strip solution. The concentration variations of Co(II) and/or Ni(II) in the strip solution were followed by the atomic absorption analysis. The temperature was kept at 298 K.

The schematic diagram of the spiral-type supported liquid membrane module is shown in Fig.1. The support is a porous membrane made of polypropylene(Duragard 2502, Polyplastics Co., Ltd., Japan, width: 30.5cm, length:1m, thickness:50μm, porosity:0.47, pore diameter:0.04x 0.4μm). The membranes and the spacers(thickness:1.1mm) were spirally wound around the pipes through which the feed and the strip solutions (2mol/L H_2SO_4 solution) were supplied, and the side and the outer surface of the modules were sealed by an adhesive. The modules were operated in a once-through mode for feed solutions and in a recycling mode for strip solutions (Figs.7 and 11), or in a once-through mode for both feed and strip solutions(Figs.9 and 10).

2. Extraction Equilibria

The equilibria in the extraction of Co(II) and Ni(II) with EHPNA at low loading ratio are expressed as follows(7).

$$2\overline{HR} \rightleftharpoons \overline{(HR)_2}, \quad K_2=[\overline{(HR)_2}]/[\overline{HR}]^2 \tag{1}$$

$$Co^{2+}+2\overline{(HR)_2} \rightleftharpoons \overline{CoR_2(HR)_2}+2H^+$$

$$K_{exCo}=([\overline{CoR_2(HR)_2}][H^+]^2/[Co^{2+}][\overline{(HR)_2}]^2)_{eq} \tag{2}$$

$$Ni^{2+}+3\overline{(HR)_2} \rightleftharpoons \overline{NiR_22(HR)_2}+2H^+$$

$$K_{exNi}=([\overline{NiR_22(HR)_2}][H^+]^2/[Ni^{2+}][\overline{(HR)_2}]^3)_{eq} \tag{3}$$

$$Na^++2\overline{(HR)_2} \rightleftharpoons \overline{NaR3(HR)}+H^+$$

$$K_{exNa}=([\overline{NaR3(HR)}][H^+]/[Na^+][\overline{(HR)_2}]^2)_{eq} \tag{4}$$

Here, $\overline{(HR)_2}$ is the dimer of the extractant. It was confirmed that the observed distribution ratios of Co(II) and Ni(II), D_M, were

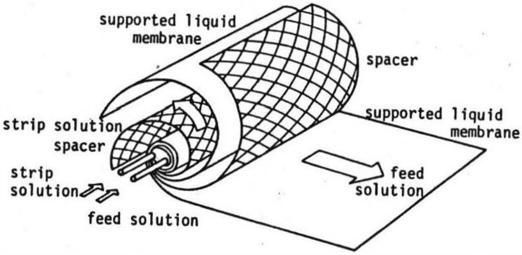

Fig.1 Spiral-type supported liquid membrane module.

approximately expressed by Eqs.(1) to (3).

The distribution ratios in the single extraction at high loading ratio are shown in Fig.2. As $[H^+]_e$ decreases, metal to extractant ratios exceed 1:2 and 1:3 for cobalt and nickel, respectively, and the ratio approaches to unity. It was confirmed by the vapor pressure osmometry(VPO) and the gel permeation chromatography(GPC) that aggregates of the metal complexes were formed which contained about 5-20 molecules of $\overline{(HR)_2}$ on the average depending on the loading ratio. For simplicity, it was assumed that the metal to carrier(dimer of the carrier) ratio in the aggregates is 1:1 regardless of the loading ratio and that the aggregates are expressed as $\overline{CoR_2}$ and $\overline{NiR_2}$, and the following empirical correlations were obtained from the data at the total carrier concentrations of 0.735 and 0.368 mol/L.

$$[\overline{CoR_2}]=0.350[\overline{CoR_2(HR)_2}]^{1.57}[\overline{(HR)_2}]^{-0.802} \qquad (5)$$

$$[\overline{NiR_2}]=0.175[\overline{NiR_22(HR)_2}]^{0.836}[\overline{(HR)_2}]^{-0.750} \qquad (6)$$

The distribution ratio calculated by Eqs.(1)-(6) are shown by the solid lines in Fig.2. It should be noted that these equations can satisfactorily predict the distribution ratios in the simultaneous extraction of cobalt and nickel as shown in Fig.3. The dotted lines in Figs.2 and 3, which are the distribution ratios calculated by Eqs.(1)-(4), are much lower than the experimental data at low $[H^+]_e$.

3. Analysis of the permeation rates through supported liquid membranes

The permeation of metal ions through supported liquid membranes consists of mamy elementary steps(8). Here, the following two steps are taken into account, i.e., (1)diffusion of metal ions through a

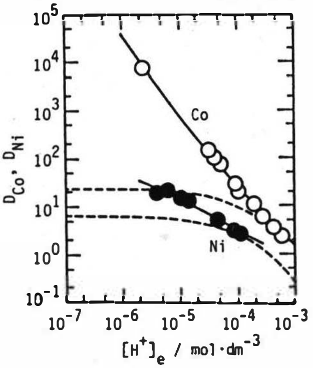

Fig.2 Distribution ratio in the single extraction. $[(HR)_2]_0$=0.735mol/L, $[Co]_0$=$[Ni]_0$=0.085mol/L, V_{aq}/V_{org}=5.

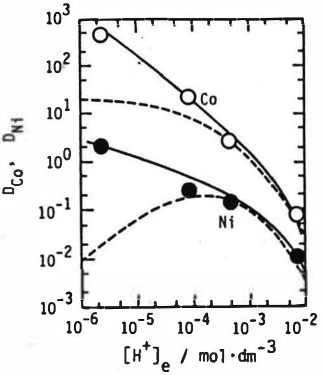

Fig.3 Distribution ratio in the simultaneous extraction. Conditions are the same as shown in Fig.2.

stagnant layer of feed solution, (2)diffusion of the carrier and the complex in the membrane, since the resistances of other steps such as interfacial reactions and the diffusion of metal ions in the strip solution can be neglected. Then the permeation rates are expressed by the following equations.

$$J_{Co}=k_{FCo}([Co^{2+}]_F-[Co^{2+}]_{Fi})=k_{mCO}[\overline{CoR_2(HR)_2}]_{Fi}+k_{mCoP}[\overline{CoR_2}]_{Fi} \tag{7}$$

$$J_{Ni}=k_{FNi}([Ni^{2+}]_F-[Ni^{2+}]_{Fi})=k_{mNi}[\overline{NiR_22(HR)_2}]_{Fi}+k_{mNiP}[\overline{NiR_2}]_{Fi} \tag{8}$$

$$J_{Na}=k_{FNa}([Na^+]_F-[Na^+]_{Fi})=k_{mNa}[\overline{NaR3(HR)}]_{Fi} \tag{9}$$

The continuity of the total flux of the carrier is expressed by

$$\begin{aligned}&k_{mB}([\overline{(HR)}_2]_{Si}-[\overline{(HR)}_2]_{Fi})+(k_{mB'}/2)\{([\overline{HR}]_{Si}/K_2)^{0.5}-([\overline{HR}]_{Fi}/K_2)^{0.5}\}\\&\quad=2k_{mCo}[\overline{CoR_2(HR)_2}]_{Fi}+k_{mCoP}[\overline{CoR_2}]_{Fi}\\&\qquad+3k_{mNi}[\overline{NiR_22(HR)_2}]_{Fi}+k_{mNiP}[\overline{NiR_2}]_{Fi}+2k_{mNa}[\overline{NaR3(HR)}]_{Fi}\end{aligned} \tag{10}$$

where k_F and k_m are the mass transfer coefficient in the feed phase and that in the membrane, respectively, and subscripts B, B', CoP, NiP, F, S and i indicate $\overline{(HR)}_2$, $\overline{HR}$, $[\overline{CoR_2}]$, $[\overline{NiR_2}]$, the feed solution, the strip solution and the interface, respectively.
The conservation of the carrier in the membrane is expressed by

$$\begin{aligned}&B_0=0.5\{[\overline{(HR)_2}]_{Fi}+[\overline{(HR)_2}]_{Si}+0.5([\overline{HR}]_{Si}/K_2)^{0.5}+0.5([\overline{HR}]_{Fi}/K_2)^{0.5}+\\&2[\overline{CoR_2(HR)_2}]_{Fi}+[\overline{CoR_2}]_{Fi}+3[\overline{NiR_22(HR)_2}]_{Fi}+[\overline{NiR_2}]_{Fi}+2[\overline{NaR3(HR)}]_{Fi}\}\end{aligned} \tag{11}$$

where B_0 is the initial concentration of the carrier.

4. Effect of experimental condition on the permeation rates

Figure 4 shows the effect of $[H^+]_F$ on the fluxes in the single permeation of Co(II) and Ni(II). As $[H^+]_F$ increases, J_M decreases due to a decrease in the distribution ratio, D_M. On the other hand, when $[H^+]_F$ is low, J_M is almost constant because most of the carrier at the feed-membrane interface is converted to the complexes, and the rate is limited by the diffusion of the carrier in the membrane.
The effect of $[H^+]_F$ in the simultaneous permeation is shown in Fig. 5. J_{CO} is approximately equal to that observed in the single permeation over the whole range of $[H^+]_F$. On the other hand, at low $[H^+]_F$, J_{Ni} is drastically lowered by the presence of Co(II) because most

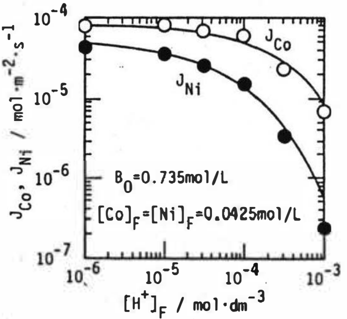

Fig.4 Effect of $[H^+]_F$ on J_{Co} and J_{Ni} in the single permeation.

of the carrier at the feed- membrane interface is exhausted by the complexation with Co(II) which has much higher distribution ratio than Ni(II). However, as $[H^+]_F$ increases J_{Ni} increases because $[\overline{(HR)_2}]_{Fi}$ also increases due to a decrease in D_{Co}. With a further increase in $[H+]_F$ both J_{Co} and J_{Ni} approach to those in the single permeation. Therefore the plot of J_{Ni} vs $[H^+]_F$ has a maximum.

Figure 6 shows the effect of the metal concentration in the simultaneous permeation. When the concentrations are low, the diffusion of metals in the stagnant layer of the feed phase is rate-determining(8), and no selectivity is obtained. On the other hand, when metal concentrations are high, J_{Ni} in the simultaneous permeation becomes much lower than that in the single permeation.

The rate parameters used for the simulation of the permeation rates were estimated as follows. The value of k_{FCo} was determined from the permeation rate under the condition of low metal concentration, high pH and high carrier concentration. k_{mCo} was calculated from J_{Co} observed in the experiment using the diffusion cell where Co(II) was transported from an organic solution loaded with a small amount of Co(II) to the strip solution through a porous membrane impregnated with the same organic solution. In this case, J_{CO} is expressed by Eq.(12), from which k_{mCo} was calculated.

$$J_{Co}=k_{mCo}[\overline{CoR_2(HR)_2}]_F \tag{12}$$

k_{mB}, k_{mB}' and k_{mNi} were estimated from k_{mCo} using the relation that the diffusivity is proportional to (molar volume)$^{-0.6}$(9). The values of k_{mCoP} and k_{mNiP} were determined so that the computed results

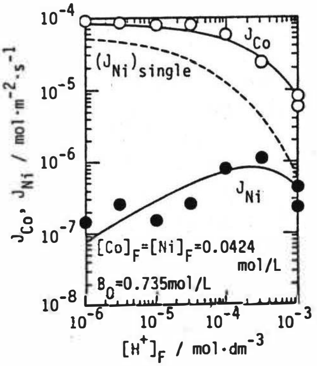

Fig.5 Effect of $[H^+]_F$ on J_{Co} and J_{Ni} in the simultaneous permeation.

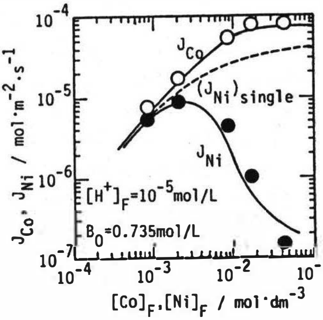

Fig.6 Effect of metal concentration on J_{Co} and J_{Ni} in the simultaneous permeation.

might compare with the observed results. The complex formations between metal ions and CH_3COO^- in the aqueous phase were taken into account in the calculation. The parameters used are as follows.

$k_{FCo}=k_{FNi}=k_{FNa}=7\times10^{-6}$m/s, $k_{mB}=1.7\times10^{-7}$m/s, $k_{mCo}=1.12\times10^{-7}$m/s, $k_{mNi}=8.8\times10^{-8}$m/s, $k_{mCoP}=8.8\times10^{-8}$m/s, $k_{mNiP}=6.5\times10^{-8}$m/s, $K_{exCo}=4.14\times10^{-6}$, $K_{exNi}=3.13\times10^{-7}$dm^3/mol, $K_{exNa}=2\times10^{-5}$dm^3/mol, $K_2=8000$dm^3/mol.

The values of k_{mCoP} and k_{mNiP} suggest that the aggregates of the complexes of Co(II) contain about 3 molecules of $\overline{(HR)_2}$, and those of Ni(II) about 5. The computed results(solid lines in Figs.4-6) are in agreement with the experimental data.

The selectivity factor, which is defined by Eq.(13), is discussed for the following special cases.

$$S=(J_{Co}/J_{Ni})/([Co^{2+}]_F/[Ni^{2+}]_F) \qquad (13)$$

Case 1. If the metal loading is low and the diffusional resistance in the feed phase is negligibly small, the formation of the aggregates is ignored. Then Eq.(14) is derived using Eqs.(2) and (3).

$$S\propto K_{exCo}/(K_{exNi}[\overline{(HR)_2}]_0) \qquad (14)$$

The region of high $[H^+]_F$ in Fig.4 corresponds to this case.

Case 2. If the metal loading is high and the diffusional resistance in the feed solution is negligibly small, then the contribution of $\overline{CoR_2(HR)_2}$ and $\overline{NiR_22(HR)_2}$ to D_M is small. Then the following equation is derived from Eqs.(5)-(6) and (13).

$$S\propto([Ni^{2+}]_F{}^{0.164}/[Co^{2+}]_F{}^{0.57})([\overline{(HR)_2}]_{Fi}{}^{0.58}/[H^+]_F{}^{1.47}) \qquad (15)$$

When $[Co^{2+}]_F$ is equal to $[Ni^{2+}]_F$ as in the case of the present experiment, S is proportional to $[\overline{(HR)_2}]_{Fi}{}^{0.58}/[H^+]_F{}^{1.47}$. According to this relation, S increases with a decrease in $[H^+]_F$. However, it should be noted that the decrease in $[H^+]_F$ loweres $[\overline{(HR)_2}]_{Fi}$. Therefore, the effect of experimental condition on the selectivity is not so simple as described by Danesi et al.(4).

Case 3. If the diffusional resistance of metal ions in the feed solution is rate-determining, the flux and S are represented by Eq.(16) and (17), respectively. This case is encountered in the region of low metal concentartion in Fig.6.

$$J_M=k_{FM}[M^{2+}]_F \text{ (M=Co, Ni)} \qquad (16)$$

$$S=k_{FCo}/k_{FNi}\cong1 \qquad (17)$$

5. Separation of metal ions by a spiral-type module

Figure 7 shows the effect of feed rate on $[Co]_{out}/[Co]_{in}$ in the recovery of Co(II). When $[\mathrm{Co}]_{in}$ is low, the diffusion of Co^{2+} in the feed phase is rate-controlling(Case 3), and 99.7% of Co(II) was recovered at low feed rate, v_F. In a similar experiment using a module with the membrane length of 2m, more than 99.9% of Co(II) was removed when v_F was 180cm^3/min. These excellent results may be due to the flow pattern in the module, i.e., plug flow. In this case, The differential mass balance equation of each metal ion is expressed by

$$d[\mathrm{M}]/dA=-(J_M/v_F) \quad (\mathrm{M=Co,Ni,Na}) \tag{18}$$

where A is the membrane area. For Case 3, Eq.(19) is derived.

$$[\mathrm{Co}]_{out}/[\mathrm{Co}]_{in}=\exp(-k_{FCo}A/v_F) \tag{19}$$

On the other hand, when $[\mathrm{Co}]_{in}$ is sufficiently high, the diffusion in the membrane is rate-determining. Then Eq.(20) is derived.

$$[\mathrm{Co}]_{out}=[\mathrm{Co}]_{in}-J_{Comax}A/v_F \tag{20}$$

Here, J_{Comax} is the maximum flux observed under the condition of high loading ratio at the feed-membrane interface and was determined experimentally using the diffusion cell. The effective membrane area A was determined approximately as 0.3m^2 from Eq.(20). Then, k_{FCo} can be estimated from Eq.(19), and is shown in Fig.8 where k_{FZn} obtained by the experiment on the removal of low concentration of Zn(II) (carrier: D2EHPA) is also shown. It can be seen that k_F is proportional to $v_F^{0.5}$. This dependency is favorable compared with that in the case of hollow fiber modules where k_F is proportional to $v_F^{0-1/3}$ because the extent of removal does not decrease remarkably with an increase in v_F. Ni(II) was also satisfactorily recovered although not shown here.

Figure 9 shows the results in the simultaneous permeation when the carrier concentration was 0.735mol/L. When both metal concentrations are low, the selectivity factor is low(Case 3). On the other hand,

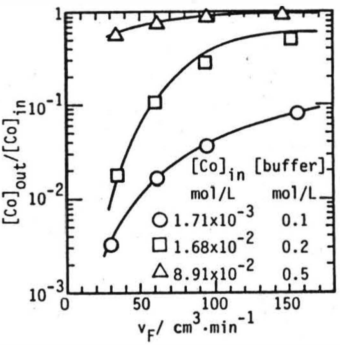

Fig.7 Effect of v_F on $[\mathrm{Co}]_{out}/[\mathrm{Co}]_{in}$.
Spiral-type module. pH_{Fin}=5.65.

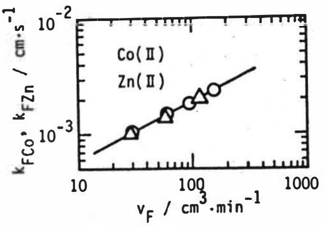

Fig.8 Effect of v_F on k_F.

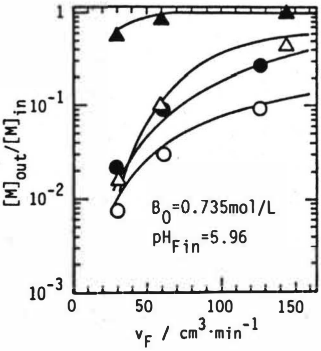

Fig.9 Simultaneous permeation of Co and Ni. Spiral-type module.

Co	Ni	$[M]_{in}$	[buffer]
○	△	0.00172mol/L	0.1mol/L
●	▲	0.0170 mol/L	0.2mol/L

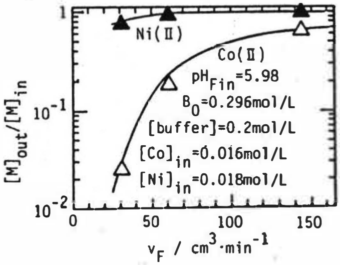

Fig.10 Simultaneous permeation of Co and Ni. Spiral-type module.

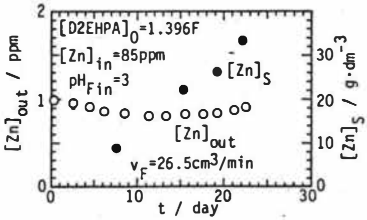

Fig.11 Recovery of Zn by spiral-type module.

when metal concentrations are high, Co(II) is selectively transported. A similar result was obtained when the carrier concentration was 0.296mol/L(Fig.10). The results calculated from Eqs.(1)-(11) and (18) are shown by the solid lines in Figs.7, 9 and 10. It is found that outlet concentrations can be satisfactorily predicted by the design equation over the whole region from Case 2 to Case 3. Figure 11 shows the time course of $[Zn]_{out}$ and $[Zn]_S$ in the recovery of Zn(II) when D2EHPA was used as a carrier. It is clearly shown that the membrane is very stable and can pump Zn(II) even when $[Zn]_S$ is about 40000 times as high as $[Zn]_{out}$.

References

1. R.Marr and A.Kopp, Chem.Ing.Tech., 52,399(1980)
2. P.R.Danesi,R.Chiarizia and A.Castagnola,J.Membr.Sci.,14,161(1983)
3. P.R.Danesi,E.P.Horwitz and P.G.Rickert,J.Phys.Chem.,87,4708(1983)
4. P.R.Danesi,L.Reichley-Yinger,C.Cianetti and P.G.Rickert,Solvent Extr.Ion Exch.,2,781(1984)
5. L.Reichley-Yinger and P.R.Danesi,ibid.,3,49(1985)
6. R.Chiarizia and A.Castagnola, ibid.,2,479(1984)
7. Komasawa,I.,T.Otake and I.Hattori,J.Chem.Eng.Japan,16,210(1983)
8. M.Teramoto,H.Tanimoto, Sep.Sci,Technol.,18,871(1983)
9. C.R.Wilke and P.Chang, AIChE J.,1,264(1965)

SEPARATION OF METAL SPECIES BY EMULSION LIQUID MEMBRANES

J. Draxler, W. Fürst, R. Marr , Technical University Graz, Austria

Nearly twenty years have passed since the first use of emulsion liquid membranes /1/ and in this time several pilot plants for the recovery of Uranium, Copper, Chromium, Mercury and Zinc /2,3,4,5,6/ have proved the technical feasibility of this Liquid-Membrane-Permeation (LMP) process and the economic superiority to comparable processes, such as solvent-extraction. But despite of it's evident advantages no large-scale plant has been built up to now in the hydrometallurgical industry. The reason for this are probably economic factors, especially the depressed state of the metal industry. There is no need for new plants and a rebuilding of an existing solvent-extraction plant to a LMP-plant is not economic, because low investment costs are the main advantage of LMP, whereas operating costs are about the same /5/.

There are two main incentives for a further developing of the emulsion liquid membrane technique. The first is the hope that the current bad situation in the hydrometallurgical industry will be improved in the near future and the second is the very promising application of liquid membranes in waste water treatment.

A prerequisite for the application of emulsion liquid membranes in waste water treatment is, that the metal ions can be separated below the limits of the environmental protection agencies of the various countries and that the solubility of the organic compounds of the membrane phase in the waste water is also below a critical value. Both requirements are met by the emulsion liquid membrane technique, as was confirmed in several pilot plants.

Contrary to solvent-extraction, which is an equilibrium-limited process, LMP is commonly regarded as a rate process, which is controlled only by the residence time in the mass transfer apparatus. For the application of emulsion liquid membranes in waste water treatment this is not always valid. To reach equilibrium once, might not be sufficient for a complete separation of the metal species. Two or more stages are necessary, so for a complete separation of the metal ions the emulsion liquid membrane technique is a rate as well as equilibrium controlles process. Using a counter-current extraction column (height: 2,7m, diameter: 50mm) following separations could be achieved in a pilot-plant with industrial solutions:

Table 1: Separation of various metals in a pilot plant

Element	Throughput (l/h)	initial concentration (mg/l)	final concentration (mg/l)
Zinc	30	4500	4
Zinc	30	500	0,8
Zinc	70	150	0,5
Copper	20	8000	27
Copper	40	800	3
Nickel	20	2200	360
Cadmium	60	14	0,01
Lead	60	8	0,01
Chromium	40	1500	4

As can be seen from table 1, Zinc, Copper, Cadmium and Lead can easily be separated down to concentrations, which are below the limits of most environmental protection agencies. This is not true for Nickel and Chromium (VI). The reason for this is that the residence time in the used column was not long enough for the Nickel-separation. Under the same conditions Nickel could be separated in a two-stage counter-current mixer-settler with sufficient residence time down to 2 ppm. The reason for the insufficient Chromium-separation was not the residence time, but, as an industrial solution containing a lot of sulfate-ions was used, the co-transport of these sulfate-ions. Although the sulfate-transport is negligible in the range of high Chromium-concentrations, it becomes dominating when the Chromium-concentration is very low. As a consequence not only the Chromium-separation is insufficient, but also a lot of NaOH-solution is consumed for the neutralisation of the transported sulfuric acid.

The other problem for the application of emulsion liquid membranes in waste water treatment is the solubility of organic substances in the aqueous phases. As can be seen from table 2, the physical solubility is much less than is usual in solvent-extraction. This is because of the different composition of the organic phase in the two processes. In solvent-extraction it is necessary to use aromatic diluents or aliphatic diluents and a modifier to prevent third phase formation. Both, aromatic diluents and modifiers, have a high solubility in water and are not necessary in LMP, where only aliphatic diluents are used. It is true, that an additional surfactant is necessary in LMP, but since the solubility of the preferrably used surfactant ECA 4360 is less than all other components, the total solubility of the membrane phase is much lower than in solvent-extraction.

Table 2: Solubility of organic compounds

	LMP (mg/l)	SX (mg/l)
Extractant	5-30	5-30
Diluent		
aliphatic	1-5	1-5
aromatic		50-100
Modifier		40-150
Surfactant	1	
Total solubility of organic phase	3-9	40-140

The treated waste water is therefore only slightly contaminated by organic substances and no problems should result. Problems might occur, if the waste water contains already high amounts of organic substances (e.g. wastes in the electroplating industry), which are extracted by the organic membrane phase, and change the characteristics and the effectiveness of the membrane in an uncontrolled manner.

The first large-scale plant for LMP was built in the Austrian viscose and rayon industry by LENZING AG for a waste water problem. The waste water is coming from spin baths and contains about 500 mg/l Zinc, which is separated selectively from Calcium down to less than 3 ppm. Several other processes, such as precipitation with H_2S and $Ca(OH)_2$, ion exchange resins and solvent-extraction had been tested, but LMP proved to be the most economic process. A pilot-plant with a throughput of 1 m^3/h waste water was operated successfully for more than 2 years. In this plant all parameters including surfactants and extractants had been optimized prior to the construction of the large scale-plant.

Fig.1 shows a flow-sheet of this plant with the throughputs and concentrations of all phases. The mass transfer apparatus is a countercurrent extraction column with a diameter of 1,6 m and an active height of 10 m. Emulsion preparation is done in a homogenizer and emulsion splitting is done in an electrostatic emulsion splitter.

A major problem in the operation of the pilot-plant was the choice of a suitable extractant. D2EHPA is commonly used for the extraction of Zinc in the hydrometallurgical industry, but the selectivity of this extractant to Calcium was not sufficient in this case. Cyanex 272 and PC-88A had the required selectivity, but the extraction efficiency was too small at the given pH-value. Only the use of Bis(2-ethylhexyl)dithiophosphoric acid made it possible to solve the problem in a satisfactorily manner.

valid and new models have to be developed which account for a mass transfer resistance of the stripping reaction.

whether ~~If~~ the Liquid-Membrane-Process will be a suitable process for the recovery of Zinc in the hydrometallurgical industry, will mainly depend on the impurities, such as Copper, Lead, Cadmium, Iron...., and whether ~~if~~ the impurities should be co-extracted, or if Zinc should be separated selectively.

Due to the combination of extraction and stripping into one step, the selectivity of the liquid membrane process is always less than it is in solvent-extraction, because the scrubbing stages are missing. The selectivity of the process is dependent on the selectivity of the extractant and there are not much possibilities to influence this selectivity. Therefore the application of the LMP-process will always be restricted to solutions, which contain only very few metals, or solutions, where all metals should be separated.

An exception of this is the separation of Copper. The hydroxioxime-extractants are very selective for Copper and impurities are extracted only to a very small extent. A lot of work has been done in the field of Copper-permeation and several pilot-plants proved the feasibility of this process. But despite of these promising reports there existed still another problem, which has not been noticed up to now, and which also causes many troubles in the permeation of other metals. This problem is the choice of a suitable surfactant. The surfactant is probably the most important component in the emulsion liquid membrane technique, for a very stable primary emulsion, where no break-up of the internal droplets occurs, is a prior condition for the application of emulsion liquid membranes. Therefore surfactants were always chosen according to their ability for stabilizing the emulsions. But for an application of emulsion liquid membranes in industrial processes a lot of other requirements have to be fulfilled by the surfactants. Important points are the capability of transporting water, the mass transfer resistance, the solubility in water and resistance to bacteria.

Mainly two surfactants - ECA 4360 and SPAN 80 - have been used up to now, and for the Zinc-permeation ECA 4360 is the most suitable surfactant, but in the Copper-permeation this surfactant has a catalytic effect on the decomposition of the hydroxioxime extractant, which is much more dramatic than is known in solvent-extraction. The chemistry of this decomposition is not quite clear, but there exist a lot of surfactants which show the same behaviour.

Bis(2-ethylhexyl)dithiophosphoric acid is a very strong extractant for many cations, but nevertheless it is nearly unknown in solvent-extraction. At least for the Zinc- and Nickelextraction this is not due to bad equilibrium conditions, but to very low kinetics of the stripping extraction. Fig.2 shows the equilibrium isotherms for the Zinc- and Nickel-extraction. It can be seen that stripping is possible with sulfuric acid, higher than about 150 g/l (3n). So there is no restriction by the equilibrium condition. But the stripping reaction for Zinc is very low and for Nickel it is extremely low, so that very large extraction apparatus would be necessary for the Zink-extraction and no conventional extraction equipment is suitable for the Nickel-extraction. In table 3 some data are listed for the stripping of Zinc and Nickel (100 % = equilibrium) in a shaker and a homogenizer with 250 g/l H_2SO_4. It can be seen that the equilibrium of the stripping reaction is reached in shaking funnel at vigorous shaking after 2 h for the Zinc-reextraction and after 4 h for the Nickel-reextraction, whereas in a homogenizer equilibrium could be reached after 4 min for Zinc and 10 min for Nickel.

Table 3: % of equilibrium for the stripping of Zinc and Nickel

Time	Shaker		Homogenizer	
	Zinc	Nickel	Zinc	Nickel
4	20	3	100	70
10	35	15	100	98
30	45	25		100
60	60	40		
120	100	70		
240		100		

These data clearly show that the equilibrium for the stripping reaction is reached much more rapidly in a homogenizer than in a shaker, because of the very large interfacial area. The reaction of Zn(Ni)-di(2-ethylhexyl)dithiophosphate and sulfuric acid takes place at the interface. Liquid membranes offer an inner interfacial area of about 10^6 m^2/m^3 and therefore the kinetics of the stripping reaction is much higher than it is in solvent-extraction.

Because of this large interfacial area, the stripping reaction was never regarded to represent a considerable mass transfer resistance, but when Bis(2-ethylhexyl)ditiophosphoric acid is used for the Zinc and especially for the Nickel-extraction, this assumption is no longer

Table 4 shows the effects of some surfactants on stability, osmosis, mass transfer resistance and on the decomposition of the extractants for the permeation of Copper with ACORGA PT5050.

Table 4: Influence of surfactants on Copper-permeation

Surfactant	Mass transfer resistance	Osmosis	Break-up (stability)	Decomposition of extractant
ECA 4360	++	+	++	--
SPAN 20	+	-	+	-
SPAN 40	-	--	++	--
SPAN 60	--	+	++	--
SPAN 65	--	++	++	++
SPAN 80	+	-	++	-
SPAN 85			--	+
TWEEN 65	-	--	+	-
TWEEN 85	-	--	+	-
ANTAROX CA420	-	--	+	++
ANTAROX CO430	-	--	+	+
PA 18	++	+	++	+

Legend: ++ very suitable for Copper-permeation with ACORGA PT5050
+ suitable
- not suitable
-- absolutely not suitable

From this table it can be seen that most SPAN-reagents are very good emulsifying agents, but all have one or more deleterious effects for the permeation of Copper. SPAN 40, 60 and 65 represent a high mass transfer resistance (nearly no Copper transported), whereas SPAN 20, 40 and 80 transport a lot of water (osmosis) from the outer to the inner phase and thereby the concentrated inner phase is diluted again. Of all the investigated surfactants only the surfactant PA 18 met all requirements and showed good results in long time pilot tests. But it should be stressed, that it is the best one only for the Copper-permeation with ACORGA PT5050 and no conclusions can be deduced for the permeation of other metals. Especially for the permeation of anionic Oxo-complexes many other surfactants have to be investigated.

CONCLUSION

With the construction of the first large-scale plant for the Zinc separation in the viscose industry, Liquid-Membrane-Permeation has grown to an industrial process and a lot of pilot-plants proved the feasibility of this process for the separation of many other metals. At the moment no large-scale plants may be expected in the hydrometallurgical industry, but waste water treatment seems to be a very promising field of application. This is because the separation of many metals is as good or even better than other processes and the metals need not to be disposed, but can be recovered.

An important feature in the application of emulsion liquid membranes is the choice of a suitable surfactant. Up to now surfactants were only chosen according to their ability of stabilizing emulsions. But there are many other important points such as mass transfer resistance, capability of transporting water, decomposition of extractant and resistance to bacteria.

The selectivity is usually worse than in solvent-extraction. But the development of new extractants may not only enhance the selectivity, but also open new fields of application.

REFERENCES

/1/ N.N. Li, US Patent 3410794 (1968)

/2/ H.C. Hayworth, W.S. Ho, W.A. Burns, N.N. Li, Sep.Sci.a.Techn. 18 (6), (1983) 493-521

/3/ N.N. Li, R.P. Cahn, D. Naden, R.W. Lai, Hydrometallurgy, 9/3 (1983) 227-305

/4/ X. Li, Y. Chang, Proc.JT Meet.Chem.Eng., Chem.Ind.Eng.Soc. China Am.Inst.Chem.Eng. 2 (1982) 571-582

/5/ S. Weiss, U. Grigoriev, P. Mühl, J.Membr.Sci. 12 (1982) 119-129

/6/ M. Prötsch, R. Marr, ISEC'83, Denver, 66-67

NOMENCLATURE

D2EHPA = Bis(2-ethylhexyl)phosphoric acid

PC-88A (Daihachi) = Bis(2-ethylhexyl)phosphonic acid

Cynex 272 (Cyanamid) = Bis(2-ethylhexyl)phosphinic acid

SPAN 80 = Sorbitanmonooleat

ECA 4360 (Exxon) = Polyamine

PA 18 = Copolymere of Maleic acid and 1-Octadecen

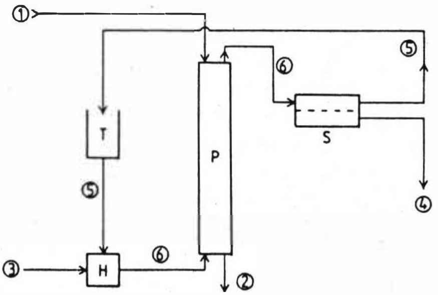

① waste water, 75 m^3/h, 500 mg/l Zn
② waste water, 75 m^3/h, 1-3 mg/l Zn
③ receiving phase, 0,5 m^3/h, 250 g/l H_2SO_4
④ receiving phase, 0,5 m^3/h, 60 g/l Zn
⑤ organic phase, 5 m^3/h
⑥ emulsion, 5,5 m^3/h
P permeation column
H homogenizer
S electrostatic splitter
T tank for organic phase

Fig 1 : Flow-sheet of a plant for Zn-recovery

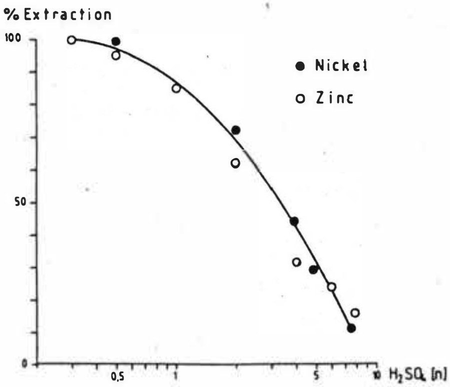

aqueous phase: 1 g/l Zn, Ni
organic phase: 5 wt% Di(2-ethylhexyl)dithiophosphoric acid
95 wt% Shellsol T
phase ratio: 1:1

Fig 2 : Equilibrium for Zn-and Ni-extraction

Metal Extraction with Liquid Surfactant Membranes: The Role of the Emulsifying Agent

B. A. Mikucki and K. Osseo-Asare
Department of Materials Science and Engineering
The Pennsylvania State University
University Park, PA 16802 USA

The relatively slow rate of metal extraction with liquid surfactant membrane (LSM) systems has been attributed to two main factors (1). First, metal extraction may be controlled by the slow diffusion rate of the complexed metal through the membrane phase (1,2). Second, the emulsifier may slow down the rate of interfacial chemical reactions (1,3). These proposals have generally been offered solely on the basis of metal extraction data. In order to gain further insight into the role played by the emulsifier in the extraction process, additional physico-chemical experimental data are needed. For example, direct measurements of interfacial reaction kinetics coupled with an investigation of the adsorption characteristics of both the emulsifier and extractant molecules would help to clarify the manner in which the presence of adsorbed emulsifier molecules influences the rate of metal extraction.

In order to investigate the role of the emulsifier type in the LSM extraction process, a comparative study of the performance of four different emulsifiers, Span 80 (active ingredient, sorbitan monooleate), Arlacel 83 (active ingredients, sorbitan mono- and di-oleates), Span 85 (active ingredient, sorbitan trioleate), and Brij 72 (active ingredient, polyoxyethylene(2)stearyl ether) in LSM copper extraction systems has been undertaken. The experimental techniques employed included the measurement of interfacial tension, membrane stability (as determined by K^+ transfer from the internal to the external phase), and copper transfer using both LSM and Lewis cell (with a conventional organic phase) systems.

Experimental

The extractant used in this study consisted of a mixture of the separately purified anti-isomers of the Henkel reagents LIX65N and LIX63 (4,5). In the discussion below, LIX65N and LIX63 refer to the respective purified anti-isomers. The emulsifiers, Span 80, Arlacel 83, Span 85, and Brij 72, (see Figure 1), were supplied by ICI Americas, Inc., and were used without further purification. Reagent grade cyclohexane was used as the organic diluent in all but the interfacial tension studies where spectroquality cyclohexane was used, and organic solutions were prepared as described previously (4,5). All inorganic chemicals were reagent grade, and doubly distilled deionized water was used to prepare the aqueous solutions.

The experimental and analytical techniques employed are discussed in detail elsewhere (4,5,6) and include interfacial tension measurements, batch LSM experiments in a baffled reactor, Lewis cell experiments, and atomic absorption spectrophotometry. In the interfacial tension studies, the aqueous phase contained 1.1 kmol m^{-3} Na_2SO_4 adjusted to pH 2.0 with H_2SO_4. The internal phase (20 cm^3) used in the LSM experiments was an aqueous solution of 1.0 kmol m^{-3} H_2SO_4 and 0.1 kmol m^{-3} K_2SO_4; the membrane phase (20 cm^3) was a cyclohexane solution of 0.10 kmol m^{-3} LIX65N, 0.014 kmol m^{-3} LIX63, and varying amounts of the emulsifier; the external phase (270 cm^3) was an aqueous sulfate solution containing 1.1 kmol m^{-3} Na_2SO_4 and 0.30 g L^{-1} Cu at pH 2.0 and this same solution was used in the Lewis cell experiments.

Results and Discussion

Interfacial Activity

Interfacial tension data for emulsifier-containing systems obtained in the absence and presence of 0.1 kmol m^{-3} LIX65N are presented in Figure 2. All the emulsifiera exhibit interfacial activity, as indicated by the decrease in interfacial tension with increase in emulsifier concentration. In the absence of LIX65N, the large decrease in the absolute value of the slopes of the interfacial tension isotherms at high concentrations of the emulsifying agents can be attributed to the aggregation of the emulsifiers to form inverted micelles. The critical micelle concentration (CMC) occurs at a concentration of about 0.1 g L^{-1} (2.3×10^{-4} kmol m^{-3}) for Span 80, 0.17 g L^{-1} for Arlacel 83, 2.14 g L^{-1} (2.2×10^{-3} kmol m^{-3}) for Span 85, and 4.0 g L^{-1} (1.1×10^{-2} kmol m^{-3}) for Brij 72. The molar concentrations were calculated by assigning molecular weights of 428, 956, and 358 to Span 80, Span 85, and Brij 72 respectively (i.e., the emulsifiers were assumed to be pure sorbitan monooleate, pure sorbitan trioleate, and pure polyoxyethylene(2)stearyl ether respectively). It is difficult to assign a molecular weight to Arlacel 83 as it contains two major constituents, sorbitan monooleate and sorbitan dioleate in unknown proportions. The observed CMC of Span 80 (0.1 g L^{-1}) agrees well with that in Diesel oil (0.45 g L^{-1} (7)), but it is somewhat different from that found by Jain and Singh for Span 80 in cyclohexane (1.9 g L^{-1}) (8). Using the Gibbs equation, limiting interfacial areas for Span 80, Span 85, and Brij 72 were calculated, i.e., 46, 64, and 66 $Å^2$/molecule respectively (4). The value for Span 80 agrees reasonably well with that found by Sherman (9) for the liquid paraffin/water interface (i.e., 40 $Å^2$).

The fact that at most concentrations Span 85, Arlacel 83, and Span 80 are all more interfacially active at the cyclohexane/water interface than is Brij 72 (see Figure 2, bearing in mind the different molecular weights) can be understood by considering the nature of the hydrophobic tails of the emulsifiers. The hydrophobic tail of a polyoxyethylene(2)stearyl ether molecule is saturated whereas the hydrophobic tails of sorbitan mono-, di-, and trioleate molecules are unsaturated (Figure 1). Since cyclohexane is a saturated hydrocarbon diluent, polyoxyethylene(2) stearyl ether will be more strongly solvated than any of the esters and, thus, less surface active. In addition, the polar head of a polyoxyethylene(2)stearyl ether molecule contains fewer hydrophilic groups than does the polar head of a sorbitan ester (Figure 1). As a result, the driving force for the transfer of emulsifier molecules from the bulk organic phase to the organic/aqueous interface may be smaller for Brij 72 than for the other emulsifiers.

Although the hydrophilic portions of sorbitan mono-, di- and trioleate molecules are all very similar, the size of the hydrophobic portion of a sorbitan trioleate molecule is greater than that of a sorbitan monooleate molecule. This is reflected in the greater value of the limiting interfacial area for Span 85 than for Span 80 (i.e., 64 and 46 $Å^2$/molecule respectively). A comparison between the oleate emulsifiers also indicates that the CMC values increase in the order Span 80 < Arlacel 83 < Span 85. This can again be understood in terms of steric factors. For example, branching of the hydrophobic portion of the molecules inhibits the packing of the molecules into micelles.

For all of the emulsifiers, the presence of LIX65N shifts the interfacial tension isotherms to the right (Figure 2). This can be understood in terms of the competitive adsorption between the emulsifier and the extractant (4,5). Qualitatively, the adsorption of the emulsifier can be considered to occur via a reaction of the type:

$$\text{n(Emulsifier)}_o + \text{(LIX65N)}_i = \text{(LIX65N)}_o + \text{n(Emulsifier)}_i \qquad (1)$$

where the subscripts o and i refer to the bulk organic phase and the organic/water interface respectively, and the coefficient n accounts for the different cross-sectional areas that molecules of LIX65N and the emulsifier occupy at the interface. Thus, a high bulk organic phase concentration of LIX65N will inhibit the adsorption of the emulsifier. For all of the emulsifiers, the CMC either disappears or shifts to higher values when LIX65N is added (Figure 2). This can be attributed to a bulk-phase interaction between the emulsifiers and the extractant (4,5).

Membrane Stability

Figure 3 presents the effects of emulsifier concentration on membrane breakdown. It can be seen that in all cases, the percent membrane breakdown decreases with increase in emulsifier concentration. As demonstrated by the interfacial tension data (Figure 2), as the concentration of the emulsifier increases, the emulsifier will be adsorbed to a greater extent. Hence, a more compact and more strongly adsorbed interfacial film of emulsifier molecules would form (i.e., film strength would increase). In addition, the emulsion will become more viscous (4). Since the resistance of an emulsion globule to membrane rupture increases as the strength of the interfacial film and the viscosity of the emulsion are increased, the observed trend is to be expected. Figure 3 also shows that membrane stability decreases in the order (bearing in mind the different molecular weights) Span 80 > Arlacel 83 >> Span 85 > Brij 72, which follows the same trend as the copper extraction results (see below). The fact that the concentration required to achieve good membrane stability varied widely with emulsifier type can be understood in terms of the relative interfacial activities of the emulsifying agents in the presence of the extractant, and the nature of the interfacial films promoted by them. For example, the fact that Span 85 is less interfacially active than Span 80 mesns that a greater molar concentration of Span 85 is needed in order to achieve good membrane stability.

Effects of Emulsifier Type and Concentration on Metal Extraction

The effects of the emulsifier type and concentration on the amount of copper extracted at 2 hours with the LSM technique are shown in Figure 4. Span 80 performed the best, followed closely by Arlacel 83. Span 85 performed poorly, and Brij 72 (not shown) gave only negligible extraction. For all the three emulsifiers indicated in this diagram, as the concentration of the respective emulsifier is increased, the amount of copper extracted at 2 hours is seen to initially increase, rise through a maximum, and then decrease. The initial increase is attributable to a decrease in membrane breakdown (see Figure 3). On the other hand, the subsequent decrease in copper extraction observed at high emulsifier concentrations may have several possible causes, including a decrease in the rate of copper complexation at the membrane phase/external phase interface, an increase in the interfacial and membrane viscosity, a decrease in the movement of the internal phase droplets within emulsion globules, and a decrease in the interfacial area at which metal extraction can take place.

The relative interfacial concentrations of emulsifier and extractant molecules would be expected to influence the rate of metal complexation as well as the magnitude of the interfacial viscosity. By coupling the Gibbs adsorption equation to a two-solute Langmuir adsorption model, the interfacial tension data can be used to estimate the adsorption densities of LIX65N and Span 80 under the conditions of the Lewis cell experiments. The results of such a calculation are presented in Figure 5 in addition to experimental data on the effects of Span 80 concentration on copper flux in a Lewis cell experiment in which an organic phase containing Span 80, LIX65N, and LIX63 was used (4,6). Three regions are apparent in the curves of Figure 5. At low Span 80 concentrations, the flux and interfacial tension are large and approximately constant. This region corresponds to a high interfacial population of LIX65N, i.e., little adsorption of Span 80 occurs under these conditions. Between about 10^{-2} and 0.5 kmol m^{-3} Span 80, both the flux and interfacial tension fall rapidly. As the concentration of Span 80 is increased in this region, the interfacial population of LIX65N decreases and that of Span 80 increases. Finally, at concentrations of Span 80 above the CMC, both the interfacial tension and flux curves level off. This third region corresponds to a constant and low interfacial population of LIX65N and a constant and high interfacial population of Span 80. Thus, it can be concluded that Span 80 significantly decreases the rate of copper extraction at the cyclohexane/water interface as a result of its preferential adsorption. The increasing displacement of extractant molecules from the interface leads to a decrease in the rate of the metal complexation reaction. Furthermore, the increasing concentration of emulsifier molecules results in increased interfacial viscosity (10) with a consequent adverse effect on mass transport in the interfacial region.

Acknowledgments

This research was supported by the National Science Foundation under Grant No. CPE 8110756. B.A.M. acknowledges the award of an MRI Fellowship by the Pennsylania Mining and Mineral Resources Research Institute.

References

1. J. Melling, Liquid Membrane Processes in Hydrometallurgy: A Review, Report No. LR330 (ME), Warren Springs Laboratory, Stevenage, U.K., 1979.
2. W. S. Ho, T. A. Hatton, E. N. Lightfoot and N. N. Li, AIChEJ, 28, 662-670 (1982).
3. T. P. Martin and G. A. Davies, Hydrometallurgy, 2, 315-334 (1977).
4. B. A. Mikucki and K. Osseo-Asare, Solv. Extr. Ion Exch., in press.
5. B. A. Mikucki and K. Osseo-Asare, Hydrometallurgy, in press.
6. B. A. Mikucki and K. Osseo-Asare, Metall. Trans. B., submitted.
7. D. N. Bhattacharyya and R. Y. Kelkar, J. Colloid Interface Sci., 92, 260-261 (1983).
8. A. K. Jain and R. P. B. Singh, J. Colloid Interface Sci., 77, 274-277 (1980).
9. P. Sherman, Rheology of Emulsions, Macmillan, New York, 1963, pp. 73-90.
10. P. Sherman, J. Colloid Sci., 8, 35 (1953).

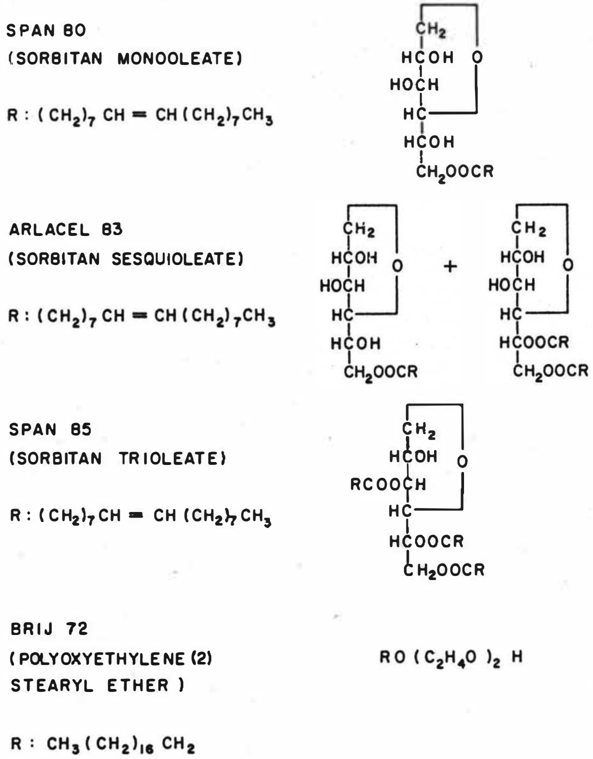

SPAN 80
(SORBITAN MONOOLEATE)
R : $(CH_2)_7CH=CH(CH_2)_7CH_3$
CH_2
HCOH
O
HOCH
HC
HCOH
CH_2OOCR
ARLACEL 83
(SORBITAN SESQUIOLEATE)
R : $(CH_2)_7CH=CH(CH_2)_7CH_3$
CH_2
HCOH
O
HOCH
HC
HCOH
CH_2OOCR
+
CH_2
HCOH
O
HOCH
HC
HCOOCR
CH_2OOCR
SPAN 85
(SORBITAN TRIOLEATE)
R : $(CH_2)_7CH=CH(CH_2)_7CH_3$
CH_2
HCOH
O
RCOOCH
HC
HCOOCR
CH_2OOCR
BRIJ 72
(POLYOXYETHYLENE (2)
STEARYL ETHER)
$RO(C_2H_4O)_2H$
R : $CH_3(CH_2)_{16}CH_2$

Figure 1. Molecular structures of the emulsifying agents.

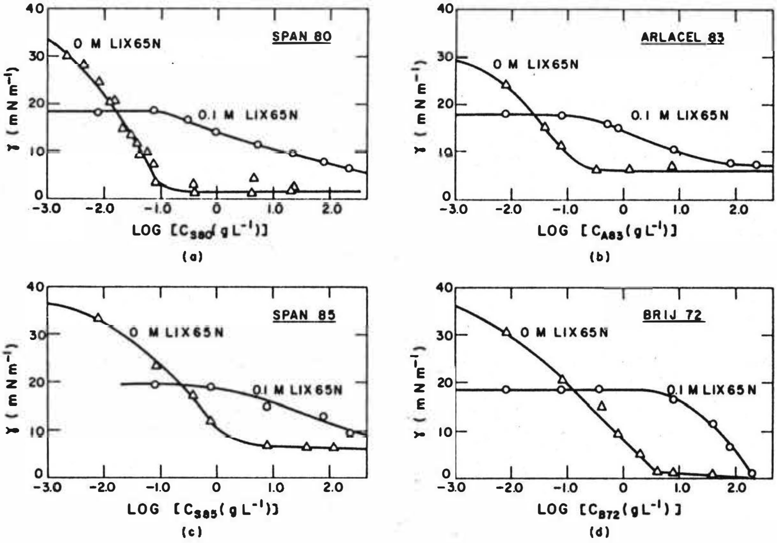

Figure 2. Effect of LIX65N on the interfacial tension isotherms of the emulsifiers at the cyclohexane/water interface.

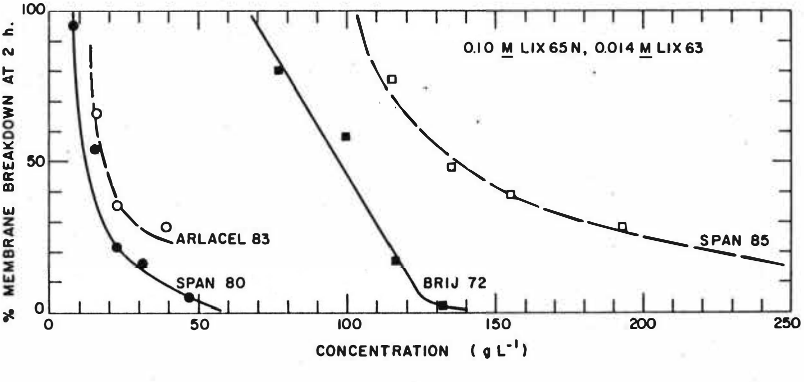

Figure 3. Effects of emulsifier type and concentration (g L^{-1}) on membrane breakdown.

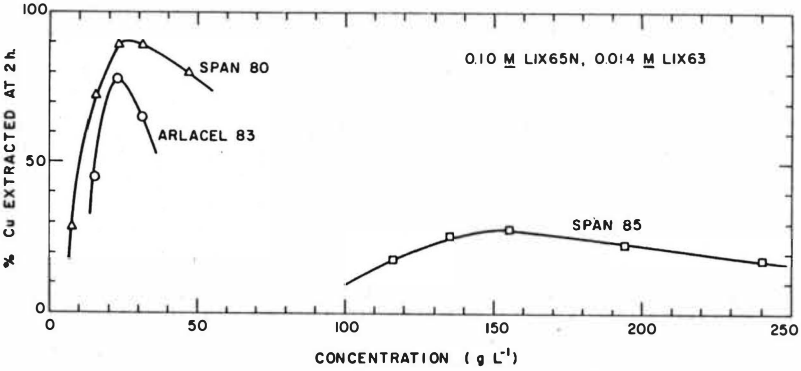

Figure 4. Effects of emulsifier type and concentration (g L^{-1}) on copper extraction in liquid surfactant membrane systems.

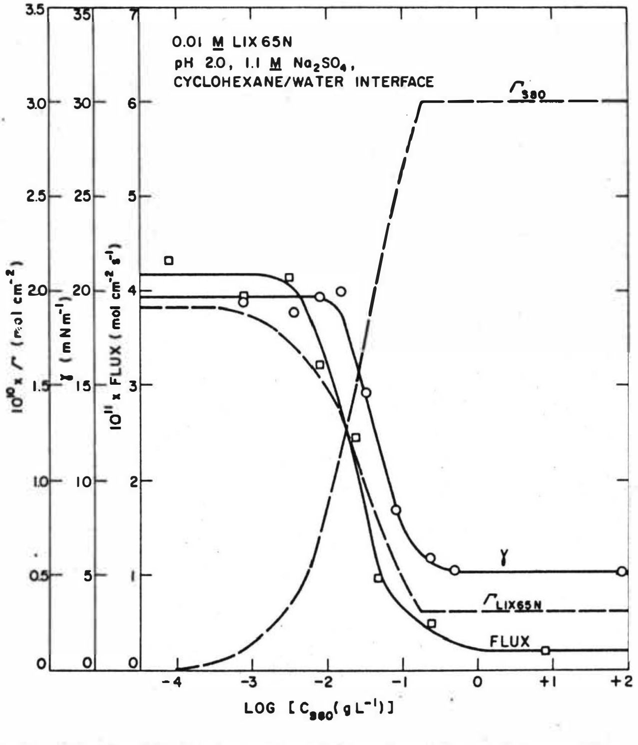

Figure 5. Relationship between competitive adsorption and copper flux. (The organic phase also contained 0.0014 kmol m^{-3} LIX63 in the Lewis cell experiments).

Separation of Copper from a Zinc Solution by Liquid Membrane Permeation

H.-J.Bart, R.Wachter and R.Marr
Techn.University Graz, A-8010 Graz, Austria

Introduction

A current problem in copper recycling process is in a separation of copper from alloy components like zinc, lead, tin, iron etc. The feed solution is leaching solution on a basis of 0,8 to 1,4 g/l Cu, 10 to 15 g/l Zn, 0,05 to 0,2 g/l Fe, traces of lead and tin and antimony in about 0,5 g/l sulfuric acid. This solution may be treated in a contercurrent column with liquid membrane permeation technique. A flow sheet of the pilot plant is in Figure 1 /1/.

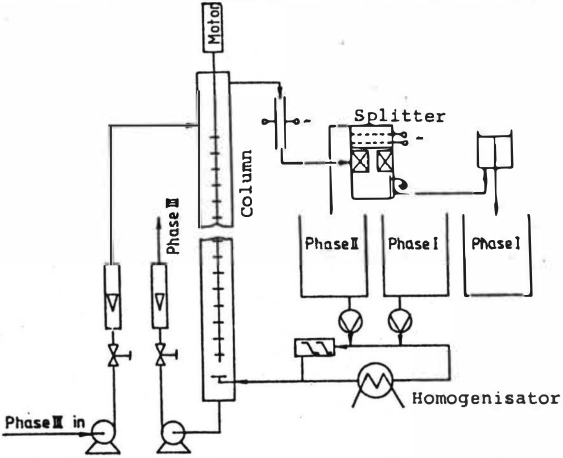

Fig. 1: Flow sheet of the pilot plant, permeation column: 6 m height, 0,1 m diameter; splitting device: 3000 V, 5mA, unisolated electrodes; emulsification: high speed emulsifier, IKA Superdispax S040.

Raffinate of this operation is considered to be of further use in a zinc recovery process. The main problem of the LMP process is the use of a membrane phase which is highly selective for copper. The optimum is to recover at minimum 97 % of the copper. The weight ratio of copper to zinc in the LMP product stream should exceed factor 1000.

After the screening program the optimum membrane phase is as follows:
- 2 % carrier, a salicyhaldoxime (e.g. Acorga P50)
- 2 % surfactant, a polyamine (e.g. Paranox 100)
- 96 % diluent, a kerosene (e.g. Shellsol T)

The internal stripping phase contains 200 g/l sulfuric acid and 15 g/l copper. Splitting and preparation of the emulsion is without special problems.

Pilot Plant Experiments

Pilot plant experiments were done by variation of three main parameters. Table 1 gives the results of different experimental conditions. Input flow of feed phase III was in the range of 50 to 125 l/h. Phase ratio of phase III to phase I was choosen to get a final inner phase I concentration of 45 g/l copper.

Phase ratio of phase II to phase I was in the range of 3 to 7 due to hydrodynamic considerations. As was obvious from the experiments, stirring speed is an dominating parameter in the column runs. The influence is on hold up, mean droplet diameter, residence time distribution function and on radial mixing. With this variation of stirring speed results in different mass transfer regimes in the column at fixed system boundaries (ion concentrations, org.phase composition etc.).

Mass transfer resistance on a liquid membrane globule can be described as following , as is indicated in Figure 2 /2/.

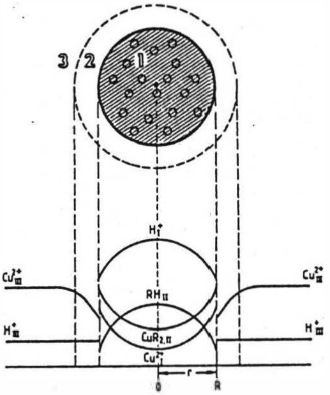

Fig. 2: Mass transfer resistance on a emulsion globule
1) quasihomogenous emulsion globule
2) aqueous film of phase III
3) bulk phase III

1.) film diffusion resistance in phase III
2.) chemical resistance due to reaction at interphase III/II
3.) diffusional resistance in the quasihomogenous emulsion globule
4.) chemical resistance due to reextraction reaction

In our earliest experiments /3/ we used membrane phases of high viscosity. This caused a high diffusional resistance in the emulsion globule. Thus all experimental data would be well described with the shrinking core model by Kopp and Marr /4/.Here a quasihomogenous description of the emulsion globule gives an $\sqrt{t}$ -dependency of the copper flux.

In low viscose systems this effect should not be becoming rate determing. Additionally resistance due to reextraction was never noted in copper systems.

With this, contribution to mass transport resistance can be expected from film diffusion resistance in phase III and chemical reaction resistance at interphase III/II. In regard to a optimum technical lay-out of the permeation column chemical reaction regime should give best results.

In the experiments listed in Table 1 we can distinguish two different regimes. Evidently at high stirring speed we enter pure chemical reaction regime. It is obvious that with a high turbulence mass transfer resistance in the film layer becomes neglegible. All data in chemical reaction regime can be fitted with a simple exponential function. This is due to a kinetical equation of first order in respect to copper. In the experimental area investigated carrier concentration and pH in a first approach enter with zero order. Thus

$$- \frac{d(Cu)}{dH} = k\ (Cu) \tag{1}$$

with

$$H = V_{III} \cdot \tau_{III}/A \tag{2}$$

Integration over the height of the column gives

$$\ln\ ((Cu)/(Cu)_0) = -k\ .\ H \tag{3}$$

For mode of comparison all concentration values should be properly normed. In a dimensionsless form in relation to equilibrium concentration, $(Cu)_{equ}$, copper concentration converts into

$$(Cu) = \frac{(Cu) - (Cu)_{equ}}{(Cu)_0} \tag{4}$$

Thus

$$\ln\ ((Cu) - (Cu)_{equ})/(Cu)_0 = -\ k\ .\ H \qquad (5$$

Table 2 gives k-values in series of tested runs (compare Tab. 1). Runs with high rpm give constant k-values at about 1,14 (1/m). At lower stirring speeds this simple law could not be verified. Data could not be fitted according an exponential function. Is is obvious that chemical reaction is not longer the only dominating factor. Here diffusion of the species act as additional resistence.

However, from this experience, batch experimental data were tested under the same assumption.
Table 3 gives a influence of LIX 64 N under different stirring conditions. All data could be well described with an exponential function and give an related k-value according Equ. 5.
With higher stirring speeds, interfacial area and turbulence degree increases. However, the k-value is expected to increase at higher rpm.

Table 4 gives the influence of different modifiers in the organic phase present. Commercial available ion exchangers have different content of modifiers. The influence is mainly on the final equilibrium value in Phase III. Inasfar, modifier has no markedly influence on the k-value.
The list of k-values of batch experimental data could be extended without difficulties. Kinetical controlled regime is found in experiments with low viscous emulsions which are under high stirring stress during the permeation process.

It can be concluded that kinetical controlled regimes offer better mass transfer results in comparison to diffusional controlled ones in the case of copper. From this point an optimal plant lay-out should be settled in the kinetical reaction regime.

Literature

/1/ R.Wachter, Doctor Thesis, TU Graz, 1986

/2/ D.Lorbach, H.-J.Bart, R.Marr:Ger.Chem.Eng. 1986, in press

/3/ A.Kopp, Doctor Thesis, TU Graz, 1971

/4/ R.Marr, A.Kopp: Chem.Ing.Techn.52 (1980), Nr.5, 399-410

Table 3: Influence of rpm in batch experiments

$V_{III}:V_{II}:V_I$ = 10:2:1

V_I: 30 g/l Cu, 192 g/l H_2SO_4

V_{II}: 4 % LIX 64 N, 2 % Paranox 100, 34 % Shellsol T, 60 % Merck Paraffine thin

V_{III}: 77 g/l zinc, 1,5 g/l Cu, pH = 4,65

n(1/min)	k	C_{equ}/C_0
300	0,11	0,325
500	0,18	0,241
700	0,33	0,261

Table 4: Influence of modifier in batch experiments

$V_{III}:V_{II}:V_I$ = 50:3:1, 250 rpm

V_I: 12 g/l Cu, 200 g/l H_2SO_4

V_{II}: 2 % P 1, 2 % Paranox 100, Shellsol T + Modifier

V_{III}: 0,8 g/l Cu, 18 g/l zinc

% Nonylphenol	k	C_{equ}/C_0
0	0,18	0,034
2	0,17	0,031
6	0,17	0,198

Table 1: Column Experiments

run No.	1	2	3	4	5	6	7	8	9	10	11	12	13	14
V_I(l/h)	2,22	2,53	4,27	6,91	5,11	3,25	3,08	4,34	4,87	3,32	4,55	4,45	4,39	3,98
V_{II}(l/h)	8,40	12,3	13,3	16,1	11,1	9,0	9,0	19,4	19,4	19,4	24,3	26,6	26,6	18,6
V_{III}(l/h)	50	75	100	125	100	100	100	100	100	100	100	100	100	100
$Cu_{I,ein}$(g/l)	15	15	15	15	15	15	15	15	15	15	15	14,5	14,5	0
$Cu_{I,aus}$(g/l)	-	-	35,3	38,7	34,8	42,3	39,1	36,9	37,0	46,5	37,2	34,6	32,4	20
$H_2SO_{4,I,ein}$(g/l)	199	199	199	199	199	199	199	199	199	199	199	199	199	232,7
$H_2SO_{4,I,aus}$(g/l)	-	-	113,2	158,3	164,5	131,2	111,8	138,1	135	111,4	136,6	136,2	124,8	133,9
$Cu_{III,ein}$(ppm)	1380	1380	1380	1380	1100	1100	1100	1400	1400	1400	1400	1140	1140	1140
$Cu_{III,aus}$(ppm)	23	32	31	38	78	44	22	229	51	25	143	34	15	9

Table 2: k-values (column-experiments)

rpm (1/min)	200	200	200	200	160	180	200	160	180	200	160	180	200	200
Cu_{equ}(ppm)	22	19	31	32	85	40	21	45	41	26	37	27	14	9
k (1/m)	1,14	1,12	1,12	1,14	1,11	-	1,11	-	-	1,15	-	-	1,06	1,13

SUPPORTED LIQUID MEMBRANE SEPARATION OF ALUMINUM FROM COPPER LEACHING LIQUORS

By L. E. Schultze, S. P. Sandoval, T. G. Carnahan, and J. A. Eisele

Reno Research Center
Bureau of Mines, U.S. Department of the Interior
Reno, NV 89512
U.S.A.

ABSTRACT

The Bureau of Mines investigated the use of a supported liquid membrane in the separation of aluminum from copper dump leaching liquors. Aluminum was selectively transported through porous polypropylene impregnated with di(2-ethylhexyl) phosphoric acid in an aliphatic diluent. The effects of variables such as solution composition, temperature, and extractant concentration were measured with a three-level factorial experimental design. Response functions were calculated for aluminum, iron, and copper. An aluminum transport rate of 2.6 g $m^{-2}h^{-1}$ was measured. The major variables influencing aluminum transport were solution temperature, pH, aluminum concentration, and extractant concentration.

As the manuscript was not available at the 28th May 1986, the deadline for printing this book, we only print the short abstract of the paper.

Development of New Surfactant in Liquid Surfactant Membrane Process

F. Nakashio, M. Matsumoto, M. Goto, J. Irie, K. Kondo;
Hakozaki, Fukuoka/JAPAN

The application of liquid surfactant membrane(henceforth LSM) to metal recovery process is an attractive approach to separation processes. To develop and design the LSM process, it is very important to elucidate the effect of surfactant on the behavior of LSM, that is, the swelling and break-up of W/O emulsion droplets, the permeation rates of solutes through LSM and the de-emulsification rate of W/O emulsion by the electrical coalescer. In most of papers on metal extraction with LSM, the commercial surfactants, e.g. Span 80 and polyamine, were used to make LSM stabilize. The study on the effect of surfactant on LSM has not been carried out so far.

The purpose of this work is to develop new surfactants for LSM because the commercial surfactants act as the carrier of water and/or solutes in the internal and feed solutions (e.g. acid and metal)(1-4).

In this study, (i) a series of derivatives of glutamic acid di-alkyl ester and di-alkyl type quaternary ammonium salts were prepared as new surfactant, (ii) copper extraction with LSM formed by W/O emulsion made of the new surfactant was carried out in a stirred tank and (iii) W/O emulsion made of the surfactant was de-emulsified by the continuous electrical coalescer.

1. Experimental

The surfactants used were shown in Fig.1.

a) Span 80 and polyamine(ECA 4360J) were used without further purification. Apparent molecular weights of Span 80 and polyamine in heptane measured by vapor-phase osmometry were 602.8 and 706.3, respectively.

b) A series of derivatives of glutamic acid di-alkyl ester(abbreviated as 2R-GE) were synthesized according to the following scheme.

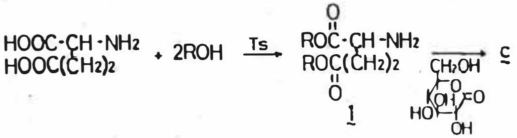

The mixture of L-glutamic acid, higher alcohol and p-toluenesulfonic acid in toluene solution was refluxed for four hours. After that, toluene was removed under reduced pressure and the reaction mixture was dissolved in chloroform, to be washed with 5% sodium carbonate solution and water, successively. Hydrochloric acid was added to the chloroform solution. The solid salt was recrystallized from acetone. The mixture of this salt and glucono-δ-lactone in ethanol solution was refluxed for three hours. After that, the solvent was removed under reduced pressure, the product(c) was recrystallized from acetone.

c) A series of di-alkyl type quaternary ammonium salts(abbreviated as 2R'-QA) were synthesized according to the following scheme(5).

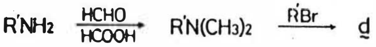

$$R'NH_2 \xrightarrow[HCOOH]{HCHO} R'N(CH_3)_2 \xrightarrow{R'Br} \underset{\sim}{d}$$

Tertiary amine was synthesized from alkylamine, formaldehyde and formic acid and purified by reduced distrillation. Product(d) was prepared from reaction of tertiary amine with alkylbromide.

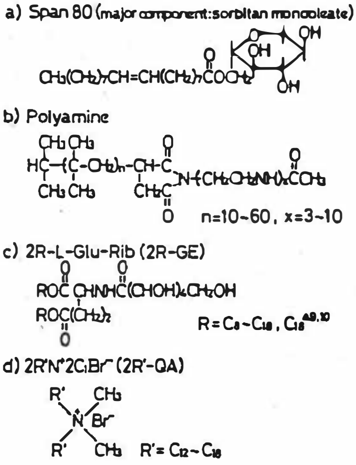
a) Span 80 (major component: sorbitan monooleate)
$CH_3(CH_2)_7CH=CH(CH_2)_7COOCH_2$
OH
b) Polyamine
n=10~60, x=3~10
c) 2R-L-Glu-Rib (2R-GE)
R = C8~C18, C18 Δ9,10
d) 2R'N+2C1Br- (2R'-QA)
R' = C12~C18

Fig.1 Molecular structure of surfactant

The experimental apparatus used for copper extraction with LSM was a batch type stirred tank which was fitted four stainless baffles. The experimental procedure was the same as that described in the previous papers(3,6). The experimental conditions were listed in Table 1.

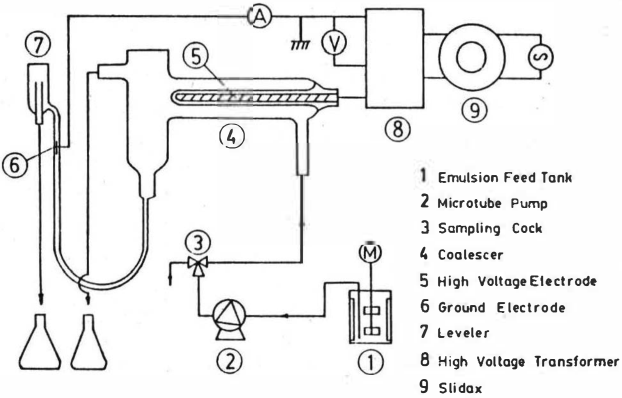
A
V
S
M
1 Emulsion Feed Tank
2 Microtube Pump
3 Sampling Cock
4 Coalescer
5 High Voltage Electrode
6 Ground Electrode
7 Leveler
8 High Voltage Transformer
9 Slidax

Fig.2 Experimental apparatus for de-emulsification

Table 1. Experimental conditions for copper extraction with LSM

Volume of feed aqueous solution (external aq. phase)	$V^{\circ}_{We} = 7\times10^{-4}\ m^3$
Concentration of copper in feed aqueous solution	$C_{CuO} = 1\ kg/m^3$
pH in feed aqueous solution	pH = 5
Extractant	LIX 65N
Extractant concentration	$C_{HRO} = 50\ mol/m^3$
Concentration of synthesized surfactant	$C_s = 10\ mol/m^3$
Concentration of Span 80	$C_s = 3$ wt%
Concentration of polyamine	$C_s = 5$ wt%
Volume of organic solution in W/O emulsion phase	$V_{org} = 5\times10^{-5}\ m^3$ (heptane)
Volume of internal aqueous solution	$V^{\circ}_{Wi} = 5\times10^{-5}\ m^3$
Concentration of sulfuric acid in internal aqueous solution	$C^{\circ}_{H} = 500\ mol/m^3$
Stirring speed	n = 300 rpm
Break-up tracer	$Ni(NO_3)_2^*$
Break-up tracer concentration in internal aqueous solution	$C^{\circ}_{Nii} = 5\ mol/m^3$
Occlusion tracer	$Mn(NO_3)_2^*$
Occlusiontracer concentration in feed aqueous solution	$C^{\circ}_{Mne} = 5\ mol/m^3$

*) Ni(II) and Mn(II) do not react with LIX 65N under this experimental conditions

Table 2. Experimental conditions for de-emulsification

Volume ratio of internal aqueous solution to organic solution in W/O emulsion phase	$V^{\circ}_{Wi}/V_{org} = 1$
Internal aqueous solution	$500 mol/m^3$, NaCl
Applied voltage	E = 1-15 kV
Mean residence time	$\bar{\theta} = 1\text{-}9$ min

The experimental apparatus for de-emulsification by the continuous electrical coalescer was shown in Fig.2. W/O emulsion in the annulus was de-emulsified by the application of AC potential of 1-15kV. The experimental conditions were listed in Table 2.

2. Results and Discussion

2.1 Copper extraction with LSM

Changes of the copper extraction in the feed aqueous solution and of the volume of the internal aqueous solution with the elapse of time are shown in Figs.3 and 4, respectively, for LSMs formed by W/O emulsion made of diverse surfactant. From these figures, it was found that the extent of copper extracted and the swelling rate of W/O emulsion phase depend on surfactant and that glutamic acid di-oleyl ester abbreviated as $2C_{18}\Delta^9GE$ is better than the other surfactants in the points of the extent of copper extracted and the permeation rate of water due to osmotic pressure.

The rate of the break-up of LSM is expressed as follows(7).

$$\frac{d\varepsilon}{dt} = k_b(1 - \varepsilon) \qquad (1)$$

$$\varepsilon = \frac{V_{We}C_{Nie}}{V^{\circ}_{Wi}C^{\circ}_{Nii}} \qquad (2)$$

where k_b is a constant for break-up, V_W is the volume of the aqueous solution, C_{Ni} is the concentration of Ni(II) as break-up tracer, the

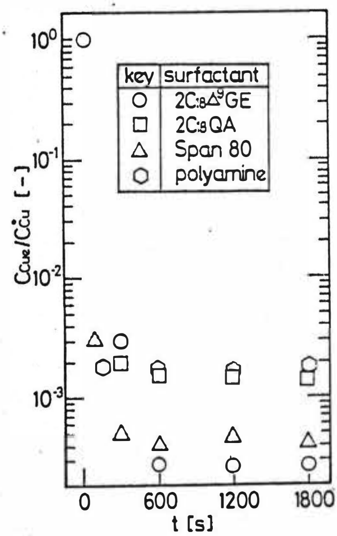

Fig.3 Change of copper extraction in feed aqueous solution

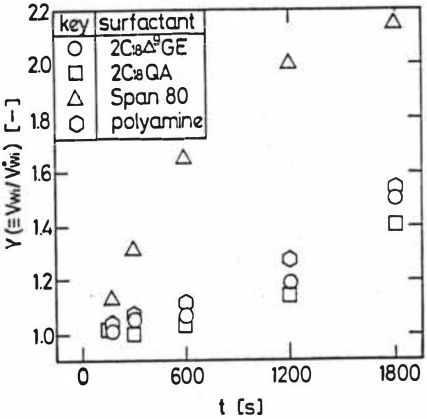

Fig.4 Volume change of internal aqueous solution

subscripts e and i denote the feed aqueous solution and the internal aqueous solution in W/O emulsion phase, respectively, and the superscript ° denotes the initial value.
Figure 5 shows the rate constant of the break-up of LSM, k_b, for each surfactant. From Fig.5, it was found that the surfactant $2C_{18}\Delta^9$GE forms the most stable LSM as compared with the other surfactants used and that k_b decreases with increasing alkyl-chain length of 2R'-QA, but in the case of 2R-GE having more than 12 carbon atoms k_b becomes constant.

The permeation rate of water through LSM due to osmotic pressure is obtained from the experimental results of V_{Wi} and ε as follows.
The mass balance of water is expressed by Eq.(3):

$$\frac{dY}{dt} = k_b Y - r_p \qquad (3)$$

$$Y = \frac{V_{Wi}}{V_{Wi}^{\circ}} \qquad (4)$$

where r_p is the rate of water permeation through LSM.
From Eqs.(1) and (3), r_p is calculated by the following equation.

$$r_p = \frac{dY}{dt} + \frac{Y}{1-\varepsilon}\,\frac{d\varepsilon}{dt} \qquad (5)$$

Figure 6(a) shows the initial permeation rate of water, r_{po}, for each

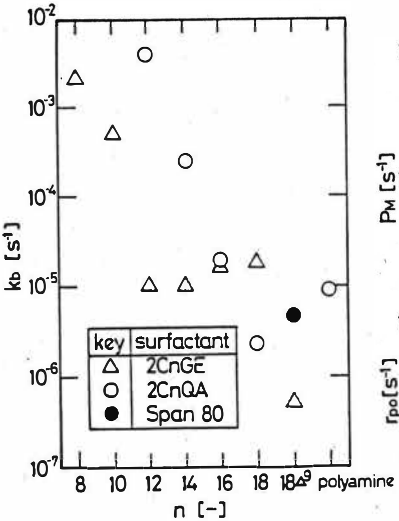

Fig.5 Effect of alkyl-chain length on break-up of LSM

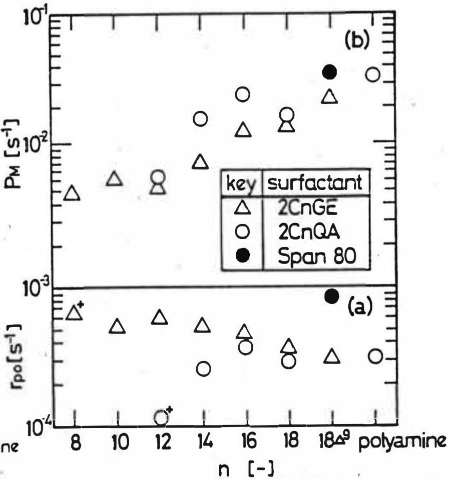

Fig.6 Effect of alkyl-chain length on permeation rates of water and copper

+ uncertainty value since break-up of LSM is large surfactant. From Fig.6(a), it was found that the effect of alkyl-chain length of the surfactant on the initial permeation rate of water through LSM is negligibly small and that Span 80 has more influence on the water permeation than the other surfactants.

From the experimental results shown in Fig.3, the permeation rate of copper through LSM is considered to be proportional to the copper concentration in the feed aqueous solution, except for high extent of copper extracted, that is,

$$-\frac{dC_{Cue}}{dt} = P_M C_{Cue} \qquad (6)$$

where P_M is a permeation coefficient of copper through LSM. P_M obtained from Eq.(6) is shown in Fig.6(b). From Fig.6(a) and (b), it was found that the LSM formed by W/O emulsion made of $2C_{18}\Delta^9$GE is better than the other surfactants used in the points of the permeation rates of copper and water.

2.2 De-emulsification by a continuous electrical coalescer

Figure 7 shows the effect of surfactants on the extent of W/O emulsion de-emulsified, Z, by the continuous electrical coalescer. Z is defined by Eq.(7).

$$Z = \frac{C_W}{C_W^o} \qquad (7)$$

where C_W is water content in the W/O emulsion. In this figure, $\bar{\theta}$ represents the mean residence time. From Fig.7, it was found that the extent of W/O emulsion de-emulsified in $\bar{\theta}$ >300s becomes greater in the order, $2C_{18}\Delta^9$GE>Span 80>polyamine>> $2C_{18}$QA. The W/O emulsion made of $2C_{18}$QA was not de-emulsified by applied voltage of 15 kV.

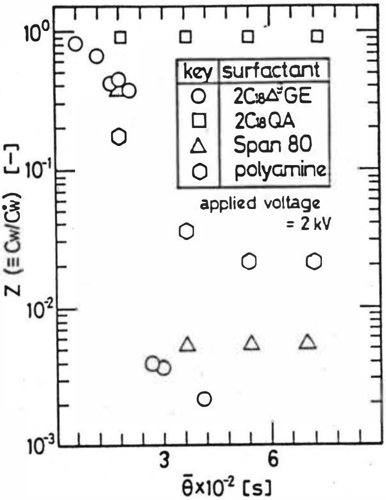

Fig.7 Effect of surfactant on extent of de-emulsified

Conclusion

The copper extraction with LSM was carried out in the stirred tank by using several new surfactants, that is, a series of derivatives of glutamic acid di-alkyl ester and di-alkyl type quaternary ammonium salts. The following results were obtained.

1) Glutamic acid di-oleyl ester forms the most stable LSM as compared with the other synthesized surfactants, Span 80 and polyamine.

2) The effect of alkyl-chain length of the surfactant on the permeation rate of water through LSM is negligibly small.

3) The LSM formed by W/O emulsion made of glutamic acid di-oleyl ester is better than the other surfactants used in the points of permeation rates of copper and water.

4) The W/O emulsion made of glutamic acid di-oleyl ester was easily de-emulsified by the continuous electrical coalescer.

References

1) J. Draxler, R. Marr;Ber. Bunsenges. Phys. Chem.,86,64(1982)
2) M. Matsumoto, K. Kondo, F. Nakashio;Nippon Kagaku Kaishi,1983,741
3) P. Colinart, S. Delepine, G. Trouve, H. Renon; J. Membr. Sci., 20,167(1984)
4) K. Fujinawa, T. Morishita, M. Hozawa, H. Ino; Kagaku Kogaku Ronbunshu 11,293(1985)
5) T. Kunitake, Y. Okahata, K. Tamaki, F. Kumamaru, M. Takayanagi; Chem. Lett.,1977,387
6) F. Nakashio, K. Kondo, J. Irie; Proc. 2nd World Congress of Chem. Eng., vol.4,p450(1981)
7) L. Boyadzhiev, T. Spundzhiev, E. Bezenshek; Separ. Sci.,12,541(1977)

Ionizable Crown Ethers for Coupled Transport of Metals across Liquid Membranes

R. A. Bartsch, W. A. Charewicz, S. I. Kang, W. Walkowiak, Department of Chemistry and Biochemistry, Texas Tech University, Lubbock, TX 79409-4260, USA

Transport of ionic species through membranes is of central importance in biological systems and is playing an increasing role in the development of practical separation schemes. Of the several transport mechanisms which have been demonstrated, coupled transport mediated by mobile carriers (ionophores) is one of the simplest mechanisms for the selective removal of a desired ion from a dilute solution. In such a system, the flux of one ion moving down its concentration gradient is used to drive the transport of the desired ion up its concentration gradient. Typically the "driving" gradient is due to protons with cations moving by countertransport from basic to acidic solution. Cation-proton-coupled countertransport has been demonstrated in natural and artifical systems for many of the carboxylate ionophore antibiotics. Thus, sodium is pumped from basic to acidic aqueous solution through a supported octanol membrane containing the sodium specific antibiotic monensin (1). Similarly calcium is transported across bulk liquid membranes and from vesicles by lascalocid (X 537-A) and calcimycin (A 23187) (2-5).

With such systems as models, we (6-9) and others (10-13) have prepared synthetic crown ether carboxylic acids and shown them to act in a completely-analogous fashion for the transport of alkali metal cations across bulk liquid organic membranes. In related studies, a 4-pyridone-fused crown ether has been utilized as the ionizable crown ether carrier in alkali metal cation transport (14).

A new series of crown ether carboxylic acids 1-3 has now been prepared and utilized as carriers for competitive transport (7) of alkali metal cations from basic aqueous solution across a bulk chloroform membrane into an acidic aqueous receiving phase. All three carriers exhibited transport ordering of K$^+$>Rb$^+$>Cs$^+$>Na$^+$>Li and similar fluxes which identifies the nature of the crown ether ring as the dominant structural factor in determining transport selectivity and efficiency for these carriers.

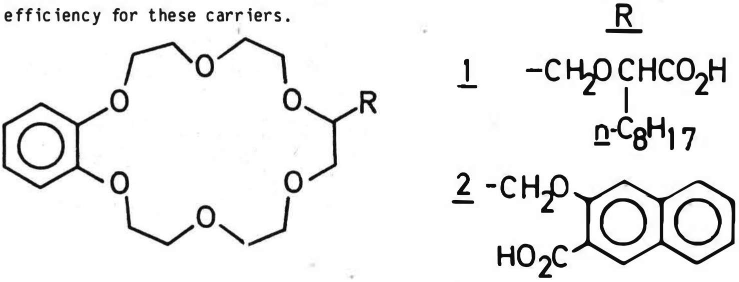

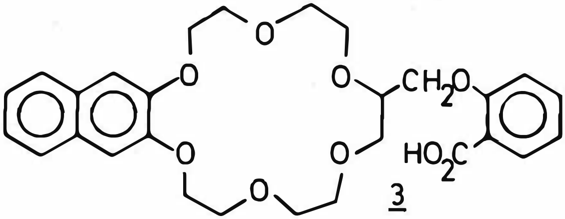

3

To systematically examine the influence of crown ether ring size variation upon the transport of alkali metal cations across bulk chloroform membranes, a series of crown ether phosphonic acid monethyl esters 4-7 was prepared. For competitive

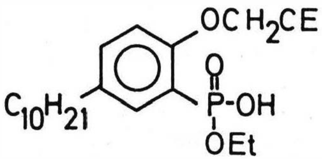

	CE		CE
4	15-Crown-5	6	21-Crown-7
5	18-Crown-6	7	24-Crown-8

transport (7) from basic aqueous solution across a chloroform membrane into an acidic aqueous receiving phase, the transport selectivity orderings were: with 4, $Na^+ >> K^+ > Li^+$, Rb^+, Cs^+; with 5, $K^+ > Rb^+ > Cs^+ > Li^+, Na$; with 6, $Rb^+ \approx Cs^+ > K^+ > Li^+, Na^+$; and with 7, $Na^+ \approx K^+ \approx Rb^+ \approx Cs^+ > Li^+$. The transport selectivities observed with 4, 5 and 6 are those which would be predicted according to the crown ether cavity sizes. The almost total loss of transport selectivity observed with 7 indicates that the crown ether ring no longer remains planar in the complex but conforms to the size of the complexed cation.

Additional results for competitive transport of alkali metal cations across emulsion (liquid surfactant) liquid membranes (15) by a crown ether phosphonic acid monoethyl ester and across polymer supported liquid membranes by crown ether carboxylic acids will be presented.

References

(1) E. M. Choy, D. F. Evans and E. L. Cussler, J. Am. Chem. Soc., 96, 7085 (1974).

(2) B. C. Pressman and N. T. Guzman, Ann. N. Y. Acad. Sci., 264, 373 (1975).

(3) W. J. Malaisse, I. Valverde, G. Devis, G. Somers and E. Couturier, Biochimie, 61, 1185 (1979).

(4) E. Couturier and W. J. Malaisee, Biochemie, 62, 177 (1980).
(5) J. Bolte, C. Demuynck, G. Jeminet, J. Juillard and C. Tisier, Can. J. Chem., 60, 981 (1982).
(6) J. Strzelbicki and R. A. Bartsch, J. Membrane Sci., 10, 35 (1982).
(7) W. A. Charewicz, G. S. Heo and R. A. Bartsch, Anal. Chem., 54, 2094 (1982).
(8) W. A. Charewicz and R. A. Bartsch, Anal. Chem., 54, 2300 (1982).
(9) W. A. Charewicz and R. A. Bartsch, J. Membrane Sci., 12, 323 (1983).
(10) L. A. Frederick, T. M. Fyles, V. A. Malik-Diemer and D. M. Whitfield, J. Chem. Soc., Chem. Comm., 1211 (1980).
(11) L. A. Frederick, T. M. Fyles, N. P. Purgrasad and D. M. Whitfield, Can J. Chem., 49, 1724 (1981).
(12) L. A. Frederick, T. M. Fyles, V. A. Malik-Diemer and D. M. Whitfield, Can. J. Chem., 59, 1734 (1981).
(13) T. M. Fyles, V. A. Malik-Diemer, C. A. McGavin and D. M. Whitfield, Can. J. Chem., 60, 2259 (1982).
(14) R. M. Izatt, G. C. Lindh, G. A. Clark, J. S. Bradshaw, Y. Nakatsuji, J. D. Lamb and J. J. Christensen, J. Chem. Soc., Chem. Comm., 1676 (1985).
(15) R. A. Bartsch, W. A. Charewicz and S. I. Kang, J. Membrane Sci., 17, 97 (1984).

Acknowledgement

This research was supported by the Office of Basic Energy Sciences of the United States Department of Energy (Contract DE-AS05-80ER-10604).

Recovery of Indium from Industrial Solutions by Supported Liquid Membranes

R. Guerriero, SAMIM Centro Ricerche Veneto, Venice, Italy
L. Meregalli, SAMIM Centro Ricerche Veneto, Venice, Italy
X. Zhang, Beijing General Research Institute of Mining and Metallurgy, Beijing China

A quite extensive literature is now available on the supported liquid membrane technique. From this literature it can be derived that the most important advantages with respect to solvent extraction and, to a lesser extent, with respect to emulsified liquid membranes are: 1) the need of very limited quantities of extractant, which permits the use of more selective extractants and of course limits quite drastically the volume of the circulating phases; 2) the achievement of the separation in one stage only; 3) no phase separation problems since the two phases are never mixed. Still, little is know on actual attempts to apply it to industrial systems and on its angineering. This study was undertaken in order to collect the necessary information on the actual applicability with tha available extractants and supports, and to examine its limits and its advantages with respect to other more traditional techniques.

From what discussed before and from experimental tests performed on already known systems (such as Cu extraction from H2SO4 solutions or Cu-Zn separation), the following preliminary observations were derived: at the present state of the art such a technique can be useful to extract metals present in relatively low concentrations (a few g/l or less) in solutions containing also high concentrations of metals and other ions (high acidities and basicities, brines, etc.). The reason for which low concentrations are preferred is that only limited metal fluxes are achievable through the membranes and do not allow a massive transfer; on the other hand, very high amounts of organic phase would be needed to treat diluted solutions with the solvent extraction technique. In addition to this, the improvement of selectivity which can be obtained with the supported liquid membrane technique, favours the separation of minor metals with respect to concentrated metals. Finally, concentrated solutions can be easily achieved with the "coupled transport" mechanisms by suitably modifying the acidity (or the ligand concentrations) of the stripping solutions.
During these studies it was also concluded that commercially available supports could satisfy the most basic requirements for their application in this field: good stability with respect to both the organic and the aqueous phases (which leads to an acceptable life-time of the support itself), good affinity with respect to the more common solvents used in the organic phase (which leads to an acceptable life-time of the liquid membrane) and availability of different configurations with which to build different modules. The possibility of working for a reasonable length of time with reactors very similar to an industrial prototype allows for the application of the technique to a system of industrial interest for the optimization both of the chemistry of the process and of its engineering. With regard to the supports, though, an important drawback of the SLM technique is their cost. Since a reduction of these costs cannot be forseen in the near future, another requirement for the application of the SLM technique is that the metal to be extracted must be quite valuable.

Based on these considerations, a hydrometallurgical system of industrial interest to be used as a test system had to be found. The extraction of indium from copper solutions from the leaching of copper drosses from lead refining process was considered to have the proper characteristics. The investigation on this system was carried out with the aim of inserting a stage of In extraction by the SLM technique, in parallel with a solvent extraction unit, in an original hydrometallurgical flowsheet for the treatment of copper drosses.

The preliminary tests carried out to optimize the operating conditions are the object of the present work.

EXPERIMENTAL

Reagents and equipment

The aqueous phase: the feed solution

The typical composition of the solution obtained from the sulfuric acid leaching of copper drosses of an I.S. plant is approximately the following:

In 0.5 – 1 g/l
Cu ≈ 70 g/l
As ≈ 3 g/l
Zn ≈ 12 g/l
Fe^{3+} ≈ 2 g/l
Sb ≈ 0.4 g/l
Bi ≈ 0.002 g/l
Ag < 0.002 g/l
H_2SO_4 ≈ 30 g/l

As discussed in the introduction, the low levels of In, the small amounts produced at an industrial level, the relatively high value of the metal (≈70 $/Kg March 1986) makes this system particularly interesting for investigation.

The organic phase

D2EHPA is already industrially used in the extraction of In and some direct experience with its application in In separation by solvent extraction and by resins was already available. For this reason it was chosen for the first application in liquid membranes. Besides, D2EHPA had been already used with success for Zn-Cu separations in previous experiments and its general behaviour with respect to its compatibility with the supports and with the other materials of the apparatus and to the life of the liquid membrane had been tested already.
The same considerations apply to the solvent, Escaid 100.

The support

Accurel (ENKA) microporous polypropylenic supports had also prooved to be quite fit for the present application since they can support a liquid film of Escaid 100 in a quite stable way (at least several weeks). No specific studies of the factors affecting impregnation had been previously carried out, but soaking the support overnight prooved to give acceptable results; the impregnation times, of approximately 60 hours, were used in this first set of experiments.
Both flat-sheet and tubolar supports were used.

The aqueous phase: the stripping solution

D2EHPA is a typical acid extractant, well suited to operate in a liquid membrane as a carrier in a coupled transport operation. The strip solution will thus need to be more acidic than the feed solution in order to allow for the reversal of the axtraction reaction. For indium, though, such a reversal is facilitated by the presence of ions, for instance chloride ions, that react with In subtracting it from equilibrium. For this reason, brines with low content of HCl, or concentrated solutions of hydrochloric acid, should be the most suitable stripping solutions.

Preliminary tests using flat-sheet supports

The first set of tests was carried out using, for semplicity, flat-sheet supports of approximately 30 cm2 in reactors containing about 150 ml of both feed and stripping solutions.

Stripping solution

Since the carrier and the solvent had already been chosen on the basis of the previous experimental experience on liquid-liquid extraction, the first factor to be optimized was the composition of the stripping solution with respect to its influence on the In flux through the membrane (expressed from now or, except when specified, as the average flux calculated over the first 8 hours of operation in µg/cm2hr. Hydrochloric solutions of different concentrations and NaCl solutions with and without addition od HCl were used. The other experimental conditions were the following: polypropylenic support, 0.1 µm pore size, impregnated with 20 % D2EHPA in Escaid 100; feed solution containing only Cu, In and H2SO4 in the aforementioned concentrations. The results of the tests are shown in fig. 1. The best results are obtained, as expected, at high HCl concentrations, but it is evident that the addition of NaCl can improve the extraction quite efficiently; further experiments will be needed to optimize the NaCl/HCl ratio. Additional tests were aimed at verifying whether the accumulation of In in solution did markedly affect the flux of In: no effect was noticed, confirming the possibility of concentrating In several folds.

D2EHPA concentration

One of the main advantages of the supported membrane technique with respect to solvent extraction is the much lower amount of axtractant that can be used in the former technique. For this reason it is possible to better optimize the concentration of the carrier in the solvent, also reaching very high concentrations.

In fig. 2, the influence of different concentrations (Vol. %) of D2EHPA in Escaid 100 on the In flux is shown for two different stripping solutions (the other conditions are the same as in the preceeding case). The increase in the concentration of the carrier does improve considerably the flux of the metal of interest, mostly in the case of the brine solution at medium D2EHPA concentrations, without considerably affecting the selectivity of the trasport that actually slightly improves.

Preliminary tests using tubular supports

Tubular supports, together with hollow fibers, are the most promising supports for industrial application due to their high surface to volume ratio. It was also experienced in our laboratories that, although their use normally requires a more complicated apparatus and larger amount of reagents, the easiness of use of the reactors and of the control of the parameters (for instance the pH) and, subsequently, the reliability of the results, advise their extensive application also on a laboratory scale.

The tubular reactors used in the tests described in the following paragraphs were prepared with supports of 1.2 mm i.d., 0.1 µm nominal pore size, with a surface of approximately 300 cm2 in all cases except for the long-term test in which a 100 cm2 reactor with supports of 0.2 µm pore size was used. Both the feed and the strip solutions (in general 1l each) were recycled countercurrently for the whole period of the test.
All the experiments were carried out at room temperature.

Feed and stripping flowrates

The fluid-dynamic conditions are very important factors affecting both the flux of the metal through the liquid membrane (by modifying the thinckness of the diffusion layer at the separation surface between the two phases) and the life span of the same. Tests at different flowrates of the feed and strip solutions through a tubular membrane reactor were thus carried out: the results are reported in Fig. 3, from which the increase in In flux with increased solution flowrates is evident. In these tests, the limit flowrate at which the liquid membrane starts to be disrupted and the metal flux through it decreases, has not been reached. Still, since the highest flowrates used corespond to a flux of solution through each tube of approximately 6 l/hr, it was considered that the flowrates used were high enough to be compared to typical industrial flowrates.

The long-term test

Once know the general behaviour of the system with respect to the most important parameters, it was necessary to prove that the life of the liquid film was reasonably long. For this "long-term test" the following conditions were choses:

feed solution: In 0.5 g/l Cu 60 g/l H_2SO_4 30 g/l
organic phase: 40 % D2EHPA in Escaid 100
support: tubular, 1.8 i.d., 0.2 µm nominal porosity, 100 cm2 total surface.
strip solution: 4.5 N NaCl 0.5 N HCl
flowrates: the total flowrate of the feed solution was kept at 70 l/hr which corresponds, because of the small number of fibers of the reactor used in this experiment, to approximately 8 l/hr per fiber.

The experiment was carried out recycling in countercurrent the two solutions and changing the feed when the concentration dropped to lower than 0.05 g/l.
The results are shown in Fig. 4, where the In flux was calculated as an average over 48 hrs. During the first part of the test (first 6 weeks) Cu increased at a steady rate of approximately 0.7 mg/l day reaching a level of approximately 0.03 g/l after 38 days of operation. The sudden change in behaviour after this period occurred because of some drastic change in the operational conditions due to the emptying of the stripping side of the module, which has favoured the ejection of the liquid film from the support, along with the sucking of part of the feed solution.
A reimpregnation of the reactor, though, restored the original efficiency for other four weeks. At this point the test had to be interrupted for thirty days during which it was left in distilled water. The soaking in water probably caused the filling of the pores by water causing a drop in the performance of the reactor. Reimpregnation did not bring the fluxes to the original values and the test was abandoned. A second test, carried out in similar conditions, showed that our supposition was correct since the efficiency of the reactor, filled with the feed and stripping solutions during the interruption period, remained the same.

Influence of other metals present in the industrial solution

Several tests were performed adding to the Cu-In artificial solution the different elements present in the "industrial" solution (that is the solution prepared in Centro Ricerche Veneto laboratories according to our own flowsheet) to verify whether there is some influence on the In flux and whether the selectivity of the system is sufficient for the application of interest.

The elements were added according to the concentrations given before. A polypropylenic (ACCUREL) reactor of approximately 300 cm2, impregnated with D2EHPA

(20 % in Escaid 100) was used in countercurrent, recycling mode (total flowrate: 70 l/hr).

In the case of As (both in the 3+ and 5+ form), Zn, Sb, Bi additions, no influence on In flux under the conditions and for the period tested were observed.

Iron was added both in the +2 and +3 form. No influence was noted within 50 hrs from the beginning of the test. It is well known though, that the +3 form is well extracted by D2EHPA, but stripped with difficulty. For this reason a building up of this ion within the liquid membrane could take place over a longer period of time. This can only be verified by the long-term tests carried out presently.

As far as selectivity is concerned the concentrations of Fe^{2+} and As are lower than the limit of detection (<0.01 and <0.05 g/l respectively).

For Zn and Fe^{+3} the concentrations in the strip solution can be controlled lower than 0.1 g/l.

From 0.015 to 0.035 % of initial Cu is coextracted in 48 hrs.

Finally, the results relative to artificial solutions at higher In concentrations and to "industrial" solutions are given in Fig. 5. No difference is evident between the two solutions.

CONCLUSIONS

The tests carried out up to now demonstrate the technical feasibility of the recovery of Indium by the SLM process from a copper-dross leaching solution.

No problems derive from the presence of other metals in solution and the long-term tests demonstrate the good behaviour of the membranes in the particular aqueous and organic environments used. We are presently starting new tests at a pilot scale with a total surface of one order of magnitude higher than that of the reactors described before. In parallel, we are designing an industrial propotype connected to a copper dross hydrometallurgical plant for the production of 10 to 30 Kg/d of In using commercial reactors.

In a first approach, the economical feasibility of such a process seems to be very interesting in comparison with the traditional processes. Of course this derives from the fact that, in the specific case, the use of membranes is applied to a system containing a quite valuable metal.

ACKNOWLEDGEMENT

We thank EEC for economic support.

FIGURE 1

INFLUENCE OF STRIPPING CONDITIONS ON In FLUX (FLAT MEMBRANE)

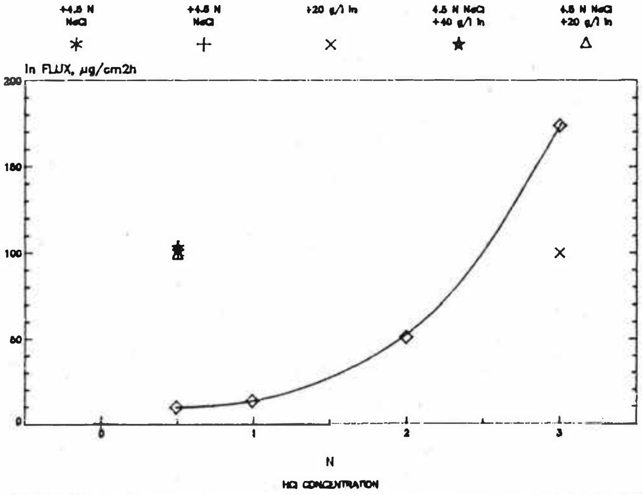

FIGURE 2

INFLUENCE OF D2EHPA CONC. ON In FLUX (FLAT MEMBRANE)

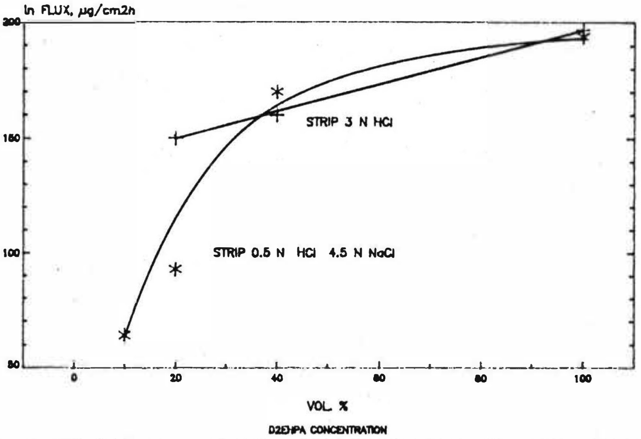

FIGURE 3

INFLUENCE OF FEED FLOWRATE ON In FLUX (CAPILLARY REACTOR)

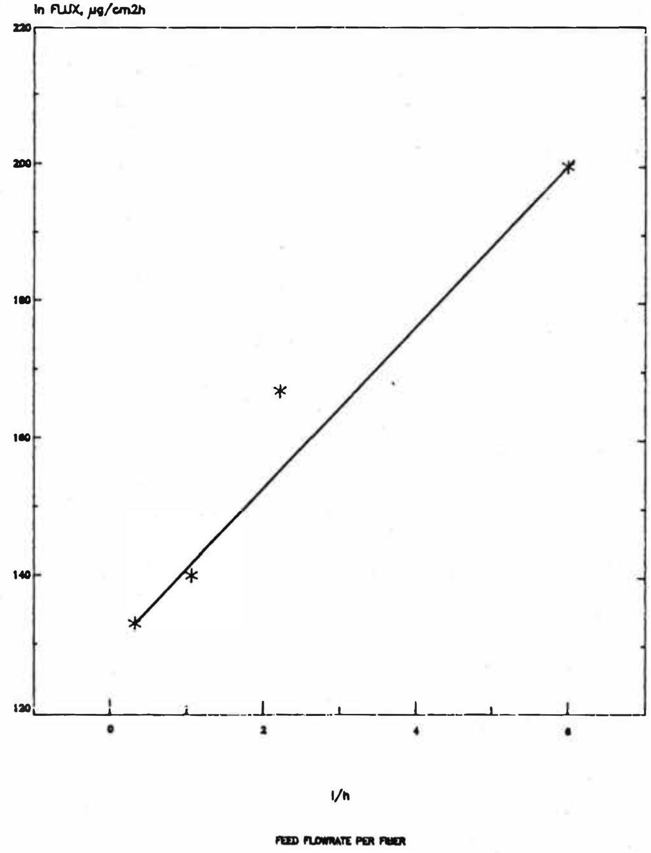

FIGURE 4

LONG TERM TEST (TUBULAR MEMBRANE)

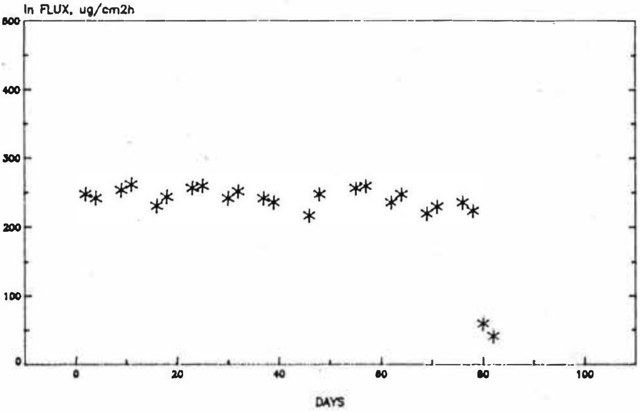

FIGURE 5

COMPARISON BETWEEN Cu-In ARTIFICIAL AND INDUSTRIAL SOLUTIONS

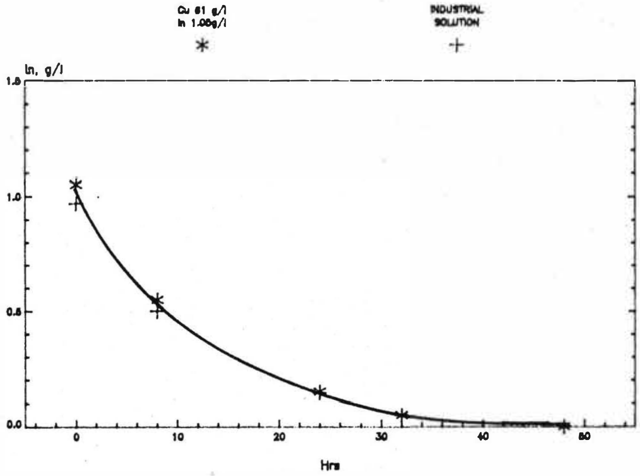

Stationary Mass Transfer at Inorganic Substances Membrane Extraction

G.A. Yagodin, S.Yu. Ivakhno, A.V. Afanasjev, O.A. Sinegribova,

Mendeleev Institute of Chemical Technology, Moscow, USSR

Introduction

Mathematical models currently available for predicting the mass transfer perfomance of liquid membrane systems are mostly based on analytical or numerical analyses of Fick's equations for molecular diffusion sometimes coupled with chemical reactions. Though theoretically reliable this method is of limited utility being associated with several assumptions wich can't be satisfied for many practically important cases [1].

In this work a simplified model of pseudo-steady state behaviour of facilitated transport across liquid membranes is developed for engineering calculations and tested experimentally using the extraction of copper (II) and chromium (VI) from diluted aqueous solutions.

Theory

The dialysis-type liquid membrane process is normally accomplished as co-transport or counter-transport of A (the permeant) and B (the agent wich provides the driving force to the uphill transport).

Under co-transport conditions A and B both present in the feed solution (phase 1) as counter-ions react with the carrier E at the interface with the membrane (phase 2):-

$$m_A A + m_B B + m_E E \rightleftarrows A_{m_A} B_{m_B} E_{m_E} \quad . \qquad (1)$$

The complex formed diffuses towards the membrane - stripping solution (phase 3) interface where the equilibrium of this reaction is strongly shifted to the left. Free carrier molecules are regenerated to recycle back and re-extract additional A by eqn.(1).

In case of A and B counter-transport an exchange reaction

$$m_A A + m_B BE_{m_A} \rightleftarrows m_A AE_{m_B} + m_B B \qquad (2)$$

proceeds at the 2/1 interface, being reversed at the other side of the membrane. As a result of this process A is transfered from the feed phase into the stripping solution while B diffuses in the opposite direction.

In the steady state the boundary concentrations of the moving species are given by partial mass transfer equations. These come for co-transport:-

$$c^A_{1/2} = c^A_1 - j/b^A_1 \; ; \; c^A_{3/2} = c^A_3 + j/b^A_3 \; ; \; c^B_{1/2} = c^B_1 - m_{BA} j/b^B_1 \; ; \qquad (3)$$
$$c^B_{3/2} = c^B_3 + m_{BA} j/b^B_3 \; ; \; c^E_{2/3} = c^E_{2/1} + m_{EA} j/b^E_2 ; \; c^{ABE}_2 = c^{ABE}_{2/3} + j/m_A b^{ABE}_2 .$$

Assuming linear concentration profiles of $A_{m_A}B_{m_B}E_{n_E}$ and E in the membrane one would be able to obtain from mass balance considerations on A, B and E :-

$$c_{10}^{A} - c_{1}^{A} = m_{AB}(c_{10}^{B} - c_{1}^{B}) \ ; \quad c_{3}^{A} - c_{30}^{A} = m_{AB}(c_{3}^{B} - c_{30}^{B}) \ ;$$

$$c_{10}^{A} + c_{20}^{A}V_{21} + c_{30}^{A}V_{31} = c_{1}^{A} + 0{,}5m_{A}(c_{2/1}^{ABE} + c_{2/3}^{ABE})V_{21} + c_{3}^{A}V_{31} \ ; \qquad (4)$$

$$0{,}5m_{E}(c_{2/1}^{ABE} + c_{2/3}^{ABE}) + 0{,}5(c_{2/1}^{E} + c_{2/3}^{E}) = c_{20}^{E}.$$

We can now substitute the boundary concentrations derived from (3)-(4) into the rate expressions for the forward (interface 1/2) and the reverse (interface 2/3) interfacial reactions (1) or (2) to arrive at a system:-

$$j = k_{1/2}(c_{1}^{A} - j/b_{1}^{A})^{\hat{m}_{1/2}^{A}}(\hat{c}_{20}^{E} - n_{1}\hat{c}_{2}^{ABE(AE)} - 0{,}5n_{2}j/b_{2}^{E(BE)})^{\hat{m}_{1/2}^{BE}} \times$$

$$(c_{10}^{B} - m_{BA}(c_{10}^{A} - c_{1}^{A}) - m_{BA}j/b_{1}^{B})^{p_1} - k_{2/1}(\hat{c}_{2}^{ABE(AE)} + 0{,}5n_{3}j \ :$$

$$: b_{2}^{ABE(AE)})^{\hat{m}_{2/1}^{ABE(AE)}} \ (c_{10}^{B} + m_{BA}(c_{10}^{A} - c_{1}^{A}) + m_{BA}j/b_{1}^{B})^{p_2} \ ;$$

$$j = k_{2/3}(\hat{c}_{2}^{ABE(AE)} - 0{,}5n_{3}j/b_{2}^{ABE(AE)})^{\hat{m}_{2/3}^{ABE(AE)}} \ (c_{30}^{B} - m_{BA}(c_{3}^{A} - c_{30}^{A}) -$$

$$m_{BA}j/b_{3}^{B})^{p_3} - k_{3/2}(c_{3}^{A} + j/b_{3}^{A})^{\hat{m}_{3/2}^{A}}(\hat{c}_{20}^{E} - n_{1}\hat{c}_{2}^{ABE(AE)} + 0{,}5n_{2}j \ :$$

$$: b_{2}^{E(BE)})^{\hat{m}_{3/2}^{E(BE)}} \ (c_{30}^{B} + m_{BA}(c_{3}^{A} - c_{30}^{A}) + m_{BA}j/b_{3}^{B})^{p_4} \ ;$$

$$\hat{c}_{2}^{ABE(AE)} = n_{3}(c_{10}^{A} + c_{20}^{A}V_{21} + c_{30}^{A}V_{31} - c_{1}^{A} - c_{3}^{A}V_{31})/V_{21} \ ;$$

where

$\hat{c}_{20}^{E} = c_{20}^{E}$; $n_1 = m_E$; $n_2 = m_{EA}$; $n_3 = 1/m_A$; $p_1 = \hat{m}_{1/2}^{B}$; $p_2 = p_3 = 0$; $p_4 = m_{3/2}^{B}$ - for the co-transport;

$\hat{c}_{20}^{E} = c_{20}^{BE}/m_A$; $n_1 = m_{BA}$; $n_2 = m_{BA}$; $n_3 = 1$; $p_1 = p_4 = 0$; $p_2 = \hat{m}_{2/1}^{B}$; $p_3 = m_{2/3}^{B}$ - for the counter-transport.

Under effective stripping condition when $c_{2/3}^{ABE(AE)} << c_{2/1}^{ABE(AE)}$ eqn.(5) becomes:-

$$j = k_{1/2}(c_{1}^{A} - j/b_{1}^{A})^{\hat{m}_{1/2}^{A}}(\hat{c}_{20}^{E} - 0{,}5n_{2}j(1/b_{2}^{ABE(AE)} + 1/b_{2}^{E(BE)}))^{\hat{m}_{1/2}^{E(BE)}} \times$$

$$\times (c_{10}^{B} - m_{BA}(c_{10}^{A} - c_{1}^{A}) - m_{BA}j/b_{1}^{B})^{p_1} - k_{2/1}(n_{3}j/b_{2}^{ABE(AE)})^{\hat{m}_{2/1}^{ABE(AE)}} \times \qquad (6)$$

$$\times (c_{10}^{B} + m_{BA}(c_{10}^{A} - c_{1}^{A}) + m_{BA}j/b_{1}^{B})^{p_2}.$$

It is also possible to recast (5) into the form of linear equation as regards to the flux:-

$$j\ (1/b_{1}^{A} + 1/\bar{K}_{2/1}b_{2}^{ABE(AE)} + \bar{K}_{2/3}/\bar{K}_{2/1}b_{3}^{A} + 1/\bar{k}_{1/2} + 1/\bar{K}_{2/1}\bar{k}_{2/3} + (1/b_{1}^{A} +$$

$$+ 1/2\bar{K}_{2/1}b_2^{ABE(AE)} + 1/\bar{k}_{1/2})\bar{K}_{2/3}V_{23}) = c_1^A(1 + \bar{K}_{2/3}V_{23} + \bar{K}_{2/3}V_{13} : \quad (7)$$

$$: \bar{K}_{2/1}) - (c_{10}^A + c_{20}^A V_{21} + c_{30}^A V_{31})\bar{K}_{2/3}V_{13}/\bar{K}_{2/1} ,$$

having defined the particular case of constant distribution coefficients by three following assumptions: a) $n = 1$ (first order reaction); b) $c_2^{ABE(AE)} \ll c_{20}^{E(BE)}$ (excess of the carrier in the membrane); c) $c_1^B = c_3^B = \text{const.}$ (excess of the driver in both aqueous phases). Effective rate constants $\bar{k}_{1/2}$ and $\bar{k}_{2/3}$ include constant values of E and B concentrations if necessary. According to eqn.(7) there should be additive 'chemical' and 'diffusion' resistances to mass transfer in liquid membrane process.

In many practically important cases chemical reactions are in fact instantaneous as compared with diffusion. That leads to the equilibrium boundary conditions for the basic model (5), i.e. one has to put zero flux values into the left parts of the kinetic equations (5). The resulting model will be:-

$$\bar{\bar{K}}_{2/1}=(\hat{c}_2^{ABE(AE)} + 0,5n_3j/b_2^{ABE(AE)})(c_1^A - j/b_1^A)^{p_5}(\hat{c}_{20}^E - n_1\hat{c}_2^{ABE(AE)} - 0,5 \times$$

$$\times n_2j/b_2^{E(BE)})^{p_6}(c_{10}^B + n_4(c_{10}^A - c_1^A) + n_4j/b_1^B)^{p_7} ;$$

$$\bar{\bar{K}}_{2/3}=(\hat{c}_2^{ABE(AE)} - 0,5n_3j/b_2^{ABE(AE)})(c_3^A + j/b_3^A)^{p_5}(\hat{c}_{20}^E - n_1\hat{c}_2^{ABE(AE)} + \quad (8)$$

$$+ 0,5n_2j/b_2^{E(BE)})^{p_6}(c_{30}^B - n_4(c_3^A - c_{30}^A) - n_4j/b_3^B)^{p_7} ;$$

$$\hat{c}_2^{ABE(AE)} = n_3(c_{10}^A + c_{20}^A V_{21} + c_{30}^A V_{31} - c_1^A - c_3^A V_{31})/V_{21} ;$$

where $n_4=-m_{BA}$, $p_5=-m_A$, $p_6=-m_E$, $p_7=-m_B$, $\bar{\bar{K}}_{2/1}= K_{2/1}$, $\bar{\bar{K}}_{2/3}= K_{2/3}$ – for the co-transport; $n_4= m_{BA}$, $p_5=-1$, $p_6=-m_{BA}$, $p_7= m_{BA}$, $\bar{\bar{K}}_{2/1} =(K_{2/1})^{1/m_A}$, $\bar{\bar{K}}_{2/3}=(K_{2/3})^{1/m_A}$ – for the counter-transport. It is possible to change concentration equilibrium constants by effective or thermodynamic ones if information on activity coefficients is available. Eqns.(6) and (7) could be also modified for transport process with instantaneous reactions.

The state of 'chemical equilibrium' for a liquid membrane system is represented by eqns.(8) at $j = 0$:-

$$\bar{\bar{K}}_{2/1}=\overset{*}{c}_2^{ABE(AE)}(\overset{*}{c}_1^A)^{p_5}(\hat{c}_{20}^E-n_1\hat{c}_2^{ABE(AE)})^{p_6}(c_{10}^B+ n_4(c_{10}^A- \overset{*}{c}_1^A))^{p_7} ;$$

$$\bar{\bar{K}}_{2/3}= \overset{*}{c}_2^{ABE(AE)}(\overset{*}{c}_3^A)^{p_5}(\hat{c}_{20}^E - n_1\hat{c}_2^{ABE(AE)})^{p_6}(c_{30}^B - n_4(\overset{*}{c}_3^A - c_{30}^A))^{p_7}; \quad (9)$$

$$\hat{c}_2^{ABE(AE)} = n_3(c_{10}^A + c_{20}^A V_{21} + c_{30}^A V_{31} - \overset{*}{c}_1^A - \overset{*}{c}_3^A V_{31})/V_{21}.$$

In case of constant distribution coefficients under the same equilibrium condition the linear equation (7) is reduced to:-

$$\overset{*}{c}{}_1^A = (c_{10}^A + c_{20}^A V_{21} + c_{30}^A V_{31})/(1 + \bar{K}_{2/1} V_{21} + \bar{K}_{2/1} V_{31}/\bar{K}_{2/3}). \qquad (10)$$

Experimental

Both copper transport in the system: aqueous $CuSO_4$, pH 2.5 (H_2SO_4) - D2EHPA (RH) in decane - aqueous H_2SO_4 and chromium transport in the system: aqueous $K_2Cr_2O_7$, pH 1.0 (H_2SO_4) - TAA (R_3N) in CCl_4 - aqueous KOH were carried out in a horizontal diffusion cell with the stirred aqueous phases and the liquid membrane supported by porous nuclear filter [1]. Except as noted below, initial concentrations of the components were, moles: $c_{10}^{Cu} = 0.183$; $c_{20}^{RH} = 0.6$; $c_{30}^{H_2SO_4} = 2.0$; $c_{10}^{Cr} = 0.2$; $c_{20}^{R_3N} = 0.1$; $c_{30}^{KOH} = 0.9$. Stripping solution samples were removed periodically and analysed by atomic absorption spectroscopy.

Partial mass transfer coefficients ($m \cdot s^{-1}$) were determined independantly by means of the nuclear filters set consisting of different units [1]: $b_1^{Cu} = b_3^{Cu} = 7.8 \cdot 10^{-4}$; $b_2^{(RH)_2} = b_2^{CuR_2} = 1.0 \cdot 10^{-5}$ (for the matrix used in experiments with variable copper concentration in the feed); $b_2^{(RH)_2} = b_2^{CuR_2} = 3.0 \cdot 10^{-5}$(for the matrix used in experiments with variable carrier concentration in the feed); $b_1^{Cr} = 1.5 \cdot 10^{-4}$; $b_3^{Cr} = 2.3 \cdot 10^{-4}$; $b_2^{R_3N} = 1.5 \cdot 10^{-5}$; $b_2^{(R_3NH)_2 Cr_2O_7} = 1.0 \cdot 10^{-5}$.

The distribution coefficients and equilibrium constants were measured by shaking the appropriate membrane and aqueous solutions.

DVK-2M computer was used for calculations.

Results and Discussion

Copper Transport

Taking into account the possibility of the carrier polymerization in organic phase one would apply (2) to the D2EHPA-mediated countertransport of copper and hydrogen cations in the form

$$Cu^{2+} + m_E(RH)_l \rightleftharpoons CuR_2(m_E - 2/l)(RH)_l + 2H^+. \qquad (11)$$

All data on kinetics of copper conventional solvent extraction by D2EHPA and consequent acidic stripping lead to the conclusion that both forward and reverse reactions (11) are fast as compared with diffusion [1]. It is most likely the case in the liquid membrane system, copper transport by D2EHPA being diffusion-controlled. The kinetic model (8) becomes:-

$$\bar{\bar{K}}_{2/1} = c_{2/1}^{CuR_2}(c_1^{Cu} - j/b_1^{Cu})^{-1}(c_{20}^{RH}/l - m_E o_{2/1}^{CuR_2} + 0.5 m_E j(1/b_2^{CuR_2} - 1/b_2^{(RH)_l}))^{-m_E};$$

$$(12)$$

$$\bar{\bar{K}}_{2/3} = (c_{2/1}^{CuR_2} - 0.5j/b_2^{CuR_2})(c_3^{Cu} + j/b_3^{Cu})^{-1}(c_{20}^{RH}/l - m_E c_{2/1}^{CuR_2} + 0.5 m_E j(1/b_2^{CuR_2} +$$

$+ 1/b_2^{(RH)_l}))^{-m_E}$;

where constant hydrogen ions concentrations c_1^H and c_3^H are included into the effective constants $\bar{\bar{K}}_{2/1} = K_{2/1}(c_1^H)^{-2}$ and $\bar{\bar{K}}_{2/3} = K_{2/3}(c_3^H)^{-2}$ because the relatively high initial values c_{10}^H and c_{30}^H wouldn't be changed significantly during the contact time (1000-2000 s) necessary for the flux measurment.

Under effective stripping condition we have from eqn.(6):-

$$\bar{\bar{K}}_{2/1} = j/b_2^{CuR_2}(c_1^{Cu} - j/b_1^{Cu})(c_{20}^{RH}/l - 0.5m_E j(1/b_2^{CuR_2} + 1/b_2^{(RH)_l}))^{m_E} \qquad (13)$$

and in case of constant distribution coefficients:-

$$j(1/b_1^{Cu} + 1/\bar{K}_{2/1}b_2^{CuR_2} + \bar{K}_{2/3}/\bar{K}_{2/1}b_3^{Cu}) = c_1^{Cu}. \qquad (14)$$

It was proved in solvent extraction experiments that $l=2$, $m_E=1$ for the systems in question [2]. With regard for these values one can obtain from (12) a cubic equation

$$G_3j^3 + G_2j^2 + G_1j + G_0 = 0 \qquad (15)$$

with coefficients dependant on c_1^{Cu}, c_3^{Cu}, c_{20}^{RH}, b_1^{Cu}, b_3^{Cu}, $b_2^{CuR_2}$, $b_2^{(RH)_2}$, $\bar{\bar{K}}_{2/1}$, $\bar{\bar{K}}_{2/3}$. Meanwhile a liquid membrane process with effective stripping is described by quadratic equation

$$\begin{aligned}(1/b_2^{CuR_2} + 1/b_2^{(RH)_2})j^2 - (c_{20}^{RH} + c_1^{Cu}(1/b_2^{CuR_2} + 1/b_2^{(RH)_2})b_1^{Cu} + \\ + 2b_1^{Cu}/\bar{\bar{K}}_{2/1}b_2^{CuR_2})j + b_1^{Cu}c_1^{Cu}c_0^{RH} = 0.\end{aligned} \qquad (16)$$

The latter relationship can be even more simplified:-

$$j = b_2^{CuR_2}\bar{\bar{K}}_{2/1}c_1^{Cu}c_0^{RH}/(2 + c_1^{Cu}\bar{\bar{K}}_{2/1}(1 + b_2^{CuR_2}/b_2^{(RH)_2})) \qquad (17)$$

by assuming $b_1^{Cu} \gg b_2^{CuR_2}, b_2^{(RH)_2}$.

Initial flux values j_{15} calculated by means of (15) at different copper and carrier concentrations are in good agreement with experimental data (tables 1 and 2). As j_{15} values are insensitive both to $\bar{\bar{K}}_{2/3}$ and b_3^{Cu} at least in the following ranges: $\bar{\bar{K}}_{2/3} \in [0.001\bar{\bar{K}}_{2/1}; 0.1\bar{\bar{K}}_{2/1}]$, $b_3^{Cu} \in [0.1b_1^{Cu}; 10b_1^{Cu}]$ neither sulfuric acid concentration in the stripping solution nor intensity of its mixing should influence the transport rate. This is also confirmed experimentally.

Thus effective stripping condition is realized. Eqn.(16) can be used for the flux calculation. It gives j_{16} values wich don't differ essentially from j_{15} and j_{exp} (tables 1 and 2).

The flux j_{15} sensitivity to the partial mass transfer coefficient b_1^{Cu} is low as well, the transfer rate j_{17} calculated by eqn.(17) being close to j_{15}, j_{16} and j_{exp} (tables 1 and 2). The reason for this comes from the comparatively high diffusion intensity in the feed phase. The second item $c_1^{Cu}\bar{\bar{K}}_{2/1}(1 + b_2^{CuR_2}/b_2^{RH_2})$ contributes from 2 to 30% to the eqn.(17) right half denominator. That's why j_{17} doesn't change much in wide range of $b_2^{(RH)_2}$ values. On the contrary c_1^{Cu}, c_{20}^{RH}, $b_2^{CuR_2}$, $\bar{\bar{K}}_{2/1}$ effects on the copper transport rate are expected to be significant. So they are in experiment.

Flux values j_{14} calculated by eqn.(14) are somewhat higher than j_{15}, j_{16}, j_{17}. However the difference of 3-6% is comparable with the experimental error. Thus there should be an excess of the carrier in the membrane leading to the phase resistances additivity.

Having assumed $l=1$, $m_E=2$ for the liquid membrane process one could transform (12) into a cubic equation wich predicts experimental results satisfactorily. A conclusion like that seems to be reasonable because the flux would hardly depend on m_E value in case of carrier excess in liquid membrane.

2. Chromium Transport

For the amine-mediated co-transport of bichromate and hydrogen ions across liquid membranes the reaction (1) is expressed as

$$Cr_2O_7^{2-} + 2H^+ + 2R_3N \rightleftharpoons (R_3NH)_2Cr_2O_7. \qquad (18)$$

Negligible effects of ionic surfactants on the mass transfer rate indicate inderectly the diffusion regime of the process [1]. Since the carrier and the transported compound molecules are able to aggregate in organic phase, the kinetic modelling is complicated. The analysis of chromium equilibrium distribution at solvent extraction and stripping gave for chromium-amine molar ratio in the membrane $\overset{*}{c}_2^{Cr}/\overset{*}{c}_2^{R_3N} > 1$. That means the real complex structure doesn't correspond to that defined by eqn.(18). Consequently equilibrium concentration constants calculated for this reaction do vary with the system composition what makes it senseless to use them in kinetic models like eqns.(8).

The measured chromium flux values appeared to be nearly the same at different c_{30}^{KOH} and mixing intensity of the stripping solution, i.e. mass transfer proceeds under effective stripping condition. Therefore by using distribution coefficients $\bar{K}_{2/1}$ instead of equilibrium constants we can formulate the kinetic system

$$c_{2/1}^{Cr} = \bar{K}_{2/1} c_{1/2}^{Cr} \; ; \quad j = b_2^{Cr} c_{2/1}^{Cr} \; ; \quad c_{1/2}^{Cr} = c_1^{Cr} - j/b_1^{Cr} . \qquad (19)$$

wich leads to the simple relationship

$$j \left(1/b_1^{Cr} + 1/b_2^{Cr} \bar{K}_{2/1} \right) = c_1^{Cr} . \qquad (20)$$

The experimental functions $j_{exp}(c_{10}^{Cr})$ and $j_{exp}(c_{20}^{R_3N})$ do correlate closely with those predicted by eqn.(20).

It is worthwhile to note that the equilibrium transport rate would be considerably decreased with the organic viscosity growth due to the partial mass transfer coefficients b_2^{Cr} and $b_2^{R_3N}$ fall.

Conclusions

The stationary liquid membrane process model developed allows not only to explain experimental results obtained for copper (II) and chromium (VI) transport across solid supported liquid membranes but also to predict effects of different chemical and diffusion parameters on the transfer rate revealing those of them wich are the most important for engineering calculatons and equipment design. The latter possibility seems to be really valuable because any experimental measurment all the more theoretical calculations of transport reactions equilibrium constants and stoichiometric coefficients as well as partial mass transfer coefficients determination are very complicated for liquid membrane systems.

Nomenclature

A - permeant, B - 'driver' compound, E - carrier, D2EHPA=RH - di-2-ethylhexylphosphoric acid, R_3N=TAA - tertiary alkylamine ($R=C_7-C_9$), b - mass transfer coefficient, c - concentration, $\overset{*}{c}$ - equilibrium concentration, $\hat{c}$ - average concentration, j - flux, K - concentration equilibrium constant, $\bar{K}$ - distribution coefficient, k - rate constant, $\bar{k}$ - effective rate constant, l - polymerization degree, m - stoichiometric coefficient, $\grave{m}$ - reaction order, n - parameter, p - formal reaction order, V - volume, G_0, G_1, G_2, G_3 - coefficients in the cubic equation.

Subscripts

A,B,E etc. - compounds; 1,2,3 - phases; i/z, where i,z=1,2,3, i≠z - interfaces or boundary layers; 21, 31, BA, EA, etc. - ratios, e.g. $m_{BA} = m_B/m_A$, $V_{21}=V_2/V_1$; 0 - initial state, 14, 15, 16, 17 (at j) - number of the equation used for the calculations, exp - experimental value.

References

1. Ivakhno S.Yu., Afanasjev A.V., Yagodin G.A. Membrannaya extractzia neorganitcheskich veschestv. Itogi nauki i techniki. Neorganitcheskaya chimiya. T.13. M., VINITI, 1985, 127 s.

2. Martynov B.V. Extractzia organitcheskimi kislotami i ich solyami. Spravotchnic po extractzii. M., "Atomizdat", 1978, 367 s.

Table 1

Calculated and experimental copper flux values ($j \cdot 10^7$, kmoles/$m^2 \cdot s$) at different c_{10}^{Cu} (kmoles/m^3).

c_1^{Cu}	0.022	0.047	0.079	0.110	0.142
$K_{2/1}$	0.93	0.72	0.56	0.50	0.42
j_{15}	1.94	3.20	4.20	5.27	5.37
j_{16}	1.96	3.21	4.18	5.16	5.61
j_{17}	1.98	3.23	4.20	5.18	5.63
j_{14}	2.02	3.35	4.39	5.46	5.93
j_{exp}	1.71±0.05	3.15±0.05	4.6±0.1	5.7±0.1	6.3±0.1

Table 2

Calculated and experimental copper flux values ($j \cdot 10^7$, kmoles/$m^2 \cdot s$) at different c_{20}^{RH} (kmoles/m^3).

c_{20}^{RH}	0.15	0.30	0.60	0.75	0.90	1.05	1.50
$K_{2/1}$	0.18	0.26	0.37	0.42	0.46	0.50	0.62
j_{15}	9.06	13.44	18.90	21.70	23.30	25.53	31.67
j_{16}	9.22	13.29	18.90	21.47	23.51	25.54	31.65
j_{17}	9.26	13.40	19.15	22.19	23.84	25.91	32.18
j_{14}	9.82	14.13	20.02	22.68	24.80	26.91	33.20
j_{exp}	10.0± 0.2	15.8± 0.3	21.5± 0.4	24.1± 0.5	25.7± 0.6	25.0± 0.6	18.5± 0.4

Use of Liquid Membrane in Metal Recovery from Metal-Containing Wastes in ppm-Range

W.Gutknecht, H.-B. Hauertmann, K. Schügerl

Institut für Technische Chemie, Universität Hannover

Introduction

In conventional solvent extraction two different processes are needed for extraction and stripping. Using liquid membrane technique, these two steps are combined to one single step . This is done by producing a water-in-oil emulsion. When the emulsion is used as the dispersed phase, the degree of extraction is not ruled by the loading capacity of the organic phase but determined mainly by the solubility of the extracted species in the stripping phase. If the solubility is high, very high enrichment factors can be obtained due low hold-ups. By choosing suitable complexing agents, a high selectivity can be achieved too. These properties of liquid membrane technique can be used for the recovery of metals from leaching solutions of low grade ores and tailings as well as for cleaning and upgrading of metal-containing waste waters.

After the extraction the emulsion must be broken in order to recover the membrane and the stripping phase. The emulsion breakdown is carried out by electrocoalescence by means of A.C. fields. Using A.C. fields, the electrocoalescence is an electrostatic process. Therefore low quantities of energy are needed.

Our investigations show the possibility of metal recovery from metal containing waste waters in the ppm-range. The experiments are divided into three parts. In the first part two copper extractions from two different waste solutions are shown. The second part deals with the emulsion breakdown and in the third part a combining of extraction and breaking is discussed.

The copper extraction

Two different waste solutions are treated by liquid membrane emulsions in a bench-scale Kühni-column. The concentrations of solution 1 and 2 are given in table 1.

table 1

metal	solution 1	solution 2
Cu	50 ppm	400 ppm
Co	50 ppm	10 ppm
Ni	50 ppm	5 ppm
Zn	50 ppm	10600 ppm

Figure 1 shows the actual concentrations in regard to their initial concentrations, declared as F, as function of the dimensionless length of the column. At a hold-up about 13 % nearly all copper is extracted from solution 1 . From the second solution only 70 % is extracted due to the short residence time, which is the same as in case of solution 1.

The influence of hold-up is demonstrated in fig. 2. The higher the hold-up the higher the degree of extraction, as it should be exspected.

Fig. 3 illustrates the possibility to use a preloaded stripping phase. There is no difference between prelaoded and unloaded stripping phase in degree of extraction.

The Emulsion Breakdown

The rate of the emulsion breakdown is shown in fig. 4. At a frequency of 1000 cps the rate increases with increasing electric field strength.

When the field strength is held constant on the other hand, the breaking degree can be increased by increasing frequency. This possibility is shown in fig. 5.

The investigations about the breakdown are suitable to optimize the content of surfactant. Optimizing surfactant content of emulsions there are two points of views. The one is to reach stable emulsions and the other is to reach unstable emulsion due to a fast and easy breakdown. In this case a stable emulsion can be built up in a certain range of surfactant content and optimization will be done by looking for a maximum in breaking-rate as illustrated in fig.6.

The organic phase, containing surfactant, carrier and solvent, must not change its properties, when it will be used many times. So the organic phase was used many times to prepare an emulsion. There was no significant difference in breaking-rate between the different cycles (fig. 7).

The Combining of Extraction and Breakdown

The extraction, emulsion breakdown and recycling of stripping and membrane phases were carried out in a combined unit. A solution containing Zn in the ppm-range was extracted by means of the liquid membrane technique. At the first time the extraction degree was 65 % in steady state, which was reached after one hour (fig.8, curve 1). The emulsion was seperated from the continuous phase and was broken up to 85 % (fig.9 ,curve 1).

The membrane and stripping phases were emulsified again and were used for a second cycle. Now the extraction degree was even higher (fig.8, curve 2). The breakdown of the emulsion was about the same as in cycle one.

Conclusions

Our experiments indicate that the use of liquid membrane technique is suitable for a nearly complete and very selective metal recovery, especially from solutions which contain very low metal concentrations. The process can be carried out continuously, and the carrier and the membrane phase as well as the stripping phase can be recycled.

Fig. 1: Influence of metal-concentration of the continuous phase

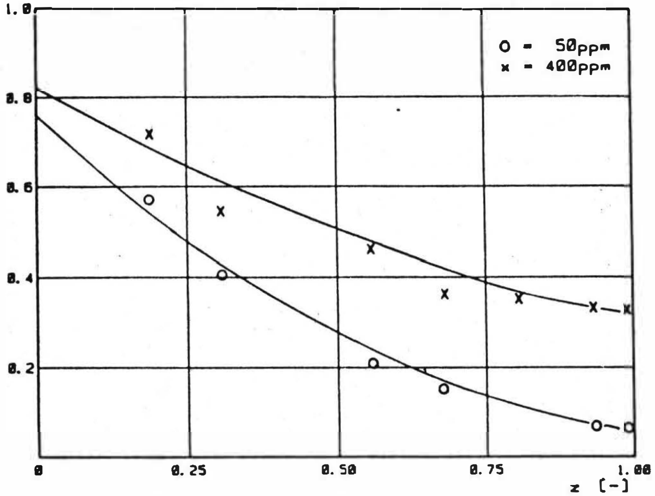

Fig. 2: Influence of the hold-up

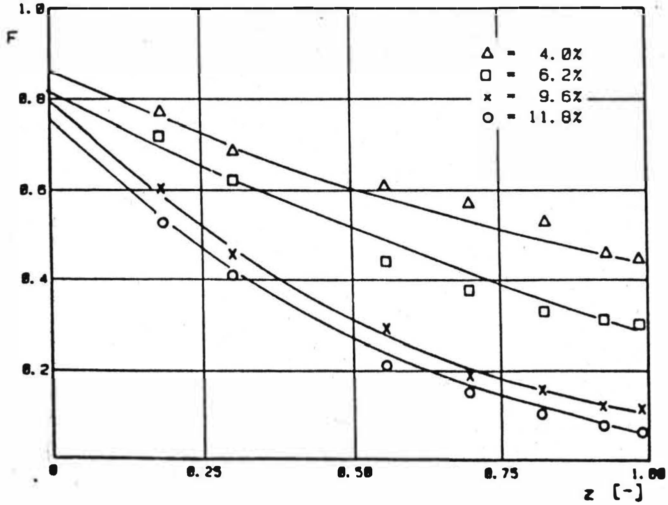

Fig. 3: Influence of unloaded and preloaded stripping phase

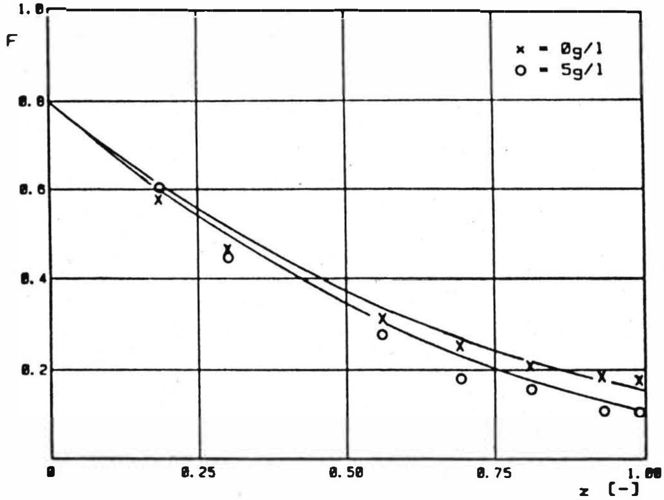

Fig. 4: Breaking rate as function of the electrical field strength

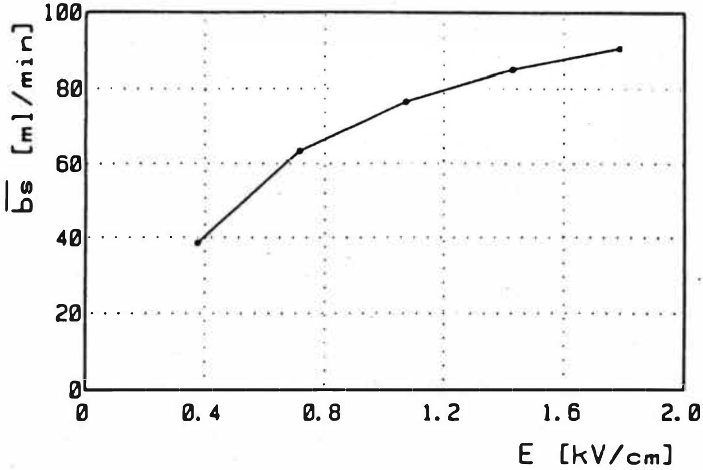

Fig. 5: Variation of the frequency
WP_{max} = 750 ml   E = 536 V/cm

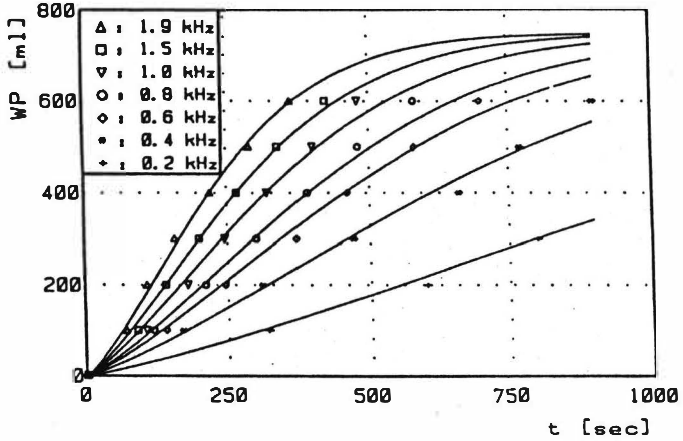

Fig. 6: Breaking rate as function of surfactant concentration

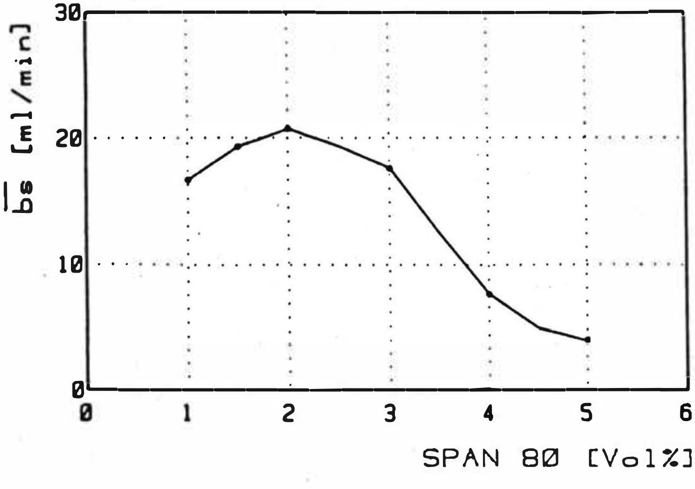

Fig. 7: Breaking rate vs numbers of cycles

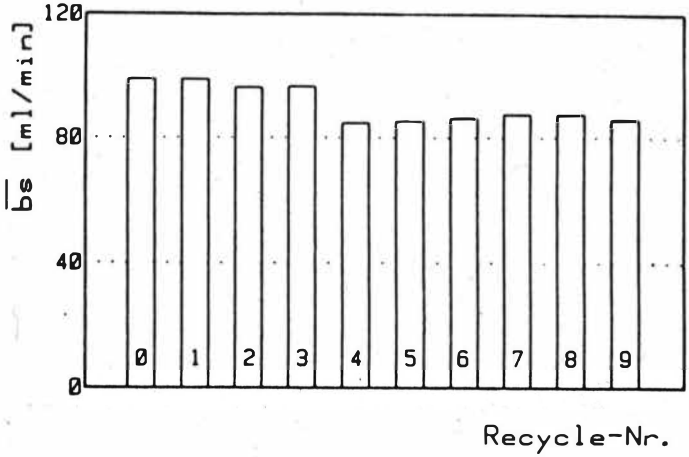

Fig. 8: The extraction at the combined process

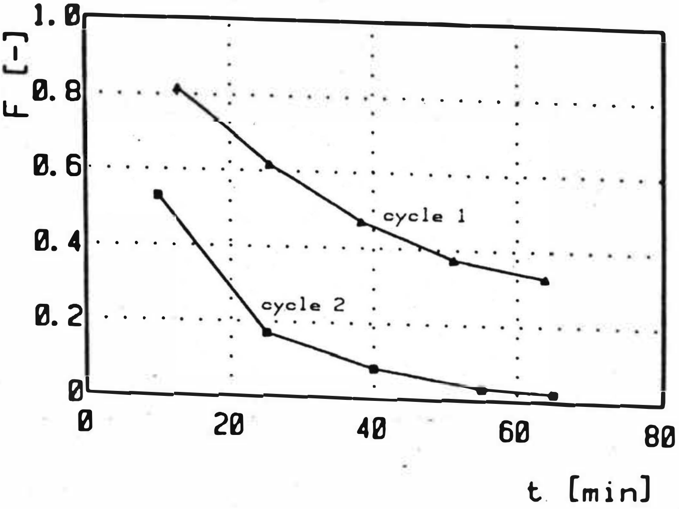

Fig. 9: Breaking degree at the combined process

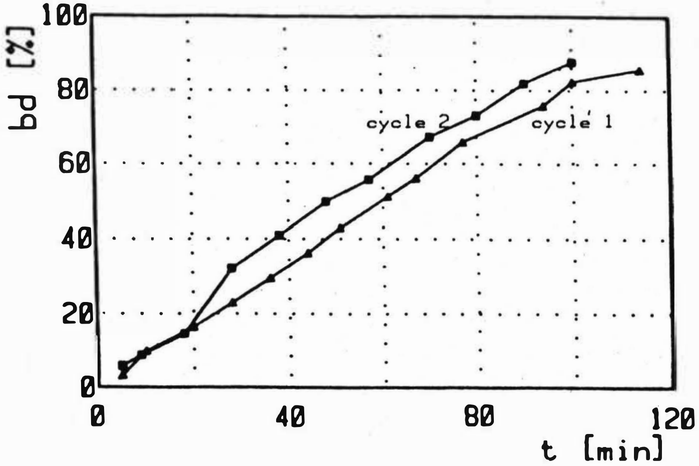

Symbols :

F	actual concentration in regard to initial concentration
z	dimensionless length of Kühni-column
bs	breaking rate in ml/min
E	electrical field strength in kV/cm
WP	volume of aequeous phase in ml
bd	volume fraction of stripping phase with regard to WP_{max}

COUPLED TRANSPORT OF ZINC USING SOLID SUPPORTED LIQUID MEMBRANES

L. Fernandez, J. Aparicio and M.Muhammed, Department of Inorganic Chemistry, Royal Institute of Technology, S-100 44 Stockholm, Sweden.

The use of Solid Supported Liquid Membranes (SSLM) as a mean for the separation and recovery of metal ions has attracted the attention of a large number of investigators in the last years (1-2). In particular situations, the use of SSLM is advantageous as compared to the more time-efficient Emulsion Liquid Membranes (ELM) processes (3-4). Complex separations requiring the use of several extraction systems or different aqueous media can also be achieved by the use of multistage SSLM processes. The "Membrane Cascade" separations reported by Danesi (5) indicate that SSLM may be a valuable alternative to ELM. The knowledge of the physico-chemical properties of the system is essential for the adequate design of SSLM separations. This requires precise information about both thermodynamic and dynamic characteristics of the system under consideration.

The study presented here deals with the coupled transport of Zn(II) and H^+ from aqueous 1.0 $mol.dm^{-3}$ $(Na,H)ClO_4$ media through a SSLM consisting of bis-(2-ethylhexyl)phosphoric acid (HDEHP = HR = $(RO)_2POOH$, where R = 2-ethylhexyl) dissolved in Isopar-H, an aliphatic kerosene (Esso), impregnated in the pores of a teflon type solid support. This system is of practical importance since several plants are operating using conventional Solvent Extraction processes based on HDEHP for the recovery of zinc (6). Furthermore, the equilibrium and kinetic behaviour of the system has also been extensively investigated by us (7,8).

EXPERIMENTAL

Zinc transfer rate experiments were conducted in a cell consisting of two compartments separated by a flat porous membrane (the solid support), which is impregnated by the organic solutions to form the Liquid Membrane. Both compartments, containing the aqueous feed and strip solutions, were stirred by means of electric motors, in order to minimize macroscopic diffusion processes. Feed solutions consisted of $Zn(ClO_4)_2$ of different concentrations. The pH of these solutions was adjusted by adittion of adequate amounts of $HClO_4$. The ionic strength was kept constant at 1.0 $mol.dm^{-3}$ $(Na,H)ClO_4$. The strip solutions consisted of 1.0 $mol.dm^{-3}$ $HClO_4$ unless otherwise stated. The solid support used in the main part of the experiments was a Durapore (Millipore) hydrophobic fluorovinilydene flat film of 125 µm thickness and 75% porosity. The characteristics of the other supports used for comparison are listed in table 1.

After impregnating = 10 µl of the HDEHP solutions in the pores of the solid support by means of a micropipette, the membrane was placed in the cell, the aqueous solutions were added and the stirrer's motors started. Zinc fluxes were experimentally evaluated by measuring the increase of zinc concentration in the strip side of the cell at fixed time intervals using an automatised Flow Injection Analysis (FIA) system (9).

RESULTS

Zinc transer rates were studied as a function of the hydrodynamic conditions, chemical composition of the system and solid support characteristics. The results are collected in figures 1 to 6.

MODELING OF THE TRANSPORT RATES

In order to model the transfer rate of zinc across the SSLM the different sources of mass transfer resistance must be taken into account. These sources are : a) diffusion of the metal ion across unstirred layers adjacent to the Liquid Membrane-aqueous interfaces, b) chemical reaction rates at the Liquid Membrane-aqueous interfaces and c) the diffusion of the Zn-HDEHP species across the Liquid Membrane itself. For such modeling, the equilibrium and kinetic characteristics of the system must be known. In our case, the equilibrium study (7) points out that the extraction of Zn(II) by HDEHP dissolved in Isopar-H proceeds by the following reactions

$$Zn^{2+} + 2\,\overline{(HR)_2} \rightleftharpoons \overline{ZnR_2(HR)_2} + 2\,H^+ \qquad [1]$$

$$Zn^{2+} + 3/2\,\overline{(HR)_2} \rightleftharpoons \overline{ZnR_2(HR)} + 2\,H^+ \qquad [2]$$

On the other hand, the extraction kinetics of this system can be explained by the following flux equation (8)

$$J = k_{ao}\,[Zn^{2+}]_i - k_{oa}\,\overline{[Zn]} \qquad [3]$$

where k_{ao} and k_{oa} are the pseudo-first order rate constants of the ITRSC mechanism. These equations are combined with Fick's first law applied to the concentration gradients originated by the diffusion layers adjacent to and inside the membrane. Assuming linear concentration gradients throughout the system and that steady state is established, the following equation, describing the initial flux through the SSLM, is obtained

$$J = \frac{[Zn^{2+}]\,[(\overline{HR})_2]^2\,F}{(\Delta_a\,[(\overline{HR})_2]^2 + k_1^{*-1})\,F\,(1+[H^+]_f^2/[H^+]_s^2) + \Delta_o k_{eq1}^{-1}\,[H^+]_f^2} \qquad [4]$$

where $F = 1+\beta[(\overline{HR})_2]^{-1/2}\,\Delta_{o,2}/\Delta_{o,1}$ [5]

DISCUSSION

The influence of the hydrodynamic conditions on the initial flux is presented in figure 1 for two different initial $[Zn^{2+}]$ in the feed solution. It can be seen that for the lower $[Zn^{2+}]$ the flux first increases as the stirring speed of the aqueous solutions is increased and then reaches a constant value. On the other hand, if the initial $[Zn^{2+}]$ is kept at a much higher level, a constant value of the flux is readily established independent of the stirring speed. These results can be analyzed in terms of equation [4]. When the $[Zn^{2+}]$ in the feed is low, the increase in the stirring speed decreases the Δ_a term. This is because the thickness of the aqueous diffusion layers are progressively decreased until Δ_a reaches a constant value. This is experimentally indicated by the apearence of the "plateau" region. For the case in which the initial $[Zn^{2+}]$ is high enough, the free carrier concentration available for transport reaches a saturation value and equation [4] can be converted to

$$J(lim) = \frac{[Zn^{2+}]\,[(\overline{HR})_2]^2\,F}{\Delta_{0,2}\,k_{eq1}^{-1}\,[H^+]_f^2} = \frac{C_{HR}}{3.5\,\Delta_{o,2}} \qquad [6]$$

being thus independent of the stirring speed of the aqueous solutions.

In figures 2 and 3 the variation of the initial flux with the initial pH_f and free carrier concentration are presented for two initial $[Zn^{2+}]$. When studying the variation of log J as a function of the free carrier concentration it is seen that, for the lower $[Zn^{2+}]$, the flux reaches a constant value

$$J = \frac{[Zn^{2+}]}{\Delta_a} \qquad [7]$$

independent of the total C_{HR} used at sufficiently high pH_f values. However, if the initial $[Zn^{2+}]$ is increased considerably, the flux progressively increases. A smilar behaviour is observed in the variation of log J when pH_f is increased. In the case of low $[Zn^{2+}]$ and at constant C_{HR}, equation [4] can be reduced to

$$J = \frac{[Zn^{2+}]\,[\overline{(HR)_2}]^2\,F}{\Delta_a[\overline{(HR)_2}]^2\,F + k_1^{*-1}\,F} \qquad [8]$$

Besides, if C_{HR} is sufficiently high eq. [8] can be further reduced to eq. [7]. When the $[Zn^{2+}]$ is increased, the effect of carrier saturation leads again to the same limiting flux value given by eq.[6]. This effect, of carrier saturation, is more pronounced when the flux is varied as a function of the total $[Zn^{2+}]$ in the feed solution at constant C_{HR} and pH_f as shown in figure 4. In this figure it is clearly noticed that the limiting value predicted by eq. [6] is obtained for both HR concentrations used.

The variation of log J vs pH_s in figure 5 gives an indication of the driving force (the excess $[H^+]_s$) which is necessary to achieve the transport of zinc without significant decrease of the flux. The initial flux is kept practically constant even for a $pH_s = 2$. This also indicates that the effective $[H^+]$ at the strip-membrane interface does not need to be substantially high in order to effectively strip the metal from the membrane. This is due to the larger diffusivity of H^+ as compared to Zn^{2+}. The solid lines of figures 2 to 5 have been constructed using the parameters obtained by fitting eq. [4] to the experimental data. From this numerical treatment the values of the different parameters given in table 2 have been evaluated.

The effect of the variation of the solid support characteristics on Δ_o, as a result of varying their ε and T values, was studied while keeping other parameters constant. In figure 6, J^{-1} is plotted vs $(\delta_o\ T^2/\varepsilon)$. It is interesting to notice that the tortuosity T, a parameter related to the degree of cross-linking of the polymeric framework of the support, affects the initial flux. Tortuosity values for the solid supports used in this work have been estimated according to the formula $T = (1+V_p)/(1-V_p)$ (10).

As a conclusion, it can be mentioned that the flux of zinc across the SSLM employed can be described by the simplified eq. [7] when the $[Zn^{2+}]$ is kept at trace level, provided that the carrier concentration and pH_f values are such that the carrier saturation phenomena and the effect of chemical reaction rates can be disregarded. The flux is described by eq. [6] if the $[Zn^{2+}]$ in the feed is high enough so that the effect of carrier saturation dominates the permeation process. This may represent a limitation in practical applications, because metal fluxes can not be undefinitely increased by the increase of C_{HR} or pH_f. Besides, further increase in the carrier concentration produces a decrease in the flux due to the higher viscosities of the resulting Liquid Membranes and the consequent decrease in the D_o values. It has also been shown that for trace concentration levels of the permeating metal ion the kinetics of chemical reaction can play a role of similar importance to diffusion. They should be thus considered when explaining the experimentally measured fluxes.

SYMBOLS AND UNITS

J : molar flux, mol cm^{-2} sec^{-1}

$k_1^* = k_1/[(HR)_i]^2$, $(cm\ sec^{-1})/(molec/Å^2)^2$

k_1 : forward rate constant of the ITRSC kinetic mechanism proposed in (8)

$\Delta = \delta T^2/(D\varepsilon)$: mass transfer coefficient, sec cm^{-1}

δ : thickness of diffusion layer, cm

D : diffusion coefficient, cm^2 sec^{-1}

β : k_{eq2}/k_{eq1}

C_{HR} : total HDEHP concentration, $mmol.dm^{-3}$

ε : porosity

T : tortuosity

V_p : volume fraction of the polymeric framework

Indexes a,o and i refer to aqueous, organic and interfacial phases and/or species respectively. Indexes f and s refer to feed and strip solutions respectively. Indexes 1 and 2 refer to $\overline{ZnR_2(HR)}$ and $\overline{ZnR_2(HR)_2}$ species respectively. The bar indicates species present in the organic phase.

ACKNOWLEDGMENTS

L. F. and J. A. gratefully acknowledge the financial support from the Basque Government through the Scholarship recieved.

REFERENCES

1 . N. N. Li, J. Membr. Sci. 3(1978)265.

2 . Proc. International Solvent Extraction Conference ISEC 83, Publised by AIChE, 1983.

3 . W. C. Babcock, R. W. Baker, E. D. Lachapelle and k. L. Smith, J. Membr. Sci. 7(1980)71.

4 . T. Largman and S. Sifniades, Hydrometallurgy 3(1978)153.

5 . P. R. Danesi, "Separations by Supported Liquid Membrane Cascades", U.S. Patent Application and Assignment, DOE Case 5-59,617, August 1983.

6 . E. D. Nogueira and J. M. Regife, Quimica e Industria, 10(1977)693.

7 . A. Sastre and M. Muhammed, Hydrometallurgy 12(1984)177.

8 . J. Aparicio, L. Fernandez and M. Muhammed, Hydrometallurgy, in press.

9 . J. Aparicio, L. Fernandez and M. Muhammed, Proc. Euroanalysis V, Cracow, Poland, August 1984.

10. J. S. Mackie and P. Meares, Proc. Roy. Soc. London, Ser A, 232(1955)498.

TABLE 1

Characteristics of the solid supports used in this work.

Membrane	Polymeric framework	Thickness	Porosity	Tortuosity
Durapore	Fluorovinilidene	125μm	75%	1.67
Fluoropore	Tetrafluoroethylene	60 "	70"	1.86
Celgard 2400	Propilene	25 "	38"	4.26
Celgard 2500	"	25 "	45"	3.44
Celgard 2402	"	50 "	38"	4.26

Durapore and Fluoropore, Celgard 2400, 2500 and 2402 are Trade Marks from Millipore Corp. and Celanese Plastics respectively.

TABLE 2

Values of the parameters obtained in the numerical treatment.

$\Delta_a = 2.40\ 10^{2}$ sec cm^{-1} $\delta_a = 1.78\ 10^{-3}$ cm

$\Delta_{o,2} = 9.87\ 10^{3}$ sec cm^{-1} $D_{o,2} = 1.70\ 10^{-6}$ cm^{2}sec^{-1}

$\Delta_{o,2}/\Delta_{o,1} = 1.12$ $D_{o,1} = 1.91\ 10^{-6}$ cm^{2}sec^{-1}

$k_1 = 15.77$ (cm sec^{-1})/(molec/A^{2})^{2}

The values $D_a = 7.2\ 10^{-6}$ cm^{2} sec^{-1}, the nominal $\delta_o = .25\ 10^{-2}$ cm, $\varepsilon = 0.75$ and $T = 1.67$ have been used in the calculation of δ_a, $\Delta_{o,2}$ and $\Delta_{o,1}$.

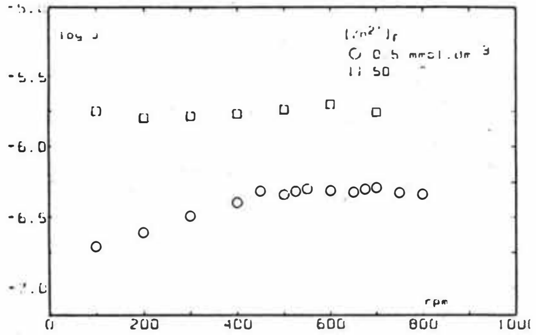

FIGURE 1 . Variation of log J as a function of the hydrodynamic conditions.
□ C_{HR} = 50 mmol.dm^{-3}, pH_f = 2.29
○ C_{HR} = 25 " , pH_f = 2.35

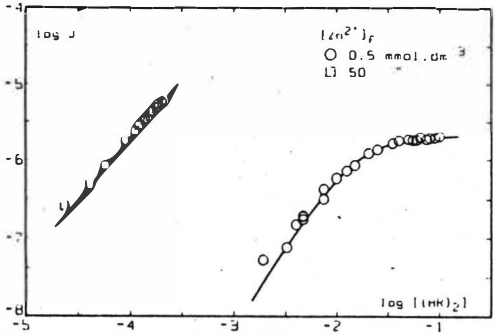

FIGURE 2 . Variation of log J as a function of the free HDEHP dimer concentration. pH_f : □ 3.45, ○ 3.43. Stirring speed = 600 rpm.

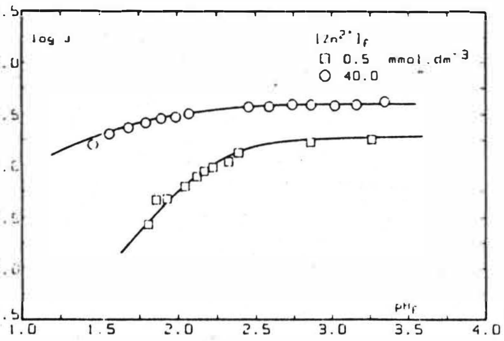

FIGURE 3 . Variation of log J as function of the aqueous feed pH.
C_{HR} : ○ 120 mmol.dm^{-3}, □ 180 mmol.dm^{-3}. Stirring speed 600 rpm.

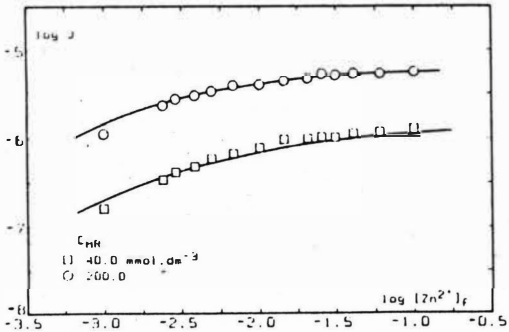

FIGURE 4 . Variation of log J as a function of the initial zinc concentration in the feed solution. pH_f = 2.00. Stirring speed = 600 rpm.

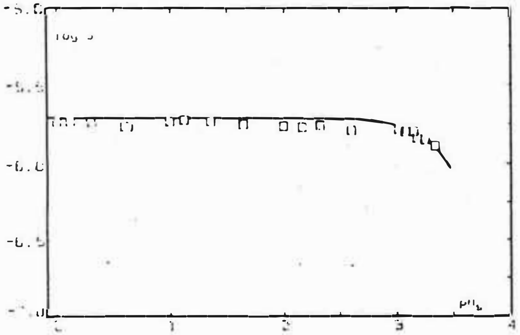

FIGURE 5 . Variation of log J as a function of the aqueous strip pH. C_{HR} = 120 mmol.dm^{-3}. pH_f = 3.43. Stirring speed = 600 rpm.

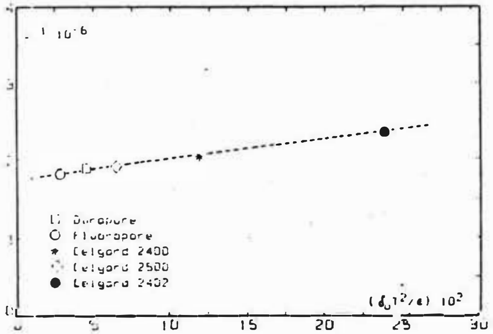

FIGURE 6 . Variation of the inverse of the flux as a function of the solid support characteristics. C_{HR} = 25 mmol.dm^{-3}. pH_f = 2.35.

Appendix

The following manuscript reached DECHEMA on 30 June 1986 and belongs to Volume III-621

Solvent Extraction of Metals by Oligomeric Extracting Agents

V.I. Bukin, A.M. Reznik, S.A. Semenov, L.D. Yurchenko, Lomonosov
Institute of Fine Chemical Technology, Moscow, USSR

At present reagents generally of phenol type (1), which in some cases have low selectivity are suggested to extract elements from alkaline solutions. A considerably greater number of reagents are known for extraction of copper, nickel and cobalt from ammonia solutions (2, 3). LIX and Kelex reagents are successfully used in industry for separation of copper, nickel and cobalt; however, these reagents have a number of disadvantages, viz., decomposition of reagents when used for a long time (4), easy oxidation of Kelex (5), and, in some cases, difficulty in re-extraction of cobalt due to its oxidation in an organic phase (6). Therefore, search and investigation of new reagents, particularly those which are able to extract metals with high selectivity, is one of the most important directions of investigations in the field of extraction.

Oligomeric derivatives of alkyl phenols are proposed to be used as extraotant for separation of metals from alkaline and ammonia media. At first these were used as extractant for alkaline elements (AE) (7). Oligomerio derivatives of alkyl phenols have a number of advantages over original alkyl phenols, viz.,: i) large effective molecular volume causing a reagent to be hydrophobic and thereby decreasing its solubility in an aqueous phase; ii) more acidic properties of oligomers as compared to alkyl phenols, e.g. pK_a of p-octyl phenol is 10.30, pK_a of ootofore OH (two benzene rings) 10.12, pK_a of SP-1047 oligomer (four benzene rings) 9.55; iii) weaker effect of diluents on extractive properties of oligomerio reagents.

Oligomeric reagents practically do not differ from alkyl phenols as to mechanism of extraction of alkaline elements (1, 7). In both cases a proton of hydroxyl group of phenol is substituted by a metal. Comparing extraction of AE it is possible to assume that their interaction with similar reagents should increase as ionic radius of AE increases. It is really observed in case of alkyl phenols and some oligomerio derivatives (e.g. novolao resins) (fig.1). However, extraotability of AE changes (fig.2) for resol resins having end methylol groups - CH_2OH; and the best extractive features are noted for lithium.

Enhanced extractability of lithium and sodium by 101 and OS reagents makes it possible to suppose that except for cation-exchange extraction, some other kind of extraction takes place. Due to its greater ability to complex formation as compared to other AE, lithium not only exchanges with a proton but also forms chelate rings as a result of its interaction with methylol group. Detailed extraction of lithium by various resol and novolac oligomers of p-isooctylphenol sulphides confirmed the above suggestion. Thus, compound of lithium with resol oligomers, being extracted by octofore 10S, can be presented as follows:

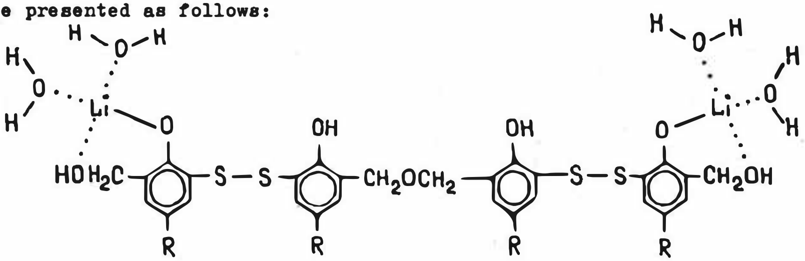

Data analysis of lithium extraction by oligomeric reagents has shown that the most effective oligomers are those containing methylol groups in a molecule; it has also made possible to suggest an extractant for separation of lithium from solutions obtained by treatment of lithium - containing catalysts of organic synthesis (8). These solutions contain 13.8 - 14.4 per cent of NaCl, 1.67 - 2.44 g/l of lithium and pH is 10.95 - 11.89.

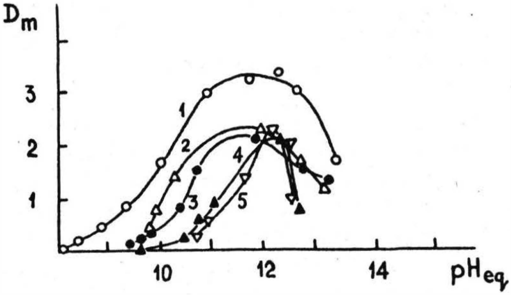

Fig. 1. The effect of pH of equilibrium aqueous phase on distribution coefficient of AE: 1-Cs, 2-K, 3-Rb, 4-Na, 5-Li.

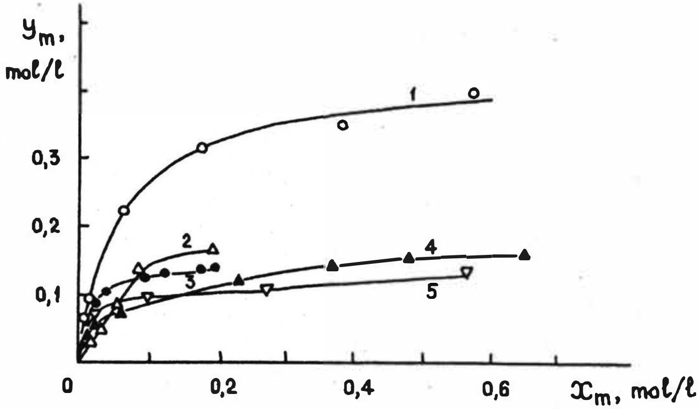

Fig. 2. The distribution of AE between their alkaline sulphate solutions and 0.24 mol/l solution of OS in kerosene (pH 12.00): 1-Li, 2-Na, 3-Cs, 4-K, 5-Rb.

101L oligomer containing 9-13 per cent of methylol groups has been suggested as an extractant (9). To prevent dilution of a solution and extraction of sodium and to more fully purify sodium chloride from lithium, sodium form of 101L oligomer in isoamyl alcohol was used. A model of crosscurrent four-stage process of extraction showed that it is possible to considerably decrease concentration of lithium in NaCl solution and extract lithium into an organic phase with 99.5% yield. Saturated solutions of Na_2CO_3 or $NaHCO_3$ were suggested as re-extracting agents for the system involved, re-extraction of lithium by $NaHCO_3$ being more complete. Recovery of lithium from re-extract is brought about by heating the solution to boiling, $LiHCO_3$ being decomposed to Li_2CO_3 and separated as a precipitate, the latter being filtered off. Lithium is recovered as a commercial product, the extent of re-extraction being approximately 98 per cent.

Sulphur-containing oligomers studied for extraction of lithium, in particular derivatives of alkyl phenol disulphides, are typical chelate-forming reagents. They contain in its molecule both OH groups replacing protons by a metal and sulphur atoms capable of coordinating metals in the process of extraction. Therefore, we investigated extraction of cobalt, nickel and copper by disulphide p-tert-butyl phenol (DSBP) in toluene.

In ammonia solutions, cobalt, nickel and copper exist in several cation forms which are in equilibrium; the change of free ammonia concentration and pH results in the change of the form of the existence of a metal, and consequently to the shift of equilibrium in the process of its extraction. Therefore, the composition of an aqueous phase will greatly affect the extraction of cobalt, nickel and copper. Extraction of nickel, cobalt and copper from 0.1 mol/l ammonia solutions by DSBP was carried out in order to investigate the influence of pH on metal extraction. Dependences of D_m vs pH(fig. 3) were shown to have an extreme character, maximum extraction of Ni, Co and Cu being observed at pH 8.0, 8.5 and 6.5 respectively. Extraction of nickel from a solution containing approximately 2 g/l of Ni was carried out to confirm a cation-exchange mechanism of metal extraction. Conditions of the experiment were such that concentration of free ammonia in all tests was kept constant and equal to 0.1 mol/l. Data obtained showed that a slope of a straight line is close to 2, which corresponds to the charge of a cation being extracted, and consequently to the number of liberated protons in extraction.

Concentration of free ammonia or ammonia ion which is associated with ammonia concentration by corresponding equilibrium exerts great influence on the process of nickel extraction. Table I shows negative influence of free ammonia concentration on nickel extraction, coefficient of nickel distribution sharply decreasing as ammonia concentration increases.

Table I. Dependence of log D_{Ni} on free ammonia concentration. $pH_{eq.}$ 8.68, Cs 0.1 mol/l, $C_{in.}$ 1.93 g/l.

log C_{NH_3}	Concentration in equilibrium phases		D_{Ni}	log D_{Ni}
	X_{Ni}, g/l	Y_{Ni}, g/l		
- 1.14	0.33	1.60	4.78	0.68
- 1.26	0.09	1.84	20.47	1.31
- 1.32	0.026	1.91	72.74	1.86
- 1.41	0.01	1.92	187.50	2.27

To determine the ratio of metal: reagent in a complex being extracted log D_m vs log C_s dependence was studied. At constant composition of an equilibrium aqueous phase, a slope in the above dependence should correspond to the number of extractant molecules taking part in extraction.

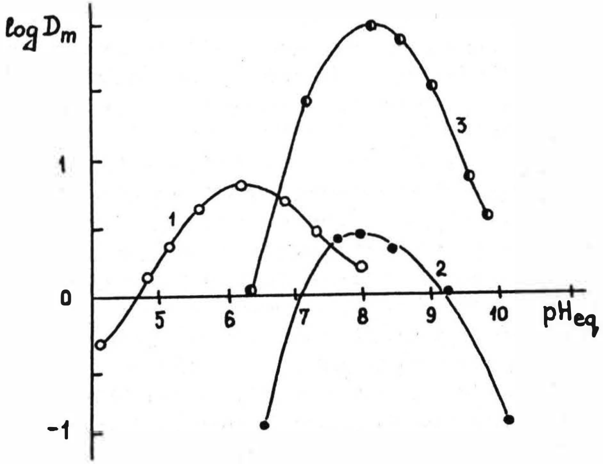

Fig. 3. Dependence log D_m vs $pH_{eq.}$: 1-Cu, 2-Ni, 3-Co.

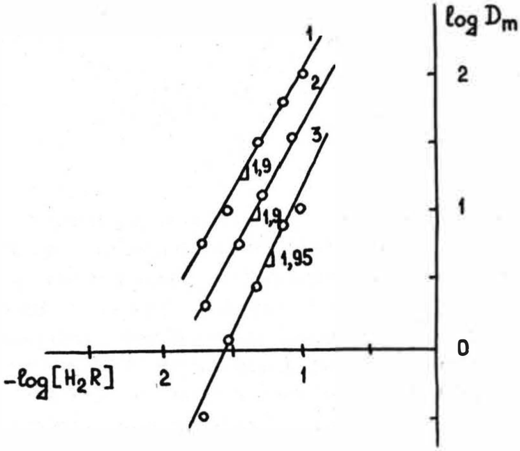

Fig. 4. Dependence log D_m vs DSBP concentration. 1-Co, 2-Ni, 3-Cu.

Experimental data in fig. 4 demonstrate that a slope of curve log D_m vs log C_s is close to 2, i.e. corresponding to ratio metal: reagent equal to 1:2 in a complex being extracted. The ratio metal: reagent close to 1:2 was also determined by isotherms of nickel, cobalt and copper extraction and confirmed by measurement of molecular weights of complexes being extracted by vapour phase osmometry.

Composition of copper, nickel and cobalt complexes being extracted was investigated by a number of physico-chemical methods, e.g., infra-red-, electron spectroscopy, X-ray electron spectroscopy. On the basis of analysis of data obtained it is possible to conclude that metal extraction by DSBP is brought about due to proton exchange of a hydroxyl group of an extractant by a metal cation and additional coordination of it by a donor sulphur atom. This results in the formation of an intracomplex compound of chelate type in which ratio metal: DSBP is equal to 1:2. A metal in the complexes formed is hexacoordinated, the coordination occurring due to the formation of two valence bonds with oxygen atoms, two coordination bonds with sulphur atoms of an extractant, and two coordination bonds with water or ammonia molecules depending on pH of an equilibrium aqueous phase. The sum of data obtained makes it possible to assume that the molecule of an extractant is a distorted octahedron the apexes of which are occupied by water or ammonia molecules:

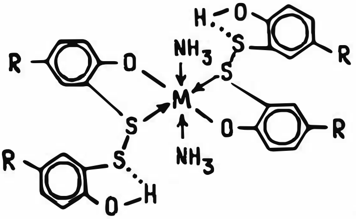

The complexes of cobalt with DSBP obtained by extraction from ammonia sulphate solutions were investigated by EPR. At first EPR signal of the samples investigated was absent, then as the time of exposure of cobalt extracts to air was prolonged, there appeared a signal in EPR spectrum. Passing oxygen through extracts of cobalt for 1hr shortened the time of signal occurrence in EPR spectra sharply. EPR spectrum of oxidised Co extracts and its parameters are evidence of the formation of paramagnetic complexes of cobalt with DSBP in the presence of oxygen and duration of time. According to literature data on the study of similar cobalt complexes by EPR method (10) it is due to addition of molecular oxygen to cobalt in one of axial positions.

On the basis of the investigation it is possible to suppose that metals are extracted from ammonia media according to the equation:

$$\left[M(NH_3)_{\bar{n}}\ (H_2O)_{k-\bar{n}}\right]^{2+}_{(w)} + 2H_2R_{(o)} \rightleftarrows \left[M(NH_3)_{\bar{m}}\ (H_2O)_{2-\bar{m}}\ (HR)_2\right]_{(o)} + $$
$$+\ 2H^+_{(w)} + (\bar{n} - \bar{m})\ NH_{3\ (w)} + (\ k - \bar{n} - 2 + \bar{m})\ H_2O$$

where k is coordination number of a metal in ammonia compound: 6 for Ni and Co, and 4 for Cu; $\bar{n}$ average number of ammonia ligands being coordinated by a metal in ammonia compound, $0 \leqslant \bar{n} \leqslant 6$; 4(Cu); $\bar{m}$ average number of ammonia molecules being coordinated by a metal in complexes being extracted, $0 \leqslant \bar{m} \leqslant 2$; H_2R - DSBP.

Re-extraction is an integral part of extraction procedure. It is known to be associated with definite difficulties for a number of chelate-forming reagents. Since Co, Ni and Cu are usually obtained by electrolysis from sulphate or chloride solutions, sulphuric acid and hydrochloric acid solutions were used for re-extraction. Study of separation of metals from extracts indicated that in the course of re-extraction Co, Cu, Ni are washed out with 95.00 - 99.75 per cent yield immediately after the extraction by 1-3N HCl or H_2SO_4.

To investigate extraction of cobalt, nickel and copper when they are mutually present a technical product, namely disulphide para alkyl C_7 - C_9 phenol (DSAP) was used (11). For extracting agent concentration (0.75 M solution of DSAP in kerosene) involved at pH 3.4, 4.7 and 6.5 of nickel, cobalt and copper respectively, extracting agent capacity of the metals concerned was determined; this capacity proved to be equal to 14.2 g/l for Ni, 14.4 g/l for Cu, and 19.2 g/l for Co (fig. 5).

In order to reveal optimum conditions for extraction separation of cobalt and accompanying metals, the influence of pH of an equilibrium aqueous phase on copper, nickel and cobalt distribution was studied. Experimental data given in fig. 6 confirmed extreme characters of dependences log D_m vs pH obtained for individual components when they were extracted by DSBP (fig. 3). Full coincidence of pH values corresponding to maximum coefficients of metal distribution when extracted by DSBP and DSAP confirmed analogy in their extraction behaviour. Coefficients of the distribution of metals were calculated in the pH range investigated on the basis of data obtained. The most favourable solutions for separation of cobalt from nickel and copper are those with pH > 9; under these conditions βCo(II)/Ni is equal to 5.01 - 7.58, βCo(II)/Cu≈70, βNi/Cu≈17. If preliminary oxidations of Co^{2+} to nonextracting Co^{3+} is carried out, separation coefficients increase considerably (e.g. β Ni/Co(III) and βCu/Co(III) > 10^3).

Taking into account the results obtained and the fact that Co^{3+} cannot be extracted from ammonia solutions by DSAP, two ways of cobalt separation from accompanying metals are possible in its technological application. The first one is based on oxidation of cobalt and further extractive separation of nickel and copper. The second way is based on multi-stage extractive separation of cobalt, nickel and copper without preliminary oxidation of cobalt.

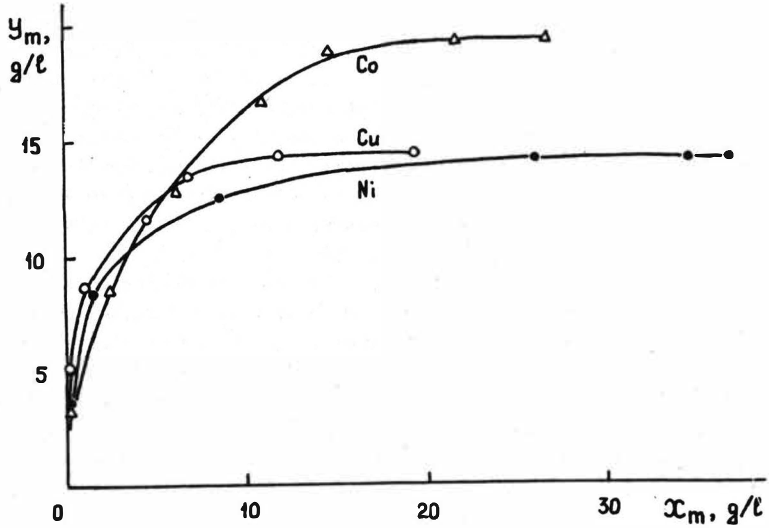

Fig. 5. Isotherms of extraction of copper, nickel and cobalt by 0.75M DSAP in kerosene.

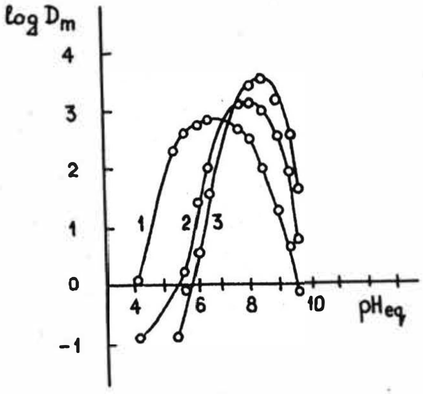

Fig. 6. Log D_m vs pH dependence at 0.75M DSAP in kerosene.
1 - Cu, 2 - Ni, 3 - Co.

References

1. A.V.Nikolaev. Extraction of Metals by Phenols, Novosibirsk, Nauka, p.196, 1976.
2. V.I.Bukin, A.M.Reznik, S.V.Vasilchenko, N.A.Granat, Moscow, TSNII tsvet met ek. i inf., No 3, 1983.
3. G.M.Ritcey, A.W.Ashbrook. Solvent Extraction. Principles and applications to process metallurgy. Amsterdam: Elsevier scientific publishing Company, 1979.
4. R.J. Whewell, H.J.Foakes, M.A.Hughes. Hydrometallurgy, v.7, No 1/2, p.726, 1981.
5. A.M.Reznik, E.I.Ponomareva, Yu.N.Silaev, Z.S.Abisheva, V.I.Bukin. Extraction and sorption in chemical technology of Gallium, Alma-Ata, Nauka, 1985.
6. P.Guesnet, D.Bauer. Analysis, v.9, No 4, p.129-134, 1981.
7. D.A.Granat, A.M.Reznik, Tallin, Est NIINTI, 1977.
8. Invention No 1111993, USSR, Bul. izobret. No 33, 1984.
9. M.M.Golberg, Moscow, Chimia, p.510, 1978.
10. J.E.Wertz, J.R.Bolton. Electron Spin resonance, New York: McGraw-Hill Book Company, 1972.
11. Invention No 1111995, USSR, Bul. izobret. No 33, 1984.

Author Index

Author	Volume/Page
A	
Abbruzzese, C., Rome/I	
Afanasjev, A.V., Moscow/USSR	I-593
Afzaletdinova, N.G., Ufa/USSR	II-527
Aguilar, M., Barcelona/E	II-239
Al Khani, A., Toulouse/F	I-151
Al-Bazi, S.J., Tucson, AZ/USA	II-393
Alessi, P., Trieste/I	III-479,III-715
Alper, E. Dharan/Saudi Arabia	III-469
Aly, G., Lund/S	III-815
Aly, H.F., Cairo/ET	II-539
Ammon von, R., Karlsruhe/D	I-223
Angelino, H., Toulouse/F	II-139
Aparcio, J. L., Stockholm/S	I-611,II-239
Aprahamian Jr., E. Tucson,AZ/USA	II-385
Aquilar, M., Barcelona/E	II-165
Arai, K., Sendai/J	III-507
Archambault, D.A., Pinawa,Manitoba/CDN	I-441
Arenson, D. R., Berkeley, CA/USA	III-741
Aufderheide, E., Clausthal-Zellerfeld/D	III-247
B	
Baba, Y., Saga/J	II-65, II-263
Bae, K., Syracuse, NY/USA	III-129
Bagreev, V.V., Moscow/USSR	I-499
Bailes, P.J., Bradford/UK	III- 63
Baird, M.H.I., Hamilton,ONT/CDN	I- 41
Balasubramanian, G.R., Kalpakkam/IND	I-413
Baradel, A., Milano/I	II-401
Bart, H.J., Graz/A	I-567,II-643,III-293,III-339,III-907
Bartsch, R.A., Lubbock,TX/USA	I-581
Bassey, E. N., Bradford/UK	III-755
Batey, W., Caithness/UK	I-371
Bathelier, A., Bessines sur Gartempe/F	I-285
Bauer, D., Paris/F	II- 91, II-463,II-503
Baumgärtner, F., Garching/D	I-253,I-293
Bautista, R. G., Nevada-Reno, NV/USA	II-107
Bautz, H., Karlsruhe/D	I-239
Becker, R., Karlsruhe/D	I-239
Beklemishev, M.K., Moscow/USSR	II-559
Bensalem, A. K., Zürich/CH	III- 99, III-191
Berger, R., Ludwigshafen/D	III- 3
Bes, R.S., Toulouse/F	III-239
Beutler, H.J., Krefeld/D	III- 51
Bhaskara Sarma, P.V.R., Bhubabeswar/IND	II-625
Billet, R., Bochum/D	III-115,III-123
Blázquez, J.C., Bilbao/E	III-839
Blaß, E., München/D	III- 11, III-379,III-387,III-445
Bleyl, H.-J., Karlsruhe/D	I-333,I-399
Bliznakovska, B., Skopje/YU	III-481

Boase, D.G., Pinawa, Manitoba/CDN I-441
Bobirenko, A.Yu. Moscow/USSR III-831
Bokobza, L., Paris/F II-131
Bonnet, J.C., Syracuse, NY/USA III-135
Borchardt, J., Jülich/D I-325
Bouwmans, I., Delft/NL III-317
Braun, Chr., Bochum/D III-123
Braun, G., Frankfurt am Main-Höchst/D III-799,III-877
Brignole, E.A., Bahia Blanca/RA I- 63
Brown, T.J., Niagara Falls, ONT/CDN III-775
Brunette, J.P., Strasbourg/F II-481
Brunner, G., Hamburg/D III-783
Bryan, S.A., Oak Ridge, TN/USA I-477
Bühlmann, U., Allschwil/CH III-167
Bukin, V.I., Moscow/USSR I-621,III-621
Bunge, A.L., Golder, CO/USA I-519
Bunzenberger, G., Graz/A III-907
Burgard, M., Strasbourg/F III-919
Byeseda, J.J., Tulsa, OK/USA II-611

C

Caldentey-Navick, M., Paris/F II- 91
Campbell, D.O., Oak Ridge,TN/USA I-301
Carlini, D., Rome/I I-355
Carnahan, T.G.,Reno, NV/USA I-572
Carvalho de, J.M.R., Lisboa/P II-295
Casamatta, G., Toulouse/F I-151,II-139,III-353,III-361
Casarci, M., Rome/I I-107,I-355
Casas, I., Barcelona/E II-165
Case, G.N., Oak Ridge, TN/USA I-477
Chachaty, C., Fontenay-aux-Roses/F I-267
Chadwick, A.T.,Oxon, OX/UK II-589
Chadwick, R.B., Oak Ridge, TN/USA I-477
Chaiko, D.J., University Park, PA/USA II-409
Chao, Shou-bai, Beijing/China III-437
Charbonnel, M.-C., Fontenay-aux-Roses/F I-261
Charewicz, W.A., Lubbock,TX/USA I-581
Chekmerev, A.M., Moscow/USSR II-195
Chen, Changqing, Beijing/China II-339
Chen, Chia-yong, Beijing/China II-447,II-565
Chen, Haijie, Shanghai/China III-183
Chen, Jiayong, Beijing/China II-573
Chen, Jinbang, Beijing/China III-667
Chen, Zhichuan, Changchun/China II-651
Chen, Zhifu, Changchun, Jilin/China II-231
Chernysheva, M.F., Kuibyshev/USSR III-747
Chesné, A., Stains/F III-739
Chiang, H.W., Pinawa, Manitoba/CDN III-369
Cichocki, M.,Wrocław/PL III-669
Coello, J., Stockholm/S II-239
Colussi, I., Trieste/I II-173,III-199
Cong, Jingyang, Beijing/China II-605
Cote, G., Paris/F II-91,II-131,II-463
Cox, M., Hatfield, Herts./UK I-537

D

Dai, Ge-sheng, Shanghai/China II-271
Dalton, R.F., Blackeley,Manchester/UK II- 11
Danesi, P.R., Vienna/ A I-527,II-255
Danilov, N.A.,Moscow/USSR II-236
Davies, G.R., Saginaw, MI/USA III-345
Davister, A., Engis/B I-177
Deák, Gy., Veszprém/H III-515
Demopoulos, G.P., Montreal,QUE/CDN II-581
Diantouba, B., Strasbourg/F II-481
Dichtl, G., Wiesbaden/D III-723
Ding, Hong-bing, Beijing/China II-122
Ding, Jian-ping, Guangzhou/China II-222
Dmitrienko, S.G., Moscow/USSR II-559
Dobrowsky, B., Zalec, YU III-639
Dohrn, R., Hamburg/D III-783
Doyle, F.M., Berkeley, CA/USA II-99
Draxler, J., Graz/A I-553
Dupire, S., Louvain-lLa-Neuve/B III-613
Dvorak, Z., Praha/CS III-765

E

Eccles, H., Preston/UK I- 13
Eiben, K., Leopoldshafen/D I-317,I-393
Eid, K., Toulouse/F III-353
Eisele, J.A., Reno, NV/USA I-572
El-Dessouky, M.M., Cairo/ET II-539
Eldridge, R.B., Austin,TX/USA III- 55
Elsässer, K.H., Allschwil/CH III-167
Elutin, A.V., Moscow/USSR II-425
Emmrich, G., Essen/D III-491
Eroglu, E., Ankara/TR III-847
Ertel, D., Karlsruhe/D I-399
Evers, H., Leopoldshafen/D I-393

F

Fair, J.R., Austin/TX/USA III- 39,III- 55
Fan, Zheng, Beijing/China III-437
Fatović, I., Zagreb/YU I-275
Faure, A., Fontenay-aux-Roses/F I-267
Fei, Weiyang, Beijing/China III-215
Feng, Hanzhen, Shanghai/China II-495
Fermeglia, M., Trieste/I III-715
Fernandez, L. A., Stockholm/S I-611,II-239,III-863
Feucht, P., Karlsruhe/D I-317,I-393
Figuerola, E., Barcelona/E II-165
Fischer, K., Dresden/DDR I-499
Fitzpatrick, L.M., Melbourne, Vic/AUS III-175,III-325
Flett, D.S., Stevenage/UK I- 3 ,II- 3
Flory, K., Karlsruhe/D I-309
Fortuin, J.M.H., Amsterdam/NL III- 31
Fredenslund, A.,Lyngby/DK I- 63
Freiser, H., Tucson,AZ/USA II-385,II-393
Friehmelt, V., Berlin (West) I-245
Fröhlich, M., Garching/D III-301
Frydrych, Ch., Berlin (West) I-245
Fürst, W., Graz/A I-553

G

Gährs, H.J., Krefeld/D III- 51
Gai, Huifa, Shandong/China II-279
Galla, U., Karlsruhe/D I-309
Gallo, V., Trieste/I II-173,III-199,III-255
Gao, Haoqi, Shanghai/China II-301
Gao, Zili, Shandong/China II-279, II-287
Gaonkar, A.G., Auburn, AL/USA II-361
Garcia, D.J., Cartagena/E II-613
Gasparini, G.M., Rome/I I-107,I-355
Gauglitz, R., Berlin (West) I-245
Gaunand, A., Fontainbleau/F II-511
Geerißen, H., Mainz/D III-807
Gelfort, E., Hannover/D I-427
Germain, M., Fontenay-aux-Roses/F I-137
Geyer, H., Potsdam/DDR II-537
Gilles, E.D., Stuttgart/D I-161
Gloe, K., Dresden/DDR II-537
Goebel, J.C., Amsterdam/NL III- 31
Goetz-Grandmont, G.J., Strasbourg/F II-481
Goklen, K.E., Cambridge,MA/USA III-587
Goldacker, Karlsruhe/D I-117
Goldmann, G., München/D III- 11
Golubkov, A.S., Moscow/USSR III-677
Goswami, A.N., Dehra Dun/IND III-539
Goto, M.,. Fukuoka/J I-573
Gourdon, C., Toulouse/F III-353,III-361
Grabas, K., Wrocław/PL I-347
Graham, F.R., Aiken, SC/USA I-381
Grilc, V., Ljubljana/YU III-639
Grizo, A., Skopje/YU III-481
Grosch, A., Bochum/D III-115
Grossi, Rome/I I-107,I-355
Grünbein, W., Frankfurt am Main-Höchst/D III-877
Guerkan, T., Ankara/TR III-846,III-847
Guerriero, R., Venezia/I I-585, II-401
Gutknecht, W., Hannover/D I-601

H

Haberland, K., Leopoldshafen/D I-317
Hänsel, R., Hannover/D III-623
Hamburger, E., Karlsruhe/D I-399
Hamza, A., Garching/D I-459
Hancil, V., Praha/CS II-57,III- 81
Harada, M., Kyoto/J II-309
Harrison, J.W., Harwell,Oxon/UK I-131
Hartland, S., Zürich/CH III- 99,III-191,III-309,III-453
Hassan, F.M., Kuwait/State of Kuwait II-113
Hatton, T.A., Cambridge,MA/USA III- 89,III-587,III-685
Hauertamnn, H.-B., Hannover/D I-601
Haydar, F., Kuwait/State of Kuwait II-113
He, Chunfu, Changchun/China II-651
Hedden, K., Karlsruhe/D III-499
Heddur, R.B., Bombay/IND II-439
Heilgeist, M., Karlsruhe/D I-309

Heits, B., Hannover/D I-427
Hemonic, D., Vert-le-Petit/F II-511
Heng, R., Frankfurt am Main/D II-613
Hodges, M.E., Aiken,SC/USA III-421
Hoecker, J., Clausthal-Zellerfeld/D III-523
Holdich, R.G., Birmingham/UK II- 19
Holt, D.L., Aiken, SC/USA I-381
Homolka, D., Darmstadt /D II-369
Horwitz, Ph., Argonne, IL/USA I- 81
Hu, Shuisheng, Shanghai/China II-487
Hua, Tingting, Beijing/China II-605
Huang, Chunhui, Beijing/China II-215
Huang, Jin-wang, Guangzhou/China II-431
Huber, A., Garching/D I-253
Hughes, M.A., Bradford/UK I- 23,III-755
Humphrey, J.L., Austin,TX/USA III- 39,III- 55
Hunag, Shulan, Beijing/China II-597
Hund, M., Saint-Etienne/F I-511
Hussain, A., Bradford/UK III-149
Hustedt, K.H., Braunschweig/D III-597,III-703

I/J

Ihle, E., Garching/D I-169
Ilic, Z., Beograd/YU I-209
Inomata, H., Sendai/J III-507
Inoue, K., Saga/J II-65, II-263
Irie, J., Fukuoka/J I-573
Ishikawa, I., Hamamatsu/J II-159
Islanova, T. Yu., Moscow/USSR II-377
Ivakhno, S.YU., Moscow/USSR I-593
Jalhoom, M.G., Baghdad/Iraq I-193
Jayasankar, P., Madras/IND I-457
Jedináková, V., Praha/CS III-765
Jeelani, S.A.K., Zürich /CH III-453
Jeffreys, G.V., Birmingham/UK III-157
Jenkins, J.A., Harwell, OX/UK I-379
Ji, Liang-nian, Guangzhou/China II-431
Jiang Dehua, Shandong/China II-279
Jiang, Yu Ming, Shanghai/China III-143,III-225
Jin, Tienzhou, Beijing/China II-215
Jing, Pinlin, Shanghai/China II-495
Jones, St., London/UK III-853

K

Khan, S.,London/UK III-853
Kafarski, P., Wrocław/PL III-669
Kalichkin, S.V., Moscow/USSR II-197
Kanellakopulos, B., Karlsruhe/D I-293
Kang, Sang Ihn, Lubbock, TX/USA I-581
Karr, A.E., Parsippany, N.J. /USA I- 41,III-943
Kása, Z., Veszprém/H III-515
Kassaczký , E., Bratislava/CS III-935
Katayama, Y., Kyoto/J I-545
Kayahara, Y., Kyoto/J II-309

Kedem, O., Rehovot/IL I-525
Keimirov. M.A., Moscow/USSR II-236
Kertes, A.S., Jerusalem/IL III-631,III-741
Keymiriv, M.A., Moscow/USSR II-236
Khalifa, S.M., Cairo/ET II-539
Khisamutdinov, R.A., Ufa/USSR II-527
Khopkar, S.M., Bombay/IND II-439
Kikic, I., Trieste/I II-173,III-479,III-715
Kim, J.I., Garching/D I-293
Kim, K.W., Chung-Nam/Korea I-215
King, C.J., Berkeley, CA/USA III-631,III-741
Kirgios, I., Hannover/D III-623
Kirkopru, A., Boulder, CO/USA I-519
Kirou, V., Syracuse, NY/USA III-135
Kiwan, A.M., Kuwait/State of Kuwait II-113
Kluth, M., Karlsruhe/D I-399
Knittel, G., Karlsruhe/D I-223
Koganti, S.B., Kalpakkam/IND I-413
Kojima, A., Kyoto/J I-545
Kolarik, Z., Karlsruhe/D I-333
Kolycheva, N.V., Moscow/USSR II-197
Kondo, K., Fukuoka/J I-573
Korchinsky, W.J., Manchester/UK III-265
Korolkova, O.V., Moscow/USSR II-197
Korpusov, G.V., Moscow/USSR II-236
Koyama, K., Ibaraki-ken/J I- 91
Kreysa, G., Frankfurt am Main/D III-461,III-767
Kriegel, S., Berlin (West) I-245
Krishna, R., Dehra Dun/IND III-539
Kroner, K.H., Braunschweig/D III-597,III-703
Krylov, Yu.S., Moscow/USSR II-236
Kube, B., Hannover/D I- 99
Kühl, H., Titz-Rödingen/D I-427
Kula, M.-R., Düsseldorf/D III-567
Kuzmin, N.M., Moscow/USSR II-559
Kuznetsov, A.H., Moscow/USSR I-433
Kwiatkowski, J., Warszawa/PL III-791

L

Lack, E., Graz/A III-645
Lackner, H., Graz/A III-339
Lackner, K., Essen/D III-491
Lahiere, R.J., Austin,TX/USA III- 39
Lancelot, F., Saint-Etienne/F I-511
Lange, H.A., Saginaw, MI/USA III-345
Lann Le, M.V., Toulouse/F I-151
Laso, M., Zürich/CH III-309
Lauprêtre, F., Paris/F II-131
Lawson, G.J., Birmingham/UK II- 19
Lawson, P.N.E. Bradford/UK I- 23
Lehmann, R., Frankfurt am Main/D II-613
Lei, Xia, Beijing/China III-215
Leif, V.E., Moscow/USSR III-223
Lejczak, B., Wrocław/PL III-669
Lenhard, U., Krefeld/D III- 51
Leroy, M.J.F., Strasbourg/F II-481,III-919

Li, Biaoguo, Beijing/China II-215
Li, Dequian, Changchun,Jilin/China II-231
Li, Han, Changchun/China II-651
Li, Ji-ding, Beijing/China II-121
Li, Jinshan, Beijing/China II-597
Li, Jokang, Shanghai/China III-423
Li, Junran, Beijing/China II-215
Li, Shushen, Shanghai/China II-487
Li, Yi-gui, Beijing/China II-121,II-122
Li, Yuan-ying, Guangzhou/China II-222
Likidis, Z.,Hannover/D III-695
Linzbach, G., Frankfurt am Main/D III-767
Lisicki, Z., Warszawa/PL III-764,III-791
Lo, T.C., Nutley, N.J./USA I- 41
Logsdail, D.H., Harwell, OX/UK I-379,II-589
Long, Haiyan, Shanghai/China II-495
Lonie, S.J., Caithness/UK I-371
Lorbach, D., Cambridge, MA/USA III-293
Lu, Jiu-fang, Beijing/China II-121,II-122
Luciani, C., Trieste/I III-199
Luerken, F., Krefeld/D III- 51
Ly, J., Gif-sur-Yvette/F I-483
Lyall, E., Harwell, OX/UK I-379
Lyaudet, G., Bessines sur Gartempe/F I-285

M

Ma, Enxin, Shanghai/China II-495
Maćkowiak, J., Bochum/D III-115
Macasek, F., Bratislava/CS I-363
Madariaga, J.M., Bilbao/E III-839
Maher, A., Chatenay-Malabry/F I-231
Majewski, W., Warszawa/PL III-791
Makryaleas, K., Hannover/D III-695
Maljković, Da., Zagreb/YU II-471
Maljković, Du., Zagreb/YU II-471
Marr, R., Graz/A I-553,II-643,III-281,III-293,III-339,III-645,III-653,III-901,III-907
Marrocchelli, A., Rome/I III-149
Martin, C.G., Pinawa, Manitoba/CON I-441
Martin, G., Engis/B I-177
Martin, P.D., Harwell,OX/UK II-589,III-331
Martinez, M., Barcelona/E II-165
Marx, G., Berlin (West) I-245
Mas, C., Karlsruhe/D I-223
Masloboeva, S.M., Moscow/USSR III-223
Massana, A., Bellaterra/E II-239
Matsubara, K., Kawasaki/J III-507
Matsumoto, M., Fukuoka/J I-573
Matt, K., Garching/D I-459
Mayer, M., Frankfurt am Main-Höchst/D III-877
McCray, C.W., Idaho Falls, ID/USA I-143
McDoughall, T.E., Pinawa, Manitoba/CON I-441
McDowell, W.J., Oak Ridge, TN/USA I-477
Mead, D.A., Hatfield, Herts./UK I-537
Mehandjiev, M.R., Sofia/BG II-331
Mehandjieva, K.R., Sofia/BG II-331
Meles, S., Zagreb/YU I-275

Melling, J., Stevenage, Herts./UK I-537
Melnyk, A.J., Pinawa, Manitoba/CDN III-405
Mendes Tasis, M.A., London/UK II- 27
Meng, Shulan, Changchun, Jilin/China II-651
Meng, Xi-quan, Beijing/China II-565
Meng, Xiangsheng, Notre Dame,IN/USA II-223
Meon, W., München/D III-379
Meregalli, L., Venezia/I I-585,II-401
Merz, A., Karlsruhe/D I-317,III-207,III-413
Mesko, V., Skopje/YU III-481
Meyer, E.-R., Hannover/D III-695
Michel, P., Velizy-Villacoublay/F I-285
Michel, Th., Garching/D I-459
Mikéta, Gy., Budapest/H II-519
Mikhailichenko, A.I., Moscow/USSR II-425
Mikucki, B.A., University Park, PA/USA I-561
Miller, J.D., Salt Lake City, UT/USA II-187
Mills, A.L., Harwell, Oxon/UK I-301,I-131,I-421
Milonjic, S., Beograd/YU I-209
Miralles, N., Barcelona/E II-165
Misek, T., Praha/CS III- 71
Missal, P., Karlsruhe/D III-499
Miyake, Y., Kyoto/J II-309,II-323
Moccia, A., Rome/I I-107
Mohan, V., Madras/IND I-457
Molinier, J., Toulouse/F III-239
Mollère, P. D., Belle Chasse, LA/USA II- 49
Moore, R.J., Melbourne, Vic/AUS III-549
Mora, J.C., Odeillo/F III-239
Morosanova, E.I., Moscow/USSR II-559
Mou, Xiru, Beijing/China III-667
Moyer, B.A., Oak Ridge, TN/USA I-477
Mrnka, M., Praha/CS II-195
Mueller, P., Dresden/DDR II-537
Muhammed, M., Stockholm/S I-611,II-237,II-239
Mumford, C.J., Birmingham/UK III-157
Munoz, M., Bellaterra/E III-863
Muratet, G., Paris/F III-353, III-361
Murinov, Y.I., Ufa/USSR II- 75,II-527
Murthy, C.V.R., London /UK II-353
Musikas, C., Fontenay-aux-Roses/F I-261,I-267, II-479
Myers, P.E., Harwell, OX/UK I-379

N

Nagata, T., Kyoto/J II-323
Najim, K., Toulouse/F I-151
Nakai, M., Kyoto/J II-323
Nakashio, F., Fukuoka/J I-573
Navratil, J.D., Golden CO/USA I-343,II-539
Naylor, A., Preston/UK I- 13
Negri, E.D., Manchester/UK III-265
Nekovár, P., Praha/CS II-195
Neuman, R.D., Auburn, AL/USA I-467,II-361
Ngoc Anh, V., Bratislava/CS I-363
Nikitin, Yu. E., Ufa/USSR II- 75
Nilsen, D.N., Albany,OR/USA II-455
Nitsch, W., Garching/D I-169,I-459,III-225,III-301
Noble, R.D., Boulder, CO/USA I-451,I-519,III-865
Noirot, P.A., Villeneuve D`Ascq/F I-491
Nothaft, A., Stuttgart/D I- 99,I-161
Nowottny, Ch., Hannover/D III-695

O

Ochkin, A.V., Moscow/USSR II-195,II-196
Ollenik, R., Garching/D I-169
Oloidi, J.O., Birmingham/UK III-157
Olson, A.L., Idaho Falls, ID/USA I-143,I-387
Orth, D.A., Aiken, SC/USA I- 75,I-381
Osseo-Asare, K., University Park, PA/USA I-561,II-175,II-345,II-409
Otillinger, F., München/D III-445
Ovejero-Escudero, F.J., Toulouse/F II-139
Ozawa, M., Ibaraki-ken/J I- 91
Ozerov, R.P., Moscow/USSR I-433,II-197

P

Paatero, E., Abo/SF II-317
Padmanabhan, K., Madras/IND I-457
Pajak, M., Bochum/D III-115
Papamichael, Braunschweig/D III-597
Pareau, D., Chatenay-Malabry/F I-231,III-739
Park, Hyun-Soo, Chung-Nam/Korea I-215,III-927
Patel, A.N., Nsukka/Nigeria III-731
Pattee, D., Fontenay-aux-Roses/F I-267
Pavasovic, V., Beograd/YU I-209,III-107
Perez de Ortiz, E.S., London/UK II-27,II-345,II-353
Pescher-Cluzeau,Y., Paris/F II-503
Peter, S., Erlangen/D III-605
Petrich, G., Karlsruhe/D I- 31,I-393,I-399
Petrukhin, O.M., Moscow/USSR II- 75,II-197,II-553
Pilhofer, Th., Wiesbaden/D III-723,III-899
Piotrowicz, J., Wrocław/PL II-205
Pitsch, H., Gif-sur-Yvette/F I-483
Plawsky, J. L., Cambridge,MA/USA III- 89
Plucinski, P., Wrocław/PL III-531,III-669
Poddubnykh, L.P., Moscow/USSR II-559
Poehlein, S.R., Atlanta, GA/USA III-659
Poitrenaud, C., Gif- sur-Yvette/F I-483
Poposka, F., Skopje/YU III-481
Popov, S.O., Moscow/USSR I-499
Porebski, T., Warszawa/PL III-885
Porta, J.J. Karlsruhe/D III-207,III-413
Pouillon, D., Berkeley, CA/USA II- 99
Pouskouleli, Ottawa, ONT/CDN II-581
Powers, L.A., Albany, OR/USA II-455
Pratt, H.R.C., Melbourne, Vic/AUS III-175,III-325,III-549
Preez du, A.C., Randburg/ZA II- 83
Preston, J.S., Randburg/ZA II- 83
Preti, U., Trieste/I III-199
Prevost, M., Vert-le-Petit/F III-919
Prior, A., Gerolfingen-Biel/CH II-643
Procházka, J., Praha/CS III-107,III-231
Prochaska, K., Poznań/PL II-35
Prostenik, M.V., Zagreb/YU I-275

R

Rajec, P., Bratislava/CS I-363
Ramanujam, S., Parsippany, NJ/USA I- 41,III-935
Ramm, H., Stuttgart/D I-161
Rashid, Z.A., Poznań/PL II- 35
Rebelein, F., München/D III-387
Rehacek, V., Bratislava/CS I-363
Reicheley-Yinger, L., Argonne, IL/USA II-255
Renon, H., Fontainbleau/F II-511
Reuben, B. G., London/UK III-853
Reznicková, J., Praha/CS III- 81
Reznik, A.M., Moscow/USSR I-621,II-377,III-621
Rhein, H.-B., Hannover/D III-273,III-623
Rice, N.M., Leeds/UK II-633
Rickel, R.L., Albany, OR/USA II-455
Rickelton, W.A., Niagara Falls, ONT/CDN III-775
Riffel, W., Karlsruhe/D I-399
Ritcey, G.M., Nepean,ONT/CDN I- 51,II-581
Robertson, A.J., Niagara Falls, ONT/CDN III-775
Rod, V., Praha/CS II- 57,III- 81
Rodrigues de Carvalho. J.M. Lisboa/P II-295
Romano, J., Zagreb/YU I-275
Ross, R., Oxford/UK I-421
Rückl, W., Graz/A III-653
Russell, J.H., Albany, OR/USA II-455
Rydberg, J., Göteborg/S III- 21

S

Saito, S., Sendai/J III-507
Sakuramoto, T., Kyoto/J I-545
Sandino, M.C., Bilbao/E III-839
Sandoval, S.P. Reno, NV/USA I-572
Sastre, A., Barcelona/E II-165
Sato, K., Hamamatsu/J II-153,II-159
Sato, T., Tokyo/J II-153,II-159
Savastano, C.A. London/UK II-345
Sazonov, V.P., Kuibyshev/USSR III-747
Schaekers, J.M., Pretoria/ZA I-185
Schaller, C., Frankfurt am Main/D III-461
Schein, R., Graz/A II-643
Scheper, T., Hannover/D III-695
Schlosser, St., Bratislava/CS III-935
Schmidt, H., Karlsruhe/D I-405
Schmieder, H., Karlsruhe/D I- 33,I-117,I-309
Schoen, J., Karslruhe/D I-399
Schouteeten, A., Stains/F III-739
Schrötterová, D., Praha/CS II-195
Schügerl, K., Hannover/D I-601,III-273,III-577,III-623,III-695
Schützeichel, P., Mainz/D III-807
Schultze, L. E., Reno,NV/USA I-572
Schulz, W.W., Richland,WA/USA I- 81

Seekamp, M., Erlangen/D III-605
Sekine, T., Tokyo/J II-179
Semenov, S.A., Moscow/USSR I-621,II-377,III-621
Seregina, I.P., Moscow/USSR II-553
Serjogina, I.F., Moscow/USSR II- 75
Seward, G.W., Phoenix, AR/USA II- 11
Shehata, F.A., Cairo/ET II-539
Shen, Jinglan, Shandong/China II-279,II-287
Shen, Haihua, Shanghai/China III-431
Shen, Zujun, Shanghai/China III-431
Shikinev, V.M., Moscow/USSR II-547
Shin, Y.J., Chung-Nam/Korea I-215
Shkil,A.N., Moscow/USSR II-553
Shuquistedt, L., Abo/SF II-247
Sibrell, P.L. Salt Lake City, UT/USA II-187
Siebenhofer, M., Graz/A III-281,III-653,III-907
Simons, A.J. F., Geleen/NL III- 31
Sinegribova, O.A., Moscow/USSR I-433,I-593,III-831
Singh, D., Pinawa, Manitoba/CDN III-369
Skarnemark, Göteborg/S III- 21
Sklokin, L.I. Moscow/USSR III-223
Slater, M.J., Bradford/UK III-149
Sluys, van, R., Geleen/NL III- 31
Smith, D.C., Leeds/UK II-633
Smith, J.K., Cumbria/UK I-201
Smith, J.M., Delft/NL III-317
Soldenhoff, K.H., Randburg/ZA II-123
Sovilj, M., Novi Sad/YU III-557
Sovová, H., Praha/CS III-231
Spivakov, B. Ya., Moscow/USSR II-547
Sreedharan, V.,Kalpakkam/IND I-413
Srinivas, V.K., Madras/IND I-475
Srinivasan, D., Madras/IND I-475
Steiner, L., Zürich/CH III- 99,III-191,III-309
Stenström, S., Lund/S III-815,III-823
Stephan, K., Garching/D I-293
Stepniak-Biniakiewicz, D., Poznań/PL II-35
Stevanovic, R., Beograd/YU I-209,III-107
Stevens, G.W., Melbourne, Vic/AUS III-175,III-325,III-549
Stieglitz, L., Karlsruhe/D I-239
Stitt, E.H., Bradford/UK III- 63
Stockwell, C.L., Oxon, OX/UK III-331
Su, Li-Min, Beijing/China III-397
Su, Yuanfu, Shanghai/China II-271,II-301,III-285,III-423
Suh, In-Suk, Chung-Nam/Korea III-927
Sun, Sixiu, Shandong/China II-279,II-287
Sun, Bing Yao, Shanghai/China III-143,III-225
Szafranski, A., Warszawa/PL III-764,III-791
Sze, Y., Pinawa, Manitoba/CDN I-441
Szilassy, I., Budapest/H II-519
Szust, J., Wrocław/PL III-531
Szymanowski, J., Poznań/PL II- 35,II-415

T

Takaya, H., Kyoto/J I-545
Takeda, T., Kyoto/J II-323
Takeuchi, Y., Hamamatsu/J II-153
Tamada, J.A., Berekley, CA/USA III-631
Tavlarides, L.L., Syracuse,NY/USA III-129,III-135
Tawfik, W.Y., Atlanta, GA/USA III-659
Tayeb, A., Strasbourg/F II-481
Tedder, D.W., Atlanta, GA/USA III-659
Teng Teng, Beijing/China II-121,II-122
Teramoto, M., Kyoto/J I-545,II-323
Textoris, A., Bessines sur Gartempe/F I-285
Thien, M.P., Cambridge,MA/USA III-685
Thompson, P.J., Caithness/UK I-371
Thornton, J.D., Caithness/UK I-371
Thyrion, F.C., Louvain-la-Neuve/B III-613
Tiegs, C., Erlangen/D III-605
Todd, D.B., Saginaw,MI /USA III-345
Todd, T.A., Idaho Falls, ID/USA I-387
Tolic, A., Belgrade/YU III-557
Tolstikov, G. A., Ufa/USSR II- 75
Tomzik, S., Warszawa/PL III-885
Torri, G., Rome/I I-355
Tromp, M., Strasbourg/F III-919
Tsien, H.H., Strasbourg/F II-481
Tzirel`son, V.G., Moscow/USSR II-197

U /V

Ueda, T., Kawasaki/J III-507
Uhlemann, E., Potsdam/DDR II-537
Vadasdi, K., Budapest/H II-519
Valiente, M., Bellaterra/E II-237,II-239,III-863
Varnek, A.A., Moscow/USSR I-433,II-197
Vernadsky, V.I., Moscow/USS I-499
Vialard, E., Fontenay-aux-Roses/F I-137
Vijayan, S., Pinawa, Manitoba/CDN III-369,III-405
Villegas, E.A., Minas Gerais/BR II- 99
Vinogradova, J.N., Moscow/USSR II-236
Vitart, X., Fontenay-aux-Roses/F II-479
Vittadini, I., Venezia/I I-585,II-401
Vogelpohl, A., Clausthal-Zellerfeld/D III-247,III-523
Vorob`eva, G.A., Moscow/USSR II-547

W

Wachter, R., Graz/A I-567,III-901
Wärnheim, T., Stockholm/S II-317
Walker, R.D., Inman, SC/USA II-107
Walkowiak, W., Lubbock, TX/USA I-581
Walter, R., Karlsruhe/D I-317,III-413
Wang, Chenguo, Changchun, Jilin/China II-232
Wang, D.I.C., Cambridge, MA/USA III-685
Wang, Jiading, Beijing/China III-215
Wang, Wenqing Xiaobo, Beijing/China I-175
Wang, Z.M., Shanghai/China III-285
Wang, Zhonghuai, Changchun, Jilin/China II-231

Warmoeskerken, M.M.C.G., Deft/NL III-317
Warshawsky, A., Rehovot/IL I-525
Wasylkiewicz, St., Wrocław/PL II-205
Watson, E.K., Niagara Falls, ONT/CDN III-775
Waubke, M., Garching/D III-255
Way, J.D., Boulder, CO/USA III-865
Weidner, E., Erlangen/D III-605
Wendt, H., Darmstadt/D II-369
West, D.W., Stevenage/UK II- 3
Westerholm, K., Abo/SF II-247
Weyer, W., Titz-Rödingen/D I-427
Wichterlová, J., Praha/CS II- 57
Wilkins, M., Harwell, Oxon/UK I-131
Will, R., Karlsruhe/D I-239
Wilson, P.D., Cumbria/UK I-201
Wingefors, S., Lund/S III-815,III-823
Wisniewski, M., Poznan/PL II-415
Wojtech, Frankfurt am Main-Höchst/D III-877
Wolf, B.A., Mainz/D III-807
Wozniak, M., Villeneuve D`Ascq/F I-491
Wu, Fubing, Shanghai/China II-495
Wu, Zhi-chun, Beijing/China II-447

X/Y

Xi, Deli, Beijing/China II-605
Xi, Zhengkai, Shandong/China II-287
Xia, Jing-mao, Guangzhou/China II-431
Xu, Guangxian, Beijing/China II-215
Xu, Zhihong, Beijing/China II-223
Yagodin, G.A., Moscow/USSR I-433,I-593,II-197,III-622,III-627,III-677
Yamanouchi, T., Ibaraki-ken/J I- 91
Yan, Jinying, Shanghai/China II-495
Yan, Xiaomin, Shanghai/China II-495
Yanagiuchi, M., Kawasaki/J III-507
Yang, Yan-sheng, Guangzhou/China II-222
Ye, Weizhen, Shanhai/China II-495
Yoo, Jae-Hyung, Chung-Nam/Korea I-215,III-927
Young, C.H., Manchster/UK III-265
Yu Ming, Jiang, Shanghai/China III-143
Yu, Han-chang, Guangzhou/China II-431
Yu, Kening, Beijing/China II-573
Yu, Qian, Beijing/China III-215
Yu, Shu-qui, Beijing/China II-447,II-565,II-573
Yuan, Chengye, Shanghai/China II-487
Yurchenko, L.D., Moscow/USSR I-621,II-377,III-621
Yurtov, E.V., Moscow/USSR III-622,III-677

Z

Zak, M., Warszawa/PL III-913
Zha, Jinrong, Beijing/China II-223
Zhang, Shouhua, Shanghai/China III-285
Zhang, Weixing, Changchun/China II-651
Zhang, X., Beijing/China I-585
Zhao, Qi, Shanghai/China III-225
Zheng, Y., Beijing/China II-175
Zhong, Yun Xiaon, Beijing/China I-175, III-667

Zhou, Xuexi, Beijing/China II-597
Zhu Jiawen, Shanghai/China III-423
Zhu, Tun, Beijing/China II-339,II-597
Zieborak, K., Warszawa/PL III-885
Zimmer, E., Jülich/D I-325
Zolotov, Yu. A., Moscow/USSR II- 75,I-499,II-547,II-553,II-559
Zvarova, T.I., Moscow/USSR II-547